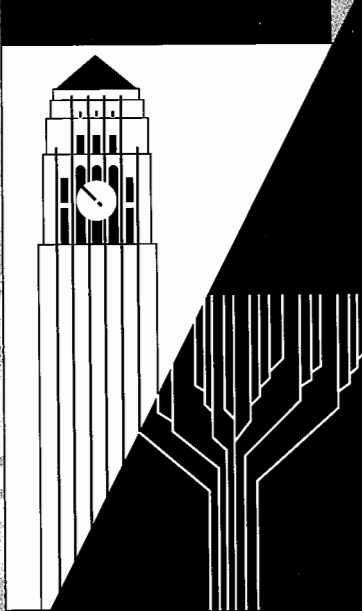


# 1993 URSI

## RADIO SCIENCE MEETING

### PROGRAM AND ABSTRACTS



JUNE 28 - JULY 2, 1993

UNIVERSITY OF MICHIGAN

ANN ARBOR, MICHIGAN, U.S.A.



## **ACKNOWLEDGEMENTS**

The Symposium Steering Committee is pleased to acknowledge the financial support of the following organizations. A final list of sponsors will be published in the Program which will be distributed at the time of the Symposium.

### **OFFICIAL SYMPOSIUM SPONSOR**

Intel Corporation

### **OTHER SPONSORS**

Environmental Research Institute of Michigan  
Air Force Institute of Technology

108  
109  
114

328

NATIONAL ACADEMIES OF SCIENCE AND ENGINEERING  
NATIONAL RESEARCH COUNCIL  
OF THE UNITED STATES



## RADIO SCIENCE MEETING

28 JUNE – 2 JULY 1993

### Program and Abstracts

SPONSORED BY  
THE UNITED STATES NATIONAL  
COMMITTEE FOR URSI

THE UNIVERSITY OF MICHIGAN  
ANN ARBOR, MICHIGAN

(ii)

## Steering Committee

**Chair:** John L. Volakis

|   |   |
|---|---|
| <b>AP-S Program Committee Chair</b><br>Linda P.B. Katehi                                | <b>URSI Program Committee Chair</b><br>Thomas B.A. Senior |
| <b>Evening Local Arrangements</b><br>Valdis V. Liepa                                    | <b>Daytime Local Arrangements</b><br>Kamal Sarabandi      |
| <b>Finance</b><br>Anthony W. England  | <b>Publicity</b><br>Gabriel M. Rebeiz                     |
| <b>Exhibits</b><br>Thomas D. Monte<br>John L. Volakis                                   | <b>Industrial Relations</b><br>Ivan J. LaHaie             |
| <b>Workshops and Short Courses</b><br>Mark A. Ricoy<br>Richard C. Compton<br>Bill Scott | <b>Publications</b><br>Brian E. Gilchrist                 |
| <b>Conference Coordinator</b><br>A. Pendleton Tully                                     | <b>Registration</b><br>M. Craig Dobson                    |
| <b>Designs and Typesetting</b><br>Marie Howard  | <b>Spouse Activities</b><br>Austra Liepa<br>Maria Volakis |
| <b>AP-S Liaison</b><br>Stuart A. Long   | <b>URSI Liaison</b><br>W. Ross Stone                      |

## **The United States National Committee for URSI**

|                      |                           |
|----------------------|---------------------------|
| Chair                | <b>Chalmers M. Butler</b> |
| Vice Chair           | <b>David C. Chang</b>     |
| Secretary            | <b>Charles M. Rush</b>    |
| Immediate Past Chair | <b>Sidney A. Bowhill</b>  |

## **URSI Technical Program Committee**

**Thomas B.A. Senior (chair)**

|                         |                       |
|-------------------------|-----------------------|
| <b>N.G. Alexopoulos</b> | <b>R.J. Mailloux</b>  |
| <b>T. Itoh</b>          | <b>J.W. Mink</b>      |
| <b>D.R. Jackson</b>     | <b>J.H. Richter</b>   |
| <b>M. Kanda</b>         | <b>F. Schwering</b>   |
| <b>R.E. Kleinman</b>    | <b>E.F. Soderberg</b> |
| <b>J.C. Lin</b>         | <b>E.R. Westwater</b> |

## Table of Contents

| Session          |  | Page |
|------------------|--|------|
| URSI B-1         | Computational RCS . . . . .  | 1    |
| URSI B-2         | Microstrip Structures . . . . .  | 13   |
| URSI D-1         | Studies of MMIC Transmission Lines . . . . .   | 25   |
| AP-S/URSI F-1    | Remote Sensing . . . . .   | 35   |
| URSI K-1         | Electromagnetic Interactions with Biological Systems . . . . .                                 | 47   |
| URSI B-3         | Time Domain Methods II . . . . .   | 57   |
| URSI B-4         | Scattering . . . . .   | 69   |
| URSI B-5         | Antenna Arrays . . . . .   | 81   |
| AP-S/URSI B-6    | Artificially Soft and Hard Surfaces for Electromagnetic Waves and their Applications . . . . . | 93   |
| URSI D-2         | Opto-Electronic Devices and Systems . . . . .  | 95   |
| URSI F-2         | Communications . . . . .   | 107  |
| AP-S/URSI K-2    | Electromagnetics in Biomedical Sensing, Diagnosis and Treatment . . . . .                      | 117  |
| URSI K-3         | Biomedical Applications of Electromagnetic Fields . . . . .                                    | 123  |
| AP-S/URSI B-7    | Radiation and Scattering from Complex Structures (Honoring Leon Peters, Jr.) . . . . .         | 129  |
| URSI B-8         | Time Domain Methods III . . . . .  | 139  |
| URSI B-9         | Integral Equation Methods I . . . . .  | 151  |
| URSI D-3         | Integrated Antennas and Feeds . . . . .  | 163  |
| URSI F-3         | Scattering and Clutter . . . . .   | 169  |
| URSI A-1         | Material Measurements . . . . .  | 175  |
| URSI B-10        | Finite Element Methods II . . . . .  | 187  |
| URSI B-11        | Antennas . . . . .   | 199  |
| AP-S/URSI D-4    | Advances in MMIC Packaging for Phased Array Antennas . . . . .                                 | 211  |
| URSI A/E-2       | Electromagnetic Field Measurements . . . . .   | 213  |
| URSI B-12        | Inverse Scattering . . . . .   | 225  |
| URSI B-13        | Complex and Chiral Media . . . . .   | 237  |
|                  | Plenary Session . . . . .  | 249  |
| URSI B-14        | Finite Element Methods III . . . . .   | 251  |
| URSI B-15        | Electromagnetic Theory III . . . . .   | 261  |
| AP 8-8/URSI B-16 | New Techniques in Computational Electromagnetics . . . . .                                     | 273  |
| URSI D-5         | Integrated Systems . . . . .   | 279  |
| URSI B-17        | Waveguides I . . . . .   | 289  |
| AP-S/URSI B-18   | W.V.T. Rusch Reflector Antenna Memorial Session . . . . .                                      | 301  |

|               |  |     |
|---------------|--|-----|
| URSI B-19     | Media Modeling . . . . .                                 | 303 |
| URSI B-20     | Integral Equation Methods II . . . . .                   | 315 |
| URSI B-21     | Diffraction . . . . .                                    | 327 |
| AP-S/URSI D-6 | Optical Controlled Arrays . . . . .                      | 339 |
| AP-S/URSI D-7 | Digital Controlled Arrays . . . . .                      | 341 |
| URSI A-3      | Antenna Measurements . . . . .                           | 343 |
| URSI B-22     | Pulse and Time Domain Analyses . . . . .                 | 355 |
| URSI B-23     | Canonical Problems . . . . .                             | 367 |
| URSI B-24     | Radiating Structures . . . . .                           | 379 |
| AP-S/URSI D-8 | Downsizing Technology in Mobile Communications . . . . . | 391 |
| URSI B-25     | Waveguides II . . . . .                                  | 393 |
| URSI B-26     | Rough Surfaces . . . . .                                 | 405 |
|               | Index . . . . .  | 417 |

**SESSION URSI B-1****MONDAY AM****COMPUTATIONAL RCS**

Chairs: C.M. Butler, Clemson University; H.B. Tran, Rockwell International

Room: Modern Languages Building, Auditorium 1      Time: 8:30-12:10

|       |  |    |
|-------|--|----|
| 8:30  | RCS OF AN EXTENDED CONDUCTING OBJECT ABOVE A DISSIPATIVE HALF SPACE<br><i>John P. Casey*, NUWC Detachment; Rajeev Bansal, The University of Connecticut</i>  | 2  |
| 8:50  | COMBINING PHYSICAL OPTICS WITH EDGE-BASED TRIANGULAR-PATCH EXPANSION FUNCTIONS IN ELECTROMAGNETIC SCATTERING PROBLEMS<br><i>P.M. Goggans*, A.W. Glisson, University of Mississippi</i>   | 3  |
| 9:10  | ELECTROMAGNETIC SCATTERING FROM 3-D TREATED CAVITIES VIA A CONNECTION SCHEME USING TRIANGULAR SURFACES PATCHES<br><i>Luiz C. Trintinalia*, Hao Ling, The University of Texas at Austin; Tai-Mo Wang, National Taiwan Institute of Technology</i> | 4  |
| 9:30  | COMPUTER SIMULATION OF INHOMOGENEOUS WAVE TRACKING<br><i>Satinath Choudhary, William Paterson College of New Jersey</i>  | 5  |
| 9:50  | IMPROVEMENT OF NUMERICAL SOLUTION FOR HIGH PERMITTIVITY DIELECTRIC TARGETS OF ARBITRARY CROSS-SECTIONS<br><i>H. Moheb, L. Shafai, University of Manitoba; S. Mishra, C. Larose, Canadian Space Agency</i>  | 6  |
| 10:10 | BREAK  |    |
| 10:30 | HIGH FREQUENCY SCATTERING BY A CONDUCTING CIRCULAR CYLINDER COATED WITH A DIELECTRIC OF NON UNIFORM THICKNESS<br><i>S. Gökhan Tanyer, Robert G. Olsen, Washington State University</i>   | 7  |
| 10:50 | FINITE VOLUME TECHNIQUE DOMAIN METHOD FOR THE COMPUTATION OF THE RADAR CROSS SECTION OF 3D BODIES<br><i>F. Hermeline, R. Le Martret, C. Le Potier*, Centre d'Etudes de Limeil-Valenton</i>   | 8  |
| 11:10 | RCS OF NON-ROTATIONAL AND DIELECTRIC TARGETS<br><i>S. Kiener*, Communications Research Laboratory; S. Mishra, C. Larose, David Florida Laboratory</i>  | 9  |
| 11:30 | OPTIMIZATION TECHNIQUES IN 2-DIM ELECTROMAGNETIC SCATTERING PROBLEMS<br><i>E. Bleszynski, M. Bleszynski, H.B. Tran*, Rockwell International</i>  | 10 |
| 11:50 | FAST RAY TRACING ALGORITHM FOR RCS PREDICTION WITH GRECO CODE<br><i>Juan M. Rius*, Merce Vall-llossera, Angel Cardama, Lluis Jofre, Universitat Politecnica de Catalunya</i>   | 11 |

## RCS OF AN EXTENDED CONDUCTING OBJECT ABOVE A DISSIPATIVE HALF SPACE

John P. Casey\*  
Submarine Electromagnetic Systems Department  
Naval Undersea Warfare Center Detachment  
New London, CT 06320

Rajeev Bansal  
Department of Electrical and Systems Engineering  
The University of Connecticut  
Storrs, CT 06269

Most RCS studies have focused on targets in free space. Common examples include the scattering from aircraft, missiles, and antennas. However, there are many cases where the target is located in the presence of a dissipative half space. Examples from the field include land-based vehicles and ships at sea. A similar problem arises in RCS measurements of large objects on an outdoor range.

This paper will try to relate the RCS of an extended object above a dissipative half space to its free space RCS using a point target formula (Knott, Shaeffer, and Tuley, *Radar Cross Section*, p. 353, Artech House, 1985). Four major scattering mechanisms that occur for a target above a half space are the direct (free space), double-bounce (image), and two single-bounce (diplane effect) returns. The relative contribution from each scattering mechanism will be discussed. Numerical results will be represented for several canonical geometries using a body of revolution algorithm based on the method of moments.

**COMBINING PHYSICAL OPTICS WITH EDGE-BASED TRIANGULAR-PATCH EXPANSION FUNCTIONS IN ELECTROMAGNETIC SCATTERING PROBLEMS**

P.M. Goggans\* and A.W. Glisson

University of Mississippi

Department of Electrical Engineering

University, MS 38677

The edged-based triangular-patch expansion function (S.M. Rao, D.R. Wilton, and A.W. Glisson, *IEEE Trans. on Antennas. and Propagat.*, AP-30, 409-418, 1982) is widely used in the moment method (MM) solution of scattering from arbitrarily shaped conducting objects. The edge based expansion function is used in conjunction with a flat triangular facet model of the scattering object. The expansion function is defined for each edge of the facet model. The current crossing an edge in the direction normal to the edge and in the planes of the two connected triangles is the to-be-determined current expansion coefficient. The current on a triangle which crosses a particular edge is assumed to flow radially from the opposite vertex and to vary linearly with the distance from the opposite vertex so that the current is zero at the vertex and has the correct normal component at the edge. The total current on a triangle is the sum of the currents crossing its three edges. For open bodies some edges are connected to only a single triangle. The value of the current expansion coefficient for these edges is zero.

Because the edge lengths in the facet model must be less than about a fifth of a wavelength, the size of scattering objects which can be reasonably considered using the MM with the edge based expansion functions is limited to the resonance region. However, the size of scatterers which can be considered can be increased using a straight forward hybrid method if some of the edge currents can be determined in advance of the MM solution. Here we investigate the use of the physical optics (PO) approximation to determine the edge currents. Because the outward surface normal on the two triangles connected to an edge are in general different, the PO approximation for the normal component of the current crossing the edge is different for each triangle. Here we use the area weighted average of the current components on the connected triangles to determine the edge current approximation.

In this paper we compare the RCS determined using three numerical methods. The three methods are the exact PO integral for triangular facets, the PO approximation with edge based expansion functions, and the hybrid PO and MM. Flat plate and spherical scatterers are considered and the RCS results are compared with the series solution or with the complete MM solution.

**ELECTROMAGNETIC SCATTERING FROM 3-D  
TREATED CAVITIES VIA A CONNECTION SCHEME  
USING TRIANGULAR SURFACES PATCHES**

Luiz C. Trintinalia\*, Hao Ling  
Department of Electrical and Computer Engineering  
The University of Texas at Austin  
Austin, TX 78712-1084

Tai-Mo Wang  
Department of Electronic Engineering  
National Taiwan Institute of Technology  
Taipei, Taiwan

Electromagnetic scattering from cavities is a problem of fundamental importance in radar cross section (RCS) reduction and in electromagnetic penetration and coupling studies. Despite of the fact that much work treating two-dimensional or specialized three-dimensional cavities can be found in the literature, data for arbitrary shaped three-dimensional geometries is relatively scarce.

Previously, a connection scheme for cavity problems was developed (Wang & Ling, IEEE-AP, 1505-13, 1991) to alleviate computational constraints for three-dimensional problems, based on microwave network theory. This scheme allows the cavity to be divided into sections and each section to be analyzed independently of the rest of the cavity. Consequently significant reduction in computational resources, both memory and processing time, can be achieved. However, since pulse basis functions were used in conjunction with point matching, problems with slow convergence and low accuracy were found.

In this work, we improve upon that formulation by the use of triangular surface patch basis functions (Rao, Wilton & Glisson, IEEE-AP, 409-18, 1982) combined with the Galerkin method to get better convergence performance. These basis functions are very suitable for modeling arbitrary shaped surfaces. Furthermore they are free of line charges, which leads, in general, to more stable solutions. In addition, the impedance boundary condition (IBC) is implemented to model wall treatment in cavities. The validity of the IBC approach for interior cavity problem is investigated by comparing the results obtained using the present formulation with mode-matching results for regular geometries.

## Computer Simulation of Inhomogeneous Wave Tracking

Satinath Choudhary

Department of Computer Science

William Paterson College of New Jersey

Wayne, NJ 07470

Waves of which intensity vary appreciably over its wave front are classified as Inhomogeneous waves, as opposed to waves with relatively constant intensity across their direction of propagation, which may be called homogeneous waves. A laser beam, or for that matter any beam (RADAR beam, SONAR beam, or sound beam) that has a beam width of only a few wave lengths, may be classified as inhomogeneous wave. If a wave has a focal point, or has a caustic, it may be considered to be inhomogeneous near the focal region and caustic region. We thus see that inhomogeneous waves are omnipresent.

In (S. Choudhary and L.B. Felsen, IEEE Trans., AP-21, No. 6, pp . 827 -842, 1973,) an Asymptotic Theory for Inhomogeneous Wave Propagation has been developed. A computer program is being developed to produce ray tracing in accordance with the said theory. It should be pointed out that if a wave is sufficiently inhomogeneous, the ray trace of the wave may be curved even in a homogeneous medium like the free space.

Computer simulation of Inhomogeneous Wave Tracking will enable us to deal with any general wave profile that may not be analytically tractable. The program developed so far has already given us very interesting results. It has indicated that the peripheral rays of a perfectly collimated gaussian beam intersect each other and form a caustic. We hope to apply it to many problems of practical interest including improvement design of optical instruments.

## IMPROVEMENT OF NUMERICAL SOLUTION FOR HIGH PERMITTIVITY DIELECTRIC TARGETS OF ARBITRARY CROSS-SECTIONS

H. Moheb, L. Shafai

*Department of Electrical & Computer Engineering*  
*University of Manitoba, Winnipeg, Manitoba, Canada R3T 2N2*

S. Mishra, C. Larose

*Canadian Space Agency Ottawa, Ontario, Canada K2H 8S2*

### Introduction

A theoretical and experimental study is undertaken to investigate the radar scattering of various three-dimensional targets. The targets considered have prismatic structure and are made of high dielectric constant materials. The surface integral equations are formulated by the equivalence principle in terms of equivalent surface electric and magnetic currents. A moment method is then used to reduce the integral equations to a matrix equation to compute the current coefficients. However, the solution accuracy deteriorates as the dielectric constant increases (A. Kishk, and L. Shafai, IEEE Trans., Antennas & Propagat., pp. 1486-1490, Nov. 1989.), and different integral equations must be used to overcome this problem (H. Moheb, and L. Shafai, IEEE Trans. Antennas & Propagat., pp. 758-766, June 1991). For instance, the E-field formulation gives more accurate results for large dielectric constants. However, the solution accuracy is still unacceptable and limited to moderate values of dielectric constant or the target size. To improve the accuracy, one may increase the number of segmentation which consequently increases the size of moment matrix and the CPU time.

As an alternative approach, in the present study the method of coordinate transformation was used to map the target cross-section onto a circle. Triangular basis functions were selected along the  $t$  vector and entire domain Fourier type basis functions were used in the cross-section. The resulting matrix equations were then a generalized form of those used for bodies of revolution, in which current modes were coupled. However, in reducing the surface integral equations to a matrix equation the surface current is modelled with fixed number of triangular pulses, regardless of the dielectric permittivity. But, for large dielectric constants each triangle is modelled with more number of pulses. The outcome of this method is that the matrix size becomes independent of the material constants and varies only with the target size.

In the measurement procedure, the amplitudes and relative phases of the scattering matrix elements were obtained. They were then used to determine the radar cross-section of the targets for linearly polarized transmitters and receivers. Both methods were then applied to study the scattering by conducting and material targets, for different polarizations and incident angles. Good agreement between numerical and experimental results is obtained and will be presented and discussed.

# HIGH FREQUENCY SCATTERING BY A CONDUCTING CIRCULAR CYLINDER COATED WITH A DIELECTRIC OF NON UNIFORM THICKNESS

S. Gökhun Tanyer

Robert G. Olsen

School of Electrical Engineering and Computer Science  
Washington State University  
Pullman, WA 99164-2752

The electromagnetic (EM) scattering from a perfectly conducting (PEC) cylinder coated with a dielectric layer of non uniform thickness is analyzed. A series solution is derived using the boundary value approach. Both the PEC cylinder and the dielectric coating are assumed to be of infinite length and of circular cross-section. The axes of the cylindrical dielectric coating and the PEC cylinder are parallel but offset by an arbitrary amount to obtain a dielectric coating of non uniform thickness. Transverse (to both of the cylinder axes) electric (TE) and magnetic (TM) plane wave excitations are considered in the analysis. To apply the boundary equations, the EM fields at the air-dielectric coating boundary were transformed to the PEC cylindrical coordinate system using the addition theorem for Bessel functions. Matching boundary conditions results in a linear matrix equation of infinite size. It is shown that for electrically small cylinders the matrices can be truncated to smaller practical sizes while preserving accuracy.

For high frequency applications, the matrix size cannot be reduced significantly and so the matrix equation is difficult to solve. Further the series is slowly converging. Using the perturbation technique an analytical solution for the matrix equation is derived which is restricted to thin coatings. This analytical expression is used to derive a rapidly convergent series solution for high frequencies by applying the Watson transform. The geometrical optics (GO) term is isolated using saddle point integration. It is shown that the GO term obtained in this work is consistent with GO terms obtained assuming locally uniform dielectric thicknesses. The remaining terms account for the diffracted fields. The electromagnetic characteristics associated with the creeping waves supported by a cylinder coated with a non uniformly thick dielectric coating are currently being investigated.

## FINITE VOLUME TECHNIQUE DOMAIN METHOD FOR THE COMPUTATION OF THE RADAR CROSS SECTION OF 3D BODIES.

F. Hermeline, R. Le Martret, C. Le Potier\*

Commissariat à l'Energie Atomique, Centre d'Etudes de Limeil - Valenton  
94195 Villeneuve St Georges Cedex, France

In this paper, we consider the problem of computing the surface currents and the Radar Cross Section (RCS) of a three dimensional perfectly conducting body. We use a finite volume technique and resolve Maxwell's curl equations in the time domain.

The finite volume method which is based on Madsen and Ziolkowski's paper (a 3D modified finite volume technique for Maxwell's equations 1990) is in fact a direct generalization of the algorithm introduced by Yee and allows the use of mixed polyhedral cells. In this kind of method, it is necessary to define a dual grid. We simplify Madsen and Ziolkowski's algorithm giving an other definition of the faces of the dual grid. Also, Absorbing Boundary Conditions (ABCs) of first order (Joly-Mercier, INRIA n° 1047 1989) which are a generalization of Engquist and Majda's ABCs for Maxwell's equations in three dimensions and a simplification of Bendali and Halpern's ABCs (CRAS Paris, Tome 307, Serie 1 n° 20 1988) are implemented on a parallelepiped which terminates the computational domain. This allows us to use grids which are composed of orthogonal hexaedral cells far from the scatterer. It is worth noting that, implementing these ABCs, we have to take into account the edges of the parallelepipedic boundary. We give some numerical results. The case of the sphere is a good validation of the computation because we have to use skewed hexaedral cells to approximate the surface of the body.

## RCS of Non-Rotational and Dielectric Targets

S. Kiener\*,

Electromagnetic Compatibility, CRL,  
4-2-1, Nukui-Kitamachi, Koganei, Tokyo 184

S. Mishra & C. Larose

CSA, David Florida Laboratory, POB 11490,  
Station "H", Ottawa, K2H 8S2 Canada

After getting a good correlation for the RCS of simple shapes ("Hotdogs": 3D cylinders with hemispherical caps; in the present case ratio height to radius 5:1), the MMP-3D is now tested for non rotational and dielectric targets. To give more information full measurements of targets at all possible incident angles have been measured and computed.

If the "Hotdog" shape is conserved, the metallic targets are now composed of two of these shapes interfering at different distances, from touching to... In all these cases, the coupling can be observed.

For dielectric targets we have also kept the basic shape and compared with measurements in the 2-18 GHz range were our targets are around 8 wave lengths long.

For that purpose, the MMP-3D code have been fully automatized to obtain the RCS of plane waves from any angle as the number of files to produce increases dramatically. Usually, the measurements are performed every  $0.25^\circ$  which is equivalent to 360 files for the simulation (for targets with 3 planes of symmetry) and for one polarization.

This automatization is only a preprocessor for the basic MMP-3D code to drive the different frequencies and incident angles and a simple post-processor to get the data in a representable form.

The basic features of the codes are conserved (direct expansion of the fields in series of multipole functions and generalized Point Matching technique for the solver).

The construction and the computation of the "double Hotdog" does not represent any difficulties. Compared with a single hotdog it has the same amount of planes of symmetry (but there are twice as many matching points) and only 1/8 of the geometry has to be constructed.

The only difference with the computation of a perfect conducting body (or even non-perfect) is the different boundary conditions:

– For perfect conductors, only the 3 tangential electric and magnetic components are matched to zero.

– For dielectric bodies, the tangential components are continuous and the normal components jump depending on the electromagnetic characteristics of the material.

Furthermore, inside the dielectric body the fields have to be modeled with multipoles (with origins located outside the body) or, if the body is smooth enough with one "normal expansion" (Hankel functions in the multipoles, Bessel functions in the normal expansion).

For the 5:1 Hotdog a normal expansion at the center of symmetry of the body is very well adapted.

## OPTIMIZATION TECHNIQUES IN 2-DIM ELECTROMAGNETIC SCATTERING PROBLEMS

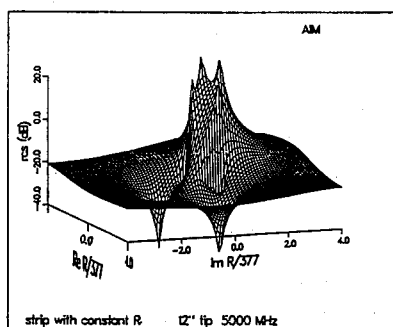
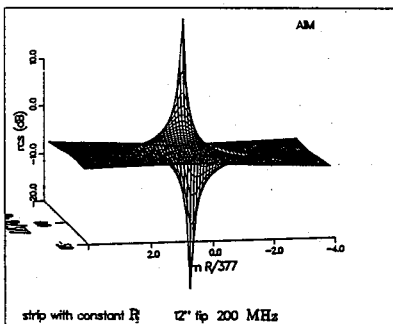
E. Bleszynski\*, M. Bleszynski† and H. B. Tran\*

\* NAA, Rockwell Int., P.O. Box 92098, Los Angeles, CA 90009

† Science Center, Rockwell Int., P.O. Box 1085, Thousand Oaks, CA 91360

We describe some aspects of optimization of 2-dim electromagnetic scattering from complex perfectly conducting targets containing regions of penetrable materials of combined dielectric and magnetic properties. Our discussion will focus on such issues as the selection of optimization methods and their effectiveness when applied to particular classes of scattering problems, physical mechanisms leading to small radar signatures, material and shape optimization at single and several frequencies. A particular stress will be put on the analysis of the structure of optimization minima and their relation to the behavior of optimization parameters.

Some numerical applications will be discussed based on the optimization version of the adaptive integral equation solver AIM developed at Rockwell.



As an example, in Fig. 1, we display radar cross section of a 6 ft wide strip terminated with a 12 inch tapered resistive termination. The cross section, for a TM polarized wave at 200 MHz and 5 GHz, and at grazing incidence is plotted as a function of the complex resistivity of the termination. The figures illustrate the increase in the number of local minima in the radar cross section with increasing frequency for this particular choice of strip termination.

More examples illustrating the usefulness of the developed optimization approaches will be presented.

## FAST RAY TRACING ALGORITHM FOR RCS PREDICTION WITH GRECO CODE

Juan M. Rius\*, Mercè Vall-llossera, Angel Cardama, Lluis Jofre  
Dpt. Teoria del Senyal i Comunicacions,  
Universitat Politècnica de Catalunya,  
Apdo. 30002, 08080 BARCELONA, (Spain)

### GRECO code for real-time RCS prediction

During the last four years, the development of graphical processing techniques for high-frequency RCS prediction has given rise to *GRECO* code (Rius et al., IEE Antennas and Propag. Magazine, Feb. 1993, and Rius, Doctorate Thesis Dissertation, Univ. Politèc. Catalunya, July 1991).

Real-time computation is achieved through graphical processing of an image of the target present at the screen of a workstation, using the hardware capabilities of a 3-D graphics accelerator. The two main advantages of the graphical processing approach over classical techniques are:

- Hardware graphics accelerator removes hidden surfaces and edges so that they do not contribute to surface or line integrals.
- CPU time and RAM requirements independent of target electrical size and complexity. Real-time computation (from 0.2 sec. to 10 sec.) is possible if hardware graphics accelerator is used.

The main features of *GRECO* code are the following:

- The I-DEAS computer aided design package for geometric modeling of solids has been used for modeling target geometry. The target is described as a collection of parametric surfaces, defined with two-dimensional NURBS (non-uniform rational B-splines). Parametric surfaces require less mass storage memory than the faceting approach, and adjust more accurately to the real target surface.
- Physical Optics (PO) for perfectly conducting surfaces, and Impedance Boundary Condition (IBC) + Physical Optics for radar absorbent coatings.
- Method of Equivalent Currents (MEC) with Physical Theory of Diffraction (PTD) and Mitzner's Incremental Length Diffraction Coefficients (ILDC) for perfectly conducting edges.
- Double reflection analysis by a ray-tracing algorithm. Bistatic GO and PO vector formulation for respectively the first and second reflections allows to obtain the scattering matrix of the target.
- Some CAD geometric modeling functions have been integrated with the real-time RCS computing code, in order to interactively modify the shape of the surface and compute the RCS. This feature provides an efficient tool for interactive modeling, design and analysis of aircraft with RCS specifications.
- Automatic optimization of low-RCS shapes has been implemented using steepest descendant and Powell (conjugate directions) algorithms. Some user-defined constraints on the surface of the target are taken into account (for example maximum or minimum dimensions, constant surface area and/or target volume).

### Ray-tracing algorithm

The fast ray-tracing algorithm that has been recently implemented in *GRECO* code will be presented in this communication. For each pixel on the target surface, a reflected ray is traced along the GO specular direction. The impact of the reflected ray with another surface is detected on the screen by comparing the z coordinates of the ray and the surface at the same x,y location. In case that there is a second reflection, the field scattered to the observer is computed using bistatic PO. Vector formulation of bistatic GO and PO for respectively the first and second reflections allows to obtain the scattering matrix of the target.



**SESSION URSI B-2****MONDAY AM****MICROSTRIP STRUCTURES**

Chairs: N.G. Alexopoulos, University of California at Los Angeles;  
D.C. Chang, Arizona State University

Room: Michigan League, Hussey Room      Time: 8:30-12:10

|       |  |    |
|-------|--|----|
| 8:30  | CPW-FED ACTIVE TWIN-SLOTS ANTENNAS RADIATING THROUGH LAYERED SUBSTRATES<br><i>Jean-Marc Laheurte*, Linda P.B. Katehi, Gabriel M. Rebeiz, University of Michigan</i>  | 14 |
| 8:50  | EFFECT OF A DIELECTRIC COVER (SUPERSTRATE) ON RADIATED EMISSIONS FROM ARBITRARILY SHAPED PRINTED CIRCUIT TRACES<br><i>Hassan A.N. Hejase*, Stephen D. Gedney, University of Kentucky</i>                               | 15 |
| 9:10  | QUASI-STATIC ANALYSIS OF A COUPLED MICROSTRIP TRANSMISSION LINE EMBEDDED IN A GROUND PLANE USING FINITE DIFFERENCE METHOD<br><i>A.Z. Elsherbeni*, B. Mourmeh, S.A. Hutchens, C.E. Smith, University of Mississippi</i> | 16 |
| 9:30  | MICROSTRIP ANTENNAS WITH MULTI-DIELECTRIC LAYERS<br><i>Wei Chen*, Kai Fong Lee, University of Toledo; J.S. Dahle, Royal Military College of Science; R.Q. Lee, NASA Lewis Research Center</i>                          | 17 |
| 9:50  | BROADBAND MICROSTRIP-FED SLOT ANTENNAS<br><i>G. Di Massa*, N. Franzese, Università della Calabria</i>  | 18 |
| 10:10 | BREAK  |    |
| 10:30 | APPLICATION OF THE TLM METHOD TO THE ANALYSIS OF SLOT-COUPLED MICROSTRIP ANTENNAS<br><i>N.R.S. Simons*, A.A. Sebak, University of Manitoba; A. Ittipiboon, Communications Research Centre</i>                          | 19 |
| 10:50 | ANALYSIS OF PARASITIC CAPACITANCES FOR SKEWED TRANSMISSION LINES IN MULTILAYERED DIELECTRIC MEDIA<br><i>J.F. Carpentier*, P. Pribetich, P. Kennis, Institut d'Electronique et de Microelectronique du Nord</i>         | 20 |
| 11:10 | EXPERIMENTAL STUDY OF THE NEW BROADBAND PRINTED ANTENNA STRUCTURE<br><i>A. Nesic*, I. Radnovic, Institute of Microwave Techniques and Electronics</i>  | 21 |
| 11:30 | THE EXACT METHOD FOR EVALUATING THE LOWER AND UPPER BOUNDARIES OF THE FILLING FACTOR OF THE COPLANAR STRIPS<br><i>S. Suvakov, A. Nesic*, I. Radnovic, Institute of Microwave Techniques and Electronics</i>            | 22 |
| 11:50 | ELECTROMAGNETIC SCATTERING FROM PERIODIC NARROW GROOVES AND SLITS<br><i>Kasra Barkeshli, Sharif University of Technology</i>   | 23 |

## CPW-FED ACTIVE TWIN-SLOTS ANTENNAS RADIATING THROUGH LAYERED SUBSTRATES

Jean-Marc Laheurte\*, Linda P.B. Katehi and Gabriel M. Rebeiz

+ NASA/Center for Space Terahertz Technology  
Electrical Engineering and Computer Science Department  
University of Michigan, Ann Arbor, MI 48109-2122

In millimeter waves applications, electrically thin substrates and substrate lenses are the two common approaches to avoid losses into guided modes and to allow printed antennas to couple efficiently to air. The main limitation of thin substrates is the increasing difficulty in fabrication as the wavelength decreases [G.M. Rebeiz, W.G. Regehr & D.B. Rutledge, 'Submillimeter-Wave Antennas on Thin Membranes', *Infrared and Millimeter Waves*, vol. 8, no. 10, Oct. 1987.]. On the other hand, lenses suffer from dielectric losses at millimeter waves frequencies and are expensive to fabricate. It has been shown that stacked substrates is an efficient solution to overcome these drawbacks [R.L. Rogers & D.P. Neikirk, 'Radiation Properties of Slot and Dipole Elements on Layered Substrates', *Infrared and Millimeter Waves*, vol. 10, no. 6, 1987]. By properly combining the layers, one can improve the slot to air radiation efficiency through the dielectrics. The use of odd quarter wavelength thicknesses allows to suppress at least all but the  $TM_0$  surface modes while still providing a useful beam pattern. Losses to the  $TM_0$  mode can be reduced with a  $\lambda_{TM_0}/2$  spacing between the in-phase driven broadside slots.

This paper first presents a theoretical characterization of a coplanar waveguide (CPW) fed twin slots antenna on a layered structure. The CPW fed antenna impedance and pattern are calculated using the Space Domain Integral Equation Technique (SDIE) [B.K. Kormanyos, W. Harokopus Jr., L.P.B. Katehi & G.M. Rebeiz, 'CPW-Fed Active Slot-Antennas', Submitted for publication in the IEEE Trans. MTT 1992]. The Green's Functions of the multilayered structure are obtained numerically with an iterative formula using the transmission line model. Dielectric losses are included in the theoretical study. A variable mesh is introduced to discretize the magnetic current in the slots and the CPW lines.

The CPW-feed and the antenna are on the same side of the substrate. Therefore, the connection and the bias of active devices is facilitated and the need for via holes is eliminated. The theoretical calculations are used in the design of a CPW active twin-slot oscillator on stacked layers in the 14-20GHz band. Results will be presented at the conference.

## Effect of a Dielectric Cover (Superstrate) on Radiated Emissions from Arbitrarily Shaped Printed Circuit Traces

Hassan A.N. Hejase\* and Stephen D. Gedney  
Dept. of Electrical Engineering, University of Kentucky  
Lexington, KY 40506

### ABSTRACT

The objective of this work is to study the effect of thickness and dielectric constant of a dielectric cover on the radiated emissions from printed circuit board traces. For EMC applications, the main task is to minimize radiated emissions from the printed circuit traces (transmission lines) in order to satisfy FCC rules. The printed traces are modeled using planar triangular patches which are capable of conforming to any geometrical surface or boundary. The Electric Field Integral Equation (EFIE) is solved using the moment method and following the approach used by Rao, Wilton and Glisson (2-D MOM patch code). The current distribution is interpolated in terms of vector-current basis functions associated with the triangular patch edges. The Galerkin procedure is then applied to yield a matrix equation in terms of the unknown current coefficients. The impedance elements represent double integrals over the triangular patches with the integrand being Sommerfeld-type integrals that represent the vector and scalar potential Green's functions. These Green's functions are derived for a two-layer microstrip with the source dipole located at the substrate-superstrate interface. For most EMC applications, the total substrate-superstrate thickness is thin enough to allow only one surface-wave mode ( $TM_0$  mode) to propagate. This surface-wave mode represents a complex singularity in the scalar potential function that defines the surface-wave power propagating in the dielectric substrate. This power contributes to the power loss when computing the radiation efficiency. To compute the Sommerfeld integrals, we follow a numerical procedure similar to that devised by Mosig and co-authors. Numerical results for the radiation efficiency as a function of frequency with the dielectric constants and thicknesses of the substrate and cover as parameters will be presented. A comparison will be made with quasi-static results in order to establish the frequency range where quasi-static or transmission line models are valid.

## QUASI-STATIC ANALYSIS OF A COUPLED MICROSTRIP TRANSMISSION LINE EMBEDDED IN A GROUND PLANE USING FINITE DIFFERENCE METHOD

A. Z. Elsherbeni\*, B. Moumneh, S. A. Hutchens, and C. E. Smith

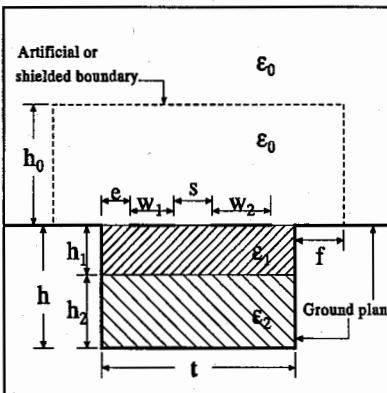
Electrical Engineering Department

University of Mississippi

University, MS 38677

### ABSTRACT

Coupled microstriplines are used in a number of microwave integrated circuits such as directional couplers, filters, and delay lines. There are numerous papers dealing with the analysis, design, and applications of coupled microstriplines. In most of these papers, the striplines are usually conformed on planar, circular, or elliptical dielectric (single or multi-layer) substrate above a planar ground plane. In this paper planar coupled lines along with two layers of dielectric substrates are embedded in a ground plane as shown in the figure. This geometrical arrangement provides less coupling between the transmission line and the surrounding transmission lines or any other microwave devices. The infinite domain above the transmission line and ground plane is terminated at an artificial boundary using an interpolating procedure that satisfies Laplace's equation at distances far from the conducting lines. The finite difference method, with non-uniform mesh, is then used to analyze this transmission line in a region bounded by an artificial boundary and the ground plane. The assumption of having a perfectly conducting ground plane (shielded boundary), in place of the artificial boundary, is also considered in our computations in order to show the effects of the assumed interpolating procedure at the artificial boundary. The potential distribution, self and mutual capacitances are computed and used to determine the quasi-TEM characteristics for the shown transmission line and for the case where the strips are located on the boundary between the two dielectric layers. It is found that distortion-less symmetric lines (where the even and odd phase velocities are equal) can be designed by properly selecting the heights and permittivities of the dielectric substrates, width and spacing between the strips.



## MICROSTRIP ANTENNAS WITH MULTI-DIELECTRIC LAYERS

Wei Chen and Kai Fong Lee

Dept. of Electrical Engineering, University of Toledo, Toledo, Ohio

J. S. Dahle

Royal Military College of Science, Shrivenham, England

R. Q. Lee

NASA Lewis Research Center, Cleveland, Ohio

Microstrip antennas with more than one dielectric layers are shown in Fig. 1. In Fig. 1(a), a superstrate cover is used to protect the patch against environmental hazards. If a naturally occurring dielectric layer such as ice is formed on top of the superstrate cover, the three-layer configuration of Fig. 1(b) results. Fig. 1(b) can also represent the situation when an unwanted air space exists between the substrate and the superstrate ( $\epsilon_{r2}=1$ ). Finally, if an airgap is deliberately introduced between the substrate and the ground plane to offset the resonant frequency decrease caused by the dielectric cover, we have the geometry shown in Fig. 1(c).

Of the three configurations depicted, only the two-layer case (1a) has been extensively studied in the literature. In this paper, we first present a spectral domain moment method analysis of multi-dielectric layer microstrip antennas. After deriving the Green's functions for plane layered media, the enforcement of the boundary condition that the tangential electric field vanishes on the patch and the probe surface leads to integral equations for the patch and the probe surface current densities. The integral equations are solved by Galerkin's method. A proper attachment mode is included to ensure current continuity at the patch-probe junction and multiple expansion modes are used on the probe current to allow for both axial and azimuthal variations. The formulation is applied to configurations 1(b) and 1(c). Theoretical and experimental results illustrating the dependence of resonant frequency and impedance bandwidth on the parameters of the various dielectric layers will be presented.

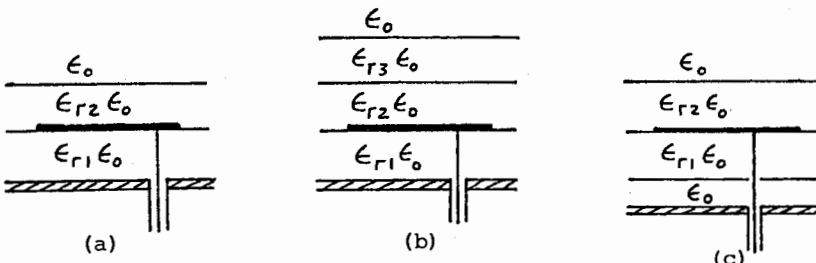


Fig. 1 Multi-dielectric layer microstrip antennas

## BROADBAND MICROSTRIP-FED SLOT ANTENNAS

G. Di Massa\*, N. Franzese

Dipartimento di Elettronica, Informatica e Sistemistica  
Università della Calabria, 87036 Rende (CS), Italy

Microstrip antennas have many interesting proprieties (e.g. low profile, light weight, cheapness), but their application in many systems is impeded by their inherent narrow bandwidth. The authors propose a new broad-band compensation-technique for bandwidth enhancement of microstrip-fed slot antennas.

A slot radiator, cut in the ground plane of a microstripline, is loaded at the ends by radial-slotline stubs. The slot excitation is achieved through electromagnetic coupling to a microstrip feedline etched on the other side of dielectric substrate. The microstrip line is properly terminated with a rectangular stub.

A simple and accurate transmission line model of the broad band microstrip-fed slot antenna is introduced. The radiating element is depicted by a transmission line loaded at the ends with reactive elements. The effect of radiation losses is accounted for by a resistor connected at the centre point of the line representing the slot. The value of the resistor is obtained via a power balance (G. Di Massa, Proc. of 2nd Int. Conf. on Electromagnetic in Aerospace Applic., Torino 1991). The Knorr model (IEEE Trans on MTT, 22, 548-554, 1974) is used in order to represent the microstrip-slotline junction. In this model the impedance of the loaded slotline is connected, through a transformer, in series to the line representing the loaded microstripline.

An experimental investigation of the proposed broadband antenna has been carried out showing a good agreement between the measured data and the results of the proposed model.

The design example concerns a slot of length  $18.5\text{mm}$  and width  $.5\text{mm}$  loaded with radial stubs of radius  $2\text{mm}$  and sectorial angle  $180^\circ$ . The  $50\Omega$  microstrip line is terminated with a matched rectangular stub of length  $4.5\text{mm}$  and width  $7.5\text{mm}$ . The antenna is etched in copper-cladbed  $1.27\text{mm}$  RT/duroid with  $\epsilon_r = 10.2$

The proposed slot antenna has its best match at  $3.3\text{GHz}$ . If the bandwidth criterion is taken to be  $WSWR \leq 2$  the measured bandwidth is given by  $B = 2.5\text{GHz}$ .

**APPLICATION OF THE TLM METHOD TO THE  
ANALYSIS OF SLOT-COUPLED MICROSTRIP ANTENNAS**

N.R.S. Simons\*, A.A. Sebak

Department of Electrical and Computer Engineering

University of Manitoba

Winnipeg, Manitoba, Canada, R3T 2N2

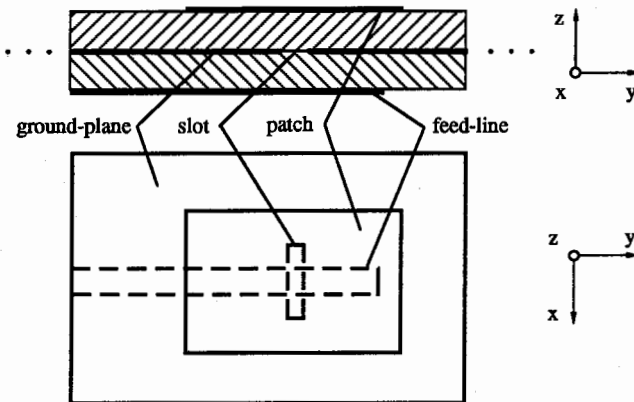
A. Ittipiboon

Communications Research Centre

P.O. Box 11490, Station H

Ottawa, Ontario, Canada, K2H 8S2

The purpose of this paper is to investigate the application of the Transmission-Line Matrix (TLM) method to the analysis of slot-coupled microstrip antennas (see figure below). The TLM method is a time-domain differential equation based numerical method and is therefore similar to the Finite-Difference Time-Domain, Finite-Volume Time-Domain, and Finite-Element Time-Domain methods. The advantages of the differential equation based methods include: minimal analytical processing; the ability to include arbitrary geometrical features (superstrates, different shaped slots, finite-sized ground planes, etc.) with minimal additional computational costs; and most importantly complete electromagnetic characterization of the problem geometry including surface wave effects and fringing fields. The main disadvantage associated with the differential equation based methods is that CPU time and memory storage exceed the requirements of integral equation based methods, and greatly exceed the requirements of modal field analysis methods and cavity models. Typical numerical results yield resonant frequencies within a few percent of measurements. A discussion of numerical convergence and detailed numerical results will be provided.



**ANALYSIS OF PARASITIC CAPACITANCES FOR SKEWED  
TRANSMISSION LINES IN MULTILAYERED DIELECTRIC MEDIA**

J.F. CARPENTIER\*, P. PRIBETICH, P. KENNIS  
*Institut d'Electronique et de Microélectronique du Nord,  
 D.H.S., U.M.R. CNRS n° 9929  
 Equipe Electromagnétisme des Circuits, Bât P4  
 Université des Sciences et Technologies de Lille  
 59650 VILLENEUVE D'ASCQ, FRANCE*

It is well known that the MMIC's design involves crossing of striplines on different dielectric layers. With the crossover's height involved and typical widths of the strips, we must take into account the associated coupling effects. We propose a quasi-static analysis to model the capacitive coupling between two microstrip lines crossing with an *arbitrary angle* in a multilayered dielectric region as shown on fig.1. The charge density along each strip is described by using basis functions chosen in such a way that they fulfil the physical constraints of the problem as accurately as possible. To relate the excess charges to the stripline potentials a pair of coupled integral equations is obtained, which are solved via the method of moments with point matching. The electrostatic 3-D Green's function which is used in our problem is an *essential step*. We carry out an approach named the complex image method. To find the complex images, we use the Prony's method (Y.L Chow, JJ Yang, G.E Howard, IEEE *TMTT*, 1120-1125, 1991). Our objective is to compute the elements of a coupling model in the form of an equivalent circuit. As example for this abstract we show typical results for the normalized lumped excess capacitances plotted versus the angle  $\theta$ .  $C_1$  and  $C_2$  are the self capacitances of the lines 1 and 2,  $C_m$  is their mutual capacitance.  $Cp_1$  and  $Cp_2$  are the capacitances per unit length of the equivalent isolated wire lines with a homogeneous medium  $\epsilon_0$ , where  $\epsilon_0$  is the permittivity of free space. As shown by these figures, this numerical tool offers the possibility to analyse the capacitive coupling for a structure with planar conductors crossed non orthogonally. This work brings an additional freedom degree for the designers. At the conference, we will present in detail the main steps of this analysis in order to describe the capacitive coupling.

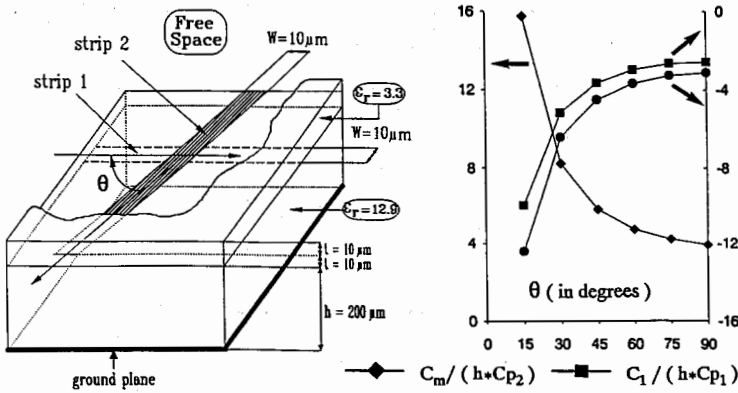


Figure 1

## EXPERIMENTAL STUDY OF THE NEW BROADBAND PRINTED ANTENNA STRUCTURE

A. Nešić\*, I. Radnović

Institute of Microwave Techniques and Electronics  
Lenjinov Bulevar 165b, 11070 Beograd, Yugoslavia

Microstrip and printed antenna structures have many advantages over conventional antennas. However, the main difficulty in design and realisation of the wideband printed antenna arrays is choosing of the radiating elements as well as the feeding network.

In this work, different types of printed dipoles - triangular (Fig. 1a), triangular with cap (Fig. 1b), trapezoidal (Fig. 1c) and slot with complementary shape with trapezoidal dipole (Fig. 2) are investigated. In the first step, the impedance measurement of the isolated printed monopoles of the three above-mentioned forms is performed. The least impedance variation is obtained in the case of monopole with trapezoidal shape. Furthermore, in order to include mutual impedance between elements, the impedance measurement of the trapezoidal monopole in array on the dielectric substrate with  $\epsilon_r=2.17$  and  $h=1.6$  mm, is performed. VSWR is below 2 with  $Z_0=75\Omega$  in the frequency range of one octave (4–8GHz). Naturally, the same conclusion is valid for trapezoidal dipoles.

Printed arrays with trapezoidal dipoles on one side of the substrate can be fed by feeding networks with coplanar strip (CPS), or with symmetrical microstrip in case when one half of dipoles is placed on one side of the substrate and another half on the other side.

Trapezoidal slot fed by coplanar waveguide (CPW) is an antenna structure which has the complementary shape with trapezoidal dipole fed by coplanar strips (CPS) (Fig. 2). VSWR of this antenna element is also less than 2 in the frequency range of one octave. Array with trapezoidal slots can be fed by feeding network with CPW.

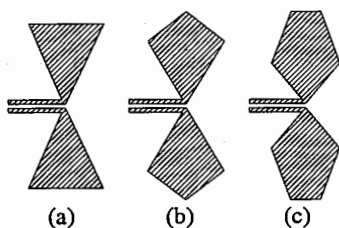


Fig. 1. Different types of printed dipoles:  
(a) Triangular, (b) Triangular with cap,  
(c) Trapezoidal.

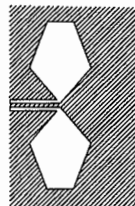


Fig. 2. Trapezoidal slot fed by coplanar waveguide

## THE EXACT METHOD FOR EVALUATING THE LOWER AND UPPER BOUNDARIES OF THE FILLING FACTOR OF THE COPLANAR STRIPS

S. Šuvakov, A. Nešić\*, I. Radnović

Institute of Microwave Techniques and Electronics  
Lenjinov Bulevar 165b, 11070 Beograd, Yugoslavia

All known quasi-static methods for coplanar strip (CPS) analysis on dielectric substrate with finite thickness such as conform mapping, variational method, moment method, etc. are, essentially, approximate. In this work, the exact method for coplanar strip analysis is presented, giving the lower and the upper boundaries for filling factor  $q$ . For the extreme values of dielectric constant - small ( $\epsilon_r \rightarrow 1$ ) and high ( $\epsilon_r \rightarrow \infty$ ) values, two models of conform mapping are defined. By means of them, the lower and upper boundaries of filling factor can be easily evaluated.

For the case when  $\epsilon_r \rightarrow 1$ , the problem is reduced to numerical calculation of two elliptical integrals with complex variables using the program package IMSL, whereas the case when  $\epsilon_r \rightarrow \infty$  is reducible to the problem of solving the complete elliptical integral of the first kind.

Since the filling factor is to be found between lower and upper boundary in real cases, we can expect that parameters of the CPS, calculated with use of different methods, are placed between limits defined in this way.

Using the above-mentioned methods, boundaries of filling factor are calculated as the function of dielectric thickness  $h$ , for very narrow strips ( $a/b=0.99$ ) and very narrow gap ( $a/b=0.01$ ), for dielectric constants  $\epsilon_r=2.5$  and  $\epsilon_r=10$ . The achieved results are compared to those obtained by quasi-static methods known so far.

We can notice that in the case of very narrow strips, the results given in Gupta and al. ("Microstrip lines and slot-lines"), are out of boundaries, whereas the results from Yamashita and Yamazaki (IEEE, MTT, Nov. 68.), Ghione, Naldi (Electronics Lett. Vol. 20, No. 4, 1984) and Đorđević and al. ("Matrix Parameters for Multiconductor Lines", Artech House), are between these boundaries. In the case of thin substrates (small  $h$ ) results from last reference, for 916 pulses are between calculated boundaries, while for 116 pulses are out of them.

ELECTROMAGNETIC SCATTERING FROM PERIODIC  
NARROW GROOVES AND SLITS

Kasra Barkeshli

Electrical Engineering Department  
Sharif University of Technology  
P.O. Box 11365-9363  
Tehran, Iran

The problem of scattering from periodic structures consisting of narrow grooves and slits recessed in a ground plane will be considered based on a quasi-static analysis of the pertaining integral equations. These configurations find numerous applications at millimeter wave, microwave, and optical frequencies.

The scattering characteristics of single narrow grooves and slits in thick conducting plates have been studied by solving (in closed-form) for the equivalent magnetic current distributions over their apertures [1]. These low frequency approximate solutions exhibit the expected edge behavior at the groove or slit terminations. They are used to derive closed-form expressions for the associated parameters such as aperture potentials, aperture admittances, and radar echo widths. The accuracy and regions of validity of these solutions have been established by comparing them with alternative formulations including full-wave [2] and impedance boundary conditions [2,3].

In this paper the above quasi-static formulation is extended to periodic structures using Floquet's theorem. The corresponding characteristic parameters are calculated and compared to the known results.

[1] K. Barkeshli and J. L. Volakis, "Scattering from narrow grooves and slits," *J. Electromag. Waves Appl.*, Vol. 6, No. 4, pp. 459-474, 1992.

[2] K. Barkeshli and J. L. Volakis, "TE scattering by a two dimensional groove in a ground plane using higher order impedance boundary conditions," *IEEE Trans. Antennas Propagat.*, Vol. AP-38, 1421-1428, Sept. 1990.

[3] T. B. A. Senior and J. L. Volakis, "Scattering by gaps and cracks," *IEEE Trans. Antennas Propagat.*, Vol. AP-37, 744-750, June 1989.



## STUDIES OF MMIC TRANSMISSION LINES

Chairs: T. Itoh, University of California at Los Angeles; F.K. Schwering, US Army CECOM

Room: Michigan League, Michigan Room

Time: 8:30-11:50

|       |   |    |
|-------|---|----|
| 8:30  | PLANAR, QUASI-OPTICAL SLAB-BEAM WAVEGUIDE FOR THE MILLIMETER-SUBMILLIMETER WAVE SPECTRUM<br><i>F.K. Schwering, U.S. Army CECOM; J.W. Mink*, U.S. Army Research Office</i>   | 26 |
| 8:50  | EXPERIMENTAL INVESTIGATION OF A QUASIOPTICAL SLAB RESONATOR<br><i>A. Schuneman, S. Zeisberg, G.P. Monahan, M.B. Steer*, North Carolina State University; J.W. Mink, US Army Research Office; F.K. Schwering, US Army CECOM</i>                          | 27 |
| 9:10  | A NEW WEIGHTED SURFACE IMPEDANCE FOR THE SPECTRAL DOMAIN APPROACH TO DETERMINE METALLIC LOSSES FOR MMIC APPLICATIONS<br><i>D. Kinowski*, E. Paleczny, J.F. Legier, P. Kennis, P. Pribetich, Institut d'Electronique et de Microelectronique du Nord</i> | 28 |
| 9:30  | CHARACTERIZATION OF DIELECTRIC STRIP WAVEGUIDES USING A GENERALIZED INTEGRAL EQUATION METHOD<br><i>Kazem Sabetfakhri*, Linda P.B. Katehi, The University of Michigan</i>  | 29 |
| 9:50  | STUDY OF MICROMACHINED QUASI-PLANAR LINES<br><i>Rhonda Franklin Drayton*, Linda P.B. Katehi, The University of Michigan</i>   | 30 |
| 10:10 | BREAK   |    |
| 10:30 | MODELING OF STRIP CIRCUITS WITH VIAS EMBEDDED IN A MULTILAYERED SUBSTRATE<br><i>Krist Blomme*, Jeannick Sercu, Niels Faché, Daniël De Zutter, University of Ghent</i>   | 31 |
| 10:50 | A QUASI-STATIC ANALYSIS OF FUZZ BUTTON INTERCONNECTS<br><i>G. Pan*, X. Zhu, B. Gilbert, University of Wisconsin-Milwaukee</i>   | 32 |
| 11:10 | CAPACITANCE AND INDUCTANCE EVALUATION OF VERTICAL INTERCONNECTIONS USING THE FINITE ELEMENT METHOD<br><i>Jong-Gwan Yook*, Linda P.B. Katehi, The University of Michigan</i>   | 33 |
| 11:30 | FULL WAVE ANALYSIS OF SUPERCONDUCTING COPLANAR WAVEGUIDE WITH METHOD OF LINES<br><i>Mingming Jiang, Yunyi Wang, Southeast University</i>  | 34 |

Mon. a.m.

PLANAR, QUASI-OPTICAL SLAB-BEAM WAVEGUIDE FOR THE  
MILLIMETER-SUBMILLIMETER WAVE SPECTRUM

F. K. SCHWERING

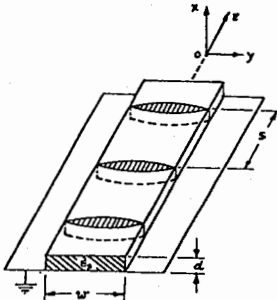
U.S. Army CECOM, ATTN: AMSEL-RD-C3-ST, Ft. Monmouth, NJ 07703

J. W. MINK\*

U.S. Army Research Office, P.O. Box 12211, Research Triangle Park, NC 27709

Abstract

A hybrid dielectric slab-beam waveguide is suggested which should be well suited as transmission medium for the design of planar quasi-optical integrated circuits and devices operating in the mm and sub-mm wave regions. The new guide consists of a grounded dielectric slab into which a sequence of equally spaced cylindrical lenses is fabricated. As indicated in the figure, the axis of the lenses coincides with the center line of the slab guide (propagation direction of the guide). The spacing of the lenses  $s$  is assumed to be in the order of many guide wavelengths  $\lambda_e$ ; the width of the slabguide  $w$  is in the order of at least several  $\lambda_e$ ; and the thickness  $d$  of the guide typically will be chosen sufficiently small so that only the fundamental surface wave mode can exist on the slab.



The structure uses two distinct wave guiding principles in conjunction with each other to guide electromagnetic waves. In the direction normal to the slab surface, the guided fields behave as surface waves of the slab guide; their energy is largely confined to the interior of the dielectric and they are guided by total reflection at the slab surface. In the lateral direction the waves behave as Gauss-Hermite beam modes that are guided by the lenses which periodically reconstitute their cross sectional phase distribution, resulting in a wave beam that is iterated with the lens spacing. The guided fields are in effect TE and TM modes, with respect to the z direction, the propagation direction of the guide. The analysis of the new guiding structure will be presented including the mode spectrum and the iteration loss due to the finite size of the lenses.

The guide suggested here bridges the gap between conventional dielectric waveguides employed in the mm-wave region and slab type dielectric waveguides used at optical wavelengths. Combining structural simplicity, approaching that of a slabguide, with the increased lateral dimensions of quasi-optical devices, it should be easy to fabricate and show good electrical performance. The new guide should be well suited in particular for the integrated design of planar quasi-optical circuits and components, including power combining of active sources.

# EXPERIMENTAL INVESTIGATION OF A QUASIOPTICAL SLAB RESONATOR

A. Schuneman, S. Zeisberg, G. P. Monahan, M. B. Steer\*,  
 High Frequency Electronics Laboratory, Department of Electrical and  
 Computer Engineering, North Carolina State University, Raleigh, North  
 Carolina 27695-7911.

J. W. Mink,

U.S. Army Research Office, P.O. Box 12211, Research Triangle Park, NC  
 27709-2211,

and F. K. Schwering,  
 CECOM, Attn. AMSEL-RD-CS-ST, Ft. Monmouth, NJ 07703-5203

Quasi-optical power combiners using open-resonators achieve efficient and robust combining at millimeter-wave frequencies and above. However systems cannot be photolithographically defined thus limiting mass production and contributing to high cost. A similar structure more amenable to photolithographic reproduction is the hybrid dielectric slab-beam waveguide (HDSBW). This structure combines the waveguiding principles of dielectric surface waves of a slab guide surface and the confined beam corresponding to Gauss-Hermite beam modes. In this presentation the HDSBW slab resonator, Fig. 1, is experimentally investigated.

Resonances were observed for different longitudinal and transverse TE and TM modes. The TE and TM modes were discerned as they are preferentially excited with the L shaped antenna parallel and normal to the ground plane respectively. The transverse order of the modes was determined by field profiling. The Q's of the observed TE modes are plotted in Fig. 2 for the antenna parallel to the ground plane. No TM modes were detected in this case. By reorienting the antenna so that it was normal to the ground plane it was possible to excite low level TM modes above 9.4 GHz in addition to small but larger TE modes.

The behavior of the fields in a HSBW resonator is similar to that in an open resonator. The Q of the dominant TE mode peaks at 3,300 around 7 GHz. This is approximately what can be expected from dielectric loss alone as the published loss tangent of Rexolite dielectric is 0.006 at 8 GHz.

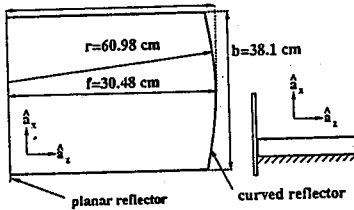


Fig. 1: Planar Quasi-Optical slab resonator

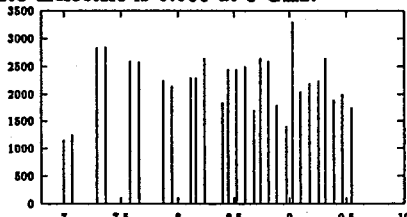


Fig. 2: Q of TE modes vs. frequency in GHz.

**A NEW WEIGHTED SURFACE IMPEDANCE FOR THE SPECTRAL DOMAIN APPROACH TO DETERMINE METALLIC LOSSES FOR MMIC APPLICATIONS**

D. KINOWSKI\*, E. PALECZNY, J.F. LEGIER, P. KENNIS, P. PRIBETICH

*Institut d'Electronique et de Microélectronique du Nord*

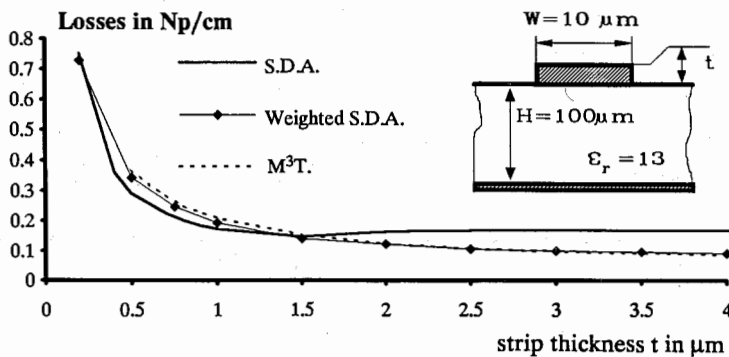
*D.H.S., U.M.R. CNRS n° 9929*

*Equipe Electromagnétisme des Circuits, Bât P4*

*Université des Sciences et Technologies de Lille*

*59650 VILLENEUVE D'ASCQ, FRANCE*

The increasing use of planar transmission lines in millimetre-wave and microwave monolithic integrated circuits has made the transmission losses of these structures an important issue. The Spectral Domain Approach (S.D.A.), which is a convenient and now a well-known method, makes it possible to take into account the conductivity and thickness of a metallic strip through the complex resistive boundary condition, and hence to evaluate the conductor losses. However S.D.A. losses results suffer from the validity and accuracy of the surface impedance concept, by comparison to heavy-built methods, such as Modified Mode Matching Techniques ( $M^3T.$ ) where no approximations are made to describe physically the electromagnetic behaviour of the strip. But  $M^3T.$ , like other heavy-built methods, needs intensive C.P.U. time. Recently the calculating, by an integral formulation, of the ac resistance of a strip over a lossy ground plane has been reported (R. Faraji-dana, Y.L Chow, IEEE *TMTTT*, 1268-1277, 1990). In a synthesis mind and in an engineering purpose, we propose, in this communication, to calculate a weighting factor for the surface impedance in order to obtain more accurate numerical data for the modified S.D.A. The weighting factor is defined by the ratio of the ac resistance of the strip on the real part of the surface impedance for a given strip width. The results obtained are compared with the  $M^3T.$  and the experiments. Here are presented some results for a typical structure. A microstrip line with  $W = 10 \mu\text{m}$  and  $\sigma = 4.1 \cdot 10^5 \text{ S/cm}$  has been considered. The weighting factor  $k$  has been calculated versus the strip thickness and implemented in S.D.A. to evaluate the structure losses (at a frequency of 10 GHz). The results compared with the  $M^3T.$  and classical S.D.A. (i.e.  $k=1$ ) are presented versus the strip thickness on figure 1. A good agreement can be seen now between  $M^3T.$  and S.D.A. with a weighted surface impedance. At the conference, we propose to present with more details this formulation. Microstrip and coplanar lines will be analysed by taking into account this new weighting factor and comparison with experiments will be presented, at the conference, for both structure.



## Characterization of Dielectric Strip Waveguides using a Generalized Integral Equation Method

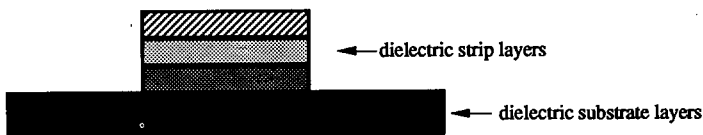
Kazem Sabetfakhri\* and Linda P.B. Katehi

Radiation Laboratory  
Department of Electrical Engineering and Computer Science  
The University of Michigan  
Ann Arbor, MI 48109-2122

Due to the importance of the dielectric strip waveguide as an efficient low-loss transmission line for submillimeter-wave applications, it is essential to have a good understanding of its performance and capabilities. To analyze such a waveguide, the majority of the available numerical methods tend to perform a fine discretization of the guide cross section which leads to practical limitations. This shortcoming becomes more tangible in the case of an open structure where the radiation spectrum usually has to be quantized. In this paper, a generalized integral equation technique is utilized to formulate a one-dimensional integral equation in the spectral domain for a dielectric strip waveguide of arbitrary guide dimensions and medium parameters. This method can handle multi-layered strips or multi-layered substrates in an open or closed configuration. It retains the continuous radiation spectrum of the open waveguide and can incorporate the effects of radiation and dielectric losses.

Given the dyadic Green's function of the substrate structure, which is in the form of Sommerfeld integrals, fictitious spectral currents are introduced as integral transforms of the volume polarization current in the dielectric strip. Then using higher-order boundary conditions on the surface of the strip, integral equations are derived which relate the unknown spectral currents through spectral-domain modified Green's functions. These equations are solved numerically using the method of moments and the characteristics of the dielectric waveguide are then determined. In addition to being a very accurate full-wave technique, because of the reduction in the dimensionality of the integral equation, the method presented here is also very efficient from a computational point of view.

### Simple Geometric Structure



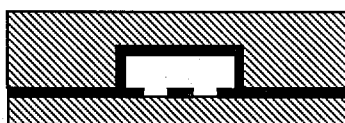
## STUDY OF MICROMACHINED QUASI-PLANAR LINES

Rhonda Franklin Drayton\* and Linda P.B. Katehi  
NASA Center for Space Terahertz Technology  
University of Michigan  
Ann Arbor, MI 48109-2122

Recent industrial trends in space and communication technology show the development of systems that have high rate information transfer as well as improved fuel economy. High rate transfer results from the improved electrical performance of circuit components while better fuel economy results from the development of smaller lightweight systems. Currently, planarized transmission lines such as microstrip, stripline, and coplanar waveguide provide enhanced flexibility in antenna and array design, compatibility with active devices and radiating elements, and reduction in size and weight. However, such lines produce unwanted frequency dependent mechanisms such as parasitic radiation and coupling which interfere with wave propagation. Consequently, a need exists for the development of transmission lines without the above limitations which exhibit improved electrical performance while offering additional reduction in the size and weight of circuits.

With recent advances in semiconductor processes, namely micromachining, Si or GaAs semiconductor substrate materials may be utilized to create planar transmission lines and their shielding cavities in monolithic form. Serving a dual purpose, the cavity can reduce electromagnetic interference and parasitic radiation while introducing additional design parameters. Geometrically, the planar transmission lines are created by metal deposition on a Si substrate whereas the shielding is created by etching a cavity into Si using KOH. After metallizing both surfaces using evaporation techniques, the two wafers are attached by electrobonding. The result is the development of lines that offer improved electrical performance and the potential to incorporate an integrated package.

In this paper a novel transmission line, which exhibits the advantages discussed above, is presented. A discussion of the fabrication procedure required to develop this line as well as the measurement technique used for characterization are presented. In addition, various line properties such as propagation constant and characteristic impedance are shown and compared to conventional lines, such as microstrip and coplanar waveguide.



Quasi-Planar Transmission Line

## MODELING OF STRIP CIRCUITS WITH VIAS EMBEDDED IN A MULTILAYERED SUBSTRATE.

Krist Blomme\* (NFWO), Jeannick Sercu(NFWO), Niels Faché  
and Daniël De Zutter (NFWO)

University of Ghent - Laboratory of Electromagnetism and Acoustics (LEA)  
Sint-Pietersnieuwstraat, 41 9000 Ghent - Belgium

### ABSTRACT

The Mixed Potential Integral Equation (MPIE) Formulation is applied to model planar strip circuits with vias embedded in a multilayered medium. The planar strip circuits are parallel to the layered medium. The focus of the presentation is on an efficient calculation technique for the via contributions.

In the classical mixed potential formulation for strip circuits the Green's functions are associated with a horizontal electric current dipole. The Green's functions are combined with the unknown two-dimensional planar current to yield the applied field on the strip surface. If this technique is simply extended to the via modelling, calculation of three dimensional Green's functions would be needed as the vias make the circuit three dimensional.

In our presentation it will be shown how for open structures the current modelling on the via can be incorporated in the (modified) two-dimensional Green's functions. In this way the additional dimension introduced by the via is included in the Green's functions and the modelling of the currents remains restricted to the strip surfaces. Vias are now represented by their projection on the plane of the circuit. Both via sheets and cylindrical vias have been implemented. Special attention will be devoted to the singular behaviour of the via Green's functions and the calculation of the corresponding matrix elements of the system matrix equation. The latter follows from the application of the method of Galerkin on the mixed potential integral equation.

## A QUASI-STATIC ANALYSIS OF FUZZ BUTTON INTERCONNECTS

G. Pan\*, X. Zhu and B. Gilbert

Department of EE&CS

University of Wisconsin-Milwaukee  
Milwaukee, WI 53201, U.S.A.

### Abstract

Fuzz buttons can interconnect up to 50 substrate layers in conjunction with metallic vias. As a result, three dimensional diamond substrate MCMs (MultiChip Modules) connected with fuzz buttons can achieve very high packaging densities. On the other hand, the vertical interconnects, surrounded by different dielectric materials and passing through many ground mesh holes, are 3D nonuniform transmission lines. Therefore, the analysis of fuzz button interconnects is not straightforward. In this paper, we propose a method to analyze fuzz buttons under quasi-static assumptions.

We first applied the electrostatic method to find the charge distribution and the distributed capacitance of the fuzz buttons; and a quasi-magnetostatic approach for the inductance. By using image theory, a free space Green's function was formulated. The effect of the via holes was taken into account by utilizing the equivalence principle. An iterative algorithm was imposed to find the magnetic current in the hole region. After the equivalent nonuniform transmission line model was established, we then applied the transmission (ABCD) matrix method so that the propagation parameters were obtained easily. Finally, we employed the FFT to convert the frequency results into the time domain. Waveform distortion, time delay and crosstalk values of a 60 ps risetime input signal were evaluated. The quasi-static approach was compared against the finite-difference-time-domain (FDTD) algorithms and good agreement was observed.

## CAPACITANCE AND INDUCTANCE EVALUATION OF VERTICAL INTERCONNECTIONS USING THE FINITE ELEMENT METHOD

Jong-Gwan Yook\* and Linda P.B.Katehi

Radiation Laboratory  
Department of Electrical Engineering and Computer Science  
The University of Michigan  
Ann Arbor, MI 48109-2122

### ABSTRACT

In high-speed high-frequency systems, signals and power are easily distorted by several sources of noise. Among the well-known sources of noise, the vertical interconnections present a rather complex problem to the circuit designer due to their high-frequency non-static properties and asymmetric overall geometry.

To tackle the complex problem of a vertical interconnection such as a via hole, the finite element method is chosen with edge-based vector basis functions and tetrahedron elements. The basis functions have divergenceless properties and allow for easy implementation of the boundary conditions on the perfect electric(pec) and perfect magnetic conductor(pm) surfaces. On the pec surface the tangential electric field and tangential vector potential are zero, but on the pmc surface the tangential magnetic field and normal vector potential component are zero. When the edge-based vector basis functions are used in the implementation of the solution, the boundary conditions on the pmc surface are automatically satisfied. Moreover, the edge-based basis function provide tangential continuity across the edge of the tetrahedron elements.

From the derived electromagnetic fields, equivalent capacitances and inductances can be calculated using well known formulas. Then,  $\Pi$ - and  $T$ - type equivalent circuits may be computed to represent the via hole and analyze its performances. The equivalent inductances and capacitances are frequency dependent. To verify this characteristic of the via, static and dynamic solutions are obtained and the results are compared in order to better understand the high frequency limitations of the static approach as it is applied to this type of circuit problems. The static capacitance of the circuit is computed from the scalar potential functional and the static inductance from the magnetic vector potential functional formulation. The node based FEM is used to solve the scalar potential problem, while the edge based FEM is used for the vector potential problem to avoid non-physical spurious modes.

The equivalent capacitances and inductances of a variety of via holes will be presented in the form of frequency dependent equivalent circuits and the performance of the via will be discussed in detail.

## FULL WAVE ANALYSIS OF SUPERCONDUCTING COPLANAR WAVEGUIDE WITH METHOD OF LINES

Mingming Jiang and Yunyi Wang

Radio Eng. Dept. Southeast Univ., Nanjing, 210018, P.R.China

### ABSTRACT

The coplanar waveguide transmission line becomes more and more important in microwave superconducting applications for its advantages of needing only single-side film and avoiding via holes. It has been analyzed by some authors. For superconducting coplanar waveguide, most authors use the concept of surface impedance to introduce the two-fluid model and London theory. As a result, the accuracy is limited to that of using quasi-TEM method. Complex dielectric constant is also used in a few papers with complicated analysis and longer calculating time.

In this paper, we base our analysis on the theory of the method of lines and use the Ohm's Law in the Maxwell Equations to substitute the complex conductivity of the superconductor,  $\sigma$ . According to the definition of the line current density, especially for the superconductor which penetration depth is very small, we build the relation between electric field and line current density involving the conductivity(complex value for superconductor) so as to introduce the lossy model into the procedure of the method of lines. In order to simplify the analysis we ignore the dielectric loss, for the conductive loss is dominant in the total losses of the coplanar waveguide in spite of the use of superconducting film.

Then we calculate the dispersion and attenuation characteristics of the superconducting coplanar waveguide as the function of frequency and temperature. Comparison with the published data verifies the reliability of this paper. At last we investigate the unloaded Q value of half wavelength superconducting coplanar waveguide resonator.

**SPECIAL SESSION AP-S/URSI F-1****MONDAY AM****REMOTE SENSING**

Chairs: E.R. Westwater, National Oceanic and Atmospheric Administration  
C.T. Swift, University of Massachusetts

Room: Michigan League, Room D      Time: 8:30-12:10

|       |  |    |
|-------|--|----|
| 8:30  | SATELLITE MICROWAVE REMOTE SENSING OF WATER VAPOR: PAST,<br>PRESENT AND FUTURE<br><i>John C. Alishouse, NOAA-NESDIS</i>  | 36 |
| 8:50  | APPLICATION OF MICROWAVE RADIOMETRY TO CLIMATE RESEARCH<br><i>Jack B. Snider, NOAA/ERL</i>   | 37 |
| 9:10  | A DUAL-CHANNEL AIRBORNE RADIOMETER FOR ATMOSPHERIC AND<br>OCEAN REMOTE SENSING<br><i>L.S. Fedor, D.A. Hazen, W.B. Madsen, J.B. Snider, E.R. Westwater,<br/>NOAA/ERL</i>  | 38 |
| 9:30  | RECENT RESULTS IN DETERMINATION OF INTEGRATED WATER VAPOR<br>BY GPS AND BY MICROWAVE RADIOMETERS<br><i>F. Solheim*, J. Johnson, T. VanHove, C. Alber, R. Ware, University Navstar<br/>Consortium</i>   | 39 |
| 9:50  | COMBINED MICROWAVE AND INFRARED SOUNDING OF THE<br>ATMOSPHERE<br><i>Yong Han, Ed R. Westwater, NOAA/ERL</i>  | 40 |
| 10:10 | BREAK  |    |
| 10:30 | MICROWAVE RADIOMETRIC SENSING OF AIRCRAFT ICING CONDITIONS<br><i>E.R. Westwater, B.B. Stankov, J.B. Snider, NOAA/ERL</i>   | 41 |
| 10:50 | QUALITY CONTROL OF GROUND-BASED RADIOMETRIC OBSERVATIONS<br><i>Maia S. Tatarskaia, Viatcheslav V. Tatarskii*, Valerian I. Tatarskii, CIRES/NOAA;<br/>Ed. R. Westwater, NOAA/ERL</i>  | 42 |
| 11:10 | MEASUREMENT OF OCEANIC PARAMETERS WITH MICROWAVE<br>RADIOMETERS<br><i>C.T. Swift, M.A. Goodberlet, University of Massachusetts</i>   | 43 |
| 11:30 | PASSIVE MICROWAVE PRECIPITATION RETRIEVAL USING THE<br>ADVANCED MICROWAVE PRECIPITATION RADIOMETER (AMPR) AND<br>DUAL-POLARIZATION RADAR<br><i>J. Turk*, Colorado State University; J. Vivekanandan, National Center for<br/>Atmospheric Research; F.S. Marzano, Universita di Roma; R.W. Spencer, R.E.<br/>Hood, NASA/Marshall Space Flight Center; A. Mugnai, Consiglio Nazionale<br/>delle Ricerche; E.A. Smith, Florida State University</i> | 44 |
| 11:50 | AIRBORNE PASSIVE MICROWAVE REMOTE SENSING DURING<br>TOGA/COARE<br><i>A.J. Gasiewski, Georgia Institute of Technology</i>   | 45 |

Mon. a.m.

SATELLITE MICROWAVE REMOTE SENSING OF WATER VAPOR:  
PAST, PRESENT & FUTURE

JOHN C. ALISHOUSE  
NOAA-NESDIS  
SATELLITE RESEARCH LABORATORY  
WASHINGTON, DC 20233

1993 marks the 25th anniversary of the launch of *Cosmos-243*, the first satellite to make microwave observations of water vapor in the earth's atmosphere. This radiometer was strictly nadir viewing and utilized channels in and near the 22.235 GHz water vapor line. In the ensuing 25 years many radiometers with scanning capabilities and channel combinations have been flown on many different satellites from many nations.

In 1987, the first operational microwave water vapor sensor, the *SSM/I*, was launched. This operational sensor, because of the high quality of its data, has inspired a great deal of additional research. Because of the weakness of the 22.235 GHz line and the high emissivity of surfaces such as sea ice and land, water vapor determinations have been limited to total columnar water over the open ocean.

An important event occurred in 1991 when the *SSM/T-2* was launched. This 5 channel radiometer uses the 183 GHz water vapor line (a much stronger line) to remotely sense the water vapor distribution in the troposphere. This instrument produces results over all surface types, but not in the presence of rain.

Future instruments promise to further enhance capabilities to determine atmospheric water vapor distributions. Beginning with the *AMSU A* and *B* instruments, an improved temperature profiling capability should enhance the retrieval of water vapor profiles. This improvement continues with the *SSM/IS* instrument which combines surface, temperature and humidity measurements into one instrument that scans conically. The *MIMR* is being developed by *ESA* for *EOS* and possible operational use on future polar orbiting environmental satellites.

APPLICATION OF MICROWAVE RADIOMETRY TO CLIMATE RESEARCH

Jack B. Snider  
NOAA/ERL/Wave Propagation Laboratory  
325 Broadway  
Boulder, CO 80303

Surface-based microwave radiometers have been employed in climate research since 1987. The ability of these systems to operate continuously and unattended for extended periods of time has provided significant new information on cloud liquid water content and atmospheric water vapor. These data have helped to improve our understanding of cloud-radiation feedback mechanisms which is fundamental to accurate prediction of global warming. In addition to collecting data on the relationship between atmospheric water substance, atmospheric transmission, and cloud albedo, the radiometric observations provide ground-truth for verification of satellite measurements of water vapor and liquid water. In this paper, results are summarized for several intensive field campaigns conducted in different geographic areas, including the western and central United States, and the Atlantic and Pacific oceans. Initial results are also presented from a long-term island-based observational program undertaken to calibrate over-water satellite measurements of water vapor and cloud liquid and to improve algorithms for the retrieval of these quantities.

Mon. a.m.

**A dual-channel airborne radiometer  
for atmospheric and ocean remote sensing**

**L. S. Fedor, D. A. Hazen, W. B. Madsen,  
J. B. Snider, and E. R. Westwater  
NOAA/ERL/Wave Propagation Laboratory  
Boulder, Colorado 80303**

**SUMMARY**

The Wave Propagation Laboratory (WPL) dual-channel (23.87 and 31.65 GHz) airborne radiometer was designed to measure the integrated water vapor and cloud liquid above the aircraft. The instrument has been modified to measure upwelling radiation; downwelling radiation; or both, by continuously rotating the antenna system. Thus by using the mobility of the aircraft the instrument is capable of measuring the three-dimensional structure of water vapor for geophysical studies, such as the clear-sky radiation budget, the formation of clouds, and the path delay of radio waves passing through the atmosphere. The three-dimensional structure of cloud liquid is significant to studies of atmospheric radiative transfer, aircraft icing, and of the energetic budget of atmospheric storm systems. The modification of the antenna system to view downward provides a capability to measure the two-dimensional structure of the sea surface or land emissivity providing important validation measurements for satellite-borne instruments. We will present data obtained during the flights to test the modified antenna system. Data from each of the modes of operation will be given.

RECENT RESULTS IN DETERMINATION OF INTEGRATED WATER VAPOR  
BY GPS AND BY MICROWAVE RADIOMETERS

F. Solheim\*, J. Johnson, T. VanHove, C. Alber, R. Ware  
UNAVCO, 3340 Mitchell Lane, Boulder, CO 80301  
solheim@unavco.unavco.ucar.edu

Data suggesting the utility of the Global Positioning System (GPS) to measure atmospheric water vapor are presented. What was once measurement noise in GPS geodesy (atmospheric water vapor) is now being viewed as a signal.

The GPS baseline measurement capability has improved in accuracy from ppm in the mid-1980s to ppb under certain circumstances. The major sources of remaining error in GPS accuracy are receiver antenna multipath and atmospheric water vapor uncertainty. Improved antenna design, site selection, and receiver software algorithms are diminishing the multipath effects, and total atmospheric water vapor can now be estimated during processing of GPS position solutions. These water vapor values agree quite well with values measured with water vapor radiometers under most meteorological conditions. Comparisons of GPS-inferred atmospheric water vapor with values measured by microwave water vapor radiometers are presented. These results were obtained from measurements at both ends of a 50 km GPS baseline over a four month period. RMS differences of GPS and WVR measurements are less than 2 mm for 10 to 25 mm of integrated water vapor.

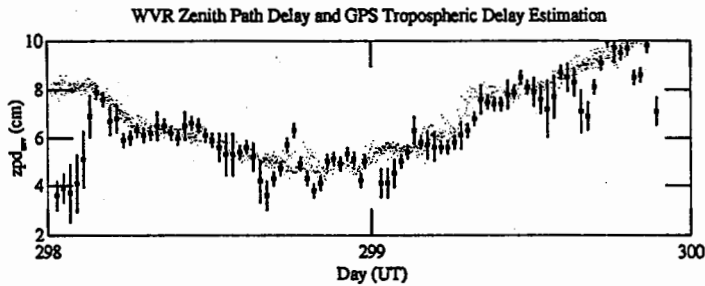


Figure 1. Symbols with error bars are GPS-derived water vapor zenith path delays (zpd); the small dots are WVR measurements. One cm of water vapor induces about 6.5 cm of path delay.

Atmospheric soundings by proposed GPS receivers in low earth orbit will also be briefly discussed. GPS soundings by this method are expected to provide globally distributed high vertical resolution refractivity, temperature, and humidity profiles.

Mon. a.m.

## COMBINED MICROWAVE AND INFRARED SOUNDING OF THE ATMOSPHERE

Yong Han and Ed R. Westwater  
NOAA/ERL/Wave Propagation Laboratory  
Boulder, Colorado 80303

A six-channel, microwave radiometer has been operated by the National Oceanic and Atmospheric Administration's (NOAA) Wave Propagation Laboratory (WPL) for about six years to provide nearly all-weather temperature profiles, integrated water vapor and liquid water. However, microwave radiometers are limited by their poor vertical resolution. An infrared sensor, the Fourier Transform Infrared Sounder (FIRS), is being developed by WPL, NESDIS/University of Wisconsin, and Colorado State University. It operates between roughly 500 and 2000 cm<sup>-1</sup> with 1 cm<sup>-1</sup> spectral resolution. Preliminary studies (Smith et al., 1990; and Joseph A. Shaw and Ed R. Westwater, 1992) have suggested that this sensor may provide high resolution temperature and water vapor profiles, as well as cloud base temperature. However, it is difficult to make profile retrievals from the FIRS sensor during cloudy conditions. A combination of the microwave radiometer and the FIRS may provide high-resolution temperature and water vapor profiles under nearly all-weather conditions. In this presentation, we evaluate the combined ground-based microwave and infrared sounding of atmospheric temperature and water vapor profiles. We focus on the cloud-free conditions.

A radiative transfer code, MODTRN (Berk et al., 1989) and a microwave radiative transfer code developed at WPL were used to provide emission spectrum and temperature and water vapor weighting functions from radiosonde profiles. The information contents on the profile retrievals were evaluated from the weighting functions. The calculated radiances with added experimental noise served as simulated FIRS and microwave radiometer measurements. Retrievals of temperature and water vapor profiles were made from the simulated measurements. These retrievals were compared with the radiosonde profiles. Both statistical and physical inversion methods were applied. Information obtained from the microwave radiometer was used as a constraint for the profile retrievals. We applied the constraint in two ways: (1) a first guess of the profiles obtained from the microwave radiometer was used to constrain the profile retrievals for the FIRS data; (2) the integrated water vapor obtained from the microwave radiometer was used to constrain the total amount of water vapor in the water vapor profile retrievals for the FIRS data.

Future work is suggested to extend current research to include cloudy conditions and field experiment.

Berk, A. ,1989: MODTRAN: A Moderate Resolution Model for LOWTRAN 7, Geophys. Lab. GL-89-0122.

Smith, W.L. et al., 1990: A Ground-Based Atmospheric Profiling Experiment. Bull. Amer. Meteor. Soc., 71(3), 310-318.

Shaw, J.A., and E. R. Westwater, 1992: Passive Remote Sensing of Boundary Layer Temperature and Water Vapor. 71st Annual AMS Meeting, New Orleans, LA.

MICROWAVE RADIOMETRIC SENSING OF AIRCRAFT  
ICING CONDITIONS

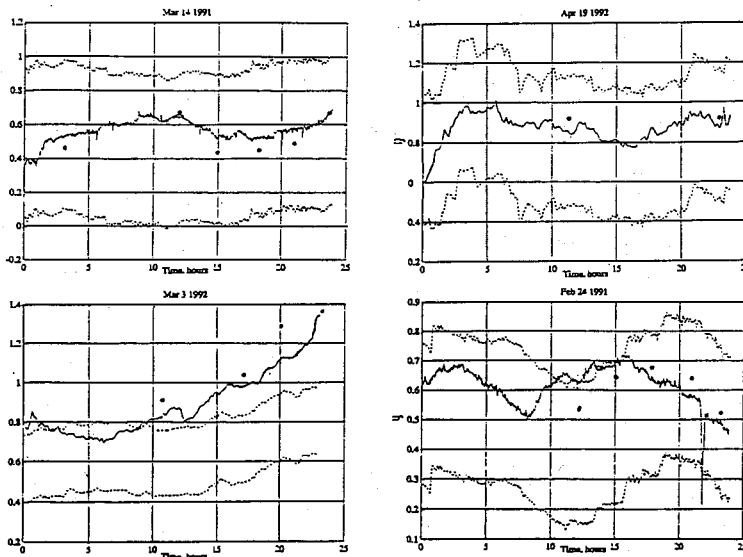
E. R. Westwater, B. B. Stankov, and J. B. Snider  
NOAA/ERL/Wave Propagation Laboratory  
Boulder, Colorado 80303

Because of their unique ability to sense liquid water in clouds, microwave radiometers have potential use in monitoring conditions for aircraft icing. Because the response of microwave radiometers to ice clouds is negligibly small, the observed signal is to liquid alone. For the past three years, an intensive program has been conducted in the front range of Eastern Colorado to determine if icing conditions can be monitored or forecast. Participants in this Winter Icing and Storms Project (WISP) include the National Center for Atmospheric Research, the NOAA Wave Propagation Laboratory (WPL), and the NOAA Forecast Systems Laboratory. During WISP 1990-1992, a limited network of ground-based dual-channel microwave radiometers was been deployed and their data were supplied to forecasters. In addition to radiometers, data from the National Weather Service's operational cloud-height sensing lidar ceilometers and a WPL Radio Acoustic Sounding Systems (RASS) were available. A combined system of radiometers, ceilometers, and RASS can in determine the vertical regions of icing potential. In this system, the ceilometer determines the cloud base, the radiometer determines the thickness of the liquid layer, and the RASS determines the temperature of the liquid. Both research aircraft and special release radiosonde soundings were used for verification of the remote sounders. We present statistical and case analyses demonstrating the potential of such remote sounders for unattended operational deployment.

QUALITY CONTROL  
OF GROUND-BASED RADIOMETRIC OBSERVATIONS

Maia S. Tatarskaia, Viatcheslav V. Tatarskii\*, Valerian I. Tatarskii,  
CIRES/NOAA WPL, Boulder, CO.  
Ed. R. Westwater,  
NOAA/ERL/Wave Propagation Laboratory, Boulder, CO.

In this work, we presented a method of quality control of integrated moisture  $Q$  measured by dual-channel microwave radiometers. Our proposed method of control is based on statistical relations between  $Q$ , dew point temperature  $t_d$ , and shelter temperature  $t$ . From data taken for 5-6 years at Denver, Colorado, USA, we calculated correlation coefficients between  $Q$ ,  $t_d$ , and  $t$ . The data base was subjected to preliminary quality control by comparing radiometer and radiosondes, as well as surface measurements taken by WPL and the NWS. As a result of this control, 25% of the data were excluded from further analysis. The values of correlation coefficients that we obtained ( $R_{t_d Q} = 0.70$ ,  $R_{t Q} = 0.30$ ) showed that supplementary information on temperature was useful for estimating  $Q$ . To estimate  $Q$  we used a linear predictor based on  $t_d$  and  $t$ . Regression coefficients were calculated for each month using the 5-6 year training set. Verification on independent data using radiosondes showed that the estimation of quality was correct 91% of the time. In addition, the method is simple and convenient, since the estimation of  $Q$  depends only on conventional meteorological surface observations of  $t_d$  and  $t$ . It is possible to obtain these quantities from the points in the northern hemisphere from the standard network of surface stations (their number in the northern hemisphere is greater than 2500, while the number of radiosonde stations is about 700). However, because of the strong horizontal variability of water vapor, it is recommended that dual-channel radiometers have their own co-located surface instrumentation, if they are not located at a standard network site.



Time series of radiometrically-measured integrated moisture  $Q$  (heavy lines), radiosonde measurements (points), and 80% confidence intervals, based on the prediction of  $Q$  from surface measurements (dotted lines).

Measurement of Oceanic Parameters  
with Microwave Radiometers

C.T. Swift and M.A. Goodberlet  
University of Massachusetts

The special Sensor Microwave/Imager (SSM/I) is a multi-frequency scanning Microwave Radiometer system that was launched in 1987. Two identical instruments have subsequently been placed into orbit. This instrument is well calibrated and produces a number of geophysical measurements, including ocean surface wind speed as an operational data product. The University of Massachusetts was heavily involved in the validation of this sensor, primarily by producing pairs of ocean surface winds derived from buoys and from the SSM/I. A description of this validation procedure and the algorithm is discussed. The shortcoming of this sensor is that the radiometer frequencies are tuned at 19 GHz and higher, which are significantly attenuated by the atmosphere, particularly if precipitation is within the instrument field of view. In preparing for the future when larger antennas become available to accommodate the lower frequencies, we have developed a C-band multi-frequency radiometer to measure windspeed in hurricanes. The operation of this instrument is described, and its capability to produce accurate measurements of both windspeed and rain rate are discussed.

## PASSIVE MICROWAVE PRECIPITATION RETRIEVAL USING THE ADVANCED MICROWAVE PRECIPITATION RADIOMETER (AMPR) AND DUAL-POLARIZATION RADAR

J. Turk<sup>1\*</sup>, J. Vivekanandan<sup>2</sup>, F.S. Marzano<sup>3</sup>  
R.W. Spencer<sup>4</sup>, R.E. Hood<sup>4</sup>, A. Mugnai<sup>5</sup>, E.A. Smith<sup>6</sup>

<sup>1</sup>Department of Electrical Engineering  
Colorado State University, Fort Collins, CO 80523

<sup>2</sup>National Center for Atmospheric Research, Boulder, CO 80307

<sup>3</sup>Dipartimento di Ingegneria Elettronica  
Universita di Roma "La Sapienza", Via Eudossiana 18, 00184 Rome, Italy

<sup>4</sup>NASA/Marshall Space Flight Center, AL 35812

<sup>5</sup>Istituto di Fisica dell'Atmosfera  
Consiglio Nazionale delle Richerche, Frascati 00044, Italy

<sup>6</sup>Department of Meteorology  
Florida State University, Tallahassee, FL 32306

Remote sensing satellites deploying combinations of active and passive microwave sensors are planned to meet the need for reliable estimates of rainfall from space. The NASA Advanced Microwave Precipitation Radiometer (AMPR), an across-track scanning, four-channel (10.7, 19.35, 37.1, 85.5 GHz) radiometer, was flown aboard a NASA ER-2 aircraft during the 1991 CaPE (Convection and Precipitation/Electrification) project in central Florida. During overflights of precipitation, coincident ground-based radar measurements were taken with the NCAR CP-2 polarimetric radar for comparison. In precipitating media, microwave radar observations are primarily sensitive to scattering and extinction characteristics of precipitation size ( $> 0.1$  mm) atmospheric particles. Techniques of estimating mass contents of liquid precipitation such as rain makes use of polarimetric measurements; however, extensions to frozen precipitation amounts are yet to be fully understood. Polarimetric studies might be relevant in pristine crystals which exhibit differential scattering characteristics, but hail, graupel and snow particles display little polarimetric dependent signatures. A hybrid statistical/physical precipitation retrieval algorithm developed by three of the authors (FSM, AM, and EAS) was tested against the radar-derived vertical profiles of rain and frozen hydrometeors. At AMPR frequencies, the upwelling brightness temperature  $T_B$  is sensitive to cloud processes originating at middle and upper altitudes within the cloud. The hybrid algorithm retrieves appropriate vertical hydrometeor profiles of liquid and frozen water contents from an explicit 3-D cloud model database. The process uses optimization techniques and fast microwave radiative transfer simulations to perturb initial guess hydrometeor profiles towards agreement with the AMPR  $T_B$  measurements. Despite differences between the cloud model and radar-derived microphysics, the hybrid model demonstrated reasonable agreement with the radar-derived rain rates and columnar mass contents. Microwave radiative transfer modeling simulations using the radar-derived drop size distributions were performed, and are compared with the observed AMPR  $T_B$ . Also, a detailed Mueller matrix based backscattering-propagation model is developed to study the radar observed propagation characteristics. Model results are shown for a typical precipitating medium.

## Airborne Passive Microwave Remote Sensing During TOGA/COARE

A.J. Gasiewski

School of Electrical Engineering  
Georgia Institute of Technology  
Atlanta, GA 30332

Among the instruments used during the Tropical Ocean Global Atmosphere/Coupled Ocean-Atmosphere Response Experiment (TOGA/COARE, January-February 1993) were several airborne passive microwave sensors. Due to their simplicity and the wealth of geophysical information available from them, passive microwave sensors have become important components of meteorological and oceanic field studies. The TOGA/COARE sensor suite was particularly innovative for several reasons: (1) sensors were flown on both high-altitude (NASA ER-2, 20 km) and medium-altitude (NASA DC-8, < 13 km) aircraft, providing diverse spatio-temporal coverage, (2) several imaging radiometers covering an unprecedented set of passive channels (all window and major tropospheric absorption features from 10 to 220 GHz) were included, and (3) a fully-polarimetric 92-GHz radiometer was included.

Three microwave sensors on the DC-8 (ESMR, AMMS, and AMMR) provide brightness measurements above, below and (subject to aircraft structural limitations) within clouds and precipitation. Due to the close proximity of the observed structures, spatial resolutions are one-to-two orders of magnitude higher than available from spaceborne sensors. Three cross-track scanning microwave imagers on the ER-2 (AMPR, MIR and MTS) provide high spatial-resolution temperature, water vapor and stormcell brightness imagery (spot sizes of  $\sim 0.6 - 3$  km at 20 km altitude) with sensitivities of  $\sim 1$  K. Collectively, these instruments measure brightness temperatures near the window-channel frequencies at 10, 18, 37, and 85 GHz (AMPR) and 90, 150, and 220 GHz (MIR), the 5-mm  $O_2$  band (MTS, one frequency-selectable nadir looking channel), the 118-GHz  $O_2$  line (MTS, 8 channels), and the 183-GHz  $H_2O$  line (MIR, 3 channels). An additional submillimeter wave receiver on the MIR will soon provide imagery at the 325 GHz  $H_2O$  line (3 channels). The composite high-resolution data will provide a unique basis for evaluating the information content of multispectral microwave imagery.

Dual-polarization radiometers (e.g., SSM/I) currently provide data for operational measurements of ocean surface wind speed. However, only recently have passive measurements of ocean surface wind direction been investigated. Included on the DC-8 is a calibrated fully-polarimetric radiometer for this purpose. The talk will focus primarily on data from this instrument and the MIR.



## SESSION URSI K-1

MONDAY AM

## ELECTROMAGNETIC INTERACTIONS WITH BIOLOGICAL SYSTEMS

Chairs: J.C. Lin, The University of Illinois at Chicago  
 T.S. Tenforde, Battelle Northwest Laboratories

Room: Alumni Center, Room 2      Time: 8:30-11:50

|       |   |    |
|-------|---|----|
| 8:30  | LEVELS OF 5'NUCLEOTIDASE: ACETYLCHOLINESTERASE AND<br>ALKALINE PHOSPHATASE IN DEVELOPING CHICK EMBRYOS FOLLOWING<br>EXPOSURE TO A 60 HZ MAGNETIC FIELD<br><i>A.H. Martin, G.C. Moses, University of Western Ontario</i>                       | 48 |
| 8:50  | CURRENT DISTRIBUTIONS IN AN INHOMOGENEOUS MODEL OF A HUMAN<br>BODY BY LIGHTNING AND NUCLEAR ELECTROMAGNETIC PULSE WAVES<br><i>Hsing-Yi Chen*, Hou-Hwa Wang, Chin-Chyang Fang, Yuan-Ze Institute of<br/>Technology</i>                         | 49 |
| 9:10  | HEATING CHARACTERISTICS OF THIN HELICAL ANTENNAS WITH<br>CONDUCTING CORES<br><i>Mark S. Mirotznik, The Catholic University of America; Nader Engheta, Kenneth<br/>R. Foster, University of Pennsylvania</i>                                   | 50 |
| 9:30  | FINITE DIFFERENCE TIME DOMAIN ANALYSIS OF COMPLEX MICROWAVE<br>HYPERHERMIA APPLICATORS<br><i>M. Okoniewski, University of Victoria</i>  | 51 |
| 9:50  | MODELIZATION OF PLANAR APPLICATORS FOR MICROWAVE<br>HYPERHERMIA BY F.D.T.D. METHOD<br><i>P.Y. Cresson*, L. Dubois, C. Michel, M. Chive, J. Pribetich, I.E.M.N.</i>  | 52 |
| 10:10 | BREAK   |    |
| 10:30 | MODELING OF ELECTRICAL DEFIBRILLATION ON A MASSIVELY<br>PARALLEL COMPUTER<br><i>S.A. Hutchinson, New Mexico State University; O.C. Deale, B.B. Lerman,<br/>Cornell University; K.T. Ng*, New Mexico State University</i>                      | 53 |
| 10:50 | INVERSION OF MEASURED SURFACE BIOPOTENTIALS TO CURRENT BIO-<br>GENERATORS INSIDE HUMAN BODY<br><i>N.K. Uzunoglu*, E. Ventouras, I. Papapolymerou, E. Thomopoulos, National<br/>Technical University of Athens</i>                             | 54 |
| 11:10 | PLANAR APPLICATORS FOR MICROWAVE HYPERHERMIA AT 434 MHZ<br><i>C. Michel*, L. Dubois, P.Y. Cresson, M. Chive, J. Pribetich, Université des<br/>Sciences et Technologies de Lille</i>   | 55 |
| 11:30 | A NON-INVASIVE WAY TO CONTROL THE TEMPERATURE IN<br>CRYOTHERAPY TREATMENTS BY MULTIFREQUENCY MICROWAVE<br>RADIOMETRY<br><i>L. Dubois*, Lecroart, F. Duhamel, M. Chive, J. Pribetich, Université des<br/>Sciences et Technologies de Lille</i> | 56 |

**LEVELS OF 5'NUCLEOTIDASE; ACETYLCHOLINESTERASE AND  
ALKALINE PHOSPHATASE IN DEVELOPING CHICK EMBRYOS  
FOLLOWING EXPOSURE TO A 60 HZ MAGNETIC FIELD**

Martin, A.H. and Moses, G.C.  
Dept. of Anatomy and Clinical Biochemistry  
Univ. of Western Ontario  
London, Ontario  
Canada

Exposure to a 60 Hz, 4  $\mu$ T split sine wave for three days did not cause an increase in the total number of dead or morphologically abnormal live embryos. The ratio of dead to abnormal embryos, however, was dramatically elevated in the exposed group. To examine this finding, embryos were exposed to the 60 Hz magnetic field for three days and the activity levels of 5'NT; AChE and ALP were determined in normal as well as abnormal live embryos. In normal-appearing embryos, the values for 5'NT were reduced by 50% while values for AChE and ALP were unchanged from controls. In exposed abnormal live embryos, the levels of all three enzymes were significantly reduced from levels found in unexposed abnormals. To determine if this effect is permanent or transitory, embryos were exposed for three days and then incubated in a field-free environment for a further 3 or 15 days. At removal on day 6, using only normal-appearing live embryos, values for 5'NT were found to be reduced again by one-third, while the levels of AChE and ALP were unchanged from controls. Following exposure and a further 15 days incubation, the brains of 18-day embryos were removed and separated into cerebellar and cortical portions. In the cerebellar segments, values for 5'NT were reduced by 1/3 with AChE and ALP unaffected. In the cortex, no effect was noted on any of the three enzymes. Finally, embryos either unexposed, exposed to the 4  $\mu$ T field or exposed to a 4  $\mu$ T magnetic field plus a superimposed random noise of equal intensity were examined at day 3. Values for 5'NT were reduced by 1/2 in the series with signal alone while values for 5'NT in the unexposed and the signal plus noise groups were identical. Embryos in the same three categories were exposed for three days, then incubated until hatching. The 4  $\mu$ T split sine wave alone had a dramatic impact with only 5 of 20 hatching while 17 and 16 hatched in unexposed and signal plus noise groups, respectively. All embryos that hatched appeared to be morphologically and functionally normal.

## CURRENT DISTRIBUTIONS IN AN INHOMOGENEOUS MODEL OF A HUMAN BODY BY LIGHTNING AND NUCLEAR ELECTROMAGNETIC PULSE WAVES

Hsing-Yi Chen\*, Hou-Hwa Wang, and Chin-Chyang Fang

Department of Electrical Engineering  
Yuan-Ze Institute of Technology  
Nei-Li, Taoyuan Shian, Taiwan 32026  
Telephone: (03) 463-8800  
Fax: (03) 463-9355

### ABSTRACT

The electromagnetic pulses (EMP) radiated from natural lightning (LEMP) and from high-altitude nuclear explosion (NEMP) have a large-amplitude transient electromagnetic phenomena. These high-intensity EM fields associated with an electromagnetic pulse have created a public concern over the potential health effects. Electric fields as high as 1-40 kV/m have been measured when the LEMP waves are close to earth (50-500 m). The intensity of electric field close to NEMP generators can reach to a very high value of 60-100 kV/m. The rise times are on the order of 1-5  $\mu$ s and 10-30 ns in the LEMP and NEMP, respectively, while the pulse durations are on the order of 50-100  $\mu$ s and 100-300 ns, respectively, in the LEMP and NEMP. Approximately, the incident EMP fields were expressed by  $E(t) = E_0 [e^{-\alpha t} - e^{-\beta t}]$  used for the calculations by using the FDTD technique in this paper, where  $E_0$  is the amplitude of the EMP,  $\alpha$  and  $\beta$  are two decay constants. Because it is a time-domain technique, and also because of its computational efficiency and accuracy, the FDTD method has become increasingly popular for computations of electromagnetic wave propagation and scattering problems and electromagnetic biological effects. In particular, it is ideally suitable for calculations involving EMP. In the study, a human body was simulated by a realistic model with 6402 cubic cells for exposure to vertically polarized LEMP and NEMP with electric fields of 40 kV/m. Since the resonant frequency of an adult human standing on a ground plane is close to 40-50 MHz, the dielectric constant and conductivity of tissues including anisotropy at 50 MHz were adopted from available literature for the worst case. The condition of exposure of the human was considered isolation from ground with shoes. The induced current densities were calculated. The maximum current density 0.46 A/cm<sup>2</sup>, induced in the location of the lower leg by the NEMP wave, is much higher than that required to influence neural activity. The minimum current density for neural activity was found in the range of 1 mA/cm<sup>2</sup> from available literature. It was also found that the maximum current density 0.018 A/cm<sup>2</sup> induced in the location of the lower leg by the LEMP wave, is much smaller than that induced by the NEMP wave. The maximum currents induced in the abdomen of the human body were found to be 3.3 and 118 amperes by the LEMP and NEMP waves, respectively. A higher value of current may be induced in the human body by the NEMP rather than by the LEMP.

## Heating Characteristics of Thin Helical Antennas with Conducting Cores

Mark S. Mirotznik\*, Nader Engheta<sup>†</sup>, and Kenneth R. Foster<sup>++</sup>

\*Department of Electrical Engineering

The Catholic University of America

Washington D.C. 20064

Departments of Electrical Engineering<sup>†</sup> and Bioengineering<sup>++</sup>

University of Pennsylvania

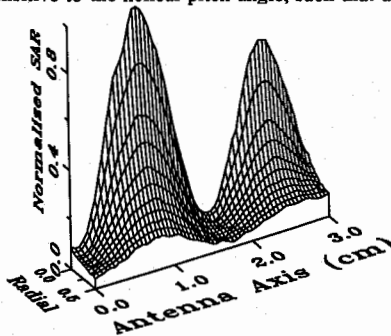
Philadelphia PA 19104-6392

### Abstract

We report a combined theoretical and experimental study of the heating characteristics of helical antennas with conducting cores in lossy dielectric media. Proposed biomedical applications of such antennas include angioplasty, hyperthermia and catheter ablation of tissue. The study focuses on helical antennas operated in the normal mode (wavelength greater than antenna diameter but comparable to antenna length), that are terminated at one end by a short circuit and at the other by a coaxial feed point.

We extend an analytical model based on the helical sheath approximation (used by Sensiper, 1955, Neurether *et. al.*, 1967 and Hill and Wait, 1980) to the case of lossy medium, and report experimental studies of the specific absorption rate (SAR) of helical antennas in aqueous electrolyte of various conductivity.

Near field SAR patterns were calculated and measured. It was found that the SAR patterns strongly reflects the presence of standing waves. These patterns depend in a complex way on the geometry of the antenna and electrical properties of the external medium. The patterns were found to be sensitive to the helical pitch angle, such that a tighter helix results in a tighter standing wave pattern. Another prominent feature is the sensitivity of the antenna SAR pattern to the conductivity of the external medium. As the conductivity was increased the SAR pattern would rapidly shift towards the antenna's tip. It was found, however, that the presence of a thin layer of insulation added to the outside of the antenna greatly reduced this effect and lead to a more uniform heating pattern. These results have significant implications for the prospective biomedical application of thin helical antennas.



Measured normalized SAR pattern of helical antenna immersed in 0.8% NaCl solution. The antenna had a length of 3.0 cm, diameter of 0.2 cm, helical pitch angle of 15° and was encapsulated in a 0.05 mm thick layer of teflon insulation.

## FINITE DIFFERENCE TIME DOMAIN ALYSIS OF COMPLEX MICROWAVE HYPERTERMIA APPLICATORS

M.Okoniewski

Dept. Of Electrical and Computer Engng, University of Victoria  
P.O.Box 3055, Victoria, BC, Canada V8W 3P6

A key technical problem in the microwave thermotherapy lies in the design of a microwave applicator able to deliver microwave power precisely to the tumor. In a typical arrangement an applicator is inserted either to a patient rectum or urethra. It was recently shown (P.Debicki *et al.*: *Urology*, v.40, no-4, pp300-307, Oct.92), that the most promising results can be obtained using a *dual applicator* procedure, where the energy is simultaneously radiated by two applicators, one located in the urethra and the other in the rectum.

Analyses of microwave hyperthermia applicators were typically carried out using a relatively simple method based on R.W.P.King theory (R.W.P.King, S.Smith: *Antennas in Matter*, MIT Pres, 1981, P.Debicki, *et al.*: in *Consensus of Hyperthermia for 90's*, Plenum, 1991). This theory fails for more complex geometries of the applicator, particularly those allowing shaping of a transverse radiation pattern (directional applicators) and those which contain tissue cooling systems and/or delay lines which improve focusing of radiated energy. Additionally, the practical applications of *dual applicator* procedure, require that not only rigorous amplitude but also phase characteristics of both applicators are known.

In this presentation an implementation of FDTD method is described for use in the analysis of hyperthermia applicators. It was necessary to implement a full 3D version of the algorithm, to account for antennae with directional beam. The method can be used to obtain both impedance properties of the applicator and its amplitude and phase radiation pattern. To save the computer memory and computation time absorbing boundary conditions are used.

In this presentation, the method was used to compute the dissipated power distribution of a multisection rectal applicator with and without transverse beam forming elements and cooling system. To the best of the author knowledge, these characteristics could not be obtained with other methods previously described. The results of computer simulations are in good agreement with data obtained with a thermographic camera during laboratory tests on a muscle model. The results also compare well with data obtained during actual prostate treatment.

The same method will be used to treat urethral applicators and to simulate and optimize the dual applicator procedure.

## MODELIZATION OF PLANAR APPLICATORS FOR MICROWAVE HYPERTERMIA BY F.D.T.D. METHOD.

P.Y. CRESSON\*, L. DUBOIS, C. MICHEL, M. CHIVE, J. PRIBETICH.

I.E.M.N. - U.M.R. C.N.R.S. N° 9929

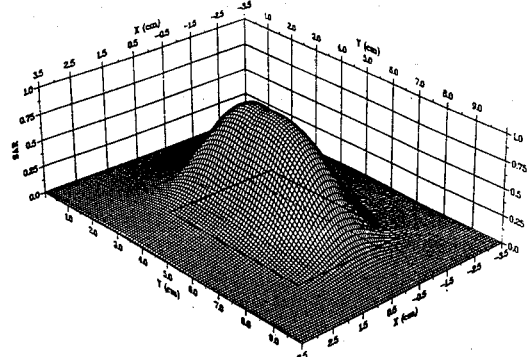
DEPARTEMENT HYPERFREQUENCES & SEMICONDUCTEURS (C.H.S.)  
UNIVERSITE DES SCIENCES & TECHNOLOGIES DE LILLE.  
59655 VILLENEUVE D'ASCQ CEDEX - FRANCE.

When planning hyperthermia treatments, it is desirable to be able to predict the complete temperature pattern both in tumor and surrounding healthy tissues in order to achieve thermal dosimetry and to optimize the efficiency of the treatment. To reach this aim, it is necessary to obtain the power deposition pattern in the heated tissues. A large number of devices have been designed for producing therapeutic heating of tumors of different sizes in a variety of anatomic locations : we are interesting in the development of planar applicators for the treatment of superficial and semi-deep tumors. Previous modelization of these applicators was based on the Spectral Domain Approach ( S.D.A. ) method which allows the calculation of the geometrical parameters, of the resonant frequency and also of the electric field from which the power deposition can be deduced.

In order to take into account the exact shape of the tissues ( which are not stratified plane structures ) and also of the applicator ( feeding line ), we are now developing a new model based on the Finite Difference Time Domain ( F.D.T.D. ) method which has been first proposed by YEE [ I.E.E.E. AP-14, n°3, 1966 ]. A three-dimensional F.D.T.D. program has been developed for the planar structure ( microstrip-microslot applicator ). The electromagnetic problem consist of numerically solving the MAXWELL's equations in which finite-difference approximation are employed for both time and space derivatives. At the boundaries of the finite grid the outgoing wave must be prevented from being reflected back into space occupied by the grid. One method of achieving this is to impose an absorption condition at the edge of the grid.

The studied structure is a microstrip-microslot applicator laid on lossy media. The heating frequency is 915MHz. The power deposition is obtained from these theoretical computations : an example is given on the figure below.

With this model, it is now possible to take into account the exact shape of both the applicator and the surrounding tissues.



## MODELING OF ELECTRICAL DEFIBRILLATION ON A MASSIVELY PARALLEL COMPUTER

S.A. Hutchinson<sup>1</sup>, O.C. Deale<sup>2</sup>, B.B. Lerman<sup>2</sup>, and K.T. Ng<sup>1\*</sup>

<sup>1</sup>New Mexico State University  
Las Cruces, NM 88003

<sup>2</sup>Cornell University Medical College  
New York, NY 10021

Electrical defibrillation is one of the most effective means to treat cardiac arrest (ventricular fibrillation). Traditionally the mechanisms of defibrillation have been investigated mainly with experimental techniques. Recent advances in digital computers have made practical the use of numerical techniques to complement the experimental study of defibrillation. The solution and memory constraints of conventional computers, however, often limit the size of realistic problems that can be investigated numerically. As a step in extending the size and complexity of the problems that can be studied, we have implemented a numerical model of electrical defibrillation on a massively parallel computer, Thinking Machine Corporation's Connection Machine 2 (CM-2). The CM-2, with up to 64k processors ( $k=1024$ ), allows a high level of parallelism and the solution of extremely large problems.

The Laplace equation governing the potential distribution during defibrillation has been solved with the finite-element method. In order to handle complex problem domains such as the thoracic cavity, we have optimized the finite-element algorithm such that a general irregular discretized problem can be mapped effectively onto the parallel architecture of the CM-2. In addition, the algorithm can handle an anisotropic medium such as the skeletal muscle which has been found to have a significant effect on the current flow in the thoracic cavity. A nodal assembly technique is used where each node in the mesh is mapped to a virtual processor in the computer. With such a technique, each processor will evaluate and store the nonzero coefficients associated with a row of the stiffness matrix. The resulting system of equations is solved with the preconditioned conjugate gradient technique.

Both first-order hexahedron and tetrahedron elements have been implemented in the computer code. Contours for major organs and the outer chest wall have been determined for a canine from transverse MRI images. These contours are digitized and imported to a pre-processing program for mesh generation. Published isotropic and anisotropic conductivity values are assigned to different tissues. Numerical results will be presented together with a description of the finite-element algorithm.

## INVERSION OF MEASURED SURFACE BIOPOTENTIALS TO CURRENT BIO-GENERATORS INSIDE HUMAN BODY

*N.K. Uzunoglu<sup>\*</sup>, E. Ventouras, I. Papapolymerou and E. Thomopoulos*

*Department of Electrical and Computer Engineering*

*National Technical University of Athens*

*Athens 10682, Greece.*

### Abstract

Measurement of biopotentials on the body surface is used widely in clinical practise. Techniques such as Electrocardiography (ECG), Electroencephalography (EEG) and Electromyography (EMG) are some examples to mention. In all these clinical diagnostic methods waveforms are observed - today using digital measurement and storing techniques - and compared to standard waveforms corresponding to healthy "curves" and already recorded pathological "curves" to provide a diagnosis. The biopotential waveforms measured on the body surface are caused by current biogenerators induced in internal organs. Then, the measured biopotential waveforms  $V_i(t)$  ( $i=1,2,\dots$ ) are complex functions of the current biogenerators inside the human body because of the highly complicated electrical structure of the human body. These current sources are characterised by the scalar current source function  $\rho(r,t) = -\nabla \cdot \underline{m}(r,t)$ , where  $\underline{m}(r)$  is the vector current density source function ( $A/m^2$ ).

In order to improve clinical diagnostic techniques mentioned before, it is highly interesting to determine the  $\rho(r)$  function in terms of the measured  $V_i(t)$  biopotentials. An alternative technique is to measure the magnetic field  $\underline{H}(r,t)$  generated by the  $\underline{m}(r,t)$  current distribution and this is already established on a limited scale in clinical practise. Taking into account the fact that the human body magnetically is passive characterised with the free space permeability, then, the  $\underline{H}(r,t)$  and  $\underline{m}(r,t)$  are related with the Bio-Saviat relation using the free-space Green's function. However, measurement of magnetic fields is very difficult and costly compared to measurement of electrical biopotentials. Then, it is necessary to pose the question on inverting the relation,  $V_i(t) = F(\rho(r,t))$  (1) to obtain  $\rho(r,t) = F^{-1}(V_i(t))$  (2)

In order to achieve the result of Eq.(2), it is necessary to take into account the electrical structure of the human body. To this end integral equation techniques are employed to derive an inversion algorithm to image the  $\rho(r,t)$  patterns in terms of the  $V_i(t)$  potentials. NMR and CT images are employed to determine accurately the conductivity  $\sigma(r)$  distribution inside the body for each subject. Then the electrostatic theory of Green's function is employed to obtain Eq.(1). In obtaining Eq.(2) the Algebraic Reversion Technique (ART) is employed. Until now the technique has been employed successfully for the imaging of  $\rho(r,t)$  distribution for the Brain Evoked potentials and ECG. Computed and measured results will be presented.

## PLANAR APPLICATORS FOR MICROWAVE HYPERTHERMIA AT 434 MHZ.

C. MICHEL\*, L. DUBOIS, P.Y. CRESSON, M. CHIVE, J. PRIBETICH.

I.E.M.N. - U.M.R. C.N.R.S. N° 9929  
DEPARTEMENT HYPERFREQUENCES & SEMICONDUCTEURS (C.H.S.)  
UNIVERSITE DES SCIENCES & TECHNOLOGIES DE LILLE.  
59655 VILLENEUVE D'ASCQ CEDEX - FRANCE

The use of the frequency bandwidth around 915 MHz for cellular phones will involve modifications in the microwave hyperthermia systems : it will be necessary either to change the heating frequency ( 2450 MHz or 434 MHz ) or to insulate the equipment ( Faraday cage ). In the case of the change of frequency, it seems judicious to choice 434 MHz because the penetration depth of the electromagnetic waves inside biological tissues is greater at this frequency. However, it will be necessary to increase the geometrical dimensions of the external planar applicators ( microstrip and microstrip-microslot ) which can be a drawback. We propose to show that the use of the applicators designed for 915 MHz is possible at 434 MHz provided that some modifications are brought.

The studied structures are planar applicators ( microstrip-microslot ) constructed on a substrate of permittivity  $\epsilon_r = 4.9$ . These applicators, covered or not with a protective dielectric superstrate, are laid on multilayered lossy media ( such as human body ). We have considered two applicators : the first one is a planar applicator constructed for a 434 MHz microwave hyperthermia ( applicator A ). The other one is an applicator designed for 915 MHz ( applicateur B ) for which the microstrip excitation line has been covered with a high permittivity layer (  $\epsilon_r = 50$  ) ( the resonant frequency is 750 MHz, but the  $S_{11}$  coefficient is  $< -10$  dB at 915 MHz and, so the applicator can be used at this frequency ). The modelization is based on the wellknown Spectral Domain Approach ( S.D.A. ) method.

In order to compare the performances of these two applicators, experimental measurements were performed on phantom models of human tissues ( saline solution or polyacrylamid gel ).

First, the return loss (  $S_{11}$  parameter ) has been measured by means of a network analyser H.P. 8510 in order to determine the resonant frequency of the applicator.

The second part of the experiment consists in the determination of the energy distribution of the applicator. This energy is obtained with a simple system for mapping the electric field pattern created in water by the microwave applicator under test. The electric probe connected to a square-law diode detector measured a quantity  $V_{det}$  which is proportional to the squared electric field intensity (  $E^2$  ). It is then possible to estimate the penetration depth ( which is defined as the distance for which the power absorbed by the medium is reduced to 37% of the incident power laid at the applicator-medium interface ). We can note that the applicateur B has the same performances that the applicator A ( better in the case of a 2 cm water bolus between the applicator and the lossy medium ).

We can conclude that the previous applicators designed for 915 MHz microwave hyperthermia can be used at 434 MHz when a high permittivity dielectric layer is laid on the microstrip excitation line.

## A NON-INVASIVE WAY TO CONTROL THE TEMPERATURE IN CRYOTHERAPY TREATMENTS BY MULTIFREQUENCY MICROWAVE RADIOMETRY

DUBOIS L.1\*, LECROART 2, DUHAMEL F.1, CHIVE M.1, PRIBETICH J.1.

1 *I.E.M.N. - DEPARTEMENT HYPERFREQUENCES & SEMICONDUCTEURS  
U.M.R. C.N.R.S. N°9929 - Bâtiment P4  
UNIVERSITÉ DES SCIENCES ET TECHNOLOGIES DE LILLE.  
59655 VILLENEUVE D'ASCQ CEDEX - FRANCE*

2 *C.H.R LILLE - Service Physiologie 59000 LILLE - FRANCE*

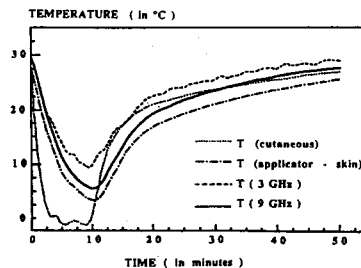
For a long time, the treatment by cryotherapy of fractures, pulled muscles or osteoarthritis was consisting in the application of an ice bolus on the zone to be treated. However the duration of the treatment is not long enough in order to reach the wanted internal temperatures. Now, we can make use of a more efficient technology by pointing a gaseous flux of nitrogen at the zone to be cooled. But for this technique the only control of temperatures is obtained superficially with thermocouples and we can not have any control in depth: so, the duration of the treatment is estimated by empirical manner.

The use of microwave radiometry is a new way allowing the non invasive control of internal temperatures and also the regulation of the flow of the gaseous nitrogen in order to obtain the required temperature in depth. The purpose of this paper is to give the first results which shows the feasibility of this new technique of control of temperatures by the use of two radiometers working around 3 and 9 GHz. The antenna used for the temperature measurement is a planar one ( slot antenna ), light and not very bulky and which is applied on the muscular zone to be cooled.

In a first step, we have compared the efficiency between the use of a flow of gaseous nitrogen and an ice bolus owing to radiometric temperatures measurements which give informations about deep-seated temperatures in the muscular tissue. These comparisons have been performed on the arm and on the thigh in the two cases ( cooling ice and nitrogen ) of several patients. The reconstruction of the thermal mapping inside tissues can be obtained with this method of control with the help of a software allowing the mono- and bidimensional resolution of the bioheat transfer equation and the calculation of radiometric temperatures at 3 and 9 GHz corresponding to these calculated temperatures.

An example of the average variations of the measured temperatures during cooling sessions performed on patient with gaseous nitrogen flow is given on the opposite figure.

The experimental results and the reconstruction of thermal mapping point out the feasibility of this new and original method of temperatures control for treatments using a gaseous nitrogen flow for cryotherapy.



**SESSION URSI B-3****MONDAY PM****TIME DOMAIN METHODS II**

Chairs: E. Heyman, Tel Aviv University; J. Litva, McMaster University

Room: Modern Languages Building, Auditorium 2      Time: 1:30-5:10

|      |   |    |
|------|---|----|
| 1:30 | GRAD, DIV, AND CURL OPERATORS, GAUSS', STOKES', AND GREEN'S THEOREMS, AND HUYGENS' PRINCIPLE IN THE FINITE DIFFERENCE WORLD<br><i>W.C. Chew, University of Illinois</i>           | 58 |
| 1:50 | A HIGHER ORDER FDTD ALGORITHM FOR SOLVING LARGE SCATTERING PROBLEMS<br><i>Charles W. Manry Jr.*, Shira L. Broschat, John B. Schneider, Washington State University</i>            | 59 |
| 2:10 | A NEW FINITE-DIFFERENCE TIME-DOMAIN TECHNIQUE IN CURVILINEAR COORDINATES<br><i>J.E. Linder*, K.T. Ng, New Mexico State University</i>   | 60 |
| 2:30 | ELIMINATION OF NUMERICAL DISPERSION IN FINITE-DIFFERENCE TIME-DOMAIN ALGORITHMS<br><i>Steven Omick*, Steven P. Castillo, New Mexico State University</i>                          | 61 |
| 2:50 | EVOLUTION OF TIME DOMAIN METHODS FOR ELECTROMAGNETIC FIELDS<br><i>J.A. Murphy*, D.P. Rowse, British Aerospace PLC; R. Mittra, University of Illinois</i>                          | 62 |
| 3:10 | BREAK   |    |
| 3:30 | A COMPARISON OF THE PROPERTIES OF RADIATING BOUNDARY CONDITIONS IN THE FDTD METHOD FOR ANTENNA AND WAVEGUIDE ANALYSIS<br><i>C.J. Railton*, E.M. Daniel, University of Bristol</i> | 63 |
| 3:50 | A UNIFIED APPROACH TO THE EFFICIENT TREATMENT OF GEOMETRICAL DETAIL IN THE FDTD METHOD<br><i>C.J. Railton, University of Bristol</i>  | 64 |
| 4:10 | A HYBRID FD-TD/SPECTRAL METHOD FOR THE ELECTROMAGNETIC ANALYSIS OF PERIODIC STRUCTURES<br><i>A. Cangellaris*, M. Gribbons, G. Sohos, University of Arizona</i>                    | 65 |
| 4:30 | A HYBRID TDFV/FDTD TECHNIQUE FOR RADIATION AND SCATTERING FROM SURFACE/WIRE STRUCTURES<br><i>Michael A. Jensen*, Yahya Rahmat-Samii, University of California, Los Angeles</i>    | 66 |
| 4:50 | ENHANCEMENTS TO THE TSAR MODELING SYSTEM<br><i>Douglas J. Riley*, Sandia National Laboratory; Steve Pennock, Lawrence Livermore National Laboratory</i>                           | 67 |

**Grad, Div, and Curl Operators,  
Gauss', Stokes', and Green's Theorems,  
and Huygens' Principle in the Finite Difference World**

W.C. CHEW

ELECTROMAGNETICS LABORATORY

DEPARTMENT OF ELECTRICAL AND COMPUTER ENGINEERING

UNIVERSITY OF ILLINOIS

URBANA, IL 61801

**Abstract**

The finite difference technique is in vogue in numerical analysis because of their simplicity. However, it does not have a rich repertoire of algebraic theory attached to it as in integral and differential calculus. For instance, in integral and differential calculus, one can have Gauss', Stokes' and Green's theorem associated with vector field. Various vector identity for grad, div, and curl operators can be derived.

In this paper, we derive the analogue of grad, div, and curl in the finite difference world. Various analogues of vector identity associated with the vector differential calculus will be derived. Consequently, the Yee algorithm (K.S. Yee *IEEE Trans. Antennas Propagat.*, 14, 302-307, 1966, W.C. Chew, *Waves and Fields in Inhomogeneous Media*, Van Nostrand Reinhold, New York, 1990) for Maxwell's equation can be written in a concise form using the new formulation. Moreover, discrete Green's theorem, Huygens' principle, Poynting's theorem, and uniqueness theorem can be derived in the finite difference world.

As an illustration, in this new formulation, Maxwell's equations appear as:

$$\tilde{\nabla} \times \mathbf{E}_m^l = -\hat{\partial}_t \hat{\mathbf{B}}_{m+\frac{1}{2}}^{l-\frac{1}{2}}, \quad (1)$$

$$\hat{\nabla} \times \hat{\mathbf{H}}_{m+\frac{1}{2}}^{l-\frac{1}{2}} = \hat{\partial}_t \mathbf{D}_m^l + \mathbf{J}_m^{l-\frac{1}{2}}, \quad (2)$$

$$\tilde{\nabla} \cdot \hat{\mathbf{B}}_{m+\frac{1}{2}}^{l-\frac{1}{2}} = 0, \quad (3)$$

$$\hat{\nabla} \cdot \mathbf{D}_m^l = \varrho_m^l. \quad (4)$$

In the above,  $\tilde{\nabla}$ ,  $\hat{\nabla}$ ,  $\hat{\partial}_t$ , and  $\hat{\partial}_t$  are the finite difference equivalence of the continuum space operators.

With the derivation of the discrete forms of various operators, theorems, and vector identities, more analysis can be added in the finite difference world. Moreover, some of these theorems can be used as checks in the validity of numerical codes.

## A HIGHER ORDER FDTD ALGORITHM FOR SOLVING LARGE SCATTERING PROBLEMS

Charles W. Manry Jr.\*, Shira L. Broschat, and John B. Schneider  
School of Electrical Engineering and Computer Science

Washington State University  
Pullman, WA 99164-2752

The Finite Difference Time Domain (FDTD) method, introduced by K.S. Yee to solve scattering problems in electromagnetics [*IEEE Trans. Antennas Propagat.*, AP-14(3), 302-307, 1966], has been widely used to solve many different electromagnetics problems. However, in problems where the scatterer is very large with respect to a wavelength, the computer memory required by Yee's FDTD algorithm to obtain an accurate solution is prohibitive due to the numerical phase anisotropy inherent in the algorithm. To minimize the error caused by this anisotropy, grid spacing must be very small relative to a wavelength.

In order to reduce the memory requirements, a second-order in time and sixth-order in space (2-6) FDTD algorithm has been developed for large dielectric-dielectric electromagnetics problems and fluid-fluid linear acoustics problems. By using sixth-order approximations to the spatial derivatives in Maxwell's equations, the anisotropy in Yee's algorithm is essentially removed and the numerical phase velocity becomes nearly constant with respect to angle. This allows a larger number of points per wavelength and leads to smaller memory requirements when compared to Yee's algorithm. The drawbacks are that the 2-6 FDTD algorithm requires more computations per time step, and the boundary conditions are more difficult to implement. However, because the number of points per wavelength is smaller, less iterations are required than for the Yee algorithm in order to achieve the same accuracy. The boundary conditions are solved using a boundary image method and pseudo-transparent boundary equations (T. Deveze, L. Beaulieu, and W. Tabbara, AP-S 1992 and AP-S 1990 Symposium Digests). Results show that the 2-6 FDTD algorithm provides an accurate method to solve large problems in electromagnetics and in linear acoustics.

## A NEW FINITE-DIFFERENCE TIME-DOMAIN TECHNIQUE IN CURVILINEAR COORDINATES

J.E. Linder\* and K.T. Ng

ECE Department  
New Mexico State University  
Las Cruces, NM 88003

The finite-difference time-domain technique originally proposed by Yee has been used to calculate electromagnetic fields in various applications. The original Yee's algorithm only applies to a rectangular grid and curved boundaries need to be approximated by staircase geometries. In order to better model curved geometries, different investigators have extended Yee's algorithm to a boundary-conforming or curvilinear grid. Recently a new finite-difference algorithm based on the Lax-Wendroff technique has been developed for a rectangular grid (S. Omick, S. Castillo & R. Hills, AP-S Symposium, 1, 398-401, 1992). The Lax-Wendroff approach eliminates the offset E- and H-grids inherent in the Yee's algorithm, thus allowing 1) the explicit enforcement of boundary conditions and 2) the use of the flux-corrected-transport algorithm to reduce numerical dispersion and better model wide-band signals.

We have generalized the Lax-Wendroff finite-difference approach to model time-domain electromagnetics problems on a curvilinear grid, while maintaining the approach's advantages mentioned above. In addition, we have formulated a new absorbing boundary condition that is self-consistent with the Lax-Wendroff approach. Following the Lax-Wendroff technique and using the Maxwell's equations, the E-field (and similarly for the H-field) at the (n+1)th time step can be obtained from quantities at the nth time step by the following expression

$$\bar{E}(n+1) = \bar{E}(n) + \frac{\delta t}{\epsilon} (\nabla \times \bar{H}(n)) - \frac{\delta t^2}{2\mu\epsilon} (\nabla \times \nabla \times \bar{E}(n)) \quad (1)$$

where  $n$  and  $n+1$  indicate quantities at the different time steps and  $\delta t$  is the time step size. The above expression is for a homogeneous medium. A more complicated expression for an inhomogeneous medium has also been derived. Expressing the vector quantities and vector operations in (1) in a curvilinear coordinate system and approximating all the derivatives by finite-difference expressions then give the algebraic equations for updating the fields.

By manipulating the equations for updating field values, we have developed expressions or absorbing conditions for terminating the simulation region. These expressions are valid for general curved boundaries and arbitrary incident waves. Details on the new FDTD algorithm will be presented together with numerical results for different cases.

## ELIMINATION OF NUMERICAL DISPERSION IN FINITE-DIFFERENCE TIME-DOMAIN ALGORITHMS

Steven Omick<sup>\*</sup>  
Steven P. Castillo

Department of Electrical and Computer Engineering  
New Mexico State University  
Dept. 3-O, Box 30001  
Las Cruces, NM 88003

The numerical solution of Maxwell's equations in the time domain for transient excitations has application in several different areas. This includes very high speed digital circuits, lightning phenomena, nuclear generated electromagnetic pulse and wide-band radar. In most cases, the design engineer for a system is concerned about electromagnetic compatibility problems. Time-domain numerical analysis of electromagnetic problems has typically been done by a direct numerical integration of Maxwell's equations. Yee developed what is commonly known in the literature as the Finite-Difference Time-Domain (FDTD) method. Although many different finite difference techniques can be applied to the numerical solution of Maxwell's equations, it is Yee's algorithm that is commonly understood to be used when referring to FDTD methods in electromagnetics. The Yee FDTD method is used extensively for modeling time-domain electromagnetics problems because it is at the same time uncomplicated to implement and reasonably accurate. However, Yee's algorithm suffers from numerical dispersion. Second-order solution techniques or in general any even-order differencing schemes are not well suited for modeling steep wavefronts encountered in transient electromagnetic phenomena. When these types of incident waves are introduced into the computational domain, non-physical oscillations are generated due to the numerical dispersion produced by the integration scheme. These oscillations worsen as the solution proceeds and are more noticeable as the algorithm is pushed closer to the stability limit. The strength of the second-order integration scheme is in the ability to model the high gradients of the transient accurately.

In this paper, we present the Flux-Corrected Transport (FCT) method for eliminating dispersion in finite-difference time-domain algorithms. FCT was first developed in computational fluid mechanics for accurately modeling shock phenomena. We present results for both one-dimensional and three-dimensional solutions of Maxwell's equations using two different finite-difference algorithms. The first is a Lax-Wendroff algorithm which is used on a non-staggered grid. The second is the standard Yee algorithm on a staggered grid. A dispersion analysis will be given so that memory and cpu time savings can be quantified. Finally, results are given for a variety of three-dimensional propagation and coupling problems using transient excitations demonstrating the effectiveness of the FCT method.

## EVOLUTION OF TIME DOMAIN METHODS FOR ELECTROMAGNETIC FIELDS

*J.A. Murphy\* and D.P. Rowse*  
**BRITISH AEROSPACE PLC**  
*Sowerby Research Centre*  
**Filton, Bristol, BS12 7QW, U.K.**

*R. Mittra*  
**Electromagnetic Communication Lab**  
*University of Illinois*  
**Urbana, IL 61801**

### Abstract

Currently, a number of time domain approaches are available for RCS computation, estimation of radiation penetration and electromagnetic hazards, and modeling of antennas mounted on complex structures. Perhaps the most widely used time domain method is the uniform grid YEE/FDTD, which is numerically straightforward and computationally efficient. However, it does suffer from a lack of systematic procedure for the geometrical representation of complex bodies, inaccuracies due to staircasing and inability to handle special features on a complex body except via a patchwork type of approach. This is especially true for complex radar targets such as stealth aircrafts, and one finds that the conventional FDTD is severely limited in its application to such bodies.

The body-conforming FDTD approach has been considered as one method for addressing some of these issues. However, efficient and flexible grid generation for complex geometrical bodies is not a feature of this approach. Grid generation can be approached via the multi-block method, developed within the CFD community, but an enormous amount of effort is required to set up the grid. Also, the geometry of grid cannot be changed without a large amount of effort. An additional difficulty relates to singularities arising in the mesh for most geometries of interest and this limits the range of application of the method. The Chimera grid generation approach, which also hails from the CFD community, involves partially overlapping grids and areas of interpolation between grids that can lead to spurious radiation.

Unstructured grids and finite elements offers solutions to the problems of body-conforming grids, efficient grid generation, variable grid sizes, and special features (special elements). Although this has to be paid for in the form of increased computational requirements, it provides the ability to employ meshes only where they are needed. This is important for applications where geometry and spatial variations dominate the meshing rather than the wavelength. The increased computational requirements, associated with unstructured methods, is also partly offset by computer technology providing more balanced architectures and better price/performance ratios.

It is clear that a range of methods have to be used in electromagnetic design, with the chosen method being dictated by the application and the objectives of the modeling. These issues are demonstrated in the paper with examples.

## A COMPARISON OF THE PROPERTIES OF RADIATING BOUNDARY CONDITIONS IN THE FDTD METHOD FOR ANTENNA AND WAVEGUIDE ANALYSIS

C. J. Railton\* and E. M. Daniel

Centre for Communications Research, Faculty of Engineering  
University of Bristol, Bristol,  
England BS8 1TR

The availability of effective radiating boundary conditions (RBCs) for use with the Finite Difference Time Domain (FDTD) method is essential for the efficient application of the technique to scattering, radiation and planar circuit analysis problems. Nevertheless a considerable amount of confusion still exists amongst practitioners of FDTD as to which of the many available published RBC algorithms is the best for a given practical analysis problem. Indeed, the writers of many commercially available FDTD codes take the view that second order RBCs actually yield no benefit over the simpler first order RBC when used in the near field of a scatterer or an antenna. Moreover, the majority of published analyses of the behaviour of various RBCs are restricted to the case of plane wave incidence and infinitely fine discretisation, situations which never occur in practice. In this contribution we present a systematic theoretical and numerical comparison of several published RBC algorithms when used in a variety of practical FDTD analysis problems. These include radiation and scattering problems both under the usual situation where the RBC is placed in the near field of the sources as well as the situation where the RBC is placed in the far field. The effect of varying the distance between the RBC and the sources is investigated by means of both a theoretical analysis and numerical tests. In addition the effect of varying the unit cell size and of using non-uniform gridding is demonstrated. We analyse the use of RBCs in waveguide analysis problems, including open planar waveguides where RBCs are required at boundary planes which are both perpendicular and parallel to the direction of propagation and where the material properties are not constant across the boundary. As well as the performance of the RBCs, their computational requirements are compared. The RBCs tested are the popular first and second order RBCs of Mur (G. Mur "Absorbing Boundary Conditions for the Finite Difference Approximation of the Time-Domain Electromagnetic-Field Equations" IEEE Trans EMC-23 pp 377-382 Nov 1981), the second order RBC of Higdon (R. L. Higdon "Numerical Absorbing Boundary Conditions for the Wave Equation" Math. Comp. vol 49 pp 65-91 July 1987) and the super-absorbing correction (SAC) applied to the first order RBC (K.K. Mei and J. Fang "Superabsorption - A method to improve Absorbing Boundary Conditions" IEEE Trans AP-40 September 1992 pp 1001-1010). In addition the use of the Poynting vector in order to optimise the parameters of a first order RBC eg. (C. L. Britt "Solution of Electromagnetic Scattering Problems using Time Domain Techniques" IEEE Trans MTT-37 pp 1181-1192 Sept 1989) is considered.

We demonstrate that in all the above mentioned cases the use of second order RBCs does give a substantial improvement over first order RBCs, usually of the order of 7dB. We show for scattering and radiation problems where the RBC is in the near field of the sources that all the second order RBCs tested perform almost identically. In particular, for Higdon's RBC which allows the parameters to be chosen so that incident plane waves of chosen angles are perfectly absorbed, in the near field performance is virtually independent of the choice of parameters. The choice of RBC, therefore, depends on the algorithm which requires the least computer resources which in this case is the SAC. For the case of waveguide termination or for scattering problems in which the boundary is placed in the far field, Higdon's RBC gives the best overall absorption, especially if the discretisation is coarse. In addition the parameters can be chosen for optimum results and variations in material parameters across the boundary causes little difficulty. This algorithm does, however, demand somewhat more computation than the SAC.

## A UNIFIED APPROACH TO THE EFFICIENT TREATMENT OF GEOMETRICAL DETAIL IN THE FDTD METHOD

C. J. Railton

Centre for Communications Research, Faculty of Engineering  
University of Bristol, Bristol,  
England BS8 1TR

The Finite Difference Time Domain (FDTD) method, implemented in Cartesian coordinates, is well proven as an efficient technique for the electromagnetic analysis of a wide variety of microwave structures. The standard FDTD method is, however, less efficient if the structure under investigation has electrically small detail or has boundaries which are not parallel to the coordinate axes. Such structures abound in the application areas of planar circuits, antennas, microwave and RF heating for food processing or therapeutic hyperthermia. Techniques designed to address these difficult structures such as staircasing, the use of locally or globally deformed grids, graded grids, sub-gridding schemes or the use of non-orthogonal coordinate systems have been reported but these impose a penalty in computational effort, accuracy or flexibility. In this contribution, an alternative technique is described whereby the standard Cartesian grid is maintained, and the existence of the material boundaries is accounted for by the use of special Finite Difference equations for the affected nodes. These equations take account not only of the positions of the boundaries but also of the asymptotic field behaviour in their vicinity. This technique results in a flexible, accurate and efficient implementation which is applicable to a wide range of structures.

The overall philosophy of the method is as follows. Having divided the computational domain into a Cartesian grid whose unit cell size is chosen purely on the basis of the wavelengths of interest, we examine the material inside each cell. The fields within a cell are approximated by means of functions  $f_1(x,z)$  and  $f_2(x,z)$  as exemplified in equation (1). The values of the four unknown coefficients,  $k_i$ , are calculated using the four known field values on the perimeter of the cell. If the cell contains only one type of material then we choose  $f_1(x,z) = z$  and  $f_2(x,z) = x$  yielding the standard FDTD approximation. For cells which contain two types of material such as shown in Figure 1, we choose functions appropriate to the type of boundary. Application of this technique leads to modified coefficients in the FD equation for the affected nodes. These coefficients are calculated once prior to the start of the FDTD iterations, the speed of the FDTD run being unaffected.

We shall demonstrate that the use of this technique yields simple and efficient implementations of FDTD for cases including curved metal edges, curved solid metal and dielectric bodies and complex biological materials and allows the range of problems amenable to accurate FDTD analysis using modest computer power to be greatly increased.

$$\begin{aligned}
 E_x &= k_1 f_1(x,z) + k_2 \\
 E_z &= k_3 f_2(x,z) + k_4 \\
 \frac{\partial H_y}{\partial t} &= \frac{\delta t}{\mu} \left( k_1 \frac{\partial f_1(\delta x/2, \delta z/2)}{\partial z} - k_3 \frac{\partial f_2(\delta x/2, \delta z/2)}{\partial x} \right)
 \end{aligned} \tag{1}$$

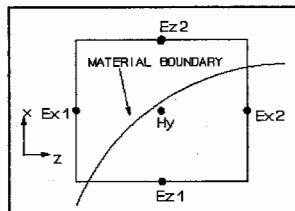


Figure 1 - FDTD cell with two material types.

A HYBRID FD-TD/SPECTRAL METHOD  
FOR THE ELECTROMAGNETIC ANALYSIS  
OF PERIODIC STRUCTURES

A. Cangellaris<sup>†\*</sup>, M. Gribbons<sup>†</sup>, and G. Sohos<sup>‡</sup>

Department of Electrical and Computer Engineering<sup>†</sup>

Program in Applied Mathematics, Mathematics Department<sup>‡</sup>

University of Arizona, Tucson, AZ 85721

This paper presents a hybrid FD-TD/spectral method developed for the efficient electromagnetic analysis of periodic structures of high complexity. More specifically, the proposed method is aimed at the computationally efficient extraction of the propagation characteristics of electromagnetic waves in two- and three-dimensional, non-homogeneous, anisotropic geometries which are periodic in one or two dimensions. In addition to their slow-wave and filter characteristics, recent applications of periodic dielectric structures for integrated optics purposes include, distributed feedback lasers, distributed Bragg reflection lasers, and quasi-phase-matched second-harmonic generation.

A brief summary of the proposed method follows. The spatial and temporal discretization of Maxwell's time-dependent curl equations over a single cell of the periodic structure is essentially performed according to the standard FD-TD method except for the following modification. Utilizing the pseudo-periodic character of the fields, Fourier series representations are used for the calculation of the spatial derivatives of all field components along the axes of periodicity of the structure. In other words, the derivatives along the axes of periodicity of the structure are computed *spectrally* at each time step utilizing standard FFT routines. This way, not only are the periodic boundary conditions enforced exactly but some of the spatial derivatives are calculated with exponential accuracy characteristic of spectral methods. Since, the propagation constant needs to be assumed known for the calculation of the Floquet expansions, the frequency becomes the eigenvalue quantity and is obtained from the solution of the hyperbolic system as an initial value problem.

The details of the mathematical formulation along with the modifications of the FD-TD lattice which are necessary for the correct implementation of the spectrally calculated derivatives will be presented. The numerical stability of the method will be discussed. In order to demonstrate the validity of the method and examine its accuracy, results will be presented from the electromagnetic analysis of periodically segmented slab waveguides and other types of periodic structures that can be analyzed using different analytical and/or numerical methods.

## A HYBRID TDFV/FDTD TECHNIQUE FOR RADIATION AND SCATTERING FROM SURFACE/WIRE STRUCTURES

Michael A. Jensen\* and Yahya Rahmat-Samii

Department of Electrical Engineering  
University of California, Los Angeles  
Los Angeles, CA 90024-1594

The rapid increases in available computing capabilities coupled with the development of sophisticated numerical differential equation solving algorithms has facilitated the solution of larger, more complex electromagnetic scattering and radiation problems. When implemented in the time-domain, these numerical techniques allow characterization of arbitrarily shaped objects for both single frequency and wideband illumination or excitation. Two such methods, the time-domain finite-volume (TDFV) and the finite-difference time-domain (FDTD) algorithms, are receiving considerable attention as viable solution techniques for complex radiation and scattering problems.

This work demonstrates the implementation of a hybrid TDFV and FDTD methodology which exploits the advantages of each algorithm. The TDFV technique, derived from established computational fluid dynamics methods, employs a characteristics-based Lax-Wendroff explicit scheme to solve Maxwell's equations in conservation law form. The use of upwinding in the difference equations makes this algorithm particularly well-suited to multi-layer problems and to geometries where grid multizoning can be used appropriately to reduce the computational complexity. Furthermore, because the technique is formulated for use with nonorthogonal body-fitted coordinates, it allows accurate representation of arbitrarily shaped objects. The more common FDTD method employs the well-known centered difference to approximate differentiation in Maxwell's equations, providing computational simplicity and increased accuracy when applied in homogeneous regions. When implemented with appropriate modifications, this technique allows improved modeling of certain fine structures such as wires. By properly joining the computational grids associated with each technique, these two algorithms may be successfully combined to allow analysis of complex objects consisting of multiple layers and wires.

The key features of both the TDFV and FDTD techniques will be summarized, and some examples will be presented to illustrate their performance for both radiation and scattering. The details of the hybrid TDFV and FDTD methodology and its application to radiation and scattering problems will be discussed, with particular emphasis being placed on the proper joining of computational grids. To illustrate the accuracy of the hybrid method, its performance in predicting the radiated and scattered fields for several canonical problems will be demonstrated. Other examples of its application to more complicated surface/wire structures will show the power and flexibility of the hybrid TDFV/FDTD algorithm.

## ENHANCEMENTS TO THE TSAR MODELING SYSTEM

Douglas J. Riley \*  
Sandia National Laboratory  
Department 9352  
Albuquerque, NM 87185

Steve Pennock  
Lawrence Livermore National  
Laboratory, L-156  
Livermore, CA 94551

### ABSTRACT

The Temporal Scattering and Response (TSAR) software has been under development at Lawrence Livermore National Laboratory, universities, and other national laboratories since 1987, with limited external distribution and use beginning in 1991. TSAR is an orthogonal-cell code based upon the Yee formulation. New features are continually being added in an effort to make it one of the most comprehensive FDTD codes available. New features include:

- 1) Thin-wire modeling. Three-dimensional arrangements of wires with narrow radii may be analyzed for input admittance and/or radiation characteristics. The wires may possess lumped or distributed loading.
- 2) Thin-slot capabilities. Slots that are narrow both in width and depth with regard to the spatial cell may be analyzed. Lossy internal gaskets and dispersive wall losses can be accommodated.
- 3) Dispersive media. Volumetric regions of dispersive material can be analyzed, allowing transient modeling of optical and semiconductor materials and devices.
- 4) Near-to-far-field transformations. Transient far-field results for various look angles and/or angular patterns for specified frequencies can be obtained.
- 5) Non-uniform multilayer analysis. A locally non-uniform mesh may be embedded within the standard mesh for analysis of complex multilayer environments consisting of electric, magnetic, and conducting materials.
- 6) Waveguide mode drivers. For waveguide-fed antenna modeling, spatial distributions of fields or currents can be specified, allowing selected modes to be driven.
- 7) Optimization on Cray YMP architectures. Extensive vector and parallel optimizations have been implemented that can provide performance well in excess of 1 GFLOP on YMP-8 class computers.
- 8) Movement to massively parallel architectures. Efforts are underway to optimize TSAR for massively parallel machines, such as the Intel iPSC/860 and the Kendall Square Research platform.
- 9) Output routines. Data can be output over planes or volumes for use with post-processors and data visualization tools.

The physics enhancements are included as new modules within the TSAR system and are activated by setting appropriate flags. Specific examples that demonstrate the capabilities and limitations of these features are discussed.



## SCATTERING

Chairs: R. Kastner, Tel Aviv University; S.W. Lee, University of Illinois

Room: Modern Languages Building, Lecture Room 2      Time: 1:30-5:10

|      |  |    |
|------|--|----|
| 1:30 | LOCATIONS AND NUMBERS OF MULTIPOLE FIELD EXPANSION<br><i>Khaled A. Ibrahim*, James E. Richie, Marquette University</i>   | 70 |
| 1:50 | ON THE COMBINATION OF MMP AND MOM<br><i>Ch. Hafner, Swiss Federal Institute of Technology; X. Shen*, Syracuse University</i>   | 71 |
| 2:10 | ON THE VALUE OF ILL-CONDITIONED MATRICES FOR COMPUTATIONAL ELECTROMAGNETICS<br><i>Ch. Hafner, G. Klaus*, Swiss Federal Institute of Technology</i>   | 72 |
| 2:30 | SCATTERING IN LOSSY RECTANGULAR CAVITIES<br><i>J. Fröhlich*, G. Klaus, Swiss Federal Institute of Technology</i>   | 73 |
| 2:50 | MODELING THREE-DIMENSIONAL SCATTERING USING A NEW NONLINEAR APPROXIMATION<br><i>Tarek M. Habashy, Carlos Torres-Verdin, Schlumberger-Doll Research; Ross W. Groom, Queen's University</i>  | 74 |
| 3:10 | BREAK  |    |
| 3:30 | PHYSICAL OPTICS SOLUTION OF SCATTERING FROM FIBER-REINFORCEMENT LAMINATED COMPOSITES<br><i>Shyh-Kang Jeng*, Jin-Yi Chu, Ming-Shing Lin, National Taiwan University</i>   | 75 |
| 3:50 | PREDICTION OF HIGH FREQUENCY RCS BY AN EXTRAPOLATION TECHNIQUE<br><i>R. Mittra*, University of Illinois; D. Bouche, CEA/CESTA Laboratories</i>   | 76 |
| 4:10 | RCS EXTRAPOLATION USING NETWORK MODELS<br><i>John Stach*, Larry Heck, SRI International</i>  | 77 |
| 4:30 | TARGET DISCRIMINATION IN RESONANCE REGION<br><i>T. Lavenan*, IRESTE; D. Le Boulch, CELAR; J. Saillard, IRESTE</i>  | 78 |
| 4:50 | RESONANT ATTENUATION IN ELECTROMAGNETIC WAVE SCATTERING FROM CONDUCTING SPHERES AND ELONGATED OBJECTS<br><i>H. Uberall*, Catholic University of America; C.R. Schumacher, David Taylor Research Center; X.L. Bao, Catholic University of America</i> | 79 |

Mon. p.m.

## LOCATIONS AND NUMBERS OF MULTIPOLE FIELD EXPANSION

Khaled A. Ibrahim\*, James E. Richie

Department of Electrical Engineering and Computer Science

Marquette University ,Milwaukee , WI 53233

The Generalized Multipole Technique, GMT, is a numerical method for solving electromagnetic boundary value problems. The accuracy of the method hinges on the location and numbers of multipole sources placed at some distances away from the surface where the boundary conditions are enforced. More specifically, each distance is a judicious choice of source location that yields minimum error and is the subject of this paper.

Accurate results have been obtained using several different criteria and through trial and error. However, each method lacks a systematic way of obtaining varying parameters that would facilitate the search for minimum error. To achieve this, a criterion is used here similar to one used in coding and sampling theory of two dimensional signal processing. The goal is to have the domain subdivided into equal areas or spheres of influence where one multipole source is placed on each of them. For example, for a cylinder or a sphere, this can be achieved by employing what is called the packing and touching numbers of a sphere as the number of multipole sources,  $m$ , and sampling points,  $n$ , respectively. The packing number is the number of identical spheres that can be densely packed in a sphere while the touching number, also fondly known as the kissing number, is the number of spheres that can be placed around a sphere in such a way that they all touch. This criterion provides a variable sampling density over the surface of a sphere or cross section area of a cylinder. Addition and translation theorems are used to translate the sources from the origin to the desired locations which are automatically determined once  $m$  and  $n$  are chosen; hence, limiting the search parameters to  $m$  and  $n$  only. Thus, by varying  $m$  and  $n$  the minimum error on the boundary condition is obtained. However, the procedure requires solving both an underdetermined and overdetermined system of linear equations. This method readily demonstrates cases of oversampling obtained by this and other criteria.

Finally, qualitative relationships of  $m$ ,  $n$ , and  $k$  can be obtained for simple scattering structures. These findings will be extended to more complex scattering structures and media.

## On the Combination of MMP and MoM

Ch.Hafner  
Swiss Federal Institute of Technology  
CH-8092 Zurich, Switzerland

X.Shen\*  
Syracuse University

The Multiple Multipole (MMP) code for computational electromagnetics is based on the Generalized Multipole Technique (GMT). This technique is very close to the analytic solution. Thus, very accurate and reliable results can be obtained. If only multipole functions are used as basis functions, the method is inefficient for structures with a relatively large surface to volume ratio. Such structures can be handled much better with well-known MoM codes. Thus, it is natural to apply the basis functions that have been shown to be useful in MoM codes in the MMP code as well. Since in the GMT the field is expanded directly whereas the current density is expanded in the MoM, this requires a translation form MoM language into GMT language. Because of the relatively close relation between MoM and GMT, this translation and the implementation of 'MoM basis functions' in MMP is quite simple.

Of course, the extended MMP code can be used like a regular MoM code but this is not the goal. For improving the MMP results for structures with a relatively large surface to volume ratio one wants to use both classical MMP expansions and 'MoM basis functions' at the same time. Usually, relatively simple geometric rules are used to find appropriate MMP expansions. Similar rules have to be found for the combination of MMP expansions with 'MoM basis functions'. Moreover, the electromagnetic field of MMP expansions usually is smooth and continuous on the surface of a domain, whereas the field of rooftop and similar functions can even have singularities. This would destroy the ability of the MMP code to accurately compute not only the far and near field but also the field on the surface of a body. To avoid this problems, rooftop functions have to be moved a little bit away from the surface. Consequently they are no longer typical MoM basis functions representing surface currents.

Rooftop functions often are used in conjunction with the simple point matching technique. In this technique, only a part of the continuity equations of the field is used in certain matching points. The location of the matching points is closely related to the location of the rooftop functions. In the MMP code, the generalized (weighted) point matching technique with overdetermined systems of equations is implemented and usually all six continuity equations of the field on a dielectric surface (three boundary conditions on an ideal conductor) are applied. Thus, the matching points for the rooftop functions in the MMP code need to be different from the matching points in regular MoM codes.

## On the Value of Ill-Conditioned Matrices for Computational Electromagnetics

Ch.Hafner and G.Klaus\*  
Swiss Federal Institute of Technology  
CH-8092 Zurich, Switzerland

Numerical methods usually implicitly or explicitly lead to matrix equations to be solved by a computer. From studying such matrix equations from a purely numeric point of view, the condition number of a matrix has been considered to be a very useful measure. Algorithms for handling ill-conditioned matrices are more complicated and time or memory consuming than algorithms for well-conditioned matrices. Thus it seems reasonable to say that numerical methods are the better the better the condition of the matrix, i.e., the smaller the condition number is. The aim of this paper is to show that this statement is wrong and can prevent designers of numeric codes from finding an optimal code.

Most of the interesting problems to be solved in computational electromagnetics and in many other areas are far beyond the problems having a solid mathematical background. Nonetheless, very often useful numerical solutions can be obtained by methods taking advantage of some 'a priori' knowledge and physical rather than mathematical reasoning. This often leads to relatively ill-conditioned matrices but to much better solutions than methods with well-conditioned or even orthogonal matrices. One finds that increasing the condition number often allows to increase the accuracy of the results until a relatively large 'optimal' condition number is reached. This 'optimal' condition number depends on the algorithm applied for solving the matrix equation. Consequently, advanced algorithms allowing to handle relatively ill-conditioned matrices allow to obtain much more accurate solutions than well-known, simple algorithms.

To illustrate the statements given above, two examples are outlined. 1) The well-known Fourier analysis of time-dependent functions leads to orthogonal matrices with the optimal condition number one. In practical applications the convergence can be very bad. An 'intelligent' Fourier analysis using non-orthogonal basis functions and taking advantage of some 'a priori' knowledge is proposed. This method is much more complicated and leads to ill-conditioned matrices but much better results for many interesting applications. 2) Working with relatively ill-conditioned matrices is the most important point for the accuracy of the results obtained by the Multiple Multipole (MMP) code. For allowing to handle such matrices, the generalized (or weighted) point matching technique in conjunction with a Givens updating procedure and block-iterative techniques have been implemented. It is expected that recognizing the value of ill-conditioned matrices will allow to improve not only the MMP code but also many other codes as well.

## Scattering in lossy rectangular cavities

J. Fröhlich\*, G.Klaus  
Swiss Federal Institute of Technology  
CH-8092 Zuerich, Switzerland

For the calculation of the field distribution in a lossy rectangular cavity a modified "image charge principle" for electrodynamics can be applied. The field is expanded as an array of exciting image sources located at the points of reflection and oriented according to the rules of reflection.

Combining this approach with the MMP code (multiple multipole program) only two or three reflections need to be taken into account. The parameters of the image sources are calculated by the MMP code according to the boundary conditions. The discretization of the model is usually depending on the frequency and on the degree and order of the used multipole expansions. But in this case the expansions are all of the same degree and order as the source. So this aspect will not influence the degree of discretization up to high frequencies. Only the number of parameters and the overdetermination factor will determine the number of matching points. This is valid as long as the wavelength is in a defined range. For smaller wavelength there is a need to take more reflections into account or to increase the overdetermination factor.

This combined approach is now applied to the problem of "3-D scattering in cavities". The model is a lossy rectangular cavity with a scatterer and an excitation (multipole source) inside. The solution is found in two steps. First the scattering problem in free space is treated separately. The obtained solution is converted to a so-called "connection" which is a feature of the MMP code and is used as excitation in the lossy rectangular cavity. Now the reflections are taken into account and the "image scattering solutions" are matched on the boundaries of the cavity and the scatterer.

This method allows to calculate models with scatterers of complex shape. It is used to calculate the field distribution around and inside scatterers with different geometries and material properties. This is of interest for the simulation, comparison and valuation of different measurement setups in EMC applications or for the study of radio communication properties inside buildings.

## Modeling Three-Dimensional Scattering Using a New Nonlinear Approximation

Tarek M. Habashy\*, Carlos Torres-Verdín\*, and Ross W. Groom†

\* Schlumberger-Doll Research, Old Quarry Road, Ridgefield, CT 06877-4108

† Queen's University, Kingston, Ontario, K7L 3N6

The Born and Rytov approximations are widely used for solving scattering problems in acoustics, elastodynamics, electromagnetics and quantum mechanics. The Born approximation and the Born series were originally developed in connection with the solution of what is now known as the Lippmann-Schwinger integral equation that describes many-body scattering in quantum mechanics. It has come to denote any approximation of the integral equation of scattering in which the total field in the integral over the scattering volume is approximated by the field in the background medium. The Born approximation is also popular in inverse scattering since it renders the scattering equations linear with respect to the material properties.

Approximating the total internal electric field by the background field is reasonable as long as the conductivity contrast is not severe, the scatterer is not too large and the frequency is not too high. However, in many low-frequency geophysical applications, moderate and high conductivity contrasts coupled with relatively large scatterers cause both the amplitude and phase of the internal electric field to differ greatly from the background values. Limitations of the Born approximation in a homogeneous background medium can often be improved by an iterative approach, where the background medium is updated at each iteration. This approach, however, does not always converge rapidly, particularly for large contrasts or at high frequencies or when the scatterer is large. In electromagnetic problems, it is also less effective for TM (transverse magnetic) and hybrid polarizations than for TE (transverse electric).

In this paper we present new and relatively simple approximations for the internal electric field which largely account for the full scattering. These approximations are designed specifically to correct the magnitude of the internal electric field, improve the estimate of the phase of the scattered field, and introduce some of the cross-polarization effects due to scattering. With these approximations, we demonstrate how complex models can be constructed using simple building blocks such as rectangular prisms or cells of appropriate sizes. Furthermore, interactions between adjacent cells are incorporated by this formulation. Results for the new approximations are superior to those derived from the Born and Rytov approximations for conductivity contrasts over several orders of magnitude. These new approximations are generally much faster to compute than the full forward problem and are comparable in efficiency to the Born or Rytov approximations. At present, the new approximations are being applied to a variety of inverse and forward scattering problems in electromagnetics particularly with geophysical applications. The general concept may also be readily applied to scattering problems in other fields such as quantum mechanics, optics, ultrasonics and seismology.

PHYSICAL OPTICS SOLUTION OF SCATTERING  
FROM  
FIBER-REINFORCEMENT LAMINATED COMPOSITES

Shyh-Kang Jeng\*, Jin-Yi Chu and Ming-Shing Lin  
Department of Electrical Engineering  
National Taiwan University  
Taipei, Taiwan, ROC

The fiber-reinforcement laminated composite material has a high strength-to-weight ratio and is very popular in the structure of modern aircrafts. Its permittivity and conductivity are anisotropic, and must be described by tensors. Scattering from such material, however, has not been dealt with thoroughly, to the authors' knowledge.

In this research, we use the Physical Optics (PO) to evaluate the scattering from structures with such material. First, we apply the Stratton-Chu formula to express the scattered far field by the tangential fields on the target surface. Next, we approximately solve the tangential field on the target surface by treating the structure as a locally-flat multi-layered anisotropic slab at each point on the surface, just like other Physical Optics (PO) approaches. Solution of the reflection from such a one-dimensional structure is easily achieved by using the wave-transmission matrix method ( see M. S. Lin and C. H. Chen, "Plane-wave shielding properties of anisotropic laminated composites," to be published in IEEE Trans. Electromagn. Compat., February 1993 ).

In this presentation we will show the RCS of some simple shells made of the composite. Typical shapes are rectangular plates, circular tubes, and aircraft wings. Also exhibited will be the effects of adding some absorbing coating on the surface of composite. The case that both PEC and composite appear will be included, since in most modern aircrafts both metal and composite material are utilized. The developed code can be incorporated to some general-purpose high-frequency scattering code like McPTD. The formulas derived in this research can be also extended for the PO/SBR ( Physical Optics/Shooting and Bouncing Rays ) technique to include multiple reflection.

## PREDICTION OF HIGH FREQUENCY RCS BY AN EXTRAPOLATION TECHNIQUE

*R. Mittra\*† and D. Bouche††*

*\*EMC Laboratory, University of Illinois, Urbana, IL, U.S.A.*

*††CEA/CESTA Laboratories, Le Barp, France*

Asymptotic methods are widely used to compute the RCS of three-dimensional targets at high frequencies, owing to their abilities to provide considerable physical insight into the diffraction mechanisms, and predict the RCS at a reasonable computational cost. For many practical configurations, for example the corner of a polyhedron or the tip of an impedance cone, exact diffraction coefficients aren't available, and one frequently resorts to Physical Optics type of approximations to derive the needed diffraction coefficients. Unfortunately, however, the computational accuracies achieved by using such approximate diffraction coefficients are often woefully inadequate.

An alternative approach would be to employ a numerically rigorous procedure, e.g., the Method of Moments, to attack the problem. However, despite a dramatic improvement in the speed and storage capacity of computers in recent years, the practical size of the object that can be handled via the MoM approach is still on the order of about ten wavelengths or less. Moreover, a purely numerical approach does not provide a good physical understanding of the various mechanisms contributing to the scattering phenomena.

Given the complementary advantages of the asymptotic methods and numerically rigorous approaches, considerable effort has been devoted in the past to the task of combining them by using a hybrid technique, that attempts to retain the advantages of both. Most of these methods employ asymptotic currents on certain parts of the object, and derive the currents on the remaining parts by using the MoM. Though such a combinational technique has been found useful for a number of interesting geometries, the method is difficult to use for a truly 3D object, which may support asymptotic current distributions that can not be predicted accurately by using the available theories. The objective of this paper is to propose a novel technique that has been designed to circumvent this difficulty. The step-by-step procedure needed to implement this approach are as follows: (i) Compute the RCS of the object at the highest frequency practicable by using the MoM; (ii) Apply a signal processing procedure to the obtained current distribution and identify the principal contributors to the RCS; (iii) Deduce the ray path lengths, and extrapolate the frequency dependence of these contributions, via an asymptotic analysis; (iv) Determine the amplitudes of the same contributions from the MoM results derived previously; (v) Combine the results from the steps (iii) and (iv) above, and derive closed-form expressions for the diffracted field.

The paper will include several examples, including that of RCS computation of targets of polyhedral shapes, to illustrate the application of the high frequency extrapolation technique described above.

## RCS EXTRAPOLATION USING NETWORK MODELS

*John Stach\* and Larry Heck*

*SRI International*

*Menlo Park, CA 94025*

*(stach@sasha.sri.com, larry@updike.sri.com)*

In this paper, we demonstrate the use of sparse radar-cross-section (RCS) measurements to predict changes in the scattered fields due to changes in target and scattering geometries. In addition to extrapolating angle, polarization and frequency, we can also extrapolate target geometry. For example, we can measure scattering from a target on a support and extrapolate the data to the target alone. This paper adds optimal model-based extrapolation and filtering to previous work (Stach, ACES conference, March 1989, Monterey, CA).

We begin with a fully interacting network model based on wire elements whose initial impedances are computed by moment methods. The resulting admittance matrix is then used as an extrapolation constraint, which allows us to use sparse measurements to predict scattering that spans the range of possible scattering angles and polarizations. The extrapolation approach that will be discussed also provides insight into an optimal choice of measurements (Heck and Reeves, ICASSP, April 1993, Minneapolis, MN).

We can predict scattered field changes due to target geometry changes by (1) modifying the extrapolation filter to include target geometry changes, or (2) using inverse scattering to modify the network model. For the inverse scattering approach, we can modify an admittance matrix directly (Stach, AP-S conference, June 1989, San Jose, CA), or iteratively modify self-impedance terms (diagonal) of an impedance matrix. A modified admittance matrix is then used to predict RCS for new target geometries. An advantage of the iterative impedance approach is that the model changes can be forced to be physically meaningful.

We will demonstrate the use of these methods by numerically removing a wire (representing a target support) from a cylinder. We will use measured scattering from the cylinder with a protruding wire and a theoretical network model to predict the measured scattering from the cylinder alone.

Mon. p.m.

## TARGET DISCRIMINATION IN RESONANCE REGION

LAVENAN T.\*, LE BOULCH D.\*\*, SAILLARD J.\*

\* : Laboratoire S2HF, IRESTE - la Chantrerie - CP3003, 44087 NANTES Cedex 03

\*\* : Centre d'Electronique de l'ARMement (CELAR) - 35170 BRUZ

Targets' stealth in high frequency region of the spectrum, has been highly improved for the last years, that is prejudicial for identification or detection of illuminated objects. That's why, it seems interesting to study these phenomena at lower frequencies, and particularly in resonance region.

The time domain response of a target illuminated by an electromagnetic wave in a frequency band corresponding to the resonance region of the object, can be determined by the knowledge of the position of the singularities and associated residues of the transfert function, in the complex plane. The time domain behavior of the response can be estimated by a sum of damped sinusoids, each multiplied by its corresponding residue.

In the complex Laplace plane, the knowledge of the position of the singularities (or complex natural poles of resonance) can be a useful information in target discrimination. The problem is to extract these poles from the target's response, response either built by calculation, or measured by a radar system. In order to extract these singularities, several methods have been existing for years but their reliability is highly function of the signal to noise ratio S/N, and decreases with N.

I - The time domain response of an object, illuminated by an EM wave can be separated in three parts which are the reflection of the wave on the target's surface, the stationary state and finally the resonant state when the wave passed beyond the object and that no more excitation still remain. In this case, the currents on the surface oscillate freely and the total resultant field can then be expressed as a sum of damped sinusoids. Thus, in frequency domain, the transfert function of the object can be expressed as a sum of an entire function (representing the early time of the response) plus a serie of rationals  $\Sigma R_\alpha / (s - s_\alpha)$  where  $s_\alpha$  and  $R_\alpha$  are respectively the natural poles of resonance (CNR) and associated residues of the object. One can notice that the CNR  $s_\alpha = \alpha + j\omega_\alpha$  are independant to the aspect angle. The study has been made on a perfectly conducting sphere in order to find analytically the CNR and associated residues.

II - The discrimination of targets measured in the resonant region requires the extraction of these CNR from the target's response. One can approximate the transfer function by a rational function of two polynomials  $P/Q$  and determine the poles by calculating the roots of the denominator  $Q$ . It is obvious that the number of poles determined will depend on the degree N of the polynomial  $Q$ . Thus only the most typical poles of the response are able to be extracted and particularly those whom damping coefficients are low. The importance of this phenomenon has been studied on the response of a sphere and significant CNR of the target have been deduced. Degradation due to noise has also been pointed out.

III - One can notice that the position of the CNR in the complex plane, for very simple geometric conducting objects as spheres, spheroids or wires, can be represented under successive branches. The first branch is particularly important for the late time part of the response. It may then be judicious to concentrate information hold by these poles, in few invariants. We analytically describe the curve drawn by the poles of the first branch. We then obtain:

$$y = 10^8 \cdot \{x\} + \epsilon$$

where  $y$  represents the frequency of the complex pole  $\omega_\alpha$ , and  $x$  its damping coefficient  $\alpha_\alpha$ . This curve becomes a line in the log-log plane:

$$\log(y - \epsilon) = \alpha \cdot \log(\{x\}) + \beta$$

If one executes a transposition of the poles, obtained by approximation of the transfert function (by a rational approximant), from the complex Laplace plane to the log-log plane, it seems possible to determine three parameters  $\alpha$ ,  $\beta$  and  $\epsilon$ . These three parameters obtained by a linear regression on the lines drawn by the poles, depend on the object and on its shape, and allow us to identify the target (connected to this group of poles). The parameter  $\alpha$  is invariable with the geometry of the object and can lead to an identification of the target. Parameters  $\beta$  et  $\epsilon$  are linked to the size of the object. So, the determination of the values of these three parameters, allow us to discriminate targets of different sizes and shapes.

RESONANT ATTENUATION IN ELECTROMAGNETIC WAVE SCATTERING FROM CONDUCTING SPHERES AND ELONGATED OBJECTS

H. Uberall\*

Department of Physics, Catholic University of America  
Washington, DC 20064, and  
David Taylor Research Center, Annapolis, MD 21402-5067

C. R. Schumacher

David Taylor Research Center, Annapolis, MD 21402-5067

X. L. Bao

Department of Physics, Catholic University of America  
Washington, DC 20064

We study the resonant attenuation (as determined by the imaginary parts of the complex eigenfrequencies) of perfectly conducting elongated objects, namely spheroids, cylinders with flat ends, or cylinders with hemispherical endcaps, including the spherical limit of the latter. Complex resonance frequencies are obtained from the principle of phase matching of surface waves. For the case where these surface waves are generated by plane waves at broadside incidence, the simultaneous presence of cylindrical circumferential-wave resonances and of the resonances of meridionally-propagating surface waves is discussed.

For the TM and TE modes of perfectly conducting, hemispherically-endcapped finite-length cylinders, we have obtained numerically the complex resonance frequencies of surface waves, circumnavigating the object both along a meridional, or along a closed equatorial path (i.e. "circumferentially"). The results were compared with earlier results for prolate spheroids or flat-endcapped cylinders with the same aspect ratio, and physical reasons for the difference were discussed.

It was found that the imaginary parts of the complex resonance frequencies (i.e., the attenuations of the surface waves) corresponding to axial incidence when plotted in the frequency plane in units of  $ka$  ( $a$  being the diameter of the oblong object) are relatively independent of aspect ratio, while those of spheroids decrease with aspect ratio. Physically, this results from the fact that for the capped cylinder, radiation takes place at always the same hemispheres, while for the spheroids, the strongly curved area at the ends where most radiation occurs, shrinks with increasing aspect ratio.



## ANTENNA ARRAYS

Chairs: Y. Rahmat-Samii, University of California at Los Angeles  
 W.L. Stutzman, Virginia Polytechnic University

Room: Michigan League, Vandenberg Room      Time: 1:30-5:10

|      |   |    |
|------|---|----|
| 1:30 | BRAGG-MODULATED PHASE SPACE GTD FOR LINE-SOURCE-EXCITED INFINITE PLANE STRIP ARRAYS<br><i>E. Gago-Ribas, L.B. Felsen, Polytechnic University</i>  | 82 |
| 1:50 | RESONANT ANTENNA ARRAYS WITH PANCAKE-SHAPED FIELD PATTERNS<br><i>George Fikioris*, Ronald W.P. King, T.T. Wu, Harvard University</i>  | 83 |
| 2:10 | MULTIPORT CIRCUIT MODEL OF AN ANTENNA ARRAY IN AN OPEN QUASI-OPTICAL RESONATOR<br><i>P. Heron, G.P. Monahan, North Carolina State University; F.K. Schwering, CECOM; J.W. Mink, US Army Research Office; M.B. Steer*, North Carolina State University</i> | 84 |
| 2:30 | EXCITATION AND RADIATION PROPERTIES OF AZIMUTHAL MODES AND THEIR ARRAYS<br><i>L. Shafai*, University of Manitoba; M. Barakat, InfoMagnetics Technologies Corporation</i>  | 85 |
| 2:50 | RADIATION PATTERN SYNTHESIS FOR ARRAY ANTENNA WITH ULTRA-LOW SIDELOBE LEVEL<br><i>Yi Hong Qi, Southeast University; Yong Chang Jiao, Guo Xiang Song*, Xidian University; Wu Tu Wang, Xian Institute of Space Technology</i>                               | 86 |
| 3:10 | BREAK   |    |
| 3:30 | THEORETICAL AND EXPERIMENTAL ANALYSES OF MULTIPLE ANTENNAS ATTACHED TO COATED BODIES OF REVOLUTION<br><i>Y. Yuan*, J.A. Kong, Massachusetts Institute of Technology; P.S. Kao, R.T. Shin, MIT Lincoln Laboratory</i>                                      | 87 |
| 3:50 | NUMERICAL SYNTHESIS OF ARBITRARY DISCRETE ARRAYS<br><i>W.A. Swart, J.C. Olivier*, Potchefstroom University for CHE</i>  | 88 |
| 4:10 | ADAPTIVE BEAMFORMING USING A BACKPROPAGATION NEURAL NET<br><i>J.C. Olivier, Potchefstroom University for CHE</i>  | 89 |
| 4:30 | ON SIDELOBE LEVEL AND GAIN OF SOLID-STATE ACTIVE PHASED ARRAY WITH TOLERANCE AND FAILURE<br><i>Li Jianxin, Gao Tie, Nanjing Research Institute of Electronics Technology</i>  | 90 |
| 4:50 | A NEW MINIMAX METHOD FOR TOLERANCE OPTIMIZATION OF LOW SIDELOBE ARRAYS<br><i>Songxin Qi, Quanrang Yang, Southeast University</i>  | 91 |

**Bragg-Modulated Phase Space GTD for Line-Source-Excited  
Infinite Plane Strip Arrays**

by

E. Gago-Ribas, L.B. Felsen  
Electrical Engineering Dept./Weber Research Institute  
Polytechnic University  
Route 110, Farmingdale, NY 11735

The time-harmonic line-source Green's function for an infinite periodic array of coplanar conducting thin strips is formulated rigorously by a) space domain and b) spectral domain analysis. These alternative formulations are shown to be equivalent via the Poisson sum formula but they parametrize the solution in terms of different wave phenomena in the configuration-spectrum phase space. This becomes apparent when the formal spectral integrals for the scattered field are evaluated approximately by saddle point asymptotics to yield wave objects which are compact in the phase space and can be parametrized in terms of Bragg-modulated GTD: each intercepted ray field emanating from the source is reflected from, or transmitted through, the grating along distinct  $m$ -indexed reflected and transmitted rays whose angles of emergence  $\theta_m$  satisfy the Bragg (periodic structure) condition for plane wave reflection with the same direction of incidence and whose reflection-transmission coefficients bear the Bragg imprint. The corresponding map in the (space)-(angular spectrum) domain identifies those local regions on the array that are activated by the  $m$ th Bragg ray congruence, which is generated by its distinct caustic. Except for the  $m=0$  congruence whose caustic collapses to the source or image points, all  $m \neq 0$  caustics are tangent to the array plane at cutoff and approach an  $m$ -dependent limiting angle  $\hat{\theta}_m$  that defines the angular coverage of the  $m$ th congruence. A typical ray and caustic configuration is shown in Fig. 1 while several caustics for an array with period  $T=10\lambda$ ,  $\lambda$ =wavelength, are shown in Fig. 2 (for these conditions, Bragg rays  $-10 \leq m \leq 10$  propagate away from the array). The presentation contains details of the space and spectral domain asymptotics, the phase space interpretation that unifies both, and various characteristics of the Bragg ray parametrization aims.

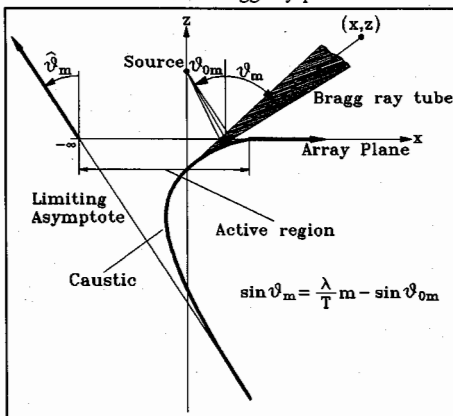


Figure 1

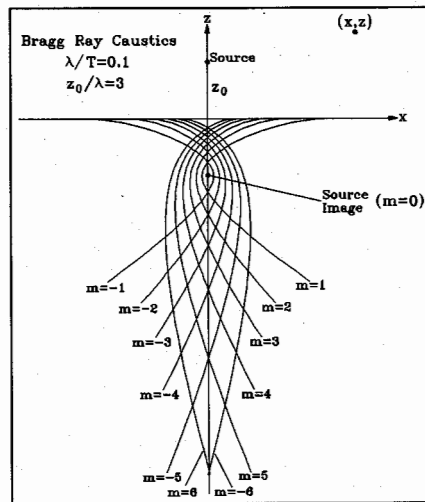


Figure 2

## RESONANT ANTENNA ARRAYS WITH PANCAKE-SHAPED FIELD PATTERNS

George Fikioris\*, Ronald W. P. King, and T. T. Wu  
Gordon McKay Laboratory, Harvard University, Cambridge, MA 02138

A novel antenna array with possible applications as a surface-wave launcher is described and analyzed. The antenna array consists of many vertical dipoles placed on a circle. Only two dipoles are driven; the rest are parasitic. When the frequency is varied, a number of narrow resonances occur in the array. At each resonance, the currents on all the dipoles become very large and nearly equal; the two driving-point reactances are zero. The field pattern at each resonance is omnidirectional in the horizontal plane and narrow in the vertical plane. The maximum radiation occurs at the plane  $\theta = \pi/2$  of the dipoles' centers so that the pattern has a pancake-like shape. Resonances associated with highly directive fields in the vertical plane can only occur if the many parameters of the problem (i.e., length and radius of the dipoles, number of elements, array diameter, and ratio of the two driving voltages) are properly chosen.

Recent theoretical and experimental studies have shown that properly dimensioned large circular arrays of dipoles may possess very narrow resonances associated with a vanishing driving-point reactance in the case where only one element is driven by a voltage  $V_1$ . The field patterns of resonant arrays with only one element driven do not have a pancake-like shape; they consist of many pencil-like beams.

This paper contains the theoretical analysis that leads to the choice of the number  $N$  of elements,  $n$  of the second driven element, and voltage ratio  $V_n/V_1$ , so that a pancake-shaped field pattern is generated while the property of zero driving-point reactance is preserved. The fact that only two elements are driven and that the two driving-point impedances are purely resistive eliminates the need for complicated feeding and matching networks.

# MUTLIPORT CIRCUIT MODEL OF AN ANTENNA ARRAY IN AN OPEN QUASI-OPTICAL RESONATOR

P. Heron<sup>†</sup>, G. P. Monahan<sup>†</sup>, F. K. Schwering<sup>◊</sup>, J. W. Mink<sup>†</sup>,  
and M. B. Steer<sup>†\*</sup>,

<sup>†</sup>High Frequency Electronics Laboratory, Department of Electrical and  
Computer Engineering, North Carolina State University, Raleigh, North  
Carolina 27695-7911.

<sup>◊</sup>CECOM, Attn. AMSEO-RD-C3-ST, Ft. Monmouth, New Jersey  
07703-5203.

<sup>‡</sup>U.S. Army Research Office, P.O. Box 12211, Research Triangle Park, North  
Carolina 27709-2211.

In a quasi-optical power combiner, Fig. 1, the output of many solid-state sources is efficiently and robustly combined. This is achieved as a result of the one-to-many coupling as the power radiated by a single element is reflected by the curved reflector on to many oscillators. The driving point impedance of each antenna is strongly effected by the presence of all other active antennas as well as by the mode structure and Q of the resonator. In this presentation the derivation of a field theoretic model describing the coupling is described. An impedance matrix is determined through use of the Lorentz reciprocity theorem and calculation of the aperture and conductor losses. A half space Green's function is used to incorporate the near-field effect of non quasi-optical fields. The result obtained can be used to impedance match each active source to its antenna and thus facilitate design of an efficient power combining system. As an example Fig. 2 shows the calculated and measured transimpedance of two antennas.

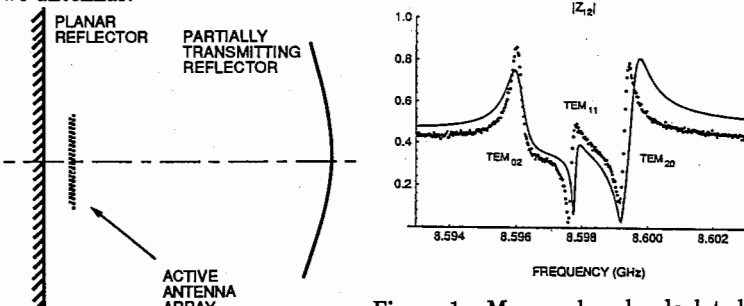


Figure 1. Cross-section of open cavity and transimpedance of cavity between two antenna ports.

## EXCITATION AND RADIATION PROPERTIES OF AZIMUTHAL MODES AND THEIR ARRAYS

L. Shafai\*

Department of Electrical and Computer Engineering  
University of Manitoba  
Winnipeg, Manitoba, Canada, R3T 2N2

M. Barakat

InfoMagnetics Technologies Corporation  
1329 Niakwa Road East  
Winnipeg, Manitoba, Canada, R2J 3T4

Properties of circular modes and their excitation in circular arrays have been known for some time and is discussed in literature (D.E.N. Davies, Chapter 12, the Handbook of Antenna Design, Vol. 2, Peter Peregrinus, 1983). In finite arrays their use facilitates the analysis and helps in design of excitation circuits, such as the Butler Matrix, to match the circuit impedance to each mode and to control the effect of mutual coupling. The latter is a rare property of the circular modes not common in linear arrays. However, because of the circular array configuration and their radiation pattern shape, their use has been limited mostly to specialized applications such as, the direction finding and null steering for navigational aids. In the communication area they have been used mostly in cylindrical arrays for broadcasting.

The concept of beam generation and scan using the azimuthal modes was recently extended to planar arrays (L. Shafai, Linear-Sum Mode Arrays and Beamforming, ANTEM'92, pp. 57-62, Winnipeg, August 5-7). In one example stacked microstrip disk antennas were used to generate the far fields of higher order  $TM_{n1}$  modes. It was shown that selecting N-azimuthal modes, for  $N=1,2,3\dots N$  can generate a pencil beam which tilts progressively towards the plane of the array by increasing the total number of azimuthal modes. A useful application of the concept for beam generation and scan in mobile communications was also described (L. Shafai, Antenna Candidates for Mobile Satellite Communications, Proc. of MM'92, pp. 255-260, Brighton, UK). The mode excitation was achieved by a symmetric geometry of multiarm spirals. This concept is now further investigated to shape the beam and scan in a three-dimensional space. Detail of the analysis and implementation of the concept for antenna designs will be discussed.

Radiation Pattern Synthesis for Array Antenna  
With Ultra-low Sidelobe Level

Yi Hong Qi

(Southeast University, Nanjing 210018, P.R.China)

Yong Chang Jiao Guo Xiang Song\*

(Xidian University, Xian 710071, P.R.China)

Wu Tu Wang

(Xian Inst. of Space Technology, Xian 710000, P.R.China)

Abstract

To eliminate the effects of noise signal, usually nulls are formed in the directions of noise source. For practical realization, there exist some difficulties in keeping the nulls at given directions. For example, within the bandwidth the positions of null will be different for different frequency point, and there are other factors that affect the positions of the null such as the tolerances of amplitudes, positions and phases of array elements. In this paper we consider the radiation pattern synthesis problem for array antenna with ultra-low sidelobe level region, the ultra-low sidelobe level region can be designed such that the noise source can always be included in this region, considering of the bandwidth and tolerance factors. Although this consideration can not totally eliminate the effect of noise signal, it can reduce this effect to a very low level, and the design is more reliable.

The problem is modelled by minimax method and is solved by newly constructed Regular Polyhedron Method (RPM). By forming a set of nulls in a limited region, a ultra-low sidelobe region is formed. The numbers and the positions of nulls can be optimized so that the ultra-low sidelobe level and the width of ultra-low sidelobe region are controlled to satisfy the given specification. In the other directions of the radiation pattern, the antenna pattern could be designed to approach to a desired pattern, for instance, Tayler radiation pattern or Chebyshev pattern. Computational results are presented, and different widths and sidelobes level in the ultra-low sidelobe level are resulted.

With draw

Mon. p.m.

## THEORETICAL AND EXPERIMENTAL ANALYSES OF MULTIPLE ANTENNAS ATTACHED TO COATED BODIES OF REVOLUTION

Y. Yuan\* and J. A. Kong  
Research Laboratory of Electronics  
Massachusetts Institute of Technology  
Cambridge, MA 02139

P. S. Kao and R. T. Shin  
MIT Lincoln Laboratory  
Lexington, MA 02173

This paper presents theoretical modeling and experimental measurements for the radiation and scattering properties of multiple wire antennas protruding from an arbitrarily shaped body of revolution (BOR). The BORs can either be perfectly conducting or partially penetrable. The wire antenna is driven by a coaxial line whose inner conductor and dielectric pierce the surface of the BOR while its outer connector is connected to it.

For numerical modeling, an integral equation/moment method formulation based on the equivalence principle is developed and applied to the structures. The formulation incorporates a rigorous model of the antenna feeding structure to properly account for the effects of layered coatings, antenna mutual couplings, and impedance loadings. The electromagnetic modeling is then divided into separate exterior and interior problems. The exterior problem consists of wire antennas/BOR with the coaxial feed replaced by a perfect conductor and an aperture magnetic current, while the interior problem consists of a coaxial line terminated by a complex voltage generator and/or load impedance at one end and short-circuited with an aperture magnetic current at the BOR surface. These two regions are connected through the aperture magnetic current.

Experimental measurements on various radiation and scattering properties were carried out for several test cases. Computational codes for the above theoretical formulations were validated with the experimental results. The test model is a cylindrical body whose height and diameter are 12 inches and 6 inches, respectively. On the surface of the body, monopole antennas (active and/or passive) can be mounted at various positions, and rotationally symmetric coatings can also be placed arbitrarily along the body axis. The validated radiation and scattering properties include input impedance, antenna gain, mutual couplings and radiation patterns, and the backscatter cross section of the antenna/BOR as a function of antenna load impedance. The effects of various dielectric coatings on the radiation and scattering properties were also investigated.

## NUMERICAL SYNTHESIS OF ARBITRARY DISCRETE ARRAYS

W.A. SWART AND J.C. OLIVIER\*  
DEPARTMENT OF ELECTRICAL ENGINEERING  
POTCHEFSTROOM UNIVERSITY FOR CHE  
P.O. BOX X6001  
POTCHEFSTROOM  
2520  
SOUTH AFRICA

A new algorithm for the synthesis of arbitrary discrete arrays is given. The method is based on a synthesis method developed by Olen and Compton [IEEE APS Vol. 38, No. 10, October 1990]. The technique uses adaptive array theory. A large number of artificial interference signals are assumed to be incident on the array. The new technique uses a different recursion equation to update the amplitudes of the artificial interference signals. It is shown that the new algorithm is able to arrive at the desired radiation pattern in a significantly reduced number of iteration steps when compared to the technique referred to above.

The technique is not a function of the type of elements used in the array, nor of the placement of the elements. Furthermore the desired radiation pattern specification may be arbitrary. If it is not attainable due to the array size being too small or poor placement of the array elements, the method will find a best or optimum solution. Hence the algorithm may be used to synthesise a conformal array which has been a difficult synthesis problem. In the special case of a linear equispaced array of isotropic elements and uniform sidelobe specification, the algorithm will converge to the classic Dolph-Chebyshev solution.

The paper will present the algorithm and extensive numerical results to indicate the validity of the new approach.

## ADAPTIVE BEAMFORMING USING A BACKPROPAGATION NEURAL NET

J.C. OLIVIER  
DEPARTMENT OF ELECTRICAL ENGINEERING  
POTCHEFSTROOM UNIVERSITY FOR CHE  
P.O. BOX X6001  
POTCHEFSTROOM  
2520  
SOUTH AFRICA

Adaptive beamforming requires the weights of an adaptive array to be updated in real time in response to a rapid time varying signal environment. Traditionally the weights of the adaptive array is computed using a digital implementation of the Widrow LMS algorithm. Digital implementation is however costly and the speed of the weight update cycle is limited by the digital processor clock rate.

Recent trends are toward analog implementation so that the real time processing requirement may be met. Neural network processors may be implemented using analog hardware and use a relatively small amount of hardware. Several neural network architectures exist. Recently the Hopfield type neural network has been used for processing a 10 element adaptive array [P-R Chang, W-H Yang and K-K Chan, IEEE APS VOL. 40, NO. 3, March 1992]. The Hopfield neural net however requires a convergence time of the order of the circuit RC time constant, and in addition the interconnection strengths between neurons are dependant on the desired and interference signal incident angles.

This paper will present an alternative approach to the Hopfield type neural net array processor, namely the backpropagation feedforward neural network array processor. The backpropagation neural net is trained prior to being used to process the adaptive array. The training procedure uses the optimal weight vectors (often referred to as the Wiener weights) as a training set. The neural net is able to generalize when confronted with situation that it has not been trained for. When used to control the adaptive array it is used in its feedforward mode, and it will therefore require no convergence time as the Hopfield net. The total delay time is simply the circuit delay time and is a function of the quality of the components used.

In addition to the proposed algorithm, the paper will present numerical results to indicate the versatility and accuracy of the neural network adaptive array processor.

## On Sidelobe Level And Gain of Solid-State Active Phased Array With Tolerance And Failure

Li Jianxin and Gao Tie

Nanjing Research Institute of Electronics Technology

P.O.Box 1315-403, Nanjing, 210013, P.R.China

**ABSTRACT** Since 1970 many active phased arrays using solid-state T / R (transmit / receive) modules have been developed. Comparing with passive phased arrays, solid-state active ones have much more advantages. However, many random errors, such as amplitude and phase errors, could give rise to sidelobe degradations and gain drop of active array antennas. In addition, elements' (or T / R modules') failures will also make antenna pattern worse. This paper mainly studies pattern statistic characteristics and discusses effects of elements' (or T / R modules') failures, amplitude and phase errors (including independent and correlative ones) on sidelobe level and gain in solid-state actived phased array antennas which transmitting sidelobes are low. With the help of probability statistic principle, the formulas are drived to estimate sidelobe degradations and gain drop of antennas. Also, the comparisons between estimations and simulations are given. The theoretical results are in good agreement with the simulated ones. In the following figures, a  $60 \times 30$  solid-state active array is analysed. Its aperture distribution is synthesised by multi-step amplitude quantization density weighting method, and the designed sidelobe levels of horizontal and vertical planes are  $-35.5\text{dB}$  and  $-29.2\text{dB}$  respectively. Fig.1 shows the PSLLs' probability curves of horizontal (left) and vertical (right) planes with indepedent amplitude-phase RMS errors 0.04, correlative ones 0.03, and failure probability 6 percent. In Fig.2, the gain drop is plotted versus the T / R module failure with amplitude and phase variance as parameter.

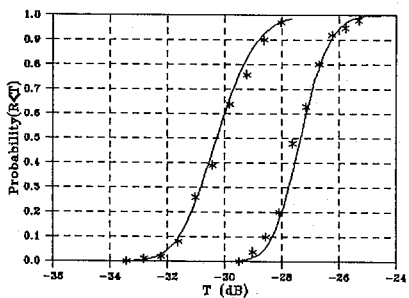


**Fig.1** Cumulative probability curves for sidelobe degradation estimates. The solid lines and astrisk represent theoretical and simulated results respectively.

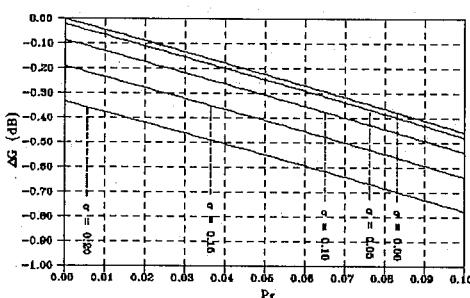


**Fig.2** Gain drop as function of T/R module failure with different amplitude and phase variance as parameter.

## A New Minimax Method For Tolerance Optimization of Low Sidelobe Arrays

Songxin Qi Quanrang Yang  
State Key Laboratory of Millimeter Waves  
Southeast University,210018,P.R.China

### ABSTRACT

In this paper, the principle of Maximum-Entropy is first introduced to develope a new efficient method to slove the tolerance optimization problems of low sidelobe arrays. With the method, the deviations of antenna actual performance from its desired one are minimized, while the design parameters deviate from its nominal values. Test results show that the new method makes the optimization process much simple and easy, meanwhile a considerable saving in CPU time and memory is obtained.



**SPECIAL SESSION AP-S/URSI B-6****MONDAY PM****ARTIFICIALLY SOFT AND HARD SURFACES FOR ELECTROMAGNETIC WAVES  
AND THEIR APPLICATIONS**

Chairs: P.S. Kildal, Chalmers University of Technology  
D. Schaubert, University of Massachusetts

Room: Michigan League, Hussey Room      Time: 3:30-5:10

|      |  |      |
|------|--|------|
| 3:30 | THICK SOLID BLOCKAGE-FREE STRUTS REALISED BY USING A HARD SURFACE<br><i>Per-Simon Kildal*, Chalmers University of Technology; Ahmed Kishk, University of Mississippi; Keyvan Forooraghi, Chalmers University of Technology</i> | AP-S |
| 3:50 | ANALYSIS OF SOFT AND HARD SURFACES USING A HYBRID FEM/FLOQUET'S MODE TECHNIQUE<br><i>M. Calamia, R. Cocciali, A. Freni, G. Pelosi*, University of Florence</i>   | AP-S |
| 4:10 | PROPERTIES OF WAVES GUIDED BETWEEN PARALLEL, ARTIFICIALLY HARD SURFACES<br><i>Jon Anders Aas, The University of Trondheim</i>  | AP-S |
| 4:30 | ANALYSIS OF CORRUGATED SOFT EDGES TO REDUCE SCATTERING FROM GAPS BETWEEN REFLECTING PANELS<br><i>Jan Carlsson*, Swedish National Testing and Research Institute; Per-Simon Kildal, Chalmers University of Technology</i>       | AP-S |
| 4:50 | INCREMENTAL DIFFRACTION COEFFICIENTS FOR ARTIFICIALLY SOFT AND HARD BOUNDARY CONDITIONS<br><i>R. Tiberio*, S. Maci, A. Toccafondi, University of Florence</i>  | 94   |

## INCREMENTAL DIFFRACTION COEFFICIENTS FOR ARTIFICIALLY SOFT AND HARD BOUNDARY CONDITIONS

*R. Tiberio\*, S. Maci, A. Toccafondi*

*Department of Electronic Engineering, University of Florence,  
via S. Marta 3, 50139, Florence, Italy.*

An accurate control of the characteristics of the radiating components of high-performance antenna systems is important in electromagnetics engineering applications. To this end, undesired scattering mechanisms may be reduced by conveniently shaping the scattering surfaces, as well as by modifying their boundary conditions (b. c.). Recently, it has been suggested that suitable combinations of corrugations and dielectric loadings may be usefully employed to devise configurations that exhibits artificially soft and hard b.c.. Also, it has been shown that the systematic use of this technology may provide effective tools to control the sidelobe level and cross-polar components of radiation patterns.

Within this framework, on one hand investigating on the characteristics of suitable periodic configurations is of interest to obtain a more complete representation of the actual b.c.. On the other hand an accurate description of diffracting mechanisms at edge discontinuities is of importance for an exhaustive examination of the polarization effects.

An Incremental Theory of Diffraction (ITD) has been developed which provides a unified framework for describing high-frequency scattering phenomena. This method is based on the appropriate use of local canonical problems, that have a uniform cylindrical configuration with arbitrary cross-section. So far, explicit expressions have been obtained for wedge shaped configurations with perfectly conducting b.c. (p.e.c.). In this paper, the procedure is extended to treat the scattering at the edge of a wedge with artificially soft and hard b.c. on one face and p.e.c. b.c. on the other face. A generalized localization process is applied to the cylindrical canonical configuration, to find the pertinent incremental diffracted field contributions.

High-frequency, dyadic expressions are obtained for the incremental diffraction coefficients, that provide the basic tool to treat the scattering at actual edges of configurations of practical interest. The solution explicitly satisfies reciprocity and the local b.c.. Thus, this procedure yields a representation of the field which is uniformly valid at any incidence and observation aspects, including caustics of the corresponding ray-field description.

**SESSION URSI D-2****MONDAY PM****OPTO-ELECTRONIC DEVICES AND SYSTEMS**

Chairs: J.W. Mink, US Army Research Office; R.C. Compton, Cornell University

Room: Michigan League, Michigan Room Time: 1:30-5:10

|      |  |     |
|------|--|-----|
| 1:30 | OPTICAL ILLUMINATION OF SERIES INTEGRATED RESONANT TUNNELING DIODES<br><i>Olga Boric-Lubecke, Tatsuo Itoh, University of California, Los Angeles</i>   | 96  |
| 1:50 | OPTICAL-BIAS-CONTROLLED AND TEMPERATURE-STABILIZED ELECTRIC FIELD SENSOR USING MACH-ZEHNDER INTERFEROMETER<br><i>Nobuo Kuwabara*, NTT Telecommunication Networks Laboratories; Ryuichi Kobayashi, University of Electro Communications</i> | 97  |
| 2:10 | ABRUPT COUPLING BETWEEN DIELECTRIC CYLINDRICAL CIRCULAR FIBERS<br><i>Tam Do-Nhat, Waterloo, Canada</i>   | 98  |
| 2:30 | COUPLING BETWEEN GAUSSIAN BEAMS AND DIELECTRIC CYLINDRICAL CIRCULAR FIBERS<br><i>Tam Do-Nhat, Waterloo, Canada</i>   | 99  |
| 2:50 | VECTOR FINITE ELEMENT ANALYSIS OF LOSSY OPTICAL FIBERS<br><i>Jin-Fa Lee*, Arthur J. Butler, Worcester Polytechnic Institute</i>  | 100 |
| 3:10 | BREAK  |     |
| 3:30 | ANALYSIS OF FUSED TAPERED OPTICAL FIBER COUPLERS WITH ASYMMETRICAL STRUCTURE<br><i>Hung-chun Chang*, Ting-Huei Lin, National Taiwan University</i>   | 101 |
| 3:50 | OPTIMIZATION OF TRAPEZOIDAL GRATINGS FOR DFB AND DBR LASERS<br><i>M.H. Rahnavard, A. Bakhtazad, H. Sarmadi, H. Abiri, Shiraz University</i>  | 102 |
| 4:10 | SYSTEM RESPONSE OF SEMICONDUCTOR PANEL TO LINEARLY GRADED MOVING RECTANGULAR SPOT ILLUMINATION AND ITS USE AS MILLIMETER WAVE IMAGE CONVERTOR<br><i>M.H. Rahnavard, A. Bakhtazad, Shiraz University</i>                                    | 103 |
| 4:30 | COMPARISON OF THREE QUASI-TEM MODELS FOR DETERMINING OPTICALLY INDUCED LOSSES IN COPLANAR WAVEGUIDES ON SEMICONDUCTOR<br><i>Zhong Liang Sun, Ao Sheng Rong, Southeast University</i>   | 104 |
| 4:50 | NUMERICALLY EFFICIENT NONUNIFORM MODEL FOR MMW OPTICALLY CONTROLLED DIELECTRIC WAVEGUIDE PHASE SHIFTERS<br><i>Ao Sheng Rong, Zhong Liang Sun, Southeast University</i>   | 105 |

## Optical Illumination of Series Integrated Resonant Tunneling Diodes

Olga Boric-Lubecke and Tatsuo Itoh  
*University of California, Los Angeles*  
*School of Engineering and Applied Science*  
*Electrical Engineering Department*  
*405 Hilgard Av.*  
*Los Angeles, CA 90024*

Excitation condition for the oscillator with several resonant tunneling diodes integrated in series is very hard to achieve. There is a need for a very fast turn-on bias voltage, in picosecond range for GHz oscillator. If turn-on is not fast enough, bias cannot be equally devided among the diodes if they are all to be biased in negative differential resistance (NDR) region.

We propose optical illumination of the device instead of biasing it with the very fast pulse. Under illumination, extra carriers will be generated in the depletion region. First, we need to apply total amount of desired bias on the series connection, which initially will not be equally devided. After that we illuminate the device, so that extra carriers generated in the depletion region reduce or overcome negative differential resistance. If NDR is overcomed, bias voltage would be devided equally, provided diodes are simillar.

We have done a preliminary experiment to investigate the change of I-V characteristic under illumination. Experiment was done on InP diode grown at UCLA. We observed small encrease in current at both the peak and the valley of the I-V (change at the peak was 1.62 mA, and at the valley 1.68 mA, which was about 2% at the peak and 4% at the valley). Voltage drop across the diode decreased under illumination by 10 mV at both the peak and the valley. Since increase in current in the valley was larger than at the peak, we can conclude that the I-V curve is changing in the right direction.

Futher experiment envolves the following: selection of the wavelength of the light depending on device material system and fabrication of the physically more suitable structure for optical illumination.

OPTICAL-BIAS-CONTROLLED AND TEMPERATURE-STABILIZED ELECTRIC FIELD SENSOR USING MACH-ZEHNDER INTERFEROMETER

Nobuo KUWABARA\*

NTT Telecommunication Networks Laboratories  
9-11 Midori-Cho 3-Chome Musashino-Shi, Tokyo 180, Japan

Ryuichi KOBAYASHI

University of Electro Communications  
1-5-1 Choufugaoka Choufu-Shi, Tokyo 182, Japan

Recent progress in electromagnetic compatibility(EMC) has created a need for a small wide-band electric field sensor to measure electromagnetic pulses and the electric field strength near radiation sources. A Mach-Zehnder interferometer with dipole element has been developed for use as a wide-band high-sensitivity sensor. However, the optical bias angle control method of the interferometer has not been clarified and the temperature stability should be improved. This paper describes on electric field sensor which can tune the optical bias angle without DC bias and improve temperature stability.

This new sensor uses a Mach-Zehnder interferometer which is formed on a 55mm by 1mm by 0.5mm LiNbO<sub>3</sub> substrate. The optical bias angle which means the phase difference between light in the two arms in interferometer should be tuned to obtain the best linearity. A stress is applied from the side of the substrate to create the phase difference between the arms. Figure 1 shows the relation between the optical power output and the electrode voltage. The dotted line shows the optical power when the stress is not applied and the solid line shows the optical power when the optical bias angle is tuned to the best angle. The optical output of the sensor drifts due to temperature changes. This mainly causes accumulation of charge between the electrodes of the interferometer. A conductive layer is formed on the LiNbO<sub>3</sub> substrate to discharge the accumulated charge. The dependence of optical output level on temperature is shown in Fig.2. The deviation is within 2dB from 5 degree to 45 degree. The sensitivity of the sensor with around 20cm long resistive element is almost flat from 1kHz to 1GHz and the minimum detective electric filed strength is about 1mV/m at 7.5kHz resolution bandwidth. This shows that the sensor can be used to measure electromagnetic pulses and electric field distributions.

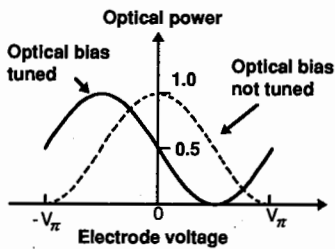


Fig.1 Relation between the optical power output and the electrode voltage

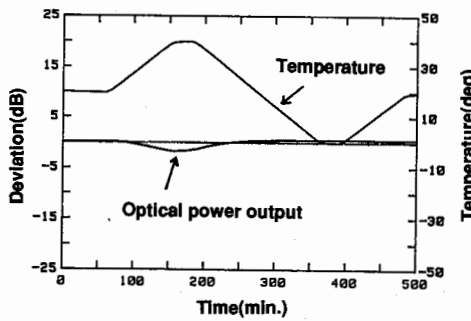


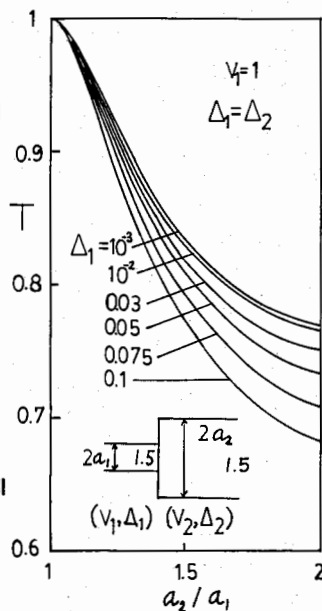
Fig.2 Dependence of optical power output level on temperature

## Abrupt Coupling between Dielectric Cylindrical Circular Fibers

Tam Do-Nhat, Ph. D.  
611-137 University Avenue W.  
Waterloo, Ontario, Canada, N2L 3E6  
Tel. (519) 725-4858

The scattering and coupling problems of abrupt dielectric waveguide discontinuities have recently been a subject of wide interest in the literature. Sophisticated numerical methods such as finite elements, finite difference time domain ( FDTD ), the least square boundary method, the method of moments, to mention just a few, are widely chosen to study abrupt discontinuities of optical planar waveguides. Traditional technique such as a full wave analysis, considered to be one of the most important methods was rigorously analysed in rib waveguide discontinuities [ T. Rozzi, L. Zappelli & M. N. Husain, IEEE MTT-40, 1879-1888, Oct. 1992 ]. Another standard technique such as the conservation of complex power technique ( CCPT ) has successfully been applied to a wide class of scattering problems including the scattering from single mode graded-index fibers [ T. Do-Nhat & R. H. MacPhie, J. Opt. Soc. Am. A, 4, 569-572, Apr. 1992 ].

The present paper studies the abrupt coupling of the fundamental  $HE_{11}$  mode of two dielectric cylindrical fibers of step-index profile by using a method which combines the modal field approach and ray Optics. In this approach the total reflected and transmitted fields at the discontinuity due to the incident  $HE_{11}$  mode are determined from the well-known Fresnel reflection formulas. This is accomplished since the  $HE_{11}$  mode can be decomposed into the spectrum of the TE and TM plane waves which rotate around the fiber axis. Then, by applying the field equivalence principle which specifies the just determined electric and magnetic current sources at the discontinuity, and by using the Lorentz reciprocity theorem in a complex conjugate form, the reflected and transmitted coefficients associated with the  $HE_{11}$  mode, all expressed in closed forms, can be isolated from those of other guided modes, as well as from the spectrum of radiation modes. Numerical results for those coefficients will be presented and this approach is expected to provide good results as long as the incident mode is paraxial, which can be applied to some incident lower order modes.



## Coupling between Gaussian Beams and Dielectric Cylindrical Circular Fibers

Tam Do-Nhat, Ph. D.  
611-137 University Avenue W.  
Waterloo, Ontario, Canada, N2L 3E6  
Tel. (519) 725-4858

The coupling problem between harmonically oscillating Gaussian beams and optical fibers has recently attracted the attention of many researchers since the day of the invention of semiconductor lasers and the fabrication of low loss optical fibers. The coupling mechanism has been analysed by either ray Optics or the scalar wave equation with the neglecting of the Fresnel reflections at the abrupt end of the fibers.

By using a combination of the modal field approach and ray Optics the present paper proposes to calculate the coupling coefficient between a beam whose beam waist located at  $z = -d$  ( see Fig. 1 ) follows the Gaussian distribution, and the HE<sub>11</sub> mode of a cylindrical circular fiber of step-index profile. First, with the help of the full wave analysis ( T. Do-Nhat & R. H. MacPhie, IEEE Antennas Propag. Symp. 4, 1839-1842, 1990 ) the Gaussian beam is explicitly expressed in terms of the TE and TM normal modes of the free space, which in turn can be decomposed into the spectrum of TE and TM plane waves rotating around the beam axis. Second, by applying the Fresnel reflection formulas to each plane wave incident upon the discontinuity the total transmitted field at the end of the fiber, i.e.,  $z = +0$ , is determined. The coupling coefficient associated with the fiber HE<sub>11</sub> mode is then calculated via the field equivalence principle with the help of the Lorentz reciprocity theorem. Finally, numerical results for the coupling coefficient will be presented and compared with those using the traditional method. The validation of the above method will also be discussed.

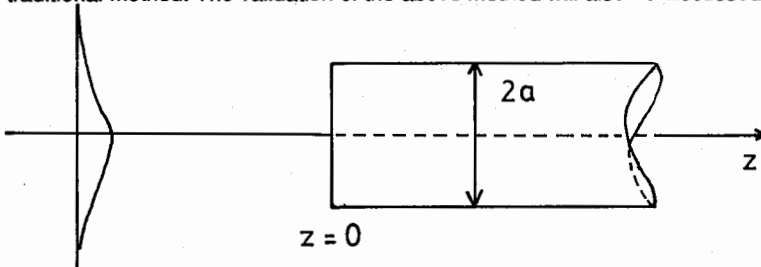


Fig. 1: A Gaussian beam at  $z = -d$  incident upon the abrupt end of a cylindrical circular fiber of step-index profile.

## VECTOR FINITE ELEMENT ANALYSIS OF LOSSY OPTICAL FIBERS

Jin-Fa Lee <sup>\*</sup> Arthur J. Butler  
Worcester Polytechnic Institute

To develop a practical/useful CAD/CAE system for analyzing propagation characteristics of lossy optical fiber, the following three issues need to be addressed: (1) A robust two-dimensional mesh generation processor; (2) A reliable and accurate vector finite element solution procedure; and, (3) An efficient sparse eigenmatrix solution technique. In this paper, we present a complete numerical procedure which is developed with these three issues beared in mind. The procedure is consisted of an automatic two-dimensional mesh generation using Delaunay triangulation, a hybrid edge-nodal finite element method for solving Maxwell's equations, minimum degree of reordering for reducing the fill-ins of the matrix equation, and the modified complex Lanczos alogirthm for solving the complex eigenmodes.

**Automatic Mesh Generation**

In WPI, we have developed an automatic triangular mesh generation program, called TESS, using Delaunay triangulation algorithm. This program takes a geometric description of the problem and breaks the problem domain automatically into triangles for the application of FEM.

**Hybrid Vector Finite Element Analysis**

To model a lossy optic fiber, we start with the vector Helmholtz equation for the electric field

$$\nabla \times \frac{1}{\mu_r} \nabla \times \vec{E} - k^2 \epsilon_r \vec{E} + j\omega \mu_o \sigma \vec{E} = 0 \quad (1)$$

where  $k$  is the wavenumber in free-space,  $\mu_r$ ,  $\epsilon_r$  are the relative permeability and permittivity, respectively, and  $\sigma$  is the conductivity of the material. In order to avoid the occurrences of spurious modes, the transverse field  $\vec{E}_t$  is being approximated by using edge-elements, and the first-order nodal basis functions are used to model the longitudinal component  $E_z$ . After applying the variational technique, the following generalized eigenmatrix equation is obtained

$$Ax = \gamma^2 Bx \quad (2)$$

where  $A$  and  $B$  are square complex matrices and  $x$  is a column vector. The element matrices for the present application have been derived analytically, in terms of geometric quantities, and will be presented in the symposium.

**Sparse Matrix Solution Techniques**

Both matrices  $A$  and  $B$  of the generalized eigenmatrix equation 2 are complex. Therefore, we have modified the non-symmetric Lanczos algorithm (Lee etc. IEEE MTT August, 1991) and extended it into solving non-symmetric complex generalized eigenmatrix equation. Furthermore, for each Lanczos iteration, we need to solve a matrix equation which is of the form

$$v = B^{-1}y, \quad (3)$$

in the present approach, this equation is solved efficiently by using the direct matrix solution technique with minimum degree of reordering.

## ANALYSIS OF FUSED TAPERED OPTICAL FIBER COUPLERS WITH ASYMMETRICAL STRUCTURE

Hung-chun Chang\* and Ting-Huei Lin

Department of Electrical Engineering and Institute of Electro-Optical Engineering  
National Taiwan University  
Taipei, Taiwan, Republic of China

The fused tapered biconical optical fiber coupler has become the key type of fiber couplers. Such coupler can be designed for wavelength-multiplexing and polarization beam splitting. In the neck region of the tapered coupler the light is guided by the boundary between the (reduced) fiber cladding and the external medium which is air unless some other potting material is employed. In practice a fused coupler can be either weakly fused or well (strongly) fused. For the weakly-fused coupler, the coupling region has the shape of two touching circular cylinders. The individual cylinders are obviously strongly-guiding fibers if the external region is air. In a previous work (Paper FA7 at OFC'92) we have provided more accurate coupling coefficients for modeling of the fused couplers by solving rigorously the (vectorial) boundary-value problem of two touching fibers. It was found that approximate calculations for the coupling coefficient and its polarization correction based on weakly guiding assumption may give large errors and thus are not suitable for use in the modeling of a coupler involving strongly guiding composite waveguide. In this paper we extend the more rigorous modeling to the case of weakly fused couplers with asymmetrical structure, i.e., structure involving touching fibers with different radii. Such couplers can achieve wavelength division multiplexing (WDM) and broad bandwidth characteristics. The solution is again based on the circular harmonics expansion method (H. S. Huang and H. C. Chang, IEEE J. Lightwave Technol., 8, 832-837, 1990). Using this method, we are able to analyze structures with large normalized frequency values and discuss the polarization splitting effect in the coupling. It is found that when the dimensions of the two fibers are slightly dissimilar, the field distribution may depart from being symmetric and antisymmetric drastically. In order to analyze a tapered coupler, we need a method to calculate the coupling in the tapered regions. We adopt the step approximation method in which the tapered region is divided into many small segments which are then analyzed as being parallel and uniformly coupled. Such segments are then connected in cascade to form the complete structure. Moreover, we adopt a simple approximation method (P. K. Ikkäinen and G. Matthaei, IEEE Trans. Microwave Theory Tech., 35, 621-628, 1987) to determine how a superposition of the local even-like and odd-like modes can approximate to fit the local total field profile and thus define the power carried in each fiber. The coupled power versus the draw length at different wavelengths and the dependence on the polarization of the input wave can then be predicted. For unpolarized powers WDM characteristics have been obtained with 3-dB power splitting at both 1.3- and 1.5- $\mu$ m wavelengths. In fact, a wavelength-flattened coupler is achieved. In summary, we have performed modeling of fused tapered asymmetrical fiber couplers based on an accurate modal analysis. It is seen that wavelength-flattened couplers can be designed by employing guided cores with different dimensions. Our model can treat the effect of different polarizations.

## OPTIMIZATION OF TRAPEZOIDAL GRATINGS FOR DFB AND DBR LASERS

M.H. Rahnavard, A. Bakhtazad, H. Sarmadi, H. Abiri  
Electrical Engineering Department  
School of Engineering  
Shiraz University

Coupled mode theory has been used to derive the coefficients of coupled wave equations, that is a key parameter describing the operation of distributed feedback (DFB), and distributed Bragg reflector (DBR). These parameters have already been calculated for trapezoidal corrugations (W. Streifer, D.R. Scifres & R.D. Burnham, *IEEE J. Quantum Electron. QE-13*, 134-141, 1977). On the other hand, fabrication of trapezoidal corrugations by dry etching has been done successfully, in which the wall angles can be modified by controlling the ion incidence angle, and analytical techniques for analysis, the problem of optimization of corrugation profile for various purposes arises. Here, both first-order and second-order gratings are taken into account.

First-order gratings are always used in DFB lasers, while second-order gratings are mainly used in DBR surface emitting lasers.

For the first-order corrugations, high effective coupling coefficient is the main figure of merit. A previous study, in which the effects of second-order coupled modes were not considered, has shown that rectangular corrugation with 1/2 duty cycle is the best profile. In this paper, the best profile, considering the contribution of the second-order modes, is obtained.

For the second-order corrugations, which are used in DBR surface emitting diodes, the side DBR reflectors must have maximum transmittivity for fixed reflectivity and corrugation length, while keeping the cladding to substrate radiation field ratio ( $E(0)/E(t)$ ) as high as possible. For this case, transmittivity for fixed corrugation length as a function of various profile parameters and reflectivity as a parameter are plotted. Also in the same figure, the cladding to substrate radiation ratio is considered.

From these graphs one may obtain the optimum trapezoidal grating profile for any case.

SYSTEM RESPONSE OF SEMICONDUCTOR PANEL TO LINEARLY  
GRADED MOVING RECTANGULAR SPOT ILLUMINATION  
AND ITS USE AS MILLIMETER WAVE IMAGE CONVERTOR

M.H. Rahnavard and A. Bakhtazad  
Electrical Engineering Department  
School of Engineering  
Shiraz University

Scanning light spot semiconductor panel has been shown to be able to convert millimeter wave images to visible displays. Reflection and transmission modes are proposed for this goal. In reflection mode reflected wave from scanning light-spot semiconductor panel is detected and in transmission mode transmitted wave through scanning shadow spot semiconductor panel is detected. The system response explains the sensitivity of this system.

In this paper the system response for scanning rectangular graded illumination for both modes are under consideration and the effects of illumination intensity, dimensions, and scanning velocity is studied. In transmission mode it is shown that an optimum illumination intensity exists, and a procedure for finding this optimum is discussed. In this mode, intrinsic attenuation of the semiconductor panel has great influence on the system response; this effect is also studied.

## Comparison of Three Quasi-TEM Models for Determining Optically Induced Losses in Coplanar Waveguides on Semiconductor

Zhong Liang Sun and Ao Sheng Rong  
State Key Laboratory of Millimeter Waves  
Department of Radio Engineering  
Southeast University  
Nanjing 210018, Jiangsu  
People's Republic of China

### Abstract

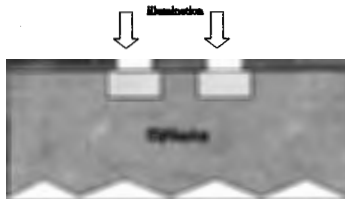
This paper presents three Quasi-TEM models—uniform, locally uniform and locally nonuniform for determining the optically induced losses in coplanar waveguides on the semiconductor. The accuracy of them is checked by comparison with experimental data available in the literature.

The uniform model assumes that optical excitation homogeneously appears in an infinite region with the depth  $H_p$  under the strip. The structure is analyzed by well known Quasi-TEM SPA.

The locally uniform model recognizes the nonuniform distribution due to the diffusion of excess carrier concentrations generated by the incident laser radiation. But the inhomogeneity is approximated by an equivalent rectangular region with the average dielectric constant  $\epsilon_p$  and the dimensions  $L_p \times H_p$ . The formulation is based on the hybrid space-spectral expression of Green's function in cooperation with the constraint conditions as follows: the constant potentials are assigned to the strips and the normal electric fluxes are continuous across the interfaces between different media.

In the locally nonuniform model, the inhomogeneous distribution of excess carrier concentrations are considered to be pseudo-two dimensional. The analytical expression of the distribution function is derived by a simplified but experimentally confirmed procedure. Hereafter, the inhomogeneity is characterized by the fictitious volume polarization charges with the density

$$\rho_p = \frac{\nabla \epsilon_p(\vec{r}) \cdot \epsilon_0 \mathbf{E}}{\epsilon_p(\vec{r})}$$



The corresponding boundary value problem is solved by the method of moments.

# Numerically Efficient Nonuniform Model for MMW Optically Controlled Dielectric Waveguide Phase Shifters

Ao Sheng Rong and Zhong Liang Sun  
 State Key Laboratory of Millimeter Waves  
 Department of Radio Engineering  
 Southeast University  
 Nanjing 210018, Jiangsu  
 People's Republic of China

## Abstract

This paper presents a numerically efficient nonuniform model for MMW optically controlled dielectric waveguide phase shifters as shown in Fig.1. The possible physical effects on the propagation are incorporated into the formulation, among which are the dielectric truncation, leaky waves, and the surface recombination and the diffusion of excess carrier concentrations generated by the incident laser radiation. The dielectric constant of the optically active regime depends on the excess carrier concentration via Drude-Lorentz formula. The nonuniform distribution due to the diffusion is characterized by a location-dependent  $\epsilon(r)$ . The latter is further approximated by many finely subdivided piecewise constant media. For a given medium, its fields are derived in a recursive manner. The propagation characteristics are obtained from the resonant condition. It is shown by typical examples that the present model provides the more subtle information than the available uniform model at the cost of a little more CPU time. Fig.2 shows the illustrative curves for the phase shifts and attenuation of  $TM_{11}$  mode versus the surface excess carrier density in SI waveguide, where the diffusion length is assumed to be  $L_s=10\mu m$  and the optically active regime is subdivided into 25 piecewise constant media. The other physical parameters read as:  $a=2.4mm$ ,  $b=1mm$ ,  $\epsilon_r=11.7$ ,  $f=94GHz$ .

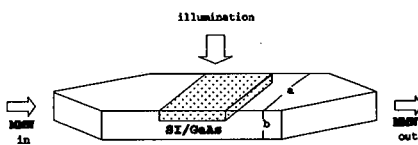


Fig.1

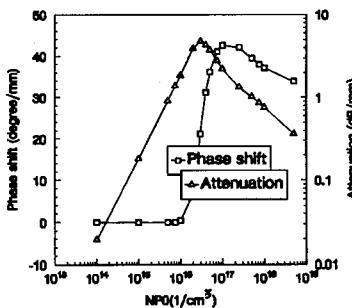


Fig.2



**SESSION URSI F-2****MONDAY PM****COMMUNICATIONS**

Chairs: W.J. Vogel, University of Texas; A. Benarroch, Universidad Politécnica de Madrid

Room: Michigan League, Room D      Time: 1:30-4:30

|      |   |     |
|------|---|-----|
| 1:30 | THE RELATIVE IMPORTANCE OF RAIN AND ICE ON CROSSLORAL DISCRIMINATION<br><i>Rolf Jakoby, Research Center of the Deutsche Bundespost Telekom</i>  | 108 |
| 1:50 | YEAR-TO-YEAR VARIABILITY OF RAIN ATTENUATION STATISTICS AT 20 GHZ ALONG EARTH-SPACE PATH<br><i>Hajime Fukuchi, Communications Research Laboratory</i>   | 109 |
| 2:10 | LARGE SCALE RAINFALL DIVERSITY FOR ACTS<br><i>H.P. Lin, W.J. Vogel*, The University of Texas at Austin</i>  | 110 |
| 2:30 | JOINT STATISTICS OF RAINFALL INTENSITY IN SPAIN<br><i>A. Benarroch*, F. Prieto, L. Mercader, Universidad Politécnica de Madrid</i>  | 111 |
| 2:50 | MILLIMETER WAVE PULSE PROPAGATION IN VEGETATION<br><i>Felix Schwerling*, US Army CECOM; Gerald M. Whitman, Anthony Triolo, New Jersey Institute of Technology; Nack Y. Cho, G.E. Aerospace Division</i> | 112 |
| 3:10 | BREAK   |     |
| 3:30 | MEASUREMENTS AND MODELING OF WIDEBAND UHF PROPAGATION INSIDE BUILDINGS<br><i>Richard Campbell*, Michigan Technological University; Kenneth Allen, Peter Papazian, NTIA/ITS.S</i>                        | 113 |
| 3:50 | THE UTILITY OF A HIGH GAIN OMNI TERMINAL ANTENNA IN A MOBILE SCATTERING ENVIRONMENT<br><i>Thomas M. Willis III, AT&amp;T Bell Laboratories</i>  | 114 |
| 4:10 | ANTENNAS FOR MOBILE ROBOTIC APPLICATIONS<br><i>Edip Niver, New Jersey Institute of Technology</i>   | 115 |

**PANEL DISCUSSION**

Room: Michigan League, Room D      Time: 4:30-6:00

|  |     |
|--|-----|
| CLASSIFICATION OF PATH-LOSS MODELS FOR MOBILE AND PERSONAL COMMUNICATION | 116 |
|--|-----|

Moderators: J. Shapira, Qualcomm Israel, Ltd.; H.L. Bertoni, Polytechnic University

Showed DCPA vs CPA for 3 yrs at 20°  
(using switched system).

6/28

Mon. p.m.

1993 URSZ Radio Science Meet (Ann Arbor)

## THE RELATIVE IMPORTANCE OF RAIN AND ICE ON CROSSPOLAR DISCRIMINATION

Rolf Jakoby

Research Center of the Deutsche Bundespost Telekom  
Darmstadt, Germany

~~CPA < 2 dB above for ice depolarization, ice effects  
dominated depolarization due to larger events for  
CPA < 0.2 B~~

The design of dually polarized satellite communication systems requires reliable and accurate information on the depolarization properties of the propagation medium. In this respect, ESA's OLYMPUS satellite offers the opportunity to study these effects at 12.5, 20 and 30 GHz. For this purpose, XPD frequency scaling and XPD-CPA relationships from three years of OLYMPUS measurements have been analyzed.

The results from equipercentage crosspolar scaling studies agree more or less with the scaling law proposed in CCIR Report 564-3. They deviate, however, from a fixed difference in XPD when scaling in frequency, depending on the depolarization mechanism. While the measured relationships at higher frequencies approach the scaling law found for "ice" (purely phase shifting medium), the curves at lower XPD values exhibit an increasing influence of rain. In addition to the equipercentage data, a variability analysis has been carried out, showing for a number of percentiles a spread which has to be taken into account in XPD scaling.

In order to both, obtain more information on the depolarization mechanisms and assess aspects of system performance, analysis have been carried out by means of XPD-CPA statistics. Because the XPD-CPA cumulative distribution, derived from the corresponding equiprobability exceedances, is lying between the 10 and 30 percentiles, the anisotropy is less than expected for a rain medium. The joint probability density statistics of instantaneous CPA and XPD allows to assess the different causes of depolarization, i. e. rain and ice, and their year-to-year variability. As expected, this statistics indicates a significant contribution from ice depolarization in the very low attenuation region, but also for CPA values between 4 and 10 dB, being associated with high depolarization.

To get a physical insight into these different depolarization effects, some typical events have been investigated by means of an XPD-analysis, in which the measured total depolarization is split into its constituents, originating from rain and ice, respectively. From these results, it is evident that not ice alone causes a wide spread in XPD versus CPA, but also rain, because of canting angle variations and a greater content of raindrops of spherical shape than expected from CCIR. This becomes evident from scatterplots XPD versus canting angle, and XPD versus differential copolar attenuation (DCPA). Furthermore, the results indicate that XPD is strongly ice induced also for CPA up to 10 dB.

# 1993 URSI Radio Science Meeting

Mon. p.m.

## YEAR-TO-YEAR VARIABILITY OF RAIN ATTENUATION STATISTICS AT 20 GHZ ALONG EARTH-SPACE PATH

Hajime FUKUCHI  
COMMUNICATIONS RESEARCH LABORATORY  
4-2-1 KOGANEI, TOKYO 184, JAPAN

[INTRODUCTION] The propagation experiments using Japanese geostationary communication satellite CS were carried out by the Communications Research Laboratory(CRL), intending to investigate precipitation effects on the millimeter wave propagation along earth-space path. Since CS was launched in 1977, the beacon signal at 19.45GHz(circular polarization, elevation angle:48 degree) have been received continuously over 8 years at the Kashima earth-station (35.95N, 140.67E) with data collection rate of 85%. In the experiment, attenuation, scintillation, cross-polarization discrimination(XPD), angle-of-arrival have been measured together with rainfall rate and other meteorological data.

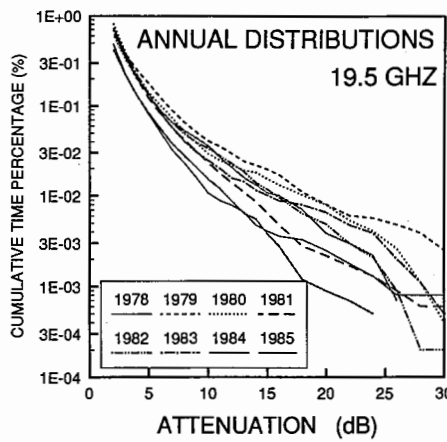
## [ATTENUATION STATISTICS]

Based on the measurements from 1978 to 1985, attenuation statistics such as yearly and worst-month cumulative distributions, cumulative distribution of attenuation duration and number of events were derived.

### [YEARLY VARIATION]

Figure shown right indicates yearly cumulative distributions derived from consecutive 8 years measurement. This indicates yearly variability of attenuation statistics and large variability can be observed.

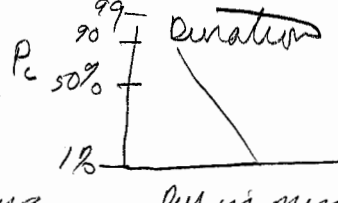
Variability of attenuation value at fixed cumulative time percentage increases as time percentage decreases. For example, standard deviation of attenuation values at cumulative time percentages of 0.3, 0.03 and 0.003% are 0.4, 1.5 and 4.3 dB, respectively, and their ratio relative to average value are 11, 15 and 19 %, respectively. These results agree with previously reported yearly variation analysis using rain rate statistics(R.K. Crane, Radio Sci. 20, 865-879, 1985). This also indicates an importance of sufficient measurement interval for propagation experiments. If statistical independence of attenuation value in each year is assumed, standard deviation of  $N$  years measurement decreases as  $1/\sqrt{N}$ .



1978.4  
to  
1986.3  
  
15 mos.  
interval,  
and typed  
1 miss ave.  
data

He says they see correlation between A and FS

$$P_c = \frac{\sum T(A) 25dB, 0.710m}{\sum T}$$



50% level of detection ( $A = 5dB$ )  
varied from 8 to 20 ms over 10 years

## LARGE SCALE RAINFALL DIVERSITY FOR ACTS

H. P. Lin and W. J. Vogel\*  
Electrical Engineering Research Laboratory  
The University of Texas at Austin  
Austin, Texas 78758

The advent of the next generation of satellites at K-Band, such as Olympus, ACTS, and others invites a study of the large scale statistics of rain attenuation [for Italy in: Barbaliscia, F., G. Ravaioli, and A. Paraboni, *IEEE Trans Ant and Prop*, 40, 1, Jan. 1992], because these satellites introduce new technologies that can make use of the fact that rainfall at any time is limited in spatial extent and has location dependent probabilities on a continental scale. Contemplated techniques are beam-shaping for satellites with CONUS coverage, such as broadcast satellites, up-link power control, and adaptive transmission rate control for multi-beam communications satellites. An example of the latter is ACTS, which will offer a certain amount of pooled resources to overcome, on demand, rain fading in a limited number of its beam locations.

The objective of this study is to predict the probable demand on shared rain fade mitigation resources of multi-beam satellites operating in the CONUS region. From the NOAA 15-minute precipitation file for the US we selected data for 128 stations covering a 17 year period and calculated the probability of simultaneous rainfall at several stations. We assumed that the chosen stations were located in separate beams of a multi-beam communications satellite with shared fade mitigation resources. In order to estimate the demands made on these resources, we determined the number of stations at which rainfall rates exceeded 10 to 40 mm/hr. We found a 1% probability that at least 5 of the 128 stations have rain at or over 10 mm/hr in any 15 minute interval. Rain at 2 stations was found to correlate over distances less than about 600 miles. A second set of 23 stations covering a 5 year period was also considered. It covers spot beam locations for ACTS and/or propagation experiment sites. Where appropriate, results are compared to those found for Italy. In order to derive ACTS specific information, we also extracted precipitation data for 23 stations that are either at locations served by the ACTS spot beams, or are at sites chosen for beacon propagation experiments. The data base yielded 5 years of concurrent information, covering the period of Jan. 1, 1984 to Dec. 31, 1988.

## JOINT STATISTICS OF RAINFALL INTENSITY IN SPAIN

\*  
A. Benarroch, F. Prieto, L. Mercader  
ETSI Telecommunicación, Universidad Politécnica de Madrid  
28040 Madrid, Spain.

Future satellite communications systems will use onboard adaptive processing techniques allowing additional resources to be employed for earth stations which require an increase of link margin or capacity due to adverse meteorological conditions. To design such systems, the probability of simultaneous request of additional resources from more than one earth station must be known. This can be easily derived from the joint cumulative distributions of rainfall intensity calculated for more than one location (L. Ordano, ICAP Proc., York, United Kingdom, 750-753, 1991; F. Barbaliscia et al., IEEE Trans. Ant. Prop. Vol. 40, No. 1, 8-12, 1992).

An extensive study of rain rate statistics is being carried out in Spain in order to obtain an accurate map of rain climatic zones (L. Mercader and A. Benarroch, URSI/APS-IEEE Proc., London, Ontario, Canada, 1808-1811, 1991). Large amounts of raingauge data from meteorological stations located all over Iberia are being analyzed. Joint distributions of rain rates have been calculated using an integration time of 5 minutes for over 200 pairs of stations, with an average of more than ten years of records per station and distances among them of up to 1000 Km.

The results obtained include as well the correlation coefficient for each pair of locations which is a function of the rain rate threshold and of the distances between the stations.

The simultaneous occurrence of rainfall of a same intensity in two locations is strongly related to their situation with respect to the more frequent movements of the rainy fronts. This climatological influence on the joint distributions and on the correlation coefficients will be discussed in the paper, together with the commented dependence of this coefficient on distance and rain rate threshold.

## MILLIMETER WAVE PULSE PROPAGATION IN VEGETATION

Felix Schwering\*, US Army CECOM; Gerald M. Whitman, Anthony Triolo, New Jersey Institute of Technology; Nack Y.Cho, G.E. AstroSpace Division

Millimeter wave communication links may have to transmit through vegetation, either by chance or, for camouflage purposes, by design. Published experimental data has shown that in a forest cw millimeter wave transmission is possible over lengths of the order of a few hundred meters and that power strongly scatters in the forward direction. Recent theoretical and experimental cw studies conducted jointly by CECOM, NJIT and NTIA have yielded the range dependency and beam broadening characteristics of millimeter wave signals in vegetation, and have provided preliminary information on depolarization effects. However, pulse broadening effects and the associated rise in bit error rate, which are important for digital signal transmission, remained to be determined. To compliment a recent experimental investigation on these effects (P.B.Papazian, D.L.Jones and R.H.Espeland, NTIA Report 92-287, US Dept. of Commerce, September 1992) and to enhance understanding, the present analytical study was undertaken. As a result, a theory of millimeter wave pulse propagation in a random medium using the scalar time-dependent equation of radiative transfer evolved.

A periodic sequence of plane wave pulses in air is assumed to impinge upon a forest half-space. The forest is taken to be statistically homogeneous and to consist of a random distribution of particles which scatter and absorb radiation. The forest is characterized by a scatter function that has a strong forward lobe superimposed on an isotropic background. The solution to the equation of radiative transfer is obtained by expanding the specific intensity in terms of Legendre polynomials and by using the least square method to satisfy the boundary condition that the incoherent (diffuse) intensity be zero at the air-forest interface. Curves of received power versus time confirm that at small penetration depths, the coherent (reduced incident) intensity dominates, whereas at large depths, the incoherent (diffuse) intensity is the strongest and causes the pulses to broaden and distort.

## MEASUREMENTS AND MODELING OF WIDEBAND UHF PROPAGATION INSIDE BUILDINGS

Richard Campbell\*

Department of Electrical Engineering  
Michigan Technological University  
Houghton, MI 49931

Kenneth Allen and Peter Papazian

NTIA/ITS.S  
U.S. Department of Commerce  
325 S. Broadway  
Boulder, CO 80303

We have measured the time delay spread at three indoor locations: a long hallway; an auditorium; and a large open plan office with movable partitions. The carrier frequency of 1.5 GHz was spread over a 1 GHz bandwidth using a PN code. The delay spread measurements were obtained using the sliding correlator technique, with a time resolution of 2 nsec. Our experiment geometry uses a fixed transmitter and a receiver that samples and records the signal as it slowly moves along preselected paths in the indoor environment. Our measurements show a consistent characteristic feature of wideband indoor scattering environments--the delay spread measurements fluctuate rapidly between two modes; a narrow delay spread mode, typically a few tens of nanoseconds; and a wide delay spread mode with delay spread strongly dependent on the dimensions of the indoor scattering environment. Because the measured delay spread distributions are bimodal, the concepts of "Average Delay Spread" and hence "Average Correlation Bandwidth" are of questionable utility in indoor environments.

A basic model for electromagnetic wave propagation inside buildings is presented which predicts the measured delay spread behavior. The model is formulated in terms of the distribution of signal arrival times (delay spread) and the distribution of signal arrival angles (angular spectrum). These two parameters are particularly useful because they are orthogonal, they are strongly dependent on the characteristics of the environment, and only weakly dependent on frequency. The model has three frequency ranges: "low frequencies," where the delay spread is less than a period of the wave; "medium frequencies," where the delay spread is greater than the period of a wave; and "high frequencies," where the delay spread is much greater than a period of the wave and all of the individual paths may be resolved. UHF and microwave signals in typical indoor environments

Mobile

# 1993 URSI Radio Science Meet (June 28)

Mon. p.m.

## THE UTILITY OF A HIGH GAIN OMNI TERMINAL ANTENNA IN A MOBILE SCATTERING ENVIRONMENT

Thomas M. Willis III  
AT&T Bell Laboratories

To provide Personal Communication Services (PCS), the next generation of mobile communications services for voice, video and data, many telecommunications companies are currently investigating the use of various new technologies. These efforts include designing and evaluating new network architectures, new radio modulation schemes, new radio terminal devices and the use of other radio bands than the current cellular communications band at 900 MHz. On such effort at AT&T is evaluating the possible use of 6 GHz for PCS. AT&T has performed numerous propagation experiments at 6 GHz in New Jersey, Atlanta, Los Angeles and Boston to determine service coverage areas as well as evaluate possible interference cases. Hundreds of miles have been logged by data acquisition vans over these areas, providing a large data set over many diverse real life scattering environments from which to draw statistical conclusions and produce propagation models.

One advantage of providing PCS at 6 GHz, compared to 900 MHz, is the ability to build a high gain directive antenna and still keep the size of such a structure small enough to be convenient for a hand held terminal device that will fit in a pocket or purse. Since it is impossible to fix the orientation of a mobile communications user, omni-directional antennas are typically used for terminal devices. Even with this constraint, the gain of an omni-directional antenna can be increased by changing its elevation pattern to be more directive. The advantage of a directive omni-directional antenna in a mobile environment, where multiple scattered waves propagating in different directions may be present, is not obvious however. Therefore, the utility of a high gain omni-directional antenna was investigated by AT&T at 6 GHz during propagation experiments performed in the Boston area.

This presentation will discuss some of the experiments performed in Boston, including a description of the data acquisition vans built for this study. Data will be presented comparing the received power levels for a high gain omni antenna compared to a quarter wave stub omni for different scattering environments. Statistical comparisons will also be made. Finally, conclusions will be drawn on the utility of the high gain omni antenna and areas for further work will be discussed.

## ANTENNAS FOR MOBILE ROBOTIC APPLICATIONS

Edip Niver

Electrical and Computer Engineering Department  
New Jersey Institute of Technology  
Newark, NJ 07102

A robot operating in a wireless environment could provide more flexibility compared to a stationary or a wired one; however, such operation, especially indoors, will introduce additional complexities. A mobile unit is equipped with an array of sensors and the obtained information has to be transmitted to the relay/remote controller as well as navigational control commands have to be received for proper operation. In such a communication system, the antenna plays an important role. Challenging problems arise in choosing the proper antenna type which necessitates consideration of multipath propagation effects, weight, polarization, bandwidth, etc. Additionally, consideration has to be given to which antenna type is to be used on a mobile platform, on a stationary receiving station or on a repeater (if there is a need for one due to the complexity of the system architecture).

Numerical simulations, fabrication and measurements have been performed on various discone, top loaded monopole and microstrip patch antennas in various frequency bands.

PANEL DISCUSSION: CLASSIFICATION OF PATH-LOSS MODELS  
FOR MOBILE AND PERSONAL COMMUNICATION

J. Shapira  
QUALCOMM Israel, Ltd.  
Haifa, Israel

Operation of modern wireless communications services based on the cellular principle is strongly influenced by channel characteristics. Originally formulated in terms of large cells for Cellular Mobile Radio (CMR) telephone service, the concept is now being applied using smaller cells (microcells) to a mixed population of pedestrian and mobile users in outdoor urban areas, and to in-building personal and data communications. Besides operating in new environments, these systems will provide new services, which itself may require a new characterization of the channel.

For macrocells employing base station antennas that are elevated above the clutter, the multiple scattering effects that lead to dispersion and fading must occur in the vicinity of the mobile, whereas the positioning of the base station only affects the range dependence. However, for urban microcellular systems using base station antennas at or below the surrounding rooftops, and for in-building systems, both the base station and mobile antennas are located in the clutter. As a result, it will be necessary to identify environmental features at both ends of the link that contribute to the dispersive and fading characteristics.

For microcellular and in-building systems, it will be possible to incorporate a more detailed model of the environment into prediction programs. Working with more detailed environmental models will in turn permit a more accurate prediction of channel characteristics. The trade-off between accuracy and cell size, as well as its implications for system design, have yet to be explored.

The panel discussion is aimed at promoting a dialogue in the community leading to the better understanding of channel model in relation to the size and environment of the coverage area, and the communication system application. This understanding will, we believe, help to bridge the gap between the communication research community and the propagation community, and will better serve communication network designers.

**SPECIAL SESSION AP-S/URSI K-2****MONDAY PM****ELECTROMAGNETICS IN BIOMEDICAL SENSING, DIAGNOSIS AND TREATMENT**

Chairs: D.R. Jackson, University of Houston  
N.G. Alexopoulos, University of California at Los Angeles  
J.C. Lin, University of Illinois at Chicago

Room: Alumni Center, Room 2      Time: 1:30-3:10

|      |   |      |
|------|---|------|
| 1:30 | APPLICATIONS OF ELECTROMAGNETIC THEORY AND TECHNIQUES IN MEDICINE<br><i>James C. Lin, University of Illinois at Chicago</i>               | 118  |
| 1:50 | ANALYSIS OF POSSIBLE HEALTH EFFECTS OF AN AIR FORCE COMMUNICATION SYSTEM<br><i>T.S. Tenforde, Battelle Pacific Northwest Laboratories</i> | 119  |
| 2:10 | ANLYSIS AND CHARACTERIZATION OF MICROWAVE INTERSTITIAL ANTENNAS<br><i>Magdy I. Iskander, University of Utah</i>                           | 120  |
| 2:30 | CURRENT STATUS AND APPLICATION OF COMPUTATIONAL ELECTROMAGNETICS IN HYPERTHERMIA<br><i>V. Sathiaseelan, Northwestern University</i>       | 121  |
| 2:50 | THE USE OF ELECTROMAGNETIC FIELDS IN MEDICAL DIAGNOSTICS<br><i>Stephen B. Baumann, University of Pittsburgh</i>                           | AP-S |

## APPLICATIONS OF ELECTROMAGNETIC THEORY AND TECHNIQUES IN MEDICINE

James C. Lin  
EECS Department, M/C 154  
University of Illinois at Chicago  
Chicago, IL 60607-7053

This paper describes several current and future applications of electromagnetic technology in service of human health and welfare. A majority of these applications have relatively short histories, their impact on diagnostic evaluation and therapeutic treatment have been most striking. Perhaps, even more significant is that recent developments promises to unveil exciting new and efficacious procedures and systems for health care applications. A number of effective and safe uses of electromagnetic energy have been developed for medicine. Magnetic resonance imaging (MRI) and spectroscopy continue as a leading noninvasive modality for diagnostic examination of tissues to detect or localize disease. Other emerging imaging modalities include electrical current, magnetic emission (MCG\MEG), microwave and thermoelastic energy sources. Microwave sensing of arterial pulse waves provides a noninvasive technique using low-power electromagnetic energy for diagnostic applications. Magnetic stimulation for the diagnosis of neurological disorders represent yet another noncontact application of electromagnetic energy that is gaining in popularity.

Some recent therapeutic practices that involve electromagnetic energy include bone healing, cardiac and vascular intervention, and hyperthermia treatment of malignant and benign tumors. Studies have demonstrated that electric and magnetic field-induced currents facilitate the healing of certain classes of nonunion bone fractures in which reparative processes have ceased. Percutaneous transluminal microwave and radio-frequency catheter technologies have been explored for ablation treatment of cardiac arrhythmias and recanalization of arterial obstructions via angioplasty. The increased interest stems in part from the nonpharmacological approach and minimally invasive nature of these procedures. Hyperthermia therapy is a treatment procedure in which tissue temperature is elevated to the range of 43° - 50°C. An important aspect of this development is the production of adequate thermal field distribution in tumors and in abnormal tissues. Interstitial and intracavitary techniques are attractive because of their ability to provide effective and uniform heating of large volumes of deep-seated tumors.

## ANALYSIS OF POSSIBLE HEALTH EFFECTS OF AN AIR FORCE COMMUNICATION SYSTEM

T.S. Tenforde  
Life Sciences Center (K1-50)  
Battelle, Pacific Northwest Laboratories  
Richland, WA 99352

The Ground Wave Emergency Network (GWEN) is a nationwide system of radio transmitters and receivers being constructed by the U.S. Air Force. The primary purpose of the GWEN system is to provide communication capabilities that would be invulnerable to electromagnetic pulses arising from the detonation of nuclear weapons over the U.S. mainland. The completed GWEN system will consist of 125 stations communicating in both the low-frequency (LF) band at 150-175 kHz, and in the ultrahigh-frequency (UHF) band at 225-400 MHz. The peak radiated power of the LF and UHF transmissions will be about 3200 W and 20 W, respectively, which are modest levels compared to most civilian radio and television stations broadcasting at similar frequencies. During peacetime the GWEN system will operate in a maintenance testing mode with an average duty cycle of 0.014. Prior to initiating construction, the Air Force completed an environmental impact statement (EIS) in 1987. The EIS concluded that GWEN emissions were within RF safety guidelines, and were therefore unlikely to have an adverse impact on public health. Because of subsequent findings on the possible health effects of electromagnetic field exposure, most notably a potential association between exposure to ELF fields and cancer risk, the U.S. Congress in 1990 required the Air Force to postpone completion of the GWEN system pending an evaluation of this new information. The Air Force subsequently requested the National Research Council (NRC) to investigate the potential health effects of GWEN emissions, and an 11-member committee prepared a report on this subject in 1991-1992. The NRC committee's report contains an analysis of both laboratory data and human epidemiological studies on the biological interactions and health effects of electromagnetic fields with frequencies ranging from ELF to microwaves. This paper will summarize the results of the NRC committee's review, which led to the conclusion that adverse effects of GWEN emissions on public health are unlikely. Based upon its findings, the NRC committee recommended that its report be used in conjunction with the original EIS as a comprehensive assessment of possible health effects of radiofrequency emissions from the GWEN communication system.

## ANALYSIS AND CHARACTERIZATION OF MICROWAVE INTERSTITIAL ANTENNAS

Magdy F. Iskander  
Department of Electrical Engineering  
University of Utah  
Salt Lake City, UT 84112

Microwave interstitial antennas have recently received increasing interest and have been used in a wide range of applications in medical diagnosis and treatment. This includes heating of brain and deep-seated tumors, microwave balloon angioplasty, measurement of dielectric properties of tissues, and in the control of hemorrhage, particularly in highly vascular organs. In the microwave hyperthermia application, for example, interstitial antennas are often used in conjunction with other types of treatments such as brachytherapy in which radioactive seeds are inserted in surgical tracks as part of clinical procedures for cancer treatment. In the microwave angioplasty treatment, on the other hand, microwaves may be used in conjunction with ultrasound to ablate plaque in arteries and to possibly remove thrombus from vessels and destroy large gall stones.

Interstitial antennas are basically monopole-type antennas inserted in catheters placed in surgical tracks inside the human body. There are many designs of interstitial antennas which are developed to provide a desired heating characteristic specific to the application in which they are being used. Designs vary from a simple uniformly insulated antenna to multisection designs which provide more uniform heating along the antenna axis.

For realistic and effective evaluation of the heating characteristics of these antennas, their radiation fields must be determined for the wide variety of designs that are often used in clinical applications. Also, to account for the variation in tissue types and their spatial distribution in the human body, 3D numerical models should be used to calculate the EM power deposition patterns of these antennas. Furthermore, various heat exchange mechanisms such as blood flow rate and thermal conduction must be accounted for in calculating the resulting heating patterns from these antennas.

In this paper, the various analytical and numerical methods used to analyze radiation characteristics of interstitial antennas will be reviewed. 3D techniques for calculating EM power deposition and heating patterns will be discussed. Experimental evaluation of the heating patterns of some of the clinically available interstitial antenna designs will be described.

## CURRENT STATUS AND APPLICATION OF COMPUTATIONAL ELECTROMAGNETICS IN HYPERTERMIA

V. Sathiaseelan  
Radiation Oncology Center  
Northwestern University and  
Northwestern Memorial Hospital  
Chicago, IL

There is a strong biological rationale for the efficacy of hyperthermia as an adjuvant to radiation therapy in the treatment of cancer. It has also been shown convincingly in a number of non-randomized clinical studies that complete response rates (CR) obtained with irradiation plus hyperthermias are more than double those obtained with the same irradiation alone, thus greatly enhancing the potential for local control and prolonged survival with improved quality of life. However, attempts to make hyperthermia treatments more routine are proving to be elusive because of the limitations of the currently available equipment and the difficulty in knowing if adequate hyperthermia treatment has been delivered. Electromagnetic (EM) heating techniques are widely used in the clinic to produce therapeutic temperatures and there is an urgent need for better design tools for building applicators and evaluating their performance in clinically realistic situations. Computer modeling can play a significant role in the design of better heating equipment and in improving the quality of the hyperthermia treatments currently being administered. There is also need for treatment planning systems that can help optimize treatments delivered with currently available equipment. Over the last five years, significant work has been carried out to advance this field of research and 3-D numerical methods that take into account the overall interaction of the irregular and heterogeneous human bodies with EM fields have been developed to predict EM power deposition and temperature distributions. However, a number of fundamental questions remain unanswered. There are several gaps in the state of the existing knowledge, which are basic to the continued clinical impact of numerical simulation and ultimately to the development of treatment planning systems similar to those used for radiation therapy. Current progress in numerical modeling and applications will be presented, following a brief review of the biological rationale and techniques presently used in the clinic.



SESSION URSI K-3

MONDAY PM

**BIOMEDICAL APPLICATIONS OF ELECTROMAGNETIC FIELDS**

Chairs: T.S. Tenforde, Battelle Pacific Northwest Laboratories  
J.C. Lin, University of Illinois at Chicago

Room: Alumni Center, Room 2      Time: 3:30-5:10

|      |   |     |
|------|---|-----|
| 3:30 | INSTRUMENTATION FOR MEASURING TRANSTHORACIC CONDUCTANCE AND CARDIAC CURRENT DISTRIBUTION DURING DEFIBRILLATION<br><i>O.C. Deale, Cornell University; K.T. Ng*, New Mexico State University; B.B. Lerman, Cornell University</i> | 124 |
| 3:50 | ANALYSIS OF THE INDUCED ELECTRIC FIELD IN A TISSUE CYLINDER IN MAGNETIC NERVE STIMULATION<br><i>Karu P. Esselle, Macquarie University; Maria A. Stuchly, University of Victoria</i>   | 125 |
| 4:10 | TRANSCATHETER MICROWAVE TECHNIQUE FOR TREATMENT OF CARDIAC ARRHYTHMIAS<br><i>J.C. Lin*, Yujin Wang, University of Illinois at Chicago; Robert J. Hariman, Hines VA Hospital</i>   | 126 |
| 4:30 | MICROWAVE INTERSTITIAL ANTENNAS FOR ARTERIAL PLAQUE ABLATION<br><i>P. McArthur, Sonic Star International Ltd.; M.F. Iskander, C. Catten, J. Hunsaker, D. Jensen, M. Orme, B. Tame, University of Utah</i>                       | 127 |
| 4:50 | DETERMINATION OF THE ELECTROMAGNETIC PATTERNS FOR R.F. AND MICROWAVE HYPERTHERMIA AND RADIOMETRY PLANAR APPLICATORS<br><i>F. Duhamel*, L. Dubois, M. Chive, J. Pribetich, Universite des Sciences and Technologies de Lille</i> | 128 |

## INSTRUMENTATION FOR MEASURING TRANSTHORACIC CONDUCTANCE AND CARDIAC CURRENT DISTRIBUTION DURING DEFIBRILLATION

O.C. Deale<sup>1</sup>, K.T. Ng<sup>2\*</sup>, and B.B. Lerman<sup>1</sup>

<sup>1</sup>Cornell University Medical College  
New York, NY 10021

<sup>2</sup>New Mexico State University  
Las Cruces, NM 88003

One of the most effective means to treat patients with cardiac arrest (ventricular fibrillation) is transthoracic defibrillation, i.e., application of high voltage shocks to the chest wall. Defibrillation is achieved when a threshold current density is reached in the heart. Thus, it is important to study the cardiac current distribution during defibrillation. In addition, as the cardiac current distribution is related to the transthoracic conductance and the circuit that delivers the defibrillation shock, a complete understanding of the relationship between the transthoracic conductance and the defibrillation system variables is important for improving the defibrillation process.

The system for measuring transthoracic conductance in this study consists of a defibrillator, a voltage divider in parallel with the defibrillator output for measuring the transthoracic voltage and a resistor in series with the defibrillator output for measuring the transthoracic current. The defibrillation electrode force is precisely controlled by a pair of balanced levers. Precision weights are used to select the desired force magnitude. All forces due to the weight of electrodes and levers are cancelled by counter-weights. Electrode area is selected by the use of a set of precision circular electrodes.

To determine the cardiac current distribution, in addition to the basic system mentioned above, bipolar electrodes are used to measure the electric field in the myocardium during defibrillation. A bipolar technique is used to avoid the sensitivity to measurement errors inherent in the conventional unipolar technique. However, the bipolar technique does introduce a common mode voltage problem that needs to be solved in order to obtain accurate measurement results. SPICE simulations and empirical investigations have been used together to obtain a circuit that allows one to minimize the common mode voltage error signal.

In this paper, we will present the details of the instrumentation system for measuring transthoracic conductance and cardiac current distribution. In particular, the analysis and design of the circuit for cancellation of the common mode voltage error signal will be described. Results obtained with the instrumentation will also be presented.

## ANALYSIS OF THE INDUCED ELECTRIC FIELD IN A TISSUE CYLINDER IN MAGNETIC NERVE STIMULATION

*Karu P. Esselle* \* and *Maria A. Stuchly* #

\* Electronics Department, School of MPC+E  
Macquarie University, Sydney, NSW 2109, Australia

# Department of Electrical and Computer Engineering  
University of Victoria, P.O. Box 3055, Victoria, B.C., V8W 3P6, Canada

Magnetic field pulses have been used to stimulate motor neurones in the cerebral cortex and nerves in upper limbs. Since its introduction (A. T. Barker, R. Jalinous & I.L. Freeston, *Lancet*, i, p. 1106, 1985), magnetic nerve stimulation has found many successful applications in medical diagnosis. In practise, the magnetic field pulse is generated by discharging a bank of charged capacitors into a specially-designed coil. The spatial distribution and temporal variation of the electric field, induced by the magnetic field pulse, are the key factors in nerve stimulation. It has been found that for long straight nerves, the "activating function" is the spatial derivative of the induced electric field along the nerve.

Analysis of the induced electric field is therefore a major step in understanding and optimising magnetic nerve stimulation. Several such analyses were done in the past but most of them were based on numerical techniques (B. J. Roth *et al*, *Electroencephal. clin. Neurophysiol.*, vol. 81, pp. 47-56, 1991). While numerical techniques are the only means for accounting heterogeneous tissue properties, they have serious limitations in coil optimisation due to the loss of the physical insight and the need for large computing resources.

Recently, two analytical techniques were developed using approximate homogeneous semi-infinite (K.P. Esselle & M.A. Stuchly, *IEEE Trans. Biomed. Eng.*, vol. 39, no. 7, pp. 693-700, 1992; K.P. Esselle & M.A. Stuchly, *ACES J.*, vol. 7, no. 2, pp. 162-178, 1992) and homogeneous spherical (H. Eaton, *Medical Biol. Eng. Comp.*, vol. 30, pp. 433-440, 1992) tissue models. This paper describes an analytical technique to compute induced electric fields in a homogeneous tissue cylinder that more closely models the stimulation of nerves in limbs. This technique is based on the expansion of induced field in terms of Modified Bessel Functions and can be applied for coils of arbitrary shapes. It can also be extended for axially heterogeneous tissue cylinders. The results obtained from this method compare very well with those obtained from previous numerical techniques yet this method is significantly (about 30 times) faster and needs less computer memory.

Because of the speed advantage and insight provided by the analytical solution, this method is ideal for the design of new coils as well as for the optimisation of new and existing coils. Even though this theory was developed primarily for the analysis, design and optimisation of magnetic nerve stimulator coils, it will also be useful in the analysis of quasi-static induced fields in other medical applications such as bone-healing (using magnetic-field pulses) and low-frequency dosimetry.

## TRANSCATHETER MICROWAVE TECHNIQUE FOR TREATMENT OF CARDIAC ARRHYTHMIAS

James C. Lin\*, Yujin Wang and Robert J. Hariman@  
@Hines VA Hospital and EECS Department  
University of Illinois at Chicago  
Chicago, IL 60607-7053

In a significant fraction of patients with ventricular tachycardias, available drug therapies have been found unsatisfactory because of a less than meaningful response or unacceptable side effects. This paper presents a microwave technique for transluminal catheter treatment of cardiac tachyarrhythmias. While other energy sources such as lasers have been used for cardiac ablation; none has achieved the desired efficacy. Some of the major limitations of these techniques include perforation of heart walls and nonfocused damage to cardiovascular tissues. A high incidence of complications involving the above mentioned issues remain to be addressed.

The propagation of microwave energy in biological tissue is governed by the source frequency, antenna configuration, tissue composition, and dielectric permittivity. Energy between the frequency of 1 to 10 GHz is readily absorbed by biological tissues and the effective absorption depth is about a few mm for tissues of high water content. The distribution of absorbed microwave energy can be controlled by judicious design of the antenna, which not only will permit radiation of microwave energy into tissue but also allow discrete localization of microwave energy absorption.

In percutaneous transluminal catheter ablation of tissue substrate responsible for tachycardia, under the guidance of fluoroscopy and endocardiac electrogram, microwave energy is delivered through a catheter to a specially designed miniature antenna to thermally ablate the cardiac conducting tissue. Since tissue heating is the principal mechanism in producing pathological alterations following microwave irradiation of biological tissue, it is possible to titrate, in stepwise manner, the microwave energy delivered to cause various degrees of tissue temperature elevation. The range of control afforded by microwave is a distinct advantage over other modalities. Lower energy levels may help to localize and confirm site to be ablated and to allow adjustment of microwave power.

## MICROWAVE INTERSTITIAL ANTENNAS FOR ARTERIAL PLAQUE ABLATION

P. McArthur,\* M. F. Iskander, C. Catten, J. Hunsaker,  
D. Jensen, M. Orme, and B. Tame

Electrical Engineering Department  
University of Utah  
Salt Lake City, UT 84112

\*Sonic Star International Ltd.  
Jamestown, NY 14702

Microwave balloon angioplasty has recently become a viable alternative to open-heart surgery. Routine balloon angioplasty involves the insertion of a catheter tipped with a deflated balloon into a human with an artery blocked by plaque. The utility of the microwave energy to soften the arterial plaque prior to and during the inflation of the balloon has resulted in improving the effectiveness of the treatment procedure. Additional benefits of the microwave energy, including the sealing of dissections and aiding in the resolution of thrombus, have also been cited [1, 2]. It is expected that the use of microwave energy in conjunction with the ultrasound procedure will help in ablating plaque, the removal of thrombus, and possibly in the destruction of large-volume gall stones.

An important part of the microwave system is the design of the interstitial antenna that heats the plaque in the balloon region. In this paper, we use the FDTD method to model and simulate the performance of several interstitial antenna designs in heating arteries. It is shown that the multisection antenna design, in which the center conductor is constructed of a few sections of varying lengths and diameters, provides many of the desirable heating characteristics. These include the uniformity of the heating pattern along the balloon and an adequate depth of penetration of 3 to 4 mm. The multisection design may be used to reduce the resonant frequency of the antenna, and this, in turn, further improves the depth of penetration of the microwave energy. To support the FDTD simulation dielectric properties of plaque, arterial tissue and blood were measured as a function of frequency using an open-ended coaxial probe. Furthermore, to help evaluate the performance of the interstitial antenna under varying rates of blood flow in an artery, a thermal model that takes into account the various heat exchange mechanisms and calculates the resulting temperature distribution was developed.

The results from the FDTD and heat transfer programs, together with results from the dielectric property measurements, will be presented. Some multisection antenna designs are constructed and their heating patterns are evaluated on phantoms using a thermographic technique. Results from these measurements will also be discussed.

- [1] A. Rosen, *et al.*, "Percutaneous Transluminal Microwave Balloon Angioplasty," *IEEE Transactions on Microwave Theory and Techniques*, Vol. MTT-38, pp. 90-92, 1990.
- [2] P. Walinsky, *et al.*, "Microwave Balloon Angioplasty," *Digest of the 1991 IEEE MTT-S International Microwave Symposium*, Vol. 2, pp. 797-800.

## DETERMINATION OF THE ELECTROMAGNETIC PATTERNS FOR R.F AND MICROWAVE HYPERTHERMIA AND RADIOMETRY PLANAR APPLICATORS .

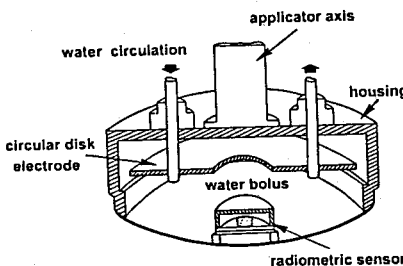
F. DUHAMEL\*, L. DUBOIS, M. CHIVE, J. PRIBETICH.

I.E.M.N. - U.M.R. C.N.R.S. N°9929  
DEPARTEMENT HYPERFREQUENCES & SEMICONDUCTEURS (C.H.S.)  
UNIVERSITE DES SCIENCES & TECHNOLOGIES DE LILLE.  
59655 VILLENEUVE D'ASCQ CEDEX - FRANCE

The present work is a continuation and a refinement of previous modelization of planar applicators used in microwave hyperthermia in which only plane multilayered and homogeneous media could be taken into account. The main characteristic of these different applicators is that they are used both to deliver the microwave heating power to the tissues and to collect the microwave thermal noise induced by the heating when the applicator operates as an antenna receiver for radiometry. We can now determine the power deposition in a completely heterogeneous medium which structure can be obtained, for instance, from CT scanner images. More, the exact shape of the water bolus coupled with the applicator can be taken into account. This calculation can also be used to determine the coupled volume to the applicator when used as a radiometric antenna to carry out non invasive temperature measurements.

This method allowing to monitor microwave hyperthermia system is also used in R.F. capacitive hyperthermia where the radiometric antenna is integrated in the heating system. The upper electrode is fitted out with a thermostated water bolus which avoid superficial burning of the tissues while allowing a better homogeneity of temperatures in the heated medium. The lower electrode is connected to the ground and covered with a water bolus. The system is monitored by a microwave radiometer operating at 1 GHz in order to control the power delivered by a generator at 13.56 MHz ( up to 600 watts ). The radiometric antenna is then situated in a complex structure as shown on the figure below. This system allow the efficient treatment of large deep-seated tumors

In order to determine the electromagnetic field diagram in such a structure, the electric fields in the aperture of a microstrip-microslot applicator are first calculated using the bidimensional S.D.A. method. This results are then used in a bidimensional F.D.T.D. modelization : the originality of our model is that it can take into account all the components of the electromagnetic fields. Comparisons with simple structures have first allowed to validate this calculation technique. This method is now used to modelize the complex capacitive system where the active heating electrode contains an integrated radiometric antenna with a water bolus..



**SPECIAL SESSION AP-S/URSI B-7****TUESDAY AM****RADIATION AND SCATTERING FROM COMPLEX STRUCTURES  
(HONORING LEON PETERS, JR.)**

Chairs: C.A. Balanis, Arizona State University; J.L. Volakis, University of Michigan

Room: Modern Languages Building, Auditorium 1      Time: 8:30-11:30

|       |  |     |
|-------|--|-----|
| 8:30  | DR. LEON PETERS, JR.: ANTENNAS, RADAR CROSS SECTION, AND<br>BASEBALL<br><i>Thomas E. Tice, Arizona State University</i>  | 130 |
| 8:50  | RCS OF CORNER REFLECTORS USING GTD-UTD AND PO-PTD<br><i>Constantine A. Balanis, Arizona State University</i>   | 131 |
| 9:10  | CHARACTERIZATION OF WIRES AND NARROW GROOVES USING<br>TRAVELLING WAVE THEORY<br><i>J.L. Volakis*, A. Alexanian, The University of Michigan</i>                 | 132 |
| 9:30  | SCATTERING CENTER MODEL REPRESENTATION OF THE SCATTERED<br>FIELD FROM A COMPLEX TARGET<br><i>W.D. Burnside*, N. Tzeng, T. Chang, The Ohio State University</i> | 133 |
| 9:50  | RADIATION AND SCATTERING FROM COMPLEX STRUCTURES USING<br>FDTD<br><i>Raymond Luebbers, The Pennsylvania State University</i>                                   | 134 |
| 10:10 | BREAK  |     |
| 10:30 | ELECTROMAGNETIC SCATTERING AND RADIATION FROM "COMPLEX<br>BODIES"<br><i>A. Dominek*, J. Young, The Ohio State University</i>                                   | 135 |
| 10:50 | ELECTROMAGNETICS AND APPLICATIONS OF CORRUGATED SURFACES<br><i>R.B. Dybdal, The Aerospace Corporation</i>  | 136 |
| 11:10 | FEED DESIGN FOR REFLECTOR ANTENNAS WITH RECTANGULAR<br>APERTURES<br><i>Roger C. Rudduck, Leon Peters, Jr., The Ohio State University</i>                       | 137 |

Tue. a.m.

**DR. LEON PETERS, JR.:  
ANTENNAS, RADAR CROSS SECTION, AND BASEBALL**

Dr. Thomas E. Tice  
Department of Electrical Engineering  
Arizona State University  
Tempe, Arizona 85287-7206

and

Radar Branch, Code 755, RDT&E Division (NRaD)  
Naval Command, Control and Ocean Surveillance Center (NCCOSC)  
San Diego, California 92152-5223

The author had the pleasure of serving as the Graduate Faculty Advisor of Dr. Leon Peters, Jr. Since that time he has maintained a close professional and personal relationship with Dr. Peters. In this paper, the author will review some of the highlights in the career of Dr. Peters, both professional and personal. The author has had the privilege of following closely the professional growth of Dr. Peters from undergraduate student, to graduate student, to research leader, to professor, to Director of the ElectroScience Laboratory, to national and international stature. Professional highlights include antenna theory and measurements, prediction and measurement of the radar cross section of complex targets, practical applications of the geometrical theory of diffraction (GTD), scattering from plasma, RFI reduction, higher efficiency and reduced sidelobes from parabolic reflectors and horns, antenna camouflage principles, and applications of ultra-wide band transient radars to subsurface radar target imaging. Personal highlights include a warm personality, a charming wife, baseball, golf, and basketball. Professor Peters has advised nineteen Ph.D. students to completion and numerous M.Sc. students. His professional and personal life are an inspiration to all -- students, faculty, staff, and professional peers throughout the world. The author is honored to count Leon as an advisee and as a friend.

## RCS OF CORNER REFLECTORS USING GTD-UTD AND PO-PTD

Constantine A. Balanis  
Department of Electrical Engineering  
Telecommunications Research Center  
Arizona State University  
Tempe, AZ 85287-7206

Some of the simplest and notable radar targets are the dihedral and trihedral corner reflectors. These configurations enhance the radar cross section of the target, and they are often used as references to measure and compare the RCS of other configurations. In addition, corner reflectors form the basic building blocks of more complex targets. Because of their importance and attractive reflections characteristics, it is desirable to understand and be able to predict accurately their scattering characteristics. In this presentation, the azimuthal plane radar cross section of dihedral corner reflectors which have right, obtuse and acute included angles is examined using high-frequency techniques such as the geometrical-uniform theory of diffraction (GTD-UTD), physical optics combined with physical theory of diffraction (PO-PTD). Both vertical and horizontal polarizations are included, and predictions are compared with measurements.

GTD-UTD allow individual backscattering mechanisms of dihedral corner reflectors to be identified and provide good agreement with measurements. Multiple reflected and diffracted fields up to third order are included in the analysis. To provide accurate representation and prediction, higher order terms may be necessary for reflectors with smaller interior angles. The total cross section is decomposed into individual components which explicitly show the dominant scattering mechanisms at specific orientations. Understanding how the total cross section is built from individual mechanisms is very important for developing methods to reduce, enhance or synthesize particular backscatter characteristics of a particular target.

Physical optics combined with physical theory of diffraction (PO-PTD) provide an alternate method to determine the backscatter cross section of dihedral corner reflectors. The analysis incorporates single, double, and triple reflections; single diffractions; and reflection-diffractions. Two techniques are contrasted. In the first, geometrical optics is used in place of physical optics to account for initial reflections in order to reduce the complexity of the analysis. The objective is to avoid any surface integrations which cannot be performed in closed form. In the second method, physical optics is used in place of geometrical optics at nearly every reflection to maximize the accuracy at the expense of utilizing numerical techniques to perform many of the integrations. However this technique yields significant improvements.

Tue. a.m.

## CHARACTERIZATION OF WIRES AND NARROW GROOVES USING TRAVELING WAVE THEORY

John L. Volakis\* and Angelos Alexanian

Radiation Laboratory

Dept. of Electrical Engineering and Computer Science

University of Michigan

Ann Arbor, MI 48109-2122

In this presentation we review the importance and utility of traveling waves for a characterization of the radiation from and scattering by thin bodies. Published and unpublished work carried out by Professor Leon Peters, Jr and his co-workers at the Ohio State University ElectroScience Laboratory will be reviewed along with work performed by other engineers. Specific attention will be also given to some recent work by the authors in modeling coated wires and grooves using physical basis functions. These basis functions consist of three traveling waves and are used in constructing simple moment method or analytical solutions of the scattering and radiation by thin wires and narrow grooves. Comparisons with measured and other reference data, including those based on a finite element formulation, will be used to demonstrate that in spite of its simplicity, the traveling wave model generates results which are very accurate. This holds even for bodies whose length is less than a wavelength.

## SCATTERING CENTER MODEL REPRESENTATION OF THE SCATTERED FIELD FROM A COMPLEX TARGET

W. D. Burnside,\* N. Tzeng and T. Chang  
The Ohio State University  
ElectroScience Laboratory  
1320 Kinnear Road  
Columbus, Ohio 43212

The high frequency scattered field from a target has been analyzed for many years using asymptotic or diffraction techniques. These methods have been very successful for studying perfectly conducting conventionally shaped structures. As one attempts to control the first-order diffraction terms by shaping and adding materials, the high frequency analysis techniques have not been able to keep up in terms of the needed new solutions because of their complexity. Nonetheless, these methods have shown that the scattered field from a complex target can be represented by a finite set of scattering centers; i.e., corners, edges, specular reflections, etc. These same scattering centers have been observed in measured data through ISAR image techniques. In fact, this image domain data represents the complex scattering of a target in its simplest form. As a result, this paper illustrates how this scattering center image data can be used to provide the scattered field properties of the target in a most efficient manner. For example, the scattering center information for a very large target at a very high frequency needs to be recorded say every five degrees. Using this approach, it will be shown that one can represent the scattered field with a fraction of the data. In addition, the desired original scattering data can be reconstructed very rapidly, because very few data points are used to represent the total scattered field.

Tue. a.m.

## RADIATION AND SCATTERING FROM COMPLEX STRUCTURES USING FDTD

Raymond Luebbers  
Department of Electrical Engineering  
The Pennsylvania State University  
University Park, PA 16802

As computers become more powerful, applied electromagnetics has seen a tendency to rely more on computation and less on analysis. Perhaps the limiting case of this trend is the Finite Difference Time Domain (FDTD) method. In FDTD, the Maxwell curl equations are directly converted to finite differences and solved by marching through time. It is arguably the simplest possible approach to solving Maxwell's equations. There are no Green's functions, no boundary conditions to apply at material interfaces, no matrices, no asymptotics, no expansions, no basis functions. The only additions to the curl equations required for antenna/scattering applications are an outer boundary to absorb the radiated/scattered fields and a transformation of these fields to the far zone.

The process of converting the curl equations to finite differences produces a mathematical grid of cells. The constitutive parameters for each cell can be assigned independently. Therefore, within the spatial approximation inherent in the method, any shape and material can be included in the calculations without any change whatsoever in the finite difference equations. Thus the method can accommodate structures of arbitrary complexity, constrained only by computer memory and speed.

During the presentation, some examples of FDTD calculation of radiation and scattering from complex structures will be given. These examples will be used to point out the current state of FDTD development (K. S. Kunz and R. J. Luebbers, The Finite Difference Time Domain Method for Electromagnetics, CRC Press, 1993) and directions of future research and application.

**ELECTROMAGNETIC SCATTERING AND RADIATION FROM  
"COMPLEX BODIES"**

A. Dominek\* and J. Young  
The ElectroScience Laboratory  
Department of Electrical Engineering  
The Ohio State University  
Columbus, OH 43212

Aircraft or helicopter structures are classified as complex bodies due to the nature of electromagnetic interactions involved. However, in this case, the complexity addressed is not the object but the environment containing the object. The "complex" environment considered here is the air/ground interface and the underlying ground in a ground penetrating radar application. An integration of various components has to be engineered to realize a usable radar system. This integration has involved studies in three primary areas: (1) antennas, (2) propagation models and (3) scattering models. These areas have been developed with a mixture of analytical and experimental efforts. This presentation reviews the development of ground penetrating radar at the ElectroScience Laboratory. Presently, the ground penetrating radar research has provided excellent graduate study activities as well as practical and marketable products to commercial and industrial communities.

Tue. a.m.

## ELECTROMAGNETICS AND APPLICATIONS OF CORRUGATED SURFACES\*

R. B. Dybdal  
The Aerospace Corporation  
Communications Systems Subdivision

Corrugated surfaces have enjoyed substantial attention in controlling electromagnetic radiation. The history of corrugated surface analyses parallels the history of analytic electromagnetic techniques. The early treatments and appreciation of corrugated surface radiation properties were based on impedance concepts, transverse resonance solutions and the Weiner-Hopf formulations. With the growth of digital computing, moment method numerical techniques were applied to provide further insight and more accurate projections of corrugated surface performance.

With the exception of conducting surfaces, the corrugated surface arguably has had the most diverse range of applications. The earliest applications used corrugated surfaces in their propagating mode to control energy on open transmission lines and surface wave antennas. Far more prominent applications result when the corrugated surface is "cutoff" and rejects energy from the surface. The widely used corrugated horn uses cutoff surfaces to maintain hybrid modes with well known high efficiency and rotationally symmetric, low sidelobe patterns. Other applications include controlling the traveling waves on radar targets and maintaining low loss modes in closed waveguides.

This paper will review the development history of corrugated surfaces and their application. Specific attention will be given to the research involvement and contributions of Dr. Leon Peters, Jr., which include controlling the traveling wave modes on radar scatterers, the corrugated horn, closed waveguide designs, and detailed analyses of their radiation properties using moment method techniques.

## FEED DESIGNS FOR REFLECTOR ANTENNAS WITH RECTANGULAR APERTURES

Roger C. Rudduck\* and Leon Peters, Jr.  
The Ohio State University  
ElectroScience Laboratory  
1320 Kinnear Road  
Columbus, OH 43212

Since the 1960's, corrugated horns have found widespread use as feeds for reflector antennas. The circularly symmetric pattern with low sidelobes, characteristic of conical corrugated horns, is very useful for circular reflectors, either direct-fed or dual reflectors. For rectangular apertures with a low aspect ratio (maximum to minimum aperture dimension), ordinary rectangular corrugated horns can compensate for the aspect ratio. For apertures with aspect ratios of 3:1 or more, the required horn flare angles are substantially different in the two principal planes. This difference results in a substantial difference in the phase center locations for each plane. Consequently, the uniform phase pattern desired for paraboloidal reflectors cannot be achieved within a reasonable accuracy.

The purpose of this paper is to discuss ways to design feeds for non-shaped main reflector surfaces with rectangular apertures that have high aspect ratios. One approach is to use a double-flare horn with a wider flare angle for the smaller horn aperture dimension. Another approach is to use an ordinary rectangular corrugated horn in conjunction with a subreflector that has a parabolic cylindrical surface. Calculated amplitude and phase patterns demonstrate the validity of these approaches.



**SESSION URSI B-8****TUESDAY AM****TIME DOMAIN METHODS III**

Chairs: A.W. Glisson, University of Mississippi; A. Taflove, Northwestern University

Room: Modern Languages Building, Auditorium 2

Time: 8:30-12:10

|       |   |     |
|-------|---|-----|
| 8:30  | APPLICATION OF FINITE-VOLUME TIME-DOMAIN METHOD TO PRINTED CIRCUITS AND ANTENNAS<br><i>A.H. Mohammadian*, V. Shankar, W.F. Hall, Rockwell International Science Center</i>  | 140 |
| 8:50  | COMBINING THE FD-TD ALGORITHM WITH AR MODEL TO ANALYZE THE MICROSTRIP PROBLEMS<br><i>Ji Chen, Chen Wu, Keli Wu, John Litva, McMaster University</i>   | 141 |
| 9:10  | FD-TD CALCULATIONS OF THE SCATTERING OF FEMTOSECOND ELECTROMAGNETIC SOLITONS IN 2-D DIELECTRIC WAVEGUIDES<br><i>Rose Joseph, Northwestern University; Peter Goorjian, NASA Ames Research Center; Allen Taflove, Northwestern University</i> | 142 |
| 9:30  | FD-TD MODELING OF DIGITAL SIGNAL PROPAGATION IN 3-D MICROSTRIP CIRCUITS WITH PASSIVE AND ACTIVE LOADS<br><i>Melinda Piket-May, John Baron, Allen Taflove, Northwestern University</i>   | 143 |
| 9:50  | FD-TD MODELING OF ELECTRICALLY LARGE 3-D STRUCTURES WITH THE CRAY EMDS SOFTWARE PACKAGE<br><i>Daniel S. Katz, Melinda Piket-May, Allen Taflove, Northwestern University</i>   | 144 |
| 10:10 | BREAK   |     |
| 10:30 | THE APPLICATION OF FINITE-DIFFERENCE TIME-DOMAIN METHOD WITH AUTOREGRESSIVE TECHNIQUE TO DESIGN THE RECTANGULAR COAXIAL LINE COMPONENTS<br><i>Chen Wu, Keli Wu, John Litva, McMaster University</i>   | 145 |
| 10:50 | FDTD SIMULATION OF MICROWAVE SINTERING IN SINGLE- AND MULTIMODE CAVITIES<br><i>M.F. Iskander, D. Roper, L. Walsh, T. Ngo, University of Utah; H. Kimrey, Oak Ridge National Laboratory</i>  | 146 |
| 11:10 | CONFORMAL FDTD MODELING OF HIGH POWER INPUT COUPLERS<br><i>M.B. Newman, P.L.E. Uslenghi, University of Illinois at Chicago; T.G. Jurgens, F.A. Harfoush, Fermi National Accelerator Laboratory</i>  | 147 |
| 11:30 | TIME DEPENDENT WAVE ENVELOPE FINITE DIFFERENCE ANALYSIS OF DIELECTRIC SLABS<br><i>Tatsuya Kashiwa, Ichiro Fukai, Hokkaido University</i>  | 148 |
| 11:50 | ELECTROSTATIC FIELD SOLUTIONS USING FDTD<br><i>Karl S. Kunz*, Lee Marshall, Pennsylvania State University</i>   | 149 |

## APPLICATION OF FINITE-VOLUME TIME-DOMAIN METHOD TO PRINTED CIRCUITS AND ANTENNAS

A. H. Mohammadian\*, V. Shankar, and W. F. Hall  
Rockwell International Science Center  
1049 Camino Dos Rios  
Thousand Oaks, California 91360

This paper addresses the application of the finite-volume time-domain (FVTD) method to the design of printed circuits and antennas. The FVTD method for solving Maxwell's equations of electromagnetics was developed by the present authors to compute the radar cross section of large aerospace configurations. A computer code known as CFDEM has been written based on the FVTD algorithm which uses zonal division with a body-fitted grid in each zone. It can handle both two and three dimensional objects with any degree of complexity. The capabilities of the code include treatment of frequency- and time-dependent materials, resistive sheets, impedance surfaces, and pulse as well as time-harmonic excitations. The algorithm, which originally came from computational fluid dynamics, has been improved over the last few years in order to address the issues peculiar to electromagnetics. These include an improved boundary condition algorithm on conducting surfaces that maintains second order accuracy, an accurate transition condition at the interface between two dielectric media with large contrast between their dielectric constants, and proper treatment for tips, edges, and corners.

In the past on certain occasions, we have used our method to investigate radiation problems such as open-ended parallel plate waveguides, two-dimensional horns, and open-ended and edge-slotted rectangular waveguides. Recently, we have revisited the subject with more defined objectives. It is our intent here to give a progress report on the application of the FVTD method to various printed circuits and antennas. Printed circuits and antennas in the microwave and millimeter wave ranges can have complex structures with several layers of dielectric materials, electromagnetic coupling among various patches, coaxial feeds, etc. Accurate prediction of mutual coupling in printed arrays and crosstalk among neighboring circuits are nontrivial matters that require a full wave solution of Maxwell's equations such as the FVTD method provides. Frequency-domain integral equation methods leading to a method of moments solution have been widely used in the past. But as the structure of these circuits and antennas become more complex, it becomes very cumbersome to formulate appropriate integral equations, let alone solve them.

Issues contributing to accurate solution for printed circuits and radiators from the FVTD method point of view will be discussed. Results of the simulation of a patch antenna, including resonance frequency and radiation pattern will be shown. Also, results for mutual coupling between two patch antennas will be presented. Simulations for a branch line coupler and a filter will be among the results that will be discussed in the talk.

## Combining the FD-TD algorithm with AR model to analyze the microstrip problems

Ji Chen, Chen Wu, Keli Wu, John Litva

Communications Reserach Laboratory, McMaster University  
Hamilton, Ontario, L8S 4K1, Canada

The Finite-Difference Time-Domain (FD-TD) method has been widely used to solve electromagnetic problems. It has been shown to give very accurate results for simulation of very complex structure. With the use of absorbing boundary conditions, it can be successfully used to simulate microstrip problems. However, to obtain accurate frequency response, the computation time is tremendous. So it is still hard to be implemented in the software. In this paper, a signal processing technique, auto-regressive (AR) method, is used to reduce the computation time. Compared with the experimental results, good agreement is obtained.

In order to extract the microstrip parameter efficiently, some consideration is still needed.

- Select the segment of FD-TD result that best reflects the characteristics of the structure been analyzed. The beginning of this segment coincides with the instant at which the launched pulse is reflected back from the farthest extremity.
- resample the FD-TD data since FD-TD algorithms usually oversamples the data necessary for implementing AR method.
- Low band pass fileter is used to process the resampled data since the higher frequency is beyond our interesting and it is also difficult to model.

Several sets of examples using AR + FD-TD algorithm is given. With the great reduction in computation time, FD-TD becomes more practical in the microstrip problems.

## FD-TD Calculations of the Scattering of Femtosecond Electromagnetic Solitons in 2-D Dielectric Waveguides

Rose Joseph<sup>1</sup>, Peter Goorjian<sup>2</sup> and Allen Taflove<sup>1</sup>

<sup>1</sup>EECS Department, McCormick School of Engineering,  
Northwestern University, Evanston, Illinois 60208-3118

<sup>2</sup>NASA-Ames Research Center, Mail Stop 202A-2, Moffett Field, CA 94035-1000

Experimentalists have produced all-optical switches capable of 100-fs responses. To adequately model such switches, nonlinear effects in optical materials (both instantaneous and dispersive) must be included. In principle, the behavior of electromagnetic fields in nonlinear dielectrics can be determined by solving Maxwell's equations subject to the assumption that the electric polarization has a nonlinear relation to the electric field. However, until our previous work [1, 2], the resulting nonlinear Maxwell's equations have not been solved directly. Rather, approximations have been made that result in a class of generalized nonlinear Schrodinger equations (GNLSE) that solve only for the *envelope* of the optical pulses.

2-D and 3-D engineered inhomogeneities in nonlinear optical circuits will likely be at distance scales in the order of 0.1 - 10 optical wavelengths, and all assumptions regarding slowly-varying parameters (which run throughout GNLSE theory) will be unjustified. For such devices, optical wave scattering and diffraction effects relevant to integrated all-optical switches will be difficult or impossible to obtain with GNLSE because its formulation discards the optical carrier. The only way to model such devices is to retain the optical carrier and solve Maxwell's vector-field equations for the material geometry of interest, rigorously enforcing the vector-field boundary conditions and the physics of nonlinear dispersion at the time scale of the carrier.

In this paper, we present first-time calculations from the vector nonlinear Maxwell's equations of femtosecond soliton propagation and scattering, including carrier waves, in two-dimensional systems of dielectric waveguides exhibiting the Kerr and Raman quantum effects. We use the finite-difference time-domain (FD-TD) method in an extension of our 1-D work (P. M. Goorjian and A. Taflove, *Optics Letters* 17, 180-182, Feb. 1, 1992; P. M. Goorjian, A. Taflove, R. M. Joseph and S. C. Hagness, *IEEE J. Quantum Electronics* 28, 2416-2422, Oct. 1992.) There, in a fundamental innovation, we treated the linear and nonlinear convolutions for the electric polarization as new dependent variables. By differentiating these convolutions in the time domain, we derived an equivalent system of coupled, nonlinear second-order ordinary differential equations (ODE's). These equations together with Maxwell's equations form the system that is solved to determine the electromagnetic fields in inhomogeneous nonlinear dispersive media. Backstorage in time is limited to only that needed by the time-integration algorithm for the ODE's (2 time steps), rather than that needed to store the time-history of the kernel functions of the convolutions (1000 - 10,000 time steps). Thus, a 2-D nonlinear optics model from Maxwell's equations is now feasible.

By retaining the optical carrier, the new method solves for *fundamental quantities* - the optical electric and magnetic fields in space and time - rather than a nonphysical envelope function. It has the potential to provide an unprecedented 2-D and 3-D modeling capability for millimeter-scale integrated optical circuits having sub- $\mu\text{m}$  engineered inhomogeneities. To illustrate the power of our new approach, we report a set of Cray supercomputer results and visualizations for the dynamics of optical solitons in such 2-D geometries as coupled and crossing dielectric waveguides.

## FD-TD Modeling of Digital Signal Propagation in 3-D Microstrip Circuits with Passive and Active Loads

Melinda Piket-May, John Baron and Allen Taflove

EECS Department

McCormick School of Engineering

Northwestern University

Evanston, Illinois 60208-3118

Most existing computer-aided design tools (primarily SPICE) are limited when digital clock speeds exceed 100 - 200 MHz. These tools do not deal with the physics of UHF and microwave electromagnetic wave energy transport along metal surfaces such as ground planes, or in the air away from metal paths, that are common above this frequency range. Effectively, high-speed electronic digital systems develop substantial analog wave effects when clock rates are high enough, and full-vector (full-wave) Maxwell's equations solvers become necessary to understand these systems.

In this paper, we first discuss models of microstrips in three dimensions using FD-TD. Parameters such as complex line impedance, propagation constant, capacitance per unit length and inductance per unit length can be easily computed as a function of frequency. We shall consider infinitely thin microstrips, finite-thickness microstrips, free-space and dielectric embedding, and multiple microstrips for even and odd mode excitation.

More important, this paper next discusses FD-TD Maxwell's equations computational modeling of lumped-circuit loads and sources in 3-D, including resistors, capacitors, inductors, voltage and current sources, diodes and transistors. We are especially interested in simulating the large-signal behavior of nonlinear logic devices in the context of the full-vector electromagnetic field. In fact, we propose that digital circuit analysis from Maxwell's equations is the *logical successor* to SPICE-like models. We believe that a synthesis of electromagnetic fields and waves and electronic circuit devices will be necessary to obtain engineering understanding of ultra-high-speed digital systems, including multilayer circuit boards and multichip modules. In such systems, the electromagnetic waves generated by digital bit streams may wash over the active devices somewhat like the surf splashing past stones on a beach.

## FD-TD Modeling of Electrically Large 3-D Structures With the Cray EMDS Software Package

**Daniel S. Katz, Melinda Piket-May and Allen Taflove**

EECS Department

McCormick School of Engineering

Northwestern University

Evanston, Illinois 60208-3118

This paper describes the EMDS (*ElectroMagnetic Design System*) software package that we have developed in collaboration with Cray Research, Inc. EMDS implements conformal curved-surface FD-TD modeling of electromagnetic wave interactions with electrically large 3-D structures of complex shape. EMDS aims to minimize computational burdens by using an almost-completely-structured FD-TD mesh, with rectangular Yee cells everywhere except for the relatively few finite-volume stretched or cut cells adjacent to the target surface. It allows the user to rapidly specify complicated structures via the General Dynamics ACAD (Advanced Computer Aided Design) system, or import appropriate files from other CAD systems. And, using Cray's MPGS (*Multipurpose Graphics System*), it provides tools to visualize the dynamics of electromagnetic wave scattering and surface current flow via color animations.

A number of examples will be presented which provide validations of EMDS modeling for perfectly electrically conducting 3-D targets. These will include the double sphere (validated versus generalized multipole theory) and the NASA almond (validated versus measurements). EMDS results for a complete General Dynamics fighter aircraft prototype will be shown and compared to scale-model scattering measurements (if the latter are available in time for this symposium).

This paper will also discuss EMDS modeling of metal scatterers with thin, high-density dielectric layers and coatings. To avoid the numerical storage, running time and stability problems experienced in directly resolving these thin layers, a "smart-cell" strategy is used wherein a surface impedance boundary condition is applied at the finite-volume stretched or cut cells adjacent to the target surface. For this case, validations will be provided for canonical 2-D and 3-D curved target shapes.

Tue. a.m.

The Application of  
Finite-Difference Time-Domain Method with  
Autoregressive Technique  
to Design  
the Rectangular Coaxial Line Components

Chen Wu, Keli Wu and John Litva  
Communications Research Laboratory, McMaster University,  
Ontario, Canada, L8S 4K1

Abstract

The Rectangular Coaxial Line (RCL) is a very attractive configuration and has been widely used in the microwave circuits, especially for beam forming network (BFN) in the satellite communications. In this paper, the Finite-Difference Time-Domain (FD-TD) method is used as a full wave analysis tool in design RCL components to achieve the stringent requirements for BFN. The Autoregressive Spectrum Estimation Technique (AR model) is used to raise the efficiency of the FD-TD method.

The typical RCL components, such as RCL step discontinuity, T-junction and coupler, are analyzed or designed. All the results obtained by the FD-TD method have very good agreements with measured results and also successfully meet design requirements. The results show that the AR model can greatly improve in efficiency of the FD-TD method and is very robust to process the data given by FD-TD method.

Tue. a.m.

## FDTD SIMULATION OF MICROWAVE SINTERING IN SINGLE- AND MULTIMODE CAVITIES

M. F. Iskander, D. Roper, L. Walsh, T. Ngo, and H. Kimrey\*

Electrical Engineering Department  
University of Utah  
Salt Lake City, UT 84112

\*Oak Ridge National Laboratory  
Oak Ridge, TN 37831

Microwave drying of polymers, sintering of ceramics, and processing of hazardous waste has been recognized as an emerging technology and is being critically evaluated by the National Materials Research Board of the National Research Council. Uniform and fast heating, improved microstructure, and in some cases the development of unique material properties are among the cited benefits from using microwaves instead of conventional heating.

Significant progress has been made towards the evaluation of the microwave technology and in assessing its potential commercial use. The majority of these efforts, however, have been experimental, which is expensive, time consuming, and, in many cases, sufficiently complex and often obscure the value of the obtained results. Our group at the University of Utah developed an FDTD code to simulate microwave sintering in single- and multimode cavities. The main objective of these simulation efforts is to identify crucial parameters involved and help guide the experimental procedures towards the routine implementation and possible optimization of the microwave sintering procedure.

In this paper, we briefly describe the FDTD simulation procedure in both single- and multimode cavities. In the single-mode cavity case, issues such as the variation in resonance frequency vs. sample size and properties, maximum sample size in a given cavity, and the effect of variation of material properties during heating on the resonant frequency and Q of the cavity are of interest. In the multimode heating, on the other hand, uniformity of field distributions and the role of the SiC rods in stimulation the sintering process are of prime interest. An experimental procedure which we used in multimode cavities to verify the results from the FDTD code will also be discussed. Results showing selection criteria for compatible samples and insulation materials, appropriate number and distribution of SiC rods to effectively stimulate sintering in multimode cavities, and guidelines for selecting the number, size, and arrangement of samples in multiple-sample sintering will be presented. Critical values of input microwave power that would eliminate the need for the SiC rods are also examined as a function of sample size, dielectric properties, and the size and properties of the surrounding insulation.

## CONFORMAL FDTD MODELING OF HIGH POWER INPUT COUPLERS

M. B. Newman and P. L. E. Uslenghi

*University of Illinois Chicago  
Chicago, Illinois 60680*

T. G. Jurgens and F. A. Harfoush  
*Fermi National Accelerator Laboratory  
Batavia, Illinois 60510*

High power klystrons are used to power particle accelerators. The energy is propagated from the klystron to the accelerating cavities via various guiding structures. In general the guiding structure is not evacuated. Ceramic windows are used in the input couplers of superconducting and conventional accelerating cavities to separate the evacuated cavity side of the structure from the source side which is under normal pressure. The window may also be subject to a temperature gradient in the case of superconducting cavities. These cavities are made of a niobium alloy and are cooled to the temperature of liquid helium.

Here we are interested in maximizing the coupling of electromagnetic fields and determining points of high fields in the ceramic. These high field points can fracture the ceramic window and is a serious problem in the design of input couplers. Since pulsed power is used to drive the cavities, a time domain analysis is used to obtain both transient and steady state responses.

This presentation reports on the extension of the contour finite difference time domain (CFDTD) algorithm for the modeling of electromagnetic fields found in high power guided wave structures. Included in this report is a description of a two dimensional cylindrically symmetric formulation of the CFDTD method. This formulation is based on the cylindrical representation of Ampere's and Faraday's laws rather than the cylindrical Maxwell curl equations. Methods for dealing with the coordinate system singularity at the origin as well as other issues not found in a cartesian formulation are discussed. Where ever possible numerical results will be compared to measured data.

## Time Dependent Wave Envelope Finite Difference analysis of dielectric slabs

Tatsuya Kashiwa, member, IEEE, and Ichiro Fukai, member, IEEE

Department of Electrical Engineering,  
Hokkaido University, Sapporo, 060 Japan

In this paper, the time dependent wave envelope finite difference approach is proposed to analyze the dielectric slabs. K. J. Baumeister have proposed the time dependent wave envelope finite difference approach for the analysis of sound propagation in scalar form (AIAA Journal, vol. 24, no.1, pp. 32-38, 1986). In this paper, this scheme is reformulated in vector form. The electromagnetic fields are described by;

$$E_y(x, y, z, t) = e_y(x, y, z, t) \exp(j\beta z) \quad (1)$$

$$H_x(x, y, z, t) = h_x(x, y, z, t) \exp(j\beta z) \quad (2)$$

where the  $E_y$  and  $H_x$  are the usual electromagnetic field quantities. The value  $\beta$  expresses the propagation constant in the  $z$  direction. By substituting these equations to Maxwell's equations, the following are obtained;

$$\partial e_y(x, y, z, t) / \partial t = \partial h_x(x, y, z, t) / \partial z + j\beta h_x(x, y, z, t) \quad (3)$$

$$\partial h_x(x, y, z, t) / \partial t = \partial e_y(x, y, z, t) / \partial z + j\beta e_y(x, y, z, t) \quad (4)$$

These equations are discretized by the usual finite difference scheme. Eqs.(3) and (4) show that the method can be considered as the expansion of the traditional FD-TD approach, associated with  $e_y$  and  $h_x$ . If  $\beta$  corresponds to the true propagation constant, waveforms of  $e_y$  and  $h_x$  coincide with the envelopes of the electromagnetic field distributions. Even if  $\beta$  is not a true propagation constant, the envelopes of  $e_y$  and  $h_x$  correspond to those of  $E_y$  and  $H_x$ . As the spatial frequency in the propagation direction is modulated by  $\beta$ , the real spatial frequency is shifted in the positive direction by  $\beta$ . That is, high spatial frequencies are transformed to low spatial frequencies. Consequently, the required amount of discretization in the  $z$  direction becomes significantly small compared with that necessary in the usual FD-TD approach which uses a direct discretization scheme. In this approach, there is no need to know the precise propagation constants and coupling constants of the component in advance, unlike in the coupled mode method. The method can be used when the reflection is small. Consequently, the method can be applied to the analysis of, for example, the weakly coupled optical directional coupler.

**Electrostatic Field Solutions Using FDTD**

Karl S. Kunz\* and Lee Marshall

Electrical Engineering Department

Pennsylvania State University

The finite difference time domain (FDTD) technique is normally employed to obtain the response of an interaction object to a transient excitation. The response can be found over a broad frequency regime a few decades above and below the first resonance. When the excitation is sinusoidal and at very low frequencies, such as 60 Hz, FDTD is not employed for interaction objects such as airplanes because of the excessively long run times required. Hence FDTD is not thought of as a low frequency tool and certainly not a tool for finding electrostatic solutions.

We have found this not to be true for electrostatics. Using two cubical metal blocks separated by a gap equal to their own dimensions a crude estimate to the static field distribution was enforced on the geometry. It was a uniform E field distribution between the adjacent faces of the two cubes. Starting with this initial distribution at time zero in the FDTD code the field was advanced in time according to the Maxwell equations. A color film made of a 2D slice through the problem space showed much of the initial field being radiated away. Rather rapidly the field distribution reached steady state leaving the electrostatic field clearly evident. What was seen was the initial distribution, which is composed of a static mode and higher radiative modes decaying to only the static mode.



**SESSION URSI B-9****TUESDAY AM****INTEGRAL EQUATION METHODS I**

Chairs: E.K. Miller, Los Alamos National Laboratory  
G. Klaus, Swiss Federal Institute of Technology

Room: Modern Languages Building, Lecture Room 2      Time: 8:30-12:10

|       |   |     |
|-------|---|-----|
| 8:30  | SPURIOUS MODES IN VECTOR ELECTROMAGNETIC EIGENVALUE PROBLEMS: A LOOK AT SEVERAL REMEDIES<br><i>Andrew F. Peterson, Georgia Institute of Technology</i>  | 152 |
| 8:50  | PHYSICAL OPTICS HYBRID METHOD (POHM) MODELLING OF LARGE COMPLEX BODIES INCLUDING DIELECTRIC SHEETS<br><i>Richard E. Hodges*, Yahya Rahmat-Samii, University of California, Los Angeles</i>  | 153 |
| 9:10  | A MOMENT METHOD SCHEME FOR THE ANALYSIS OF SCATTERING AND RADIATION PROBLEMS OF BODIES MODELLED BY MESHS OF NURBS AND BEZIER SURFACES<br><i>Fernando Rivas*, Luis Valle, M. Felipe Catedra, Universidad de Cantabria</i>                    | 154 |
| 9:30  | A THREE-DIMENSIONAL METHOD OF MOMENTS SURFACE SCATTERING CODE USING A SAMPLING-THEORETIC CURRENT EXPANSION<br><i>G.E. Mortensen*, C.C. Cha, T.G. Krauss, Syracuse Research Corporation</i>  | 155 |
| 9:50  | THE SPATIAL BANDWIDTH OF INDUCED CURRENTS AND IMPLICATIONS IN THE METHOD OF MOMENTS<br><i>G.E. Mortensen*, C.C. Cha, D.L. Wilkes, Syracuse Research Corporation</i>   | 156 |
| 10:10 | BREAK   |     |
| 10:30 | A SIMPLE AND ACCURATE TECHNIQUE FOR THE ANALYSIS OF COUPLED TAPERED LINES IN THE MOMENT METHOD<br><i>G.E. Howard*, The University of British Columbia, Y.L. Chow, University of Waterloo</i>  | 157 |
| 10:50 | ELECTROMAGNETIC SCATTERING ANALYSIS OF ARBITRARILY SHAPED THIN METALLIC PLATES USING MOMENT METHOD<br><i>M.D. Deshpande*, Vigyan Inc.; C.R. Cockrell, F.B. Beck, NASA Langley Research Center; T.X. Nguyen, Research Triangle Institute</i> | 158 |
| 11:10 | CALCULATION OF TRANSMISSION LINE PARAMETERS USING THE BOUNDARY ELEMENT METHOD<br><i>R. Remmert, University of Paderborn; W. John, E. Griese, Siemens Nixdorf Informationssysteme AG; M. Vogt, University of Paderborn</i>                   | 159 |
| 11:30 | FORMULATION AND APPLICATION OF A HYBRID NUMERICAL - ASYMPTOTIC INTEGRAL EQUATION TECHNIQUE<br><i>Keith R. Aberegg*, Andrew F. Peterson, Georgia Institute of Technology</i>   | 160 |
| 11:50 | THE APPROXIMATION PROPERTY OF THE EXTENDED BOUNDARY ELEMENT SPACE<br><i>Song Guoxiang*, Xidian University; Qi Yihong, Southeast University</i>  | 161 |

## SPURIOUS MODES IN VECTOR ELECTROMAGNETIC EIGENVALUE PROBLEMS: A LOOK AT SEVERAL REMEDIES

Andrew F. Peterson  
School of Electrical Engineering  
Georgia Institute of Technology  
Atlanta, GA 30332-0250

Since vector formulations for the numerical analysis of dielectric-loaded waveguide structures were first investigated two decades ago, the most difficult obstacle to overcome has been the appearance of spurious eigenvalues. Vector formulations for scattering and radiation problems involve a matrix operator that is similar to that used for waveguide analysis, and are also expected to encounter difficulties. Although the spurious eigenvalues are known to be associated with the nullspace of the curl-curl operator, discretization schemes that attempt to properly model the equation are not always completely successful. Proposed methods include the so-called penalty function approach, several different ways of numerically enforcing zero divergence throughout the region of interest, and the use of special vector "edge elements." Although all of the proposed remedies seem to provide some relief from the problem, none completely eliminate it without an increase in computational cost and complexity.

In this presentation, the "spurious mode" problem and several remedies will be described and illustrated through numerical examples. The penalty function approach, which is probably the most widely-used remedy for waveguide applications, does not actually eliminate spurious eigenvalues. Several of the other remedies seem to eliminate spurious eigenvalues for waveguide problems, but can not be easily adapted for radiation and scattering applications. Vector basis functions (edge elements) satisfying the Nedelec constraints (J. C. Nedelec, *Numer. Math.*, vol. 35, pp. 315-341, 1980) are successful at separating the spurious eigenvalues from the desired set, but do not eliminate them. Details of the construction of vector basis functions for linear and quadratic order will be presented. Other types of edge elements in use do not conform to the Nedelec spaces and only provide partial relief from the spurious mode problem.

## PHYSICAL OPTICS HYBRID METHOD (POHM) MODELLING OF LARGE COMPLEX BODIES INCLUDING DIELECTRIC SHEETS

Richard E. Hodges\* and Yahya Rahmat-Samii

Department of Electrical Engineering

University of California, Los Angeles

Los Angeles, CA 90024-1594

Dielectric sheets are commonly used in microwave antenna applications such as aircraft radomes, wind screens, covers for aperture antennas and dielectric windows. These dielectrics can have a significant effect on the radiation patterns of a microwave system. Thus, a practical method of analysis is needed for problems involving radiators mounted on (or near) complex bodies which may include both conductors and dielectrics. In principle, one may obtain accurate results with the Method of Moments (MM), but the method is only applicable for objects smaller than a few wavelengths. The Physical Optics Hybrid Method (POHM), a technique which combines the strengths of Physical Optics and the Moment Method, has previously been shown to provide an accurate analysis of electromagnetic radiation in the presence of large complex conducting bodies. Also, it has been found that Dielectric Physical Optics can adequately characterize the scattering from relatively large stratified dielectric sheets. This suggests that POHM may be extended to include both conductors and dielectric sheets.

This paper presents an overview of our work on extending POHM to include layered dielectric sheets in the analysis of large complex radiation problems. In this approach, the PO analysis of both conductors and dielectrics is introduced as a means of approximating the Moment Method matrix equations. Thus, the presence of bodies approximated by PO is properly accounted for in the matrix equation used to solve for currents in the MM region. This results in good accuracy for both radiation patterns and input impedance. An overview of the theory will be given. In addition, potential cost savings from *zero order* and *first order* approximations of the dielectric PO analysis are discussed.

Several examples are given to establish the accuracy and limitations of the dielectric POHM analysis. For reasons of practicality, accuracy checks comparing pure Moment Method results and POHM are made for a two-dimensional structure. This includes multi-element line source radiators mounted on a finite ground plane with dielectric skirts. In addition, example calculations for a three-dimensional geometry demonstrate the potential of this technique for problems such as multi-element wire antennas mounted on curved finite ground constructed with a combination of conductors and dielectrics.

A MOMENT METHOD SCHEME FOR THE ANALYSIS  
OF SCATTERING AND RADIATION PROBLEMS OF BODIES  
MODELED BY MESHES OF NURBS AND BEZIER SURFACES

Fernando Rivas\*, Luis Valle, M. Felipe Cátedra  
Departamento de Electrónica  
Universidad de Cantabria  
39005-SANTANDER, SPAIN

Meshes by simple elements (triangles, polygonal plates, parallelepipeds, tetrahedrals) are used by electromagnetic computational methods like Finite Element (FE), Finite Difference - Time Domain (FD-TD) and Moment Methods (MM). These meshes are commonly obtained from precise geometrical models of the bodies using some pre-processing software. The precise geometrical models are generated in the industries by using Computer Aided Geometrical Design (CAGD) tools which provides representations of the bodies by meshes of NURBS (Non-Uniform Rational B-Splines) surfaces. Although a mesh of NURBS elements is the best tools to generate and to store the surface of an arbitrary body, it is better to obtain a new mesh based in Bézier patches for the rendering and for the numerical treatment of the surface. It is quite easy and fast to obtain the Bézier mesh from the data of a representation by NURBS by applying the Cox-de Boor's transformation algorithm. Bézier patches allow a quite accurate and efficient representation of complex bodies using only a small number of them, (for instance a complete aircraft can be modeled using a mesh with several hundreds of Bézier patches).

In this communication a MM approach to solve scattering and radiation problems using directly Bézier meshed is presented. The approach is a precise and powerful tools because, avoiding the re-meshing by simple elements, complex shaped bodies are treated exactly by using a few number of MM unknowns.

In the approach a surface Mixed Potential Electrical Field Integral Equation is solved. New basis functions have been developed. These functions can be considered as a generalization of the "rooftops" functions introduced by Wilton: a basis function is associated to each one of the boundary lines between pairs of Bézier patches, each basis function spread only over the surfaces of the patches that shares the common boundary line, and in each one of these surface the divergence of the basis function (the charge density) is constant. As testing functions we have considered "Razor-Blades", defined over the isoparametric curve lines which joins the centres of the Bézier patches of the pair associated to each basis function. Special basis functions has been developed to treat the join of a wire antenna to a Bézier patch.

Results of current distributions and scattering and radiation parameters for different geometries will be presented. From the convergence studies performed and from the comparisons with results obtained by others methods or measurements it can said that the scheme appears to be efficient and accurate.

## A THREE-DIMENSIONAL METHOD OF MOMENTS SURFACE SCATTERING CODE USING A SAMPLING-THEORETIC CURRENT EXPANSION

*G.E. Mortensen\*, C.C. Cha, and T.G. Krauss*  
Syracuse Research Corporation

*Merrill Lane  
Syracuse, NY 13210*

In this paper a three-dimensional method of moments (MOM) surface scattering code is described which uses a current expansion based on the concepts of sampling theory. We present results which show that in many cases this code requires significantly fewer unknowns to achieve a given RCS accuracy than an equivalent code using the common Rao-Wilton-Glisson (RWG) basis functions.

We briefly summarize previous results which demonstrate that the induced surface current is generally quasibandlimited (most of the energy in the spatial frequency spectrum of the current is confined to some finite interval) and that sampling theory leads to an efficient expansion for quasibandlimited currents. We then extend these results to an implementation for general three-dimensional parametric surfaces. The surface basis functions used are truncated (finite domain) two-dimensional sampling functions in the parametric space used to define the target geometry. The properties of sampling functions such as the sinc function and self-truncating (ST) sampling function are compared to those of triangle and pulse basis functions. The effects of truncating the sampling functions on solution accuracy and convergence is discussed.

Implementation issues such as potential and testing integration and surface edge boundary conditions will be addressed. Target geometry parameterization and its effect on the solution will be discussed. It is demonstrated that use of the sampling-theoretic basis functions increases the matrix fill time per unknown, but that the reduction in the matrix size can result in substantially reduced total computation time for moderate to large problems.

We present results of the MOM code for targets of various sizes and geometries. RCS curves, matrix sizes, and timing results are compared to results from a well-validated MOM code with RWG basis functions.

## THE SPATIAL BANDWIDTH OF INDUCED CURRENTS AND IMPLICATIONS IN THE METHOD OF MOMENTS

*G.E. Mortensen\*, C.C. Cha, and D.L. Wilkes  
Syracuse Research Corporation*

*Merrill Lane  
Syracuse, NY 13210*

The number of unknowns required for an accurate method of moments (MOM) scattering solution is driven by the spatial bandwidth of the induced current. Sampling theory places a lower bound (in the absence of additional information) on the number of expansion functions required to guarantee an exact expansion of a bandlimited current, and provides guidance on reaching that bound.

We have recently developed an approach to MOM which provides close to optimal expansion efficiency while retaining many of the advantages of common subdomain expansions. In order to utilize this approach effectively, a good estimate of the current spatial bandwidth in the current expansion domain is required. In this paper we discuss the current spatial frequency spectra of arbitrary wires and surfaces and present results to illustrate the current characteristics for a variety of target geometries. We show that in general induced currents are quasibandlimited; i.e. that most of the spectral energy is confined to some lowpass band. Methods for analyzing and measuring spatial bandwidth on wires and surfaces are discussed. The effects of geometrical parameterization on the measured apparent bandwidth are also discussed. The effects of length, radius, and curvature on the induced currents of wire targets will be demonstrated. The effects of overall target size, curvature, bends, apertures, and sharp edges on induced surface currents of three-dimensional targets will be demonstrated.

We show, via a thin wire code, that the MOM results using the sampling theoretic approach are consistent with the bandwidth findings and that accurate results may be obtained with a sampling rate only slightly higher than the spatial bandwidth cutoff.

## A Simple and Accurate Technique for the Analysis of Coupled Tapered Lines in the Moment Method

G.E. Howard\* and Y.L. Chow

Department of Electrical Engineering, The University of British Columbia  
Department of Electrical and Computer Engineering, University of Waterloo

### Abstract

A simple and efficient tapered line model for use in the moment method is introduced. The model accounts for the taper in a continuous manner for accuracy. The model also accounts for mutual coupling in an analytic fashion for speed and simplicity.

Recently digital circuit board design has progressed to designs which can have signals with significant frequency content up to 10's of Gigahertz. Due to such high frequencies, and the tendency for the frequencies to go higher, accurate electromagnetic characterization of these structures is necessary. In digital circuit boards, the tapered line plays an important role in bringing the interconnect lines of the printed circuit board to the chip. When tapered lines are used in this manner the near field and discontinuity effects are important so that a three dimensional (3D) analysis which includes these effects is necessary. A software package which provides a full wave 3D analysis of arbitrarily shaped conductor layouts on a multilayered dielectric medium using the method of moments (MoM) is used in this paper to analyze the tapered line effects. Since this software package is ideally suited to the analysis of complex circuits, the inclusion of a simple model for the tapered line structure in this package would allow it to be used for analyzing complicated digital circuit board problems, as well as enabling it to analyze curved line sections in a piecewise linear fashion. This paper describes the extension of the multipipe technique for the tapered line in the 3D MoM mentioned above.

The technique used involves the description of the strip conductors in terms of a multi-pipe model. In this model the strip conductor is replaced by a series of pipes, the number depending on the length to width ratio of a segment in the Method of moments. By modeling the strip in this fashion, the charge distribution of the strip is automatically accounted for via a Gauss-Tchebyshev quadrature distribution of the pipe locations. This removes the edge singularity in the charge distribution just as in the original multipipe model.

Using the multipipe model accounts for the taper in a continuous manner through the use of a continuously tapered pipe. Thus the accuracy of the model is due to a correct description of the transverse charge/current distribution on the conductor in a continuous taper just as in the physical structure. The efficiency of the model is obtained by transforming the mutual coupling surface integrals to line integrals which can be performed analytically. The Green's function singularity in the tapered strip method of moments self term is automatically accounted for when using this model, due to the finite radii of each of the pipes.

In the presentation, results for continuous tapered lines will be compared to theoretical tapered line transformers, as well as published results.

## Electromagnetic Scattering Analysis of Arbitrarily Shaped Thin Metallic Plates Using Moment Method

M. D. Deshpande \*, Vigyan Inc., Hampton, VA..

C. R. Cockrell & F. B. Beck, NASA LaRC, Hampton, VA..

T. X. Nguyen, Research Triangle Institute, Hampton, VA.

### Abstract

The Electromagnetic Surface Patch ( ESP ) code developed at The ElectroScience Laboratory, Ohio State University, is a widely used code to determine EM scattering due to metallic objects. The ESP code is based on a segmentation technique which results in a symmetrical but not necessarily a Toeplitz impedance matrix in the moment method solution of scattering problems. This results in large CPU time for filling the impedance matrix for large size objects.

In this work a new segmentation technique which leads to a symmetrical and block Toeplitz impedance matrix will be presented to analyze the EM scattering from thin polygonal flat metallic plates. Comparison of numerical results on the EM scattering due to various nonrectangular plates with the results obtained from the ESP code and the experimental data measured in the NASA/LaRC's Experimental Test Range facility will be presented. As an example, the EM scattering due to a plate shown in Fig. 1 is computed using the present segmentation technique, the ESP code technique and the measured results. Some of the advantages and disadvantages of the present technique will also be discussed.

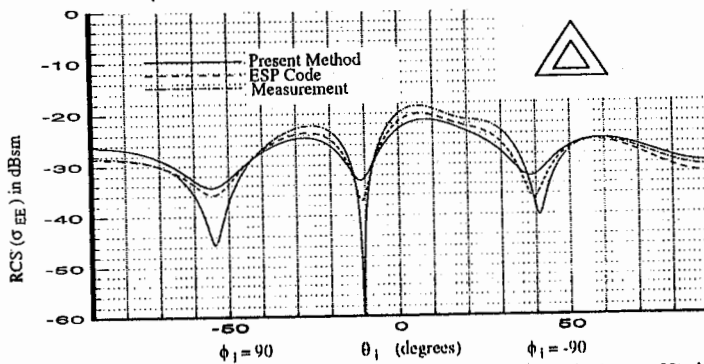


Fig. 1 Monostatic RCS of a plate as shown, which is excited by an E-polarized ( $\alpha_0 = 90$ ) plane wave as a function of  $\theta_1$  for frequency = 11.81GHz,  $N=M=19$ .

## Calculation of Transmission Line Parameters Using the Boundary Element Method

R. Remmert\*\*, W. John\*, E. Gries\*, M. Vogt\*\*

\*Siemens Nixdorf Informationssysteme AG/Cadlab — Analog System Engineering

\*\*University of Paderborn/Cadlab — Analog System Engineering

Bahnhofstraße 32  
4790 Paderborn, Germany

During the design process of printed circuit boards, EMC-effects like reflexion and crosstalk have to be taken into consideration. To decrease the number of redesigns and to reduce the time to market, simulation tools which are based on exact theoretical approaches, have to be employed. The simulation of the electrical behaviour of direct or indirect nets on printed circuit boards, requires the knowledge of transmission line parameters like characteristic impedance and phase velocity. These parameters can be determined by the constant capacitance and impedance matrices per unit length. Assuming the quasi-TEM mode, a fast computation of this characteristic quantities can be carried out by using the Boundary Element Method (BEM).

In the frequency range up to 10  $GHz$ , the longitudinal components of the field strengths outside of the conducting areas can be neglected in comparison to the transversal ones. Therefore, the electric and magnetic field strength in these areas can be described with sufficiently accuracy by transversal electromagnetic waves. This type of propagation is called quasi-TEM mode. Assuming this simplification, Maxwells equations lead to the Laplace equation which has to be solved. After a transformation of this differential equation into an integral equation, the application of the Boundary Element Method yields a system of linear equations. By solving this linear system, the charge distribution on the boundaries can be determined. The requested transmission line parameters are calculated by the integration of the charge distribution.

The position of the nodes on the boundaries is of great importance for the accuracy of the results. In those program systems concerning the Boundary Element Method known from literature, the node distribution is provided by the user. This requires some knowledge about the expected result. To avoid this problem, an algorithm was developed and implemented, which produces the node distribution automatically. Starting from a linear distribution of nodes, the number of nodes is increased at every step. It emerges that the choosen iteration algorithm converges very well.

Using this method the characteristic parameters of any structure of single and coupled transmission lines can easily be calculated. Also transmission lines which are located within multilayered dielectrics can be analyzed. Numerical results and a comparison with other methods show the precision of this method.

## FORMULATION AND APPLICATION OF A HYBRID NUMERICAL - ASYMPTOTIC INTEGRAL EQUATION TECHNIQUE

*Keith R. Aberegg \**

*Georgia Tech Research Institute  
Georgia Institute of Technology  
Atlanta, GA 30332-0800*

*Andrew F. Peterson*

*School of Electrical Engineering  
Georgia Institute of Technology  
Atlanta, GA 30332-0250*

When applied to electrically large electromagnetic scatterers, numerical methods are generally limited by the fact that they require the solution of a matrix equation whose size grows in proportion to the surface area or volume of the target. Asymptotic procedures, on the other hand, are computationally efficient for large geometries but often fail to produce accurate solutions in regions of geometric complexity. Consequently, there are two types of electromagnetic analysis tools in existence, one suited for large simple targets and one suited for small complex targets. Unfortunately, there is a broad intermediate range where neither approach works well.

Several authors have proposed numerical procedures that attempt to incorporate a priori knowledge of the phase variation of the field, obtained from simple asymptotic solutions, in an attempt to reduce the wavelength-order variation of the primary unknown in a numerical formulation. Ling (*AIAA Journal*, vol. 25, pp. 560-566, April 1987) developed a differential equation approach that factored out the first-order phase progression of the outward-propagating part of the field, permitting a more efficient numerical solution using larger cells. James (*IEEE Trans. Antennas Propagat.*, vol. 38 pp. 1625-1630, Oct. 1990) developed a similar approach based on a surface integral equation, and demonstrated its efficiency for 2D circular cylinders.

A hybrid approach similar to James' will be described, and illustrated for 2D scatterers of general cross-sectional shape, including those with edges or corners. Although the cell sizes may be reduced if necessary to ensure the same accuracy as the underlying integral equation method, the goal of the hybrid approach is to permit the use of cells that are much larger than a wavelength. Since the cells may be large, the success of the hybrid procedure is highly dependent on an efficient evaluation of the matrix entries. Details of the implementation will be discussed. The hybrid formulation will be evaluated by comparing its computational efficiency (execution time and storage) with a traditional combined-field integral equation approach.

## THE APPROXIMATION PROPERTY OF THE EXTENDED BOUNDARY ELEMENT SPACE

Song Guoxiang\*  
(Xidian University, China)      Qi Yihong  
(South-east University, China)

### Abstract

Many problems in physics, mechanics and engineering may be sorted out to solutions of boundary value problems of partial differential equations. With the rapid development and wide application of computer technology in the recent 30 years, numerical methods have become the chief measure for solving such boundary value problems. The boundary element method (BEM) became an important branch of numerical methods, and exhibits its special feature in computing some electromagnetic engineering problems. In solving boundary value problems by using BEM, we first must transform the differential equation in certain regions into integral equations along the boundary by following Green's formula. Then, we must make the boundary discrete in order to obtain a set of linear algebraic equations for the solution. Lowering the dimension and reducing unknown variables during computation, the BEM is characterized by the superiority through less input of data and shorter computing time. As with FEM, BEM uses piecewise polynomials to replace global approximations in Ritz's method and simple functions in a single element are used to replace complicated functions in the whole domain for approximation. Traditionally, there are two ways to improve the computing accuracy: the first is to dissect the boundary more finely; the second is to raise the order of interpolation functions. Both measures mentioned above will expand the scale of the discrete system. Since the coefficient matrix of boundary element equations is full and asymmetric, a high price will be paid for enlarging the scale in computation. To deal with the above-mentioned dilemma, an idea of extended element method has been proposed<sup>2</sup>, i.e. to construct extend basis functions by using information in neighboring elements to realize higher-order interpolation to improve accuracy without increasing the total number of nodes (or degrees of freedom). This is the so-called extended boundary element method. Computed examples demonstrate favorable effect. The approximation property of the extended boundary element space is discussed from the viewpoints of subspace and projective operator in this paper, in order to guarantee the approximate solution obtained from Extension-BEM.



**SESSION URSI D-3****TUESDAY AM****INTEGRATED ANTENNAS AND FEEDS**

Chairs: G. Rebeiz, University of Michigan; D.J. Roscoe, Communications Research Center

Room: Michigan League, Michigan Room      Time: 8:30-10:10

|      |   |     |
|------|---|-----|
| 8:30 | POWER COMBINING DESIGNS WITH CPW-FED SLOT ANTENNAS<br><i>B.K. Kormanyos*, L.P.B. Katehi, G.M. Rebeiz, University of Michigan</i>  | 164 |
| 8:50 | A 10 GHZ Y-BA-CU-O/GAAS ACTIVE MICROSTRIP PATCH ANTENNA<br><i>M.A. Richard, Case Western Reserve University; Kul B. Bhasin*, NASA Lewis Research Center; Norman J. Rohrer, George J. Valco, The Ohio State University</i> | 165 |
| 9:10 | DEVELOPMENT OF A NOVEL, COMPACT RECTENNA FOR CONVERTING MICROWAVE POWER TO DC POWER<br><i>C. Nguyen*, M. Tran, Texas A&amp;M University</i>   | 166 |
| 9:30 | A 25-40 GHZ FREQUENCY TRIPPLER FOR ARRAY APPLICATIONS<br><i>W. Wright*, R.C. Compton, Cornell University</i>  | 167 |
| 9:50 | FREE SPACE WAVE POWER COMBINING ON MILLIMETER WAVE<br><i>JunXiang Ge, University of Electronic Science and Technology of China</i>  | 168 |

## POWER COMBINING DESIGNS WITH CPW-FED SLOT ANTENNAS

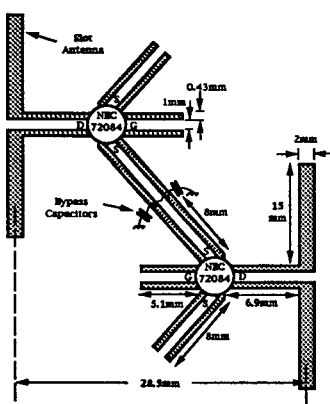
B. K. Kormanyos\*, L. P. B. Katehi, and G. M. Rebeiz  
NASA/CSTT University of Michigan, Ann Arbor 48109

A two-element quasi-optical power combining array of active slot oscillators has been constructed at 5.4GHz. The oscillators are synchronized by mutual coupling between antenna elements.

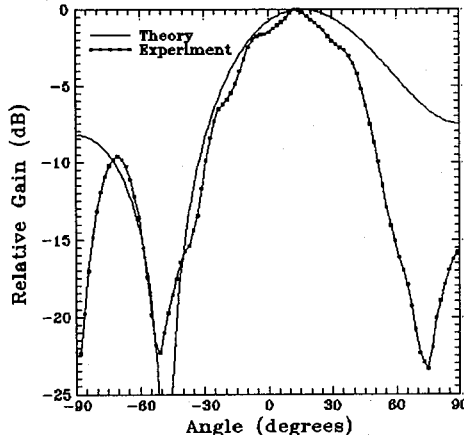
Quasi-optical power combining is a practical way to increase the power available from solid state sources at millimeter wave frequencies. Other groups have achieved successful power combining with grid oscillators and arrays of active antennas. We have developed a CPW-fed slot antenna oscillator [1] with several advantages over previously used active antennas. The oscillator is uniplanar and compatible with the integration of transistors. The oscillator circuit is very simple because it requires no external feedback mechanism and the slot antenna is designed to match directly to the transistor through a single length of CPW.

The oscillator array is constructed on a very thin substrate so slot impedance and mutual coupling are calculated with standard equations. For slot arrays on substrate lenses which act as infinite substrates, the antenna Z parameters are calculated using a full wave moment method analysis. The terminals of the FETs are DC isolated from each other to allow bias voltages to be applied. This is done by integrating metal-insulator-metal capacitors and bypassed slits in the ground plane. The spectrum of the oscillator array indicates stable operation at a single frequency of 5.4GHz. The radiation patterns of the array are consistent with two antenna elements oscillating with a phase difference of 48 degrees given by the phase of the mutual coupling. The measured E-plane pattern has false nulls at the pattern edges created by blockage from the mount. The total power radiated by the array is measured to be 34.0mW with a DC to RF efficiency of 19%. The power combining efficiency is 91% with 18.7mW radiated by a single oscillator. Results for a larger two dimensional array will be presented at the conference.

[1] B. K. Kormanyos, W. Harokopus Jr., L.P.B. Katehi, and G.M. Rebeiz "CPW-fed active slot antennas," Submitted for publication in *IEEE Trans. Microwave Theory Tech.*, Oct. 1992.



5.4GHz CPW-fed slot oscillator array



E-plane pattern of oscillator array

A 10 GHZ Y-Ba-Cu-O/GaAs ACTIVE MICROSTRIP PATCH ANTENNA

M.A. Richard<sup>1</sup>, Kul B. Bhasin<sup>2\*</sup>, Norman J. Rohrer<sup>3</sup>, and George J. Valco<sup>3</sup>

<sup>1</sup>Department of Electrical Engineering  
Case Western Reserve University, Cleveland, OH 44106

<sup>2</sup>National Aeronautics and Space Administration,  
Lewis Research Center, Cleveland, OH 44135

<sup>3</sup>Department of Electrical Engineering  
The Ohio State University, Columbus, OH 43210

Because of the limited amount of available space in high frequency arrays, some authors have suggested the use of active patch antenna as the radiating element. By using active patch antennas, the problem of rf distribution to each radiating element is minimized and space is made available for phase shifters and power amplifiers. In this paper, we report a first demonstration of a HTS/GaAs hybrid active patch antenna consisting of a hybrid oscillator on one substrate, and a feedline proximity coupled to a circular microstrip patch antenna on a second substrate.

A 10 GHz hybrid Y-Ba-Cu-O/GaAs microwave oscillator proximity coupled to a circular microstrip antenna has been designed, fabricated and characterized. The oscillator was a reflection mode type using a GaAs MESFET as the active element. The feedline, transmission lines, rf chokes, and bias lines were all fabricated from  $YBa_2Cu_3O_{7-x}$  superconducting thin films on a 1 cm x 1 cm lanthanum aluminate substrate. The output feedline of the oscillator was wire bonded to a superconducting feedline on a second 1 cm x 1 cm lanthanum aluminate substrate, which was in turn proximity coupled to a circular microstrip patch antenna. The patch antenna was printed on alumina ( $\epsilon_r = 9.9$ ) to reduce the effective permittivity seen by the radiator. Antenna patterns from this active patch antenna and the performance of the oscillator measured at 77 K are reported. The oscillator had a maximum output power of 11.5 dBm at 77 K, which corresponded to an efficiency of 10 %. In addition, the efficiency of the microstrip patch antenna together with its high temperature superconducting feedline was measured from 85 K to 30 K and was found to be 71 % at 77 K, increasing to a maximum of 87.4 % at 30 K.

Tue. a.m.

## DEVELOPMENT OF A NOVEL, COMPACT RECTENNA FOR CONVERTING MICROWAVE POWER TO DC POWER

C. Nguyen\* and M. Tran  
Department of Electrical Engineering  
Texas A&M University  
College Station, Texas 77843-3128

### ABSTRACT

Beamed microwave power transmission is a viable means to provide power for use in various space activities. Applications include beaming power from space to Earth, from Earth to space, and from space to space. The Solar Power Satellites (SPS), established in 1968 by Glasser, is a proven demonstration of this technology. Its objective is to convert solar energy in space for use on Earth. And the rectenna (RECTifier + anTENNA), invented by W.C. Brown in 1969, is the key of the beamed microwave power transmission technology. The rectenna consists of a rectifier integrated with an antenna, and is used to receive and convert microwave power into DC power. Several rectennas have been developed using dipole and patch antennas. There are two main drawbacks of these rectennas. First of all, they are narrow-band due to the use of dipole and patch antennas. A reduction in efficiency can thus occur if the frequency is shifted. Also, for the dipole antennas, if the angle of the linearly polarized incident field is shifted, due to atmosphere, etc., the efficiency of the rectenna will be reduced. Second, these rectennas employ separate DC-pass filters to pass the DC and reject harmonics, making the rectenna size large.

In this paper, we present the development of a novel, compact rectenna using a Schottky-barrier diode directly integrated on a bow-tie antenna, with DC buses connected at the wider ends of the bow-tie. Principal advantages include a broad bandwidth and the elimination of a DC-pass filter. A very good microwave-to-DC conversion efficiency of 79% has been measured at 2.45 GHz.

## A 25 - 40 GHz Frequency Tripler for Array Applications

W. Wright\* and R. C. Compton

*School of Electrical Engineering  
Cornell University, Ithaca, NY 14853*

Combining the output of a large number of individual generators to produce a high power microwave source is an attractive strategy which is readily implemented by planar semiconductor fabrication techniques. Such approaches to arrays of generators (either oscillators or frequency multipliers) fall into two categories. Firstly, arrays in which a generator significantly interacts with its neighbours. Examples in this class are diode or MESFET oscillators embedded in a periodic grid structure (D. B. Rutledge et al, Proc. 1990 IEEE MTT-S Dig. p.1201). Secondly, arrays in which the generators are weakly interacting, as for example with an array of weakly coupled, mutually synchronised diode or MESFET oscillators (R. A. York and R. C. Compton, IEEE MTT 39, 1000, 1991). An important advantage in the second approach is the ability to separately fabricate and optimize a single generator element.

We are adopting the weakly interacting array approach to generate radiation using a frequency tripler. The fundamental input power is in the range 8.5 to 13.5 GHz and the output from each tripler is fed to a single antenna. The total output from an array of such tripler-antenna sources is then combined using quasi-optical techniques.

In this paper we will describe progress in the development of a prototype hybrid tripler-antenna element. This element, when optimized, is to serve as the design basis for a fully integrated monolithic array of tripler elements fabricated in GaAs in future work. The prototype element is configured in coplanar waveguide with two anti-parallel, beam lead Schottky diode pairs - one pair from the center conductor to each ground plane. Separate DC biasing can be applied to each diode in the anti-parallel pair to vary the pair's I-V characteristics for optimum frequency tripling performance. The output from the tripler is fed to a broadband antenna.

## Free Space Wave Power Combining On Millimeter Wave<sup>\*</sup>

JunXiang Ge

Institute of Applied Physics  
University of Electronic Science and Technology of China  
Chengdu 610054, P. R. China

### ABSTRACT

The space wave power combining methods on millimeter wave region have two types, that is, quasi-optical cavity power combining and free space wave power combining. The research on the quasi-optical cavity power combining has been done much [1-4]. Little work, however, have been done in the study on free space wave power combining. In this paper, a new kind of free space wave power combining method is proposed on the basis of compound quasi-optical power combining method [4]. The power combining system consists of some single-cavity multiple-devices power combiners and a dielectric antenna array. We call such a power combining system a 'Compound Free Space Wave Power Combining System'. Because it has well impedance matching and injection locking characteristic and is not restricted by the number of the single-cavity multiple-devices power combiners, this free space wave power combining system has higher output power and combining efficiency.

\*The project was supported by National Natural Science Young Foundation of China.

### REFERENCES

- [1] W. Lothar & N. Vahakn, IEEE-MTT, 31, 189-193, 1983
- [2] M. James, IEEE-MTT, 34, 273-279, 1986
- [3] D. B. Rutledge, Z. B. Popovic & R. M. Weikle, MTT-S, 1209-1212, 1990
- [4] J. X. Ge, S. F. Li & Y. Y. Chen, Electron. Lett., 27, 880-882, 1991

## SCATTERING AND CLUTTER

Chairs: G.S. Brown, Virginia Polytechnic Institute & State University  
R.H. Ott, General Research Corporation

Room: Michigan League, Room D      Time: 8:30-10:10

|      |  |     |
|------|--|-----|
| 8:30 | 36 GHZ OFF-NADIR, BEAMWIDTH-LIMITED WAVEFORMS OVER OCEANS AND CONTINENTAL ICE<br><i>Michael H. Newkirk*, Gary S. Brown, Virginia Polytechnic Institute and State University; Douglas C. Vandemark, NASA Goddard Space Flight Center</i>  | 170 |
| 8:50 | SCATTERING AND DIFFRACTION FROM OCEAN AND SEA ICE STRUCTURES<br><i>Robert Nevels*, Zuoguo Wu, Chenhong Huang, Texas A&amp;M University</i>   | 171 |
| 9:10 | MEASUREMENTS AND THEORETICAL MODELING OF RADAR SEA BACKSCATTER (CLUTTER) AND MULTIPATH (FORWARD SCATTER) IN THE FREQUENCY RANGE FROM 60 TO 400 MHZ<br><i>R.H. Ott*, General Research Corporation; Michael A. Pollock, Robert J. Dinger, Thomas E. Tice, Naval Command, Control and Ocean Surveillance Center</i> | 172 |
| 9:30 | DIFFERENCES IN CLUTTER AMPLITUDE ECHOES FOR VERTICALLY OR HORIZONTALLY POLARIZED ILLUMINATORS<br><i>W.G. Stevens*, Daniel Fallon, K.V.N. Rao, Rome Laboratory</i>  | 173 |
| 9:50 | RADIATIVE TRANSFER MODEL FOR ACTIVE AND PASSIVE REMOTE SENSING OF VEGETATION CANOPY<br><i>Hsiu C. Han*, Iowa State University; Jin A. Kong, Massachusetts Institute of Technology</i>  | 174 |

Tue. a.m.

## 36 GHz OFF-NADIR, BEAMWIDTH-LIMITED WAVEFORMS OVER OCEANS AND CONTINENTAL ICE

Michael H. Newkirk\* and Gary S. Brown  
Bradley Department of Electrical Engineering  
Virginia Polytechnic Institute and State University  
Blacksburg, VA 24061-0111

Douglas C. Vandemark  
Observational Sciences Branch  
NASA Goddard Space Flight Center - Wallops Flight Facility  
Wallops Island, VA 23337

There has been very significant interest in monitoring the thickness of the Greenland ice sheet (H. J. Zwally, *et al*, *Science*, 246, 1587-1591, 1989; C. T. Swift, *et al*, *J. Geophys. Res.*, 90, B2, 1983-1994, 1985). One of the instruments that has recently been used to measure elevation profiles of the ice shelf is the Multimode Airborne Radar Altimeter (MARA) operated by NASA Goddard Space Flight Center - Wallops Flight Facility. Its unique design allows for the simultaneous measurement of the waveforms from a nadir beam and four off-nadir beams (nominally at 12° with respect to the vertical). These data provide local surface slope measurements from the range measurements for each beam. While surface slope measurements are desirable, it is also important to understand the complete scattering process on the ice sheet because this tells where the scattering originates, i.e. the surface or volume. To do so requires the inclusion of volume scattering in the scattering model used for the ice sheet (J. K. Ridley & K. C. Partington, *Int. J. Remote Sensing*, 9, 601-624, 1988) and the recognition that the volume component can have a significant effect on measured waveforms.

A great deal of 36 GHz, beamwidth-limited scattering data were obtained during MARA's recent August-September, 1991 mission to Greenland. This data set includes waveforms from the shelf ice, sea ice and open ocean. Before examining the complicated problem of surface and volume scattering, it is desirable to ensure that the system is operating as expected. To do this, the much simpler and better understood process of only sea surface scattering is investigated. Validation of the MARA system data can be achieved by comparing an average of the measured sea surface-scattered individual waveforms to a convolutional waveform model (M. H. Newkirk & G. S. Brown, *IEEE Trans. Ant. and Prop.*, 40, no. 12, 1992). The above model allows for the short pulsedwidth (6 ns) and small beamwidth (0.6°) of the beamwidth-limited MARA system, as well as for off-nadir pointing angles greater than 12°. In this summary, we present the results of the comparison of the off-nadir MARA ocean data to the convolutional model. We then take a preliminary look at the scattered waveforms from the ice shelf and compare to the open ocean-scattered waveforms, revealing the importance of volume scattering in the waveform structure. Since the Greenland mission took place when the MARA system was still undergoing engineering checkout, the waveform data are not perfect. We discuss some potential causes of the anomalies and, where possible, resolve what is surface- and what is sensor-induced by comparison of the data to the waveform model.

## Scattering and Diffraction from Ocean and Sea Ice Structures

Robert Nevels\*, Zuoguo Wu and Chenhong Huang  
 Department of Electrical Engineering  
 Texas A&M University  
 College Station, Texas 77843-3128

Several studies have been carried out concerning radar backscatter from ocean waves and sea-ice. Some of the original experimental work on the polarization features of radio signals scattered from the sea surface at grazing angles was done by A. Kalmikov and V. Pustovoytenko (J. Geophys. Res. 81, 1960-1964, 1971). Later R.L. Lewis and I.D. Olin (Radio Sci. 15, 815-826, 1980) in an independent study accounted for the 'spiky' radar return characteristic by a model in which the normalized radar backscatter from the ocean surface is based on wedge shaped 'whitecaps'. In this paper we will present the results of a numerical analysis of the electromagnetic field scattered by an ocean surface 'whitecap'. The newly developed Fourier transform path integral (FTPI) method will be used. A particular feature of the FTPI method is that any changes in shape of the scattering structure are accounted for by changing only the dielectric constant description of the scattering region. This will allow calculations of the scattered field spanning a period of time including the formation and complete evolution of whitecaps.

Floating sea ice is another feature of the ocean surface. Again we will use the FTPI method to show the electromagnetic field scattered from two sea ice structures carried through a complete pitch cycle. Finally stationary sea ice structures will be investigated, in this case as a function of changes in under-sea features of the ice structures. In each case illumination will be via an incident plane wave at several incidence angles.

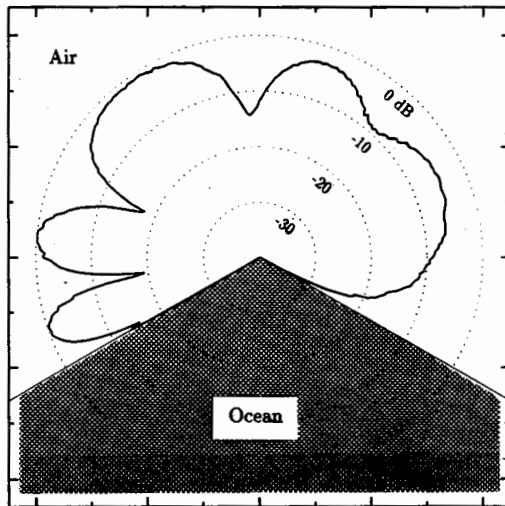


Fig. Pattern for wedged ocean whitecap with an interior angle of  $120^\circ$ .

Tue. a.m.

Measurements and Theoretical Modeling of Radar Sea Backscatter  
(clutter) and Multipath (forward scatter) in the Frequency Range  
from 60 to 400 MHz

R.H. Ott<sup>(1)\*</sup>, Michael A. Pollock<sup>(2)</sup>, Robert J. Dinger<sup>(2)</sup>,  
and Thomas E. Tice<sup>(2)</sup>

<sup>(2)</sup>Radar Branch  
Naval Command, Control and Ocean Surveillance Center  
San Diego, CA 92152

<sup>(1)</sup>General Research Corporation  
Albuquerque, NM 87106

Measurements of low-grazing-angle radar sea backscatter and multipath in the frequency range from 60 MHz to 400 MHz, along with the supporting theoretical modeling, have been relatively lacking because of the practical difficulties (primarily related to antenna size and frequency allocation) associated with fielding radars in this band. An ultra-wideband radar that radiates waveforms encompassing this band has recently been installed at a seaside location near San Diego, CA. The radar uses two 10-m reflector antennas to radiate and receive impulse (3-ns pulselength) signals. This paper will summarize the results of comparisons of clutter and multipath as a function of grazing angle and sea state. The backscatter measurements are made without a man-made target in the scene, and the multi-path measurements are made with spheres, dipoles, and active calibration sources at various altitudes above the ocean.

The theoretical model is based upon an integral equation solution for the surface fields on deterministic or random ocean profiles. The surface fields are then integrated to obtain either the forward scatter (multi-path) or backscatter (clutter) for the illuminated surface patch. The surface fields are obtained using a new mathematical derivation for the integral equation for the surface fields (R.H. Ott, Radio Science, Vol. 27, No. 6, pages 867-882, November-December, 1992). This new integral equation extends the frequency range of the former algorithm, PROGRAM WAGNER, to the VHF band. The new computer algorithm is named RING (Radio Integral over Ground).

**DIFFERENCES IN CLUTTER AMPLITUDE ECHOES FOR VERTICALLY  
OR HORIZONTALLY POLARIZED ILLUMINATORS.**

W. G. Stevens\*, Lt. Daniel Fallon and K. V. N. Rao  
Environmental Effects Branch  
Applied Electromagnetics Division  
Electromagnetics and Reliability Directorate  
Rome Laboratory  
Hanscom AFB MA 01731

The objective of this experiment is to compare the cumulative density functions of the clutter amplitude echoes seen by an elliptically polarized receiver from clutter patches which are illuminated by a transmitter that was either vertically or horizontally polarized. The transmitter, clutter patch and the receiver are located such that the clutter patch was illuminated at an incidence angle of 80 degrees, and an elevation scattering angle of 75 degrees. We estimate that the 3-dB beamwidth of the transmitter antenna and the receive antenna intersected a volume of the clutter patch .75 meters in range, surface area of 20 square meters, and a height of approximately 3 meters. Thus the transmitter illuminated both the trunks and the branches of the trees in the clutter patch. The clutter echo amplitudes were recorded every 200 milliseconds for 500 pulse repetition intervals. In this paper we report the data taken from three contiguous range bins. The bistatic configuration allowed us to collect the echo data from only five or six range bins. The experimentally derived temporal cumulative density functions of the received echo amplitudes are different for vertical and horizontal illuminators. We speculate that the differences observed in the density functions arise due to scattering dominated by either vertically or horizontally oriented scatterers. Further analytical investigation is needed to confirm these experimental observations.

## RADIATIVE TRANSFER MODEL FOR ACTIVE AND PASSIVE REMOTE SENSING OF VEGETATION CANOPY

Hsiu C. Han\*

Department of Electrical Engineering and Computer Engineering  
Iowa State University  
Ames, Iowa 50011

Jin A. Kong

Department of Electrical Engineering and Computer Science  
and Research Laboratory of Electronics  
Massachusetts Institute of Technology  
Cambridge, Massachusetts 02139

Based upon the vector radiative transfer (RT) equations, we present a theoretical model for calculating the radar backscattering coefficients and the brightness temperatures of multi-layered vegetation canopy for active and passive microwave remote sensing, respectively. Effects of the underlying rough surface have been taken into account through the Geometrical Optics approximated coupling matrix in the radiative transfer formulation. The solutions of the RT equations are derived iteratively to the second order for the active case, and first order for the passive case. The particular physical scattering or emission mechanism associated with each term in the iterative solution is identified. Numerical examples for the backscattering coefficients and brightness temperatures of a two-layer vegetation-like medium are presented.

Vegetation canopy can be modeled as either a mixture of multiple-species discrete scatterers described by a certain size, shape, and orientation distributions, or a continuous random medium characterized by correlation functions. In this paper, the phase matrix and emission vector under both approaches are evaluated for a collection of randomly oriented spherical inhomogeneities. Numerical comparison for the resulting backscattering coefficients is performed. The relation between the correlation lengths used in the continuous random medium model to describe the shape of inhomogeneities and the dimensions of the scatterer in the discrete model are discussed. More specifically, the scattering amplitudes, attenuation rates, and the albedo's, or the amplitude ratio between scattering and attenuation, predicted under both approaches are compared, and the causes giving rise to the discrepancies in the scattering and emission computation are identified.

## MATERIAL MEASUREMENTS

Chairs: W.R. Scott, Jr., Georgia Institute of Technology  
 C.M. Weil, National Institute of Standards and Technology

Room: Alumni Center, Room 2      Time: 8:30-12:10

|       |   |     |
|-------|---|-----|
| 8:30  | INVESTIGATION OF A WAVEGUIDE TECHNIQUE FOR MEASURING THE CONSTITUTIVE PARAMETERS OF PLANAR MATERIALS<br><i>Gregory S. Warren*, Waymond R. Scott, Jr., Georgia Institute of Technology</i>   | 176 |
| 8:50  | NEW METALLIZED CERAMIC COAXIAL PROBE FOR HIGH-TEMPERATURE DIELECTRIC PROPERTY MEASUREMENTS<br><i>S. Bringhurst, O.M. Andrade, M.F. Iskander, University of Utah</i>   | 177 |
| 9:10  | MATERIAL CHARACTERIZATION USING A STRIPLINE RESONATOR<br><i>Chriss A. Jones*, John H. Grosvenor, Michael D. Janezic, National Institute of Standards and Technology</i>   | 178 |
| 9:30  | DETERMINING THE PERMITTIVITY OF PRINTED CIRCUIT BOARD SUBSTRATES USING A QUASI-ANALYTIC MICROSTRIP MODEL<br><i>Shankar Chidambaram*, George Hanson, University of Wisconsin-Milwaukee</i>   | 179 |
| 9:50  | MEASUREMENT PROBLEMS INVOLVING THE BROADBAND CHARACTERIZATION OF HIGH-PERMITTIVITY MATERIALS<br><i>James R. Baker-Jarvis, Eric J. Vanzura, Michael D. Janezic, Claude M. Weil*, National Institute of Standards and Technology</i>  | 180 |
| 10:10 | BREAK   |     |
| 10:30 | NUMERICAL IMPULSE CHARACTERIZATION OF THE EFFECTIVE PERMEABILITIES FOR THE NONLINEAR RESPONSE OF FERROMAGNETIC SHIELDS WITH AN EXPONENTIAL DIFFERENTIAL MAGNETIC PERMEABILITY MODEL<br><i>W.J. Croisant*, C.A. Feickert, M.K. McInerney, U.S. Army Construction Engineering Research Laboratory</i> | 181 |
| 10:50 | EFFECT OF MACROSCOPIC INHOMOGENEITY ON FERRITE LOSS<br><i>Richard G. Geyer, National Institute of Standards and Technology</i>  | 182 |
| 11:10 | COMPUTING PORT PARAMETERS AND EIGENMODES FOR STRUCTURES LOADED WITH GENERAL LOSSY MATERIALS<br><i>G. William Slade*, Kevin J. Webb, Purdue University</i>   | 183 |
| 11:30 | NON-INVASIVE MEASUREMENT TECHNIQUE FOR MONOLITHIC CIRCUITS BASED ON FORCE MICROSCOPY<br><i>R.A. Said*, G.E. Bridges, D.J. Thomson, University of Manitoba</i>   | 184 |
| 11:50 | MICROWAVE CHARACTERIZATION OF SLOTLINE ON HIGH RESISTIVITY SILICON FOR ANTENNA FEED NETWORK<br><i>Rainee N. Simons*, Susan R. Taub, Richard Q. Lee, Paul G. Young, NASA Lewis Research Center</i>   | 185 |

## INVESTIGATION OF A WAVEGUIDE TECHNIQUE FOR MEASURING THE CONSTITUTIVE PARAMETERS OF PLANAR MATERIALS

Gregory S. Warren\* and Waymond R. Scott, Jr.

School of Electrical Engineering  
Georgia Institute of Technology  
Atlanta, Georgia 30332-0250

A technique using a waveguide fixture to measure the constitutive parameters (complex permittivity and complex permeability) of planar materials is examined in this work. Figure 1 is a sketch of the fixture that is used in the technique; the material to be measured is placed between the two conducting plates which are attached to the waveguides. The reflection and transmission coefficients of the fixture are measured, and the constitutive parameters are determined from these measurements. A planar material can be placed in the fixture without any preparation; this is a substantial advantage over techniques which require the sample to be machined to fit into a waveguide, coaxial line, or other measurement fixture. In many techniques, the preparation of the sample is the most difficult part of the measurement procedure.

The feasibility of the technique is investigated in this work. An accurate model for the measurement fixture is formulated. Since a closed form analytical solution does not exist for the fixture, the finite element and the finite-difference time-domain methods are examined as suitable solutions. The reflection and transmission coefficients must be sensitive to changes in the constitutive parameters for the technique to be accurate; thus, a parametric study of the sensitivity is performed. In addition, the reflection and transmission coefficients must be insensitive to the small air gaps that will exist in practice between the material being measured and the conducting walls; consequently, the effect of the air gaps is investigated.

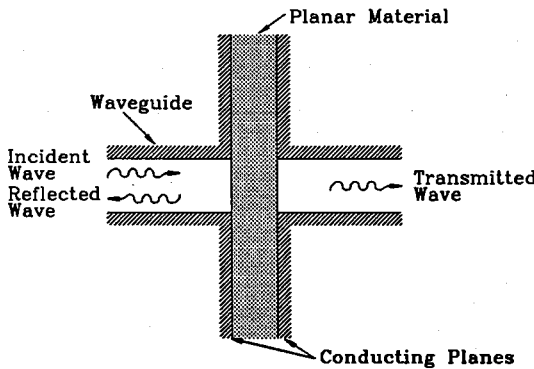


Figure 1. Measurement Fixture.

## NEW METALLIZED CERAMIC COAXIAL PROBE FOR HIGH-TEMPERATURE DIELECTRIC PROPERTY MEASUREMENTS

S. Bringhurst, O. M. Andrade, and M. F. Iskander  
Electrical Engineering Department  
University of Utah  
Salt Lake City, UT 84112

Broadband dielectric property measurement is important in characterizing the atomic and molecular structure of materials. In the area of microwave sintering of ceramics, which is of interest to us, it is also important that these measurements be made as a function of temperature up to 1400°C. Data obtained from these measurements are used to support numerical modeling and simulation efforts as well as to characterize the absorption characteristics of ceramic materials vs. temperature and frequency. Issues such as sample/insulation compatibility and parameters involved in optimizing the heating process also benefit from the results of these measurements. High-temperature dielectric properties are only known for a limited number of materials, and there are serious frequency gaps in the available dielectric property database.

We have developed a novel metallized ceramic open-ended coaxial probe for making broadband dielectric property measurements for temperatures up to 1400°C. In this paper, the design aspects of this probe will be described. This includes the metallization process by depositing platinum (melting temperature of 1780°C) on AD-998 alumina (the bulk of the probe) to a thickness of a few skin depths calculated at the lower frequency of interest. It also includes a unique design and fabrication of the connector (modified GR-874 type) and its interface with the probe. A procedure was devised to obtain high-temperature calibration using a network analyzer and a short, open, and a ceramic sample of known properties vs. temperature as a standard material.

Additionally, results of measurements on some ceramic samples as a function of temperature will be presented and compared with data obtained from highly accurate cavity perturbation measurements also developed in our laboratories.

# MATERIAL CHARACTERIZATION USING A STRIPLINE RESONATOR

Chriss A. Jones\* John H. Grosvenor

Michael D. Janezic

National Institute of Standards and Technology  
Electromagnetic Fields Division  
325 Broadway, Boulder, CO 80303

## Abstract

The aerospace industry has looked at techniques for the accurate characterization of dielectric and magnetic materials. Such techniques include transmission lines, cavities, non-destructive probes and resonant fixtures. There are advantages and disadvantages for each of these techniques. For example, one advantage of a 7mm coaxial transmission line is that it provides very broadband measurements. On the other hand, a disadvantage is the uncertainty due to airgap. Although much could be written of the other techniques as well, this presentation will focus on the stripline resonator method for measuring dielectric and magnetic properties.

The main advantage of the stripline resonator is the simple sample geometry. The dimensions for a rectangular sample geometry can be machined more accurately than the dimensions for a coaxial sample geometry, thus reducing the uncertainty in the airgap. Another advantage is that the electric and magnetic fields are decoupled which allow independent measurements of permittivity and permeability, as long as the sample is small or the permittivity or permeability is low. Among the disadvantages are limited bandwidth with measurements at only discrete frequencies and possible radiation leakage due to the open stripline geometry.

The real parts of permittivity and permeability were calculated using the measured frequency shift which results when the empty cavity is partially filled with a sample. The losses can be calculated from the change in the quality factor of the resonance. The dielectric measurements were made on cross-linked polystyrene, leaded glass, nylon, and two different ferrite-loaded polymers. Magnetic measurements were made on the ferrite-loaded polymers. Details and explanations of the measurements are presented.

DETERMINING THE PERMITTIVITY OF PRINTED CIRCUIT  
BOARD SUBSTRATES USING A QUASI-ANALYTIC  
MICROSTRIP MODEL

Shankar Chidambaram\* and George Hanson  
Department of Electrical Engineering and Computer Science  
University of Wisconsin-Milwaukee, Milwaukee, Wisconsin, USA 53201

The measurement of the material property permittivity can be accomplished using a variety of techniques. For dielectric materials used in printed circuit boards, transmission line and resonator methods are commonly used. Although transmission line methods provide data over a wide range of frequencies, resonator methods are generally considered to provide more accurate results for the dissipation factor of low loss dielectrics. Resonator measurements are often done in stripline, although this geometry has several drawbacks. For instance, stripline measurements require two pieces of material of equal thickness, and a method of clamping the stripline together such that air gaps are eliminated. Resonator measurements made in microstrip requires less sample material and no clamping, although there are additional losses due to surface-wave and space-wave radiation.

A method for measuring the complex permittivity of printed circuit board substrates by a microstrip resonator technique is presented. This method accounts for all loss mechanisms in an efficient manner. Well-known formulae for effective permittivity, including dispersion, and the open-end effect are used in an iterative solution for the real part of permittivity. Dielectric and conductor losses can also be accounted for with simple expressions. The work presented here will concentrate on studying the influence of surface-wave and space-wave radiation losses on the dissipation factor. These loss mechanisms will dominate over other losses when the substrate is electrically thick, and can perhaps be ignored for electrically thin substrates. We will identify regimes where radiation losses can be ignored, and investigate the accuracy of methods to include the effect of radiation where necessary.

MEASUREMENT PROBLEMS INVOLVING THE BROADBAND  
CHARACTERIZATION OF HIGH-PERMITTIVITY MATERIALS

James R. Baker-Jarvis, Eric J. Vanzura,  
Michael D. Janezic, Claude M. Weil\*  
Electromagnetic Fields Division (813.08),  
National Institute of Standards and Technology,  
325 Broadway, Boulder, CO 80301

The Transmission/Reflection (T/R) method is a widely used measurement technique for characterizing the dielectric and magnetic properties of homogeneous and isotropic solid materials over broad ranges of the RF/microwave spectrum. The transmission line geometry of choice is generally the 7 mm diameter coaxial air line, owing to its very broadband coverage (0.001-18 GHz), but other geometries such as the 14 mm diameter air line, as well as waveguides, are also used. The Electromagnetic Properties of Materials Program at NIST has recently developed some improved algorithms for this technique which yields measurement accuracies of the order of  $\pm 5\%$  for low-to-medium permittivity ( $\epsilon_r < 50$ ) materials. NIST has also organized a national intercomparison of such materials using the 7 mm coax line; major variations in the measured data submitted by participants were evident.

This talk will primarily address the problems associated with attempting to apply this technique to the accurate characterization of high-permittivity ( $\epsilon_r > 50$ ) materials. Some of the factors causing such problems include: a) the newer iterative reduction algorithms, including that developed by NIST, require a close initial guess for  $\epsilon_r$  that usually is not available, b) these same algorithms have difficulty resolving closely separated roots and c) the inevitable presence of an air gap between sample and the coax line inner conductor always biases measured data low, thus creating major measurement uncertainties ranging to 100% or more. All three factors will be discussed in turn, with emphasis on the air gap problem. Initial guess data can be derived using the explicit Nicholson-Ross solution and supplemented in the low frequency region (<10 MHz) using a parallel plate capacitor fixture and in the microwave range (>500 MHz) using resonant cavities. Routines that correct for the effects of air gaps are available, but do not work satisfactorily for high- $\epsilon_r$  materials. Improved routines, based on Marcuvitz's full-field analysis, are being developed. Other techniques being investigated for the mitigation of air-gap problems include the use of larger-diameter coax lines (e.g. 80 mm diameter), a mode-filtered coaxial air line in which the  $TE_{0n}$  mode is the principal mode rather than the TEM mode and the use of conductive pastes and solders to fill in the gap.

NUMERICAL CHARACTERIZATION OF THE EFFECTIVE PERMEABILITIES  
FOR THE NONLINEAR IMPULSE RESPONSE OF FERROMAGNETIC SHIELDS  
WITH AN EXPONENTIAL DIFFERENTIAL MAGNETIC PERMEABILITY MODEL

W. J. Croisant\*, C. A. Feickert, and M. K. McInerney  
U.S. Army Construction Engineering Research Laboratory  
Champaign, IL 61826-9005, USA

The analysis of pulsed electromagnetic field interactions with ferromagnetic shields is complicated by the variation with magnetic field intensity,  $H$ , of the differential magnetic permeability,  $\mu_d(H) = dB(H)/dH$ , which makes the phenomenon nonlinear. For a planar approximation to a thin-walled cylindrical impulse surface current problem, the nonlinearity of the peak transient electric field induced at the inner surface,  $E_{peak}$ , can be expressed in terms of an effective permeability  $\mu_E(\beta)$

$$E_{peak} = 5.9220537270 \frac{O_o}{\mu_o \mu_E(\beta) \sigma^2 d^3} \quad (1)$$

and that of the time of the peak,  $t_{peak}$ , in terms of an effective permeability  $\mu_T(\beta)$

$$t_{peak} = 0.091751715 \mu_o \mu_T(\beta) \sigma d^2, \quad (2)$$

for sheet thickness  $d$ , electrical conductivity  $\sigma$ , permeability of free space  $\mu_o$ , charge per unit length  $O_o$  (transported along the outer surface), and applied pulse parameter  $\beta$ , which is a fundamental combination of nonmagnetic quantities

$$\beta = \frac{O_o}{\sigma d^2}. \quad (3)$$

In general, the effective permeability curves  $\mu_E(\beta)$  and  $\mu_T(\beta)$  that correspond to a given differential permeability representation  $\mu_d(H)$  have to be characterized via numerical calculations. For a set of values of  $d$ ,  $\sigma$ , and  $O_o$ , the electric field response is calculated numerically, and  $E_{peak}$  and  $t_{peak}$  are evaluated. The value of  $\beta$  for the particular case is determined from Eq. 3. The value of  $\mu_E(\beta)$  is determined from

$$\mu_E(\beta) = 5.9220537270 \frac{O_o}{\mu_o E_{peak} \sigma^2 d^3}, \quad (4)$$

and the value  $\mu_T(\beta)$  is determined from

$$\mu_T(\beta) = 10.898979 \frac{t_{peak}}{\mu_o \sigma d^2}. \quad (5)$$

A detailed numerical characterization of  $\mu_E(\beta)$  and  $\mu_T(\beta)$  over a wide range of  $\beta$  has been performed for an exponential relative differential permeability model

$$\mu_d(H) = 1 + \frac{B_s}{\mu_o H_c} \exp \left( -\frac{H}{H_c} \right), \quad (6)$$

where  $H_c$  is a characteristic value and  $B_s$  is the saturation magnetization of the material. For intermediate pulses ( $0 < \beta < B_s/2$ ),  $\mu_E(\beta)$  and  $\mu_T(\beta)$  are distinctly different. Exponential behavior is not observed in  $\mu_E(\beta)$ . For moderate  $\beta$ ,  $\mu_E(\beta)$  is nearly linear. In limiting cases,  $\mu_E(\beta)$  and  $\mu_T(\beta)$  exhibit similar behavior: for very small pulses both approach the initial value of the relative differential permeability so that to a good approximation  $\mu_E(0) = \mu_T(0) = \mu_d(0) = 1 + B_s/\mu_o H_c$ ; near  $\beta = B_s/2$  both exhibit the onset of saturation (which is in close agreement with the prediction of the limiting nonlinear theory for a step magnetization curve); and for very large pulses both approach the permeability of free space so that to a good approximation  $\mu_E(\infty) = \mu_T(\infty) = \mu_d(\infty) = 1$ .

## EFFECT OF MACROSCOPIC INHOMOGENEITY ON FERRITE LOSS

Richard G. Geyer

National Institute of Standards and Technology  
325 Broadway, Boulder, CO 80303

### Abstract

Accurate broadband spectral characterization of ferrites is of paramount importance to improved rf design of many devices as well as in microwave and millimeter wave applications that enable ferrites to be used in isolators, phase shifters, and circulators. Several goals of the National Institute of Standards and Technology (NIST) are to evaluate measurement techniques currently being used in industry, to provide reference materials that serve to validate techniques, and to provide a measurement service for materials submitted by industry. Desired characteristics of magnetic reference materials are

- Homogeneity of all electrical and magnetic properties
- Insignificant anisotropy in polycrystalline form
- Linearity of complex permeability at field levels used in measurement and in device application
- Minimal electromagnetic property variations with temperature
- No significant "built-in" dc bias fields so that scalar permeability evaluation is sufficient
- Low magnetic coercivity and remanent induction; low temperature coefficient of contraction; high Curie temperature.

Magnetic reference materials must have repeatable, predictable spectral loss behaviors. In polycrystalline ferrites magnetic loss mechanisms are those due to hysteresis, eddy currents, domain wall movement, domain rotation, and gyromagnetic resonance phenomena. Gyromagnetic resonance phenomena include coupling from the dominant excited spin mode into other spin modes, spin-lattice scattering energy from spin modes into elastic modes of the lattice, and interactions between frequency of electron transfer among ferrous and ferric ions and the precession frequency of total internal magnetization.

Loss from domain wall movement is dependent on the low-frequency permeability, resonant frequency for wall motion, and domain width. Loss from domain rotation varies directly with the saturation magnetization and inversely with the anisotropy constant and is a strong function of granularity or porosity. The effects of porosity on the magnetic and dielectric behavior of polycrystalline ferrites may be evaluated by treating the ferrite as a binary composite exhibiting macroscopic inhomogeneity. It is shown that porosity strongly affects the presence of domain wall movement resonances and the spectral location of maximum magnetic loss.

## COMPUTING PORT PARAMETERS AND EIGENMODES FOR STRUCTURES LOADED WITH GENERAL LOSSY MATERIALS

G. William Slade\* and Kevin J. Webb

School of Electrical Engineering

Purdue University

West Lafayette, IN 47907

In order to realistically model three-dimensional structures, it is necessary to allow for the presence of lossy bulk materials and the ability to interface with the outside world. The method we present here is based on a three-dimensional magnetic field vector finite element algorithm. The finite element method is based on a weighted residual method similar to Paulsen, et al. (*IEEE Trans. Microwave Theory Tech.*, pp. 682-693, Apr. 1988) with a couple of extensions.

One of the useful additions to the modeler is the capability to compute eigenmodes of a structure which can be arbitrarily shaped and possess arbitrary loss. We have incorporated a general non-self-adjoint subspace iteration algorithm similar to Fernandez et al. (*Electronics Lett.*, pp. 1824-1826, 26 Sept. 1991) into the finite element code. Several interesting effects can be observed as losses are introduced. The skin effect becomes readily apparent as well as several numerical peculiarities; namely, the limitations of the interpolation and the limitations of mode identification for inhomogeneous dielectric problems.

In order to be useful for an investigator, some method for coupling to the outside world is desirable. We have extended the weighted residual formulation to include a waveguide absorbing boundary condition as well as an input boundary condition. This allows the user to excite a structure with an incoming wave and to observe the resultant outgoing modes. The obvious result of this ability would be the computation of multiport parameters.

## Non-invasive Measurement Technique for Monolithic Circuits Based on Force Microscopy

R. A. Said\*, G.E. Bridges, and D. J. Thomson

*Department of Electrical and Computer Engineering*

*University of Manitoba, Winnipeg, Man., Canada R3T 2N2*

As the speed and density of monolithic circuits is enhanced, their experimental measurement has become an increasingly difficult task. Many times network analyzer measurements at a circuits terminal ports is no longer adequate to perform complete diagnostics. In these cases non-invasive measurements at the circuits internal nodes are desired, and may require a micron scale resolution. Conventional measurement techniques, that usually rely on direct electrical contact with a point in the circuit being monitored, are unsuitable for this purpose due to difficulties in performing the measurement without disturbing the circuits operation and are often impossible in the presence of insulating passivation layers. To overcome this problem, electro-optic and electron beam probing measurement techniques have been under development, but at present are still relatively complex or expensive. Simpler measurement methods utilizing reactive coupling between a localized probe and the circuit under test have been developed(S.S. Osofsky and S.E. Schwarz, IEEE Trans. Microwave Theory Tech., MTT-40, 1701-1708, 1992), but current resolutions are still inadequate for measurements on a micron scale. More recently circuit measurement techniques based on scanning tunneling microscopy and attractive mode force microscopy(J.M.R. Weaver and D.W. Abraham, J. Vac. Sci. Technol. B., 9, 1559-1561, 1991) have been under investigation. The new techniques allow the submicron static potential measurement of integrated circuits. An instrument based on the attractive mode force principle has been constructed and has demonstrated micron resolution measurement capabilities(R.A. Said, G.E. Bridges, and D.G. Thomson, Dept. Elect. and Comp. Eng., Univ. of Man., UMECE TR-93-10, 1993).

In this paper a technique based on attractive mode scanning force microscopy is presented as a non-contact high resolution diagnostic tool for monolithic circuits. The measurement system constructed consists of a wire cantilever probe with a very sharp tip at its end, which is held in close proximity to the circuit under test. The probe can be scanned over the test circuit using an x-y positioner with a sub-micrometer resolution. The probe is excited by a signal at the same frequency as the circuit under test with a controllable amplitude and phase. Due to probe-sample potential differences, the probe tip will experience a capacitively induced attractive force, causing a mechanical deflection of the probe cantilever. The probe deflection is detected using a fiber interferometer. The signal at a desired location on the circuit under test can then be extracted by adjusting the probe amplitude and phase so that the deflection force acting on the probe is eliminated. This nulling force technique is used as it overcomes the calibration problems encountered in other methods. Results obtained using this diagnostic tool will be presented from measurements performed on typical monolithic test structures.

**MICROWAVE CHARACTERIZATION OF SLOTLINE ON HIGH RESISTIVITY SILICON FOR ANTENNA FEED NETWORK**

Rainee N. Simons\*, Susan R. Taub, Richard Q. Lee and  
Paul G. Young  
NASA Lewis Research Center, Mail Stop 54-5  
21000 Brookpark Road, Cleveland, Ohio 44135

Silicon MOSFETs with cutoff frequency of 89 GHz have been recently reported and silicon MMIC amplifiers and mixer chips are commercially available. Some advantages of silicon technology over GaAs and InP technology are: more maturity, availability of wafers of very large diameters, and lower cost. Further, integration of MMICs with digital control circuits and radiating elements on a single silicon wafer can enhance the reliability and efficiency and lower the cost of phased array antenna systems. Conventional silicon wafers have low resistivity and consequently an unacceptable high dielectric attenuation. Therefore, microwave circuits for phased array antenna systems fabricated on these wafers have low efficiency. By choosing a silicon substrate with sufficiently high resistivity the dielectric attenuation of the interconnecting microwave transmission lines can be made to approach those of GaAs or InP. In order for this to be possible, the transmission lines on silicon must be characterized.

In this presentation, the effective dielectric constant ( $\epsilon_{eff}$ ) and attenuation constant ( $\alpha$ ) of a slotline on high resistivity (5000-10000  $\Omega$ -cm) silicon wafer will be discussed. The  $\epsilon_{eff}$  and  $\alpha$  are determined from the measured resonant frequencies and the corresponding insertion loss of a slotline ring resonator. Figs. 1 and 2 show typical results for slot width, substrate thickness,  $\epsilon_r$ , and metal (gold) thickness equal to 0.1 mm, 0.381 mm, 11.7, and 2.5  $\mu$ m respectively. The results for slotline will be compared with microstrip line and coplanar waveguide on other materials.

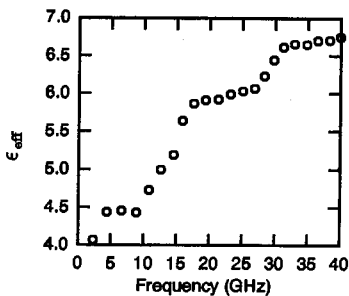


Fig. 1 Effective Dielectric Constant

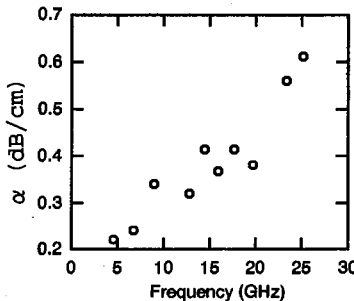


Fig. 2 Attenuation Constant



## FINITE ELEMENT METHODS II

Chairs: D.R. Wilton, University of Houston; R. Lee, The Ohio State University

Room: Modern Languages Building, Auditorium 1      Time: 1:30-5:10

|      |   |     |
|------|---|-----|
| 1:30 | HIGH ORDER DIVERGENCELESS EDGE ELEMENTS<br><i>J. Jevtic*, R. Lee, The Ohio State University</i>   | 188 |
| 1:50 | NUMERICAL, DIVERGENCELESS SHAPE FUNCTIONS FOR THREE<br>DIMENSIONAL FINITE ELEMENT ANALYSIS<br><i>Daniel C. Ross*, John L. Volakis, University of Michigan</i>                                 | 189 |
| 2:10 | FINITE ELEMENT MODELING OF SCATTERING FROM ANISOTROPIC<br>MATERIALS WITH ARBITRARY PRINCIPAL AXES<br><i>J.W. Parker, Jet Propulsion Laboratory</i>  | 190 |
| 2:30 | A COMPARATIVE STUDY OF NODE AND VECTOR APPROACHES FOR THE<br>FINITE ELEMENT SOLUTION OF WAVEGUIDE PROBLEMS<br><i>A. Khebir*, A.B. Kouki, F.M. Ghannouchi, Ecole Polytechnique de Montreal</i> | 191 |
| 2:50 | THE INCLUSION OF RESISTIVE SHEETS IN A 3-D VECTOR FINITE<br>ELEMENT ANALYSIS OF A DOUBLY INFINITE PERIODIC ARRAY<br><i>Thomas Fontana*, Eric Lucas, Westinghouse Electric Corporation</i>     | 192 |
| 3:10 | BREAK   |     |
| 3:30 | A 3-D VECTOR FINITE ELEMENT ANALYSIS FOR INFINITE DOUBLY<br>PERIODIC RADIATING ARRAYS<br><i>Eric Lucas*, Thomas Fontana, Westinghouse Electronic Corporation</i>                              | 193 |
| 3:50 | A HYBRID FINITE ELEMENT-MODAL FORMULATION FOR INLET<br>SCATTERING<br><i>Daniel C. Ross*, John L. Volakis, Hristos Anastassiou, University of Michigan</i>                                     | 194 |
| 4:10 | A NEW E-B FORMULATION FOR MODELING ARBITRARY THREE-<br>DIMENSIONAL MICROWAVE DEVICES<br><i>Din Kow Sun*, Xingchao Yuan, Zoltan Cendes, Ansoft Corporation</i>                                 | 195 |
| 4:30 | A FAST METHOD FOR COMPUTING THE SPECTRAL RESPONSE OF<br>MICROWAVE DEVICES OVER A BROAD BANDWIDTH<br><i>Xingchao Yuan*, Zoltan Cendes, Ansoft Corporation</i>                                  | 196 |
| 4:50 | A SEQUENTIAL AND PARALLEL IMPLEMENTATION OF A PARTITIONING<br>FINITE ELEMENT TECHNIQUE FOR ELECTROMAGNETIC SCATTERING<br><i>Y.S. Choi-Grogan*, R. Lee, The Ohio State University</i>          | 197 |

## HIGH ORDER DIVERGENCELESS EDGE ELEMENTS

J. Jevtić\* and R. Lee

ElectroScience Laboratory  
Department of Electrical Engineering  
The Ohio State University  
1320 Kinnear Rd.  
Columbus, Ohio 43212-1191

Edge elements offer elegant ways of treating some of the problems inherent to the nodal elements. Sharp edges, spurious modes and dielectric interfaces pose no problem. However, the efficient application of conventional edge elements has long been hindered by the low accuracy and corresponding large number of unknowns associated with problems of practical size.

We are proposing a new way of constructing vector edge basis functions that enables us to preserve the essential properties of the conventional edge elements while providing for higher order approximation. To fully utilize the advantages of this approach a new method of implementing edge elements into the finite element scheme is presented. At this time, the method is limited to two dimensional problems with homogeneous triangular elements.

For the vector basis function within each element we choose the actual electromagnetic field that would exist inside it assuming that all element boundaries except one are made perfectly conducting. The modes of the analytical solution are used to obtain various orders of the basis function. Since our basis functions already satisfy Maxwell's equations it only remains to match the tangential electric and magnetic fields between neighbouring elements. This is accomplished by a set of orthogonal one dimensional matching functions associated with each edge.

As it turns out, the use of high order divergenceless edge elements leads to major qualitative and quantitative improvements over the conventional finite element scheme. Both electric and magnetic fields are approximated to the same degree of accuracy. Single elements of several wavelengths in size, suitable for large homogeneous parts of the problem, are easily coupled to the tiny elements that follow the geometry of the problem. The completely edge based formulation leads to an order of magnitude improvement in the computation time and memory requirements. Preliminary studies indicate numerical dispersion of less than one degree phase error after more than 300,000 wavelengths of plane wave propagation through a free space mesh where we assume 8.8 unknowns/wavelength.

## Numerical, Divergenceless Shape Functions for Three Dimensional Finite Element Analysis

*Daniel C. Ross\*, John L. Volakis*

Radiation Laboratory

University of Michigan, Ann Arbor MI 48109-2122

Standard finite element analysis of three dimensional electromagnetics problems result in spurious solutions unless the divergenceless character of the field is enforced. One technique to resolve this problem is to use shape functions that are themselves divergenceless. Currently, vector shape functions which are edge based are used for this purpose. These shape functions, while having zero divergence, are of zeroth order along element edges. To remove this lower level of approximation while retaining the simplicity of the linear shape functions, we will introduce new divergenceless node based shape functions.

In contrast to the edge based elements, these shape functions are linear in all three directions and are derived from the traditional node based functions upon enforcement of the divergenceless condition. The divergenceless condition eliminates one of the degrees of freedom and as a result, only eleven coefficients are present in the representation of the element fields. Using these shape functions, one can proceed with the traditional finite element formulation without a need to introduce a penalty term for eliminating spurious solutions (*Paulsen and Lynch*, IEEE Trans. MTT, vol. 39, no. 3 pg. 395).

Results will be presented to assess the accuracy of these shape functions over the edge elements.

Tue. p.m.

FINITE ELEMENT MODELING OF SCATTERING  
FROM ANISOTROPIC MATERIALS WITH ARBITRARY PRINCIPAL AXES

J. W. Parker, Jet Propulsion Laboratory, California Institute of Technology  
Pasadena, California, USA 91109

A full 3-D definition of electromagnetic fields in anisotropic materials is implied by the standard frequency-domain Galerkin bilinear functional, with relative permeability and/or permittivity given in explicit tensor form. Materials with arbitrarily directed principal axes afford simplicity in description and solution as compared to gyroscopic materials. For principal axis materials, a material tensor  $A$  is expressible in the form  $C^{-1}DC$ , where  $D$  is diagonal ( $= \text{diag}(d_{ii})$ ) and  $C$  is orthogonal ( $C^{-1} = C^T$ ). A convenient interface description has been adopted which may be produced by standard graphical design programs, consisting of values of the relative material constants on the diagonals of the tensors as interpreted in a principal axis coordinate system, plus a coordinate frame record indicating the relative directions of the principal axes to a global coordinate system. This form of material description is interpreted by a finite element code enforcing the functional. The matrix inverse  $A^{-1}$  of one of the tensors may be required, and this inverse is remarkably simple to compute given the diagonal values and the auxiliary coordinate axis description:  $A^{-1} = C^T \text{diag}(d_{ii}^{-1}) C$ .

The finite elements used are tetrahedral Whitney edge elements, which automatically enforce the boundary conditions at material interfaces, including anisotropic material boundaries. The domain of the computation is terminated by a local wave-absorbing boundary condition. This condition, used with the restriction of materials to those with principal axes, results in a matrix system which is symmetric and highly sparse.

Implementation on a message-passing distributed-memory computer allows rapid solution of problem domains larger than one wavelength across. Initial test cases examined include a DC-biased Kerr cell, which demonstrably transforms linearly polarized incident radiation to circular polarization, and an anisotropic rectangular slab with a result we compare to a finite-difference time-domain solution.

## A COMPARATIVE STUDY OF NODE AND VECTOR APPROACHES FOR THE FINITE ELEMENT SOLUTION OF WAVEGUIDE PROBLEMS

*A. Khebir\*, A. B. Kouki, and F. M. Ghannouchi*

Microwave Research Laboratory

Department of Electrical and Computer Engineering

Ecole Polytechnique de Montreal

3333 Queen Mary Blvd. 2nd Floor

Montreal, Quebec, H3V 1A2, CANADA

The finite element method is the most general and versatile method for the solution of dielectric waveguides partially because of its ability to use triangular elements and different order-polynomials. However, it has a serious difficulty that researchers have been wrestling with since 1971 when it was first applied for the solution of waveguide problems, namely, the occurrence of nonphysical solutions better known as spurious modes. Various remedies have been suggested for their elimination. Before the appearance of the so called tangential vector finite elements (*J. F. Lee, et al., IEEE MTT-39, 1262-1271, 1991*), approaches based on nodal finite elements, at best, shifted the wave number of the spurious modes to high frequency range. In addition to its ability to eliminate those modes, tangential vector finite elements approach has some other advantages. Namely, it imposes only the continuity of the tangential component, it naturally handles structures that have both electric and magnetic inhomogeneities, and it easily enforces the Dirichlet boundary conditions. However, it requires special elements not normally available in finite element meshing and display programs, it significantly increases the number of degrees of freedom in the model, and it uses only lower-order polynomials.

Recently, a new approach, that uses the conventional nodal based finite elements but without spurious modes, has been used for the solution of 3D cavities (*J. Bardi, et al., IEEE-Magnetics, Vol. 27, 4036-4039, 1991*). It consists of using a fixed Coulomb gauge and, hence, no spurious modes appear even in the case of zero wavenumber. We have extended this approach to the solution of general guiding structures. We have also developed a code based on the tangential vector finite elements approach. We have performed a comparative study of both approaches in terms of the memory requirement, the speed of computation, the accuracy of the solutions, etc. The results of this study will be presented and discussed.

THE INCLUSION OF RESISTIVE SHEETS IN A 3-D VECTOR  
FINITE ELEMENT ANALYSIS OF A DOUBLY INFINITE PERIODIC  
ARRAY

Thomas Fontana\* and Eric Lucas  
Westinghouse Electric Corporation  
Antenna/Aperture & Integrated Sensor Department  
P.O. Box 746  
Baltimore, Maryland, 21203

Resistive sheets have been used in Salisbury Screen absorbers, circuit analog absorbers, or as a mechanism to attenuate unwanted mode propagation. In this work, ohmic resistive sheets have been rigorously included in a vector finite element solution for the periodic volume using the partial variational principle, PVP (S. J. Chung and C. H. Chen, IEEE, MTT-36, March 1988). The PVP uses the variational properties of the reaction of the adjoint field with trial currents that are derived from the field discontinuities and the form of the basis. A E-field formulation has been constructed using a basis of second order vector edge elements in a tetrahedral mesh. Vector Floquet harmonics are used in a boundary element formulation at the top and bottom of the periodic cell. Appropriate periodic constraints are placed at the other sides of the cell.

Using the PVP technique, a trial current is calculated at the facets of all the tetrahedra from the tangential fields. Typically, the reaction of the adjoint field with this current cancels with the surface integration associated with a volume reaction term and results in the natural boundary condition. However, for a resistive sheet at the facet, a residual surface integration remains. An additional case of walls with finite conductivity was also examined. Using the same methodology, a slightly modified surface integration must be included.

We have used resistive sheets in the modeling of 3-D periodic scatterers and radiators. Comparisons are made with results from a method of moment analysis using rooftop current functions for the case of resistive patches. An array of hexagons formed from resistive sheets is also examined. For surfaces with finite conductivity, the quality factors of rectangular cavity resonances are compared with those derived from direct computations.

A 3-D VECTOR FINITE ELEMENT ANALYSIS FOR INFINITE  
DOUBLY PERIODIC RADIATING ARRAYS

Eric Lucas\* and Thomas Fontana  
Westinghouse Electric Corporation  
Antenna/Aperture & Integrated Sensor Department  
P.O. Box 746  
Baltimore, Maryland, 21203

In this work, a vector finite element analysis has been applied to a general periodic 3-D cell that describes a phased array radiator. The configuration is arbitrary in that conductors, lossy electric and magnetic media, and current sources are located by means of a tetrahedral mesh covering the cell. This has enabled diverse classes of radiators to be analyzed by a single analytical tool.

The finite element analysis uses the E-field formulation which follows from the fundamental variational principle (S. K. Jeng and C. H. Chen, IEEE, AP-32, Sept. 1984) and the partial patial variational formulation, PVP (S. J. Chung and C. H. Chen, IEEE, MTT-36, March 1988). The basis for the field consists of second order vector edge functions that ensure continuity of the tangential electric field and avoid spurious mode problems (A. Bossavit & I. A. Mayergoz, IEEE, MAG-25, July 1989). The cell is periodic in an infinite doubly periodic triangular array. Periodic constraints are rigorously enforced within the non-self-adjoint formulation of PVP. At the top and bottom of the cell, vector Floquet harmonics have been included to satisfy the radiation boundary condition. Using a PVP approach, this results in a hybrid finite element / boundary element solution.

The analysis has been successfully applied to a variety of 3-D radiators on transmit and receive. Complex structures have been modeled on an engineering work station using as many as 50,000 degrees of freedom. Engineering design information such as driving point impedance, element patterns, and axial ratio has been computed. Examples of analyzed radiators include a wide band notch radiator with its printed circuit board and stripline feed, patch radiators with coaxial feeds, and waveguide apertures. Comparisons of predictions with measurements in waveguide simulators are shown.

# A HYBRID FINITE ELEMENT-MODAL FORMULATION FOR INLET SCATTERING

*Daniel C. Ross\*, John L. Volakis and Hristos Anastassiou*

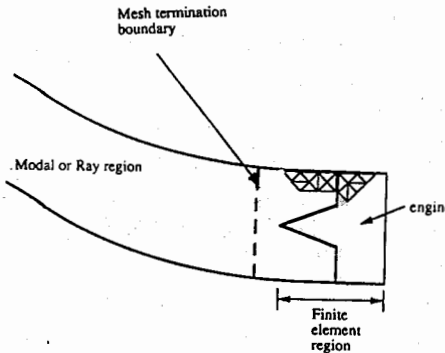
Radiation Laboratory

University of Michigan, Ann Arbor MI 48109-2122

The scattering mechanisms in jet engine inlets are complex and difficult to accurately simulate. The difficulty being the geometrical complexity and the large size of the problem. Most previous techniques have employed some high frequency solution (*Burkholder and Pathak IEEE AP Trans. vol. 37 pg. 194* and *Chuang and Lee IEEE AP Trans. vol. 23, pg. 770*) and recently, a boundary integral-modal technique (*Ling, IEEE AP Trans. vol. 38, pg. 1413*) was also employed.

A difficult aspect of the inlet problem is the accurate simulation of the engine face. This complex target can be efficiently modelled by the finite element method where the high frequency techniques break down. Away from the engine face, the fields within the inlet can be expanded as a modal solution and connected to the finite element solution through a connectivity matrix. Or, if the inlet is very large, ray tracing techniques can be used to construct the connectivity matrix.

In this paper, a hybrid finite element-modal formulation for the inlet scattering problem will be presented. This formulation uses three-dimensional finite element analysis for the engine face and a modal expansion for the solution in the inlet away from the engine. The finite element solution uses divergenceless shape functions that are linear in all directions and have eleven degrees of freedom as apposed to the traditional edge elements which have only six degrees of freedom. The overall storage requirement however remains the same. Part of this presentation will include a discussion of the fully automatic geometry pre-processing package, the advantages of the flexible finite element-modal connectivity scheme, and efficient, preconditioned iterative solution schemes. Results will be shown for cylindrical, simply terminated inlets to verify the procedure and for more complex configurations.



## A New E-B Formulation For Modeling Arbitrary Three-Dimensional Microwave Devices

Din Kow Sun\*, Xingchao Yuan, and Zoltan Cendes  
Ansoft Corporation  
Pittsburgh, PA 15129

A new transfinite element formulation of Maxwell's equation is obtained by solving for the electric field (**E**) and magnetic field (**B**) simultaneously. The electric field is approximated by using tangential vector finite elements and the magnetic field is approximated by using normal vector finite elements. In this way, the tangential continuity of the electric field and the normal continuity of the magnetic field is automatically satisfied.

This formulation offers three distinctive advantages over the standard method that solve the vector wave equation: (a) **E** and **B** are obtained in one step, (b) the resulting matrix is very sparse and can be solved very efficiently, and (c) it is well suited for use with the asymptotic waveform evaluation. As shown in our companion paper (X. Yuan and Z.J. Cendes, "A Fast Method for Computing the Spectral Response of Microwave Devices Over a Broad Bandwidth", IEEE APS/URSI 1993 Joint Symposia), the frequency response of a structure over a broad bandwidth is obtained very efficiently. Factors of ten or more speed improvement over traditional formulations can be obtained in analysing typical microwave devices such as microstrip bends and waveguide filters.

To show accuracy and efficiency of the new approach, a number of practical microwave devices are simulated and the numerical results are compared with measurements and those obtained by solving the problem at each single frequency directly.

## **A Fast Method for Computing the Spectral Response of Microwave Devices Over a Broad Bandwidth**

Xingchao Yuan\* and Zoltan Cendes

Ansoft Corporation

Pittsburgh, PA 15129

The finite element method has been applied successfully to solve the vector wave equation using tangential vector elements. Applications of this procedure range from simulating complicated three dimensional microwave devices to predicting the power deposition inside complex human models. As with other frequency domain formulations, the vector wave equation is solved at a single frequency. If solutions are required at more than one frequency, the solution must be repeated. This is computationally intensive because the solution of a matrix equation at each frequency is required. The CPU time required to simulate microwave resonators or filters having a complex spectral response is often prohibitive with this traditional approach.

In this paper, the vector wave equation is solved with a new technique that couples the finite element method with a procedure called asymptotic waveform evaluation. The scattering parameters and electromagnetic fields of arbitrary three-dimensional structures are obtained over a broad bandwidth. Specifically, the frequency response is computed by solving the structure at a single frequency and performing a few additional forward/backward substitutions to obtain the solution at other frequencies. The computational cost of obtaining the spectra response of a typical microwave device is at least one order magnitude less than with the traditional approach. Furthermore, the new method predicts device resonances and nulls analytically. Hence, it can be used to solve problems that are not well handled by other methods.

**A SEQUENTIAL AND PARALLEL IMPLEMENTATION OF  
A PARTITIONING FINITE ELEMENT TECHNIQUE  
FOR ELECTROMAGNETIC SCATTERING**

Y.S. Choi-Grogan\* and R. Lee

ElectroScience Laboratory  
Department of Electrical Engineering  
The Ohio State University  
1320 Kinnear Rd.  
Columbus, Ohio 43212-1191

A partitioning finite element method, which is capable of efficiently solving electromagnetic scattering problems involving electrically large scatterers, is presented. In this method the computational domain is divided into subregions. Within each subregion, finite element solutions are generated independent of the other subregions. The solution within each subregion is then coupled together by a global matrix equation. On a single processor computer, it can be shown that this method requires a significantly smaller amount of memory than the traditional finite element method (a typical example: 3 megaword versus 28 megaword on a Cray YMP). In addition, there is a significant computational savings for many problems involving electrically large scatterer. To account for the region exterior to the computation domain, the bymoment method is used for the boundary truncation.

To demonstrate this method, we consider the two dimensional problem of electromagnetic scattering from a penetrable cylinder. Two methods of partitioning are presented. In the first method, the partitioning is done only along one direction, so that the subregions are lined up along a single axis. In the second method, the partitioning is performed in two directions, so that the subregions form a two dimensional mesh structure. Both methods are used because their efficiency depends upon the geometry of interest.

The partitioning technique is also very suitable for implementation on a parallel computer. Because the finite element solution for each subregion is computed independently, the computation for each subregion can be done on separate processors without any need for interprocessor communication until the solution of the global matrix equation is performed. Thus, this method is ideal for the parallel computer. The major drawback is that the memory savings achieved on a single processor computer is negated because the memory information for all the subregions must be available to perform the computations on the parallel computer, whereas the memory information for each subregion is accessed sequentially on a single processor machine. Numerical results are presented for both single and multiple processor computers.



## ANTENNAS

Chairs: R.C. Hansen, R.C. Hansen, Inc.; T.G. Campbell, NASA Langley Research Center

Room: Michigan League, Vandenberg Room

Time: 1:30-5:30

|      |  |     |
|------|--|-----|
| 1:30 | INTERACTIVE DESIGN OF IMPEDANCE MATCHING NETWORKS FOR BROADBAND ANTENNA APPLICATIONS USING THE REAL FREQUENCY METHOD<br><i>Steven D. Eiken*, Omar Ramahi, Raj Mittra, University of Illinois</i>   | 200 |
| 1:50 | COMPARISON BETWEEN INDUCED EMF AND MOM METHOD IN MODELING A CIRCULAR LOOP ANTENNA ABOVE A FINITE REFLECTOR<br><i>Hassan A.N. Hejase*, Keith W. Whites, Stephen D. Gedney, University of Kentucky</i>   | 201 |
| 2:10 | A GENERALIZED RAY EXPANSION FOR COMPUTING THE EM FIELDS RADIATED BY AN ANTENNA IN A COMPLEX ENVIRONMENT<br><i>Robert J. Burkholder*, Prabhakar H. Pathak, The Ohio State University</i>  | 202 |
| 2:30 | A SIMPLE GAUSSIAN BEAM ANALYSIS OF THE FIELDS RADIATED BY TWO-DIMENSIONAL PARABOLIC REFLECTOR ANTENNAS ILLUMINATED BY A FEED ARRAY<br><i>Hristos T. Anastassiou*, University of Michigan; Prabhakar H. Pathak, The Ohio State University</i> | 203 |
| 2:50 | ANALYSIS OF LOG-PERIODIC DIPOLE ARRAY ANTENNAS FOR GROUND WAVE RADARS<br><i>S.A. Saoudy, Dion Pike, Memorial University of Newfoundland</i>  | 204 |
| 3:10 | BREAK  |     |
| 3:30 | AN EFFICIENT PLANAR ANTENNA NEAR FIELD ANALYSIS USING GAUSSIAN ELEMENTS<br><i>George Zogbi*, Robert J. Burkholder, Prabhakar H. Pathak, The Ohio State University</i>  | 205 |
| 3:50 | MOM SOLUTION OF A MODERATELY THICK WIRE ANTENNA<br><i>Xianneng Shen*, Joseph R. Mautz, Roger F. Harrington, Syracuse University</i>  | 206 |
| 4:10 | ON THE ACCURACY OF SEVERAL CAPACITANCE FORMULAS FOR ELECTRICALLY SMALL TUBULAR ANTENNAS<br><i>David F. Rivera*, John P. Casey, Naval Undersea Warfare Center</i>   | 207 |
| 4:30 | L-BAND ANTENNAS FOR MSAT TERMINALS<br><i>A. Kumar, AK Electromagnetique Inc.</i>   | 208 |
| 4:50 | GLINT NOISE REDUCTION BY FREQUENCY AGILITY FOR AN ANTI-COLLISION AUTOMOTIVE RADAR<br><i>Vahid Badii, Indiana-Purdue University</i>   | 209 |
| 5:10 | NECESSARY AND SUFFICIENT CONDITION FOR THE EXISTENCE OF AN INFLECTION POINT AND ITS APPLICATION TO REFLECTOR ANTENNA ANALYSIS<br><i>M.H. Rahnavard, Shiraz University</i>  | 210 |

**INTERACTIVE DESIGN OF IMPEDANCE MATCHING NETWORKS  
FOR BROADBAND ANTENNA APPLICATIONS  
USING THE REAL FREQUENCY METHOD**

*Steven D. Eiken\*, Omar Ramahi, and Raj Mittra  
Electromagnetic Communication Laboratory  
University of Illinois  
Urbana, Illinois 61801*

The development of broadband antenna technology, and the ability of the antenna designer to provide a good match of its impedance to the generator over the frequency band of interest, must go hand-in-hand in order to exact the best possible performance from the antenna. Optimal matching assures maximum power transfer to the load, increases the system efficiency and allows one to make the best use of the broadband characteristics of the antenna.

Numerous methods are available in the literature for broadband impedance matching using the gain-bandwidth theories. However, these methods require an analytical model of the load structure, which may be extremely complicated, or even impossible to obtain, especially for complex broadband antenna systems. An additional drawback of the analytical approaches is that they work only when the power gain of the system has been prescribed, and this is often not possible in practice. Although there are some computer packages available for generating simple matching networks, they neither offer the flexibility needed in the design process, nor do they guarantee an optimal performance. The Real Frequency Method (RFM), developed by Carlin, overcomes the shortfalls of the approaches mentioned above, and has been applied recently by Ramahi and Mittra (O. M. Ramahi and R. Mittra, *IEEE Trans. Antennas Propagat.*, vol. AP-37, no. 4, pp. 506-509, April 1989) to the problem of matching two loaded monopoles. They have not only carried out a numerical simulation of the design of a matching network, but have also verified their results through laboratory experiments. In light of the above background, the RFM method was judged to be best-suited for the broadband impedance matching problem investigated in this paper.

The Real Frequency Method is a numerical technique that requires only the input impedance data for the antenna to be matched. The method first develops a piecewise linear impedance function that optimizes the transducer power gain (TPG), which, in turn, is used to determine the impedance matching function. A computer code based on the RFM technique has been developed to synthesize the matching networks for arbitrary antennas, using only the input impedance of the antenna over the desired frequency range as the given data. A major advantage of RFM is that the designer can choose the topology of the matching network and can exercise some degree of control over the optimization results to fit the design specifications. The RFM matching code is very efficient and requires only a few seconds to run on a conventional computer or a workstation. This enables the user to adjust the design constraints in on the fly and develop matching networks in an efficient manner.

Numerical results illustrating the application of the method to the problem of matching a multi-octave antenna system will be presented in the paper.

## Comparison Between Induced EMF and MOM methods in Modeling a Circular Loop Antenna Above a Finite Reflector

Hassan A.N. Hejase\*, Keith W. Whites, and Stephen D. Gedney  
Dept. of Electrical Engineering, University of Kentucky  
Lexington, KY 40506

### ABSTRACT

This work studies the effect of image plane (reflector) dimensions on the radiated emissions from a circular loop antenna. Two methods are employed to compute the z-directed power gain from a circular loop antenna above a finite square reflector. The first is the Induced EMF method which computes the far-zone radiated fields as the superposition of two terms: The fields radiated from the loop currents (found by assuming an infinite plate) in the absence of the reflector, and the fields radiated from the induced reflector currents. The currents induced on the plate (obtained from a Physical Optics solution) are computed using a mixed FFT- Quadratic interpolation algorithm. The plate is discretized into triangular patches and the integration over each triangle is performed by making use of normalized area coordinates. This approach neglects the effect of plate edges when computing the current distribution on the loop. The edge effect becomes more pronounced as the plate dimensions decrease or as the loop is moved farther from the plate. A correction term is added to the fields to account for the edge effects using equivalent edge currents. The second approach uses a full-wave MOM code which will accommodate arbitrarily shaped 3-D PEC bodies and thin wires. In contrast to the first approach, no approximations to the scattering are made, but the computational costs are much larger. For numerical computations a loop one wavelength in circumference is chosen. Preliminary results obtained when the loop is placed a distance  $\lambda/4$  above the plate show that both the Induced EMF and MOM patch codes differ by less than 0.5 dB for plate widths larger than  $1\lambda$ . Further results for the power gain will be presented with the loop height and plate width as parameters.

Tue. p.m.

## A GENERALIZED RAY EXPANSION FOR COMPUTING THE EM FIELDS RADIATED BY AN ANTENNA IN A COMPLEX ENVIRONMENT

Robert J. Burkholder\* and Prabhakar H. Pathak

The Ohio State University

Dept. of Electrical Engineering/ElectroScience Laboratory  
1320 Kinnear Road, Columbus, Ohio 43212

A method is presented for computing the electromagnetic (EM) fields radiated by an arbitrary antenna in a complex environment using a generalized ray expansion (GRE).<sup>1</sup> Typical applications include the EM analysis of ship and airborne platforms with large antennas that may rotate and/or be electronically steered. In the GRE method the antenna is first replaced by electric and magnetic surface currents, using the equivalence theorem, which exist over a conveniently chosen surface which encapsulates the antenna and excludes all exterior obstacles. Next, the encapsulating surface is discretized into a small number of surface patches, or "subapertures," and the equivalent currents of each subaperture then radiate independently in the complex environment. The subaperture sizes are chosen so that all nearby obstacles, such as masts, turrets, and other antennas, are in the far zones of all the subapertures. This allows conventional ray methods to be used to track the fields radiated by each subaperture (assuming that the antenna environment is amenable to ray analysis), even though obstacles may exist in the near zone of the original antenna.

In the GRE method, rays are launched radially outward from the phase centers of the subapertures and tracked throughout the complex environment to a field observation point using high-frequency asymptotic ray methods, such as geometrical optics (GO) and the uniform theory of diffraction (UTD). The observation point could be in the far zone of the original antenna (e.g., for pattern prediction), or in the shipboard environment (e.g., for antenna coupling or onboard radiation hazard prediction). The amplitude of each ray is weighted by the far field radiation pattern of its subaperture evaluated in the direction in which the ray was initially launched. An advantage of the GRE method is that only the amplitude weighting of the rays changes with antenna excitation and not the ray paths. Therefore, the rays only need to be tracked once, independently of the antenna rotation or electronic steering angle.

---

<sup>1</sup>The GRE method has previously been used for computing the EM scattering by large open-ended waveguide cavities (Pathak & Burkholder, *Radio Science*, Vol. 26, No. 1, pp. 211-218, Jan.-Feb. 1991).

**A SIMPLE GAUSSIAN BEAM ANALYSIS OF THE FIELDS  
RADIATED BY TWO-DIMENSIONAL PARABOLIC REFLECTOR  
ANTENNAS ILLUMINATED BY A FEED ARRAY**

Hristos T. Anastasiu\*

Dept. of Electrical Engineering  
and Computer Science  
University of Michigan  
Ann Arbor, Michigan, U.S.A.

Prabhakar H. Pathak

Dept. of Electrical Engineering  
The Ohio State University  
Columbus, Ohio, U.S.A

A simple and physically appealing Gaussian Beam Analysis is presented for predicting the fields radiated by an electrically large reflector antenna illuminated by a primary feed. The fields radiated by a single feed or by an array of feed elements for illuminating a reflector antenna are first expanded into a set of relatively few, well focussed Gaussian beams (GB's). The coefficients of this expansion, which constitute the GB amplitudes, can be found in a relatively simple fashion. In particular, a sufficient number ( $N$ ) of identical GB's are launched radially from a preselected periodic array of lattice points ( $M$ ). Furthermore, each beam set  $N$  has a constant angular interbeam spacing for every  $m (= 1, 2, \dots, M)$ . In the present work, the feed and the parabolic reflector are assumed to be 2-D for the sake of illustrating the main ideas in the GB approach, without the additional work required for the 3-D case. The set of well focussed GB's launched from the feed plane next illuminate the reflector and thus undergo reflection and diffraction at the parabolic surface. Only incident GB's which strongly illuminate the reflector edges contribute significantly to the fields diffracted by the edges. The composite reflection and diffraction of an incident GB by an edge is found via the solution to an appropriate canonical problem. For incident GB's whose beam axes strike the reflector sufficiently far from the edges, the above composite GB scattering solution reduces simply to the reflected GB as predicted by the simple rules of beam optics. Thus, the present GB based approach is expected not only to be physically appealing, but also extremely efficient as it would completely avoid the need for evaluating any radiation integrals over the reflector boundary or its projected aperture as is required in the conventional approaches for reflector antenna analysis. The present GB approach is different from that presented previously by others in that it does not use a combination of the complex source point (CSP) method in combination with the uniform geometrical theory of diffraction (UTD) which to date has been shown to yield only the far out sidelobes and back lobes of reflectors, while failing in regions where the reflected GB's exist and provide the dominant contribution to the radiated field. In contrast, the present approach accurately provides the main lobe, side lobes as well as the backlobes. The extension to 3-D reflectors is currently in progress. Numerical examples based on the present GB approach will be illustrated for 2-D feed-reflector configurations.

Tue. p.m.

**ANALYSIS OF LOG-PERIODIC  
DIPOLE ARRAY ANTENNAS  
FOR GROUND WAVE RADARS**

**S.A. Saoudy and Dion Pike**  
Centre for Cold Ocean Resources Engineering  
Memorial University of Newfoundland  
St. John's, Newfoundland, Canada A1B 3X5

Attention has been paid to ground wave radar (GWR) research over the past decade due to its potential for over-the-horizon detection of surface based and low flying objects.

A vertical log-periodic dipole array (VLPDA) antenna can be used as the transmitting antenna in a GWR system since it offers various advantages: a wide operational bandwidth; a high power rating and directivity; a wide azimuth beamwidth; high front to back ratio; and a deep null in the vertical direction.

Since the early development of the log-periodic antenna concept in free space by D. Isbell (1960), considerable work has been done for the VLPDA that is applicable to high frequency GWR systems. Most importantly, the presence of ground requires that the array be skewed to overcome frequency sensitivity, and so allows broadband application.

This work establishes a procedure for determining the particular geometry of a skewed VLPDA antenna with certain radiation characteristics. Based on three parameters: scale factor  $r$ , spacing factor  $\sigma$ , and a newly introduced height factor  $B_1$  within a specified frequency band, numerous graphs of antenna characteristic have been developed. The radiation characteristics of a particular skewed VLPDA configuration over perfect ground have been evaluated using the Numerical Electromagnetics Code (NEC-2) which employs the method of moments. For a particular application with required radiation characteristics, these graphs are used 1) to determine if the skewed VLPDA can deliver such characteristics and 2) to determine the closest values of  $r$ ,  $\sigma$ , and  $B_1$  which furnish these characteristics. In producing these graphs account was taken of the presence of a metallic tower whose position satisfies the scale factor  $r$ .

Also, a quantitative investigation has been carried out into the change in radiation characteristics due to 1) the relative location of the tower with respect to the elements, 2) the height above ground of the entire VLPDA, and 3) the relative height of the lower tip heights of the elements over ground. Illustrations of the VLPDA active region and current distribution along the array elements have also been developed.

## AN EFFICIENT PLANAR ANTENNA NEAR FIELD ANALYSIS USING GAUSSIAN ELEMENTS

George Zogbi,\* Robert J. Burkholder and Prabhakar H. Pathak  
The Ohio State University ElectroScience Laboratory  
Department of Electrical Engineering  
Columbus, Ohio 43212

An efficient approach is presented in which a relatively few Gaussian basis elements are employed to represent the field distribution over an electrically large planar antenna which may be electronically scanned. This representation leads to simple closed form expressions for the radiated antenna fields. The near fields obtained are valid at distances substantially less than the conventional Fresnel zone distance and the field expressions are automatically valid in the far zone as well. The Gaussian expansion coefficients are easily found using Galerkin's method and once obtained are valid for all frequencies. An efficient calculation of antenna near fields is invaluable for such applications as radiation hazard analysis, near field antenna coupling, and planar near to far field transformations.

Recently, Gaussian expansions have been utilized by others based on a Gabor representation that reproduces the required distribution over the finite equivalent source region on the antenna aperture plane and zero fields elsewhere on the plane. This enables one to employ a paraxial approximation which gives the radiated fields in terms of simple Gaussian beams. In contrast, in the present formulation the field in the antenna aperture plane is expanded in terms of substantially fewer Gaussian elements by not forcing the distribution to go to zero outside the finite extent of the source region. Consequently, the radiated field expression will now contain error functions associated with the end elements while the near in elements generate essentially Gaussian beams.

One pleasing aspect of the present formulation is that the resulting radiated field expressions are accurate at all distances from the aperture except in the extreme near zone. Thus, if the antenna near fields are measured over a finite region on a plane away from the physical antenna, they can be expressed in terms of the Gaussian elements as discussed above and the resultant near and far fields may then be easily computed. These expressions are more physically insightful than an FFT technique which would simply yield numerical values for the far field; it is also more efficient than employing a vector wave function expansion which is slowly convergent for electrically large, or high gain antennas. Examples illustrating these concepts will be presented.

## MOM SOLUTION OF A MODERATELY THICK WIRE ANTENNA

Xianneng Shen\*, Joseph R. Mautz, Roger F. Harrington  
Department of Electrical & Computer Engineering  
Syracuse University  
Syracuse, NY, 13244-1240

The problem considered is that of obtaining a MoM (method of moments) solution of a thick wire antenna. The thin wire antenna model assumes that the electric current at the two ends is zero, which is only valid for the wire whose radius is electrically small. In modelling the moderately thick wire antenna, we must be aware that the two ends give a considerable contribution to the scattering or radiation field. The currents on the top and the bottom disks are in the  $\rho$ -direction and uniformly distributed along the  $\varphi$ -direction. The requirement of the continuity of the currents at the centers of the disks forces the currents to be zero at the center of the top disk and the bottom disk. It may be reasonable to assume that the current on the disks is a linear function of  $\rho$  along the  $\rho$ -direction between the center and the edge of the disk. On the top disk, the current can be visualized as turning sharply from the  $z$ -direction to the  $-\rho$  direction and flowing continuously from the  $z$ -direction to the  $-\rho$  direction. On the bottom surface, the current starts from zero at the center of the disk and increases linearly as it flows towards the corner  $\rho = a$ . Then the current turns sharply from the horizontal  $\rho$ -direction to the vertical  $z$ -direction, flowing continuously. From this picture, it may be sufficient to approximate the current on each disk by a half triangle. The expansion functions are chosen to be triangle functions. The testing functions consist of the triangle expansion functions on the lateral surface of the wire displaced to the axis of the wire. The testing functions at the ends of the axis are half triangles.

A set of linear equations is obtained for the unknown coefficients of the expansion functions by requiring that the net  $z$ -directed electric field on the axis be orthogonal to each testing function. This set of linear equations is the MoM matrix equation. This matrix equation is solved for the unknown coefficients. Numerical results will be presented, and further discussion will be given.

## ON THE ACCURACY OF SEVERAL CAPACITANCE FORMULAS FOR ELECTRICALLY SMALL TUBULAR ANTENNAS

David F. Rivera\* and John P. Casey  
Submarine Electromagnetic Systems Department  
Naval Undersea Warfare Center Detachment  
New London, CT 06320

The design of an electrically small dipole or monopole antenna involves the calculation of its input impedance. The input impedance of such an antenna can be modelled by a capacitor C in series with a resistance R, where  $R \ll 1/j\omega C$ . R represents the radiation resistance of the antenna plus any dissipative losses. The antenna capacitance C is obtained through electrostatics (Schelkunoff and Friis, *Antennas: Theory and Practice*, Ch. 10, J. Wiley & Sons, 1952).

Simple formulas for determining the capacitance of an electrically small tubular antenna have been published by Grover (*Bureau of Standards Scientific Papers*, 22, 569 - 629, 1928) and by Casey and Bansal (*Electron. Lett.*, 24, 1021 - 1022, 1988). The accuracy of each formula depends on the ratios of various parameters such as  $h/l$  and  $d/l$ , where  $h$  is the separation of the tube from the ground plane (monopole case) or one-half of the feed gap (dipole case),  $d$  is the tube diameter, and  $l$  is the tube length (monopole case). The absence of a parametric study that determines the region of validity of each formula has led to confusion regarding their applicability in practical design problems.

This simple parametric study determines the accuracy of the capacitance formulas by comparing them against numerical results obtained from the method of moments. Data will be presented and regions that are accurate to within 10% of the method of moments results are identified.

Tue. p.m.

*No Shows*

## L-BAND ANTENNAS FOR MSAT TERMINALS

A. Kumar  
AK Electromagnetique Inc.  
P. O. Box 240  
30 Rue Lippee  
Coteau Station  
Quebec  
Canada J0P 1EO

This paper describes the design and performance of a family of fixed and mobile antennas developed at AK Electromagnetique Inc., Communications Research Centre and other organizations in support of an emerging North American Mobile Satellite Service (MSS) system. The noise temperature and G/T parameters are compared for these antennas at various elevation angles. Measured radiation patterns and return loss are described in this paper. The design for each of the key elements are carefully reviewed to see how the designs could be modified so as to best represent a commercially produced antenna. The results of the costs are discussed for each antenna.

**GLINT NOISE REDUCTION BY FREQUENCY AGILITY  
FOR AN ANTI-COLLISION AUTOMOTIVE RADAR**

Vahid Badii  
Assistant Professor of Electrical Engineering  
Indiana-Purdue University at Fort Wayne  
Fort Wayne, IN 46805

Monopulse radar has been proposed for possible automotive use as an anti-collision sensor. A system entitled "cradar" (Dale Grimes and Craig Grimes, 'Cradar - An Open-Loop Extended-Monopulse Automotive Radar', IEEE Trans. on Vehicular Tech., Vol. 38, No. 3, August 1989) was introduced to provide such target information as range, bearing and closing speed. Cradar uses three waveguide propagation modes to sequentially drive a single horn antenna. Because of the simplicity of cradar, the ultimate cost is expected to be quite low.

Monopulse radar has a basic unresolved difficulty: Glint noise. It refers to the perceived deviation from the true center of the target being tracked. This deviation can cause false alarms. Glint noise or target scintillation is essentially a wave-interference phenomena. Target glint occurs when the object being tracked is several times larger than the radar wavelength, as is the case in the highway environment. Aperture-averaging and frequency-averaging are two commonly used methods to overcome glint noise.

Previous results (Vahid Badii and Dale Grimes, 'Glint Noise Cancellation Methods for an Open Loop, Extended Monopulse Automotive Radar', 1990 URSI Meeting, Sponsored Jointly by the IEEE and URSI, Dallas, TX. May 7-11, 1990) have shown that aperture-averaging alone is not enough to mitigate the effects of glint noise.

A computer model has been developed to simulate the automotive radar. The model tests cradar's monopulse radar tracking system. A two point target model is used to test the effects of frequency averaging. A considerable improvement is detected with the addition of two frequencies to the center frequency. Further improvement will result as more frequencies are used. The results prove frequency averaging shows promise as a method of reducing glint noise in the automotive radar studied.

Tue. p.m.

NECESSARY AND SUFFICIENT CONDITION FOR THE EXISTENCE  
OF AN INFLECTION POINT AND ITS APPLICATION TO  
REFLECTOR ANTENNA ANALYSIS

M. H. Rahnavard  
EE Dept., School of Engg.  
Shiraz University  
Shiraz, Iran

In the study and analysis of surface curvature induces shadow which is encountered in dual shaped reflector, Glaindo-Williams surface and unstable optical resonator inflected point has important role. In this paper necessary and sufficient condition for the existence of inflected point is studied. The role of inflected point in analyzing an ideal cubic phase front is considered.

**SPECIAL SESSION AP-S/URSI D-4****TUESDAY PM****ADVANCES IN MMIC PACKAGING FOR PHASED ARRAY ANTENNAS**

Chairs: R.N. Simons, NASA Lewis Research Center; S.R. Taub, NASA Lewis Research Center

Room: Michigan League, Michigan Room

Time: 1:30-5:10

|      |  |      |
|------|--|------|
| 1:30 | THE ROLE OF EM MODELING IN INTEGRATED PACKAGING<br><i>Linda P.B. Katehi, The University of Michigan</i>  | AP-S |
| 1:50 | ELECTROMAGNETIC DESIGN ASPECTS OF PACKAGES FOR PHASED ARRAY MODULES THAT MAY INCORPORATE MONOLITHIC ANTENNA ELEMENTS<br><i>D.W. Griffin*, A.J. Parfitt, The University of Adelaide</i> | AP-S |
| 2:10 | GAAS MMIC MULTICHP MODULES<br><i>Susan M. Collette, Motorola Inc.</i>  | AP-S |
| 2:30 | ADVANCED CERAMIC PACKAGING FOR MICROWAVE AND MILLIMETER WAVE APPLICATIONS<br><i>Deborah S. Wein, StratEdge Corporation</i>   | AP-S |
| 2:50 | MICROMACHINED SILICON AS A MODULE PLATFORM FOR MULTIPLE FIBER I/O'S<br><i>Paul G. Haugsjaa, GTE Laboratories</i>   | AP-S |
| 3:10 | BREAK  |      |
| 3:30 | OPTICAL INTERCONNECTION AND PACKAGING FOR ACTIVE ARRAY ANTENNAS<br><i>Nick J. Parsons, GEC - Marconi Research Center</i>   | AP-S |
| 3:50 | THE EVOLUTION OF MMIC PACKAGING<br><i>H.J. Kuno, T.A. Midford, J.J. Woodridge, Hughes Aircraft Company</i>   | AP-S |
| 4:10 | MULTI-ELEMENT MULTI-LAYER PACKAGING FOR PHASED ARRAY ANTENNA APPLICATIONS<br><i>Kurt A. Shalkhauser*, NASA Lewis Research Center; Martin P. Goetz, StratEdge Corp.</i>                 | AP-S |
| 4:30 | A MULTILAYERED PACKAGE TECHNOLOGY FOR MMICS<br><i>Masao Ida, Toshio Nishikawa, Murata Mfg. Co.</i>   | AP-S |
| 4:50 | DISCUSSION   |      |



## ELECTROMAGNETIC FIELD MEASUREMENTS

Chairs: K.M. Chen, Michigan State University  
 M. Kanda, National Institute of Standards and Technology

Room: Michigan League, Room D Time: 1:30-5:10

|      |   |     |
|------|---|-----|
| 1:30 | VHF-UHF UWB MEASUREMENT OF SCATTERING AND SUPPORT<br>INTERACTIONS FOR A CONDUCTING CYLINDER<br><i>J.D. Young*, B. Chan, The Ohio State University</i>   | 214 |
| 1:50 | RADAR TARGET DISCRIMINATION USING E-PULSES WITH THE EARLY-<br>TIME AND LATE-TIME RESPONSES<br><i>J. Ross*, P. Ilavarasan, E. Rothwell, R. Bebermeyer, K.M. Chen, D. Nyquist, Q. Li, Michigan State University</i>                                     | 215 |
| 2:10 | RADAR DETECTION OF TARGETS IN A SEA CLUTTER ENVIRONMENT<br>USING E-PULSE TECHNIQUE<br><i>P. Ilavarasan*, J. Ross, R. Bebermeyer, E. Rothwell, K.M. Chen, D. Nyquist, Michigan State University</i>  | 216 |
| 2:30 | COUPLING THROUGH DEEP, TORTUOUS PATH AND BOLT-LOADED<br>NARROW SLOT APERTURES WITH DEPTH AND LOSS<br><i>Russell P. Jedlicka*, Steven P. Castillo, New Mexico State University; Larry K. Warne, Sandia National Laboratories</i>                       | 217 |
| 2:50 | INFRARED MEASUREMENTS OF ELECTROMAGNETIC FIELDS IN A<br>COMPACT, EFFICIENT CIRCULAR WAVEGUIDE MICROWAVE ANTENNA<br>USING A COMBINED MODE CONVERTER/RADIATOR<br><i>Norgard, Sega, Harrison, Komar, Pohle, Prather, Smith, USAF Phillips Laboratory</i> | 218 |
| 3:10 | BREAK   |     |
| 3:30 | RADAR TARGET DISCRIMINATION USING NEURAL NETWORKS AND THE<br>DISCRETE WAVELET TRANSFORM<br><i>C.Y. Tsai*, R. Bebermeyer, E. Rothwell, K.M. Chen, D. Nyquist, Michigan State University</i>  | 219 |
| 3:50 | SPACE SHUTTLE EMC STUDY FOR THE WISP/HF EXPERIMENT<br><i>K.G. Balmain*, C.C. Bantin, M.A. Tilston, M.M. Reeves, University of Toronto</i>   | 220 |
| 4:10 | CALIBRATION OF MICROSTRIP & STRIPLINE FIELD APPLICATORS USING<br>TIME DOMAIN TECHNIQUES<br><i>D. Infante*, D.P. Nyquist, J. Ross, Michigan State University; M. Havrilla, General Electric Aircraft Engines</i>                                       | 221 |
| 4:30 | THE CHARACTERISTICS OF METEOROLOGICAL NOISES RELATED WITH<br>WEATHER<br><i>Eikichi Asari, Hokkaido College of Arts and Sciences</i>   | 222 |
| 4:50 | ABOUT THE MATCHED SIGNALS OF SUBSURFACE SURVEYING RADARS<br><i>Fang Guangyou*, China Research Institute of Radiowave Propagation; Wang Wenbing, Xian Jiaotong University</i>  | 223 |

## VHF-UHF UWB Measurement of Scattering and Support Interactions for a Conducting Cylinder

J. D. Young\* and B. Chan  
The Ohio State University ElectroScience Laboratory  
Department of Electrical Engineering  
Columbus, Ohio 43212

A 2:1 conducting cylinder is a typical scattering calibration target. There are accurate analytical models for its response over a wide range of frequencies and angles, and its shape and symmetries make it easy to mount and measure accurately. In particular, the cylinder exhibits strong specular scattering at broadside and endfire which are useful for target electrical alignment as well as for simple calibration at high frequencies. A common mounting technique for the cylinder target involves an ogival pylon, which either contacts the bottom surface of the target or is spaced a small distance away using a foam saddle. The subject of this presentation are a series of measurements to determine the error effects of the pylon support on the data, for a wide frequency range (200 to 2000 MHz), a wide selection of orientations, and for two polarizations.

The data were recorded at the Ohio State University "Big Ear" compact radar scattering range. The experimental equipment and the experimental technique will be described. The presentation will describe a tether mounting apparatus for the target, so the pylon could be slid in underneath the target without disturbance and a differential image could be measured.

Both conventional UWB ISAR and superresolution processing were done on the data base. This paper presents the conventional processing, and a companion presentation (Gerry and Walton) will discuss superresolution results. The processing has arrived at impulse waveforms and frequency spectra for several support interaction terms. The quantitative data will be presented to support the conclusion that pylon errors over the total 200 to 2000 MHz frequency band are more than 30dB down from the specular scattering echos of this calibration target.

## RADAR TARGET DISCRIMINATION USING E-PULSES WITH THE EARLY-TIME AND LATE-TIME RESPONSES

J. Ross\*, P. Ilavarasan, E. Rothwell, R. Bebermeyer,  
K.M. Chen, D. Nyquist and Q. Li  
Department of Electrical Engineering  
Michigan State University  
E. Lansing, MI 48824

Radar target discrimination using aspect angle independent E-pulse methods and the late-time resonant response have been developed and applied successfully to measured scale model responses. Unfortunately, for targets with low Q or targets whose dominant natural resonances are not excited by the interrogating waveform, the late-time signal energy is very small. This leads to great difficulty in discrimination using late-time E-pulses.

To avoid this problem, it is desirable to use the early-time response which in these cases contains most of the received signal energy. The early-time response is generally composed of specular reflections from various target structures such as fuselage, wings, engines, etc. In some cases there are also components arising from substructure resonances and building global resonances. When the specular reflections dominate, it has been found that the Fourier transform of the early-time response can be approximated as a sum of exponentially damped sinusoidal waveforms in the frequency domain. This approximation allows a frequency domain analog of the late-time E-pulse to be constructed for the early-time response. Unlike the late-time E-pulse which is aspect independent, the early-time frequency domain E-pulse is aspect dependent. Thus, many early-time E-pulses are required for each target. This problem of aspect dependency however is characteristic of all potential discrimination schemes based on the early-time. It is apparent that the amount of data storage required for the E-pulses is generally orders of magnitude less than may be required for correlation based methods. Moreover, the scheme may prove useful for targets that have both a strong early-time and late-time response since the discrimination process can be easily combined with existing late-time E-pulse algorithms.

This paper will discuss the early-time frequency domain E-pulse and discrimination will be demonstrated using measured short pulse radar returns from scale model aircraft. Methods for combining these results with results obtained from late-time E-pulse methods to enhance the discrimination decision process will be discussed.

Tue. p.m.

## RADAR DETECTION OF TARGETS IN A SEA CLUTTER ENVIRONMENT USING E-PULSE TECHNIQUE

P. Ilavarasan\*, J. Ross, R. Bebermeyer, E. Rothwell,  
K. M. Chen and D. Nyquist

Department of Electrical Engineering  
Michigan State University  
East Lansing, MI 48824

The radar detection of a target flying just above the ocean surface is difficult because the target response is usually overwhelmed by strong sea clutter. Recently, we have studied the feasibility of using an ultra wide band, pulse-type radar combined with the E-pulse technique to address this problem.

To study the nature of sea clutter, the ocean wave is modeled by a sinusoidal conducting surface and a theoretical analysis conducted to calculate the scattering of a short EM pulse from this ocean wave model. An experiment was also conducted to measure the scattering from a simulated ocean wave model illuminated by a short EM pulse either synthesized by sweeping the 1-7 GHz frequency band using a network analyzer or generated by an EM pulse generator. Theoretical and experimental studies indicate that a short EM pulse is reflected principally from the tops of the ocean wave crests. This results in a sea clutter that is periodic with the period determined by the distance between the ocean wave crests.

To increase the probability of detection of the target it is desirable to minimize the sea clutter return. Generally, the application of post-receive processing methods are less desirable than optimization performed in the transmit portion of the system. Thus, one would like to determine if there is an optimal transmitted pulse waveform that would minimize the clutter return. By examining the damped periodic nature of the sea clutter return, it can be seen that a significant portion of the signal can be approximately represented as a sum of exponentially damped sinusoids. Thus, a finite duration E-pulse may be constructed and transmitted such that when it illuminates the ocean wave the sea clutter is minimized while the target response is enhanced.

This paper will demonstrate the utility of the E-pulse method in sea clutter reduction using both theoretical and measured clutter returns from a simulated ocean wave model of sinusoidal conducting surface. It will also be shown that the E-pulse spectrum can be further modified to increase the target response without losing the clutter reduction capability.

## COUPLING THROUGH DEEP, TORTUOUS PATH AND BOLT-LOADED NARROW SLOT APERTURES WITH DEPTH AND LOSS

Russell P. Jedlicka<sup>1</sup>, Steven P. Castillo<sup>1</sup> and Larry K. Warne<sup>2</sup>

<sup>1</sup>Department of Electrical & Computer Engineering  
New Mexico State University Las Cruces, New Mexico

<sup>2</sup>Electromagnetic Analysis Division  
Sandia National Laboratories Albuquerque, New Mexico

Electromagnetic coupling to shielded systems is an important problem. The energy can penetrate to the interior via antennas as well as through seams in otherwise shielded enclosures. Bowing of the metal at seams in an overlap joint can create entry points. These can be viewed as narrow slot apertures. Previously an experimental study was commenced to validate the antenna/local transmission line model (L.K. Warne and K.C. Chen, AP-37, No. 7, July 1989, pp. 824-834 and EMC-32, No. 3, August 1990, pp 185-196) for rectangular narrow slot apertures with depth. An equivalent antenna radius is used to account for depth. The model also accounts for losses in the walls of the slot as well as the surrounding ground plane. The work was performed in the 2-4 GHz range and the slot length was chosen such that the first resonance was in the frequency band of interest. The coupling for slots of varying geometry, in a large ground plane, was found to decrease with increasing depth, increase for larger widths and showed a decided dependence upon the conductivity of the wall material. In fact, for small widths, the effect of changing wall conductivity changed the coupling by as much as 10 dB.

The slots considered in the original study had a right rectangular cross section and were terminated with a short on either end. This investigation extends the earlier experimental work to consider the limiting case of a very deep rectangular slot. Additionally, it considers a tortuous path slot which is representative of an aperture in a system with an overlap joint. Furthermore, rectangular and tortuous path slots with bolt loads were measured. The deep slot, which is 2" in length, 2.75" deep and 0.005" wide, displays two peaks which reflect the length and depth resonances. The peak coupling values and Q factors agree quite well with the predicted results of the model. The tortuous path slot dimensions were chosen to model a typical joint which might occur in an actual system. It's length is 2.8", width is 0.010" and the tortuous path depth is 0.50". The overlap section of this slot was chosen to be 0.25". This slot was measured with, and without, a center bolt load. Without the bolt, the computed and measured results are in good agreement in terms of the peak coupling level at resonance as well as the Q factor. When the bolt is in place, there is a definite upward frequency shift which is due to the small inductive load at the center of the slot. Additionally, the coupling is reduced at this higher frequency. The coupling through the bolt-loaded, overlapped joint is also compared to that of bolt loads in simple rectangular slots.

In summary, measurements were performed to characterize the coupling through narrow slot apertures with depth. In this work more realistic slot apertures were considered; that is, configurations that are representative of riveted and bolted seams at joints of shielded enclosures.

Tue. p.m.

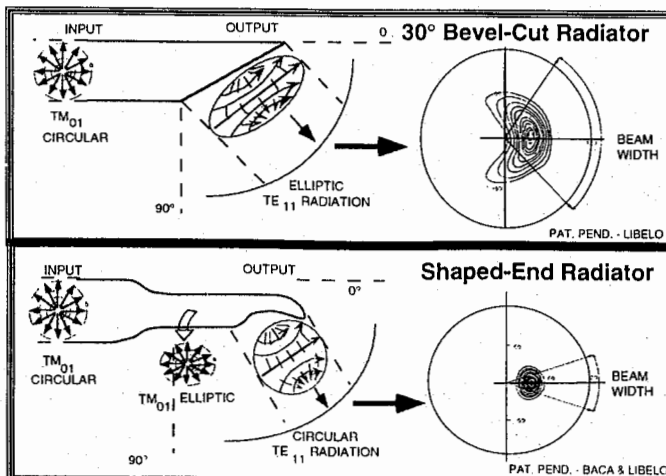
**INFRARED MEASUREMENTS OF ELECTROMAGNETIC FIELDS  
IN A COMPACT, EFFICIENT CIRCULAR WAVEGUIDE MICROWAVE ANTENNA  
USING A COMBINED MODE CONVERTER/RADIATOR**

Norgard, Sega, Harrison, Komar, Pohle, Prather, Smith

Microwave Research Laboratory  
USAF Phillips Laboratory  
Kirtland AFB, NM 87117-6008

An infrared (IR) measurement technique is described that can be used to measure electromagnetic (EM) fields. This IR technique is based on the Joule heating that occurs in a lossy material as an EM wave passes through the material. The absorbed heat energy is converted into conducted and convected heat energy and into re-radiated EM energy. This EM energy is concentrated in the IR band, and is detected with an IR camera as the energy radiated from a "blackbody". This technique involves placing a thin lossy planar detection screen in the plane over which the fields are to be measured. The absorbed energy causes the temperature of the detector to rise above the ambient temperature of the surrounding environment by an amount proportional to the local electric and/or magnetic field intensity (energy) at each point in the screen material. The temperature distribution in the screen material is a map of the intensity of the electric or magnetic field distribution absorbed in the screen.

This IR measurement technique is applied to determine the electromagnetic characteristics of a combined mode converter/radiator in a circular waveguide microwave antenna. The antenna is fed with a coaxial  $TM_{01}$  mode for compact size and efficient operation. From symmetry, the  $TM_{01}$  mode does not radiate in the bore-sight direction; therefore, a mode converter/radiator is used to convert this mode to the dominant  $TE_{11}$  mode. A 30 degree bevel-cut radiator and a shaped-end radiator are examined. Near-field and far-field radiation patterns of the antenna are also measured with the IR technique.



RADAR TARGET DISCRIMINATION USING NEURAL NETWORKS  
AND THE DISCRETE WAVELET TRANSFORM

C.Y. Tsai\*, R. Bebermeyer, E. Rothwell, K.M. Chen and D. Nyquist

Department of Electrical Engineering

Michigan State University

E. Lansing, MI 48824

It is well known that the early-time specular portion of the transient scattered-field response of a radar target is highly aspect dependent. Using early time for target discrimination thus requires the storage of target information for a large number of aspect angles. Storing the target responses themselves is highly inefficient, and a variety of techniques have been devised for reducing storage requirements. One of the most promising of these approaches is to store the aspect information within a neural network.

One popular approach to pattern recognition uses a multi-layer nonrecurrent neural network trained using the backpropagation algorithm. For radar target identification, each anticipated target is assigned a desired sequence which will appear at the output of the network when the input is the response of the target measured at any aspect angle. Thus, a single network can recognize several targets, regardless of aspect.

Several difficulties arise when implementing the backpropagation algorithm. First, there is no guarantee that training will converge, and the learning process may be very slow. More importantly, the nonrecurrent network tends to assign an unknown input to an output state of a known waveform. That is, the network has trouble discerning when an input was not used in the training process, leading to a false identification of an unknown target. This also leads to a high occurrence of error in the presence of random noise.

The noise sensitivity of a nonrecurrent network can be reduced by first processing the input waveforms through the discrete wavelet transform (a hierarchical decomposition into wavelet basis functions), and then truncating the wavelet spectrum, keeping only the largest coefficients. The temporal positions of these coefficients are relatively insensitive to random noise and can be used as the input to the neural network. This also serves to dramatically reduce the size of the neural network.

Both noise sensitivity and the misclassification of unknown targets can be overcome using associative memory networks. These recurrent networks use feedback to create an output which settles to a stable state. Thus, an input which is only partially correct (or contaminated by random noise) may still produce the correct output. Similarly, an unknown input tends to produce an output which settles at a stable state not associated with a known input. Networks can be either autoassociative as with Hopfield networks or heteroassociative as with bidirectional associative memory networks. The drawback with associative memory networks lies with capacity. It is not always possible to associate all desired inputs with a stable state, and a large network may be required to store a modest amount of information.

This paper will discuss the applicability of neural networks to target discrimination and compare the performance of the above neural networks using the measured responses of several aircraft target models at a variety of aspect angles.

## SPACE SHUTTLE EMC STUDY FOR THE WISP/HF EXPERIMENT

K.G. Balmain\*, C.C. Bantin, M.A. Tilston, and M.M. Reeves

Department of Electrical and Computer Engineering

University of Toronto

Toronto, Ontario, Canada M5S 1A4

Waves-in-Space-Plasmas/High-Frequency (WISP/HF) is a proposed Space Shuttle experiment intended for radiated-wave studies of the F-region ionosphere. It covers the frequency range 0.1-30 MHz, utilizing radiation from a dipole antenna with pre-selected tip-to-tip lengths of 5 m (extending from sill to sill across the Shuttle's payload bay), 15 m (extending out over the wings) and 50 m (extending beyond the wings). The available power into a  $100\Omega$  matched load will be 50 W peak from 0.1 to 2.0 MHz, and 500 W peak from 2.0 to 30 MHz. These power levels are sufficient to indicate the need for detailed EMC study, and two such studies have been carried out, by the Canadian Space Agency and by NASA: this paper reports some of the results of the CSA study, with emphasis on frequencies high enough to be largely free of effects due to the ionospheric plasma.

Computations were carried out using a thin-wire moment-method computer program based on a piecewise-sinusoidal current expansion (M.A. Tilston and K.G. Balmain, IEEE Trans. A.P., vol. 38, no. 10, pp. 1636-1644, Oct. 1990), so that any metal surface had to be modeled as a wire mesh. In this way the payload bay with its interior ribs, the bay doors, the bay heatshields and the wings were modeled, along with the payload itself consisting of the WISP pallet (near the rear), the ATLAS pallet (an unrelated scientific experiment) and the support frame for SPARTAN (a free-flying subsatellite to be used as a receiver platform for WISP). In addition, the covered cable tray on each side of the bay was modeled, the tray containing a typical coaxial cable whose induced interior voltage could be calculated.

The open forebay region between the SPARTAN support and the crew cabin bulkhead is approximately  $\lambda/2$  wide and a little over  $\lambda/2$  long at 30 MHz, at which frequency it exhibits a standing-wave interior field pattern indicative of a relatively low-amplitude resonance. A much stronger 30 MHz resonance was identified in the narrow space between the pallets and the bay ribs, a resonance which had the effect of injecting current into the cable tray. The high fields around the pallets and the cable interference level were effectively reduced by ground strapping and partial shielding, as shown by computation.

Experimental validation was carried out using scale models with scale factors of 200:1, 73:1 and 10:1 (the 10:1 scale experiments having been done at NASA Marshall Space Flight Center). The bay fields and antenna impedance were measured using half-models over ground, while antenna radiation patterns and some bay field measurements were done using complete models. The paper will assess the validation and will relate the estimated full-scale interference levels to susceptibility standards and known component susceptibilities. The results underline the importance of detailed EMC evaluations for large and complex systems.

## CALIBRATION OF MICROSTRIP & STRIPLINE FIELD APPLICATORS USING TIME DOMAIN TECHNIQUES

D. Infante\*, D.P. Nyquist, J. Ross  
Department of Electrical Engineering  
Michigan State University  
E. Lansing, MI 48824

M. Havrilla  
General Electric Aircraft Engines  
One Neumann Way, MD-G50  
Cincinnati, OH 45215

Microstrip and stripline field applicators have found increasing use for broadband measurement of the electrical properties of materials. The usual frequency domain calibration methods employed for field applicators require measurement of several standards or a single standard located at different positions within the field applicator. These methods are reliable and provide good results for most materials of interest.

Recently, however, there has been increased interest in measurement of the electrical properties of materials at microwave frequencies for wider ranges of temperature. This is important for microwave heating applications and for situations where stealth type coatings are subjected to high temperature as in the exhaust regions of aircraft engines.

Unfortunately, the usual method of calibration becomes cumbersome and of questionable accuracy for high temperature measurements since the applicator must be heated and cooled several times to allow placement of the various standards. The extra measurements of standards also increase total measurement time and cost. Thus, it is important to make calibrations using the minimum number of standards.

The number of standard measurements can be significantly reduced by taking advantage of the inherent properties of the time domain response of the field applicator. By careful design of the field applicator and use of time domain filtering, the applicator can be calibrated with measurement of only one standard. This greatly reduces calibration time and measurement uncertainties due to repeated thermal heating and cooling cycles.

This paper will discuss a calibration method using time domain principles and will provide a comparison of material properties measured using both the time domain method and the usual frequency domain method.

Tue. p.m.

## THE CHARACTERISTICS OF METEOROLOGICAL NOISES RELATED WITH WEATHER

Eikichi Asari

Department of Management and Information Science,

Hokkaido College of Arts and Sciences

Bunkyoudai-Midori-machi 582, Ebets, Hokkaido, JAPAN

Various kinds of electromagnetic radiations are caused by atmospheric actions such as turbulent air flows, precipitations, thunders and electric discharge from artificial and natural electric conductive constructions. These noises are called generally as meteorological noises.

Since 1974, author has detected these noises and investigated the characteristics of their that related with weather conditions. Noise detection executed in frequency band from 150kHz to 30MHz by receivers adjusted to broad pass-band and non-linear sensitivity. Non-linear sensitivity is effective to separate the detected noises from receiver's internal noise make use of difference between both noises. Noise's kinds recognized at receiver's audio out-put point.

According to author's experiments, there are relations of specific types of noises and weather conditions. For example, the precipitation noise detected before rainfall and snowfall. And spherics noises received before thunderstorm.

Author introduced the classifications of meteorological noises according to analyzing to noise's spectrum, crest value, periods, intensity and other characters. And author discovered that various kinds of weather conditons related peculiar types of noises. This phenomenon contributes to developing of a new method of weather forecasting.

## ABOUT THE MATCHED SIGNALS OF SUBSURFACE SURVEYING RADARS

Fang Guangyou\*

China Research Institute of Radiowave Propagation  
P.O.Box 138(27), Xinxiang, Henan, P.R.China.

Wang Wenbing

Xi'an Jiaotong University

There have always been requirements for high-resolution surveying of the underground. Subsurface surveying radars have been used for shallow detection for many years. The resolution and penetration depth of subsurface surveying radars are antagonistic since lossy media having much attenuation to higher frequency electromagnetic waves. So, the radars sources have been taken as a series of baseband pulses and each pulse width is about  $0.01\mu\text{s}$  in order to mitigate such antagonistic problem. If a carrier wave and narrow band signal is used there will be a little penetrating depth through lossy media.

The EM wave  $X(\omega)$  emitted from the transmit antenna penetrates into lossy media, The reflected / scattered wave will be partly received by another antenna in air. Suppose the total transfer function is  $H(\omega)$ . According to the matched filter theory, the S / N (Signal / Noise) ratio is maximum at a given arbitrary time  $t_0$  in the receiving antenna when the emitted signal  $X(\omega) = KH^*(\omega)\exp(-\omega t_0)$ , here  $K$  is an arbitrary constant and  $H^*(\omega)$  is the complex conjugate of  $H(\omega)$ . Then, one can get the time domain emitted wave  $x(t)$  from  $X(\omega)$ , it will be seen that the matched transmitted signal  $x(t)$  is a baseband pulse whose shape is determined by the parameters  $(\epsilon, \sigma, \mu)$  of the lossy media, the scatterers and their buried depth.

When priori information about the lossy medium and the kind of buried object (such as a kind of metal pipe), the matched signal can be used to detect the presence of the object and its buried depth. Though it is difficult to determine the matched signals in actual engineering surveying, it is much favourable to use different waveforms when surveying above different media (such as soil, sand, ice or snow and so on).



**SESSION URSI B-12****TUESDAY PM****INVERSE SCATTERING**

Chairs: T.M. Habashy, Schlumberger-Doll Research; A.K. Jordan, Naval Research Laboratory

Room: Alumni Center, Room 1      Time: 1:30-5:30

|      |  |     |
|------|--|-----|
| 1:30 | GEOMETRICAL CONSIDERATIONS IN GEOPHYSICAL DIFFRACTION<br>TOMOGRAPHY<br><i>Pawan Chaturvedi*, Richard G. Plumb, The University of Kansas</i>  | 226 |
| 1:50 | IMAGING A 2-D AXISYMMETRIC INHOMOGENEOUS MEDIUM USING LOW-FREQUENCY TM MEASUREMENTS<br><i>Qing-Huo Liu, Schlumberger-Doll Research</i>   | 227 |
| 2:10 | AN IMPROVED LIMITED ANGLE IMAGING ALGORITHM FOR METALLIC OBJECTS<br><i>Gregory P. Otto*, Weng Cho Chew, University of Illinois</i>   | 228 |
| 2:30 | A NEW INVERSION TECHNIQUE FOR SHAPE RECONSTRUCTION<br><i>T.S. Angell*, Xinming Jiang, R.E. Kleinman, University of Delaware</i>  | 229 |
| 2:50 | INVESTIGATING ANGLE SCATTERING STATISTICS FOR AUTOMATIC TARGET RECOGNITION<br><i>E.K. Miller*, J.T. Chen, Los Alamos National Laboratory; G.J. Burke, Lawrence Livermore National Laboratory; R.L. Haupt, C.J. McCormack, US Air Force Academy</i> | 230 |
| 3:10 | BREAK  |     |
| 3:30 | SCATTERING CENTERS ANALYSIS BY USING A ONE STEP PARALLEL ESTIMATOR<br><i>Mohcine Zouak, Joseph Saillard*, IRESTE</i>   | 231 |
| 3:50 | AEROSPACE TARGET IDENTIFICATION - COMPARISON BETWEEN THE MATCHING SCORE APPROACH AND THE NEURAL NETWORK APPROACH<br><i>Hsueh-Jyh Li*, Vicent Chiou, National Taiwan University</i>   | 232 |
| 4:10 | MICROWAVE IMAGING FOR SHIP OBJECTS<br><i>Hsueh-Jyh Li*, Gen-Tay Huang, National Taiwan University</i>  | 233 |
| 4:30 | DETERMINATION OF MULTIPLE CRACKS FROM BOUNDARY MEASUREMENTS<br><i>Kurt Bryan, NASA Langley Research Center; Valdis Liepa, University of Michigan; Michael Vogelius, Rutgers University</i>   | 234 |
| 4:50 | AN ADAPTIVE RECONSTRUCTION ALGORITHM FOR 2-D MICROWAVE IMAGING<br><i>Selcuk Paker, Bingul Yazgan*, Istanbul Technical University</i>   | 235 |
| 5:10 | USE OF WAVELETS AND CHEBYSHEV POLYNOMIALS IN K-PULSE SYNTHESIS AND TARGET IDENTIFICATION<br><i>Gönül Turhan-Sayan*, Kemal Leblebicioğlu, Middle East Technical University</i>  | 236 |

## GEOMETRICAL CONSIDERATIONS IN GEOPHYSICAL DIFFRACTION TOMOGRAPHY

Pawan Chaturvedi\* and Richard G. Plumb

Radar Systems and Remote Sensing Laboratory  
Electrical and Computer Engineering  
The University of Kansas, Lawrence, KS

Diffraction Tomography provides a powerful technique for imaging objects buried in optically opaque media. Besides its application in medical imaging, it can also be used in the fields of non-destructive evaluation and subsurface imaging. In geophysical imaging, several different geometries of the transmitter and receiver locations are possible. The geometry chosen for a specific problem is usually application dependent. In this paper, Diffraction Tomography is discussed in terms of the various geometries of the setup. The discussion in this paper is valid for plane wave illumination under the weak scattering approximation.

The geometrical arrangement of the transmitters and receivers for subsurface imaging determines the k-space coverage of the object. Although theoretically, data can be obtained over a full disc of radius  $2k$  in k-space, where  $k$  is the wavenumber of the illuminating wave in the background medium, this is possible only if the transmitters and receivers can be rotated in a full circle around the object being imaged. For geophysical applications, the limited number of viewing angles available impose a limitation on the k-space coverage. Since the k-space coverage directly affects the quality of the image, the image quality for an application depends on the geometry of the transmitter and receiver locations.

The images of a given object achieved by offset Vertical Seismic Profiling (VSP), borehole-to-borehole, and surface-to-surface arrangements are compared. The results are valid for a weak scattering approximation and a homogeneous background medium. Images are reconstructed for Born and Rytov approximations.

The borehole-to-borehole arrangement results in the best coverage of the k-space, but provides the most complicated arrangement for implementation. Although surface-to-surface arrangement is the easiest to implement, it also provides the worst k-space coverage among the three geometries. In many applications, offset VSP results in images of sufficient quality, and a convenient geometry compared to the borehole-to-borehole arrangement. Since none of these arrangements provides isotropic k-space coverage, artifacts in the image are present in all three cases. These artifacts appear in the direction of lower k-space coverage. Using a combination of two or more of these geometries, or using offset VSP with receivers placed in two boreholes on either side of the object would provide better k-space coverage than any single arrangement and eliminate most of these artifacts. Using a range of frequencies instead of a single frequency increases the k-space coverage, but does not result in any substantial improvement along the direction of lower k-space coverage since the coverage in any particular direction is determined by the geometry used, not by the operating frequency.

## IMAGING A 2-D AXISYMMETRIC INHOMOGENEOUS MEDIUM USING LOW-FREQUENCY TM MEASUREMENTS

QING-HUO LIU  
SCHLUMBERGER-DOLL RESEARCH  
OLD QUARRY ROAD  
RIDGEFIELD, CT 06877

In electromagnetic well logging, electrode-type resistivity tools are often used instead of induction tools to measure the formation conductivity. It is well known that when the formation conductivity is much lower than the borehole mud conductivity, the electrode-type tools give much more reliable measurements than the induction tools. It is the purpose of this work to invert for the conductivity distribution of an axisymmetric inhomogeneous medium using measurements from electrode-type tools.

A fundamental electrode-type resistivity tool consists of a ring electrode emitting low frequency current into the inhomogeneous medium to be probed; the potentials measured at several voltage electrodes contain the information of the conductivity distribution of the formation. A coaxial ring electrode in an axisymmetric inhomogeneous medium generates a pure transverse magnetic (TM) field. In comparison, an induction tool with a coaxial ring antenna generates a pure transverse electric (TE) field. For the TM field, there is a charge buildup in the medium due to the inhomogeneous dielectric constant  $\epsilon_r(\rho, z)$  and conductivity  $\sigma(\rho, z)$ ; while for the TE field, if the magnetic permeability  $\mu$  of the medium is constant, there is no such a charge buildup. Therefore, the inverse scattering problem of TM measurements is usually much more nonlinear than that of TE measurements.

In this paper, we present the inversion of borehole TM measurements for the conductivity distribution of axisymmetric inhomogeneous media. We first present a numerical mode-matching (NMM) method developed for solving the forward problem of TM (electrode-type) sensors in an axisymmetric medium. This efficient forward solver greatly helps speed up the nonlinear iterative inversion. For the inversion, we use the distorted Born iterative method (DBIM) to linearize the nonlinear inverse scattering problem. Several numerical examples will be shown along with the comparison between the inversion results from TM and TE measurements.

Tue. p.m.

## AN IMPROVED LIMITED ANGLE IMAGING ALGORITHM FOR METALLIC OBJECTS

GREGORY P. OTTO\* AND WENG CHO CHEW

Electromagnetics Laboratory  
Department of Electrical and Computer Engineering  
University of Illinois  
Urbana, IL 61801

Multiple scattering effects are the primary cause of nonlinearity in inverse scattering problems. This effect commonly presents itself as multiple-scattering ghosts in linear theories such as pulse-echo radar imaging and Diffraction Tomography. Ghost images are more prevalent for limited angle problems than full angle problems because of shadowing. This significantly reduces the range resolution of linear methods. Therefore, the scattering model should account for multiple scattering in order to reduce the number of phantom objects and increase the range resolution. Also, since the number of data measurements is small in limited angle imaging problems, nonlinear algorithms are necessary to squeeze as much information as possible from the small data set.

This paper shows how the LSF imaging algorithm [W.C. Chew & G.P. Otto, IEEE Trans. MGWL 2, 284-286, 1992] can be used for the limited angle reconstruction of metallic objects in 2-D. For this method, the resolution limit for separating two metallic point objects is 0.4 wavelengths in both the range and cross-range directions, which is better than delimited by the Rayleigh criterion. The LSF reconstructions are sharper and contain fewer false ghost images than either pulse-echo radar imaging or Diffraction Tomography with multi-frequency scattering data. The current bottleneck in these solutions is the computational speed of the forward solver, but strides have been made with fast forward solvers such as RATMA and NEPAL to make the reconstruction time reasonable. This method is useful for target identification, medical diagnostics, geophysical exploration, and nondestructive testing. Also, actual microwave measurement data will be used to reconstruct physical objects.

## A NEW INVERSION TECHNIQUE FOR SHAPE RECONSTRUCTION

T. S. Angell\*, Xinming Jiang, and R. E. Kleinman  
Department of Mathematical Sciences  
University of Delaware  
Newark, DE 19716

A new method is presented for reconstructing the shape of an axially symmetric scatterer from a knowledge of the far scattered field produced by a known incident plane wave, of the approximate location of the scatterer, and of the boundary condition satisfied at the surface of the scattering object. The class of scattering objects is restricted to bodies of revolution in three dimensions. The technique may be easily extended in theory to objects without symmetry however the complexity of numerical implementation dramatically increases.

Essentially the method involves the simultaneous determination of two coefficient vectors, one made up of the coefficients of a representation of the unknown surface in an expansion in terms of known functions (spherical harmonics) and the second consisting of coefficients of a representation of the scattered field in terms of elementary sources located within the scatterer. We take advantage of axial symmetry and represent the scattered field as a superposition of ring sources. These two sets of coefficients are determined iteratively by minimizing two cost functionals, one representing the  $L_2$  error in fulfilling the boundary condition and the second representing the  $L_2$  error in matching the given "measured" data. This "measured" data is synthesized by solving the direct problem for a known surface and determining the far scattered field, then suppressing the knowledge of surface. The location of the ring sources is not fixed and is taken to lie on a cone of rays approximately three quarters of the distance along a ray from the origin to the boundary corresponding to an initial guess. Since the boundary changes with each iteration the location of the ring sources also changes. The number of ring sources is fixed and the cones on which the rings lie are chosen to have equal angular separation. A conjugate gradient technique is used to minimize a linear combination of the functionals and each iteration requires two steps, one to update the surface and one to update the field.

Convergence of the method to a simultaneous minimizer of the two functionals is established. The technique has been implemented for a variety of shapes and for both Dirichlet and Neumann boundary conditions for scalar scattering and perfectly conducting for electromagnetic scattering. Remarkably faithful reconstructions are obtained and compared with those found by other methods.

## INVESTIGATING ANGLE SCATTERING STATISTICS FOR AUTOMATIC TARGET RECOGNITION

E. K. Miller\* & J. T. Chen, Los Alamos National Laboratory, Los Alamos, NM

G. J. Burke, Lawrence Livermore National Laboratory, Livermore, CA  
R. L. Haupt & C. J. McCormack, US Air Force Academy, CO

Radar, sonar, and other active interrogation techniques are used for a variety of applications. In order of increasing difficulty, these applications involve answering generic questions such as:

- 1) Detection--Is there a target?
- 2) Classification--Is the target in a class of interest?
- 3) Identification--Which one of that class is the target?

and

- 4) Reconstruction--What are the geometrical and electrical parameters of an otherwise unidentified target?

The problem of noncooperative target identification (NCTI), or equivalently, automatic target recognition (ATR), remains one of the most important goals in radar applications. Approaches being pursued for ATR can be described as being either feature-based or image-based schemes, or some combination thereof. Representative of the former is the use of body resonances, while the latter includes range profiling. Body resonances provide an intuitively attractive approach and are aspect independent, but can exhibit limited observability in noisy data and may not exploit the total scattered field. On the other hand, profiling and imaging can be very data intensive since aspect dependence must be explicitly accounted for. Both approaches continue to be investigated however, as the payoff from developing a practical ATR technique could be significant.

The ideas described here incorporate some aspects of both feature-based and imaging techniques. We assume access to a data base like that needed for an imaging approach, where wideband RCS data over  $4\pi$  steradians of viewing angle is available, but we attempt to reduce the data-processing burden by using those data to develop features useful for identification. The least data-intensive approach considered is that of using expected values of the frequency- and angle-dependent RCS as a target-feature library. Somewhat more data intensive is use of RCS probability density functions, where aspect angle is the random variable, again as a function of frequency. Most data intensive, aside from imaging, is determining whether the measured RCS from an unknown target, when compared with stored angle-scattering patterns, is consistent over the available frequencies, with a single incidence angle for one of the library targets. Results from testing these various techniques for ATR against a set of simple targets will be summarized.

SCATTERING CENTERS ANALYSIS  
BY USING A ONE STEP PARALLEL ESTIMATOR

Mohcine ZOUAK and Joseph SAILLARD\*

S2HF, IRESTE, La chantrerie, C.P.3003, 44087 Nantes cedex 03 France  
Phone (33) 40 68 30 20 & 40 68 30 64, telefax: (33) 40 68 30 66

During the last decades, several papers addressed the problem of characterizing radar signatures based on the concept of scattering centers. It is well known that high-frequency scattering can often be described in terms of a finite number of scattering centers, each with a different phase and magnitude [1]. The reflection/diffraction phenomena determine the relative magnitude of each contribution while the phase is dependent on the distance from the scattering center to the observation point.

Under the exponential model assumption of scattering, the problem studied can be reformulated in terms of a parameter estimation problem for the exponential model [2]. Hence, significant progress has been made by the use of parametric scattering models and high resolution spectrum analysis techniques. However, in a nonstationary environment i.e. when the target sources are moving or when the frequencies are continuously or abruptly varying in time, all the conventional block processing methods (FFT, Prony, ...) estimating radar signatures become inefficient.

Conceptually, these classical algorithms for characterizing and tracking radar signatures are implemented in three steps: The sequential estimation of AR parameters step, the adaptive AR polynomial root solving step and the Van Der Monde system solving step.

In this paper, we seek to locate and characterize the discrete scattering centers of an object by using a parametric time dependent scattering model. We suggest a one step adaptive algorithm. For this, we use an adaptive AR filter which can directly estimate and track its own zeros without any root finding or a "pick picking" procedure [3]. The time updates of the zeros are chosen optimally to minimize the mean output power of the filter so that the accuracy of the equivalent standard filter's coefficients estimators is maintained. The Van Der Monde system solving is avoided by an approximation technique based on an appropriate polynomial approximation of the model data in the  $z$  - transform domain [4]. This approximation is held in a sliding window of the same length as the model order so that we incorporate a forgetting window in the algorithm. In addition, the used approximation is easily derived by the adaptive filter equations so that no more computations are needed and yielding to a parallel one-step algorithm. Finally, a performance discussion and a simulation study are presented for illustration.

**References**

- [1] Saillard J., 10<sup>ème</sup> Col. Trai. Sig. & Applications. Nice, 1985
- [2] S. L. Marple Jr., Prentice-Hall, Englewood Cliffs, N.J., 1987
- [3] Zouak M et al., IMACS Sym. Mod. & Cont. Tech Syst., Vol 2, 455, 1991
- [4] Lambert C. and Castanie F., Signal Processing IV, 571, 1988

AEROSPACE TARGET IDENTIFICATION — COMPARISON  
BETWEEN THE MATCHING SCORE APPROACH AND  
THE NEURAL NETWORK APPROACH

Hsueh-Jyh Li <sup>\*</sup> and Vicent Chiou  
Department of Electrical Engineering  
National Taiwan University  
Taipei, Taiwan, R. O. C.

ABSTRACT

Three phases are usually involved in automatic target identification. They are: data acquisition, data representation, and data classification. Selection of proper feature vectors is key to the success of target identification. In this paper we will use range profiles as the feature vectors. The decision rule also plays a very important role in target identification. An intuitive decision rule is to compare the similarity between the feature vector of the unknown target with those stored in the data base, and choose the class which has the greatest correlation coefficient. This method is referred to as the matching scored method. This approach is simple and is invariant to the range-shift of the feature vector. Neural networks have the properties of fault tolerance, capability to reconstruct image from incomplete information, and parallel computation. The backpropagation model is one of the most well-known and powerful algorithm of neural networks. It is a multi-layered network with hidden nodes.

In this paper five different airplane models are used as the known targets. Their range profiles at aspects within certain angular windows are measured and employed to establish the data base. We then apply the matching score method to identify an unknown target which belongs to the known target set. With the same data base we also employ the backpropagation model to train the neural network using different training parameters. Recognition performances using the matching score approach and the neural network approach without and with the presence of Gaussian noise are experimentally compared and discussed. The neural network approach may fail to recognize a shifted feature vector. We propose a centroid-aligned method to overcome the range shift problem. Simulated results show that this method is simple and effective.

## MICROWAVE IMAGING FOR SHIP OBJECTS

Hsueh-Jyh Li<sup>\*</sup> and Gen-Tay Huang  
Department of Electrical Engineering  
National Taiwan University  
Taipei, Taiwan, R. O. C.

### ABSTRACT

Imaging of aircraft objects and ship objects belongs to moving object imaging. However, the motion modes and environments for aircrafts and ships are quite different. The speed, range, aspect, and direction of flight of an aircraft usually can be estimated by a modern radar. The effect of clutter usually can be ignored for a ground-to-air radar. But as to ship objects, their motion and environments are more complicated. For example, the ship object has motions both in translation and rotation and it is hard to estimate the instantaneous directions of the bow and hull. In addition, strong reflection from the sea wave may override the echo from the target and preclude detecting the target. As a consequence, ISAR imaging of a ship object by utilizing ship's motion to synthesize an aperture is more difficult than that by a flying airplane.

In this paper we focus on the problem concerning imaging of ship objects using the radar on an aircraft. During the image coherent processing interval, the radar antenna on the aircraft synthesizes an aperture, and the ship object also inversely synthesizes an aperture arising from the ship's translating and/or rotating motion. Consequently this problem is a combination of SAR/ISAR imaging. Due to the unpredictable sea waves, it is difficult to predict the ship motion, making the imaging problem very complicated. Fortunately, the speed of aircrafts or missiles is usually very fast so that an aperture, large enough to give acceptable resolutions, can be synthesized in a short time interval (e.g. in one second). During this short interval the ship motion caused by the sea wave may be assumed uniform. In that case, the range-Doppler reconstruction method and the preprocessing techniques can be employed to overcome the above difficulties.

In this paper the scattering of ship objects situated in the sea ocean is discussed and how the presence of sea surface affects the reconstructed image is numerically examined. It is found that in most cases sea clutters and multiple reflections have little effect on obtaining a focused image. Because an aperture size can be synthesized in a short time interval due to the fast speed of the flying vehicle, it is concluded that object motion has little effect on the image reconstruction if the object is moving or rotating along the same direction during the data collection interval. An experiment for imaging a boat model has been designed and conducted in a big water tank and focused images have been obtained in the presence of man-made water waves. The simulated and experimental results verify the effectiveness of our proposed algorithms.

## DETERMINATION OF MULTIPLE CRACKS FROM BOUNDARY MEASUREMENTS

**Kurt Bryan**  
ICASE, NASA Langley Research Center  
Hampton, VA 23681

**Valdis Liepa**  
Radiation Laboratory, Dept. EECS  
University of Michigan  
Ann Arbor, MI 48109

**Michael Vogelius**  
Department of Mathematics  
Rutgers University  
New Brunswick, NJ 08903

### Abstract

The objective is to develop mathematical and computational techniques for the nondestructive evaluation of materials using impedance imaging. The focus is on the detection and location of cracks in electrically conductive materials. In our model the "specimen" takes the form of a planar domain with a number of electrodes attached to the boundary. Current flows in at one electrode, out at another, and the induced potential is measured at all the "inactive" electrode locations. The goal is to use the current flux and voltage data to locate any cracks inside the specimen.

A numerical algorithm for locating a collection of linear cracks in an otherwise uniform conductive object has been developed. The algorithm is a natural extension of one developed by Santosa and Vogelius for the recovery of a single linear crack. The technique is a variation of Newton's method; it uses adaptively chosen two-electrode current fluxes to generate the boundary voltage data for updating the estimate of the crack locations. At each iteration the electrode locations are adjusted to ensure maximal sensitivity (in a sense which is made precise) to the location of the cracks. Numerical simulations have shown that our approach converges quite rapidly to the correct cracks and is not as prone to becoming trapped in local minima as a more traditional optimization/least-squares approach.

An experimental device for generating actual data has also been constructed. Application of the algorithm to data generated by this device has yielded good results for both single and multiple crack location problems.

## AN ADAPTIVE RECONSTRUCTION ALGORITHM FOR 2-D MICROWAVE IMAGING

Selçuk PAKER      Bingül YAZGAN\*

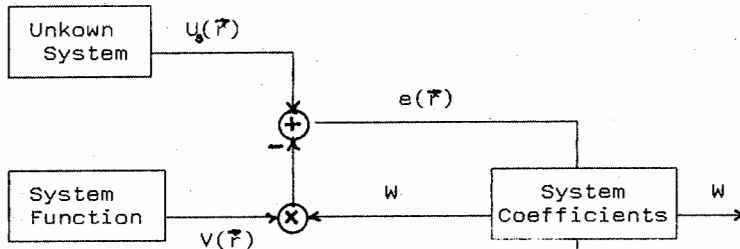
Electrical & Electronics Engineering Faculty  
Istanbul Technical University, 80626, Maslak, Istanbul, Turkey

In this paper, a different numerical method for image reconstruction in EM diffraction tomography is presented. An adaptive algorithm is proposed for the reconstruction of the complex permittivity of an inhomogeneous lossy dielectric object having arbitrary shape. Starting from the integral representations of the scattered electric field and using the moment method, an algorithm based on adaptive LMS is applied to 2-D problem. Using simulated data, successful results are obtained with this adaptive reconstruction algorithm.

Consider the two dimensional inverse scattering problem where the object is characterized by an index of refraction over some finite region that is contained between the source and receiver arrays. No assumption will be done concerning the magnitude of index  $n(\vec{r})$  so that the developed theory will be valid for both strongly and weakly scattering object. The scattering system models a general linear system. For each scattered wave, one equation can be written relating unknowns to the measured field data. Doing this for each scattered wave enables one to obtain a system of  $K$  equations with  $L$  unknowns. The minimum mean-square error criterion is used to optimize the coefficients. Specifically, the weighing factors are chosen so as to minimize an index of performance mean squared error. The problem of estimating medium parameter  $w$  has now been reduced to solving the set of linear equations. However, several problems remain to be considered. Firstly, the data  $U_s(\vec{r})$  is not known exactly in any practical case as a result of various sources of noise in the system and approximations in the discrete model. Generally this will cause some inconsistency. Secondly, the number of independent equations, determined by the scanning geometry, are usually insufficient to determine  $w$  uniquely. Finally, in many cases the number of equations are too large for direct matrix inversion or pseudo-inversion solution techniques previously used by others. For the reasons mentioned above, we use an adaptive method which treats one equation at a time.

This adaptive system identification algorithm does not require a priori knowledge of, or assumptions about the unknown object function. The LMS algorithm lead to a computational complexity of  $O(L)$ , otherwise the usual way of solving linear equations ( deterministic inverse scattering problem ) requires an  $O(L^3)$  computation. Our proposed imaging algorithm can be used for strong dielectric scatterers and allows high resolution with less computation for this type of image reconstruction.

Flowchart of the adaptive imaging algorithm.



USE OF WAVELETS AND CHEBYSHEV POLYNOMIALS  
IN K-PULSE SYNTHESIS AND TARGET IDENTIFICATION

Gönül Turhan-Sayan<sup>(\*)</sup> and Kemal Leblebicioğlu  
Middle East Technical University  
Department of Electrical and Electronic Engineering  
06531 Ankara, Turkey

The K-pulse of a finite dimensional electromagnetic scatterer is a special excitation waveform which is of minimal finite duration. The Laplace transform of a K-pulse should be an entire function whose complex zeros must coincide with the complex natural resonance (CNR) frequencies of the scatterer. Theoretically, the K-pulse of an object is completely and uniquely characterized by infinitely many CNR frequencies. Therefore, it produces time-limited target responses for all possible orientations and polarizations of excitation. In practical problems, however, the available data from radar or compact-range measurements are always band limited and noisy, leading to an approximate K-pulse which usually has only the dominant CNR frequencies excited in a certain bandwidth as its Laplace transformation zeros. Obviously, such a practical K-pulse is not unique but it is still useful for target identification purposes.

To achieve a reasonably low error rate in target identification procedure, especially when the measurement data have a low signal-to-noise ratio (SNR), the K-pulse waveforms of the library targets must be synthesized with a good accuracy in the sense of producing the CNR frequencies of each library target as the spectrum zeros of its K-pulse over a certain bandwidth. The main factors which determine the accuracy of the synthesized K-pulse are the choice of basis functions used to expand the K-pulse waveform in time domain and the optimization procedure utilized to obtain the expansion coefficients.

In this paper, we will use two different complete and orthogonal bases of time-limited functions which are Wavelets and Chebyshev polynomials. The advantages of using these special basis functions in K-pulse synthesis and target identification will be demonstrated for different target geometries at various SNR levels. Possible improvements to the present optimization approach, which depends on multi-combinational late-time K-pulse response energy minimization, will be also discussed.

## COMPLEX AND CHIRAL MEDIA

Chairs: P.L.E. Uslenghi, University of Illinois at Chicago; D.G. Dudley, University of Arizona

Room: Alumni Center, Room 2

Time: 1:30-5:30

|      |  |     |
|------|--|-----|
| 1:30 | THE PROPAGATION OF A RADAR PULSE IN SEA WATER<br><i>R.W.P. King*, T.T. Wu, Harvard University</i>  | 238 |
| 1:50 | FDTD MODELING OF OPTICAL PULSE PROPAGATION IN LINEAR<br>DISPERSIVE, NONLINEAR MATERIALS<br><i>Richard W. Ziolkowski, Justin B. Judkins*, The University of Arizona</i>   | 239 |
| 2:10 | MASSIVELY PARALLEL PROCESSOR COMPUTER FDTD MODELING OF<br>OPTICAL PULSE PROAGATION IN LINEAR AND NONLINEAR MATERIALS<br><i>Richard W. Ziolkowski*, Justin B. Judkins, The University of Arizona; David B. Davidson, University of Stellenbosch</i> | 240 |
| 2:30 | ACTIVE REMOTE SENSING OF THREE-LAYERED ANISOTROPIC RANDOM<br>MEDIA<br><i>Jay K. Lee*, Yun Hee Lee, Syracuse University</i>   | 241 |
| 2:50 | COMPARISON OF LONG WAVELENGTH AND MULTIPLE SCATTERING<br>MODELS FOR MICROWAVE CHIRAL COMPOSITES WITH EXPERIMENTAL<br>RESULTS<br><i>Vasundara V. Varadan*, Vijay K. Varadan, The Pennsylvania State University</i>                                  | 242 |
| 3:10 | BREAK  |     |
| 3:30 | SURMOUNTING NUMERICAL LIMITATIONS IN THE FULL-WAVE SIMULATION<br>OF CHIRAL MATERIALS<br><i>Keith W. Whites, University of Kentucky</i>   | 243 |
| 3:50 | RECTANGULAR WAVEGUIDE PARTIALLY FILLED WITH BIAXIAL AND<br>CHIRAL MATERIAL<br><i>Lizhen Li*, P.L.E. Uslenghi, The University of Illinois at Chicago</i>  | 244 |
| 4:10 | APPLICATIONS OF EIGENFUNCTION THEORY TO GUIDED WAVE CHIRAL<br>ELECTROMAGNETICS<br><i>C.A. Moses, I.M. Besieris, Virginia Polytechnic Institute and State University</i>  | 245 |
| 4:30 | ACTIVE CHIRAL MEDIA AND DISTRIBUTED FEEDBACK DEVICES<br><i>Kevin M. Flood, Dwight L. Jaggard, University of Pennsylvania</i>   | 246 |
| 4:50 | INVARIANT EMBEDDING AND CHIRAL MATERIAL<br><i>D.L. Jaggard, J.C. Liu, University of Pennsylvania</i>   | 247 |
| 5:10 | PLANE WAVE PROPAGATION IN A UNIAXIAL CHIRAL MEDIUM<br><i>I.V. Lindell*, A.J. Viitanen, Helsinki University of Technology</i>   | 248 |

## THE PROPAGATION OF A RADAR PULSE IN SEA WATER

Ronald W. P. King\* and Tai T. Wu  
 Gordon McKay Laboratory, Harvard University, Cambridge, Massachusetts 02138

The propagation in sea water of an electromagnetic field in the form of a semi-infinite wave train or a radar pulse generated by an electric dipole is investigated analytically for low frequencies. The frequency-domain formula for the downward-traveling field of a horizontal electric dipole excited by a sinusoidally modulated electric-current pulse is Fourier transformed to obtain an explicit expression for the field at any distance in the time domain. Specific application is made to a wave packet of  $f_0 = \omega_0/2\pi = 25.5$  cycles in a time duration of one second. The amplitude and phase velocity of the wave packet are determined together with the amplitudes of the initial and final transients. Graphs are displayed and discussed for a range of distances; these show that the amplitude of the wave packet decays more rapidly than the amplitudes of the transients. Possible application to remote sensing in the ocean is considered.

The formula for the electric field of an electric dipole with effective length  $2h_e$  in sea water when excited by the current pulse

$$I_x(t) = I_x(0) \frac{[U(t) - U(t - 2t_1)]}{2t_1} \sin \omega_0 t \quad (\text{in Amp/sec}),$$

where  $U(t)$  is the step function, is

$$\frac{E_x(t, z)}{2I_x(0)h_e} = \frac{\mu_0 \omega_0 \beta_{10}}{16\pi^2 t_1} \times \begin{cases} 0, & t \leq 0, \\ \pi e^{-\beta_{10}z} \left[ \left( \frac{1}{\beta_{10}^3 z^3} + \frac{1}{\beta_{10}^2 z^2} \right) \sin(\omega_0 t - \beta_{10}z) \right. \\ \left. + \left( \frac{1}{\beta_{10}^2 z^2} + \frac{2}{\beta_{10} z} \right) \cos(\omega_0 t - \beta_{10}z) \right] \\ + \frac{2\sqrt{\pi}}{\omega_0 t} e^{-\beta_{10}^2 z^2 / 2\omega_0 t} \left( \frac{1}{\beta_{10}^3 z^3} - \frac{1}{\beta_{10} z \omega_0 t} + \frac{\beta_{10} z}{\omega_0^2 t^2} \right), & 0 < t \leq 2t_1, \\ \frac{2\sqrt{\pi}}{\omega_0 t} e^{-\beta_{10}^2 z^2 / 2\omega_0 t} \left( \frac{1}{\beta_{10}^3 z^3} - \frac{1}{\beta_{10} z \omega_0 t} + \frac{\beta_{10} z}{\omega_0^2 t^2} \right) \\ \pm \frac{2\sqrt{\pi}}{\omega_0(t - 2t_1)} e^{-\beta_{10}^2 z^2 / 2\omega_0(t - 2t_1)} \\ \times \left( \frac{1}{\beta_{10}^3 z^3} - \frac{1}{\beta_{10} z \omega_0(t - 2t_1)} + \frac{\beta_{10} z}{\omega_0^2(t - 2t_1)^2} \right), & 2t_1 < t. \end{cases}$$

Here,  $2t_1$  is the width of the pulse,  $k_1 = \beta_1(1 + i) = \sqrt{\omega\mu_0\sigma_1/2}(1 + i)$  is the wave number of sea water, and  $\beta_{10} = \sqrt{\omega_0\mu_0\sigma_1/2}$ .

## FDTD MODELING OF OPTICAL PULSE PROPAGATION IN LINEAR DISPERSIVE, NONLINEAR MATERIALS

Richard W. Ziolkowski and Justin B. Judkins\*  
Electromagnetics Laboratory  
Department of Electrical and Computer Engineering  
The University of Arizona  
Tucson, AZ 85721

Full-wave vector Maxwell's equations solvers, such as the finite difference time domain (FDTD) approach, are rapidly becoming mainstream computational electromagnetics tools. FDTD codes have been used and validated in a wide range of applications including radar cross section, HPM aperture coupling, and device interconnects. Recently, the FDTD technique has been extended to problems dealing with the modeling of pulsed optical beam propagation in nonlinear materials [(Ziolkowski and Judkins, J. Opt. Soc. Am. B, vol. 10(2), 75-87, 1993)]. This extension was accomplished by incorporating into the linear FDTD solver a vector extension of a Debye model of a nonlinear Kerr material.

This NL-FDTD approach has already revealed a number of physical effects that are not recovered from the standard one-dimensional, scalar, nonlinear Schrödinger equation models used by the optics community. For instance, when an intense, ultrashort, optical pulse propagates in a Kerr medium, the medium responds to the leading edge of the pulse by forming an effective tapered waveguide which focuses the anterior portion of the pulse. This self-focusing can cause catastrophic failure of the host optical material. The full-wave, vector, NL-FDTD method has shown that the transverse and reflected power flows, which are absent in the scalar models, actually limit the self-focusing process, thus avoiding the catastrophic focusing results predicted by the scalar models. Moreover, the NL-FDTD results have revealed the formation of optical vortices in the wakefield of the self-focusing region (mild turbulence in the neck of the tapered waveguide region).

Despite these initial successes, many aspects of this simple NL-FDTD model are inadequate for complete understanding or design purposes. Ultrashort pulses have frequency spectra that can encompass both resonant and non-resonant effects in a semiconductor material. The resonant effects are not treated well with the Debye model and one must incorporate a Lorentz model of the medium. Moreover, linear dispersion begins to play a significant role, particularly in nonlinear guided wave problems dealing with propagation over long distances. Our NL-FDTD algorithm will be discussed in detail, particularly the inclusion of the linear dispersion and nonlinear Debye and Lorentz material models into the FDTD approach. The resulting model incorporates the linear and nonlinear effects of dispersion, diffraction (spatial dispersion), compression (temporal dispersion), time retardation, and resonances. Typical examples of applications of this approach to studies of pulsed-beam propagation in nonlinear waveguides will also be presented. New effects observed when the linear dispersive and resonant material models are included in the NL-FDTD model will be emphasized.

Tue. p.m.

## MASSIVELY PARALLEL PROCESSOR COMPUTER FDTD MODELING OF OPTICAL PULSE PROPAGATION IN LINEAR AND NONLINEAR MATERIALS

Richard W. Ziolkowski\* and Justin B. Judkins  
Electromagnetics Laboratory  
Department of Electrical and Computer Engineering  
The University of Arizona  
Tucson, AZ 85721  
(602) 621-6173

David B. Davidson  
Department of Electrical and Electronic Engineering  
University of Stellenbosch  
Stellenbosch 7600  
South Africa

Full-wave, vector Maxwell's equations solvers, such as the finite difference time domain (FDTD) approach, are rapidly becoming mainstream computational electromagnetics tools because of their versatility and ease of implementation. Recently, the FDTD technique has been extended to problems dealing with the modeling of pulsed optical beam propagation in nonlinear materials (Ziolkowski and Judkins, *J. Opt. Soc. Am. B*, vol. 10(2), 75-87, 1993). The interest in this class of problems has been driven by the anticipation of enormous technological dividends from linear and nonlinear optical-based devices and the subsequent need for more accurate and realistic numerical simulations of these devices and systems. The NL-FDTD full-wave, vector approach offers several benefits to modeling optical devices and systems including the potential of understanding the basic device physics; of encouraging multiple engineering concept and design iterations that result in enhanced performances; of system integrations of these devices; and of providing frameworks in which one can interpret complex experimental results and suggest further diagnostics or alternate protocols.

The need for modeling optical phenomena with an massively parallel processor (MPP) computer has been driven by our desire to model fully three-dimensional real-world problems. There are very large scale variations between wavelength, device size, and material response times in a typical optical problem; and the resulting FDTD models are extremely memory and compute intensive, generally surpassing the limits of most serial machines. Our recent activities into porting our linear and nonlinear optical device and systems modeling approaches to a MPP environment will be discussed. Particular attention will be given to how the Debye and Lorentz materials models are incorporated in the FDTD approach to make effective use of the MPP computer. It will be demonstrated that the NL-FDTD modeling approach maps well onto a MPP environment. Typical examples of applications of the NL-FDTD approach for studying the physical mechanisms associated with the self-focusing of pulsed-beams and for modeling basic nonlinear guided optical wave devices will also be presented.

## ACTIVE REMOTE SENSING OF THREE-LAYERED ANISOTROPIC RANDOM MEDIA

Jay K. Lee \* and Yun Hee Lee

Department of Electrical and Computer Engineering  
Syracuse University  
Syracuse, NY 13244-1240

In this paper, we consider the problem of electromagnetic wave scattering from three-layered anisotropic random media, where two anisotropic random media are bounded by air above and an isotropic homogeneous half space below. The two random media have different permittivity tensors  $\tilde{\epsilon}_i$ ,  $i = 1, 2$ , each with different optic axis tilted by some angle  $\psi_i$ ,  $i = 1, 2$ , from the normal (z-) axis and different three dimensional correlation functions. The layer boundaries are parallel and smooth. Based on the wave theory under the Born approximation where a single scattering process is considered and all the multiple reflections at the boundaries are taken into account, the backscattering coefficients are derived for application to active microwave remote sensing. For this work, the dyadic Green's functions for three-layered anisotropic media are developed and used.

Our results are first confirmed by those of the two-layered anisotropic random media (J. K. Lee and J. A. Kong, *IEEE Trans. Geosci. Remote Sensing*, Vol. GE-23, pp. 910-923, Nov. 1985) and three-layered isotropic random media (Zuniga, Habashy and Kong, *IEEE Trans. Geosci. Electronics*, Vol. GE-17, pp. 296-302, Oct. 1979). The frequency and viewing-angle responses of the backscattering coefficients are illustrated numerically along with their dependence on the variances, the correlation lengths and the permittivities, all of which are assumed to be anisotropic. It is shown that the single scattering process leads to strong cross-polarization due to anisotropy of each layer. The oscillating behavior of the backscattering coefficients of the three-layer model is also observed as a function of both frequency and viewing angle. Finally the theoretical results will be used to interpret the experimental data obtained from active remote sensing of sea ice.

## COMPARISON OF LONG WAVELENGTH AND MULTIPLE SCATTERING MODELS FOR MICROWAVE CHIRAL COMPOSITES WITH EXPERIMENTAL RESULTS

Vasundara V. Varadan\* and Vijay K. Varadan  
Research Center for the Engineering of Electronic and Acoustic Materials  
Department of Engineering Science and Mechanics  
The Pennsylvania State University  
University Park, PA 16802

At microwave and millimeter wave frequencies materials described by the constitutive relations  $D = \epsilon(E + \beta \nabla \times E)$  and  $B = \mu(H + \beta \nabla \times H)$  can only be constructed by embedding non-centro symmetric or chiral inclusions in a dielectric host material. Such materials are effectively chiral and  $\epsilon, \mu, \beta$  are the effective properties describing the propagation of the *coherent field* in such a material. Several theoretical models have been developed to describe the effective properties. They fall into two classes, long wavelength and sparse concentration models and multiple scattering models suitable for dense concentrations and higher frequencies. The long wavelength models use a dipole approximation for the inclusion and are limited to single scattering effects only. Thus they cannot predict losses due to geometrical dispersion. The multiple scattering model overcomes some of these limitations and in addition, can take into account the effects of different distribution functions for the inclusions. The disadvantage is that results can only be obtained numerically whereas the simpler models can yield closed form results. All theories are restricted to modeling the inclusion to be made of a chiral material, not chiral in shape or geometry. This is a serious limitation on all these models, which can be overcome only by developing numerical methods to solve scattering from helical objects. Recently experimentally measured values of the effective properties for random dispersions of miniature helices have also become available. Thus it is useful to compare all of the available theoretical models and compare their predictions with experimental data. The objective is to study the robustness of the models and also compare effectively racemic and effectively chiral composite materials with composites that have no microstructural chirality whatsoever.

# SURMOUNTING NUMERICAL LIMITATIONS IN THE FULL-WAVE SIMULATION OF CHIRAL MATERIALS

*Keith W. Whites*

Department of Electrical Engineering  
University of Kentucky  
Lexington, KY 40506-0046

The research of many investigators in the recent past has revealed many of the substantial electromagnetic benefits of chiral materials as compared with normal dielectric/magnetic materials. Applications ranging from radar absorbing materials to micropatch antenna substrates have been reported (for a review, see N. Engheta and D. L. Jaggard, "Electromagnetic chirality and its applications," *IEEE APS Newsletter*, Oct. 1988). While these materials occur naturally at optical frequencies, at microwave wavelengths they must be manufactured giving rise to the concept of an "artificial" material. These chiral materials, which on a macroscopic scale have been modeled by the constitutive parameters  $\bar{D} = \epsilon \bar{E} + \alpha \epsilon \nabla \times \bar{E}$  and  $\bar{B} = \mu \bar{H} + \beta \mu \nabla \times \bar{H}$ , provide extra "degrees of freedom" which can be exploited to satisfy problem constraints in the above mentioned, or other, applications.

The design and implementation of these artificial materials require a predictive power of analysis. The aim of this research is toward a full-wave numerical simulation of artificial materials composed of *handed* inclusions (chromophores). A full-wave analysis has many favorable attributes including a complete accounting of all multiple interactions between inclusions, which is often neglected. Additionally, no assumptions are required as to the shape or composition of the chromophores.

However, the full-wave analysis of any material is severely hampered by obvious computational constraints including the number of unknowns, the size of the inclusions and the density of the inclusions. These constraints are naturally imposed by the fact that a *material* is being modeled; that is, the scattering by all chromophores is accounted for using only the lowest-ordered terms in the Taylor's expansion of the scattered fields. While large inclusions (greater than  $0.1 \lambda$ ) provide more scattering with fewer numbers of unknowns, these are not materials but rather a complex collection of scatterers.

This talk will focus on two primary topics. The first is the efficient implementation of the full-wave numerical simulation. In this work, a moment method solution combined with a Monte Carlo method is used to obtain the averaged scattered fields produced by a random ensemble of chromophores grouped in an imaginary free-space enclosure. The use of parallel computational platforms and their advantages will also be discussed. The second topic is a discussion of the results and their comparison with the traditional chiral macroscopic model.

RECTANGULAR WAVEGUIDE PARTIALLY FILLED  
WITH BIAXIAL AND CHIRAL MATERIAL

Lizhen Li\* and P.L.E. Uslenghi

Department of Electrical Engineering and Computer Science  
University of Illinois at Chicago, Box 4348, Chicago, IL 60680

A metallic rectangular waveguide whose cross-section occupies the region  $0 \leq x \leq a, 0 \leq y \leq b$  in the (x,y) plane is partially filled with a material which is both biaxial and chiral. The material occupies the portion  $0 \leq x \leq a, 0 \leq y \leq d \leq b$  of the waveguide cross-section, and air the remainder. The material is characterized by a tensor permittivity  $\bar{\epsilon}$ , a tensor permeability  $\bar{\mu}$  and a chiral admittance  $\Upsilon_0 \xi_c$ , where  $\Upsilon_0 = Z_0^{-1} = \sqrt{\epsilon_0 / \mu_0}$ . The relative chiral admittance  $\xi_c$  and the relative permittivity and permeability tensors  $\bar{\epsilon}$  and  $\bar{\mu}$  are dimensionless quantities which characterize the electromagnetic behavior of the material; in air  $\xi_c = 0$  and  $\bar{\epsilon} = \bar{\mu} = \bar{I}$ ,  $\bar{I}$  being the identity. If the fields are three-element column vectors, then  $\bar{\epsilon}$  and  $\bar{\mu}$  are 3x3 matrices in the (x, y, z) coordinate system.

By normalizing the magnetic field  $\mathbf{H}$  to  $\mathbf{H} = Z_0 \mathbf{H}$  and with time-dependence factor  $\exp(j\omega t)$ , Maxwell's curl equations in a source-free region are:

$$(1) \quad \nabla \times \underline{\underline{\mathbf{H}}} = j k_0 \bar{\epsilon}_c \underline{\underline{\mathbf{E}}} + k_0 \xi_c \bar{\mu} \underline{\underline{\mathbf{H}}}, \quad \nabla \times \underline{\underline{\mathbf{E}}} = k_0 \xi_c \bar{\mu} \underline{\underline{\mathbf{E}}} - j k_0 \bar{\mu} \underline{\underline{\mathbf{H}}}$$

where  $\bar{\epsilon}_c = \bar{\epsilon} + \xi_c^2 \bar{\mu}$ ; the divergence equations are:

$$(2) \quad \nabla \cdot (\bar{\epsilon}_c \underline{\underline{\mathbf{E}}}) - j \xi_c \nabla \cdot (\bar{\mu} \underline{\underline{\mathbf{H}}}) = 0, \quad \nabla \cdot (\bar{\mu} \underline{\underline{\mathbf{H}}}) + j \xi_c \nabla \cdot (\bar{\mu} \underline{\underline{\mathbf{E}}}) = 0.$$

We assume modal propagation in the z-direction, and set:

$$(3) \quad \left. \begin{aligned} \underline{\underline{\mathbf{E}}}(x, y, z) \\ \underline{\underline{\mathbf{H}}}(x, y, z) \end{aligned} \right\} = e^{-j\beta k_0 z} \cdot \left\{ \begin{aligned} \underline{\underline{\mathbf{E}}}(x, y) \\ \underline{\underline{\mathbf{h}}}(x, y) \end{aligned} \right\}$$

Also, we assume that  $\bar{\epsilon}$  and  $\bar{\mu}$  are biaxial:

$$(4) \quad \bar{\epsilon} = \begin{pmatrix} \epsilon_1 & 0 & 0 \\ 0 & \epsilon_2 & 0 \\ 0 & 0 & \epsilon_3 \end{pmatrix}_{xyz}, \quad \bar{\mu} = \begin{pmatrix} \mu_1 & 0 & 0 \\ 0 & \mu_2 & 0 \\ 0 & 0 & \mu_3 \end{pmatrix}_{xyz}.$$

Substitution of (3-4) into (1-2), solution of the resulting equations and imposition of the boundary conditions results in a complete characterization of the various propagating modes. Several numerical results are presented, and particular cases are discussed.

## APPLICATIONS OF EIGENFUNCTION THEORY TO GUIDED WAVE CHIRAL ELECTROMAGNETICS

C. A. Moses and I. M. Besieris  
Bradley Department of Electrical Engineering  
Virginia Polytechnic Institute and State University  
Blacksburg, VA 24061

In recent years, a large number of potential applications for microwave chiral materials have been suggested: anti-reflection coatings, radomes, waveguides, microstrip antennas, phase shifters, and absorbers. One expects novel features from each of these devices due to mode bifurcation arising from the bi-isotropic nature of chiral media. The chirality parameter that lends itself to the double modes allows one an extra degree of freedom to optimize devices for certain applications.

In order to examine the interaction of a chiral medium with an electromagnetic wave, one should consider both bounded and unbounded domains. One bounded problem considered by Pelet and Engheta is the chirostrip antenna [*"Chirostrip antennas: line source problem," J. of Elect. Waves and Appl.* (1992)]. They determined the complex modal structure necessary to satisfy the chiral vector wave equation (within the antenna substrate) and the boundary conditions (on the ground-plane and at the interface). When a source is embedded within a chiral medium, it generally becomes difficult to obtain full-wave analytic solutions for the radiation fields. A specific technique, the standard eigenvalue-eigenfunction Ohm-Raleigh method, is useful in this respect because it lends itself well to asymptotic expressions; however, certain precautions must be taken. For the chirostrip antenna, Pelet and Engheta have utilized the Ohm-Raleigh method with great success.

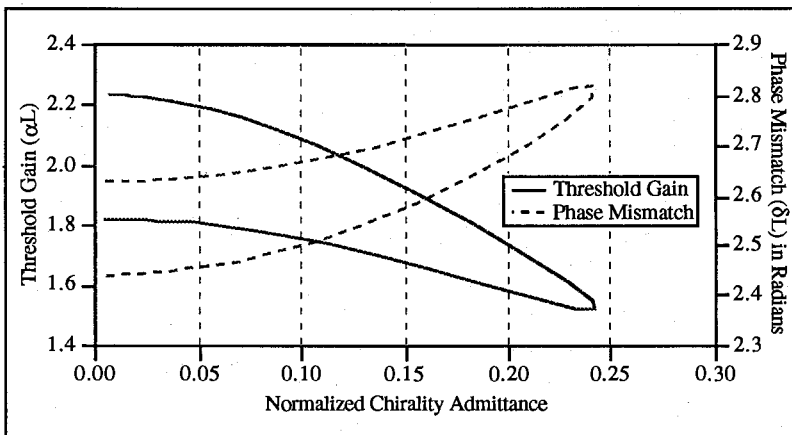
A problem of recent interest is the chirowaveguide suggested by Pelet and Engheta, *"The Theory of Chirowaveguides," IEEE Trans. on Ant. and Prop.* (1990). The authors have discussed in depth topics including the dispersion relationship, cut-off frequencies, propagation modes and evanescent modes for the parallel plate chirowaveguide. In this presentation, we are considering a source embedded within a chirowaveguide. The solution for the guided modes is obtained via an eigenvalue-eigenfunction approach akin to the Ohm-Raleigh method. Numerical analysis of the asymptotic expression for the full-wave solution is presented to highlight novel features of the chirowaveguide.

## ACTIVE CHIRAL MEDIA AND DISTRIBUTED FEEDBACK DEVICES

Kevin M. Flood and Dwight L. Jaggard  
Complex Media Laboratory  
Moore School of Electrical Engineering  
University of Pennsylvania  
Philadelphia, PA 19104

Distributed feedback (DFB) devices use the Bragg effect of periodic structures to provide coupling between modes throughout the device. In chiral media, there are two wavenumbers and a richer coupling mechanism available for DFB devices made of chiral material. For active material combined with chirality and periodicity, gain is available to the electromagnetic wave. Under appropriate conditions, such devices operate as chiral DFB lasers.

The combined effect of chirality and gain (or loss) on wave propagation and coupling in periodic structures is investigated here for transversely unbounded structures. The focus is on DFB lasers in a transversely unbounded periodic slab with spatially modulated electromagnetic parameters. The analysis uses a coupled mode approach employing a canonical physical model of chiral materials to predict the effects of chirality on DFB lasers. Results for DFB laser behavior in chiral media are compared and contrasted to the achiral case. We find that electric and magnetic field coupling characteristic of chiral materials can result in a lower threshold gain for DFB lasers in media with a given index of refraction and characteristic impedance. It is also found that chiral index-coupled or gain-coupled DFB lasers exhibit the same spectral mode properties as their achiral counterparts. An example of threshold gain ( $\alpha L$ ) and phase mismatch ( $\delta L$ ) is given in the plot below as a function of chirality for a device of length  $L$ .



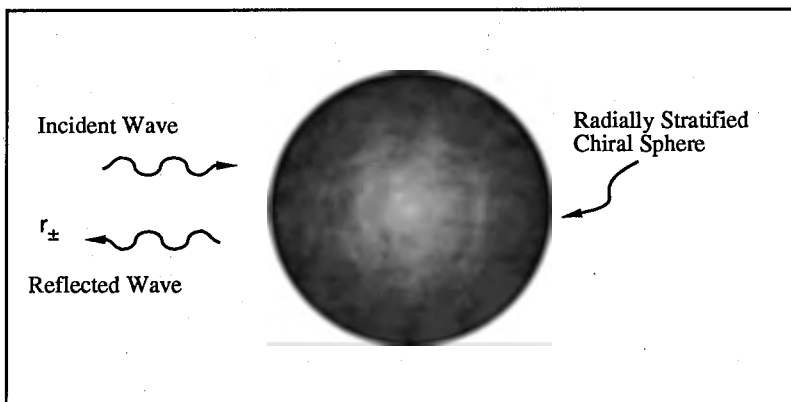
Example of threshold gain and phase mismatch as a function of normalized chirality admittance for DFB laser of constant electrical length. Values of relative electric and magnetic susceptibility vary along each curve.

## INVARIANT EMBEDDING AND CHIRAL MATERIAL

D. L. Jaggard and J. C. Liu  
 Complex Media Laboratory  
 Moore School of Electrical Engineering  
 University of Pennsylvania  
 Philadelphia, PA 19104

Methods of invariant embedding find their roots in the work of Ambarzumian [*Comptes Rendus (Doklady) de L'Academie des Sciences de l'URSS* 38, 229-232 (1943)] on light reflection in diffuse media. More recently, these methods have been used for scattering and inverse scattering problems of planar structures. Here we review and examine a generalization of these methods to chiral structures, both planar and spherical.

We start with a review of invariant embedding methods for planar layered chiral structures [see e.g., D. L. Jaggard, X. Sun and J. C. Liu, *Microwave and Optical Technologies Letters* 5, 107-112 (March 1992); D. L. Jaggard and X. Sun, *J. Opt. Soc. Am. 9*, 804-813 (1992)]. Although the problem of scattering from homogeneously layered chiral spheres and cylinders has been previously examined [see, e.g., D. L. Jaggard and J. C. Liu, *J. Electromagnetic Waves Applic.* 5/6, 669-694 (May - June 1992).], little has been done for the problem of spherical structures with radially varying properties. One exception is the work of R. W. Lathem [*Can. J. Phys.* 46, 1463-1468 (1968)] on dielectric cylinders and spheres. Continuing and generalizing this work, we develop a spherical chiral Riccati equation scattering from a radially stratified chiral sphere, as indicated in the figure below. As with its planar counterpart, the spherical Riccati equation transforms the boundary value problem to an initial value problem. Reflection coefficients  $r_{\pm}$  appear for the two circular eigenmodes of the scattered field. We compare and contrast the planar and spherical cases in addition to the chiral and achiral cases.



Geometry for scattering from a radially stratified chiral sphere.

## PLANE WAVE PROPAGATION IN A UNIAXIAL CHIRAL MEDIUM

I.V. Lindell\*, A.J. Viitanen  
 Electromagnetics Laboratory  
 Helsinki University of Technology  
 Otakaari 5A, Espoo SF-02150 FINLAND

Propagation of a plane wave in a uniaxially bianisotropic (reciprocal or nonreciprocal chiral) medium is considered. Such a medium is obtained, e.g., by mixing in an isotropic base material a number of metal helices with random locations but parallel axes. (This may actually be simpler than producing a truly isotropic, i.e., bi-isotropic, chiral medium.) When the axial direction is defined by the unit vector  $u_z$ , the constitutive equations of such a medium can be written in first approximation as

$$\mathbf{D} = (\epsilon_t \bar{\bar{I}}_t + \epsilon_z u_z u_z) \cdot \mathbf{E} + \xi u_z u_z \cdot \mathbf{H},$$

$$\mathbf{B} = (\mu_t \bar{\bar{I}}_t + \mu_z u_z u_z) \cdot \mathbf{H} + \zeta u_z u_z \cdot \mathbf{E},$$

with  $\bar{\bar{I}}_t$  denoting the two-dimensional unit dyadic transverse to the  $z$  axis. This means that, instead of four parameters as in a bi-isotropic medium, we have six scalar parameters describing the uniaxial medium.

Plane wave propagation in such a medium is considered. It is shown that there are two eigenwaves which individually see the uniaxial bianisotropic medium as a uniaxial anisotropic medium with respective effective parameter dyadics  $\bar{\bar{\epsilon}}_+ = \epsilon_t \bar{\bar{A}}_+$ ,  $\bar{\bar{\mu}}_+ = \mu_t \bar{\bar{A}}_+$  and  $\bar{\bar{\epsilon}}_- = \epsilon_t \bar{\bar{A}}_-$ ,  $\bar{\bar{\mu}}_- = \mu_t \bar{\bar{A}}_-$ , with  $\bar{\bar{A}}_{\pm} = \bar{\bar{I}}_t + A_{\pm} u_z u_z$ . The parameters  $A_{\pm}$  are simple functions of the original parameters:

$$A_{\pm} = \frac{1}{2} \left( \frac{\mu_z}{\mu_t} + \frac{\epsilon_z}{\epsilon_t} \right) \mp \sqrt{\frac{1}{4} \left( \frac{\mu_z}{\mu_t} - \frac{\epsilon_z}{\epsilon_t} \right)^2 + \frac{\xi \zeta}{\epsilon_t \mu_t}}.$$

This kind of anisotropic media can be reduced through certain affine transformations to equivalent isotropic media, in which the dispersion equation can be easily solved. When transformed back to the bianisotropic medium, the wave numbers for the two eigenwaves are obtained in the form

$$k_{\pm} = \frac{k_t}{\sqrt{\cos^2 \theta + A_{\pm}^{-1} \sin^2 \theta}},$$

where  $k_t = \omega \sqrt{\mu_t \epsilon_t}$  and  $\theta$  is the angle of the direction of propagation from the axis of the medium. For  $\xi = \zeta \rightarrow 0$ , the solutions reduce to  $A_+ \rightarrow \epsilon_z / \epsilon_t$  and  $A_- \rightarrow \mu_z / \mu_t$  corresponding to the well-known TM and TE polarized eigenwaves of the uniaxial anisotropic medium. The polarizations of the two plane eigenwaves in the uniaxial bi-isotropic medium are also easily found. The results can be directly applied to plane-wave propagation and reflection problems in layered uniaxial bianisotropic media.

**WEDNESDAY AM**  
**PLENARY SESSION**

Moderator: Peter M. Banks, Dean, College of Engineering, The University of Michigan

Rackham Auditorium      Time: 8:00-12:00

|             |  |
|-------------|--|
| 8:00-8:15   | WELCOMING REMARKS<br><i>James J. Duderstadt, President, The University of Michigan</i>                                 |
| 8:15-8:45   | REMOTE SENSING AND SIGHTED AUTOMATION<br><i>William Brown, President, Environmental Research Institute of Michigan</i> |
| 8:55-9:25   | SPACE TECHNOLOGY INITIATIVES<br><i>Dan Goldin, Administrator, National Aeronautics and Space Administration</i>        |
| 9:35-10:05  | STEALTH<br><i>John F. Cashen, Vice President, Northrop Corp. B2-Division</i>   |
| 10:15-10:40 | BREAK  |
| 10:40-11:10 | HIGH PERFORMANCE COMPUTING TRENDS<br><i>Justin R. Rattner, Director, INTEL Corporation</i>                             |
| 11:20-11:50 | FUTURE TRENDS OF INTELLIGENT VEHICLE HIGHWAY SYSTEMS<br><i>Don A. Savitt, Program Manager, Hughes Aircraft Co.</i>     |



**SESSION URSI B-14****WEDNESDAY PM****FINITE ELEMENT METHODS III**

Chairs: A. Peterson, Georgia Institute of Technology  
T. Fontana, Westinghouse Electric Corporation

Room: Modern Languages Building, Auditorium 1      Time: 1:30-4:50

|      |   |     |
|------|---|-----|
| 1:30 | VARIATIONAL FORMULATION OF ELECTROMAGNETICS FOR FIELD COMPUTATION<br><i>Jianming Jin, Otsuka Electronics, Inc.</i>  | 252 |
| 1:50 | A COMPARISON OF PARTITIONED AND NON-PARTITIONED MATRIX SOLUTIONS TO COUPLED FINITE ELEMENT-INTEGRAL EQUATIONS<br><i>Tom Cwik, Vahraz Jamnejad*, Cinzia Zuffada, Jet Propulsion Laboratory</i>                   | 253 |
| 2:10 | A NEW SELF-ADJOINT FORMULATION FOR THE COUPLED INTEGRAL EQUATION/FEM SOLUTION FOR THE BOR<br><i>Larry W. Epp*, Daniel J. Hoppe, Jet Propulsion Laboratory; Jin-Fa Lee, Worcester Polytechnic Institute</i>      | 254 |
| 2:30 | RADIATION BOUNDARY CONDITIONS FOR THE VECTOR HELMHOLTZ EQUATION<br><i>Douglas B. Meade, University of South Carolina; Andrew F. Peterson, Georgia Institute of Technology; Kevin J. Webb, Purdue University</i> | 255 |
| 2:50 | AN ANALYSIS OF THE MEASURED EQUATION OF INVARIANCE<br><i>J. Jevtic, R. Lee*, The Ohio State University</i>  | 256 |
| 3:10 | BREAK   |     |
| 3:30 | THEORETICAL ASPECTS ON THE MEASURED EQUATION OF INVARIANCE<br><i>Jeffrey L. Young, University of Idaho; John B. Schneider, Robert G. Olsen, Washington State University</i>                                     | 257 |
| 3:50 | MEI-BASED MESH TRUNCATION CONDITIONS FOR THE FINITE-ELEMENT MODELING OF EM SCATTERING BY TWO-DIMENSIONAL PENETRABLE TARGETS<br><i>D.B. Wright, A.C. Cangellaris*, University of Arizona</i>                     | 258 |
| 4:10 | FINITE ELEMENT ANALYSIS OF BODIES OF REVOLUTION USING THE MEASURED EQUATION OF INVARIANCE<br><i>T.L. Barkdull*, R. Lee, The Ohio State University</i>   | 259 |
| 4:30 | ELECTROMAGNETIC MODELING USING GRAPHICAL WORKSTATIONS - A CASE STUDY<br><i>H.T. Shmansky*, E.H. Newman, R.G. Rojas, The Ohio State University; G.C. Barber, NASA Langley</i>                                    | 260 |

## VARIATIONAL FORMULATION OF ELECTROMAGNETICS FOR FIELD COMPUTATION

Jianming Jin

Otsuka Electronics, Inc.  
Fort Collins, Colorado 80525

In finite element analysis two methods are often employed to formulate the system of equations. One is Galerkin's method and the other is the Rayleigh-Ritz variational method. Whereas Galerkin's method starts directly with the differential equations to be dealt with, the Rayleigh-Ritz variational method starts from a variational formulation, or the so-called functional, of the original boundary-value problem. Therefore, the applicability of the method depends directly on the availability of such a variational formulation. In this presentation we will discuss the methods for establishing the variational formulation, or for constructing the functional, for a given boundary-value problem defined by a differential equation and associated boundary conditions. Specifically, we will first discuss the applicability of a standard variational principle, which will show that this variational principle is limited to lossless boundary-value problems with homogeneous boundary conditions. Then we will modify this variational principle to accommodate inhomogeneous boundary conditions, and finally we will present a general variational principle which can be applied to boundary-value problems involving lossy media and/or lossy boundaries. With this general variational principle, we will be able to formulate most boundary-value problems encountered in electromagnetics. Specific examples will be given in the presentation.

**A COMPARISON OF PARTITIONED AND NON-PARTITIONED MATRIX SOLUTIONS TO  
COUPLED FINITE ELEMENT-INTEGRAL EQUATIONS**

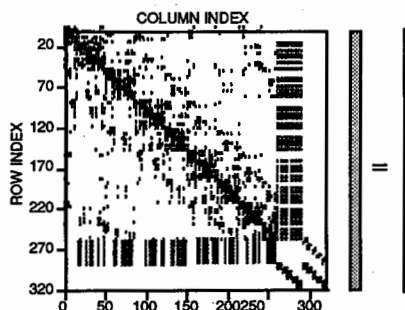
**Tom Cwik, Vahraz Jamnejad\*, and Cinzia Zuffada**

**Jet Propulsion Laboratory  
California Institute of Technology  
Pasadena, CA 91109**

The coupled finite element-integral equation technique is developed for solving radiation and scattering problems involving inhomogeneous objects with large dimensions in terms of wavelength. This method incorporates an exact integral equation outside an arbitrary surface, very near the object and circumscribing it, instead of an approximate absorbing boundary condition on a surface much farther away from the object, which is typically employed in finite element solutions (T. Cwik, et al., IEEE-APS Symposium, June 1993). As shown in the figure below, the complete matrix equation resulting from the coupled approach involves a large sparse submatrix  $K$  which is due to the finite-element mesh within a body of revolution (BOR) boundary, relatively small and banded submatrices  $Z_M, Z_J$  describing the integral equation, and two rectangular strip submatrices,  $C$  and  $C^T$  which represent the coupling between the finite element and the integral equation at the boundary. The unknowns are the magnetic field inside the BOR and the fictitious surface currents  $M$  and  $J$  on the BOR.

The system may be solved in three ways. In a single-step non-partitioned solution, an iterative solver is used. A complex non-Hermitian quasi minimal residue (QMR) algorithm is applied. This is simple and straight-forward but has to be repeated for multiple right-hand sides. In a two-step approach, the unknown magnetic field  $H$ , is eliminated by applying a complex but symmetric QMR to the symmetric  $K$  matrix. The problem is then reduced to a system for  $M$  and  $J$  currents and is solved by a direct method (i.e., LU factorization) which can handle multiple right-hand sides, while the operation on  $K$  is performed only once. Finally, in a three-step partitioned solution, the  $M$  or  $J$  unknown is eliminated by yet another direct solver. Then, the final matrix equation for the remaining unknown current,  $J$  or  $M$ , can be broken down into individual submatrix equations for each Fourier mode of the current, each of which can be solved for by applying a direct solver. The results obtained by the above methods are compared and the relative speed, memory requirement, and accuracy issues are discussed.

$$\begin{array}{c|c|c|c|c}
 K & C & 0 & H & = 0 \\
 \hline
 C^T & 0 & Z_o & M & 0 \\
 0 & Z_M & Z_J & J & V
 \end{array}$$



## A NEW SELF-ADJOINT FORMULATION FOR THE COUPLED INTEGRAL EQUATION/FEM SOLUTION FOR THE BOR

Larry W. Epp\*, Daniel J. Hoppe  
California Institute of Technology  
Jet Propulsion Laboratory  
Pasadena, CA 91109

Jin-Fa Lee  
Worcester Polytechnic Institute  
Worcester, MA 01609-2280

Finite element methods have proven to be very useful for the solution of complex bodies in enclosed spaces. Their uses in open region problems is only limited by the method in which the Sommerfeld radiation condition is imposed on the boundary. Absorbing boundary conditions can be applied that maintain the sparsity of the matrix equation to be solved, and are readily solvable by the sparse matrix techniques already employed in the finite element solution of the closed region interior problem. With sparse matrix solvers, the use of absorbing boundary conditions is limited by the extent to which the desired matrix structure is preserved and by the accuracy that is needed. When accuracy becomes an important issue on a large complex body, an exact truncation on the boundary through integral equation methods becomes attractive. These methods enforce the Sommerfeld radiation condition, but the large non-sparse matrix that results can be difficult to solve. An iterative matrix solution of the exact case holds the promise of effectively competing with the sparse matrix solution in terms of storage, speed, and accuracy of solution.

In the past application of the exact boundary condition not only destroyed the sparsity of the matrix equation, but destroyed the symmetry of the matrix equation. This made solution with existing symmetric iterative solvers based on the conjugate gradient method impossible. It can also lead to a large condition number causing poor convergence when using more general iterative methods. Interestingly before enforcing necessary continuity of tangential fields, the finite element solution of the closed region problem and the integral equation solution of similar open region problems by themselves can be made symmetric. In this work we have re-examined the fundamental formulation of the exact boundary condition approach in cylindrical coordinates for objects that are azimuthally symmetric. By deriving the variational form for the problem, the resulting solution was self-adjoint. Application of this exact boundary destroys sparsity, but since symmetry is preserved storage is decreased by a factor of two. Taking advantage of the physical symmetry of the body further reduces the number of unknowns to a two-dimensional slice of the problem. These methods are currently being compared to the integral equation solution of bodies of revolution consisting of conducting objects coated by layered dielectric material.

## RADIATION BOUNDARY CONDITIONS FOR THE VECTOR HELMHOLTZ EQUATION

Douglas B. Meade<sup>1,\*</sup>

Andrew F. Peterson<sup>2</sup>

Kevin J. Webb<sup>3</sup>

<sup>1</sup> Department of Mathematics, University of South Carolina, Columbia, SC 29208

<sup>2</sup> School of Electrical Engineering, Georgia Institute of Technology, Atlanta, GA 30332

<sup>3</sup> School of Electrical Engineering, Purdue University, West Lafayette, IN 47907

### Abstract

The solution of three-dimensional variational or Galerkin forms of the vector Helmholtz equation in open regions presents a challenging numerical problem. Of particular importance is the treatment of the unbounded spatial domain. In order to solve realistic three-dimensional problems, it is necessary to use a computational domain that is as small as possible. For this to be effective the truncation boundary should be conformal with the scatterer and the radiation boundary condition must be appropriately specified.

The basic idea is to introduce an artificial boundary and reformulate the problem on the truncated domain. Considerable work has been done on this for the scalar problem on planar and circular boundaries (Engquist and Majda, *Comm Pure Appl Math* (32), 313-357, 1979; Bayliss, Gunzburger and Turkel, *SIAM J Appl Math* (42), 430-451, 1982). The success of these methods depends critically on the selection of both the artificial boundary and the boundary condition applied on this boundary.

The purpose of this paper is to present a class of approximate radiation boundary conditions for the vector Helmholtz equation. The form of these boundary conditions is suitable for use with a general-shaped artificial boundary. This is an extension of our earlier work that applied to the scalar case with an arbitrary convex truncation boundary (Meade, Slade, Peterson, and Webb, 1992 *IEEE APS Digest*, 540-543, 1992).

In the three-dimensional vector field case, the derivation of the approximate radiation boundary conditions is based on the vector Wilcox (far-field) expansion for the solution of the time-periodic wave equation in the exterior of a scatterer (Peterson, *Microwave and Optical Technology Letters* (1), 62-64, 1988). For a non-spherical boundary, the surface curvature must be incorporated in the representation of the curl term in the surface integral.

Particular attention is given to the implementation of the boundary conditions in the finite element method. The performance of these boundary conditions is evaluated on the basis of the two criteria: approximation error and computational complexity. The trade-offs between these competing objectives are identified, illustrated and analyzed.

## AN ANALYSIS OF THE MEASURED EQUATION OF INVARIANCE

J. Jevtić and R. Lee\*

ElectroScience Laboratory  
Department of Electrical Engineering  
The Ohio State University  
1320 Kinnear Rd.  
Columbus, Ohio 43212-1191

The measured equation of invariance (MEI), which has been previously introduced by Mei (AP/URSI meeting, Chicago, 1992), is a boundary truncation technique for finite element/finite difference methods. Although the method has been shown to produce accurate solutions for several simple geometries, at this point, it is unclear as to exactly why the method works. Furthermore, its capability in modeling geometries of arbitrary size and shape has not yet been established. In fact, our results indicate that a significant error is present for electrically large geometries. In order to improve upon the current method, it is necessary to obtain a better understanding of MEI.

In this paper, we present an alternate formulation which provides several important insights into the capabilities of MEI. It provides a suitable explanation for the corresponding loss in accuracy as the electrical size of the geometry increases. In addition, it provides several possible explanation as to why the accuracy decreases as the boundary is brought closer to the geometry. It can be shown that the finite difference approximation used in MEI for the boundary condition cannot be excitation independent. Our study indicates that the metrons currently used to find the coefficients associated with the finite difference equation on the boundary only guarantees invariance over a small set of excitations and has not been optimized for all possible excitations, including in most cases the excitation of interest.

We will introduce metrons which perform an optimization over all possible excitation. This optimization may produce a more accurate boundary condition than the current metrons. We will demonstrate that it is better for the case of a perfectly conducting circular cylinder as well as other more complex geometries.

THEORETICAL ASPECTS  
ON THE MEASURED EQUATION OF INVARIANCE

Jeffrey L. Young\*, John B. Schneider<sup>+</sup> and Robert G. Olsen<sup>+</sup>

\*Department of Electrical Engineering  
University of Idaho  
Moscow, ID 83843

+School of Electrical Engineering and Computer Science  
Washington State University  
Pullman, WA 99164-2752

The measured equation of invariance method, recently put forth by Mei et al. [URSI Digest, p. 544, APS/URSI Joint Symposium, Chicago, 1992] combines the relative merits of the integral equation approach (i.e. satisfaction of the radiation condition, geometry conforming) and the finite difference method (i.e. sparse matrices) into a single algorithm. As with the finite difference method, the matrix equation  $\mathbf{Ax} = \mathbf{b}$  is formed by approximating the Helmholtz operator (or the Laplacian) at each nodal point in the computational domain in terms of a discrete sum. However in the MEI method, there is no restriction to the number of nodes in the sum nor how the nodes are configured with respect to the reference node. The unknown coefficients, say  $\alpha_n$ , appearing in the sum are not the central difference coefficients but are derived from a set of  $N - 1$  linearly independent equations:

$$\sum_{n=1}^{N-1} \alpha_n \Phi^k(\mathbf{r}_n) = -\alpha_o \Phi^k(\mathbf{r}_o) \quad (1)$$

Here  $k = 1, 2, \dots, N - 1$  and  $\Phi^k$ , called a measuring function, is a known solution to the homogeneous Helmholtz equation.

In this presentation, we discuss theoretical aspects of the MEI method by considering various analytical examples. First, it is shown that the  $\alpha_n$ 's of Equation (1) are the central difference coefficients when a) the mesh points form a cross, b) the  $\Phi^k$ 's form an independent set, c) the  $\Phi^k$ 's satisfy the Helmholtz equation, and d)  $h^4$  terms and higher in the Taylor series of  $\Phi^k$  are identically zero. Second, by considering Laplace's equation associated with a perfectly conducting cylinder in free-space and using the MEI method, we can generate a closed-form solution; the MEI solution and the physical solution are identical. Finally, we show that the sum of (1) can be generated from the method of moments, under certain restrictions.

MEI-BASED MESH TRUNCATION CONDITIONS  
FOR THE FINITE-ELEMENT MODELING OF EM SCATTERING  
BY TWO-DIMENSIONAL PENETRABLE TARGETS

D. B. Wright and A. C. Cangellaris\*

Electromagnetics Laboratory

Department of Electrical and Computer Engineering  
University of Arizona, Tucson, AZ 85721

The *Measured Equation of Invariance* (MEI) is a new concept, proposed by K.K. Mei (K.K. Mei, et al, *Proc. of the First European Conference on Numerical Methods in Engineering*, Brussels, Belgium, Sept. 1992), which can be used to develop accurate, local mesh truncation conditions for the finite element/finite difference solution of electromagnetic scattering and radiation problems. Such mesh truncation conditions have been successfully implemented in the finite-difference solution of electromagnetic scattering by two- and three-dimensional conducting targets in free space, two-dimensional scattering by perfectly conducting discontinuities in waveguides, as well as two-dimensional scattering by penetrable scatterers. In all of the above applications, the MEIs are generated by means of an integral expression for the scattered fields in the unbounded region in terms of the field and(or) its normal derivative on the surface of the scatterer.

This presentation considers three different approaches for developing MEI-based truncation conditions for use in the finite element modeling of two-dimensional electromagnetic scattering problems. The first approach is based on Huygen's principle and follows rigorously the MEI postulates. Thus, both the shape of the scatterer and its composition are taken into account in the development of the MEIs. The second approach is a less "rigorous" approach, since only the shape of the scatterer is accounted for in the generation of the MEIs. However, it is computationally less demanding from the first approach. Finally, in the third approach distributions of cylindrical multipoles are used to generate the MEIs. From a computational point of view, this last approach is the most efficient.

The presentation provides a detailed comparison of the performance of the three approaches in conjunction with finite-element calculations of scattering by a variety of two-dimensional penetrable targets. The numerical examples include scatterers of various shapes and electrical sizes ranging from a fraction of a wavelength to several wavelengths. In order to examine the accuracy of the proposed approaches, comparisons are made between our results and those obtained using other hybrid finite element and/or integral equation techniques.

## FINITE ELEMENT ANALYSIS OF BODIES OF REVOLUTION USING THE MEASURED EQUATION OF INVARIANCE

T.L. Barkdoll\* and R. Lee

ElectroScience Laboratory  
Department of Electrical Engineering  
The Ohio State University  
1320 Kinnear Rd.  
Columbus, Ohio 43212-1191

This paper is concerned with the finite element solution of the problem of an axially symmetric conducting body of arbitrary cross-section, which is excited by an incident plane wave in an isotropic homogeneous infinite media. The coupled azimuthal potential (CAP) formulation, which is valid in isotropic, inhomogeneous, rotationally symmetric media, is used to express the field values in terms of the two potentials which are proportional to  $E_\phi$  and  $H_\phi$  (M. Morgan, *IEEE Transactions on Antennas and Propagation*, vol. AP-27, March 1979). Due the rotationally symmetric nature of the geometry, the three dimensional problem can be decomposed into an infinite sum of two-dimensional problems. Four node quadrilateral elements are used to model the geometry.

The measured equation of invariance (MEI), which was developed by Mei (AP/URSI meeting, Chicago, 1992), is used to perform the boundary truncation. This method uses a set of finite difference equations as the boundary condition for the problem domain. These finite difference equations are based on a set of "measures" which are found from the placement of a set of linearly independent currents on the boundary. The nodes associated with each equation are chosen such that it does not increase the bandwidth of the finite element matrix; therefore, the solution of the problem is expected to very efficient. One of the interesting features of applying MEI to this problem is that  $E_\phi$  and  $H_\phi$  are coupled together in the boundary condition. The manner in which they are coupled will be presented.

One possible problem with the MEI boundary condition is that it is approximate. The accuracy of the solution is a function of the scatterer's shape and electrical size. Also, it depends upon the distance between the mesh boundary and the scatterer. To determine the accuracy of this method, we will present results for several canonical geometries. In addition, we plan to consider several more complex geometries to demonstrate the versatility of this method.

## Electromagnetic Modeling Using Graphical Workstations – A Case Study

H.T. Shamansky\*, E.H. Newman and R.G. Rojas  
The ElectroScience Laboratory  
The Ohio State University  
1320 Kinnear Rd.  
Columbus, Ohio 43212

G.C. Barber  
Antenna and Microwave Research Branch  
NASA Langley  
Hampton, Virginia 23665

As electromagnetics applications involve more realistic and geometrically complex shapes, modern high-performance graphical workstations find an increasing role in the complete solution. This paper looks in detail at a variety of pitfalls and hurdles encountered in the transformation of well-established electromagnetic codes into a graphically assisted generalized helicopter radiation package. As a case study, the *Helicopter Antenna Radiation Prediction* code, (HARP), is examined from a perspective of the integration of traditional electromagnetic codes with user guided graphical pre- and post-processing enhancements.

Aspects including such issues as graphical user interfaces (GUI's), depth and position perception as it applies to interactive applications in electromagnetics, uses of color and three dimensional viewing versus more traditional black and white, two dimensional images are considered in this paper. A summary of the experiences gained from this case study will provide one look into the pros and cons of advanced visualization tools to expand and enhance the core electromagnetic solutions.

**SESSION URSI B-15****WEDNESDAY PM****ELECTROMAGNETIC THEORY III**

Chairs: R.G. Rojas, The Ohio State University; A. Ishimaru, University of Washington

Room: Modern Languages Building, Auditorium 2      Time: 1:30-5:30

|      |   |     |
|------|---|-----|
| 1:30 | WAVE GUIDING PROPERTIES OF PARALLEL RESISTIVE SHEETS<br><i>John R. Natzke*, Thomas B.A. Senior, University of Michigan</i>  | 262 |
| 1:50 | TIME DOMAIN LEAKY MODES IN SCATTERING BY AN INFINITE PERIODIC ARRAY OF FLAT CONDUCTING STRIPS ON A GROUNDED DIELECTRIC SLAB<br><i>M. Jaureguy, P. Borderies, Onera-Cert; L.B. Felsen, Polytechnic University</i>                | 263 |
| 2:10 | TOWARDS A UNIFIED ANALYTICAL MODEL OF DISPERSIVE MATERIALS<br><i>Nicolaos G. Alexopoulos, University of California, Los Angeles; Rodolfo E. Diaz, Hexcel APD</i>  | 264 |
| 2:30 | A NEW IMPEDANCE BOUNDARY CONDITION FOR NON-PERFECT CONDUCTORS<br><i>S. Kiener*, A. Nishikata, Communications Research Laboratory</i>  | 265 |
| 2:50 | THE ARTIFICIAL PUCK FREQUENCY SELECTIVE SURFACE<br><i>Robert G. Schmier, Westinghouse Electronic Systems Group</i>  | 266 |
| 3:10 | BREAK   |     |
| 3:30 | ELECTROMAGNETIC BACKSCATTERING BY A THREE-DIMENSIONAL PLATE OF ARBITRARY SIZE<br><i>Y.J. Stoyanov*, M.A. Sekellick, A.J. Stoyanov, National Surface Warfare Center</i>  | 267 |
| 3:50 | ELECTROMAGNETIC SCATTERING BY A TWO-DIMENSIONAL PERIODIC ARRAY OF ELECTRICALLY SMALL BIISOTROPIC/CHIRAL SPHERES<br><i>Asoke K. Bhattacharyya, New Mexico State University; Akhlesh Lakhtakia, Pennsylvania State University</i> | 268 |
| 4:10 | VECTORIAL DIFFRACTION ANALYSIS OF PERIODIC DIELECTRIC GRATINGS WITH ARBITRARY SURFACE<br><i>E. Griese, Siemens Nixdorf Informationssysteme AG</i>   | 269 |
| 4:30 | ADAPTATION OF SPATIAL NETWORK FOR VECTOR POTENTIAL TO ELECTROMAGNETIC FIELDS WITH MEDIUM CONDITIONS<br><i>Norinobu Yoshida, Hokkaido University</i>   | 270 |
| 4:50 | TIME-DOMAIN UTD COEFFICIENT FOR SCATTERING FROM A WEDGE WITH TWO FACE IMPEDANCES AND SOME APPLICATIONS<br><i>Asoke K. Bhattacharyya, New Mexico State University</i>  | 271 |
| 5:10 | PENETRATION CHARACTERISTICS OF EM WAVES IN SEMICONDUCTING MATERIALS<br><i>C.S. Guttu, G.S.N. Raju, P.M. Rao, K.R. Gottumukkala, K.V. Rao, Andhra University</i>   | 272 |

Wed. p.m.

## WAVE GUIDING PROPERTIES OF PARALLEL RESISTIVE SHEETS

John R. Natzke\* and Thomas B. A. Senior  
Radiation Laboratory

Department of Electrical Engineering and Computer Science  
University of Michigan  
Ann Arbor, MI 48109-2122

In this paper, the scattered field of a pair of parallel resistive half planes under plane wave illumination is determined using the angular spectrum method of Booker and Clemmow. The solution is obtained upon splitting the associated Wiener-Hopf functions via a numerically efficient routine. The diffraction coefficient is derived, and far field data are presented for various resistivities and separation distances. The field guided by the structure is investigated and found to be comprised of surface waves associated with each half plane and a waveguide modal field. For edge-on incidence, this guided field is characterized as a function of the resistivity and separation distance of the half planes. Based on the results for the parallel resistive half planes, a high frequency model is developed for a pair of parallel resistive strips. A transmission line analysis is used in the model to account for the multiple interactions between the edges of the strips. The scattered far field is verified using a moment method solution.

## Time domain leaky modes in scattering by an infinite periodic array of flat conducting strips on a grounded dielectric slab

M. Jaureguy, P. Borderies  
 Onera-Cert 2-Ave E. Belin  
 31055-Toulouse-Cedex-FRANCE

and

L.B. Felsen

Polytechnic University 5 Metrotech Center  
 Brooklyn, New York 11220

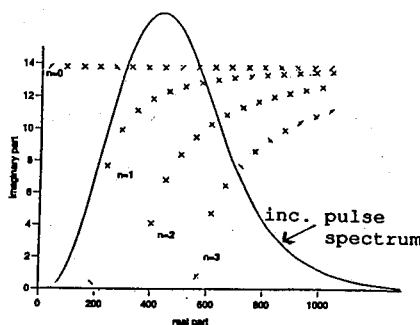
An infinite array of perfectly conducting strips printed on a dielectric slab backed by a perfectly conducting ground plane is illuminated by a very short plane pulse incident obliquely in the plane perpendicular to the strips. We calculate the transient signal at any observation point above the array by using array-modulated leaky modes (LM) in the Fourier integral relating the time and frequency domains.

First, the response to a unit current located in the strip plane is derived in the spectral wavenumber domain and extended to the periodic configuration through Poisson's sum formula giving a field expansion in terms of Floquet modes (FM). The strip currents are expanded on a set of basis functions with unknown coefficients which will be determined by enforcing boundary conditions on the strips and solving the resulting linear system via the method of moments. The composite Green's function obtained in this manner has frequency dependant poles singularities which couple the FM and smooth-slab LM effects. Those FM-LM poles also appear in the complex frequency plane and determine there the behaviour of the corresponding time domain FM-LM.

The non-dispersive fundamental mode ( $n=0$ ) has all its complex frequency poles lying on a straight line parallel to the real axis; thus, all of the associated oscillations are equally damped and summing their contributions rebuilds the incident pulse shape without distortion from successive reflections on the metallic ground plane. However, the higher order modes exhibit the behaviour depicted in Fig.1: real poles from DC to FM-LM modes cut-off (surface wave poles, trapped and undamped) whereas above cut-off complex poles tending toward the fundamental mode at high frequencies. In the presentation the build-up of the transient signal in relation with these FM-LM modes will be discussed and their role in the asymptotic evaluation of the complex frequency inversion integral will be demonstrated.

Fig.1

poles position  
 in the complex  
 frequency plane  
 $(n = \text{FM-LM index})$



Wed. p.m.

## TOWARDS A UNIFIED ANALYTIC MODEL OF DISPERSIVE MATERIALS

Nicolaos G. Alexopoulos<sup>1</sup> and Rodolfo E. Diaz<sup>2</sup>

<sup>1</sup>Department of Electrical Engineering  
University of California  
Los Angeles, CA 90210

<sup>2</sup>Hexcel APD  
2500 W. Frye Rd.  
Chandler, AZ 85224

### ABSTRACT

All dielectric materials, by nature, exhibit a frequency dependent permittivity. The traditional approach to modeling this property, termed dispersion, is to postulate physical mechanisms such as rotations, vibrations and elongations of the constituent molecules and then derive from these an equation for the permittivity. As a result of this procedure the material models obtained are considered to be only useful approximations, valid only over finite bands of frequency. The classic material behaviors of Debye relaxations and Lorentz resonances can be mimicked but they are considered to be mutually exclusive and of limited validity (see A. Von Hippel, "Dielectrics and Waves", Wiley, 1954, p. 178 and J. B. Hasted, "Aqueous Dielectrics", Chapman and Hall, 1973, pp. 56-58). With the ever increasing bandwidth of operation of electromagnetic devices and with the advent of dispersive time domain numerical electromagnetics codes, such band limited models of questionable rigor are no longer adequate. A compact analytic representation of all physically realizable dielectric materials is needed for the analysis and design of realistic electromagnetic devices. Such a representation is presented in this paper.

Using the consequences of causality and a minimum number of physical assumptions it is shown that all physically realizable dielectric materials can be modeled by a special set of complex functions. In special cases these functions reduce to the classic Debye relaxation and Lorentz resonance phenomena; but they are not limited to them. As a particular example of the completeness and compactness of this representation a model for the water substance is obtained which includes the phenomenon of optical transparency.

## A New Impedance Boundary Condition for Non-Perfect Conductors

S. Kiener\* & A. Nishikata,  
Electromagnetic Compatibility, CRL,  
4-2-1, Nukui-Kitamachi, Koganei, Tokyo 184

The purpose of this communication is to compute the **inside** field of a closed cavity which boundaries are made of arbitrarily shaped non-perfect conductors (see also A. Nishikata & S. Kiener, "Non-Perfect Conducting Enclosure's Shielding: Characterization of Walls and Numerical Application", in *Proc. EMC Zurich*, Zurich, 1993).

The classical surface impedance boundary condition (Leontovich-Schelkunoff) is defined as:

$$\vec{E}_t = Z_S (\vec{n} \times \vec{H}_t), \quad Z_S = \sqrt{\frac{\mu}{\epsilon}}, \quad \epsilon' = \epsilon - j \frac{\sigma}{\omega}.$$

$E_t$  and  $H_t$  are the components tangential to the surface of the conductor (and perpendicular to one another).

This boundary condition is valid under the following assumptions:

- The conductor is much thicker than the skin depth and
- the radius of curvature is larger than the same skin depth.

This condition is used to take into account the finite conductivity of materials for the "outside" problem, but not to compute the electromagnetic "pollution" which is penetrating through the material.

Moreover, the minimum thickness condition, necessary to the Schelkunoff impedance boundary condition, does not make it usable for thin metallic shields which are precisely of interest as they may let an appreciable portion of the field go through.

For all these cases a new surface impedance boundary condition had to be developed.

One can show that, for the 1D case (an infinite shielding plane of finite thickness with normal incident plane waves) and 2 polarizations, the tangential fields on the source side before the shield ( $z = 0$ ) and after ( $z = d$ ) are related by the following exact relations:

$$\begin{pmatrix} E_x(z=0) \\ E_y(z=0) \\ E_x(z=d) \\ E_y(z=d) \end{pmatrix} = \begin{pmatrix} 0 & Z_s & 0 & -Z_{tr} \\ -Z_s & 0 & Z_{tr} & 0 \\ 0 & Z_{tr} & 0 & -Z_s \\ -Z_{tr} & 0 & Z_s & 0 \end{pmatrix} \begin{pmatrix} H_x(z=0) \\ H_y(z=0) \\ H_x(z=d) \\ H_y(z=d) \end{pmatrix}$$

The  $Z_s$ ,  $Z_{tr}$  are function of the propagation constant in air, the electromagnetic characteristics of the shielding material as well as its thickness.

In the 3D case, we assume that the following vector form is valid:

$$\begin{aligned} \vec{E}_t &\simeq Z_s [\vec{n} \times \vec{H}_t] + Z_{tr} [-\vec{n} \times \vec{H}_\tau] \\ \vec{E}_\tau &\simeq Z_s [-\vec{n} \times \vec{H}_\tau] + Z_{tr} [\vec{n} \times \vec{H}_t] \end{aligned}$$

where  $t$  denotes the tangential components on the source side,  $\tau$  on the opposite side and  $\vec{n}$  is pointing at the source.

This is the definition of our impedance boundary condition which has been implemented in a numerical code (MMP-3D) to compute a 3D enclosures of general shape.

Wed. p.m.

## THE ARTIFICIAL PUCK FREQUENCY SELECTIVE SURFACE

Robert G. Schmier  
Westinghouse Electronic Systems Group  
P.O. Box 746, MS 55  
Baltimore, MD 21203

In this paper the analysis and performance of a new type of filter element used in frequency selective surface applications is introduced. The element introduced is a symmetric, two-pole, iris-loaded circular waveguide element. Construction employing this type of element centers around a conductive plate with holes drilled in it in a predetermined grid pattern. These holes are filled with a variable dielectric constant, pourable, dielectric material. Circular conductive patches are then concentrically deposited on the dielectric filler on either side of the drilled waveguide holes. Finally, sheets of dielectric are added to each side of the conductive plate to fine tune the frequency selective surface.

This paper will describe the design of this filter element which began with a complete electromagnetic analysis employing a spectral moment method solution of the magnetic field integral equation, rigorously taking into account various dielectric layers and waveguide fillers. The key to the analysis of this element is setting up an equivalent problem. In the equivalent problem, the apertures formed by the irises are replaced by perfect conductors and a sheet of magnetic current is placed on top of the conductor on both sides of the aperture. The currents on opposite sides of the aperture are of equal magnitude and opposite sign. By employing this equivalent problem, the analysis can be conveniently separated into three distinct regions - free space to the left side of the surface, a waveguide region in the surface itself, and a free space region to the right side of the surface - which are coupled together by the magnetic currents. The analysis allows for any number of stratified dielectrics in all three regions.

This paper will show comparisons between calculated performance, based on the computer code ARTPUCK.FOR generated as a result of the analysis, and data measured from frequency selective surfaces designed to resonate at X, Ku, and Ka bands.

## ELECTROMAGNETIC BACKSCATTERING BY A THREE-DIMENSIONAL PLATE OF ARBITRARY SIZE

Y. J. Stoyanov,\* M. A. Sekellick, and A. J. Stoyanov

Carderock Division, NSWC, Bethesda, MD 20084-5000

The electromagnetic backscattering from a three-dimensional flat rectangular plate is examined at Horizontal-polarization including traveling surface waves at grazing angles of incidence. The backscattering pattern of a long, perfectly conducting plate exhibits a traveling wave lobe near end-on incidence when illuminated by an H-polarized electromagnetic field. Conventional theories including Physical Optics (PO) and the Uniform Theory of Diffraction (UTD) cannot account for the traveling wave (TW) contributions to the backscattering pattern. In this paper the Geometrical Theory of Diffraction (GTD) is used in conjunction with a traveling surface wave representation to yield a solution which provides an accurate backscattering from a plate of arbitrary size. This solution provides insight into the relative contributions of the various scattering mechanisms excited on the three dimensional plate. The GTD-TW method extends the applicability of GTD and can be used to isolate traveling wave contributions (Y. J. Stoyanov et al., Proceedings of the 1992 URSI International Symposium on Electromagnetic Theory). The edge thickness modifies radar returns at grazing angles and contributes to the total radar cross section (RCS) of the plate. The edge thickness contribution is observed clearly by comparing RCS patterns of beveled edge and thick edge plates. The edge contributions to the RCS diminish in magnitude for aspects close to the normal angle of incidence. Comparisons with measured RCS data are used to demonstrate the accuracy of this high frequency asymptotic solution. The hybrid GTD-TW approach substantially improves the accuracy of predictions in the non-specular area.

Wed. p.m.

ELECTROMAGNETIC SCATTERING BY A TWO-DIMENSIONAL PERIODIC ARRAY OF  
ELECTRICALLY SMALL BIISOTROPIC/CHIRAL SPHERES

Asoke K. Bhattacharyya

Tel: (505)-522-9468

Research Center, Physical Science Laboratory,  
New Mexico State University, Las Cruces, NM 88003-0002.

Akhlesh Lakhtakia

Tel: (814)-863-4319

Department of Engineering Science and Mechanics,  
Pennsylvania State University, University Park, PA 16802-1401.

**Abstract**

Considerable interest has recently been shown in fabricating artificial chiral composites as well as on the possibilities of their use in components and devices for radar and communications applications. Canonical chiral problems have been well-documented [e.g., C.F. Bohren, *Chem. Phys. Lett.* **29**, 458 (1974); A. Lakhtakia (ed): *Selected Papers on Natural Optical Activity* (1990)]. Work has been reported on the estimation of effective dipole moments of electrically small chiral spheres [A. Sihvola and I.V. Lindell, *Electron. Lett.* **26**, 118 (1990); A. Lakhtakia et al, *Appl. Opt.* **29**, 3627 (1990)] as well as bianisotropic spheres [A. Lakhtakia, *J. Phys. France* **51**, 2235 (1990); Z. *Naturforsch.* **46a**, 1033 (1991)]. Linear arrays of electrically small chiral spheres have also been investigated [D.L. Jaggard et al, *IEEE Trans. AP* **36**, 1007 (1988)].

In this presentation we will address scattering by a periodic planar array of small biisotropic/chiral spheres, with special emphasis on the co- and cross-polarization scattering characteristics of arrays of chiral spheres. Mutual coupling between the spheres will be ignored. It will be shown that the chirality parameter -- in conjunction with other array and radar parameters -- can help control the RCS of the array to the considerable advantage of a radar engineer.

## Vectorial Diffraction Analysis of Periodic Dielectric Gratings with Arbitrary Surface

E. Griese

Siemens Nixdorf Informationssysteme AG · Cadlab — Analog System Engineering  
Bahnhofstraße 32 · 4790 Paderborn · Germany

The vectorial diffraction problem of a homogeneous plane wave of arbitrary incidence by an infinite dielectric grating is solved by computing a transmission matrix. It transforms the boundary conditions of the plane above the grating region into the plane below the grating region.

The method of solution is based on the Coupled-Wave-Theory. The whole space is divided into different areas, into the areas with homogeneous permittivity and into the grating region. The problem is described in cartesian coordinates  $(x, y, z)$ . The wave vector of the incident plane wave is given by the three cartesian components. Its direction can be described by two angles  $\varphi_0$  and  $\vartheta_0$  with respect to the  $z$ -coordinate. The geometrical arrangement does not depend on the  $y$ -coordinate and is periodical in the  $x$ -direction. The normal to the planar grating boundaries (global normal to the grating) is given by the unit vector  $e_z$ . With respect to the independence of the  $y$ -coordinate, the  $y$ -dependence of the resulting field strengths will be identical with that of the incident plane wave. Therefore, the complete field distribution can be determined, if only the  $y$ -components of the electric and magnetic field strengths are given.

Within the homogeneous regions, these field components satisfy the homogeneous Helmholtz equation. Due to the periodicity of the grating surface, the solutions are given by Fourier series. Therefore, the electromagnetic field strength in each homogeneous region can be described by a discrete spectrum of plane waves.

Inside the periodic modulated region the  $y$ - and  $z$ -components of the electric and magnetic field strengths have to satisfy a coupled system of partial differential equations with variable ( $z$  dependent) coefficients. This system is obtained from Maxwell's equations. After discretization of the grating surface by an approximation with staircase functions, a planar layer model of the grating is obtained. The permittivity and its reciprocal value in each layer depend only upon the coordinate  $z$  and they are periodical in  $x$ -direction. So they can be expanded into Fourier series with constant coefficients. The field strengths within the grating region are also as those in the homogeneous space domains pseudo periodical in the  $x$ -direction. Therefore, the approaches for the unknown field describing functions are given by Fourier series with  $z$ -dependent coefficient functions. These approaches lead with respect to the orthogonality of the exponential functions to a fourth order system of vectorial ordinary differential equations with an infinite dimension. It can be shown that in the case of non lossy structures the necessary reduction to a finite system does not change its characteristic of being free from losses. The reduced ordinary differential equation system is solved by computing the exponential of the system matrix. This is done without computing the eigenvalues and eigenvectors, but by using a Padé approximation. This method is faster and numerical more accurate than the computation by the corresponding Taylor series. With the continuity of the tangential components of the electric and magnetic field strengths, the state variables (field describing functions) are continuous in the planes between the side by side arranged layers. Therefore, the transmission matrix of the grating region is given by the product series of the matrix exponentials of each layer and the matrices, which take the boundary conditions of the planes above and below the grating region into consideration.

A special choice and arrangement of the state variables lead to the same structure of the system matrix which is obtained in the case of the scalar diffraction problem. (If the field strengths of the incident wave do not depend on the coordinate  $y$ , the general diffraction problem can be divided into the two not coupled scalar problems  $TE$ - and  $TM$ -polarization.) Therefore, the same numerical algorithms for computing the matrix exponential and the coefficients of the Fourier series in the homogeneous space domains can be used. Numerical results show the validity of this method.

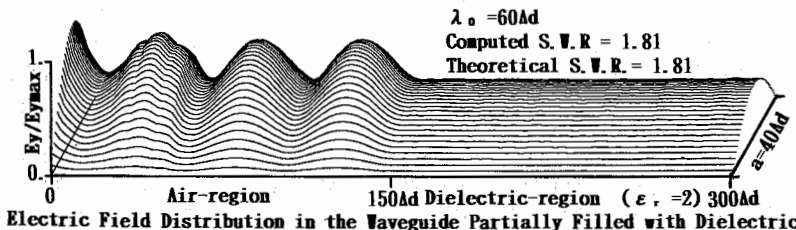
## ADAPTATION OF SPATIAL NETWORK FOR VECTOR POTENTIAL TO ELECTROMAGNETIC FIELDS WITH MEDIUM CONDITIONS

Norinobu Yoshida

Department of Electrical Engineering  
Hokkaido University, Sapporo 060 Japan

In the analysis of electromagnetic fields, the vector potential has important roles especially when sources exist. I have already proposed the treatment of the vector potential for the Coulomb's gauge condition in the three-dimensional space and time domain [N. Yoshida; "Transient Analysis of Vector Potential in Three-Dimensional Space by Spatial Network", *Radio Science*, **26**, 1, pp.259-264 (Jan. 1991)]. In the treatment, both the magnetic vector potential and the electric vector potential are used, and each component of the vector potential variables is arranged at each lattice point in the three-dimensional lattice network. Further, I proposed the unified formulation including both the vector and scalar potentials with the Lorentz gauge condition [N. Yoshida; "Time-dependent Formulation of Scalar Potential Field with Lorentz Gauge Condition for Lossive Field", Proc. 1992 URSI Int. Symp. on Electromagnetic Theory, pp.240-242, 1992]. In the formulation, the new variables 'F', 'F'' and the conventional static electric and magnetic field variables 'Es', 'Hs' correspond to the voltage and current variables, respectively.

The computation by using the vector potential usually confronts the problems in treating the boundary conditions at the interface between different medium. In this paper, to examine the validity of the formulation in treating the boundary condition, the electromagnetic fields in the waveguide partially filled with dielectric medium are analyzed. In the waveguide, the fundamental component of the wave propagates obliquely repeating reflections on the side walls. Therefore on the surface of dielectric medium perpendicular to the longitudinal axis, the incident wave can have the both tangential and normal components of the electromagnetic fields. The following figure shows the steady state electric field distribution of the TE mode in the waveguide as a basic example of the computation. In this case, only tangential component exists on the surface. The standing wave ratio agrees well with the theoretical one for every used frequency, that is, for resultant correspondent incident angle.



**TIME-DOMAIN UTD COEFFICIENT FOR SCATTERING FROM A  
WEDGE WITH TWO FACE IMPEDANCES AND SOME APPLICATIONS**

**Asoke K. Bhattacharyya**

(505) 522-9468

Research Center

Physical Science Laboratory  
New Mexico State University  
Las Cruces, NM 88003-0002

A time-domain uniform diffraction coefficient(TDUTD) for electromagnetic scattering from wedge with two face impedance has been presented[Bhattacharyya-1992 IEEE EMC Conference, Anna Heim,CA, Aug 1992, pp 499-502] based on the work of Tiberio, Pelosi and Manara in the frequency domain on the same problem. The TDUTD was obtained by transformation from frequency domain results as in the work of Verrutipong for PEC wedges. A Fortran code for time-domain scattering from impedance wedges of various exterior wedge angles including a half plane has been developed. This code has been applied to some practical problems of scattering from a flat plate with any combination of two face impedances and a finite cylinder with any combination of surface impedances of the curved and flat surfaces. A few scattering results have been discussed with various target parameters and input waveforms. The nature of the induced current on the surface of the scatterers will be presented.

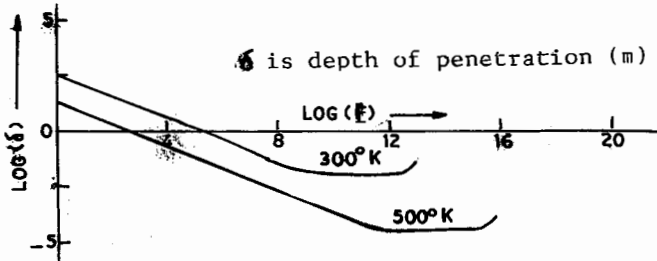
The problem of time-domain scattering from composite structures is of interest to researchers. It appears to the author that less research has been done on the analytical formulations of the problem than on the numerical methods particularly, the time-domain finite difference (FDTD) and experiments. Recently, a key contribution on the analytical modeling was reported by Verrutipong[T.W. Verrutipong-IEEE APS-38, Nov 1990, pp. 1757-1764] presenting a time-domain diffraction coefficient for a PEC wedge but with no practical applications. Also this valuable work restricts to plots of surface current and charge densities on the PEC 90° wedge, a PEC half plane and a PEC strip and does not address the scattering aspects as such. The frequency domain analysis of the diffraction coefficient was done by Tiberio et al [ IEEE AP-33, No.8, Aug 1985, pp. 867-873] for the general wedge of two face impedances. In this paper, a TDUTD coefficient obtained by the transformation from the FD results for the more general case of the wedge with two face impedances has been applied to two cases of time domain scattering (1) a flat plate scattering with any arbitrary impedances and (2) a finite cylinder with various combinations of impedances of the curved and flat surfaces.

## PENETRATION CHARACTERISTICS OF EM WAVES IN SEMICONDUCTING MATERIALS

C.S.Gutti, G.S.N. Raju, P.M. Rao, K.R. Gottumukkala, K.V.Rao  
College of Engineering, Andhra University  
Visakhapatnam-530 003, India

The conducting properties of conductors and dielectrics are already reported in the literature. One of the important property for such materials is penetration depth when an EM wave is incident upon the material of interest. However, there is no information on the penetration behaviour of EM waves on a semiconducting material like Ge or Si. This information is found to be vital to study the negative/damaging characteristics of a semiconducting material situated in an Electromagnetic environment. To obtain such important information the knowledge of a typical semiconducting material is not just sufficient as the conducting properties are also influenced by dielectric constant, permeability, frequency and temperature.

It is, therefore, of interest to obtain the variation of the penetration depth as a function of frequency with temperature as a parameter. In the present work, pure germanium and silicon are considered to be homogeneous and isotropic and the penetration depths of EM waves are evaluated for frequencies ranging from very low to very high. This data is infact obtained from the real part of the propagation constant, which is also a function of the basic parameters of the medium, frequency and temperature. The data so obtained for a germanium material is presented in the following figure for temperatures 300°K and 500°K. For the sake of convenience, the logarithmic varations of penetration are presented. It is found from the results the penetration depths are found to rapidly fall as the frequency increases.



## JOINT SESSION: NEW TECHNIQUES IN COMPUTATIONAL ELECTROMAGNETICS

Chairs: F.X. Canning, Rockwell International Science Center  
 S.R. Laxpati, University of Illinois at Chicago

Room: Modern Languages Building, Lecture Room 2      Time: 1:30-4:50

|      |   |      |
|------|---|------|
| 1:30 | METHOD OF MOMENTS SCATTERING COMPUTATIONS USING HIGH-ORDER BASIS FUNCTIONS<br><i>L.R. Hamilton, M.A. Stalzer, R.S. Turley*, J.L. Visher, S.M. Wandzura, Hughes Research Laboratories</i>  | AP-S |
| 1:50 | THE IMPORTANCE OF ACCURATE SURFACE MODELS IN RCS COMPUTATIONS<br><i>L.R. Hamilton, Hughes Research Laboratories; V. Rokhlin, Fast Mathematical Algorithms and Hardware Corporation; M.A. Stalzer, R.S. Turley, J.L. Visher, S.M. Wandzura, Hughes Research Laboratories</i> | AP-S |
| 2:10 | A NEW COMBINED FIELD INTEGRAL EQUATION FOR IMPEDANCE MATRIX LOCALIZATION (IML)<br><i>Francis X. Canning, Rockwell Science Center</i>  | AP-S |
| 2:30 | WAVELET-LIKE BASIS FUNCTIONS FOR EFFICIENT WAVEGUIDE MODE COMPUTATION<br><i>Robert L. Wagner*, Gregory P. Otto, Weng Cho Chew, University of Illinois</i>   | AP-S |
| 2:50 | ON THE APPLICATION OF QUASI-WAVELET EXPANSIONS TO OPEN DIELECTRIC WAVEGUIDE PROBLEMS<br><i>Kazem Sabelfakhri, Linda P.B. Katehi, The University of Michigan</i>   | AP-S |
| 3:10 | BREAK   |      |
| 3:30 | WAVELETS: WHAT DOES IT MEAN TO AN ENGINEER?<br><i>Tapan K. Sarkar, Syracuse University; Luis-Emilio García-Castillo, Magdalena Salazar-Palma, Universidad Politécnica de Madrid</i>   | 274  |
| 3:50 | INTRODUCTION OF WAVELET CONCEPTS INTO FINITE ELEMENT TECHNIQUES<br><i>Luis-Emilio García-Castillo, Magdalena Salazar-Palma, Universidad Politécnica de Madrid; Tapan K. Sarkar, Syracuse University</i>   | 275  |
| 4:10 | ELECTROMAGNETIC WAVE SCATTERING BASED ON THE PATH INTEGRAL WITH A WAVELET TRANSFORM<br><i>Robert Nevels*, Chenhong Huang, Zuoguo Wu, Texas A&amp;M University</i>   | 276  |
| 4:30 | MODELING OF ELECTROMAGNETIC SCATTERING USING WAVELET TECHNIQUES FOR GEOMETRY MODELING AND EXPANSION FUNCTIONS<br><i>D.-S. Wang, McDonnell Douglas; Grant Welland, University of Missouri</i>  | 277  |

## WAVELETS: WHAT DOES IT MEAN TO AN ENGINEER?

*Tapan K. Sarkar\*,  
Luis-Emilio García-Castillo\*\*, Magdalena Salazar-Palma\*\**

*\*Dept. Electrical and Computer Engineering, Syracuse University,  
121 Link Hall, Syracuse, New York 13244-1240, USA*

*\*\*Grupo Micrornas y Radar, Dpto. Señales, Sistemas y Radiocomunicaciones,  
E.T.S.I. Telecomunicación, Universidad Politécnica de Madrid,  
Ciudad Universitaria, s/n, Madrid 28034, SPAIN*

In recent times Wavelets have been an active area of research in the abstract mathematical sciences and they have been applied in certain specific areas as image coding and filter theory. It is quite important to point out that there is a fundamental difference between what the engineers call wavelets and what the mathematicians call wavelets. To a mathematician, a wavelet is basically a transform technique which produces local information about the waveform both in the original and in the spectral domain. Specifically, the Wavelet Transform defines a transform of a function  $f$  as:

$$W(f) = \frac{1}{\sqrt{|a|}} \int_{-\infty}^{\infty} f(t) \bar{\Psi}\left(\frac{t-b}{a}\right) dt \quad \text{for } f \in L^2(R)$$

So the Wavelet Transform localizes a signal with a time window

$$[b + a t^* - a \Delta \Psi; b + a t^* + a \Delta \Psi]$$

where the center of the window is at  $b + a t^*$  and the width is given by  $2a\Delta\Psi$ . The signal is also localized in the frequency domain. For the Wavelet Transform this analysis is done in a natural way, namely by "constant-Q" analysis. This means that the window dilates at low frequencies and shrinks at high frequencies. One important aspect of this phenomena is that the first step of signal processing carried out by the human ear is done in a fashion described above. One fundamental aspect that the basic wavelet must satisfy is:

$$\int_{-\infty}^{\infty} \Psi(x) dx = 0$$

This is an admissibility condition. However, interestingly, for most practical applications, where the wavelets have been found numerous engineering applications, this condition is often "ignored". This admissibility condition implies that the dc value of the function is zero, hence one has to carefully define convergence when such types of basis functions are employed to approximate a function that has non zero dc values.

The objective of the paper is to outline the mathematical definitions and engineering applications of wavelets. Examples will be presented to illustrate where this technique is applicable and where it is not.

A companion paper illustrates how this concept can be used for numerical techniques applied to differential form of operator equations, namely for the Finite Element Method.

## INTRODUCTION OF WAVELET CONCEPTS INTO FINITE ELEMENT TECHNIQUES

*Luis-Emilio García-Castillo<sup>\*</sup>, Magdalena Salazar-Palma<sup>\*</sup>, Tapan K. Sarkar<sup>\*\*</sup>*

*<sup>\*</sup>Grupo Microondas y Radar, Dpto. Señales, Sistemas y Radiocomunicaciones,  
E.T.S.I. Telecomunicación, Universidad Politécnica de Madrid,  
Ciudad Universitaria, s/n, Madrid 28040, Spain.*

*<sup>\*\*</sup>Dept. Electrical and Computer Engineering, Syracuse University,  
121 Link Hall, Syracuse, New York 13244-1240, USA.*

The Finite Element Method is a differential operator based approach to solve practical engineering problems. Even though the system matrix structure of the Finite Element Method is quite sparse, yet the condition number of the system matrix increases somewhere between  $\log(N_T)$  to  $\exp(N_T)$  (where  $N_T$  is the total number of unknowns) depending on the problem and on the proper choice of expansion functions. A detailed explanation may be found in Mikhlin ["The Numerical Performance Of the Variational Method"]. The ultimate dream of a numerical technique practitioner would be to choose a set of basis functions which will make the system matrix diagonal. If the system matrix is made diagonal then the solution technique becomes trivial.

This paper is an attempt to describe a set of basis functions for a certain class of finite element discretization so that the major part of the system matrix is diagonal. Specifically, the paper describes how much a concept related to wavelets is utilized and applied successfully to the solution of differential equations employing the finite element approach. It is shown that for 2D problems if a rectangular discretization is used, then for the TM problem the system matrix size becomes  $(LN^2 + NN_{EI} + N_{Vi})^2$  with a diagonal submatrix of dimensions  $LN^2 \times LN^2$ . Thus the system matrix is mostly diagonal and the computation is strongly reduced. L is the number of rectangular elements, N is a parameter that determines the order of the approximation,  $N_{EI}$  is the number of internal edges and  $N_{Vi}$  the number of internal vertices. For the TE case, the system matrix size becomes  $(LN^2 + NN_E + N_V)^2$ . Again, a major portion  $LN^2 \times LN^2$  of the system matrix is made diagonal by a suitable choice of basis functions.  $N_E$  is the number of edges and  $N_V$  is the number of vertices.

The paper explains the choice of the basis functions, how the system matrix is approximately diagonalized and what is the order of the increment of the computational complexity as N and L go up. Convergence studies and numerical results illustrate the features of the method.

## Electromagnetic Wave Scattering Based on the Path Integral with a Wavelet Transform

Robert Nevels\*, Chenhong Huang and Zuoguo Wu  
Department of Electrical Engineering  
Texas A&M University  
College Station, Texas 77843-3128

The path integral is in a class of expressions known as functional integrals which are solutions to parabolic and, by a suitable transformation, elliptic or Helmholtz type differential equations. The path integral has been described as a universal (infinite inhomogeneous region) Green's function. In fact the path integral expression is that of a universal Green's function, however the fast Fourier transform (FFT) upon which the recently developed Fourier transform path integral (FTPI) scattering method depends, places limitations on the physical size of the scattering structure or equivalently the size of the scattering region. Here we will show the size of the scattering region can be extended by using the wavelet transform.

The form of the path integral is not unique, but depends upon the chosen 'basis' function. In the FTPI method, Fourier exponentials were chosen as a basis because this leads to a nested Fourier transform expression which can be evaluated by taking advantage of FFT routines. However, two and three dimensional FFT's require computations that must be carried out at every point on a square grid. This means that the entire scattering region must be spanned by the FFT range. The size of a square grid that accurately accounts for all the features of the scatterer and includes the remainder of the region inside and surrounding the scatterer is limited by the available *in core* computer memory. Accurate results have been obtained for example for a  $2\lambda$  (wavelength) circular cylinder lying inside a  $15\lambda \times 15\lambda$  region with 8 points per wavelength. The wavelet transform on the other hand can be adjusted so that basis functions are concentrated in the vicinity of surface features. By doing so, fewer grid points are required and the scatterer itself can be more detailed or larger in size. A family of wavelets will be constructed and moment method, Fourier transform path integral and wavelength transform path integral method results will be presented for some simple scattering structures illuminated by a line source and a plane wave. The relative merits of the three methods will be discussed.

**Modeling of Electromagnetic Scattering  
Using Wavelet Techniques for Geometry Modeling  
and Expansion Functions**

**D. -S. Wang**

**McDonnell Douglas Research Laboratories**

**P.O. Box 516**

**St. Louis, MO 63166, USA**

**Grant Welland**

**Department of Mathematics and Computer Science**

**University of Missouri, St. Louis**

**8001 Natural Bridge Rd.**

**St. Louis, MO 63121, USA**

Choices of geometry representations and expansion basis functions are two important issues in the electromagnetics (EM) modeling. For example, the application of method of moments (MM) for studying electromagnetic (EM) scattering of 3D arbitrary-shaped bodies requires sophisticated geometric modeling techniques for the boundary surfaces that support currents to be used in the integral equations. Most of these techniques employ either planar-faceted or curve-patched models for the surfaces. For planar-faceted models, the linear (roof-top) expansion functions are commonly used for the surface currents. For curve-patched models, there are choices of expansion functions including both the linear and higher order ones. The computational efficiency depends on the choice of these basis functions. Recent advances in wavelet techniques and multi-resolution analyses enable the development of a new solution technique for the MM formulation. We have demonstrated that a set of wavelet basis functions can be incorporated into the MM formulation to obtain a highly sparse matrix to save both memory and computing time requirements. (D. - S. Wang, G. Welland, and S. Zhao, 1992 International IEEE/URSI Meeting, Chicago, IL)

In this presentation, we report the development of an MM formulation incorporating a wavelet technique that is used to develop both a geometry modeling technique and a set of expansion functions. This technique provides not only accurate geometry modeling, but also an efficient representation of highly oscillatory surface currents. Our goal is to develop an EM modeling technique that couples the basis functions with the geometry representations to not only minimize the computation requirements, but also extend the analysis to arbitrary 3D geometries. We emphasize the accuracy and computational efficiency of the present formulation.



## INTEGRATED SYSTEMS

Chairs: M. Shur, University of Virginia; M. Steer, North Carolina State University

Room: Michigan League, Michigan Room Time: 1:30-4:50

|      |  |     |
|------|--|-----|
| 1:30 | NOVEL MMIC 31/93 GHZ FREQUENCY TRIPLEXER<br><i>R. Bradley*, National Radio Astronomy Observatory; S. Weinreb, S. Duncan, E. Schlecht, Martin Marietta Labs</i>   | 280 |
| 1:50 | A DUAL DIELECTRIC RESONATOR FREQUENCY DISCRIMINATOR<br><i>Sabah Khesbak*, Thomas T.Y. Wong, Illinois Institute of Technology</i>   | 281 |
| 2:10 | POUND DISCRIMINATOR REALIZED WITH DIELECTRIC RESONATOR<br><i>Thomas Nagode*, Thomas T.Y. Wong, Illinois Institute of Technology</i>  | 282 |
| 2:30 | MODIFIED BROADSIDE-COUPLED MICROSTRIP LINES AND THEIR USE IN NEW COUPLED-LINE BAND-PASS FILTERS FOR ACHIEVING WIDE BANDWIDTHS<br><i>C. Nguyen*, M. Tran, Texas A&amp;M University</i>  | 283 |
| 2:50 | HYSTERETICAL BEHAVIOR OF THE CURRENT NOISE IN HIGH TEMPERATURE SUPERCONDUCTORS<br><i>A. Masoero, Modena University; P. Mazzetti, A. Stepanescu, Politechnic of Torino; G. Cone, D. Grobnić, I. Pop, I. Stirbat, Politechnic Institute of Bucharest</i> | 284 |
| 3:10 | BREAK  |     |
| 3:30 | 2.8 TIME REDUCTION IN THE TEMPORAL RESPONSE OF PIN PHOTODIODES WITH A TRANSMISSION LINE TRANSFORMER<br><i>M.C.R. Carvalho, W. Margulis, J.R. Souza, Pontifical Catholic University of Rio de Janeiro</i>   | 285 |
| 3:50 | INTEGRALIZATION DESIGN OF T/R MODULES AND FEEDING NETWORKS FOR SOLID-STATE ACTIVE PHASED ARRAYS<br><i>Yin Liansheng, Gao Tie, Li Jianxin, Nanjing Research Institute of Electronics and Technology</i>   | 286 |
| 4:10 | FIGURE OF MERIT FOR ESTIMATING THE HIGH FREQUENCY PERFORMANCE OF MICROWAVE ICS<br><i>T. Mallikarjun, Queen's University</i>  | 287 |
| 4:30 | ON THE PERFORMANCE ANALYSIS OF SUBCARRIER MULTIPLEXED LIGHTWAVE SYSTEMS<br><i>T. Mallikarjun, Queen's University</i>   | 288 |

Wed. p.m.

## NOVEL MMIC 31/93 GHZ FREQUENCY TRIPLER

**R. Bradley\***

National Radio Astronomy Observatory<sup>†</sup>  
2015 Ivy Road  
Charlottesville, VA 22903

**S. Weinreb, S. Duncan, and E. Schlecht**

Martin Marietta Labs  
1450 S. Rolling Road  
Baltimore, MD 21227

A monolithic 31/93 GHz frequency tripler was designed, fabricated, and evaluated. The tripling performance of the GaAs abrupt-junction Schottky diode, with 20 micron anode diameter,  $2.5 \times 10^{16} \text{ cm}^{-3}$  active layer doping, and reverse breakdown greater than 20 volts, was analyzed using both Fourier and harmonic balance techniques. A balanced diode configuration was chosen to increase the output power and effectively separate the even and odd harmonic frequencies. A linear circuit simulator was used to design the input, output, idler, and bias embedding circuitry. Conductor-backed coplanar waveguide (CBCPW) on a semi-insulating GaAs substrate was chosen for circuit realization to improve heat dissipation and eliminate complicated flip-chip mounting. Unwanted modeing was reduced by the use of numerous via hole connections between the upper and lower ground planes and by proper air bridging around CBCPW discontinuities. Tuning stubs were used to separate the dc and commensurate frequencies. Novel features include a mutual-inductance air bridge scheme to simultaneously tune the idler and output, stacked dc and rf lines to provide diode bias while preserving isolation, and a wide bandwidth coplanar waveguide to rectangular waveguide transition in the output circuit. The overall fabricated chip size was 177 x 49 mils. Four versions of the tripler design were fabricated on a single wafer. Return loss measurements at the input and output indicate proper circuit tuning as a function of bias voltage. Output power greater than 24 mW from 90 to 95 GHz was measured with 500 mW input power. The best results obtained occurred at 93.45 GHz with an output power of 34 mW and an efficiency of 6.7 percent.

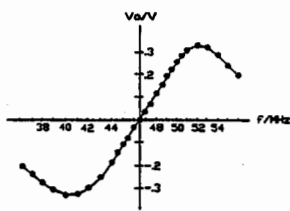
---

<sup>†</sup>The National Radio Astronomy Observatory is operated by Associated Universities, Inc. under cooperative agreement with the National Science Foundation.

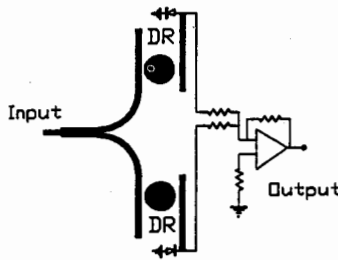
## A Dual Dielectric Resonator Frequency Discriminator

Sabah Khesbak\* and Thomas T.Y. Wong  
 Department of Electrical and Computer Engineering  
 Illinois Institute of Technology  
 Chicago, Illinois 60616

The design and implementation of a frequency discriminator employing two dielectric resonators are described. This is a planar circuit with dielectric resonators realization of the classic dual-tank-circuit frequency discriminator employed in FM receivers. The input RF signal is evenly coupled to a pair of oppositely connected diodes through the two dielectric resonators, which function as high-Q filters with resonant frequencies close to each other, as shown in the figure below. Outputs from the diodes are summed to give the S curve response. The slope of the S curve can be adjusted by tuning the resonant frequencies of the resonators. The linearity can be optimized by varying the coupling of the resonators to the microstrips which tends to offset any asymmetry in the circuit and any mismatch between the diodes. With an input power of 20 dBm at 4.246 GHz the maximum sensitivity of the circuit was measured to be 170mV/MHz. The implementation offers a versatile and cost-effective approach to the realization of frequency discriminators.



The frequency response

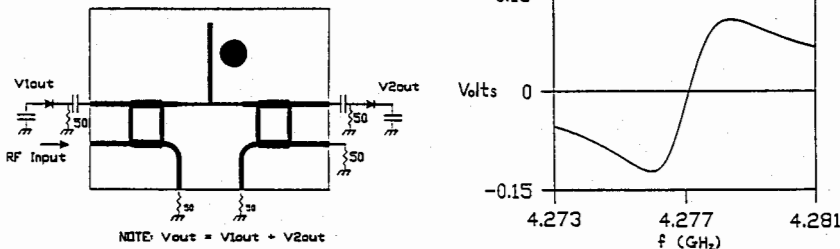


The circuit diagram

## Pound Discriminator Realized with Dielectric Resonator

Thomas Nagode\* and Thomas T.Y. Wong  
Department of Electrical and Computer Engineering  
Illinois Institute of Technology  
Chicago, Illinois 60616

Originally implemented with waveguide junctions and cavity resonator, the Pound frequency discriminator has over the years found many applications in RF and microwave phase-locked loops, receivers and source stabilizers. An advantage of the design is only one resonator is required. A cost effective realization of the Pound discriminator in microstrip circuit is now made possible by the availability of high-Q dielectric resonators. In this paper, the design and implementation of a dielectric resonator based Pound discriminator are described. As illustrated by the figure below, it consists of a dielectric resonator coupled to a microstrip line which is branch connected to two diodes through two  $70-50\Omega$  step transitions. Two 3-dB couplers combine the RF signals and reduce possible mismatch. With a 20 dBm input at 4.277 GHz center frequency, typical measured value for the slope of the S curve was around 150mV/MHz. Design procedures and comparison of the simulated and measured responses will be presented.



\* Present Address: Motorola Inc., International Cellular Subscriber Division, Libertyville, Illinois.

**MODIFIED BROADSIDE-COUPLED MICROSTRIP LINES AND THEIR  
USE IN NEW COUPLED-LINE BAND-PASS FILTERS  
FOR ACHIEVING WIDE BAND-WIDTHS**

C. Nguyen\* and M. Tran  
Department of Electrical Engineering  
Texas A&M University  
College Station, Texas 77843-3128

**ABSTRACT**

The broadside-coupled stripline structure, first reported by J.E. Dalley in 1969, has an inherent broad-band property, resulting from the strong coupling between the two broadside-coupled strips. Since then, different configurations of the broadside-coupled lines have been proposed. However, they are all stripline-type transmission lines, and thus clearly not suitable for microwave and millimeter-wave monolithic integrated circuits (MMICs) and, to some extent, microwave and millimeter-wave integrated circuits (MICs).

The microstrip and stripline half-wavelength coupled-line band-pass filters developed by S.B. Cohn in 1958 have perhaps been the most widely used microwave band-pass filters in the past several decades. One drawback of this class of filters is the limited bandwidth due to the use of microstrip and stripline parallel-coupled transmission lines that have inherent weak coupling characteristics.

In this paper, we report modified symmetric and asymmetric broadside-coupled microstrip lines (Fig. 1), suitable for MIC and MMIC applications requiring wide bandwidths and tight couplings. Their analysis based on the spectral-domain method will be described. The development of various new half-wavelength coupled-line band-pass filters using the proposed broadside-coupled structures will be presented. Fig. 2 shows the performance of one of the new filters. The reported transmission lines and filter structures should be very useful for MICs as well as MMICs as they show a great capability in achieving broad bandwidths and tight couplings.

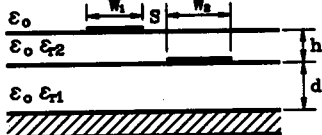


Fig. 1 A modified broadside-coupled microstrip line.

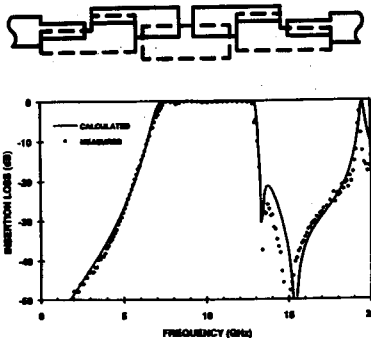


Fig. 2 Performance of a new broadside-coupled filter

## HYSERETICAL BEHAVIOR OF THE CURRENT NOISE IN HIGH TEMPERATURE SUPERCONDUCTORS

A.MASOERO<sup>1</sup>, P.MAZZETTI<sup>2</sup>, A.STEPEANESCU<sup>2</sup>, G.CONE<sup>3</sup>, D.GROBNIC<sup>3</sup>, I.POP<sup>3</sup>, I.STIRBAT<sup>3</sup>

1 - Phisics Department of Modena University, Italy

2 - Phisics Department - Politecnic of Torino, Italy

3 - Phisics Department - Politecnic Institute of Bucharest, Romania

It is known that the ceramic superconductors exhibit properties that are characteristic to the type II superconductors. In addition to the flux expulsion of the Meissner state, a type II superconductor may also exhibit a mixed state in which the magnetic flux penetrates the sample in the form of the quantized flux lines. The inhomogenous nature of this materials determines the occurrence of regions with weak links, where the fluxoids mobility gives rise to dissipative effects.

In this paper are reported measurements, obtained with an improved experimental technique, of this effect, concerning a hysteretical behavior of the current noise in YBCO superconducting samples brought to a resistive state by a magnetic field. The results confirm the already published ones and are in agreement with a model where noise is generated by motion of fluxoids in weak superconducting regions under the percolation threshold. Hysteresis effects should arise because the pattern of the region where the current density is supercritical depends on the internal field and the field generated by trapped fluxoids.

Also, the results of the current noise vs variables values of the temperature and injection currents for different magnetic fields are presented.

The experimental evidence of the hysteretical behavior of the noise was interpreted in terms of a mathematical model, that simulate the properties of a granular superconductor by means of a random Josephson junction network, where the granular superconducting islands are coupled to one another through Josephson-like weak links. The behavior of this disorderly system in a strong magnetic field is modeled buy the parameter of the simple overdamped Josephson junction. The statistical distribution of normal junction resistance as well as the critical temperature distribution of the grains are taken into account.

The hysteretical behavior of the noise is explained in terms of the intrinsec behavior of the Josephson junction and of the percolative properties of the superconductor network.

The mathematical model generate a 3-dimension random resistor network with the values of the resistors comanded in temperature, field and electrical current. The RRN was solved using a sparse program pakage.

## 2.8 TIME REDUCTION IN THE TEMPORAL RESPONSE OF PIN PHOTODIODES WITH A TRANSMISSION LINE TRANSFORMER

M. C. R. Carvalho, W. Margulis and J. R. Souza

Center for Telecommunication Studies - Pontifical Catholic University of Rio de Janeiro  
Rua Marquês de São Vicente, 225; 22453 Rio de Janeiro-RJ, Brazil

In this paper we describe how the temporal response of PIN photodiodes can be improved by using a compact transmission line impedance transformer, shown in Figure 1.

Initially, an InGaAs PIN photodiode was employed, with a capacitance of  $1.4\text{pF}$ , and  $20\Omega$  series resistance. The dashed line in Figure 2 represents the response of the photodiode when illuminated by  $30\text{ps}$  pulses from a gain switched BH semiconductor laser, and coupled to the  $50\Omega$  load (scope) through a  $50\Omega$  microstrip line. In order to reduce the rise and fall times of the photodiode, the output signal was coupled on to the  $50\Omega$  load through a transmission line impedance transformer (TLT), whose impedance varied from  $5\Omega$  at the diode side to  $50\Omega$  at the scope side. In this new arrangement, the characteristic photodiode RC time is dramatically reduced. The impedance variation along the TLT was confirmed through time domain reflectometry. The TLT incorporating a new transmission line configuration composed of combined CPW-slotline structures, as illustrated in Figure 2, was designed using a full wave spectral domain analysis/synthesis routine, and was built via standard etching techniques on a ceramic substrate with  $\epsilon_r=80$ . The total length of the TLT was  $14\text{mm}$ , yielding a lower frequency cutoff of  $\sim 300\text{MHz}$ , and the total width of the substrate was limited to  $3.0\text{mm}$  to avoid higher order modes up to  $\sim 20\text{GHz}$ . The measured return loss of the TLT was better than  $15\text{dB}$  from  $500\text{MHz}$  to  $18\text{GHz}$ .

The response of the same PIN diode when connected to the oscilloscope through the TLT is shown by the solid line in Figure 2. The fall time is seen to have been reduced by 2.8 times, while the rise time is improved by 1.2 time, when compared with the arrangement used for the result in Figure 2-a. The ringing observed at the tail of the pulse can be avoided by increasing either the repetition frequency of the laser or the length of the TLT. Other commercial photodiodes were also tested, showing improved performance as compared to the  $50\Omega$  arrangement. An even more drastic reduction in temporal response is expected for faster photodiodes, which present lower series resistance.

The same TLT can be also used with advantage in the pumping of semiconductor lasers. In this case, the impedance matching between the generator and the laser allows greater usage of the available electrical power. Also, an improvement on the temporal response of the laser is expected. The reduced dimensions of the TLT make integration within the small packing of commercial photodiodes and laser diodes feasible, yielding faster devices for optical communication systems.

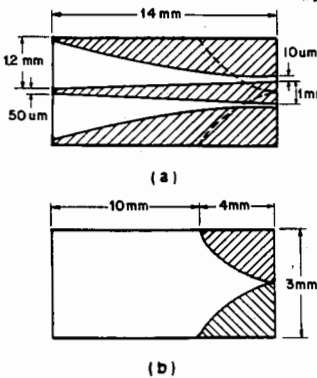


Figure 1: Transmission line impedance transformer

(a): upper face    (b): lower face

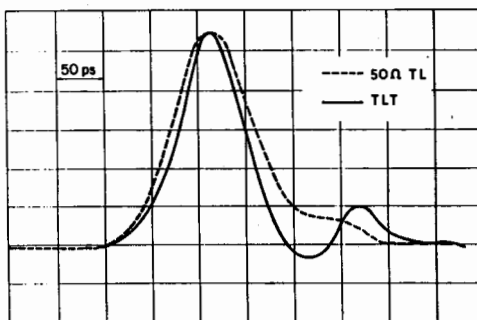


Figure 2: Comparison of the response of a PIN photodiode to short optical pulses, when the diode is coupled through the TLT (solid curve) and through a conventional  $50\Omega$  microstrip line (dashed curve).

## Integralization Design of T / R Modules and Feeding Networks for Solid-State Active Phased Arrays

Yin Liansheng, Gao Tie and Li jianxin

Nanjing Research Institute of Electronics and Technology  
P.O.Box 1315, Nanjing, 210013, P.R.China

**ABSTRACT** In a solid-state active phased array, each element is linked with a T / R module. In general, transmitting networks provide exciting powers for power-amplifiers in T / R module, and the output receiving signals from T / R modules are to be formed sum and difference beams with receiving networks. Thus, there will be much more T / R modules and feeding networks in the antenna array. So, the space is very crowded, and it is very difficult to ventilate air and radiate heat. In this paper, a integralization design method of T / R modules and column feeding networks are proposed. The elevation sum and difference beamforming networks and transmitting column feeding ones use the common, so that the column feeding ones will be reduced by half. Therefore, the weight of the array antennas are to be decreased significantly, which is benificial to ventilate air and radiate heat. The block diagram is shown in Fig.1 and the some relationships are as follows:

$$T_N(n) = T(n) \quad R_{\Sigma N}(n) = T_N(n)$$

$$R_{\Sigma N}(n) \cdot R_A(n) = R_{\Sigma}(n) \quad R_A(n) \cdot R_{\Delta N}(n) = R_{\Delta}(n)$$

where

- $T_N(n)$  the column distribution function (CDF) required by transmitting beam
- $R_{\Sigma}(n)$  CDF required by receiving sum beam
- $R_{\Delta}(n)$  CDF required by receiving difference beam
- $T(n)$  CDF of transmitting beam performed with column feeding network
- $R_{\Sigma N}(n)$  CDF of receiving sum beam performed with column feeding network
- $R_{\Delta N}(n)$  CDF of receiving difference beam performed with column feeding network
- $R_A(n)$  the distribution function of transportation coefficients' amplitude of digital control attenuator

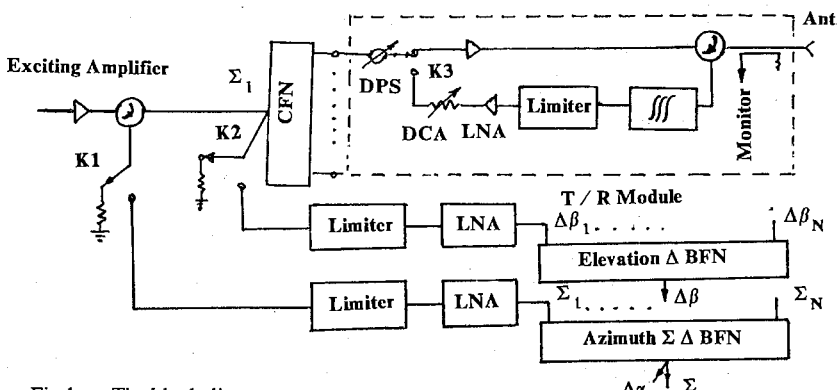


Fig.1 The block diagram

## FIGURE OF MERIT FOR ESTIMATING THE HIGH FREQUENCY PERFORMANCE OF MICROWAVE ICs

T.Mallikarjun

Department of Electrical Engineering

Queen's University at Kingston

Kingston, Ontario, CANADA K7L 3N6.

e-mail: [mallik@qucdnee.bitnet](mailto:mallik@qucdnee.bitnet)

There are several IC processes for high frequency applications, such as Si-bipolar, GaAs MESFET/HEMT, HBT and so on. The maximum frequency of oscillation ( $f_{max}$ ) and the unity current gain frequency ( $f_t$ ) are used as figures of merit for estimating the high frequency performance of these MICs. Both of these figures of merit are not quite suitable to the design of either monolithic or hybrid microwave integrated circuits. This is because,  $f_{max}$  is measured only by matching the transistor conjugatively to the source and load impedances respectively, which is quite impractical in integrated circuits, and  $f_t$  is obtained with the output short-circuited and thus has no relevance to a practical application.

Recently, a more practical figure of merit  $F_{pmax}$  was suggested by Taylor et al [Solid State Elect., vol. 29, pp. 941-946] for integrated Si-bipolar transistors.  $F_{pmax}$  is defined as the frequency, where the ratio of power transferred between the identical transistor amplifiers goes to unity. This  $F_{pmax}$  does not suffer from the limitations mentioned in the case of  $f_t$  and  $f_{max}$ . The circuit designers can estimate the actual bandwidths of MESFETs/HEMTs or HBTs for the design of MICs, based on a small signal model of the devices, by means of  $F_{pmax}$ .

In this paper, based on the concept proposed by Taylor for integrated Si-bipolar transistors, the maximum frequency  $F_{pmax}$  for unity power transfer ratio of a transistor amplifier based on GaAs MESFETs/HEMTs, which is preceded and followed by identical amplifiers, has been determined. An analytical expression for calculating  $F_{pmax}$  of GaAs MESFET/HEMT has been derived based on small signal equivalent circuit of MESFET/HEMT. The impact of different circuit elements of MESFETs/HEMTs on  $F_{pmax}$  has been investigated and clarified. The numerical results are shown and discussed. The parameters which have strong influence on  $F_{pmax}$  are pointed out. The comparison between  $F_{pmax}$ ,  $f_t$  and  $f_{max}$  is made and significant differences between these figures of merit have been observed.

## ON PERFORMANCE ANALYSIS OF SUBCARRIER MULTIPLEXED LIGHTWAVE SYSTEMS

**T. Mallikarjun**

**Department of Electrical Engineering  
Queen's University at Kingston  
Kingston, Ontario, CANADA K7L 3N6.  
e-mail: mallik@qucdnee.bitnet**

This paper attempts to provide design principles which identify quantitative limits to sub-carrier multiplexed (SCM) broadcast network performance and in some cases indicate optimum performance criteria. Three main areas are being investigated. First, the influence of various noise impairments on subscriber carrier-to-noise ratio (CNR) is assessed. These noise impairments include a) laser overall non-linearity b) laser related noises, such as laser relative intensity noise (RIN), mode partition noise, modal and chirp induced noises, and c) receiver noise. Second, the issue of receiver design is being studied. This includes, receiver front-ends with PIN-APD followed by GaAs MESFETs/HEMTs, HBTs in tuned and untuned configurations. This paper also presents complementary studies for increasing the power budget and distribution capacity of SCM networks, through enhanced receiver sensitivity by using resonant receivers. Receiver sensitivity using the FM and QAM modulation formats is analyzed for realistic values of receiver thermal noise, RIN and non-linear distortions. Finally, use of multilevel QAM to SCM-IM/DD system is studied. The effect of coding to increase the channel capacity in QAM-SCM-IM/DD system has been investigated.

The limitations due to second order and third order intermodulation products (IMPs), and clipping effects on RIN limited SCM lightwave system performance has been examined. The penalty incurred by the use of multiple sub-carriers is being studied. The optimum operating condition for any SCM system constrained by non-linearity is a balance between distortion and noise. Increasing the modulation depth provides greater signal power to overcome noise, but increases the magnitude of the distortion products generated. This trade-off has been investigated for system optimization.

## WAVEGUIDES I

Chairs: L. Shafai, University of Manitoba; J.M. Besieris, Virginia Polytechnic University

Room: Michigan League, Henderson Room

Time: 1:30-5:30

|      |  |     |
|------|--|-----|
| 1:30 | ON THE TANGENTIAL MAGNETIC FIELD IN AN APERTURE IN A CYLINDRICAL WAVEGUIDE OR CYLINDRICAL CAVITY WHERE THE TANGENTIAL ELECTRIC FIELD IS GIVEN<br><i>Joseph R. Mautz*, Roger F. Harrington, Syracuse University</i>       | 290 |
| 1:50 | A NUMERICAL TECHNIQUE FOR THE ANALYSIS OF MODAL PROPAGATION IN CURVED WAVEGUIDES<br><i>Michael Kaye, Daniel D. Reuter*, Gary A. Thiele, The University of Dayton</i>   | 291 |
| 2:10 | WAVEGUIDE MODE SOLUTION USING HYBRID EDGE ELEMENTS AND INTEGRAL FORMULATION<br><i>Gregory M. Wilkins, Madhavan Swaminathan, IBM Corporation; Jin-Fa Lee, Worcester Polytechnic Institute</i>                             | 292 |
| 2:30 | EDGE ELEMENT ANALYSIS OF DIELECTRIC-LOADED WAVEGUIDES<br><i>Zeng Ying*, P. Luypaert, ESAT Laboratory</i>   | 293 |
| 2:50 | CONCEPTUALIZATION OF THE CONTINUOUS SPECTRUM AND LEAKY-WAVE MODES OF INTEGRATED DIELECTRIC WAVEGUIDES<br><i>Jerry M. Grimm*, Center for Naval Analyses; Dennis P. Nyquist, Byron Drachman, Michigan State University</i> | 294 |
| 3:10 | BREAK  |     |
| 3:30 | TE AND TM WAVES IN THE NONLINEAR SLAB WAVEGUIDES<br><i>Mitsuhiro Yokota, Kyushu University</i>   | 295 |
| 3:50 | COMPUTER AIDED DESIGN OF DIELECTRIC WAVEGUIDE CIRCULAR BEND OF FINITE LENGTH<br><i>Kazuo Tanaka, Masahiro Tanaka, Hisamitsu Tashima, Akinao Takagi, Gifu University</i>  | 296 |
| 4:10 | NUMERICAL EVALUATION OF THE PERFORMANCE OF A TM01 CIRCULAR TO TE10 RECTANGULAR WAVEGUIDE MODE CONVERTER<br><i>Roger F. Harrington*, Joseph R. Mautz, Syracuse University</i>   | 297 |
| 4:30 | RIGOROUS ANALYSIS OF POSTS IN RECTANGULAR AND CIRCULAR WAVEGUIDES<br><i>J.M. Garai*, J. Zapata, Universidad Politécnica de Madrid</i>  | 298 |
| 4:50 | USE OF A BEND WAVEGUIDE TO CONSTRUCT KA BAND-PASS FILTERS<br><i>H. Tertuliano, P. Jarry, L.A. Bermudez, Université de Bordeaux</i>   | 299 |
| 5:10 | ANALYSIS OF COPLANAR WAVEGUIDE LOADED INSET DIELECTRIC GUIDE BY THE EXTENDED TRANSVERSE RESONANCE DIFFRACTION METHOD<br><i>Z. Fan*, S.R. Pennock, University of Bath</i>   | 300 |

ON THE TANGENTIAL MAGNETIC FIELD IN AN  
APERTURE IN A CYLINDRICAL WAVEGUIDE OR  
CYLINDRICAL CAVITY WHERE THE TANGENTIAL  
ELECTRIC FIELD IS GIVEN

Joseph R. Mautz\* and Roger F. Harrington  
Department of Electrical and Computer Engineering  
Syracuse University, Syracuse, NY 13244-1240

Solution of electromagnetic field problems involving waveguides and/or cavities requires knowledge of the tangential magnetic field on the wall of the waveguide or cavity when a magnetic current expansion function is placed on the inside surface of the wall. This tangential magnetic field is usually extracted from the electromagnetic field obtained by using the series expansion of the dyadic Green's function (Robert E. Collin, Field Theory of Guided Waves, IEEE Press, 1991). The series expansion for the tangential magnetic field thus obtained is accompanied by a discontinuous series expansion for the tangential electric field, one that jumps from  $M \times n$  near the wall to zero on the wall ( $M$  is the magnetic current and  $n$  is the exterior unit normal vector).

The above-mentioned discontinuity of the accompanying series for the electric field can be eliminated by replacing the magnetic current source  $M$  by the boundary condition that the tangential component of the electric field be  $M \times n$  on the wall of the waveguide or cavity. With this replacement, the electric field in a cavity can be expanded as a series of vector functions, each of which satisfies the Helmholtz equation and has a tangential component that reduces to  $M \times n$  on the wall. However, for a waveguide where  $M$  is confined between  $z = 0$  and  $z = d$ , this replacement leads not to a series expansion of the field but to a continuous spectrum in  $z$  where  $z$  is the axial coordinate. Fortunately, this continuous spectrum has an equivalent series which can be found by proceeding as follows: The dyadic Green's function is used to obtain a series expansion for the field everywhere in the waveguide. The tangential magnetic field at the magnetic current is extracted from the sum of two source-free fields in the section of waveguide between  $z = 0$  and  $z = d$ : the electromagnetic field whose electric field is  $M \times n$  on the lateral wall and zero on the end faces at  $z = 0$  and  $z = d$  and the electromagnetic field whose tangential electric field is zero on the lateral wall and is that given by the previously obtained series expansion at  $z = 0$  and  $z = d$ .

Series expansions are obtained for the tangential magnetic field at the magnetic current  $M = u_\phi \cos(\pi z/d) + u_z \sin(\pi z/d)$  on the lateral wall of the circular box whose end faces are at  $z = 0$  and  $z = d$ . The rate of convergence of the series expansion obtained by using the method described in the previous paragraph is compared with that of the series expansion obtained by using the dyadic Green's function.

## A NUMERICAL TECHNIQUE FOR THE ANALYSIS OF MODAL PROPAGATION IN CURVED WAVEGUIDES

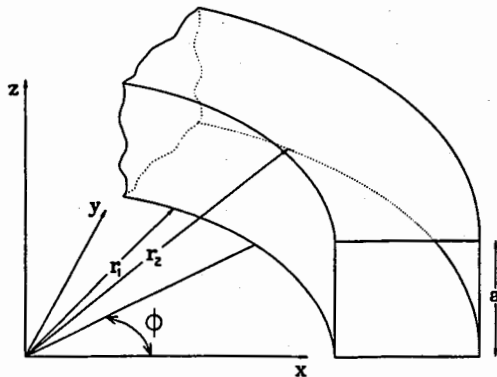
Michael Kaye, Daniel D. Reuster\* and Gary A. Thiele  
 Department of Electrical Engineering  
 The University of Dayton  
 Dayton, OH 45409-0226

The analysis of modal propagation in straight waveguides is well understood and can be found in most textbooks on electromagnetics. Modal propagation in curved waveguides is more difficult to analyze and although the subject has received fairly extensive attention in the literature, the computation of the admissible angular propagation constants ( $\nu$ ) is still considered a complex procedure. The difficulty in computation arises from the fact that the propagation constants are, in general, non-integer in nature and are computed from a transcendental equation involving Bessel functions:

$$Y_\nu(k_x r_1) J_\nu(k_x r_2) - Y_\nu(k_x r_2) J_\nu(k_x r_1) = 0 \quad (LM \text{ modes})$$

$$Y'_\nu(k_x r_1) J'_\nu(k_x r_2) - Y'_\nu(k_x r_2) J'_\nu(k_x r_1) = 0 \quad (LE \text{ modes})$$

This paper presents a generalized numerical technique for determining the admissible propagation constants for modes present in curved waveguides. The method proposed bypasses the necessity of computing the Bessel functions. The technique is based upon expanding the unknown radial functions in a series of Chebyshev polynomials and using the method of collocation to obtain a well conditioned system of linear homogeneous equations, transcendental in ( $\nu$ ), which incorporates the boundary conditions. The admissible values of ( $\nu$ ) are then found by applying a bracketing and bisection technique to the determinant of the system of equations. The algorithm requires only the computation of the sign of the determinant of the system; and hence, common numerical problems, associated with determinant computation, are avoided.



Wed. p.m.

## Waveguide Mode Solution using Hybrid Edge Elements and Integral Formulation

Gregory M. Wilkins\*  
Madhavan Swaminathan\*  
Jin-Fa Lee\$

\* IBM Technology Products  
E.Fishkill, NY 12533

\$ Worcester Polytechnic Institute  
Worcester, MA

Knowledge of existing modes of operation is essential in the complete analysis of waveguide field behavior. This is particularly important when enforcing absorbing boundary conditions at waveguide ports. Closed-form solutions are readily obtainable for homogeneously-filled waveguides which are uniform along the longitudinal axis and which have rectangular or circular cross sections. However, difficulties arise when the cross sections are irregular and/or inhomogeneous. A common problem is the generation of spurious modes due to the inability to satisfy the Dirichlet boundary condition at the perfect electric conductor boundaries and dielectric interfaces. Techniques have been implemented for isolating the spurious modes [1]–[2] but they nonetheless exist. An approach which totally eliminates the spurious modes is the use of hybrid edge elements. This approach allows us to model a three-dimensional field quantity over a two-dimensional boundary, namely the waveguide cross section. The electric field is decomposed into its transverse and longitudinal components which are modeled in terms of two-dimensional edge elements and scalar nodal elements, respectively. Another approach, the method of moments, serves as an excellent means of verifying the results obtained through use of hybrid edge elements. A comparison of these techniques is presented along with the associated field plots for several geometries.

### References:

- [1] A.J.Kobelansky and J.P.Webb, "Eliminating Spurious Modes in Finite-Element Waveguide Problems by using Divergence-Free Fields", *Electronics Letters*, May '86, Vol. 22, No. 11.
- [2] Kazuya Hayata et al, "Vectorial Finite-Element Method without any Spurious Solutions for Dielectric Waveguiding Problems using Transverse Magnetic-Field Component", *IEEE Transactions on Microwave Theory and Techniques*, Nov '86, Vol. 34, No. 11.
- [3] M. Swaminathan et al, "Computation of TM and TE Modes in Waveguides Based on a Surface Integral Formulation", *IEEE Transactions on Microwave Theory and Techniques*, Feb '92, Vol. 40, No. 2.

## EDGE ELEMENT ANALYSIS OF DIELECTRIC-LOADED WAVEGUIDES

Zeng Ying\*, P. Luypaert

K. U. Leuven - ESAT

Kardinaal Mercierlaan 94, B-3001 Heverlee, Belgium  
Tel:32.16.220931.ext 1070 email:zeng@esat.kuleuven.ac.be

### abstract

*This paper presents a efficient application of finite-element analysis of dielectric-loaded waveguide. An emphasis attention is paid to study the problem of spurious modes.*

*For the conventional finite element analysis of dielectric-loaded waveguides, the magnetic fields are approximated by interpolation from nodal values, considering a vector as a triplet of scalar fields. By setting the common nodal values in adjacent elements to be identical, all of three components between elements are imposed to be continuous. That is surely not the nature of electric and magnetic field, which have particular properties: tangential continuity across all surfaces, as its normal component may have a discontinuity across a material interface. So the spurious modes were still appearance, even several different vector variational expressions are tried. The special triangular edge-elements, which were a approach solution suggested by Fumio Kikuchi for mixed finite model, were tried to be employed to eliminate the spurious modes. The tangential components of magnetic fields are interpolated by the unknown field values along each edge of element with a two-component vector shape function  $u_h = \{u_x \ u_y\}^T$ . The coefficients in the shape function, which depend upon the geometrical parameters of the elements, can be determined by the following conditions: (1) The tangential component of  $u_h$  is constant on each side of triangles; (2)  $\nabla \cdot u_h = 0$  on the triangular element. Moreover, we should point out that the tangential component of  $u_h$  is zero on the boundaries and continuous along the interelement boundaries. And it can be proved that  $\nabla \times u_h$  is constant in each triangle. On the other hand, the z-component of the magnetic field is modeled by the normal Lagrange interpolation.*

*The finite element discretization for those special elements are derived for established an eigenvalue equation, and adapted to a final eigenvalue equation in terms of the transverse magnetic fields and the propagation constant itself. A scientific program based on this method for the rectangular dielectric-loaded waveguide is developing by using the software MATLAB. Several cases of the rectangular dielectric-loaded waveguide are investigated. The solution can be presented at the conference.*

## CONCEPTUALIZATION OF THE CONTINUOUS SPECTRUM AND LEAKY-WAVE MODES OF INTEGRATED DIELECTRIC WAVEGUIDES

Jerry M. Grimm\*  
Center for Naval Analyses  
Alexandria, VA 22302

Dennis P. Nyquist  
Department of Electrical Engineering  
Michigan State University  
E. Lansing, MI 48824

Byron Drachman  
Department of Mathematics  
Michigan State University  
E. Lansing, MI 48824

Integrated dielectric waveguides (IDWGs) possess both bound, propagating modes and a continuous distribution of radiation modes (the continuous spectrum). While the bound modes are relatively well-understood, the continuous spectrum has not been investigated, save for the simplest of configurations. We present a method by which to characterize the continuous radiation spectrum for practical, IDWGs of finite cross-section or integrated within a planarly layered background structure.

The electric field of an IDWG is described by the well-known axial transform domain electric field integral equation

$$\bar{\mathbf{e}}(\bar{p}, \zeta) - \int_{CS} \frac{\delta n^2(\bar{p}')}{{n_c}^2} \bar{\mathbf{g}}^0(\bar{p} | \bar{p}', \zeta) \cdot \bar{\mathbf{e}}(\bar{p}', \zeta) d\bar{s}' = \bar{\mathbf{e}}^i(\bar{p}, \zeta) \quad \forall \bar{p} \in CS \quad (1)$$

In this EFIE,  $\zeta$  is the complex-valued axial (or propagation) wavenumber,  $\bar{\mathbf{g}}^0$  is the electric-field dyadic Green's function for tri-layered background media,  $\bar{\mathbf{e}}(\bar{p}, \zeta)$  is the electric field supported by the waveguide of finite cross-section  $CS$ ,  $\bar{\mathbf{e}}^i(\bar{p}, \zeta)$  is the electric field impressed upon the waveguide, and  $\delta n^2(\bar{p})$  is the contrast between the waveguiding region and the cover region. The scalar components of the electric-field dyadic Green's function are, as with all exact formulations for layered media, Sommerfeld integrals upon *transverse* spectral frequency  $\zeta$ .

The spatial fields are recovered by an inverse Fourier transform on the *axial* wavenumber  $\zeta$ . This complex-valued wavenumber requires that branch cuts in the axial transform domain (complex  $\zeta$ -plane) be defined to maintain a single-valued integrand and restrict the inversion contour to the top (spectral) Riemann sheet. These needed axial transform plane branch cuts are chosen to restrict the migration of singularities in the Green's function integrands, guaranteeing the existence of those integrals.

These axial transform-domain branch cuts define a multi-sheeted Riemann surface in the complex  $\zeta$ -plane and play an important role in the characterization of radiation loss effects. The continuous radiation spectrum is identified by a singularity expansion upon the axial transform domain singularities, and is associated with the branch cuts. A radiation mode is a solution to the forced EFIE for  $\zeta$  restricted to a deformation about the branch cut. Also, the branch cuts separate the spectral top Riemann sheet from other non-spectral sheets. Leaky waves for IDWGs are identified by solving the homogeneous EFIE for axial wavenumbers on non-spectral sheets. In this case, the Green's function singularities migrate and necessitate a deformation of the integration path. The method presented here is then applied to the integrated dielectric rib waveguide, and various types of its leaky wave modes are quantified.

## TE AND TM WAVES IN THE NONLINEAR SLAB WAVEGUIDES

Mitsuhiro Yokota  
Department of Computer Science  
and Communication Engineering,  
Kyushu University 36, Fukuoka 812, Japan

In the linear system, TE and TM waves can be analyzed separately because the superposition is satisfied. However in the nonlinear system, the superposition is not satisfied as is well known. So, it is important to examine the electromagnetic waves in the nonlinear slab waveguides where TE and TM waves exist simultaneously. Here, we investigate the guided TE and TM waves in the slab waveguide with a weakly nonlinear film by using the singular perturbation technique with multiple space scales theoretically. Consider the symmetric slab waveguide which consists of a thin, optically nonlinear, dielectric film bounded by semi-infinite linear dielectrics. The optically nonlinearity is assumed to be of the Kerr type self-focusing, isotropic and electrostriction.

In order to apply the perturbation technique, we first introduce the perturbation parameter concerned with the nonlinear coefficient and the multiple space scales in the propagation direction. Then, the electromagnetic field components are expanded by using the perturbation parameter. Substituting the expansion of the field and the multiple space scales into the Maxwell's equation and equating coefficients to equal powers of the perturbation parameter to zero, we can get the governing equations to each order of the perturbation. The analytical solutions of these equations to satisfy the boundary conditions are derived. From the solvability conditions to have nontrivial solutions for each perturbation solutions, it can be shown analytically that the effective index for the nonlinear waves changes corresponding to the incident power of TE and TM waves.

As a numerical example, the effective index for the nonlinear waves are examined. It is found that the effective index changes proportional to the zero-order power given at the initial plane. And it is shown that the effective index of the nonlinear TE and TM waves are different with that of only TE wave or only TM wave. The results presented here give the correct solutions in the limit of weak nonlinearity because the wave equations and the boundary conditions satisfy exactly.

## Computer Aided Design of Dielectric Waveguide Circular Bend of Finite Length

Kazuo TANAKA, Masahiro TANAKA, Hisamitsu TASHIMA and Akinao TAKAGI

Department of Electronics and Computer Engineering,

Gifu University

Gifu City, Yanagido 1-1, Japan 501-11

In this paper, we present the computer-aided design (CAD) of asymmetric dielectric waveguide circular bend of finite length. In the analysis, new integral equation method, which is called guided-mode extracted integral equation method, is used. It is shown that numerical results satisfy the energy conservation law within an accuracy of 1%.

The the problem considered in this paper can be stated as follows: The dielectric slab waveguide 1 of width  $2a_1$  and waveguide 2 of width  $2a_2$  ( $a_1=a_2$ ), are joined together throuth a circular bend of finite length. It is assumed that both dielectric waveguides satisfy the single-mode condition and that a TE or TM dominant-mode is incident from waveguide 2 to the circular bend.

We consider that the field  $\psi^C$  which presents the difference between total field and transmitted wave in the waveguide 1, and the difference between total field and incident+reflected waves in the waveguide 2. Field  $\psi^C$  represents the total field in the circular bend section for convenience of notation. If we adopt the condition that the radiation filed cannot exist at points far away from the circular bend in the dielectric waveguides, we can derive the boundary integral equations for the field  $\psi^C$  which can be called guided-mode extracted integral equations (GMEIE's)(K. Tanaka & M. Kojima, J. Opt. Soc. Am. A **6**, 667-974, 1989).

Since the fields  $\psi^C$  in the both waveguides will vanish at points far away from the bend section, we can regard the propagation characteristics in the circular bend of finite length as the scattering problem by the isolated finite-sized dielectric object. The structure of GMEIE's is identical to that of conventional integral equations. So, GMEIE's can be solved by the conventional moment-method or boundary-element method by applying boundary conditions.

The propagation characteristics of circular-bend of finite length of asymmetric optical thin-film waveguide i.e., the dependences of power transmission coefficient  $\Gamma_T$ , normalized scattering power  $\Gamma_S$  and their total  $\Gamma_{TOTAL} = \Gamma_T + \Gamma_R + \Gamma_S$  on the curvature-radius of the bend, are evaluated. It is found that all results of  $\Gamma_{TOTAL}$  satisfied energy-conservation law within an accuracy of 1%.

The basic idea used in GMEIE's is very general. Hence, the theory is applicable to the more complicated waveguide discontinuity problems such as dielectric waveguide branches. The theory is also applicable to problems of other fields such as acoustic and elastic waves.

**NUMERICAL EVALUATION OF THE PERFORMANCE OF A  
TM<sub>01</sub> CIRCULAR TO TE<sub>10</sub> RECTANGULAR WAVEGUIDE  
MODE CONVERTER**

Roger F. Harrington\* and Joseph R. Mautz

Department of Electrical and Computer Engineering  
Syracuse University, Syracuse, NY 13244-1240

Consider the waveguide mode converter that consists of a circular waveguide with two symmetrically placed apertures backed by rectangular waveguides. Both rectangular waveguides run along the  $x$ -axis, which is perpendicular to the  $z$ -axis of the circular waveguide. The rectangular waveguides, whose smaller dimension is in  $z$ , are identical but can be terminated with different loads. The circular waveguide is shorted at one end. A wave of the TM<sub>01</sub> mode comes from the other end. Some TM<sub>01</sub> power is reflected in the circular waveguide. The rest of it is converted into TE<sub>10</sub> power in the rectangular waveguides. By assumption, only the nonexcited TE<sub>11</sub> mode and the excited TM<sub>01</sub> mode can propagate in the circular waveguide, and only the TE<sub>10</sub> mode can propagate in the rectangular waveguides.

The power transmitted into the rectangular waveguides is calculated by using the method of moments to solve the integral equations obtained from application of the equivalence principle. Each aperture is closed with an infinitely thin perfectly conducting plate, a magnetic current is placed on the side of the plate facing the rectangular waveguide, and the negative of this magnetic current is placed on the other side. Integral equations for the magnetic currents are obtained by not allowing any net electric current to flow on the plates. The magnetic current on the rectangular waveguide side of each curved plate is approximated by a linear combination of the magnetic currents which, placed on a flat plate that resembles the curved one as much as possible, launch a finite number of rectangular waveguide modes. The magnetic current on the circular waveguide side of the plate is approximated by a magnetic current that is as much as possible like the negative of this linear combination. The electric current induced by the magnetic current on the rectangular waveguide side of a plate is obtainable in terms of the coefficients in the expansion of this magnetic current. The electric current induced by the magnetic current on the circular waveguide side of one of the plates is obtained by using the dyadic Green's function (C. T. Tai, Proc. IEEE, **61**, 480-481, 1973) to express the magnetic field of this magnetic current.

A computer program was written to calculate the power transmitted into the rectangular waveguides. Some numerical results obtained by means of this program are shown.

## RIGOROUS ANALYSIS OF POSTS IN RECTANGULAR AND CIRCULAR WAVEGUIDES

J. M. Garai\*, J. Zapata

Grupo de Electromagnetismo Aplicado y Microondas  
Ciudad Universitaria, E.T.S.I. Telecommunicación, U.P.M.  
28040 Madrid Spain

Posts inside waveguides play an important role in developing a great number of microwave circuits like filters, polarizers, etc.

Posts in rectangular waveguide have been broadly studied by different methods in order to obtain equivalent suitable circuits that were appropriate for CAD. However, for the case of cylindrical post inside circular waveguide, a few references are found in the literature.

In our study, cylindrical posts have been modelled like posts with square cross section. This makes possible to apply Mode-Matching Technique in the analysis.

As the waveguide cross section is circular or square in shape, analytic modes are utilized in those parts of the circuit, but when the cross section of the structure made difficult or impossible to obtain analytic modes, as it happens in the sections that contains the metallic posts, a numerical technique (Finite Element) has been employed (J. Zapata et al., URSI SYM 1991 London, Canada, p.146)

Two examples have been analyzed. The first one is an square waveguide with posts in the center of the four walls and all of them located in the same cross section (fig.1). Different depths of the posts have been simulated. The second one is a post inside a circular waveguide (fig.2). In this case the maximum of  $TE_{11}$  electric field is in the same plane of the post.

In both cases numerical results show very good agreement with the measurements or data in the literature. Convergence studies, in order to obtain the adequate mode-relation in both sides of each discontinuity, have been accomplished.

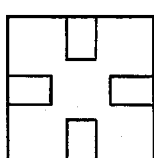


fig. 1

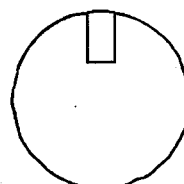


fig. 2

# USE OF A BEND WAVEGUIDE TO CONSTRUCT Ka BAND-PASS FILTERS

H. TERTULIANO, P. JARRY, L.A. BERMUDEZ

Université de Bordeaux I - Laboratoire de Télécommunications - E.N.S.E.R.B  
34, Chemin de Pomerol 82-B 33000 BORDEAUX - FRANCE

## SUMMARY

We present here the results of a precise numerical computations and an analytical investigation of a band-pass filter constituted of two rectangular guides binded with them by a bend waveguide. Dielectrics resonators are used to change the electromagnetic champ distribution.

We devide the structure into waveguide discontinuities and sections (Fig.1). From Maxwell's equations, we demonstrate that two scalaires fonctions  $E_{z1}$  and  $H_{z1}$  are simultaneously solutions of the Helmholtz equation and take into account the boundary and limit conditions, we found the matrix [S] associated with each section. The discontinuity between the rectangular guides are characterized by the modal analysis method. The same procedure is used in order to characterize the bend waveguide. The junction between a straight and a curved guide is make connecting incident and reflected waves. After considering the concept of characteristic impedance and the wave and voltage-current formalisms, we can deduce for each basic element of the structure an elementary corresponding network (Fig.2). By using the equivalence properties between the quadripoles, we can transform the initial network of the structure into the one show in Fig.3. The results obtained for a 4 poles evanescent curved filter with bandpass 14-14.5GHz and a radii of 13.6mm are choosen in Fig.4. All peaks which characterize the Chebyshev response can be remarqued and when taking into account the nature of the distributed elements we can explain the variation of ondulation in the band for  $S_{11}$ .

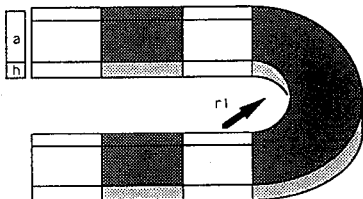


Fig. 1

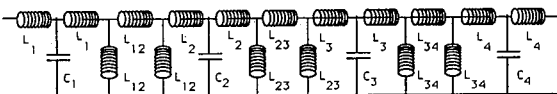


Fig. 2

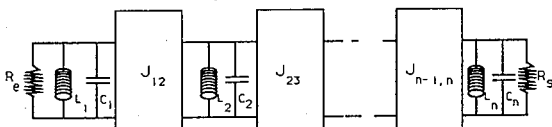


Fig. 3

Bandpass of the filter: 14 - 14.6 GHz

Number of pole: 4

Minimal frequency: 14 GHz

Maximal frequency: 14.6 GHz

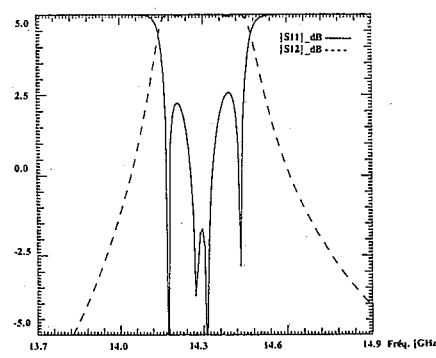
Undulation in the band: 0.01 dB

Width: 12 mm

Height: 6 mm

Curvature ray: 38.1 mm

| 1st element: | length: | 3 mm | permittivity: 2.5 |
|--------------|---------|------|-------------------|
| 2nd element: |         | 5 mm | 1.0               |
| 3rd element: |         | 5 mm | 2.5               |
| 4th element: |         | 5 mm | 1.0               |
| 5th element: |         | 3 mm | 2.5               |



299

## ANALYSIS OF COPLANAR WAVEGUIDE LOADED INSET DIELECTRIC GUIDE BY THE EXTENDED TRANSVERSE RESONANCE DIFFRACTION METHOD

Z. Fan\* and S.R. Pennock

School of Electronic and Electrical Engineering  
University of Bath, Bath BA2 7AY, U. K.

A new quasic-planar structure, coplanar waveguide loaded inset dielectric guide (CPWLIDG) is proposed as a quasic-TEM transmission line appropriate for microwave and millimeter wave integrated circuit applications. This structure is derived by placing a coplanar waveguide on the air dielectric interface of an inset dielectric guide, retaining many advantages of coplanar waveguide. The configuration offers several advantages over coplanar waveguide: excellent confinement of the electromagnetic field, lower radiation loss from discontinuities, two additional flexibilities in obtaining a wide range of characteristic parameters and no excitation of the surface waves which often affect the performance of coplanar waveguide.

The transverse resonance diffraction method is extended to analyze CPWLIDG with a two-layer dielectric substrate or with a two-layer ferrite-dielectric substrate. In the extended method, electromagnetic fields in the groove and air regions are expressed in terms of discrete and continuous Fourier transforms, respectively and related to the aperture electric field at the upper interface by applying the boundary conditions across the lower interface. By enforcing the continuity of the magnetic field at the aperture surface, integral equations for the aperture electric field are obtained. By employing Galerkin's procedure, the determinantal equation for the propagation constants of odd and even modes is derived. In addition, characteristic impedances are calculated based on the voltage-power definition. Convergence and numerical efficiency of the analysis are demonstrated to be very good.

Numerical results for CPWLIDG with a dielectric substrate are obtained for various values of structural and material parameters. The effects of uniaxial dielectric anisotropy on the propagation characteristics are illustrated and found to increase with increasing frequency. The results for CPWLIDG with a one-layer isotropic dielectric substrate are compared with measured data and a good agreement between theory and experiment is found. Numerical results for nonreciprocal propagation characteristics of CPWLIDG with a two-layer ferrite-dielectric substrate are also obtained for various values of the thickness of a ferrite layer and the permittivity of a dielectric layer. It is found that the nonreciprocity increases with the increase in the thickness of the ferrite layer and the permittivity of the dielectric layer. It is shown from the numerical results that the two-layer ferrite-loaded CPWLIDG exhibits adequate nonreciprocal characteristics in order to realize efficient nonreciprocal devices.

**SPECIAL SESSION AP-S/URSI B-18****WEDNESDAY PM****W.V.T. RUSCH REFLECTOR ANTENNA MEMORIAL SESSION**

Chairs: A. Prata, University of Southern California  
Y. Rahmat-Samii, University of California at Los Angeles

Room: Alumni Center, Room 1      Time: 1:30-4:30

|      |   |      |
|------|---|------|
| 1:30 | A TRIBUTE TO PROFESSOR WILLARD VAN TUYL RUSCH<br><i>Aluizio Prata, Jr.*, Hans H. Kuehl, University of Southern California</i>   | AP-S |
| 1:50 | NOVEL SUPERQUADRIC APERTURE BOUNDARIES FOR REFLECTOR<br>ANTENNAS<br><i>Yahya Rahmat-Samii*, Dah-Wei Duan, University of California at Los Angeles</i>   | AP-S |
| 2:10 | RADIATION FROM A REFLECTOR IN THE NEAR FIELD OF A CIRCULAR<br>APERTURE<br><i>D.C. Jenn*, Naval Postgraduate School; R.J. Pogorzelski, General Research<br/>Corporation</i>  | AP-S |
| 2:30 | SEMI-ACTIVE REFLECTOR ANTENNAS<br><i>Antoine G. Roederer, ESA-ESTEC</i>   | AP-S |
| 2:50 | ADAPTIVE NULLING IN HYBRID ANTENNAS<br><i>Robert Shore, Rome Laboratory, Hanscom AFB</i>  | AP-S |
| 3:10 | BREAK   |      |
| 3:30 | SUBREFLECTOR AND FEED SCATTERING IN DUAL-SHAPED REFLECTOR<br>SINGLE CHAMBER COMPACT RANGES<br><i>Victor Galindo-Israel, William Imbriale, Jet Propulsion Laboratory; Raj Mittra,<br/>University of Illinois</i>                     | AP-S |
| 3:50 | APPLICATION OF INCREMENTAL LENGTH DIFFRACTION COEFFICIENTS<br>TO CALCULATE THE PATTERN EFFECTS OF THE RIM AND SURFACE<br>CRACKS OF A REFLECTOR ANTENNA<br><i>Robert A. Shore, Arthur D. Yaghjian*, Rome Laboratory, Hanscom AFB</i> | AP-S |
| 4:10 | MULTIPLE CONTOURED BEAM REFLECTOR ANTENNA SYSTEMS<br><i>P. Balling*, Antenna System Consultant; K. Tjønneland, L. Yi, INTELSAT; A.<br/>Lindley, EUTELSAT</i>  | AP-S |



**SESSION URSI B-19****WEDNESDAY PM****MEDIA MODELING**

Chairs: Y. Kuga, University of Washington; B.E. Gilchrist, University of Michigan

Room: Alumni Center, Room 2      Time: 1:30-5:30

|      |   |     |
|------|---|-----|
| 1:30 | ELECTROMAGNETIC PROPERTIES AND MODELING OF THE NON-LOCAL $\Omega$ MEDIUM<br><i>Mamdouh M.I. Saadoun, Nader Engheta, University of Pennsylvania</i>  | 304 |
| 1:50 | REFLECTION AND SHIELDING CHARACTERISTICS OF THE LAYERED LOSSY NON-LOCAL $\Omega$ MEDIUM<br><i>Mamdouh M.I. Saadoun, Nader Engheta, University of Pennsylvania</i>   | 305 |
| 2:10 | CALCULATION OF THE EFFECTIVE PERMITTIVITY OF A RANDOM COLLECTION OF DIELECTRIC CYLINDERS<br><i>M. Moghaddam*, Jet Propulsion Laboratory; B. Houshmand, University of California at Los Angeles</i>                      | 306 |
| 2:30 | SYMMETRY ANALYSIS OF LARGE TWO-DIMENSIONAL CLUSTERS OF COUPLED CAVITY RESONATORS<br><i>Ross A. Speciale, Hughes Missile System Company</i>  | 307 |
| 2:50 | INTEGRAL EQUATION ANALYSIS OF ARTIFICIAL MEDIA<br><i>E.H. Newman*, M.E. Peters, The Ohio State University</i>   | 308 |
| 3:10 | BREAK   |     |
| 3:30 | A PROCEDURE FOR DEVELOPING COMPACT MODELS OF MATERIALS FOR NUMERICAL ELECTROMAGNETICS<br><i>Nicolaos G. Alexopoulos, University of California, Los Angeles; Rodolfo E. Diaz, Hexcel APD</i>                             | 309 |
| 3:50 | PROPAGATION CONSTANT OF COHERENT MICROWAVES IN A DENSE DISTRIBUTION OF NONTENUES SPHERES<br><i>Daniel J. Rice, Yasuo Kuga, Akira Ishimaru, University of Washington</i>   | 310 |
| 4:10 | EFFECT OF INCLUSION GEOMETRY, SIZE, CONCENTRATION AND ORIENTATION ON THE EFFECTIVE PROPERTIES OF DISCRETE RANDOM MEDIA<br><i>Vasundara V. Varadan*, Yushieh Ma, Vijay K. Varadan, The Pennsylvania State University</i> | 311 |
| 4:30 | DISPERSION PROPERTIES OF BULK ANISOTROPIC DIELECTRIC MEDIA<br><i>E.A. Skirta*, N.A. Khizhniak, IRESTE</i>   | 312 |
| 4:50 | ANALYSIS OF FERRITE LOADED STRUCTURES WITH FINITE DIFFERENCE TIME DOMAIN TECHNIQUE<br><i>M. Okoniewski, University of Victoria</i>  | 313 |
| 5:10 | DIFFRACTION BY TWO-DIMENSIONAL CANTOR APERTURES<br><i>D.L. Jaggard, T. Speilman, M. Dempsey, University of Pennsylvania</i>   | 314 |

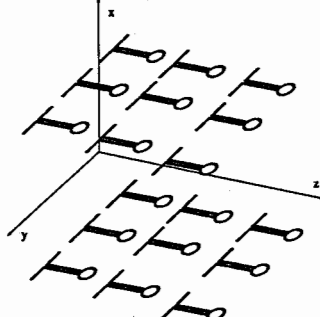
## ELECTROMAGNETIC PROPERTIES AND MODELING OF THE *NON-LOCAL* $\Omega$ MEDIUM

Mamdouh M. I. Saadoun and Nader Engheta

Moore School of Electrical Engineering  
University of Pennsylvania  
Philadelphia, Pennsylvania 19104

The idea of  $\Omega$  medium, which is a subset of the class of bianisotropic media, was recently introduced and some of its electromagnetic properties and potential applications were discussed [M. M. I. Saadoun and N. Engheta, A Reciprocal Phase Shifter Using Novel Pseudochiral or  $\Omega$  Medium, *Microwave and Optical Technology Letters*, 5, 184-188, 1992; M. M. I. Saadoun and N. Engheta, Novel Pseudochiral or  $\Omega$  medium and Its Applications, *Proc. of the 1991 Progress in Electromagnetic Research Symposium*, p. 339, 1991]. It was suggested that this medium could be composed by embedding planar conducting (or dielectric)  $\Omega$ -shaped microstructures in a simple host medium. The loop portion of the  $\Omega$ -shaped elements is in the same plane as its stems. The orientation of these seeding inclusions is not random and can be along a preferred direction.

Recently in our theoretical analysis, we have generalized and extended the idea of  $\Omega$  medium further to the *non-local*  $\Omega$  medium wherein the  $\Omega$ -shaped microstructures are assumed to be "stretched". More explicitly, the loop portion and the stems of each element are separated and connected via parallel wires (See Figure below). A non-local  $\Omega$  medium can, in principle, be constructed by spreading a large number of these non-local  $\Omega$  elements in an otherwise simple host dielectric as sketched in Figure below. The non-local  $\Omega$  elements must have a fixed orientation throughout the medium. In such a medium shown below, due to the shape of the stretched  $\Omega$  elements, the y-component of  $\mathbf{E}$  field at any point is coupled to the x-component of  $\mathbf{B}$  at another point. This "non-local" coupling introduces some interesting electromagnetic properties for this medium. In this talk, we will present some of the electromagnetic properties such as constitutive relations, wave equations, and dispersion relations of this medium. Plane waves and eigenmodes of propagation will also be discussed, and physical insights into analytical results along with some potential applications of this medium will be given.



The non-local  $\Omega$  medium can be thought of as an artificial dielectric wherein a large number of "non-local" or "stretched"  $\Omega$ -shaped microstructures are embedded in an otherwise host dielectric.

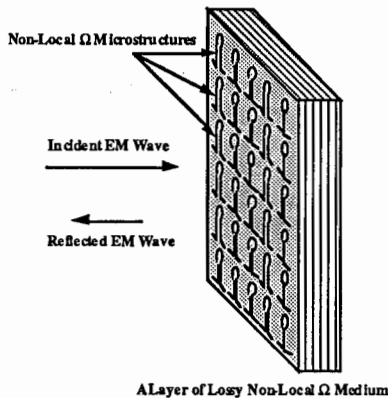
## REFLECTION AND SHIELDING CHARACTERISTICS OF THE LAYERED LOSSY NON-LOCAL $\Omega$ MEDIUM

Mamdouh M. I. Saadoun and Nader Engheta

Moore School of Electrical Engineering  
University of Pennsylvania  
Philadelphia, Pennsylvania 19104

In our theoretical analysis of electromagnetic wave propagation in  $\Omega$  media, we have studied some of the electromagnetic properties of these media and have addressed some of their potential applications [M. M. I. Saadoun and N. Engheta, The Pseudochiral  $\Omega$  Medium: What Is It? and What Can It Be Used For?, *Digest of the 1992 IEEE AP-S Symposium, Chicago*, pp. 2038-2041, 1992]. Recently we have theoretically extended this concept to the non-local  $\Omega$  medium. In such a medium, the loop portion and stems of the  $\Omega$ -shaped elements are separated and then connected by parallel wires. Some of the waveguiding properties of the non-local  $\Omega$  medium have been studied and presented elsewhere [M. M. I. Saadoun and N. Engheta, Pseudochiral  $\Omega$  medium and Guided-Wave Structures: Theory and Principles, *Proc. of the 1992 URSI Electromagnetic Theory Symposium, Sydney, Australia*, pp. 302-304, 1992].

In this talk, we present the results of our theoretical study of reflection and absorption properties of layered lossy non-local  $\Omega$  media. The role of *lossy* host material on the dispersion characteristics of the bulk medium will be discussed and the effect of non-locality of the  $\Omega$ -shaped microstructures will be addressed. We will also present shielding and absorption properties of a metal-backed layer of lossy non-local  $\Omega$  medium. The effect of parameters such as loss tangent of the host and shape of the non-local  $\Omega$  elements on the reflection and absorption characteristics of the grounded layer will be mentioned. Potential applications of these analyses to microwave shielding and absorption will be addressed.



Reflection of electromagnetic waves from a layer of lossy non-local  $\Omega$  medium. The non-local  $\Omega$  medium can, in principle, be constructed by spreading "stretched"  $\Omega$ -shaped microstructures in a host medium. The  $\Omega$  elements should have a fixed orientation throughout the medium.

Wed. p.m.

## CALCULATION OF THE EFFECTIVE PERMITTIVITY OF A RANDOM COLLECTION OF DIELECTRIC CYLINDERS

M. Moghaddam<sup>\*1</sup> and B. Houshmand<sup>2</sup>

<sup>1</sup> Jet Propulsion Laboratory  
California Institute of Technology  
4800 Oak Grove Drive  
Pasadena, CA 91109

<sup>2</sup> Department of Electrical Engineering  
University of California at Los Angeles  
Los Angeles, CA 90024

### ABSTRACT

Characterization of scattering by multiple objects is of importance in several areas such as remote sensing, random media, and mixing laws. Here, we utilize inverse scattering to calculate the equivalent dielectric constant of a random mixture of two-dimensional scatterers with circular cross sections. First, we use the recently developed fast algorithms for scattering by multiple objects (e.g., see Chew, W. C., *Waves and Fields in Inhomogeneous Media*. New York: Van Nostrand Reinhold, 1990) to find the average scattered field from a collection of randomly distributed cylinders. This is done by specifying the fraction of the simulation area occupied by the scatterers, the average scatterer diameter, and dielectric constant. The scattering problem is then solved several times, each time with a new arrangement for the location of the randomly distributed cylinders. The scattered field is found at many points around the simulation region by statistically averaging the field due to each arrangement. Normal plane wave incidence is assumed. If the cylinders have low permittivity such that they are weak scatterers, we can use a number of linear inverse scattering techniques to find the equivalent dielectric constant of an object with the same scattered field as the above collection of cylinders. Here, we use diffraction tomography for linear inversion. The results of this approach will be presented. For the case where scatterers are not weak, it is also possible to carry out a nonlinear inversion using the Born iterative method.

This work was performed in part by the Jet Propulsion Laboratory, California Institute of Technology, under a contract from the National Aeronautics and Space Administration.

**SYMMETRY ANALYSIS OF LARGE TWO-DIMENSIONAL  
CLUSTERS OF COUPLED CAVITY RESONATORS**

Ross A. Speciale  
Hughes Missile System Company  
Pomona, California 91769-2507

**ABSTRACT**

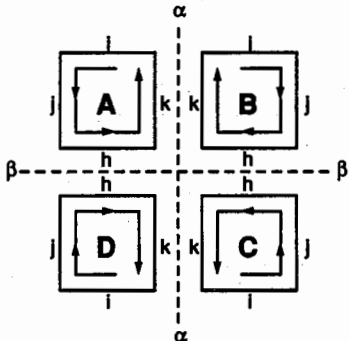
Electrically large, two-dimensional clusters of directly-coupled cavity resonators, ordered in a square or in an hexagonal lattice, perform and can be used as doubly-periodic wave-guiding structures. The considered two-dimensional clusters may extend hundreds of free-space wavelengths in length and width, and can be designed to exhibit wide relative transmission bandwidths. The transmission losses within such large passbands are very low if high-Q cavity resonators are used as 'unit-cells' of such clusters.

Large relative transmission bandwidths are obtained by using resonant-iris coupling between resonators. Further, because of the intrinsic 'multiport image impedance match' between mutually-identical multiport resonators, guided traveling electromagnetic waves propagate without reflection through such structures in every arbitrary direction.

Such two-dimensional clusters of coupled cavity resonators can be excited by any arbitrary topological distribution of multiple, mutually-coherent signal sources. Practical cluster-structures of finite physical extent can be excited by sets of signal sources properly aligned around the structure perimeter. Numerous, and very complex two-dimensional patterns of guided, traveling-wave fields can be obtained, by properly controlling the relative amplitudes and phases of the coherent driving sources.

A comprehensive symmetry analysis of such two-dimensional clusters, with either a square or an hexagonal lattice, is being performed, to determine the dependence of the wave-impedance and of the propagation constant upon the frequency and the azimuthal direction of wave-propagation. Further, the boundary conditions for reflection-free, multiport impedance matching around the perimeter of finite clusters are being formally defined.

Generalized matrix-algorithms have been derived that formally express the open-circuit impedance matrix of a cluster of finite extent, as seen from the 'external' ports, aligned around the structure perimeter. The derived generalized matrix-algorithms use a multi-level diakoptic approach, by tearing the cluster into progressively smaller subdivisions, while maintaining geometrical similarity, and conserving the translation-, rotation-, and reflection-symmetry of the whole system. Finally, formal expressions are obtained for the two-dimensional traveling-wave amplitude and phase patterns, generated by any given distribution of mutually-coherent excitation sources.

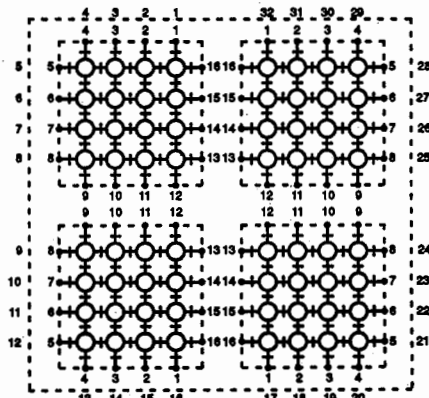


$$i = 1, 2, \dots, n$$

$$h = 2n+1, 2n+2, \dots, 3n$$

$$j = n+1, n+2, \dots, 2n$$

$$k = 3n+1, 3n+2, \dots, 4n$$



*Port Numbering Sequence For The Four Blocks Of A  $2n \times 2n$  Cluster Of Directly-Coupled Cavity Resonators.*

Wed. p.m.

## INTEGRAL EQUATION ANALYSIS OF ARTIFICIAL MEDIA

E.H. Newman\* and M.E. Peters  
The Ohio State University  
Department of Electrical Engineering  
ElectroScience Laboratory  
1320 Kinnear Rd.  
Columbus, OH 43212

An artificial medium consists of a large number of scattering elements placed in some homogeneous background or host medium. Typically there will be a large number of identical electrically small scatterers per cubic wavelength. When an electromagnetic wave propagates through the artificial medium, it will induce currents on or in the scatterers. Thus, the scatterers can be viewed as macroscopic electric and/or magnetic dipole moments, in analogy with the microscopic molecular electric and/or magnetic dipole moments in a real dielectric and/or ferrite medium. These macroscopic dipole moments modify the net electric and/or magnetic dipole moment per unit volume, and thus they also modify the effective permittivity and permeability of the medium. An interesting and potentially useful feature of artificial media is that by adjusting the size, shape, material composition, and density of the scatterers, one may be able to engineer or design a medium which has desirable permeability, permittivity, and dispersion characteristics.

This paper will present an integral equation and method of moments solution for the effective permittivity and permeability of the artificial medium. The scatterers are assumed to be on a periodic lattice, and the periodic moment method is used to set up a matrix equation for the currents induced in the reference element by a plane wave propagating through the artificial medium in a given direction. By setting the determinant of the impedance matrix to zero, one can determine the eigenfunctions of the periodic medium and their corresponding eigenvalues, i.e., the propagation constant of the plane wave. Once this propagation constant is known, the effective permittivity and permeability can be determined.

## A PROCEDURE FOR DEVELOPING COMPACT MODELS OF MATERIALS FOR NUMERICAL ELECTROMAGNETICS

Nicolaos G. Alexopoulos<sup>1</sup> and Rodolfo E. Diaz<sup>2</sup>

<sup>1</sup>Department of Electrical Engineering  
University of California  
Los Angeles, CA 90210

<sup>2</sup>Hexcel APD  
2500 W. Frye Rd.  
Chandler, AZ 85224

### ABSTRACT

The analytic model of physically realizable dielectrics presented in the companion paper<sup>1</sup> results in a compact ultrabroadband representation of dispersive materials. With such a representation, Time Domain Computational Electromagnetics codes can finally realize their full potential; since now a single pulse solution of the problem truly contains the behavior of the entire spectrum of the pulse. Using the important case of materials with multiple Debye relaxations, a method for obtaining the model from experimental data is disclosed. Since the method, derived from the work of F. A. Grant ("Use of Complex Conductivity in the Representation of Dielectric Phenomena", *J. Appl. Phys.*, vol. 29, 1958, pp.76-80), yields an analytic model of the material, band-limited data can be analytically continued into a full spectrum representation. As a particular example experimental data from a carbon loaded absorbing foam, taken over three frequency bands (10KHz-1MHz, 500MHz-1.5GHz, 1.5GHz-20GHz), is used to yield a model valid over a 2,000,000:1 bandwidth.

When the analytic model is expressed as a circuit model, it is readily implemented in numerical electromagnetics methods. The model of the absorbing foam is incorporated into a Physical Transmission Line Model of Maxwell's equations and the propagation of picosecond pulses through the foam calculated. Finally, using a two-dimensional Dispersive Finite Difference Time Domain computer code, the broadband focusing properties of a dispersive lens are studied.

---

<sup>1</sup> N. G. Alexopoulos and R. E. Diaz, "Towards a Unified Analytic Model of Dispersive Materials."

## PROPAGATION CONSTANT OF COHERENT MICROWAVES IN A DENSE DISTRIBUTION OF NONTENUOUS SPHERES

Daniel J. Rice, Yasuo Kuga and Akira Ishimaru  
Department of Electrical Engineering

University of Washington  
Seattle, Washington 98195

In a discrete random medium, the effective propagation constant depends on the volume fractional density of particles. The extinction rate is an important quantity in scattering and emission problems in remote sensing. For a sparse concentration of spheres with  $N$  sizes of radii  $a_1, a_2, \dots, a_N$  that are randomly positioned, the particle positions are usually uncorrelated for all order statistics. In this case, the extinction rate for the coherent wave is given by summing  $n_j \sigma_j(a_j)$ , where  $n_j$  is the number of spheres per unit volume with radius  $a_j$  and  $\sigma_j(a_j)$  is the extinction cross section of a sphere of radius  $a_j$ . This is known as independent scattering. In certain types of media, such as snow and ice, the concentration of scatterers is quite high (10-40%) and the extinction rate does not obey this simple relation.

We conducted experiments to study the characteristics of coherent microwaves propagating through a random medium. The medium consisted of layers of styrofoam with spherical glass particles embedded at predetermined random positions generated by computer. The magnitude and phase of the transmitted field were measured over the frequency range 10-40 GHz for media with volume fractional densities ranging from 1 to 11%. The glass particle size was adjusted such that the size parameter  $ka$  covered both Mie resonance and Rayleigh scattering regions. The results are compared with independent scattering, Foldy's approximation, and the quasicrystalline approximation (QCA) using the solution of the Percus-Yevick (PY) equation for the pair-distribution function. The effects of size distribution are included.

## **EFFECT OF INCLUSION GEOMETRY, SIZE, CONCENTRATION AND ORIENTATION ON THE EFFECTIVE PROPERTIES OF DISCRETE RANDOM MEDIA**

Vasundara V. Varadan\*, Yushieh Ma and Vijay K. Varadan  
Research Center for the Engineering of Electronic and Acoustic Materials  
Department of Engineering Science and Mechanics  
The Pennsylvania State University  
University Park, PA 16802

It is well known that the effective properties of discrete random media are dictated by the geometry, size, concentration and orientation of the inclusions that are dispersed therein. These properties define the behavior of the coherent field in the medium. In general, a multiple scattering formalism that takes into account the statistical correlations in position and orientation will be best suited to describe such a problem. Monte Carlo and Percus - Yevick models are adequate to describe the statistics of the problem. The single scattering response can be conveniently described by a T - matrix. The solution is necessarily numerical. At long wavelengths, approximate models based on a dipole approximation to the single scattering problem result in Maxwell-Garnett type expressions for the effective properties. The objective of this presentation is to compare the effect of inclusions of different shape - prolate and oblate spheroids, needle and disc shaped objects, chopped fibers and rings, spheres and helices; on the propagation characteristics of the coherent wave especially attenuation due to multiple scattering in such media. The literature in this area is quite large, but a critical comparison is lacking. The effective parameters are studied as a function of frequency and concentration for the different cases.

Wed. p.m.

## DISPERSION PROPERTIES OF BULK ANISOTROPIC DIELECTRIC MEDIA

E. A. SKIRTA\* and N. A. KHIZHNIAK

\* Laboratory S2HF, IRESTE

La Chantrerie - CP 3003- 44087 NANTES Cedex 03, FRANCE

Ph: (33) 40 68 30 66 & (33) 40 68 30 64, Fax: (33) 40 68 30 66;

Physical and Technical Institute of Ukrainian Academy of Sciences, Kharkov,  
Ukraine, Ph: 7(0572) 35 64 14

The electrodynamic averaging method that has been developed on the basis of integral-differential equations allows to derive the medium effective dielectric permittivity tensors determined by geometrical and electromagnetic parameters of scattering particles and geometrical properties of their spatial structure. Such dielectrics can be formed by cubic, orthogonal, tetragonal, monocline and other types of spatial gratings in scattering nodes of which particles of an arbitrary shape are positioned (ellipsoids, spheroids, cylinders, discs, and spheres). In this paper the main attention is focused on the study of dispersion properties of such an anisotropic structure with anisotropy which may be caused by either anisotropic scattering of the electromagnetic field by particles of the dielectric or the grating anisotropic structure.

Nature of spread of particles in the structure, their orientation, shape and size, and a complex dielectric permittivity determine the dielectric permittivity tensor component expressions which can be found from the equations describing the mean dielectric field variance in a homogeneous isotropic medium. An averaging procedure of the field in an "elementary volume" is formulated for the structure formed by the different geometrical dimensions of particles positioned in nodes of different subgratings, as well as for the medium formed by alternating grating in scattering nodes of which particles of different geometrical shapes and electromagnetic parameters are positioned.

A series of known formulae of mixture theory which describe the dielectric permittivity of random media follow from the obtained results. These are the formulae of Rayleigh, Maxwell-Garnett, and Clausius-Mossotti for spherical particles, as well as the results similar to Taylor formulae for randomly oriented needles and discs.

Dispersion dependences are calculated for dielectric permittivity tensor components of regular structures and three-component ones formed by two kinds of particles with random spread of geometrical and electromagnetic parameters. Such media can serve as models of some ice and snow covers, specifically, ice ones for which air bubbles and water drops are inclusions and snow covers being a mixture of water drops and ice particles in air. Dielectric properties of media being a mixture of dielectric and perfectly conducting particles in a nonmagnetic medium are analysed. Such structures can serve as models of soil and rock. The calculations have been carried out for the real and imaginary parts of dielectric permittivity according to the three-component model versus the volume fraction of both kinds of scatterers and spread of their geometrical dimensions. The frequency dependence of cylindrical or spheroidal inclusions with a high dielectric permittivity (saline water pockets in sea ice, for example) that is described by two different expressions, allows to investigate anisotropic properties of such structures, and compares these results with the reference ones.

## ANALYSIS OF FERRITE LOADED STRUCTURES WITH FINITE DIFFERENCE TIME DOMAIN TECHNIQUE

M.Okoniewski

Dept. Of Electrical and Computer Engng., University of Victoria  
P.O.Box 3055, Victoria, BC, Canada V8W 3P6

In this presentation modifications to the basis FDTD algorithm (Yee, K.S.Yee, IEEE Trans. AP-14, 302, 1966) which let one use FDTD method to treat structures loaded with magnetized ferrites are described. In a standard approach to the analysis of a ferrite loaded structure the permability tensor is used to account for wave interactions with the ferrite medium. This tensor is however defined in a frequency domain and therefore its use in a time domain method would require time-consuming computations of convolutions. In this formulation the basics of ferrite physics are exploited. The equation of motion  $\frac{d}{dt}\vec{M} = -\gamma(\vec{M} \times \vec{H})$  which relates magnetization vector  $\vec{M}$  magnetic strength vector  $\vec{H}$  is solved simultaneously with Maxwell *curl* equations, and thus the permability tensor is avoided altogether. A similar approach was used to treat ferrite media by Bergeron method (N.Kukutsu *et al.*, IEEE trans MTT-36, 114, 1988). In that method however, the transformation of the electromagnetic wave problem into an equivalent circuit, where the ferrite medium was represented by complicated mutual inductances between spatial nodes of the model mesh, yielded complex formulae in which the elegance and simplicity of time domain methods were lost. In the approach presented here, the basic field vectors are simulated directly, and the resulting algorithm is surprisingly simple.

It is assumed that  $\vec{M} = \vec{M}_s + \vec{m}$ ,  $\vec{H} = \vec{H}_i + \vec{h}$ , where  $\vec{M}_s$  and  $\vec{H}_i$  are the saturation magnetization and the biasing magnetic field respectively. Assuming also that  $\vec{M}_s \gg \vec{m}$ ,  $\vec{H}_i \gg \vec{h}$  and eliminating magnetic flux vector  $\vec{B}$  from Maxwell equations the following three equations are obtained:

$$\frac{d}{dt}\vec{h} = -\frac{1}{\mu_0}\nabla \times \vec{E} + \frac{d}{dt}\vec{m}; \quad \frac{d}{dt}\vec{E} = \frac{1}{\epsilon}\nabla \times \vec{h}; \quad \frac{d}{dt}\vec{m} = -\gamma(\vec{m} \times \vec{H}_i + \vec{M}_s \times \vec{h})$$

A pair of vectors  $\vec{m}$  and  $\vec{h}$ , as opposed to  $\vec{h}$ , and  $\vec{E}$  is defined in the same time and space point. Thus, care must be taken in casting the motion equation into the finite difference form in order to maintain the second order accuracy of the central difference Yee algorithm. applied along one of the coordinate system axis (this can always be achieved by a proper coordinate rotation) only magnetization vectors perpendicular to that axis need to be considered.

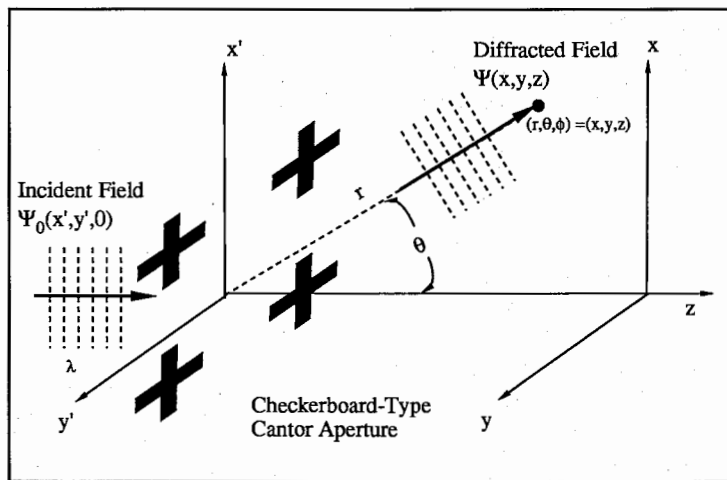
The method was validated against the data obtained with the mode-matching analysis and measurements of a resonator (M.Okoniewski, J.Mazur: IEEE MTT-S Symp, 181-184, 1991). A lowest order resonance frequency, for a resonator consisting of a ferrite rod in a metal box (22.86x10.16x28.85mm, ferrite:  $M_s=950$ Gs,  $r=2$ mm,  $l=22.85$ mm,  $H_i=0.57*H_s$ ) was found at 7.51GHz in measurements, and was computed at 7.40GHz and 7.50Ghz for FDTD and mode matching respectively.

## DIFFRACTION BY TWO-DIMENSIONAL CANTOR APERTURES

D. L Jaggard, T. Spielman, and M. Dempsey  
Complex Media Laboratory  
Moore School of Electrical Engineering  
University of Pennsylvania  
Philadelphia, PA 19104

Fractal electrodynamics combines classic electromagnetic theory with the recursive properties of fractal geometry [see e.g., D. L. Jaggard, "Fractal Electrodynamics," in *Recent Advances in Electromagnetic Theory*, H. N. Kritikos and D. L. Jaggard, eds., Springer-Verlag (1990)]. Electromagnetic waves can be used to remotely gather information on the fractal nature of a structure through observation of the scattered fields. Here, the wavelength of the incident fields is used as a variable electromagnetic yardstick to interrogate the multi-scale nature of a fractal aperture.

We investigate the far-zone diffracted fields for checkerboard-type apertures. These apertures are represented by two-dimensional separable patterns derived from the Cantor bar. This work is a continuation of work on rotationally separable targets reported elsewhere [D. L. Jaggard and T. Spielman, *Microwave and Optical Technologies Letters* 5, 460-466 (August 1992)]. Examination of the diffraction patterns for various stages of growth of these Cartesian targets (see below) lead to an iterative solution. These solutions are employed to find the characteristic spatial frequency dependence relation to stage of growth and fractal dimension.



Problem Geometry: Diffracted field  $\Psi$  from a sample two-dimensional fractal aperture as a function of scattering angle  $\theta$  for a time harmonic incident plane wave  $\Psi_0$ .

**SESSION URSI B-20****THURSDAY AM****INTEGRAL EQUATION METHODS II**

Chairs: T.S. Angell, University of Delaware; R.F. Harrington, Syracuse University

Room: Modern Languages Building, Auditorium 1

Time: 8:30-12:10

|       |   |     |
|-------|---|-----|
| 8:30  | APPLICATION OF DOMAIN DECOMPOSITION METHODS FOR THE ELECTROMAGNETIC ANALYSIS OF LARGE TWO- AND THREE-DIMENSIONAL STRUCTURES<br><i>C.T. Spring*, A.C. Cangellaris, University of Arizona</i>   | 316 |
| 8:50  | AN APPLICATION OF NESTED EQUIVALENCE PRINCIPLE ALGORITHM (NEPAL) IN MATRIX-VECTOR MULTIPLICATION OF ITERATIVE ALGORITHMS<br><i>Jiun-Hwa Lin, Weng Cho Chew, University of Illinois</i>  | 317 |
| 9:10  | CONVERGENCE OF SUCCESSIVE IMAGES WITH RELAXATION<br><i>Raphael Kastner, Tel Aviv University</i>   | 318 |
| 9:30  | A MULTILEVEL-DISCRETIZATION FAST INTEGRAL-EQUATION SOLVER FOR LARGE SCALE ELECTROMAGNETIC COMPUTATIONS<br><i>M. Bleszynski, Rockwell International; T. Jaroszewicz, University of California at Los Angeles</i>                                     | 319 |
| 9:50  | SCATTERING BY AN IMPEDANCE BODY OF REVOLUTION WITH AN ARBITRARY PATCH<br><i>S.F. Kawalko*, S.R. Laxpati, P.L.E. Uslenghi, University of Illinois at Chicago</i>   | 320 |
| 10:10 | BREAK   |     |
| 10:30 | TRANSVERSE ELECTRIC SCATTERING FROM CLOSED SURFACES: AN INTEGRAL EQUATION FORMULATION IN TERMS OF CHARGE AND AVERAGE CURRENT<br><i>K.M. Mitzner*, Northrop Corporation; J.L. Volakis, L.C. Kempel, University of Michigan</i>                       | 321 |
| 10:50 | A NOVEL TECHNIQUE TO CALCULATE THE ELECTROMAGNETIC SCATTERING BY SURFACES OF ARBITRARY SHAPE<br><i>J.S. Lim, S.M. Rao*, Auburn University; D.R. Wilton, University of Houston</i>   | 322 |
| 11:10 | VECTORIZATION OF THE PATH INTEGRAL FOR 3-D ELECTROMAGNETIC SCATTERING APPLICATIONS<br><i>Robert Nevels*, Zuoguo Wu, Chenhong Huang, Texas A&amp;M University</i>  | 323 |
| 11:30 | SURFACE INTEGRAL EQUATIONS FOR ELECTROMAGNETIC SCATTERING PROBLEMS INVOLVING THIN SHEETS OF COMBINED DIELECTRIC AND MAGNETIC PROPERTIES FOR NEAR-GRAZING INCIDENCE ANGLES<br><i>E. Bleszynski, M. Bleszynski, H.B. Tran, Rockwell International</i> | 324 |
| 11:50 | RIGOROUS ANALYSIS OF VARIOUS COAXIAL LINES WITH ARBITRARY CROSS-SECTION USING HIGH-ORDER BEM<br><i>Zhang Feng, Fu Junmei, Xi'an Jiaotong University</i>   | 325 |

APPLICATION OF DOMAIN DECOMPOSITION METHODS  
FOR THE ELECTROMAGNETIC ANALYSIS  
OF LARGE TWO- AND THREE-DIMENSIONAL STRUCTURES

C. T. Spring\* and A. C. Cangellaris  
Department of Electrical and Computer Engineering  
University of Arizona, Tucson, AZ 85721

A domain decomposition method is implemented for the electromagnetic modeling of electrically large structures. The objective is to develop the solution in a piecewise manner over properly defined subregions of the structure and then to couple in the subregions in a rigorous and computationally efficient manner. The total structure is logically partitioned into smaller regions, and numerical solutions are calculated in each of the small regions using a superposition of basis excitations. These bases are equated with field derivatives on the boundaries. By invoking the continuity of the fields themselves at the boundaries, a matrix is formed to solve for the fields throughout the entire structure. This final matrix has a sparse character that allows for very efficient inversion.

The advantages of this decomposition approach are improvements in flexibility, accuracy, and timesavings over conventional methods. Gains in flexibility are made by being able to model each region with a different numerical technique best suited for the geometry of the particular region. Two- and three-dimensional studies of guided structures using the scalar and vector Helmholtz equations demonstrate its flexibility. By working with smaller areas, the numerical mesh generation is greatly simplified. Gains in accuracy are made by eliminating the ill-conditioning associated with very large matrices, thus diminishing the round-off error associated with large matrix inversion. Accuracy is also increased by avoiding multiple analysis of repetitive regions; this is especially useful in analyzing periodic or nearly periodic structures.

In addition the decomposition approach is ideally suited for parallel processing. Each region can be analyzed independently, and each basis excitation can be analyzed independently; therefore, at least two levels of parallelism can be exploited in the decomposition approach. Finite numerical techniques also have several levels of parallelism that can be exploited. Examples from a two-dimensional parallel code on the Connection Machine illustrate the utility of the approach.

## An Application of Nested Equivalence Principle Algorithm (NEPAL) in Matrix-Vector Multiplication of Iterative Algorithms

JIUN-HWA LIN\* AND WENG CHO CHEW

ELECTROMAGNETICS LABORATORY  
DEPARTMENT OF ELECTRICAL AND COMPUTER ENGINEERING  
UNIVERSITY OF ILLINOIS  
URBANA, IL 61801

Solving the matrix equation iteratively has gained a lot of attention since the matrix storage is not required and for each iteration, only some matrix-vector multiplications are performed. So, if the converging rate is reasonably fast, the iterative approach is an efficient method to solve large problems. For example, conjugate gradient (CG) type algorithms are very popular. Performing the matrix-vector multiplication directly requires  $O(N^2)$  operations, which is still computationally intensive, where  $N$  is the number of unknowns. Exploiting the convolution feature of the matrix equation, we can use fast Fourier transform (FFT) to speed up the calculation of matrix-vector multiplications. The complexity of this method is  $O(N \log N)$ . But in order to prevent aliasing problems, zero-padding scheme is necessary. This renders FFT not as efficient as it should be.

Recently, we have developed NEPAL [W.C. Chew and C.C. Lu, *IEEE Antennas and Propagation Society International Symposium Digest*, pp. 184-187, July 18-25, Chicago, 1992] to perform a fast matrix inversion. The basic idea is that the object is appropriately divided into many small groups, and then, using Huygens' principle, the sources in each small group can be replaced with the surface sources on the boundary. Next, we group four small groups as a subgroup and again, replace sources inside the subgroup with the surface sources on the boundary of each subgroup. Repeated nesting of the subgroups with larger subgroups, we eventually obtain four largest groups with surface sources representing the effects produced by those original sources within the groups. Therefore, in order to find the field on one group from the other three, we only need to calculate the contributions directly from the surface sources instead of from each original source inside those three groups. Furthermore, to find out the field at some specific point due to the other sources, we just replace those outside sources with surface sources on the group where that point belongs to. By repeated nesting, it reduces to the smallest group, where the contributions from many outside sources are accounted for by a dozen of surface sources lying around the smallest group. The complexity of this algorithm is  $O(N \log N)$  principally. But techniques can be employed to speed up the calculations of finding surface sources, therefore to reduce the prefactor using, e.g., wavelet transforms or fast multipole method. An  $O(N)$  algorithm is possible.

## CONVERGENCE OF SUCCESSIVE IMAGES WITH RELAXATION

Raphael Kastner

Department of Electrical Engineering, Physical Electronics  
Tel Aviv University, Tel Aviv 69978, Israel

The method of successive images has been presented recently (R. Kastner, 1992 AP Symposium). The basic idea is based on the availability of the exact solution for an impressed tangential electric current near a perfect electric conductor (PEC) surface, i.e., its image. Therefore, if any incident field could be expressed via its equivalent incident current over a surface adjacent to the scatterer, the solution would be straightforward. In general, however, both electric and magnetic equivalent currents describe the incident wave. The method of successive images overcomes this problem by successively deducting portions of the equivalent magnetic current and transforming them into terms of the unknown equivalent electric current. The basic algorithm is modified here with a relaxation stage, as follows:

1. Given an incident field, determine the equivalent incident electric and magnetic sources from the incident magnetic and electric fields, respectively.
2. Store the electric contribution  $J^{eq}$ .
3. Split  $M^{eq}$ , the magnetic contribution, into two parts, #1 and #2 (normally, 50% each). Compute the new electromagnetic field (both electric and magnetic) generated over the surface by part #1 only. Store part #2.
4. Determine the additional component of the electric field from the new magnetic field. Add it to  $J^{eq}$ . Check for convergence.
5. Compute the new equivalent magnetic current by adding two components: (1) the new component resulting from the new electric field, (2) component #2 of step 3.
6. Go to step 3.

This algorithm now weighs the new value of  $M^{eq}$  with the previous one, as seen in step 5. This relaxation feature of the algorithm serves to enhance convergence considerably. The efficiency of the method is dependent upon the number of iterations P. At each iteration, step 3 requires an integration of the source and Green's function over the scatterer. It is an operation of the order of  $N^2$ , where N is the number of unknowns over the surface. The total number of operations is thus  $PN^2$ .

In several examples we show that the number of iterations is quite low. We have also observed that this number is almost independent of the size of the scatterer. Typically, ten to twenty iteration steps have been sufficient for reconstructing MoM solutions for two dimensional scatterers. One can see that indeed an  $N^2$  algorithm has been devised.

## A MULTILEVEL-DISCRETIZATION FAST INTEGRAL-EQUATION SOLVER FOR LARGE SCALE ELECTROMAGNETIC COMPUTATIONS

M. Bleszynski<sup>+</sup> and T. Jaroszewicz<sup>++</sup>

<sup>+</sup> Science Center, Rockwell International Corporation

P.O. Box 1085, Thousand Oaks, CA 91360

<sup>++</sup> Physics Department, UCLA, Los Angeles, CA 90034

We describe a new fast integral-equation solver applicable to large-scale electromagnetic scattering problems. As it is based on an iterative solution of the linear system of equations obtained as a result of discretization, its most essential part is a fast convolution method (physically, a fast evaluation of a field generated by a given current distribution).

The fast convolution algorithm (of complexity  $O(n \log n)$ , where  $n$  is the number of unknowns) is based on:

1. Recursive approximation of the original (full) matrix of the linear system by a sum of a sparse matrix and a smaller full matrix; physically, the former corresponds to the "near-field", and latter to the "far-field", generated by a coarsened current distribution (hence smaller matrix size).
2. The use of a uniform regular grid at each resolution level; this discretization results in a Toeplitz matrix, for which convolutions can be evaluated by means of fast Fourier transformations.

The algorithm utilizes multilevel adaptive discretization, in which the resolution may be different in various regions of the scatterer, resulting in significant memory saving (compared to a uniform discretization). Corrections to the discretization based on uniform grids are systematically implemented by local grid deformations (e.g., at interfaces), and by evaluating corrected short-range convolutions. The method takes also into account restrictions following from the oscillatory behavior of the integral kernel (Green's function of the Helmholtz equation).

The convolution algorithm employs restriction and prolongation operations analogous to those of multigrid methods; they are implemented in a way ensuring continuity of the field at the boundaries between the discretization subdomains. Evaluation of far-field contributions from various domains is organized, by utilizing Fourier transforms, in a way minimizing the number of terms in the explicit sum over distant subdomains; as a result, only nearest-neighbor subdomains have to be summed over explicitly.

Because of the local character of the convolutions (only nearest-neighbor subdomains involved at every discretization level), the algorithm is well suited for massive parallelization.

## SCATTERING BY AN IMPEDANCE BODY OF REVOLUTION WITH AN ARBITRARY PATCH

S. F. Kawalko(\*), S. R. Laxpati and P. L. E. Uslenghi

Department of Electrical Engineering and Computer Science, M/C 154

University of Illinois at Chicago

851 S. Morgan Street

Chicago IL 60607-7053

This paper will present some results on the scattering of a linearly polarized, obliquely incident plane electromagnetic wave by a scatterer with a rotationally symmetric body of uniform surface impedance with a small region (patch) of different surface impedance. The body is rotationally symmetric with respect to the z-axis. Previously, results of scattering from such a body with arbitrary varying surface impedance and with fins has been reported by the authors [URSI International Symp. on EM Theory, Sydney, Australia, August 1992].

The generalized Maue integral equation formulation for the surface currents on the body is carried out. Either the magnetic field, electric field or combined field integral equation is solved numerically for the vector electric surface currents. The method of moment procedure with parametric elements is employed in the numerical solution. To implement this, the generating curve for the body of revolution is described in parametric form along the arc length. This permits the mapping of the surface of the body as well as the patch into rectangular regions. These regions are then subdivided into smaller rectangular regions (surface patches). The electric surface current density on a surface patch is represented by two-dimensional Hermite expansion functions. This choice of basis function permits discontinuities in the surface currents as well as their derivatives and yet permits the use of the Dirac delta function as the testing function to transform the integral equations into a matrix equation.

The matrix equation is solved for the coefficients of the expansion function at each node via LU decomposition technique. From the knowledge of the surface current densities on the surface patches, the far scattered fields are derived; the integral representation of the far field is evaluated numerically. The bistatic radar cross section is then calculated for various angles of incidence and the results are plotted as 3-D surface plots.

The Fortran -77 computer code which has been previously validated has been modified for the present case. The results for the scattering by a cone-cylinder geometry with a patch on the cylindrical as well as conical part of the body will be presented. These results will be compared with the results for scattering by a cone-cylinder geometry with a constant surface impedance.

TRANSVERSE ELECTRIC SCATTERING FROM CLOSED SURFACES:  
AN INTEGRAL EQUATION FORMULATION  
IN TERMS OF CHARGE AND AVERAGE CURRENT

K. M. Mitzner\*

MS W944/UB Northrop Corporation  
8900 Washington Blvd., Pico Rivera, California 90660

J. L. Volakis and L. C. Kempel  
EECS Department University of Michigan  
Ann Arbor, MI 48109

It was shown in a recent paper (K. M. Mitzner, J. L. Volakis, J. M. Jin, L. C. Kempel, and D. Ross, "An Integral Equation in Terms of Charge for TE Scattering by Curved Open Surfaces", July 1992 URSI Radio Science Meeting Digest, p. 85) that TE scattering from an open surface of constant section can be calculated using a charge integral equation (CIE) rather than an integral equation in terms of current.

This paper extends the approach to bodies with closed surfaces, including perfect electric conductors, impedance boundaries, and tubes of resistive (and complex impedance) card.

For the closed surface it is necessary to introduce one additional unknown, the spatial average of the current. If the surface is divided into  $N$  zones, there will then be  $N+1$  unknowns, the average current and  $N$  values of charge. The condition that total charge vanish provides the required additional equation.

The formulation makes use of a representation of the current as the sum of its average value plus an integral of the charge, a representation that follows from the current being a periodic function of the arc length parameter on the surface. The integral of the charge leads numerically to matrix elements that are defined by double integrals, but the double integrals have special structure that makes it still possible to fill the matrix in  $O(N^2)$  operations.

The new formulation is well-behaved down to arbitrarily low frequency and indeed has been designed to separate correctly in the static limit into an electric polarizability problem and the problem of determining the current induced by the applied magnetic field. The latter problem is trivial for a uniform applied field.

Thu. a.m.

**A NOVEL TECHNIQUE TO CALCULATE  
THE ELECTROMAGNETIC SCATTERING BY  
SURFACES OF ARBITRARY SHAPE**

J. S. Lim and S. M. Rao, Department of Electrical Engineering,  
Auburn University, Auburn, AL 36849.

D. R. Wilton, Department of Electrical Engineering, University of  
Houston, Houston, TEXAS 77004.

Much progress has been accomplished in the last decade in the development of numerical solution procedures for handling radiation and scattering by arbitrarily shaped, three dimensional conducting/material bodies. These procedures, primarily, are based on the application of the surface equivalence principle and the well-known method of moments solution procedure to solve the integral equations. For conducting bodies, the solution to the electric field integral equation (EFIE), obtained by enforcing the total tangential electric field component to zero on the scattering surface, is a preferred choice. This is because, the EFIE is applicable to both open and closed bodies. At present, there exist many user-oriented computer codes, based upon the EFIE solution, capable of predicting the surface currents and scattered fields accurately in the resonance region which may be defined as the range of frequencies for which the maximum dimension of the structure is of the order of wavelength. Although the EFIE solutions are highly accurate in the resonance region, problems of inaccuracy and ill-conditioning have been reported at very low frequencies. Some work has been done in this area to alleviate the ill-conditioning problem but these methods are cumbersome to apply for a general arbitrarily shaped geometry. In this work, we present an alternate method which is easily applicable to both low and resonance frequency ranges. The new method is simple, efficient, accurate, and robust at all frequencies. In the present method, we approximate the scattering surface by planar triangular patches and define a new pair of basis functions for the method of moment solution. These basis functions decompose the surface current density into divergence-less and curl-free parts which essentially get decoupled at the very low end of the frequency spectrum. Further, these new pair of basis functions are also used as testing functions to generate a diagonally dominant moment matrix which is well-conditioned at all frequencies. Numerical results for various structures are presented and compared with other methods.

## Vectorization of the Path Integral for 3-D Electromagnetic Scattering Applications

Robert Nevels\*, Zuoguo Wu and Chenhong Huang  
Department of Electrical Engineering  
Texas A&M University  
College Station, Texas 77843-3128

The path integral was originally developed as a Green's function for a parabolic or Schrödinger type equation. By a suitable transformation the parabolic equation and its associated path integral expression can be converted into an elliptic or scalar Helmholtz type equation. The recently developed Fourier transform path integral (FTPI) numerical method has been successful in evaluating the path integral for a number of scalar scattering problems. However, because to date only a scalar formulation has been available, the usefulness of path integral has been limited to one and two dimensional scattering geometries. An example which will yield a scalar form of Helmholtz equation solvable by the path integral method is the two dimensional case in which a TM incident wave is scattered from an inhomogeneous cylinder. The TE incidence case could not be solved by this method.

In this paper we will present a general path integral solution for the vector Helmholtz equation. The method is based on a dyadic formalism and the result is valid for scatterers composed of any combination of conducting, inhomogeneous or anisotropic materials. The result is fully programmable by the FTPI method. Sources of any polarization may be used and the method can be applied in three dimensions. As in the scalar case the size of the scatterer is still restricted to a few (generally less than 5) wavelengths due to limitations imposed primarily by the fast Fourier transform code upon which the FTPI method is based. However, it will be shown that many of the scalar FTPI method advantages are still true for the general vector case. These advantages include programming ease and versatility.

**SURFACE INTEGRAL EQUATIONS FOR ELECTROMAGNETIC  
SCATTERING PROBLEMS INVOLVING THIN SHEETS  
OF COMBINED DIELECTRIC AND MAGNETIC PROPERTIES  
FOR NEAR-GRAZING INCIDENCE ANGLES**

E. Bleszynski\*, M. Bleszynski† and H. B. Tran\*

\* NAA, Rockwell Int., P.O. Box 92098, Los Angeles, CA 90009

† Science Center, Rockwell Int., P.O. Box 1085, Thousand Oaks, CA 91360

Scattering and radiation properties of thin layers of combined dielectric and magnetic properties are of considerable interest in radar cross section reduction applications and antenna design. Calculations of fields generated by such systems simplify considerably if the layers can be modeled by infinitesimally thin sheets of electric and magnetic currents on which suitable boundary conditions are imposed which allow one to reduce the volume integral equations to approximate surface integral equations. We derive such surface integral equations for electromagnetic scattering problems involving thin penetrable layers of combined dielectric and magnetic properties as well as impenetrable sheets with two different face impedances.

Our formulation is based on the surface integral representation for the fields outside a thin material layer in terms of two surface polarization currents  $\mathbf{J}$  and  $\mathbf{M}$ .

$$\mathbf{J}(\mathbf{r}) = \mathbf{J}_N(\mathbf{r}) + \mathbf{J}_T(\mathbf{r}), \quad (1a)$$

$$\mathbf{M}(\mathbf{r}) = \mathbf{M}_N(\mathbf{r}) + \mathbf{M}_T(\mathbf{r}), \quad (1b)$$

where  $\mathbf{J}_N$ ,  $\mathbf{M}_N$  and  $\mathbf{J}_T$ ,  $\mathbf{M}_T$  are the normal and tangential current components with respect to the sheet surface. By evaluating the fields values following from this representation on two sides of the layer and subjecting them to the boundary conditions in a form of generalized "Ohm's laws" for the polarization currents, we obtain a set of two coupled surface integral equations for  $\mathbf{J}$  and  $\mathbf{M}$ . The generalized "resistivity" coefficients appearing in these "Ohm's laws" depend on the material properties of the layers or on the values of surface impedances. For some particular cases, the integral equations decouple.

While simulation of thin sheets by currents with tangential components only yields accurate results for near normal incidence, the inclusion of normal components of the currents substantially improves the thin sheet approximation for the near grazing incidence. Also, our formulation is valid for *inhomogeneous* layers with position-dependent material properties. We discuss the relation of our method to that of Ref. [1] where integral equations involving tangential and normal field components for a thin dielectric strip were presented and the boundary conditions for a thin penetrable, *homogenous* dielectric/magnetic layer have been proposed. We also analyze the relation of the parameterization of the material properties of the sheet used in our approach to that based on the higher order impedance boundary conditions, considered recently in [2].

- [1] T. B. A Senior and J. Volakis, "Sheet simulation of a thin dielectric layer", *Radio Science*, Vol. 22(7), pp. 1261-1272, 1987.
- [2] T. B. A Senior "Generalized boundary and transition conditions and the question of uniqueness", *Radio Science* Vol. 27(6), pp. 929-2934, 1992.

RIGOROUS ANALYSIS OF VARIOUS COAXIAL LINES WITH  
ARBITRARY CROSS-SECTION USING HIGH-ORDER BEM

Zhang Feng      Fu Junmei

(Dept. of Information and Control Engineering  
Xi'an Jiaotong University, Xi'an 710049, P.R.C.)

With the development of microwave technique, various coaxial lines are utilized for numerous cases. Thus, it is necessary to determine the characteristic impedance of a coaxial line with arbitrary cross-section. There are many available analytical and numerical approaches. Generally, we may use conformal transformation or the finite element method. But the former is constrained to some complex cases, the latter will consume huge computation time. It is the main purpose to develop a simple, efficient and general method to improve the accuracy of the calculation of the characteristic impedances.

In coaxial lines, the potential  $u$  is satisfied to two-dimensional Laplace equation ( $\partial^2 u / \partial x^2 + \partial^2 u / \partial y^2 = 0$ ). With the Green theorem and Cauchy principal value integral, the Laplace equation is converted to a new equation, as the similar one (C.A.Brebbia et al., Boundary element technique in engineering, London: Butterworth, 1980, pp.36-65). Discretizing the boundary with high-order boundary element, linear equations can be obtained which is derived from that equation. Solving these equations, the potential distribution is determined, then the characteristic impedances can be calculated easily.

Compared with the analytical solution of coaxial lines with circular or elliptical cross-section, the accuracy of this approach has been verified. Then the characteristic impedances of several kinds of noncircular coaxial lines with arbitrary cross-section are calculated. Compared with the existing data, all our results are as accurate as the data available in literatures. Some results are believed to be more accurate than those reported in the literature. Furthermore, the computation time is less than that of other approaches. Thus, the presented method is a simple, rigorous and general method for this kind of problems.



**SESSION URSI B-21****THURSDAY AM****DIFFRACTION**

Chairs: C.A. Balanis, Arizona State University; E. Bahar, University of Nebraska

Room: Modern Languages Building, Auditorium 2      Time: 8:30-12:10

|       |  |     |
|-------|--|-----|
| 8:30  | PO/PTD ANALYSIS OF ARRAY-FED SINGLE- AND DUAL-REFLECTOR ANTENNAS<br><i>Dah-Wei Duan*, Yahya Rahmat-Samii, University of California at Los Angeles</i>                                      | 328 |
| 8:50  | NUMERICAL COMPARISON OF ASYMPTOTIC AND EXACT FORMULATIONS FOR FIELDS NEAR CONVEX SURFACES<br><i>D. Chatterjee*, R.G. Plumb, University of Kansas</i>                                       | 329 |
| 9:10  | SLOPE DIFFRACTION AT PERFECTLY CONDUCTING EDGES: A PTD CONSTRUCTION<br><i>P. Ya. Ufimtsev*, Y. Rahmat-Samii, University of California, Los Angeles; K.M. Mitzner, Northrop Corporation</i> | 330 |
| 9:30  | AN INCREMENTAL SLOPE DIFFRACTION COEFFICIENT<br><i>S. Maci, R. Tiberio, A. Toccafondi, University of Florence; G. Manara*, University of Pisa</i>  | 331 |
| 9:50  | DIFFRACTION OF AN INHOMOGENEOUS PLANE WAVE BY AN IMPEDANCE WEDGE<br><i>G. Manara*, P. Nepa, University of Pisa; R.G. Kouyoumjian, The Ohio State University; B.J.E. Taute, CSIR</i>        | 332 |
| 10:10 | BREAK  |     |
| 10:30 | A UNIFORM ASYMPTOTIC ANALYSIS FOR THE SCATTERING AND DIFFRACTION BY SMOOTHLY INDENTED BOUNDARIES CONTAINING EDGES<br><i>E.D. Constantinides*, R.J. Marhefka, The Ohio State University</i> | 333 |
| 10:50 | HYBRID RAY-MODE REPRESENTATION OF ELECTROMAGNETIC PULSE PROPAGATION ON CONCAVE BOUNDARY<br><i>T. Ishihara*, K. Yukutake, K. Goto, National Defense Academy</i>                             | 334 |
| 11:10 | SCATTERING FROM IMPEDANCE POLYGONAL CYLINDERS AT RESONANCE USING HIGH FREQUENCY METHODS<br><i>G. Muller, F. Molinet*, Société Mothesim</i>   | 335 |
| 11:30 | A UNIFORM GTD TREATMENT OF SURFACE DIFFRACTION BY IMPEDANCE AND COATED CYLINDERS<br><i>Paul E. Hussar, IIT Research Institute</i>  | 336 |
| 11:50 | COMPARISON OF NUMERICAL AND EXPERIMENTAL COUPLING RESULTS BETWEEN ANTENNAS MOUNTED ON A CIRCULAR CYLINDER<br><i>D. Chatterjee*, R.G. Plumb, The University of Kansas</i>                   | 337 |

1993 Radar Science Meeting (Ann Arbor, MI)  
July 1, 1993

Thu. a.m.

## PO/PTD ANALYSIS OF ARRAY-FED SINGLE- AND DUAL-REFLECTOR ANTENNAS

Dah-Weih Duan\* and Yahya Rahmat-Samii

Department of Electrical Engineering  
University of California, Los Angeles  
Los Angeles, CA 90024-1594

Efficient and accurate high frequency diffraction techniques for reflector antenna analysis have been of interest for many years. Among these techniques, Physical Optics (PO) has been widely used because it is accurate in the main beam region and the first few sidelobes. However, for far-angular regions and the cross-polarized fields, the PO solution may not be as accurate. The Physical Theory of Diffraction (PTD) modifies the PO field by adding a fringe field that asymptotically approximates the diffraction from the edge of the scatterer. In the past, attempts have been made to apply the PTD analysis to single-reflector antennas. In this paper, the PTD technique is applied to analyzing array-fed single- and dual-reflector antennas. It must be emphasized that the PTD fringe field analysis presented in this work is readily applicable to existing PO computer programs for reflector antenna analysis, and only marginally increases the CPU time required by the PO analysis.

In the formulation, a thorough singularity analysis of the PTD diffraction coefficients is conducted in order to avoid the apparent singularities. Secondly, surface derivatives and local coordinate systems that are required in the PO/PTD analysis are developed systematically for commonly used reflector surfaces (such as paraboloid, hyperboloid, ellipsoid, and shaped surfaces represented by a Jacobi-Fourier global expansion) with superquadric aperture boundaries. Furthermore, a general computation scheme employing the Eulerian rotations is developed to handle array feeds with arbitrary excitations, positions, and orientations. The feed elements can be modeled by various methods such as sources of  $\cos^q$  or Gaussian type, various aperture type horns, models based on measurement data, or the outcome of a complex diffraction analysis program.

A computer program has been developed based on the above formulation for PO/PTD analysis of array-fed single- or dual-reflector antennas. Comparisons with published computational and experimental data, and with other techniques such as GTD and MoM are carried out. Representative examples such as the antennas used in direct-broadcast satellite communications (DBS) are presented to demonstrate the effectiveness of the PTD fringe field. In particular, a method for determining the incident angles in computing the PTD fringe field for array feed and subreflectors is presented. The effect of the fringe field in a dual-reflector antenna is also carefully investigated.

## NUMERICAL COMPARISON OF ASYMPTOTIC AND EXACT FORMULATIONS FOR FIELDS NEAR CONVEX SURFACES.

D.Chatterjee\* and R.G.Plumb

Radar Systems and Remote Sensing Laboratory,  
University of Kansas, Lawrence, KS 66045-2969Abstract

The problem of calculating the creeping wave fields in the neighborhood of a smooth convex surface is of fundamental importance in predicting EMI coupling for antennas mounted on or near aircraft fuselages [T.E.Durham, *IEEE Symp. Electromagn. Compat. Rec.* pp. 420-427, Aug. 1987]. To analyze the EMI coupling at high frequencies and for large aircrafts, the UTD coupling formulation [P.H.Pathak & N.N.Wang, *IEEE-T-AP-29*, pp. 911-922, Nov. 1981] generally yields correct results for sources on the curved surface. When sources are off, but, still shadowed by the cylinder, the UTD scattering formulation [P.H.Pathak, W.D.Burnside & R.J.Marhefka, *IEEE-T-AP-28*, pp. 631-640, Sept. 1980] provides an alternate way of computing the surface field. In both cases, coupling depends on the *geodesic* path length between the *attachment & launch* points of the surface ray traveling from the source to the receiver. By invoking the principle of locality of high-frequency radiation [B.R.Levy & J.B.Keller, *Commun. Pure & Applied Math.*, v. XII, pp. 159-209, 1959], one can study the special case of scattering by a conducting circular cylinder, which is a *canonical* problem in this case.

The UTD scattering and coupling formulations are basically different asymptotic approximations to the general problem studied earlier [V.A.Fock (ed.), *Electromagnetic Propagation & Diffraction Problems*, Pergamon Press, 1965, U.S]. This difference arises because of the two different asymptotic approximations to the Hankel function,  $H_\nu^{(1,2)}(kr)$ , [N.Bleistien & R.A.Handelsman, *Asymptotic Expansions of Integrals*, pp. 268-273, Dover 1986, N.Y.], where  $\nu$  and  $kr$  are the order and argument of the Hankel function, respectively. Such approximations result in the Pekeris caret  $\hat{P}_{s,h}(\xi)$  (UTD scattering) & surface-Fock functions  $U_0(\xi), V_0(\xi)$  (UTD coupling). The quantity  $\xi$  is the universal Fock parameter and depends on the location of the sources and the frequency of propagation. It was observed that the UTD scattering and coupling were *mutually exclusive* in nature [D.Chatterjee, *M.A.Sc thesis*, E&CE Dept. Concordia University, Montréal, 1992]. The mutual exclusivity being manifested w.r.t the height  $kh$  from the curved surface of the cylinder. (Here  $k$  is the wavenumber and  $h$  is the actual height from the curved surface.) Near the cylinder ( $kh \rightarrow 0$ ), the UTD scattering yields *infinite* fields, while, far away from, the cylinder ( $kh \rightarrow \infty$ ), UTD coupling is invalid due to limitations in the pertinent formulations. Thus, it is important to identify the accuracy of the formulations at a specific distance ( $kh$ ) from the curved surface of a cylinder.

In the recent past improved UTD scattering formulation [P.Hussar & R.Albus, *IEEE-T-AP-39*, pp. 1672-1680, Dec. 1991] was obtained. This improvement gave better numerical agreement with the earlier UTD scattering result when both were compared to the exact (eigenfunction) result for the same problem - near the shadow boundary and in the deep shadow regions. However, this new UTD formulation, still contains terms that might lead to incorrect results in the deep shadow as  $kh \rightarrow 0$ .

This paper will thus examine the two UTD scattering, UTD coupling (asymptotic) formulations and compare them with the TE eigenfunction (magnetic line source) case. Results for  $|\vec{E}_s|$  vs.  $kh$  will be presented for different values of  $\phi$  (beyond & near the shadow boundary) and  $ka = 10, 20, 100, 500, 1000$ . The results will provide further insight into developing uniform asymptotic formulations when sources are at different heights from the cylinders surface.

Thu. a.m.

## **SLOPE DIFFRACTION AT PERFECTLY CONDUCTING EDGES: A PTD CONSTRUCTION**

**P.Ya. Ufimtsev\* and Y. Rahmat-Samii**

Electrical Engineering Department  
University of California, Los Angeles  
Los Angeles, California 90024-1594

**K.M. Mitzner**

Northrop Corporation  
MS W944/UB  
8900 East Washington Boulevard  
Pico Rivera, California 90660

Slope diffraction is a special case of edge diffraction, when a scattering edge is situated in the direction in which the directivity pattern of an incident wave has a zero. One distinguishes slope diffractions of different orders. Here we consider the most important one to be the slope diffraction of the first order. In this case, the directivity pattern has a zero but its first derivative is not equal to zero. Such a phenomenon occurs in reflector antennas, when one tries to decrease side lobes, and in the diffraction process, when several scatterers (or different parts of the same scatterer) interact.

The slope diffraction is investigated within the framework of the Physical Theory of Diffraction (PTD). The basic idea of PTD consists of the separation of surface currents into two parts: The uniform (geometrical optics) current  $j^0$ , and the nonuniform (diffraction) current  $j^1$ . A scattered field created by the uniform current  $j^0$  is known as the Physical Optics approximation. In this paper we investigate corrections to the Physical Optics approach caused by the nonuniform current  $j^1$ . These corrections are found for diffraction fields both in ray regions and in diffraction regions such as the vicinity of shadow boundaries, smooth caustics, and focal lines. The general theory is illustrated by some representative examples.

## AN INCREMENTAL SLOPE DIFFRACTION COEFFICIENT

*S. Maci, R. Tiberio, A. Toccafondi  
University of Florence, via S. Marta 3, 50139 Florence, Italy.*

*G. Manara<sup>\*</sup>  
University of Pisa, via Diotisalvi 2, 56126 Pisa Italy*

Accurate calculations of the radiation pattern of reflector antennas, as well as predicting the characteristics of antennas mounted on complex structures are of interest in several practical applications.

Recently, an Incremental Theory of Diffraction (ITD) has been developed to provide a unified framework for describing high-frequency phenomena. This method is applicable to any local shape, where a uniform, cylindrical, local canonical configuration with arbitrary cross-section is appropriate. Also, its formulation is uniformly valid at any incidence and observation aspects, including caustic of the corresponding ray-field representation. The procedure is essentially based on a localization process, developed by a rigorous Fourier transform analysis of canonical problems. This allows to define local incremental field contributions that are adiabatically distributed either on the actual lit surface or at its shadow boundary line. This leads to a representation of the total field which consists of a Generalized Geometrical Optics (GGO) field and incremental diffracted field contributions.

So far, explicit ITD formulations have been obtained only for a plane wave incident at a wedge and for an observation point at a finite distance from its edge. By reciprocity, the same result is used to treat the scattering in the far zone of an incident field with a local, spherical wavefront.

In this paper, the formulation is extended to treat the case of an incident wavefront which may exhibit rapid spatial variations. To this end, the incremental, diffracted field contribution is augmented by an incremental, slope diffraction contribution. In a local, incident ray-fixed coordinate system, slope effects are accounted for that may occur in the angular coordinates both perpendicular ( $\phi'$ ) and parallel ( $\beta'$ ) to the plane of incidence. The asymptotic analysis shows that such slope contributions may be calculated as the directional derivatives of the incident field times their pertinent, incremental slope diffraction coefficients. It is found that this latter involve only very familiar transition functions. A dyadic expression is obtained for the electromagnetic vector problem.

The effect of a radial component of the incident field is also considered. Eventually, the use of a plane wave spectral representation of the incident field is investigated.

## DIFFRACTION OF AN INHOMOGENEOUS PLANE WAVE BY AN IMPEDANCE WEDGE

G. Manara\*, P. Nepa

Dept. of Information Engineering, University of Pisa, Italy

R. G. Kouyoumjian

Dept. of Electrical Engineering, The Ohio State University, USA

B.J.E. Taute

CSIR, Aeronautical Systems Technology, Pretoria, South Africa

Recently, a high-frequency solution was presented for the diffraction of an inhomogeneous plane wave by a perfectly conducting wedge (R.G. Kouyoumjian et al., Proc. IXth Italian Nat. Meeting on Electromagnetics, 53-56, Assisi, Italy, 1992). In that paper an exact integral representation of the field was determined by an analytic continuation of the integral representation for the homogeneous plane wave case. Then, the integral representation was evaluated asymptotically to obtain a uniform, high-frequency expression for the diffracted field.

In this paper the same procedure is applied to treat the more general case of the diffraction of an inhomogeneous plane wave by a wedge with different impedance faces. Uniform asymptotic expressions are derived which contain the UTD transition function but with complex arguments. Particular attention is devoted to the description of the discontinuity compensation mechanism which takes place at the shadow boundaries of the incident and reflected fields. The displacement of these boundaries from their conventional locations in the case of homogeneous plane wave incidence is described. The dependence of these displacements on losses in the medium surrounding the wedge is discussed, and the the locations of the transition regions are given.

Of considerable interest in the scattering from an impedance wedge is the excitation of surface waves at the edge of the wedge (G. Manara et al., IEEE AP-S Int. Symp. Dig., 14-17, London, Ontario, 1991). The dependence of the surface wave parameters on the evanescence angle associated with the incident plane wave is investigated in detail. The surface wave shadow boundary is geometrically determined and the continuity of the solution at that boundary is described.

Several numerical results will be shown both to demonstrate the continuity of the total field across the shadow boundaries of the incident field, the reflected field and the surface waves and to show the importance of the different field contributions.

**A UNIFORM ASYMPTOTIC ANALYSIS FOR THE SCATTERING  
AND DIFFRACTION BY SMOOTHLY INDENTED BOUNDARIES  
CONTAINING EDGES**

E. D. Constantinides\* and R. J. Marhefka  
The Ohio State University, ElectroScience Laboratory  
Department of Electrical Engineering  
Columbus, Ohio 43212

It is well known that the classic geometrical optics solution fails near transition regions where the scattering mechanism is no longer localized and the field behaves in a more complicated manner. It is therefore necessary to analyze the fields within such regions by employing uniform asymptotic procedures. In this paper, uniform asymptotic expressions for the reflected and diffracted fields will be presented for both two and three dimensional smoothly indented (concave or concave-convex) boundaries containing edges. Such surfaces give rise to composite shadow boundaries resulting from the confluence of a smooth caustic of singly reflected rays and a reflection shadow boundary (RSB) associated with an edge in the reflecting surface. When the RSB is not in the immediate vicinity of the caustic, the conventional UTD edge diffraction coefficient developed by Kouyoumjian and Pathak and involves the Fresnel integral as a canonical function can be used to effectively describe the edge diffracted field behavior in the neighborhood of the RSB. Furthermore, the ordinary Airy integrals and their derivatives are the appropriate canonical functions for the description of the high-frequency fields in the neighborhood of the smooth caustic (Pathak and Liang, T-AP 38, 1192-1203, 1990). However, when there is a confluence of both reflected and caustic type shadow boundaries, neither the Fresnel integral nor the ordinary Airy integrals adequately describe the transition region phenomena, and they must be appropriately replaced by the incomplete Airy functions (Levey and Felsen, Radio Sci. 4, 959-969, 1969).

The expressions for the reflected and diffracted fields derived in this paper are casted in a UTD format; they remain valid across the composite shadow boundary and reduce to the known expressions in the exterior. The new edge diffraction coefficient involves the incomplete Airy function and is in agreement with the usual UTD diffraction coefficient when the RSB is sufficiently isolated from the smooth caustic. The new solution is applicable to both near-zone (antenna) and far-zone (RCS) problems, and its accuracy is verified via an independent moment method analysis.

## HYBRID RAY-MODE REPRESENTATION OF ELECTROMAGNETIC PULSE PROPAGATION ON CONCAVE BOUNDARY

T.Ishihara\*, K.Yukutake and K.Goto  
Dept. of Electrical Engineering,  
National Defense Academy,  
Hashirimizu, Yokosuka, 239, JAPAN

High-frequency propagation along and near a concave boundary excited by a time harmonic source close to the boundary exhibits anomalous effects attributable to the failure of ray theory for the high-order multiply reflected fields. The high-order reflected rays have been treated collectively, either in terms of a selected number of the lowest-order whispering gallery(WG) modes that are guided along the surface or in the integral form [T.Ishihara, L.B.Felsen, Radio Science, 1988]. Geometrical ray convergence problems can be avoided if the fields is expressed as a sum over all excited WG modes. However, a modal representation is inconvenient to calculate the fields at high frequency, and is difficult to interpret the propagation phenomena physically. A hybrid ray-mode representation can overcome the deficiencies of the ray representation.

In the present investigation, various representations derived for the time-harmonic regime are extended to account for the electromagnetic pulse propagation excited by a high-frequency pulsed source with a Gaussian envelope located on a concave boundary. Numerical comparison of the asymptotic solutions with a reference solution calculated from the modal representation reveals the accuracy and utility of the various representations. Included are ray-optical, whispering-gallery mode, and canonical integral, and various combination of these. Of special interest from a physical standpoint is the hybrid ray-mode representation that comprises a mixture of  $(N(\omega)+1)$  geometric optical rays and  $M(\omega)$  ( $\omega$ :angular frequency) whispering gallery modes, with criteria provided for the proper choice of  $N(\omega)$  and  $M(\omega)$ . One may observe the ray-like behavior of the waveform at early times and mode-like behavior at late times.

SCATTERING FROM IMPEDANCE POLYGONAL CYLINDERS AT RESONANCE  
USING HIGH FREQUENCY METHODS

G. Muller, F. Molinet (\*)

Société MOTHESIM, La Boursidière, 92357 Le Plessis-Robinson, France

The launching coefficient of a TM surface wave tends to unity when the real part of the surface impedance is negligibly small and its imaginary part becomes large. As a consequence, the surface wave launched at an edge of a polygonal cylinder is practically not attenuated by further diffractions at the other edges. Hence high order multiple scattering of surface waves occur and produce resonance effects which must be taken into account in the calculation of the scattered field.

The direct summation of all the individual contributions of surface waves having encountered one to  $n$  interactions with the edges of a polygonal cylinder is very cumbersome and time consuming.

A more efficient method has been developed which leads to the exact summation of the series of multiple interactions. On each face of the polygonal cylinder, the diffracted field due to a surface wave of amplitude unity propagating along this face is chosen as an unknown. If the cylinder has  $N$  faces, a total number of  $2N$  unknowns occur. It is shown that these unknowns verify a system of  $2N$  linear equations. The total diffracted field which is expressed as a linear combination of the solutions of this system, with known coefficients is then readily obtained.

The method has been applied to a cylinder with a triangular cross section as shown on Fig. 1. The surface impedance with respect to vacuum is constant and equal to  $5j$ . Fig. 2 shows the echo width divided by the wavelength as a function of the relative wave number  $k/k_0$  calculated by this method.

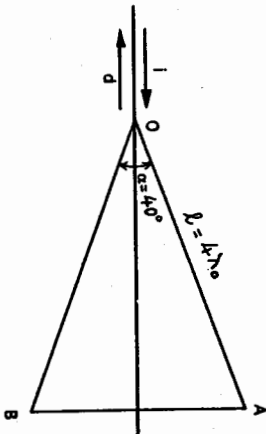


Fig. 1 : Cross section of the polygonal cylinder and direction of observation

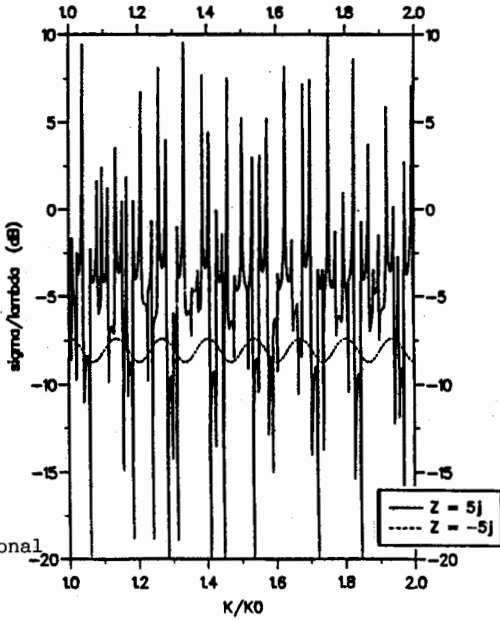


Fig. 2 : Echo width in dB

A UNIFORM GTD TREATMENT OF SURFACE DIFFRACTION  
BY IMPEDANCE AND COATED CYLINDERS†

Paul E. Hussar  
IIT Research Institute  
185 Admiral Cochrane Drive  
Annapolis, MD 21401

The uniform geometrical theory of diffraction (UTD) permits the analysis of electromagnetic scattering by electrically large conductors at modest computational expense. If the UTD is to be extended to treat scattering by curved surfaces which are either coated or characterized by a constant surface impedance, the problem of rapidly calculating the fields in the vicinity of the shadow boundary (i.e. the transition region) must be solved. Historically, UTD results for the transition region (conducting case) have relied on tabulated values of the hard and soft Pekeris functions obtained via numerical integration. While this approach can be adapted to cover other cases, function values would need to be tabulated over an immense material parameter space to satisfactorily cover the range of practical problems. The eigenfunction summation method proposed by Kim and Wang (H. T. Kim and N. Wang, IEEE Trans. Antennas Propagat., pp. 1463-1472, Nov. 1989) can be used as an alternative to numerical integration, but remains far too computationally intensive to be directly included within UTD field-computation algorithms. The purpose of the present paper is to provide a uniform GTD technique that is applicable to impedance and coated scatterers and satisfies the demands of computational efficiency. In the case of a conducting cylinder, a recently derived residue series representation (P. Hussar and R. Albus, IEEE Trans. Antennas Propagat., pp. 1672-1680, Dec. 1991) is known to accurately describe the field throughout the shadow region. Analogous representations are shown to permit rapid field computations everywhere in the shadow region of an impedance or coated cylinder. Only the shadow region is considered, and the discussion is limited, for simplicity, to two-dimensional problems.

**COMPARISON OF NUMERICAL AND EXPERIMENTAL COUPLING  
RESULTS BETWEEN ANTENNAS MOUNTED ON A CIRCULAR  
CYLINDER**

D.Chatterjee\* and R.G.Plumb

Radar Systems and Remote Sensing Laboratory,  
Electrical and Computer Engineering  
The University of Kansas, Lawrence, KS

**Abstract**

Modeling of EMI coupling between antennas mounted on a circular cylinder is a *canonical* case that provides answers to similar problems arising in more real-world situations. EMC analysis codes, routinely employed in predicting EMI coupling for fuselage- and wing-mounted antennas [H.P.Widmer, ECAC-CR-83-048, DoD EMC Analysis Center, North Severn, MD, U.S.A., 1983], generally contain the state-of-art formulations for accurate quantification of EM fields in these situations. For fuselage-mounted antennas, the canonical geometry of a circular cylinder serves as a fundamental model in computing the *creeping wave* fields over smooth convex surfaces. To validate such user-oriented codes, for more advanced applications, it is necessary to perform periodic validation of these formulations in the codes by either comparing them against experimental or other theoretical results.

In the recent past, efforts in such direction were attempted by many workers [G.C.Genello & A.F.Pesta, *IEEE Symp. Electromagn. Comp. Rec.*, pp. 72-74, 1985], [T.E.Durham, *IEEE Electromagn. Comp. Rec.*, pp. 420-427, Aug. 1987]. The work of Durham contains enough information on the behavior of a class of *high-frequency* (asymptotic) formulations for creeping waves and their comparisons with experimental data. The coupling gain between antennas was computed by using the Numerical Electromagnetics Code-Basic Scattering Code (version 2) (NECBSC2) [R.J.Marhefka and W.D.Burnside, Tech. Rep. # 712242-14, ESL, OSU, Dec. 1982], and the Aircraft inter-Antenna Propagation with Graphics (AAPG) codes. (The AAPG code has been described in the report by Widmer, cited above.) The verification of Durham's results via alternate techniques and additional comparisons have been performed [D.Chatterjee, *M.A.Sc thesis*, E&CE Dept., Concordia University, Montréal, 1992] and presented elsewhere [D.Chatterjee, S.J.Kubina & R.J.Paknys, *3rd Canadian Conf. Elec. & Comp. Engng.*, Ottawa, Sept. 1990], [D.Chatterjee, R.J.Paknys & S.J.Kubina, *ANTEM*, Winnipeg, Manitoba, August 1992].

However, it appears that by employing the technique used earlier [S.A.Davidson & G.A.Theile, *IEEE-T-EMC-26*, pp. 90-97, May 1984] in evaluating the AAPG code, it should be possible to rigorously verify the experimental data in Durham's report. This is important because the data refer to the measurements for the canonical case of the circular cylinder. Since NECBSC2 code demands that antennas be located *off* by at least a  $\frac{\lambda}{4}$  from the curved surface, this verification will also provide information on the usage of the code in modeling on-surface EMI coupling. Results from the NECBSC2 code, the MM-GTD technique and experimental data will be presented for coupling vs. frequency cases for both large and small  $\phi$  angles and *torsional* & *torsionless* paths.



**SPECIAL SESSION AP-S/URSI D-6****THURSDAY AM****OPTICAL CONTROLLED ARRAYS**

Chairs: F. Schwering, US Army CECOM; M.B. Steer, North Carolina State University

Room: Michigan League, Michigan Room

Time: 8:30-10:10

|      |  |      |
|------|--|------|
| 8:30 | PHOTONICS AS APPLIED TO ANTENNA SYSTEMS - BENEFITS AND RISKS<br><i>Brian M. Hendrickson, Air Force Rome Laboratory</i>                       | AP-S |
| 8:50 | OPTICAL CONTROLLED PHASED ARRAY RADAR RECEIVERS<br><i>H.R. Fetterman*, S.R. Forrest, D.V. Plant, University of California at Los Angeles</i> | AP-S |
| 9:10 | APPLICATIONS OF OPTICS IN ARRAYS<br><i>Richard R. Kunath, NASA Lewis Research Center</i>   | AP-S |
| 9:30 | OPTICALLY CONTROLLED PHASED ARRAYS - LATEST TECHNIQUES<br><i>A.S. Daryoush, Drexel University; R.R. Kunath, NASA Lewis Research Center</i>   | AP-S |
| 9:50 | AM/FM NOISE IN FIBER OPTIC LINKS FOR RADAR ANTENNA REMOTING<br><i>M. Wechsberg*, D.E. Snyder, Hughes Aircraft Company</i>                    | AP-S |



**SPECIAL SESSION AP-S/URSI D-7**

**THURSDAY AM**

**DIGITAL CONTROLLED ARRAYS**

Chairs: R.J. Mailloux, Hascom AFB; H. Steyskal, Hascom AFB

Room: Michigan League, Michigan Room

Time: 10:30-12:10

|       |  |      |
|-------|--|------|
| 10:30 | OPENING REMARKS<br><i>H. Steyskal, Hascom AFB</i>  |      |
| 10:50 | BEAM FORMING AND ARRAY PROCESSING WITH ACTIVE ARRAYS<br><i>W.D. Wirth*, U. Nickel, FGAN-FFM, EL</i>  | AP-S |
| 11:10 | ANTENNA PATTERNS FOR PROTOTYPE TWO-DIMENSIONAL DIGITAL BEAMFORMING ARRAY<br><i>John F. Rose*, Brent A. Worley, Michael M. Lee, U.S. Army Missile Command</i> | AP-S |
| 11:30 | ERROR ANALYSIS IN A PRACTICAL DIGITAL BEAMFORMER<br><i>William R. Humbert*, Warren F. Brandow, Rome Laboratory</i>   | AP-S |
| 11:50 | AN EXPERIMENTAL UHF RADAR USING DIGITAL ADAPTIVE BEAMFORMING<br><i>Blair D. Carlson, MIT Lincoln Laboratory</i>  | AP-S |



## ANTENNA MEASUREMENTS

Chairs: K.C. Gupta, University of Colorado  
 M. Kanda, National Institute of Standards and Technology

Room: Michigan League, Room D      Time: 8:30-12:10

|       |  |     |
|-------|--|-----|
| 8:30  | PERFORMANCE EVALUATION OF SYMMETRIC AND OFFSET NEAR-FIELD REFLECTOR ANTENNAS<br><i>B. Houshmand*, M. Zimmerman, University of California at Los Angeles</i>  | 344 |
| 8:50  | OPTIMIZING THE FEED IMPEDANCE OF REFLECTOR IMPULSE RADIATING ANTENNAS<br><i>Everett G. Farr, Farr Research</i>   | 345 |
| 9:10  | NEW IDEAS ON COMMON-MODE RADIATION FROM PRINTED CIRCUIT BOARDS<br><i>J.L. Drewniak*, T.H. Hubing, T.P. VanDoren, University of Missouri-Rolla</i>  | 346 |
| 9:30  | MICROSTRIP PATCH ANTENNAS WITH LEAKY-WAVE EDGE REGIONS<br><i>Azar S. Ali*, US Air Force Academy; Kuldip C. Gupta, University of Colorado</i>   | 347 |
| 9:50  | FREQUENCY AND TIME DOMAIN CHARACTERIZATION OF UWB ANTENNAS<br><i>J.S. Gwynne*, J.D. Young, The Ohio State University</i>   | 348 |
| 10:10 | BREAK  |     |
| 10:30 | DESIGN OF ARRAYS TO RADIATE SHORT PULSES<br><i>Victor K. Tripp*, Scott R. Crowgey, Georgia Tech Research Institute</i>   | 349 |
| 10:50 | G/T AND TRACKING FEATURES OF A BROADBAND, LOW-COST, AND LOW-PROFILE LAND-MOBILE SPIRAL-MODE MICROSTRIP ANTENNA<br><i>J.J.H. Wang*, J.K. Tillery, V.K. Tripp, C.B. Chambers, G.O. Hirvela, Wang-Tripp Corporation</i> | 350 |
| 11:10 | NOISE MODEL OF SERIES DISTRIBUTED ACTIVE ANTENNAS<br><i>D.J. Roscoe*, A. Ittipiboon, Communications Research Centre; L. Shafai, University of Manitoba; M. Cuhaci, Communications Research Centre</i>                | 351 |
| 11:30 | ELECTROMAGNETIC PENETRATION OF CAVITY-BACKED APERTURES WITH INTERNAL LOADING<br><i>Russell P. Jedlicka*, Steven P. Castillo, New Mexico State University; Larry K. Warne, Sandia National Laboratories</i>           | 352 |
| 11:50 | OPTIMISING PATTERN SYNTHESIS USING CLASSICAL VARIATIONAL METHOD<br><i>Xian-zhong Zhang, Nanjing Research Institute of Electronics Technology</i>   | 353 |

## Performance Evaluation of Symmetric and Offset Near-field Reflector Antennas

B. Houshmand<sup>1</sup> and M. Zimmerman<sup>2</sup>

<sup>1</sup>University of California  
Los Angeles, CA 90024-1594

<sup>2</sup>Analex Corporation, Brookpark, Ohio

### ABSTRACT

A Near-field reflector antenna provides an effective structure to magnify a small phased array into a much larger aperture antenna. This type of antenna system is particularly suitable for rapid scanning of a limited view angle. This type of antenna system consist of a parabolic main reflector and a confocal parabolic subreflector in a concave or convex configuration. A phased array with the dimensions comparable to the subreflector is positioned in the near field of the subreflector. The phased array elements collectively produce a collimated beam in the near field of the array which is transformed to a tapered but larger collimated beam after reflecting from the sub- and main reflectors. The increase in the effective aperture is proportional to the square of the ratio of reflector diameters. For this type of antenna system, scanning is achieved by introducing a linear phase taper on the phased array elements.

Performance of near-field antennas is dependent on geometrical arrangements as well as the phased array parameters such as number of elements, element size, and excitation coefficients. By considering the field contributions due to individual elements, the performance of this antenna system can be evaluated. This is in contrast to the collimated beam approach where the phased array is replaced by an ideal collimated beam. Including the array element effects are particularly important for accurate evaluation of the scan performance where the near field phase variations deviate from an ideal collimated beam. A computational method based on the geometrical theory of diffraction is available to account for the effects of individual phased array elements. Forward and inverse ray tracing methods can be employed to compute the main reflector aperture field. For the forward ray tracing approach, the incident field from each element is traced as it bounces from the sub- and main reflectors. The total aperture field is the sum of the fields produced by the individual elements. The inverse ray tracing approach relies on computation of the reflection points on the subreflector for each feed array element. In this approach, the total field is computed on a grid on the surface of the main reflector. For each grid point, the total field is the sum of the contributions for the individual elements. While both methods are equivalent, each can offer computational advantages depending on the geometrical arrangements of the antenna system. For example, the symmetrical configurations are well suited for the inverse ray approach. The forward ray approach can be used for the offset configurations where the reflection point computation can be particularly time consuming. In this talk the performance of symmetric and offset near-field reflector antennas with concave and convex subreflectors are evaluated. Methods to improve the scan performance by geometrical and phased array considerations, and implementation of the forward and inverse ray tracing approaches on a parallel machine are presented.

## OPTIMIZING THE FEED IMPEDANCE OF REFLECTOR IMPULSE RADIATING ANTENNAS

Everett G. Farr  
Farr Research

When designing a reflector Impulse Radiating Antenna, one must choose an appropriate feed impedance. Using the simplest approximations valid for high feed impedances, one finds that lower feed impedances are always preferable. However, low feed impedances imply thick feed arms, which increase feed blockage for many designs, thus reducing the radiated field. Low feed impedances also lead to a breakdown of the approximation that the effective aperture height is equal to the radius of an aperture for circular apertures. Thus, even when there is no feed blockage, there is a reduced aperture height at low feed impedances.

We calculate the radiated field based on a contour integration technique that takes into account feed blockage. With these calculations, one can find the optimal feed impedance for a given configuration of feed arms. The analysis is valid in the limit of fast risetimes, and is carried out for three different feed structures.

Consider the IRA of Figure 1, with diameter  $D$ , focal distance  $F$ , and feed impedance  $Z_c = Z_o f_g$ . The simple model of the radiated field on boresight is

$$E_y(r, t) = \frac{V_o}{r} \frac{D}{4\pi c f_g} \left[ \delta_a(t - 2F/c) - \frac{c}{2F} [u(t) - u(t - 2F/c)] \right] \quad (1)$$

where the driving voltage across the feed arms is a step function,  $V(t) = V_o u(t)$  and  $\delta_a(t)$  is an approximate delta function. If we now keep power constant, the radiated field is proportional to  $f_g^{-1/2}$ . If we choose to keep voltage constant, the radiated is proportional to  $1/f_g$ . In either case, these simple models suggest a small  $f_g$  is always preferable. This would imply, however, a large aperture blockage, so we must find a way to compromise.

The problem arises because the field in (1) is calculated by using a contour integral that includes the entire aperture. A better approximation is obtained by excluding the portion of the aperture that is blocked by the feed, as shown in Figure 1. By doing so, one can find an optimal feed impedance.

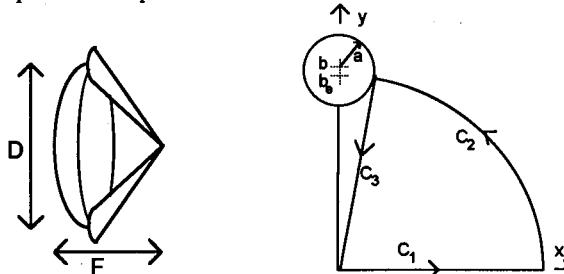


Figure 1. An Impulse Radiating Antenna (left), and the contour one integrates to find the corrected radiated field (right).

## NEW IDEAS ON COMMON-MODE RADIATION FROM PRINTED CIRCUIT BOARDS

J. L. Drewniak\*, T. H. Hubing, T. P. VanDoren  
Department of Electrical Engineering  
University of Missouri-Rolla  
Rolla, MO 65401

Radiation from printed circuit boards (PCBs) with attached cables is of increasing concern to industry and government organizations. As digital data rates continue to increase with an accompanying increase in PCB radiation problems, the need for adequately characterizing and modeling this radiation grows. Typical PCB designs complete with attached I/O and signal return cables, and possibly contained within an enclosure, are too complex to model every feature with current full-wave numerical analysis packages. It is common practice to make simplifying assumptions concerning the source of radiation from the PCB and then proceed to calculate the radiation. Often the assumptions made eliminate aspects of the problem which are primary contributors to the radiation. The currents on PCBs are typically broken down into two components, differential-mode and common-mode. Drawing an analogy to a folded-dipole antenna, the differential-mode currents are analogous to the transmission-line currents of the folded dipole, and the common-mode currents are analogous to the antenna currents. Most often it is the common-mode current that is the primary contributor to radiation from PCBs even though the common-mode current might be several orders of magnitude lower than the differential-mode currents. Understanding the fundamental physics and origin of common-mode currents is therefore essential so that physical attributes of the PCB design which produce these currents are incorporated into sophisticated numerical modeling codes.

Most fundamentally, radiation can be reduced to a source driving an antenna. In the case of common-mode radiation the antenna is the conductors on which the common-mode current exists, which usually include conductors that extend well beyond the signal conductors which carry the differential-mode or signal currents. The source driving this antenna results from differential-mode signals on the PCB, but the mechanisms by which differential-mode signals produce common-mode sources are not well understood. Two fundamental source mechanisms resulting from common design configurations on PCBs have been identified, a point differential-mode voltage, and a loop differential-mode current which produces a common-mode antenna voltage source. These sources drive the two common-mode antenna halves to which they are connected. Experimental results indicate that in many cases the loop-current mechanism is dominant. Finding and eliminating this mechanism of common-mode radiation can be more difficult than the point-voltage source mechanism, because the two antenna halves which the resulting common-mode source drive appear to be at the same potential in the design. Numerical and experimental results that demonstrate the two mechanisms of common-mode radiation will be presented.

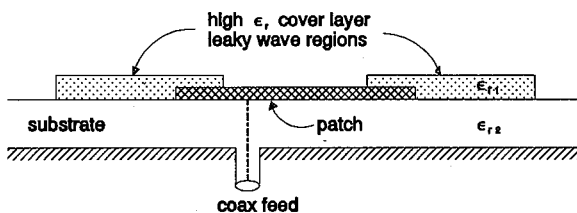
## MICROSTRIP PATCH ANTENNAS WITH LEAKY-WAVE EDGE REGIONS

Azar S. Ali\*, Department of Electrical Engineering, US Air Force Academy, Colorado Springs, CO 80840  
 Kuldip C. Gupta, Department of ECE, University of Colorado, Boulder, CO 80309-0425

This paper presents a microstrip antenna configuration wherein the regions in the vicinity of the radiating edges are modified such that leaky-waves are excited in these regions. This modification consists of adding two overlays of a higher dielectric constant cover layer as shown in the figure below. Excitation of leaky-waves increases the radiation conductance associated with the edges of the patch. This increased radiation enhances the bandwidth as compared to traditional microstrip patch antennas.

From expressions for the fields in the grounded substrate and the leaky wave propagation constants, an equivalent edge conductance is defined. This edge conductance along with the characteristic impedance of ordinary microstrip patches are used to develop an equivalent transmission line model. The equivalent transmission line model for these novel antenna configurations will be discussed and results indicating the possibility of much wider bandwidths will be presented.

This phenomenon of enhanced radiation by the excitation of leaky waves is also indicated by a study of the radiation from a magnetic current line source on a grounded dielectric slab when it is covered by a dielectric layer such that the resulting structure can support leaky waves.



## Frequency and Time Domain Characterization of UWB Antennas

J.S. Gwynne\* and J.D. Young  
The Ohio State University ElectroScience Laboratory  
Department of Electrical Engineering  
Columbus, Ohio 43212

The standard narrow band antenna parameters are inadequate in characterizing an antenna for use in an ultra-wide bandwidth (UWB) system where the antennas are expected to operate with bandwidths of at least 25%. In this paper, the antenna is viewed as a transducer in which the transmitting and receiving cases are fully described by complex transfer functions that provide a more natural means of characterizing the antenna for UWB applications. Calibrated measured results are presented that characterize the performance as a function of angle for three common antennas and a three octave band limited impulse waveform. Considered are a rhombic shaped TEM parallel plate horn, an AEL double ridged horn, and an AEL pyramidal log periodic antenna.

The time domain transmit and receive transfer functions of our test antennas are presented in a contour map as a function of angle for the two principle planes and co- and cross-polarized cases. Radiation centers are identified and correlated to physical attributes. In addition, the waveform dispersion, the peak radiated energy, and the total radiated energy for a band limited impulse excitation are compared to an ideal antenna and are used to characterize the antennas performance for UWB applications.

## DESIGN OF ARRAYS TO RADIATE SHORT PULSES

Victor K. Tripp\* and Scott R. Crowgey

Georgia Tech Research Institute

Microwave and Antenna Technology Development Lab.

Atlanta, Georgia 30332

A recent surge of interest in impulse radar has necessitated the design of arrays for very broad-instantaneous-band signals, rather than for more typical narrowband signals. In this paper, we present the performance of various array geometries, calculated in the time domain for impulse signals. Besides the elimination of grating lobe problems (except for very high repetition rates), interesting features are observed related to design requirements. For instance, it is found that a close relationship exists between the beamwidth and sidelobe envelope for the CW array and those of the pulse array. A very interesting result is that the array factor directivity can rise above the nominal limit of  $2N$  for CW arrays simply by separating the elements. Where space is limited, it was discovered that "half-wavelength" spacing offers no significant advantage over a spacing of  $3/4$  wavelength or more. Where endfire operation is feasible, the directivity was shown to be at least  $N$ , even for closely spaced arrays whose broadside gain dropped significantly below  $N$ . Design principles derived from this investigation include the fact that the best element spacing often will be greater than a half wavelength.

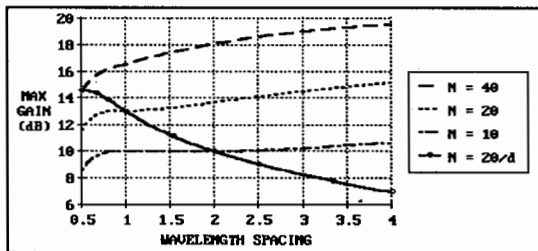


Figure 1. Array Gain vs. Spacing.

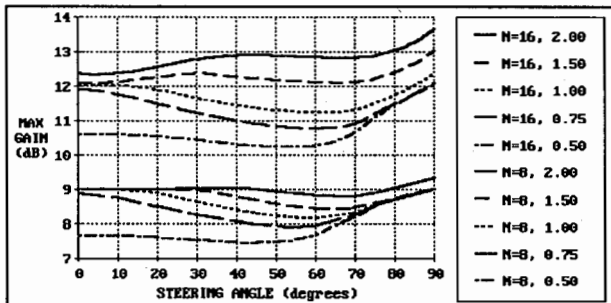


Figure 2. Array Gain vs. Steering.

## G/T AND TRACKING FEATURES OF A BROADBAND, LOW-COST, AND LOW-PROFILE LAND-MOBILE SPIRAL-MODE MICROSTRIP ANTENNA

J. J. H. Wang<sup>\*\*</sup>, J. K. Tillery<sup>\*</sup>, V. K. Tripp<sup>\*\*</sup>, C. B. Chambers<sup>\*</sup>,  
and G. O. Hirvela<sup>\*</sup>

<sup>\*</sup>Wang-Tripp Corporation  
1710 Cumberland Point Drive, Suite 17  
Marietta, Georgia 30067  
and  
<sup>+</sup>Georgia Tech Research Corporation  
Georgia Institute of Technology  
Atlanta, Georgia 30332

The spiral-mode microstrip antenna (J. J. H. Wang and V. K. Tripp, *IEEE AP Trans.* 39, 332-335, 1991) has a number of attractive features for applications as a land-mobile antenna: low profile, broadband, aesthetic appeal, and potentially low cost. When used in a multi-mode configuration, low-cost beam-steering using a single phase shifter is feasible (J. J. H. Wang, G. D. Hopkins, and V. K. Tripp, *Proc. ISAP'92*, Sapporo, Japan, 789-792, 1992). In this paper, experimental work on a tracking scheme for this antenna and measurements and improvements of its G/T, antenna gain over system noise temperature, are discussed.

The tracking feature of this antenna is aimed at geostationary MSS (Mobile Satellite System) applications. The antenna gain G ranges between 6 and 8 dB over wide elevation angles, which is lower than the typical 10 to 16 dB gain enjoyed by many mobile antennas currently in use. However, since G/T, rather than the antenna gain G, should be used as the final figure of merit for communication antennas, we tried to focus on narrowing the G/T gap. It is often feasible to increase G/T by 2 dB or so by reducing the noise temperature T instead of increasing the antenna gain G. Since it may be more costly to increase G than G/T, especially for the forthcoming LEO (Low Earth Orbit) satellites, the present antenna with a low G yet a moderate G/T could be a practical solution for cost-driven consumer applications.

Measurements of the antenna temperature, and thus G/T, of the present antenna were carried out using a spectrum analyzer (P. Estabrook and W. Rafferty, *39th IEEE Veh. Tech. Conf.*, 757-762, San Francisco, 1989) at Wang-Tripp Corporation's field sites and anechoic chamber. The removal of edge loading used in the earlier model reduces the antenna temperature. Attention is also paid to the radiation pattern and the feed network to reduce both the external and internal noises of the antenna.

## Noise Model of Series Distributed Active Antennas

D.J. Roscoe\*, A. Ittipiboon, L. Shafai^, M. Cuhaci

Communications Research Centre  
3701 Carling Ave., P.O. Box 11490, Station H  
Ottawa, Ontario, K2H 8S2, Canada

<sup>^</sup>Department of Electrical Engineering  
University of Manitoba  
Winnipeg, Manitoba, R3T 2N2, Canada

A cascaded network model has been developed to analyse the noise characteristics of a previously developed antenna. This antenna, shown in Figure 1, is travelling wave in nature and has active components integrated within it. An interesting problem exists when calculating the system temperature of this structure. Each section of the antenna contributes to the system noise temperature and each section is weighted by the active devices. The noise sources present may be identified as: i) device noise; ii) sky noise, and; iii) ohmic losses. The developed model utilizes a network equivalent of the antenna that is a combination of resistors, attenuators, and active devices. These components are referenced to their environment temperature; the radiation resistance is thus referenced to the sky temperature.

The developed model was verified with experimental measurements. A "Y-factor" measurement approach was used where the antenna under test was placed in a controlled environment. The measured and calculated results presented in Figure 2 show good agreement. Note that the large temperatures obtained are due to the noisy amplifiers used in the fabricated prototype, i.e.  $NF \sim 12$  dB.

The details of the model and measurement procedure will be presented at the conference.

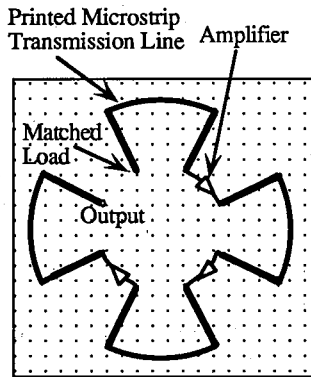


Fig. 1 : Fabricated active integrated antenna.

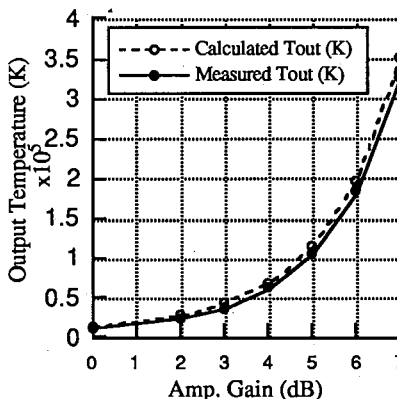


Fig. 2 : Calculated and measured output temperature, referenced to 295 K.

## ELECTROMAGNETIC PENETRATION OF CAVITY-BACKED APERTURES WITH INTERNAL LOADING

Russell P. Jedlicka<sup>1</sup>, Steven P. Castillo<sup>1</sup> and Larry K. Warne<sup>2</sup>

<sup>1</sup>Department of Electrical & Computer Engineering  
New Mexico State University Las Cruces, New Mexico

<sup>2</sup>Electromagnetic Analysis Division  
Sandia National Laboratories Albuquerque, New Mexico

Coupling to systems can cause upset or, in the extreme, component burnout. The energy can penetrate the shield through radiating structures such as antennas or through seams created by bowing at overlap joints. The coupling through narrow slot apertures with depth and loss has previously been studied, and an antenna/local transmission line model has been validated by measurements. Furthermore, rudimentary cavity-backed apertures have been considered. Coupling through narrow slot apertures, representative of seams in shielded systems, has been shown to be dependent upon aperture width, slot depth and the conductivity of the walls. Moreover, the effect on slot coupling when the aperture is backed by a resonant structure has been investigated. The original study considered rectangular apertures backed by simple cavity structures. This has been extended to observe the effects of loading within the cavity. In this experiment, wires and monopoles, which are terminated with resistive and reactive loads, are placed within the cavity and the effect upon coupling through the slot apertures is observed.

The work was performed in the 2-4 GHz range. The two inch aperture length assured that the first resonance of the slot was excited in this frequency band. The widths varied between 0.010 to 0.125 inches. The depths from 0.125 to 0.50 inches. The cavity dimensions were chosen to be 3.4" x 1.7" x 3.94". Thus, the resonant frequency of the rectangular unloaded cavity was also in the frequency band of interest. The fields within the cavity were measured with an electrically small probe while the cavity was loaded with a 1.25" long monopole as well as a 1.7" long wire which was attached between the top and bottom walls. The coupling to the cavity was modified by the presence of the conductor as well as the load on the end of the wire. The fields within the cavity were found to be significantly reduced (on the order of 20 or more dB) when the wire was terminated in a resistive load. Additionally, the frequency response was considerably broadened.

In addition to knowing how much energy is coupled to this configuration, it is interesting to study how the power is distributed. That is, of the incident power, how much is dissipated in the slot walls, how much in the metallic surfaces of the cavity and how much is delivered to loads within the cavity? To investigate these effects, the power delivered to a  $50 \Omega$  load on the end of the wire was also measured. In order to determine a bound on the power which would have been delivered to a matched load, the input impedance was measured at the bottom of the wire so that the mismatch could be determined. The power delivered to a matched load was then determined and the effective aperture of the configuration, with and without a resistive load on the opposite end of the wire, was computed. The effects of internal loading are observed and presented.

**OPTIMISING PATTERN SYNTHESIS  
USING  
CLASSICAL VARIATIONAL METHOD**

Xian-zhong Zhang  
Nanjing Research Institute of Electronics Technology  
Nanjing, Jiangsu 210013, PRC

**Abstract**

Many papers on pattern synthesis have been published. This paper tries to use Classical Variational Method (CVM) to optimise pattern synthesis of a line source and got success. The word "optimisation" used here means that the distribution has the highest aperture efficiency with meeting arbitrary given pattern restrictions.

The idea applied in this paper is ,first, suppose the radiation pattern  $F(u)$  is a real function and take the radiation field amplitude on the biggest field strength direction as a functional of aperture distribution  $f(x)$  which can be proven to be the form of  $f_1(x)-if_2(x)$ , where  $f_1(x)$  and  $f_2(x)$  are even and odd functions respectively. Second, using that 1) the energy on the line source is constant, 2)the given relationship between the desired pattern amplitude and main lobe, 3)derivative of  $F(u)$  with respect to  $u$  at peak position should be zero, one can establish isoperimetric condition set.

$$\int_{-1}^1 [f_1^2(x) + f_2^2(x)] dx = \text{const} \quad (1)$$

$$F(u_i) = a_i F(u_0) \quad i=1,2,\dots,n \quad (2)$$

$$\frac{dF}{du}(u=u_i) = 0 \quad i=1,2,\dots,n \quad (3)$$

where,  $n$  is the number of sidelobes to be controled. Third, construct a new functional and use well-known Euler-Lagrange equation to make up a set of equations. Finally, solve this equation set.

Optimising the pattern synthesis using CVM has the following advantages, 1)can flexibly control beam shape,null positions, sidelobe level and positions, and make one parameter optimised at the same time. 2)the results ( $f(x)$ ,  $F(u)$  and aperture efficiency) are expressed by analytic forms, which is much helpful for further analysis. 3)with clear geometrical and physical sense.



**SESSION URSI B-22****THURSDAY AM****PULSE AND TIME DOMAIN ANALYSES**

Chairs: R.W. Ziolkowski, University of Arizona; M.A. Ricoy, ERIM

Room: Alumni Center, Room 2

Time: 8:30-12:10

|       |   |     |
|-------|---|-----|
| 8:30  | APERTURE SYNTHESIS FOR ULTRAWIDEBAND/SHORT-PULSE RADIATION<br><i>Ehud Heyman, Tel-Aviv University</i>   | 356 |
| 8:50  | ON THE TRANSMISSION OF AN UNDISTORTED BROADBAND PULSED BEAM<br><i>Itshak Dvir*, Pinchas D. Einziger, Technion - Israel Institute of Technology</i>                      | 357 |
| 9:10  | DISTORTION OF TRANSIENT PULSED FIELDS IN PROPAGATION ABOVE A HIGHLY REFRACTIVE HALF-SPACE<br><i>Thomas Alan Winchester, Defense Science and Technology Organisation</i> | 358 |
| 9:30  | PULSED FIELD DIFFRACTION BY A PERFECTLY CONDUCTING WEDGE: A SPECTRAL THEORY OF TRANSIENTS ANALYSIS<br><i>Reuven Ianconescu, Ehud Heyman*, Tel-Aviv University</i>       | 359 |
| 9:50  | PULSED BEAM DIFFRACTION BY A PERFECTLY CONDUCTING WEDGE: EXACT SOLUTION AND PARAXIAL APPROXIMATIONS<br><i>Reuven Ianconescu, Ehud Heyman*, Tel-Aviv University</i>      | 360 |
| 10:10 | BREAK   |     |
| 10:30 | IMPROVING THE STABILITY OF MARCHING ON IN TIME METHOD USING FIR DIGITAL FILTERS<br><i>Ali Sadigh*, Ercument Arvas, Syracuse University</i>                              | 361 |
| 10:50 | APERTURE EXCITATION OF LW PULSES<br><i>A.M. Shaarawi, Cairo University; A.A. Chatzipetros, I.M. Besieris, Virginia Polytechnic Institute and State University</i>       | 362 |
| 11:10 | HIGH RESOLUTION TIME DOMAIN ANALYSIS OF VHF/UHF RCS MEASUREMENTS<br><i>M.J. Gerry, E.K. Walton, The Ohio State University</i>   | 363 |
| 11:30 | WIDEBAND SCATTERING ANALYSIS OF AN ARCHIMEDEAN SPIRAL ANTENNA<br><i>T.G. Moore, F.P. Hunsberger, Massachusetts Institute of Technology</i>                              | 364 |
| 11:50 | A MECHANISM FOR THE PRODUCTION OF ELECTROMAGNETIC RADIATION DURING FRACTURE OF BRITTLE MATERIALS<br><i>Steven G. O'Keefe*, David V. Thiel, Griffith University</i>      | 365 |

## APERTURE SYNTHESIS FOR ULTRAWIDEBAND/SHORT-PULSE RADIATION

Ehud Heyman

Tel-Aviv University, Faculty of Engineering,  
Dept. of Electrical Engineering - Physical Electronics,  
Tel-Aviv, 69978, Israel

### ABSTRACT

The paper discusses some basic principles in aperture synthesis for radiation of impulse-like fields. It is well known that there is a time-derivative relation between the aperture field and the field in the far radiation zone. In the frequency domain, this relation has the form of a  $j\omega$  term in the transfer function that connects the spatial Fourier transform of the aperture field with the far zone radiation pattern. One way to compensate for this relation in order to radiate impulse-like fields is to use wideband sources whose frequency spectrum is proportional to  $(j\omega)^{-1}$  [C.E. Baum, "Aperture efficiencies of impulse-like transient fields", SSN-328, 1991]. In the present paper we show that a major disadvantage in this realization is that the low frequency components diffract at wide angles near the source plane, thereby hampering the effective efficiency of the impulse antenna. We also show that it is possible to compensate for the aforementioned time derivative relations by using aperture synthesis in space-time. It is demonstrated that this relation is a direct consequence of the frequency dependence of the Fresnel distance of the aperture. The time-derivative relation can therefore be compensated for by choosing an aperture distribution that has a frequency independent Fresnel distance. The resulting time-dependent field has the form of a pulsed beam (PB), i.e., a collimated impulse-like space-time wavepacket that remains confined all the way from the near to the far zone. No field components are therefore lost due to diffraction. We present expressions for the time-dependent source distribution for this case.

## ON THE TRANSMISSION OF AN UNDISTORTED BROADBAND PULSED BEAM

Itshak Dvir\* and Pinchas D. Einziger  
 Department of Electrical Engineering,  
 Technion - Israel Institute of Technology Haifa, Israel 32000

Pulsed beams characterized by highly localized electromagnetic energy in space-time have received a due attention recently (e.g., R. W. Ziolkowski, IEEE Trans. Antennas Propagat., 40, 8, 888-905, 1992, P.D. Einziger & S. Raz, J. Opt. Soc. Am. A, 4, 3-10, 1987). The localization characteristic hold promising in applications such as ultra-wide bandwidth pulse-driven arrays, covert broadband communication, artificial vision, and high resolution detection and reconstruction. Unfortunately, while for properly executing some of these applications the pulsed beam time-envelope has to be maintained undistorted, strong distortion is unavoidable due to the space-time dispersion associated with the broadband signal propagation mechanism, even in homogenous-nondispersive media. Thus, it would be desirable to synthesize the space-time source distribution, aiming to support an undistorted time-signal.

The proposed synthesis scheme, obtained through a direct inversion of the space-time radiation integral connecting the source plane ( $z=0$ ) and the arbitrary observation plane ( $z=z_0$ ), results in an explicit expression for the spectral content of the source distribution, a necessary and sufficient constraint for an undistorted signal at  $z_0$ :

$$\mathbf{e}_t(\mathbf{r}, \omega) = \frac{\omega}{\omega_0} \mathbf{e}_t \left( \mathbf{r} \frac{\omega}{\omega_0}, \omega_0 \right) \exp \left[ ik \frac{r^2}{2z_0} \left( \frac{\omega}{\omega_0} - 1 \right) \right] ,$$

where  $\mathbf{e}_t(\mathbf{r}, \omega_0)$  is the tangential field source distribution at  $\omega=\omega_0$ ,  $\mathbf{r}$  and  $k$  are the source coordinates,  $\mathbf{r}=(x, y, 0)$ , and the wave number,  $k=\omega/v$ , respectively. It should be noted that the source distribution undergoes frequency dependent focusing, scaling, and amplitude variations. The focusing term depends also on the observation plane location  $z=z_0$ , continuously varying from the near field to the far field zones, and can be implemented by a dispersive thin lens. Finally, the above expression may be utilized for synthesizing pulse-driven array-elements.

## DISTORTION OF TRANSIENT PULSED FIELDS IN PROPAGATION ABOVE A HIGHLY REFRACTIVE HALF-SPACE

Thomas Alan Winchester  
Defence Science and Technology Organisation  
PO Box 1500,  
Salisbury SA 5108 Australia

**Abstract** In this discussion we examine the pulse distortion of a transient electromagnetic pulse generated by an arbitrarily oriented transient current element propagating over a highly refractive half-space. Both electric and magnetic current sources are considered. The technique is based upon the Exact Image Theory developed by Lindell and Alanen, thus avoiding many of the problems associated with the evaluation of the Sommerfield integrals (IEEE Trans. Antennas Propagat., Vol.AP-32: no.2 pp 126-133 Feb.1984, no.8 pp 841-847 Aug.1984, no.10 pp 1027-1032 Oct.1984).

In this formulation, the image currents are allowed to exist in a complex space. Asymptotic expressions for the image currents are available when the refracting effect of medium is large. When a Taylor series expansion of the complex distance to the image current is used, the integrals can be evaluated analytically. FFT techniques are then used to obtain time domain results for a given electric or magnetic current pulse. The validity of the Taylor Series approximation used is discussed in further detail. A simple formulae is obtained from which validity of the Taylor Series approximation can be assessed for a given physical application. With due regard given to the spectral content of the transient pulse, it is shown that the propagation of transient pulses close to the interface, and direct reflections from below the current element, can be analysed accurately using this technique.

The formulae obtained can be written in terms of the complementary error function of a complex argument. The asymptotic expansion of this formulae yields a result which, close to the interface, is essentially that of the Surface-Wave expansion. However, the formulae discussed here are valid for all angles and in the extreme far-field reduce to the Reflection Coefficient Method (RCM). The efficiency of this computational technique enables the practical use of frequency domain methods to analyse the reflection of transient pulses over a highly refractive half-space. Example calculations are provided using a Gaussian current pulse, and the validity of the RCM is discussed. Regimes in which significant distortion of a transient pulse occurs are identified.

**PULSED FIELD DIFFRACTION BY A PERFECTLY CONDUCTING WEDGE:  
A SPECTRAL THEORY OF TRANSIENTS ANALYSIS**

Reuven Ianonescu and Ehud Heyman\*

Tel-Aviv University, Faculty of Engineering,  
Dept. of Electrical Engineering - Physical Electronics,  
Tel-Aviv, 69978, Israel

**ABSTRACT**

The canonical problem of pulsed field diffraction by a perfectly conducting wedge is analyzed directly in the time domain via the spectral theory of transients (STT). Within this framework, the diffracted field is expressed as a spectral integral of time-dependent (pulsed) plane waves. Closed form expressions for the pulse response are obtained via analytic evaluation of this integral. For impulsive excitation, the final results are identical to those obtained previously via time-harmonic spectral integral techniques; the STT route, however explains explicitly in the time domain how the spectral contributions add up to construct the field. Via the STT route we also derive new solutions for a *finite* (non-delta) incident pulse. The finite pulse response parametrizes the field in terms of the ratio  $vT/\ell_0$ , where  $v$  is the wave speed,  $T$  is the pulse length and  $\ell_0$  is the ray path. Special attention is given to the field structure near the wavefront and in various transition regions. Finally, an important feature of the present STT solution, which in fact motivated this study, is that it can be extended to wedge-diffraction of pulsed beam fields (i.e. space-time wavepackets). This subject is addressed in a companion paper.

**PULSED BEAM DIFFRACTION BY A PERFECTLY  
CONDUCTING WEDGE:  
EXACT SOLUTION AND PARAXIAL APPROXIMATIONS**

Reuven Ianconescu and Ehud Heyman\*

Tel-Aviv University, Faculty of Engineering,  
Dept. of Electrical Engineering - Physical Electronics,  
Tel-Aviv, 69978, Israel

**ABSTRACT**

Pulsed beam (PB) are highly localized space-time wavepackets that propagate along ray trajectories. Because they have these properties they are useful in modeling applications addressing highly focused energy transfer, local (high resolution) interrogation or probing of the propagation environment, etc. In previous publications we showed how the complex source model can be used to derive exact closed form solution for certain pulsed beam scattering problems. The present paper addresses the new canonical problem of PB scattering by a perfectly conducting wedge. The exact field solution for the diffracted wavepacket is derived using a systematic procedure based on the previously introduced spectral theory of transients (STT). Further insight into the structure of the local scattering mechanism is gained by developing uniform local models for the diffracted wavepacket. They explain, uniformly, the full richness of the scattering phenomena as a function of the incident wavepacket parameters: Its direction and distance from the vertex and its spatial and temporal collimation. It is shown that if the incident wavepacket strikes near the vertex, it generates a toroidal diffracted wavepacket that propagates essentially along Keller cone, as well as shadow boundaries effects in the geometrical optics transition regions. As the distance from the vertex grows this diffraction model is gradually deformed into a geometrical optics model. The excitation strength of these phenomena are parametrized in terms of the space-time collimation properties of the incident wavepacket. The results demonstrate how highly focused pulsed fields can be used to probe the scatterer locally.

## IMPROVING THE STABILITY OF MARCHING ON IN TIME METHOD USING FIR DIGITAL FILTERS

Ali Sadigh\* and Ercument Arvas

Department of Electrical and Computer Engineering  
Syracuse University, Syracuse, NY 13244

The Integral equation formulation along with the marching on in time method is a well known procedure to solve the scattering from objects in time domain. Unfortunately, these solutions tend to be unstable in the late times. These instabilities are often observed in an exponentially growing form which make the solution of certain problems inaccurate if not impossible.

In this study, an EFIE formulation in time domain is applied to perfectly conducting bodies of arbitrary shape. Triangular patches and expansion functions are employed to approximate the surface and the equivalent electric current on the object, respectively. The formulation of the problem involves only the first derivative of the magnetic vector potential. The system is excited by a plane Gaussian pulse and the marching on in time method is used to solve for the unknown current coefficients by stepping in time. In order to eliminate/reduce the oscillatory behavior of the solution in late times, a finite duration impulse response (FIR) digital filter is used. Since the bandwidth of the incident wave is known, it is possible to design an FIR filter prior to the solution and use it to filter out the unwanted responses throughout the stepping process. The method is very similar to block convolution. Here after computing all the currents for some certain number of steps, each of them is convoluted (either directly or by using FFT) with the impulse response of the FIR filter. Using this method, the components of the solution outside the bandwidth of the filter are reduced each time we apply the convolution. These "clean" currents are then used in the next time steps and the process repeats. This has proved to be very effective in eliminating the spurious late time oscillations or reduce them to a trivial level. FIR filters introduce a constant group delay. This translates to a known constant time delay which is compensated for in the course of solution. This method in a special case reduces to the three point averaging scheme used by Rynne and Smith (JEWIA, Vol. 4, No. 12, pp. 1181-1205, 1990). The numerical results, while agreeing very well with the published data, show great improvement in the late times.

## APERTURE EXCITATION OF LW PULSES

by

A. M. Shaarawi

Department of Engineering Physics and Mathematics

Cairo University, Giza, Egypt

and

A. A. Chatzipetros, I. M. Besieris

Bradley Department of Electrical Engineering

Virginia Polytechnic Institute and State University

Blacksburg, Virginia 24061

It is known that FWM-like solutions can be synthesized as a superposition of Bessel beams with appropriate choice of spectra. It has been shown that a Bessel beam defined initially on an infinite plane (e.g. the  $z = 0$  plane) will propagate under the effect of Huygen's operator in the positive  $z$ -direction and that the contributions from the acausal negative  $z$ -components sum up to zero. Such a proof can be applied directly to the FWM pulse to show that, under certain conditions on the free parameters  $a_1$  and  $\beta$ , it has no acausal incoming wave contributions. In fact, for a particular choice of  $a_1$  and  $\beta$ , it will be shown that the FWM pulse can be launched from an aperture with radius that shrinks from infinity to a finite value and expands once more to infinity. Such a time-varying aperture needs an infinite time of excitation. In contradistinction to the other solutions that could be excited from an infinite aperture, like plane waves and Bessel beams, the FWM pulse does not require infinite power for the aperture excitation. This is the case because as the aperture becomes infinitely large, the power density of the field exciting the aperture decreases to zero at a rate  $(ct)^{-2}$  while the area of the aperture increases as  $(ct)^2$ . These two effects balance each other and the energy on the aperture remains constant. Such an excitation acts like a temporal focusing aperture, concentrating an extremely weak field distributed over a huge aperture onto a much smaller one, which in turn expands once more to infinity.

In this work, we shall also present results of finite-time excitation of time-varying apertures mentioned above. The analysis is carried out by keeping the excitation time of the FWM aperture finite. This can be done by imposing a Gaussian time window on the excitation field of the aperture. The resulting solution has finite energy and it is dispersive, unlike the FWM pulse. The Rayleigh range of such a pulse is calculated and compared to three different diffraction lengths: the Gaussian pulse diffraction length for a static aperture, the Hafizi-Sprangle diffraction length for an expanding aperture, and the plane-wave diffraction length for an aperture excited by a plane wave. Under special conditions and using the above Gaussian time-window, the diffraction length of the finite-energy FWM pulse can be made larger than the diffraction lengths mentioned above. Other finite-energy pulses, e.g., MPS pulse, are also examined.

## HIGH RESOLUTION TIME DOMAIN ANALYSIS OF VHF/UHF RCS MEASUREMENTS

M. J. Gerry\* and E. K. Walton  
The Ohio State University ElectroScience Laboratory  
Department of Electrical Engineering  
1320 Kinnear Rd  
Columbus, Ohio 43212-1191

The experimental study of the backscatter of a cylinder and an ogive support structure is presented. The emphasis of the study is on the signal processing used to observe the electromagnetic interaction of the cylinder with the ogive. These interaction terms are found to be very small in amplitude and localized in frequency. As a result, the resolution and signal to noise ratio of the algorithms used in the signal processing are very important. For this reason, both parametric and classical methods are studied, with the parametric method displaying high resolution at small bandwidths, thus providing unique insight in the behavior of the target.

It is well known that radar data measured in the frequency domain is more readily analyzed in the time domain. Classical time domain analysis involves using the Fourier Transform to find the impulse response of a target. It is known that the resolution of the FT is the inverse of the measured bandwidth. In this case, where two GHz of frequency (50-2000MHz) data are available, the FT has a time domain resolution of only 0.5 nanoseconds which corresponds to approximately six inches.

Parametric spectral estimation can greatly increase resolution by assuming a model for the scattering behavior of the target and solving for the parameters of that model. More specifically, the scattering behavior of the target is assumed to be a sum of complex sinusoids with unknown amplitudes and phase centers. A Forward Backward Linear Prediction technique is used to solve for the phase centers. A singular value decomposition is used to solve for the amplitudes of the sinusoids. Moreover, because the algorithm involves the use of a model the resolution is not dependent on measured bandwidth. In fact, very narrow bands of data can be analyzed with very high resolution, allowing for the use of these algorithms in the study of frequency dependent scattering.

High resolution time domain analysis using narrow bands of data allows for the location of the interactions between the cylinder and its ogive support structure. Bandwidths as narrow as 200 MHz are used in the signal processing to isolate the frequency behavior of various scattering mechanisms.

## **WIDEBAND SCATTERING ANALYSIS OF AN ARCHIMEDIAN SPIRAL ANTENNA**

T. G. Moore  
F. P. Hunsberger

Lincoln Laboratory  
Massachusetts Institute of Technology

When detailed examination of radar images is performed there can be significant information obtained about particular scatterers based upon information in the image. An antenna is a typical scatterer which presents a unique signature in a radar image, and typically provides sufficient information in the scattered field to estimate important parameters.

In this paper we consider the wideband scattering response of a two-arm Archimedian spiral antenna. The investigation is performed using the Finite-Difference Time-Domain method. Computed wideband monostatic radar cross sections for various look angles are reported, along with comparisons to Method of Moments solutions. The near-field mechanisms responsible for the scattering are discussed.

Based upon the detailed analysis of the scattering mechanisms, an approach is presented to estimate the critical parameters of a spiral antenna from the wideband scattered field response. A particular example is presented to demonstrate the estimation of these parameters.

# A MECHANISM FOR RADIATION-INDUCED PRODUCTION OF ELECTROMAGNETIC FRACTURE OF BRITTLE MATERIALS.

en G. O'Keefe\* and David V. Thiel  
chool of Microelectronic Engineering  
Griffith University  
Nathan, Brisbane 4111 Australia.

For effects have investigated rock and ice. Many theories have been  
suggested especially for rock fracture, but this theory  
is the crack propagates more charge will cause current to flow around the edges of the  
apex of the crack. This process and the EM radiation produced can be  
predicted by a Sturm Liouville solution of the apex current for a one dimensional case.

expression was verified using a one dimensional finite difference model and gives  
dimensions which allows examination of the potential over a crack surface. When two  
crack is symmetrical, the currents flowing in the parallel surfaces of the crack are the  
equal amplitude and opposite direction. Because these sheet currents are very close together  
the EM radiation produced by these sheet currents will cancel. The current flowing  
around the crack apex is however not mirrored and will produce EM radiation. This  
radiation will be polarised according to the orientation of the crack. Both of these  
effects have been observed after rock blasting in quarries. After the blast the newly  
exposed rock face will relax after the rock in front of it has been removed. This causes  
cracking. The cracks will form in approximately the same plane to relieve this stress.  
The EM radiation produced by each crack should therefore be similarly polarised. This  
effect has been observed by receiving the EM radiation on differently polarised. This  
antennas. Some antennas receive strong signals while others receive very little. The  
stress relieving cracks, (or crack extensions), occur in long strings where a crack  
produces a pulse of radiation. These strings are often started or terminated with a large  
pulse indicating a larger crack. These strings are often started or terminated with a large  
stress from an area. The shape of the signal received on an antenna will correspond to  
the current around the crack apex. Because of the relatively small capacitance produced by  
the crack surfaces the time over which radiation is produced is predicted to be quite  
short. The relationship between the model and measured signals is predicted to be quite  
information about crack formation and propagation. Recent experimental and numerical  
results will be presented.



THURSDAY PM

SESSION CANONICAL PROBLEMS

R.G. Plumb, University of Kansas; J.W. Burns, ERIM  
anguages Building, Lecture Room 1

Time: 1:30-5:10

SESSION ELECTRIC SCATTERING BY AN OPEN-ENDED CONDUCTING 368  
is\*, Robert W. Scharstein, The University of Alabama

SESSION FOR THE DIELECTRIC WEDGE 369  
'ein, The University of Alabama

SESSION AND RADIATION IN THE PRESENCE OF A MATERIAL 370  
F. Otero\*, Roberto G. Rojas, The Ohio State University

SESSION A COMPARISON OF THE IMPEDANCE BOUNDARY CONDITION 371  
SPHEROID FORMULATION AND EXACT SOLUTION FOR A COATED PROLATE

J.D. Kotulski, Sandia National Laboratories

SESSION THEORETICAL STUDY AND OPTIMIZATION OF A BIDIMENSIONAL 372  
CAPACITIVE GRATING STANDING ABOVE A BACKED METAL SUBSTRATE

J.Y. Suratteau, Aérospatiale Espace et Défense; D. Maystre, M. Saillard,

SESSION Faculté des Sciences de St-Jérôme

SESSION BREAK 373

SESSION POLARIZED RESPONSE TO WEDGE SHARPNESS

Richard S. Grannemann\*, Charles S. Liang, General Dynamics

SESSION SCATTERING OF A TUBULAR CYLINDER WITH DIFFERENT INSIDE AND 374  
OUTSIDE SURFACE IMPEDANCES

Hung-Mou Lee, Naval Postgraduate School

SESSION DIFFRACTION BY A PARALLEL-PLATE WAVEGUIDE CAVITY WITH TWO- 375  
LAYER MATERIAL LOADING

Takeshi Momose, Shioichi Koshikawa, Kazuya Kobayashi\*, Chuo University

SESSION ANALYSIS OF A WIRE IN THE PRESENCE OF A HOLLOW BODY OF 376  
REVOLUTION WITH AN APERTURE

Zhiqiang Qiu\*, Chalmers M. Butler, Clemson University

SESSION DIFFRACTION OF ELECTROMAGNETIC WAVES AT BLACK BODIES 377  
THE PROBLEM OF INVISIBLE OBJECTS

P. Ya. Ufimtsev, University of California, Los Angeles

2:50

3:10  
3:30

3:50

4:10

4:30

4:50

367

ELECTROMAGNETIC SCATTERING BY A  
OPEN-ENDED CONDUCTING FRUSTUM

ANTHONY M. J. DAVIS\*  
DEPARTMENT OF MATHEMATICS  
UNIVERSITY OF TORONTO

AND

ROBERT W. SCHARSTEIN  
DEPARTMENT OF ELECTRICAL ENGINEERING  
UNIVERSITY OF ALABAMA  
TUSCALOOSA, ALABAMA 35487

W. SCHARSTEIN  
OF ELECTRICAL ENG.  
THE UNIVERSITY OF ALABAMA 35487  
TUSCALOOSA, ALABAMA

DEPARTMENT OF ELECTRICAL ENGINEERING  
THE UNIVERSITY OF ALABAMA  
TUSCALOOSA, ALABAMA 35487

## HIGH RESOLUTION TIME DOMAIN ANALYSIS OF VHF/UHF RCS MEASUREMENTS

M. J. Gerry\* and E. K. Walton  
The Ohio State University ElectroScience Laboratory  
Department of Electrical Engineering  
1320 Kinnear Rd  
Columbus, Ohio 43212-1191

The experimental study of the backscatter of a cylinder and an ogival support structure is presented. The emphasis of the study is on the signal processing used to observe the electromagnetic interaction of the cylinder with the ogive. These interaction terms are found to be very small in amplitude and localized in frequency. As a result, the resolution and signal to noise ratio of the algorithms used in the signal processing are very important. For this reason, both parametric and classical methods are studied, with the parametric method displaying high resolution at small bandwidths, thus providing unique insight in the behavior of the target.

It is well known that radar data measured in the frequency domain is more readily analyzed in the time domain. Classical time domain analysis involves using the Fourier Transform to find the impulse response of a target. It is known that the resolution of the FT is the inverse of the measured bandwidth. In this case, where two GHz of frequency (50-2000MHz) data are available, the FT has a time domain resolution of only 0.5 nanoseconds which corresponds to approximately six inches.

Parametric spectral estimation can greatly increase resolution by assuming a model for the scattering behavior of the target and solving for the parameters of that model. More specifically, the scattering behavior of the target is assumed to be a sum of complex sinusoids with unknown amplitudes and phase centers. A Forward Backward Linear Prediction technique is used to solve for the phase centers. A singular value decomposition is used to solve for the amplitudes of the sinusoids. Moreover, because the algorithm involves the use of a model the resolution is not dependent on measured bandwidth. In fact, very narrow bands of data can be analyzed with very high resolution, allowing for the use of these algorithms in the study of frequency dependent scattering.

High resolution time domain analysis using narrow bands of data allows for the location of the interactions between the cylinder and its ogive support structure. Bandwidths as narrow as 200 MHz are used in the signal processing to isolate the frequency behavior of various scattering mechanisms.

## **WIDEBAND SCATTERING ANALYSIS OF AN ARCHIMEDEAN SPIRAL ANTENNA**

T. G. Moore  
F. P. Hunsberger

Lincoln Laboratory  
Massachusetts Institute of Technology

When detailed examination of radar images is performed there can be significant information obtained about particular scatterers based upon information in the image. An antenna is a typical scatterer which presents a unique signature in a radar image, and typically provides sufficient information in the scattered field to estimate important parameters.

In this paper we consider the wideband scattering response of a two-arm Archimedean spiral antenna. The investigation is performed using the Finite-Difference Time-Domain method. Computed wideband monostatic radar cross sections for various look angles are reported, along with comparisons to Method of Moments solutions. The near-field mechanisms responsible for the scattering are discussed.

Based upon the detailed analysis of the scattering mechanisms, an approach is presented to estimate the critical parameters of a spiral antenna from the wideband scattered field response. A particular example is presented to demonstrate the estimation of these parameters.

## A MECHANISM FOR THE PRODUCTION OF ELECTROMAGNETIC RADIATION DURING FRACTURE OF BRITTLE MATERIALS.

Steven G. O'Keefe\* and David V. Thiel  
School of Microelectronic Engineering  
Griffith University  
Nathan, Brisbane 4111 Australia.

For some time electromagnetic radiation has been associated with the fracturing of brittle solids. The authors have investigated rock and ice. Many theories have been suggested as the cause of this radiation but none has been completely validated. Piezoelectric effects have been suggested especially for rock fracture, but this theory does not explain radiation from non-piezo materials. A charge separation mechanism is proposed as the source of this radiation. As a crack forms in a material, charge will be separated and stored on each side of the crack. This charge would be produced by breaking chemical bonds and may also be aided by piezo effects in suitable materials. In a conducting material this charge will cause current to flow around the edges of the crack. As the crack propagates more charge is produced and more current will flow around the apex of the crack. This process and the EM radiation produced can be described by a Sturm Liouville solution of the apex current for a one dimensional case.

This expression was verified using a one dimensional finite difference model and gives good agreement to the analytical expression. The model was extended into two dimensions which allows examination of the potential over a crack surface. When the crack is symmetrical, the currents flowing in the parallel surfaces of the crack are of equal amplitude and opposite direction. Because these surfaces are very close together the EM radiation produced by these sheet currents will cancel. The current flowing around the crack apex is however not mirrored and will produce EM radiation. This radiation will be polarised according to the orientation of the crack. Both of these effects have been observed after rock blasting in quarries. After the blast the newly exposed rock face will relax after the rock in front of it has been removed. This causes cracking. The cracks will form in approximately the same plane to relieve this stress. The EM radiation produced by each crack should therefore be similarly polarised. This effect has been observed by receiving the EM radiation on differently polarised antennas. Some antennas receive strong signals while others receive very little. The stress relieving cracks, (or crack extensions), occur in long strings where each crack produces a pulse of radiation. These strings are often started or terminated with a large pulse indicating a larger crack which shifts stress into a new area of rock or relieves stress from an area. The shape of the signal received on an antenna will correspond to the current around the crack apex. Because of the relatively small capacitance provided by the crack surfaces the time over which radiation is produced is predicted to be quite short. The relationship between the model and measured signals allows one to deduce information about crack formation and propagation. Recent experimental and numerical results will be presented.



## CANONICAL PROBLEMS

Chairs: R.G. Plumb, University of Kansas; J.W. Burns, ERIM

Room: Modern Languages Building, Lecture Room 1      Time: 1:30-5:10

|      |   |     |
|------|---|-----|
| 1:30 | ELECTROMAGNETIC SCATTERING BY AN OPEN-ENDED CONDUCTING FRUSTUM<br><i>Anthony M.J. Davis*, Robert W. Scharstein, The University of Alabama</i>   | 368 |
| 1:50 | STATIC SOLUTION FOR THE DIELECTRIC WEDGE<br><i>Robert W. Scharstein, The University of Alabama</i>  | 369 |
| 2:10 | SCATTERING AND RADIATION IN THE PRESENCE OF A MATERIAL LOADED IMPEDANCE WEDGE<br><i>Michael F. Otero*, Roberto G. Rojas, The Ohio State University</i>  | 370 |
| 2:30 | A COMPARISON OF THE IMPEDANCE BOUNDARY CONDITION FORMULATION AND EXACT SOLUTION FOR A COATED PROLATE SPHEROID<br><i>J.D. Kotulski, Sandia National Laboratories</i>   | 371 |
| 2:50 | THEORETICAL STUDY AND OPTIMIZATION OF A BIDIMENSIONAL CAPACITIVE GRATING STANDING ABOVE A BACKED METAL SUBSTRATE<br><i>J.Y. Suratteau, Aérospatiale Espace et Défense; D. Maystre, M. Saillard, Faculté des Sciences de St-Jérôme</i> | 372 |
| 3:10 | BREAK   |     |
| 3:30 | POLARIZED RESPONSE TO WEDGE SHARPNESS<br><i>Richard S. Grannemann*, Charles S. Liang, General Dynamics</i>  | 373 |
| 3:50 | SCATTERING OF A TUBULAR CYLINDER WITH DIFFERENT INSIDE AND OUTSIDE SURFACE IMPEDANCES<br><i>Hung-Mou Lee, Naval Postgraduate School</i>   | 374 |
| 4:10 | DIFFRACTION BY A PARALLEL-PLATE WAVEGUIDE CAVITY WITH TWO-LAYER MATERIAL LOADING<br><i>Takeshi Momose, Shoichi Koshikawa, Kazuya Kobayashi*, Chuo University</i>  | 375 |
| 4:30 | ANALYSIS OF A WIRE IN THE PRESENCE OF A HOLLOW BODY OF REVOLUTION WITH AN APERTURE<br><i>Zhiqiang Qiu*, Chalmers M. Butler, Clemson University</i>  | 376 |
| 4:50 | DIFFRACTION OF ELECTROMAGNETIC WAVES AT BLACK BODIES AND THE PROBLEM OF INVISIBLE OBJECTS<br><i>P. Ya. Ufimtsev, University of California, Los Angeles</i>  | 377 |

Thu. p.m.

**ELECTROMAGNETIC SCATTERING BY AN  
OPEN-ENDED CONDUCTING FRUSTUM**

**ANTHONY M. J. DAVIS\***  
DEPARTMENT OF MATHEMATICS

AND

**ROBERT W. SCHARSTEIN**  
DEPARTMENT OF ELECTRICAL ENGINEERING

**THE UNIVERSITY OF ALABAMA  
TUSCALOOSA, ALABAMA 35487**

A mixed boundary value problem is formulated for the surface currents that are induced by a time-harmonic plane wave incident upon an open-ended conductor whose shape is a frustum, namely a finite length portion of a cone. Scattered fields are represented in terms of the uncoupled azimuthal Fourier modes of this body of revolution. Physically, the scattering may be regarded as a distortion of that previously determined for an open-ended tube since the same essential features must be exhibited. This reasoning provides an appropriate mathematical formulation for this more complicated geometry. Thus, after a suitable change of the radial coordinate, the integral equation for the surface currents can be reduced, for each azimuthal mode, to a set of linear equations by means of a Galerkin expansion of the currents in terms of Chebyshev polynomials with edge-condition weighting. Resultant surface currents and axial fields are calculated for several combinations of scatterer geometry and frequency. Induced vector currents on the frustum can exhibit extreme variation over the conducting surface, in both the azimuthal and radial directions. The numerical implementation of this mathematical analysis yields a complete and accurate solution for both the circumferential and radial currents, as a function of electrical length, frustum angle and aspect ratio, and the polarization and orientation of the incident plane wave. The standing wave nature of the surface currents indicates that the interaction between the exciting plane wave and the frustum ends occurs via the external surface and internal guided waves of the nonuniform waveguide.

## NOTION FOR THE DIELECTRIC WEDGE

STATY

ROBERT W. SCHARSTEIN  
DEPARTMENT OF ELECTRICAL ENGINEERING  
THE UNIVERSITY OF ALABAMA  
TUSCALOOSA, ALABAMA 35487

The Mellin transform is applied to the classical boundary value problem of a line source excitation for Poisson's equation in a two-media geometry. The wedge angle  $2\alpha$  and the dielectric contrast  $\epsilon_1/\epsilon_2$  are arbitrary. Even symmetry about the wedge bisector is employed to simplify the mathematics. The radial coordinate is transformed according to the Mellin transform, upon which boundary conditions are applied in the remaining azimuthal coordinate of the polar system. Although this important static problem is of great interest in dynamic wave problems, and in particular as a canonical geometry for the study of dielectric edge conditions, and is often hinted at in the literature, no complete solution has been uncovered by this author. The occurrence of complete even symmetry where the line source lies on the wedge bisector is treated in a soviet text (N.N. Lebedev, I.P. Skalskaya, and Y.S. Uflyand, *Worked Problems in Applied Mathematics*, Dover, 1965). In the case where the wedge angle is a rational multiple of  $\pi$ , the poles of the transform can be nicely represented and the inverse Mellin transform becomes a sum of analytic terms. This unique solution satisfies all of the physical boundary conditions plus Laplace's equation. Resultant static field distributions are presented for several example geometries, and the exact edge behavior is extracted from the analytic solution. Besides the present interest in the potential behavior for the penetrable wedge, this is a pretty example problem to use in a graduate course on boundary value problems or complex variable theory.

SCATTERING AND RADIATION  
PRESENCE OF A MATERIAL IN THE  
IMPEDANCE WEDGE <sup>ED</sup>

Michael F. Otero\* and Roberto G. Rojas  
Ohio State University ElectroScience Lab.  
Columbus, Ohio 43212

A two dimensional Green's function for a wedge whose faces satisfy the Tovtovich boundary conditions, which is very efficient for numerical computation, was developed last year (R.G. Rojas & M.F. Otero, 1992 URSI Digest, 444). The present paper discusses the use of this Green's function to solve scattering as well as radiation problems. The scattering problem involves the diffraction of an incident plane wave by a two-dimensional material body of arbitrary shape which is in the vicinity of or attached to the tip of the wedge. The purpose of this study is to investigate how the material parameters and shape of the body affect the diffraction from the tip of the wedge. The radiation problem involves the study of the radiation of two dimensional slot antennas mounted on the faces of the impedance wedge. As in the scattering problem, the effect of the material body on the radiation pattern of the antennas will be investigated.

The method of analysis is the Moment Method/Green's function scheme where a set of integral equations with as few unknowns as possible has been developed. Note that due to the presence of the material body which couples the various components of the electric and magnetic fields, it is important to obtain integral equations with this property; otherwise, the resulting matrix equation becomes too large for practical applications. Several examples will be shown illustrating the effect of the impedance values of the faces of the wedge as well as the shape and material parameters of the material body on the scattering and radiation problems discussed above.

Comparison of the Impedance Boundary Condition  
and Exact Solution for a Coated Prolate Spheroid

J. D. Kotulski  
Sandia National Laboratories  
Radiation and Electromagnetic Analysis, Dept. 9352  
Albuquerque, NM 87185-5800

Impedance boundary condition has been used effectively to analyze conductive scatterers coated with a dielectric or magnetic material. The applicability of this method has been described by previous investigators and depends on a number of parameters that include the refractive index, radius of curvature, and the thickness of the coating layer with respect to frequency. A test problem to examine the accuracy of this boundary condition is the coated conducting spheroid. This problem can be formulated using an eigenfunction expansion when an impedance boundary condition is used or when the coated conducting spheroid is retained. This is due to the separable nature of the coordinate system. Additionally, the surface of the prolate spheroidal scatterer can be varied to examine two limiting cases -- the wire and the sphere.

The purpose of this paper is to compare the solutions of a coated conducting spheroid excited by an equatorial gap using two different assumptions that account for the coating. The first assumption uses the impedance boundary condition on the surface to account for the coating while the second solves the coated spheroid with no simplifications for the coating layer. The coating can be magnetic or dielectric with conductivity or loss. The input admittance values obtained using both methods are compared. Furthermore, the poles of the input admittance are examined in the complex s-plane. This allows a closer look at the resonance structure of the antenna in the context of the Singularity Expansion Method (SEM). Once this comparison has been made the limiting cases can be considered (the wire and the sphere) where previous results will be compared and discussed.

THEORETICAL STUDY AND OPTIMIZATION OF  
BIDIMENSIONAL CAPACITIVE GRATING STANDING AB  
A BACKED METAL SUBSTRATE.

J.Y. Suratteau\*, D. Maystre, M. Saillard

Laboratoire d'Optique Electromagnétique, Faculté des Sciences  
de St-Jérôme, 13397 Marseille Cedex 20 France, and \*Aérospatiale  
Espace et Défense, 78133 Les Mureaux Cedex France

We are seeking structures able to absorb waves in the radar range and not to emit in the infrared spectrum. For that we have studied and optimized a device composed of a metallic material backed plane substrate covered with a bidimensional capacitive grating of infinitely conducting metallic plates. With this aim in view, we have used the Wood anomalies which are close linked with the absorption of the incident energy and the excitation of a leaky wave in the vicinity of the structure.

The phenomenological theory of the Wood anomalies, elaborated by one of the authors ( D. Maystre ) for classical gratings, was applied to the present structure and we have shown that there exists an absorption which is linked with a complex pole and a complex zero of the scattering matrix of the device. In particular, in the vicinity of the absorption, when there is one propagating reflected Rayleigh order, the reflectivity, considered as a function of the wavelength of the incident wave, is very accurately described by an homographic function, depending of the pole and the zero. The localization of the pole and the zero in the complex plane of the wavelengths allows us to predict quantitatively the wavelength where there is a maximum absorption, the value of the minimum reflectivity and the bandwidth of the absorption.

We used a modal method to compute the reflected Rayleigh orders and to numerically determine the scattering matrix. The numerical computation of the pole and the zero of this matrix allows us to optimize the device by minimizing ( with the Powell algorithm ) a function which depends of the parameters of the structure.

PL  
absorbs how numerical results which prove the connection between the location of the reflected and the absorption of energy. In particular, the phenomenon of total reflection is pointed out when the zero lies on the real axis. Next, we will show some results from the Powell optimizing procedure.

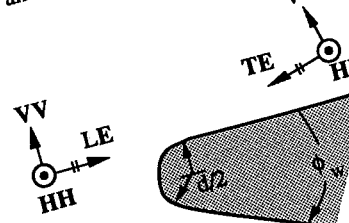
## NORMALIZED RESPONSE TO WEDGE SHARPNESS

Richard S. Grannemann\* and Charles S. Liang  
 General Dynamics/Fort Worth Division  
 Fort Worth, TX 76101

Magnetic scattering from a semi-infinite wedge with a blunt tip is an idealized wedge problem with relevance to many aerospace applications. A. Ross and M. A. K. Hamid, IEEE Trans. AP-19, No. 4, 509-515, 1971. The approximation of the blunt wedge with a sharp wedge is inadequate at sufficiently high, and approximation by variously shaped thin wedges which can artificially model these semi-infinite targets to a high degree of accuracy with finite targets with absorbing characteristics. This paper discusses the normalized radar signature design data for the blunt wedge by comparing the normalized response of a cylindrically capped wedge as a function of diameter and wedge angle over the spectrum between the high and low frequency limits.

The target geometry used in the computation is shown in the figure. The HH and VV polarization conventions and computation is shown in the figure. The illumination directions are indicated. In the LE case with a leading edge (LE) (cylindrically capped thick half-plane case), both the VV and HH returns converge asymptotically to the physical optics solution of a cylinder as tip diameter (in wavelengths) increases. For VV polarized response, the convergence is oscillatory due to the sensitivity of VV waves to first derivative surface discontinuities at the end-cap junctions producing small superimposing reflections. For HH polarized response, the convergence is smooth since generated surface irregularities are orthogonal to surface smoothness. As tip diameter becomes small, both returns approach that of a sharp half-plane. In the TE case of a cylindrically capped thick half-plane, both polarizations show attenuation from that of the thin half-plane. Curves representing the radar return for both polarizations and incidence directions over a four-decade range in tip diameter are presented. Deviation from the return of a sharp half-plane answers quantitatively the question "How sharp is sharp?".

As wedge angle is allowed to increase, the radar return, as expected, increases. Again, high and low frequency limits for the cylindrically capped wedge approach the physical optics blunt wedge solution and sharp edge wedge respectively. The design challenge is to derive the shape of the wedge in order to reduce the blunt wedge response to close to that of a half-plane with a corresponding tip thickness.



## SCATTERING OF A TUBULAR CYLINDER WITH DIFFERENT INSIDE AND OUTSIDE SURFACE IMPEDANCES

Hung-Mou Lee

Department of Electrical and Computer Engineering (EC/Lh)  
Naval Postgraduate School, Monterey, CA 93943-5100

Very accurate theoretical results on the scattering of a perfectly conducting tubular cylinder was reported [H.-M. Lee, *IEEE Trans. AP-35* (4), 384-390, 1987]. This was achieved through utilizing the double series representation for the Green's function [H.-M. Lee, *Radio Science*, 18 (1), 48-56, 1983] in solving the integrodifferential equations governing the surface current distribution on the cylinder.

Extension of this problem to include the case when the cylinder is coated differently on the inside and outside walls has been carried out. Each coated surface is modelled in terms of an impedance boundary condition. Because the cylinder is no longer perfectly conducting, the magnetic surface current, which is equivalent to the tangential components of the electric field intensity on the surface of the cylinder, has to be determined together with the electric surface current.

It can be deduced from the Stratton-Chu equations [J. A. Stratton, *Electromagnetic Theory*, Sec. 8.14, McGraw-Hill, 1941] that the sums, respectively of the magnetic and the electric types, of the surface currents on both sides of the infinitesimally thin wall of the cylinder determine the radiation completely. The tangential components of the sums of the radiated field intensities on both sides of the wall are then linked to the incident fields through the impedance boundary condition, thus completing the integrodifferential equations for the sum currents. Note that the tangential components of the differences of the radiated field intensities across the wall of the cylinder are consistency conditions intrinsic within the Stratton-Chu equations and do not contribute to the solution of this problem.

Once the sum currents generate the radiation, the edge condition applies to assure that the radiated power is finite and the field intensities are zero in the space away from the cylinder. The double series representation is based on the convergence of the Green's function over the Chebyshev polynomials in solving this problem.

A characteristic of the Green's function creates the discontinuity in the tangential components of the electric field across the wall of the cylinder. Due to the presence of this discontinuity, the double series representation of the sum of the Green's function approaching the wall from inside and from the outside is required. This representation has been found.

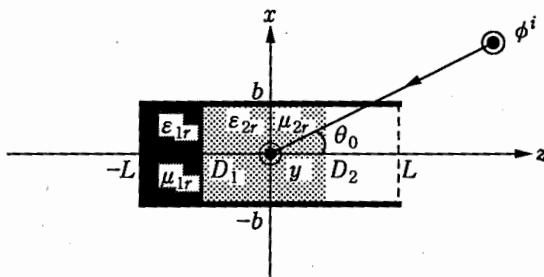
## DIFFRACTION BY A PARALLEL-PLATE WAVEGUIDE CAVITY WITH TWO-LAYER MATERIAL LOADING

Takeshi Momose, Shoichi Koshikawa and Kazuya Kobayashi\*

Department of Electrical and Electronic Engineering, Chuo University  
1-13-27 Kasuga, Bunkyo-ku, Tokyo 112, Japan

The problem of scattering from open-ended metallic waveguide cavities has received much attention recently in radar cross section (RCS) reduction and electromagnetic penetration/coupling studies. As an example of simple two-dimensional cavity structures, we have previously considered a finite parallel-plate waveguide with a planar termination at the open end and solved rigorously the plane wave diffraction using the Wiener-Hopf technique (K. Kobayashi and A. Sawai, *J. Electromagn. Waves Appl.*, Vol. 6, 475-512, 1992). The analysis has also been extended to treat the case where the region inside the cavity is partially filled with a material layer (K. Kobayashi et al., presented at 1992 *IEEE-APS/URSI/NEM Joint Symposia*, Chicago, Illinois, July 1992).

In this paper, as a generalization to our previous treatment on the material-loaded case, we shall rigorously analyze the plane wave diffraction by a parallel-plate waveguide cavity with two-layer material loading as shown in the figure using the Wiener-Hopf technique, where  $\phi^i$  is the incident field. The surface of the cavity is infinitely thin, perfectly conducting, and uniform in the  $y$ -direction, and the media inside the cavity for  $-L < z < D_1$  and  $D_1 < z < D_2$  are characterized by the relative permittivity/permeability  $(\epsilon_{1r}, \mu_{1r})$  and  $(\epsilon_{2r}, \mu_{2r})$ , respectively. Both  $E$  and  $H$  polarizations will be considered. Introducing the Fourier transform for the unknown scattered field and applying boundary conditions in the transform domain, the problem is rigorously formulated in terms of the simultaneous Wiener-Hopf equations. The Wiener-Hopf equations are then solved via the factorization and decomposition procedure to yield the exact and approximate solutions. The scattered field inside and outside the cavity is evaluated by taking the inverse Fourier transform together with the use of the saddle point method. The scattering characteristics of the cavity will be discussed via illustrative numerical examples of the RCS.



## ANALYSIS OF A WIRE IN THE PRESENCE OF A HOLLOW BODY OF REVOLUTION WITH AN APERTURE

Zhiqiang Qiu\* and Chalmers M. Butler

Department of Electrical and Computer Engineering  
Clemson University, Clemson, SC 29634-0915

Interest in this paper focuses upon the electromagnetic response of a wire in the presence of a hollow body of revolution (*bor*) with an aperture. Both bodies are perfect conductors and they share a common axis. The wire is thin and the *bor* is a shell of vanishing wall thickness. The surface of the *bor* is continuous except, at its upper end, a circular aperture is cut, exposing its interior to any field created by an exterior source. Aside from the conducting wire and *bor* shell, all space is filled with material characterized by  $(\mu, \epsilon)$ . Cases are considered in which the axially-directed wire is inside the hollow *bor*, outside the *bor*, or partially inside and partially outside, *i.e.*, the wire passes through the aperture. Excitations of interest are due to sources both inside and outside the *bor* and are not limited to circularly symmetric cases.

An integro-differential equation is derived for the current induced on the wire in the presence of the body of revolution. The coupling between the *bor* and wire is accounted for by a numerical Green's function, which is essentially the response (axial component of electric field) of the *bor* to an axial elementary dipole source. The wire equation, with its kernel (exact) modified by the numerical Green's function, is solved by numerical techniques to obtain the wire current distribution. When the incident field is known, the scattered field is computed from knowledge of the wire current, thereby allowing one to compute the total field. By localizing the independent source, the scattering problem can be interpreted as an antenna problem, from whose solution one can determine input impedance and admittance.

Data depicting the current induced on the wire scatterer/antenna and the input admittance of the wire in the presence of the *bor* are presented for several *bor*-wire geometries. The configuration is modified to comply with special cases found in the literature in order to corroborate our results. In addition, results of the wire in the presence of a large (relative to  $\lambda$ ) circular disk are checked against data approximated from image theory. Good agreement is obtained in all cases. Copious data are presented for the *bor* specialized to be of a missile-like shape for alternate locations of the wire (inside and outside the body, as well as partially inside and partially outside).

## **DIFFRACTION OF ELECTROMAGNETIC WAVES AT BLACKBODIES AND THE PROBLEM OF INVISIBLE OBJECTS**

**P.Ya. Ufimtsev**

Electrical Engineering Department  
University of California, Los Angeles  
Los Angeles, California 90024-1594

The Kirchhoff-Kottler model of plane black plates is extended for volumetric bodies with arbitrary shapes. This definition of blackbodies (BBs) can be considered as an idealized model of large scatterers with good radio absorbing coatings. Basic properties of the field scattered by BBs are established in the analytical form. Among the properties of BBs, the most important ones are the following. The field scattered by BBs almost does not depend on their shapes and are only determined by the size and geometry of the shadow contour which is the boundary between the illuminated and shadowed sides of the body. Different BBs with the same shadow contour create the same scattered field. The bi-static radar cross section of BBs does not depend on the polarization of the incident wave. The total power scattered by BB in all directions are only two times less than the total power scattered by the perfectly reflecting (metallic) body with the same shape and size. The scattered field created by BB is a constituent part of the field scattered by any large opaque object. This part of the scattered field cannot be removed by any absorbing coatings and can be used for detection of scattering objects by multipositioned radars. Some details of this phenomenon can be found in "Journees Internationales de Nice Sur Les Antennes", a conference held in Nice, November 12-14, 1992. See the Ufimtsev paper in Section 5, pp. 461-464.



SESSION URSI B-24

THURSDAY PM

## RADIATING STRUCTURES

Chairs: R.J. Mailloux, Hanscom AFB; D.L. Sengupta, University of Detroit

Room: Michigan League, Vandenberg Room Time: 1:30-5:30

|      |   |     |
|------|---|-----|
| 1:30 | AN ASYMPTOTIC CLOSED FORM APERTURE GREEN'S FUNCTION WITH APPLICATIONS TO RADIATION AND SCATTERING BY SLOTS IN MATERIAL COATED GROUND PLANES<br><i>Gary A. Somers*, Prabhakar H. Pathak, The Ohio State University</i> | 380 |
| 1:50 | RADIATION FROM AN OPEN-ENDED COAXIAL LINE THROUGH A MATERIAL LAYER<br><i>Ching-Lieh Li, Kun-Mu Chen, Michigan State University</i>  | 381 |
| 2:10 | FAR FIELD RADIATION PATTERN DUE TO A PERFECTLY CONDUCTING WEDGE EMBEDDED IN A FINITELY CONDUCTING EARTH<br><i>Minish Sinha, S.A. Saoudy, John Walsh, Memorial University of Newfoundland</i>                          | 382 |
| 2:30 | THE EFFICIENT PREDICTION OF THE RADIATED EMISSIONS FROM LARGE AND COMPLEX PRINTED CIRCUIT<br><i>Yuan Zhuang, Ke-Li Wu, John Litva, McMaster University</i>  | 383 |
| 2:50 | AN ANTENNA ENERGY PROPAGATION MODEL: APPLICATION TO DISTANCE MEASUREMENT SYSTEMS<br><i>J.M. Tranquilla, Radha Telikepalli*, University of New Brunswick</i>   | 384 |
| 3:10 | BREAK   |     |
| 3:30 | SPHERICAL NEAR-FIELD TO FAR-FIELD TRANSFORMATION USING EQUIVALENT MAGNETIC AND ELECTRIC CURRENT APPROACHES<br><i>Ardalai Taagholt, Tapan K. Sarkar, Mark Miller, Syracuse University</i>                              | 385 |
| 3:50 | A DOMAIN DECOMPOSITION TECHNIQUE FOR ELECTRICALLY LARGE RADOMES<br><i>M.P. Hurst, McDonnell Douglas</i>   | 386 |
| 4:10 | DIELECTRIC LENS ANTENNA AT EHF<br><i>A. Kumar, AK Electromagnetique Inc.</i>  | 387 |
| 4:30 | THE USE OF MODEL BASED PARAMETER ESTIMATION (MBPE) FOR THE DESIGN OF CORRUGATED HORNS<br><i>L.R. Fermelia, G.Z. Rollins, P. Ramanujam, Hughes Space and Communications Company</i>                                    | 388 |
| 4:50 | GENERALIZED COORDINATE TRANSFORMATION MATRIX IN ANTENNA APPLICATIONS<br><i>Feng Cheng Chang, National Chung Cheng University</i>  | 389 |
| 5:10 | L-BAND PATH LOSS MEASUREMENTS INSIDE A 350 CUBIC INCH ENGINE BLOCK CAVITY<br><i>Brian M. Bock*, Richard Campbell, Douglas Brumm, Carl Anderson, Glen Barna, Michigan Technological University</i>                     | 390 |

## AN ASYMPTOTIC CLOSED FORM APERTURE GREEN'S FUNCTION WITH APPLICATIONS TO RADIATION AND SCATTERING BY SLOTS IN MATERIAL COATED GROUND PLANES

Gary A. Somers\* and Prabhakar H. Pathak  
The Ohio State University ElectroScience Laboratory  
Department of Electrical Engineering  
Columbus, Ohio 43212

An asymptotic closed form dyadic aperture Green's function,  $\bar{\bar{G}}_a$ , which has been developed recently, will be applied to efficiently treat the electromagnetic radiation and scattering by a variety of interesting large but finite material coated slot array configurations in PEC ground planes. The highlights of the asymptotic development of  $\bar{\bar{G}}_a$  will be presented. The asymptotic  $\bar{\bar{G}}_a$  will be shown to remain uniformly valid within the surface and leaky wave transition regions, and to remain accurate even for separations of source and field points, along the ground plane, which are as small as a quarter wavelength (in free space) or so.

Conventional integral equation approaches for analyzing the radiation and/or scattering by a large array of material covered slots in PEC ground planes require the extremely time consuming numerical computation of the exact Sommerfeld integral form of  $\bar{\bar{G}}_a$ , which in general has to be done repeatedly. Another commonly used method is the Floquet mode analysis which is based on an approximate model of an infinite periodic array for the finite array case which therefore does not include array end effects. These end effects can play a significant role in the performance of low sidelobe arrays. In contrast, the present asymptotic closed form  $\bar{\bar{G}}_a$ , which needs no numerical integration takes into account the array end effects when used within the integral equation formulation and provides a very efficient solution which is orders of magnitude faster than the numerical implementation (with envelope extraction) of the Sommerfeld integral.

This computation technique will be applied to several element configurations. First we will consider the case of the linear polarization array where the array consists of parallel slots. Second, an array configuration that can produce either dual linear or circular polarization is considered. This consists of arrays of subarrays such that the elements within the subarray are orthogonal. Third, we will consider the external coupling of the inclined slots on a waveguide array. This coupling will be computed for numerous tilt angles and slot separations. In this paper, we will discuss both rectangular and triangular lattice configurations and a variety of stratification schemes.

## RADIATION FROM AN OPEN-ENDED COAXIAL LINE THROUGH A MATERIAL LAYER

Ching-Lieh Li\* and Kun-Mu Chen  
Department of Electrical Engineering  
Michigan State University  
East Lansing, MI 48824

In this paper, the radiation from an open-ended coaxial line through a material layer is studied. Our objectives are to investigate the effects of a dielectric material layer on the radiation characteristics of an annular slot antenna, and to study the excitation of the complex waves in a dielectric layer by an open-ended coaxial probe.

This problem is analyzed by using the integral equation formalism. By suitable representations for the EM fields inside and outside the coaxial line, an integral equation for the aperture electric field can be derived by matching the boundary conditions across the aperture plane and the air-material layer interface. The integral equation is solved by applying the method of moments, where the basis and weighting functions are chosen to be the modal functions of the coaxial line.

Once the aperture electric field is obtained numerically, the quantities such as the input impedance, the EM fields at various regions, and the far-field pattern can be calculated. The excitation of surface waves and the radiated wave is also identified through the poles and the branch cuts in the complex plane by a deformed contour integration for the EM fields. The far zone fields can be evaluated by using the saddle-point method of integration along the steep descent path. After that the power carried by surface waves and the radiated wave can then be calculated by numerically integrating the Poynting vector over a suitable surface.

The distribution of power into the surface waves and the radiated wave is examined. As required by the conservation of energy, the sum of the power for the surface waves and the radiated power is found to be equal to the transmitted power from the coaxial line. Also it is noted that the power of the surface waves depends strongly on the physical parameters such as the permittivity, permeability and the thickness of the material layer. The radiation pattern as a function of frequency and the properties of the material layer is also presented for various cases. Moreover, the effect of a multi-layer material medium upon the radiation pattern is examined.

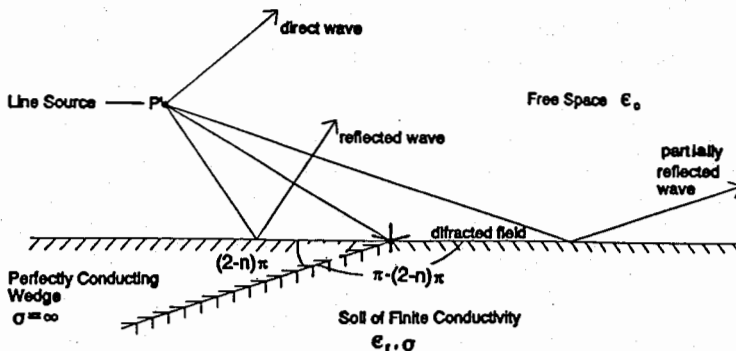
FAR FIELD RADIATION PATTERN DUE TO  
A PERFECTLY CONDUCTING WEDGE EMBEDDED  
IN A FINITELY CONDUCTING EARTH

Manish Sinha\*, S.A. Saoudy\*\*, and John Walsh\*  
\*Faculty of Engineering and Applied Science  
\*\*Centre for Cold Ocean Resources Engineering  
Memorial University of Newfoundland  
St. John's, Newfoundland, Canada A1B 3X5.

The problem of a ground screen situated on real earth can be modelled as a perfectly conducting wedge of angle  $(2-n)\pi$  imbedded in an imperfect ground medium. By equating  $n$  to 2, the conducting wedge is transformed into a half plane interfacing with a real earth terrain.

In this work, the geometrical theory of diffraction is utilized, along with geometrical optics, to determine the far field radiation pattern due to a line source located parallel to a perfectly conducting wedge of angle  $(2-n)\pi$  with one of its surfaces aligned to a ground of finite conductivity as shown in figure. In this geometry, there are four radiation mechanisms that must be considered in determining the far field pattern in free space.

The first component is the incident field, which is direct radiation from the line source to the observation point. The second component is the field reflected from the surface of the perfectly conducting wedge due to oblique incidence. Beyond the wedge, partial reflection takes place on the imperfect ground interface. This third component of partial reflection is dependant on soil conductivity and permittivity. The diffraction coefficient for this particular wedge geometry, where the surrounding medium is not fully free space, will be studied from first principles. The resulting diffraction field will be added to the previous three field components. Comparisons will be made with available literature.



WAVE MECHANISM AT A WEDGE  
IMPEDED IN A SOIL OF FINITE CONDUCTIVITY

## THE EFFICIENT PREDICTION OF THE RADIATED EMISSIONS FROM LARGE AND COMPLEX PRINTED CIRCUIT

Yuan Zhuang, Ke-Li Wu and John Litva

Communications Research Laboratory, McMaster University  
Hamilton, Ontario, Canada L8S 4K1

With the working frequency becoming higher and higher, electromagnetic interference (EMI) is becoming a major constraint in the design of printed circuit boards (PCB's) used in computers and communication equipments. Some strict specifications have already been set for the radiated emissions from PCB's. The circuit equivalent approach is first used for modelling PCB's. Full-wave analysis methods, such as Moment Methods, are also adopted to simulate the currents on PCB's, and then the radiations. The former approach is limited by its accuracy and frequency range. The later ones are accurate but usually the size and the complexity of the PCB's being able to analyzed is constrained by the computer memory, computing time, and the model used. In this presentation, an efficient full-wave analysis technique, modified CG-FFT is utilized to simulate the radiated emissions from large and complex PCB's. The CG-FFT algorithm is modified to include the opens, shorts, complex components (R,C,L) and source drives which can be located in arbitrary positions within electronic circuits. These modifications, combined with the intrinsic merits of CG-FFT, high efficiency ( $O(N)$  in computer memory and  $O(4N(1 + \log_2(N)))$  in computing time), propose a robust tool for the accurate prediction of large and complex PCB's. To demonstrate this technique, some PCB's are analyzed. The radiation emission (from 20MHz up to 1GHz), caused by a non-ideal square-wave typically transmitted in digital PCB's, are calculated and compared with the measured results done by a cooperative company. Some discussions are made at last. The details will be presented in the symposium.

## AN ANTENNA ENERGY PROPAGATION MODEL: APPLICATION TO DISTANCE MEASUREMENT SYSTEMS

J.M. Tranquilla and Radha Telikepalli\*  
Radiating Systems Research Laboratory  
Department of Electrical Engineering  
University of New Brunswick  
Fredericton/N.B., Canada E3B 5A3

Energy propagation can be represented geometrically by means of Poynting vector flow lines or energy flow lines. Energy flow thus represented gives the direction of the time-average Poynting vector at any point in space and the density of lines in a particular area is proportional to the average power flow per unit area. This type of geometrical representation gives a convenient physical interpretation for propagation phenomena. For antennas, the antenna pattern amplitude characteristics are represented by Poynting vector flow lines and the phase characteristics are presented by phase contours. The amplitude maxima and minima are identified by closely spaced and deflected flow lines respectively. The phase contours appear to converge around amplitude pattern nulls.

The Poynting vector flow lines from an ideal point source radiator are radial with respect to the source, however practical antennas differ from a point source and there are corresponding changes in the energy flow lines. These lines appear in the far field to be directed (converge) toward an imaginary point which gives rise to the concept of phase center. For many practical antennas the location of this apparent point of convergence is direction dependent.

In radio positioning systems an observation point is assumed to be located radially from the antenna source. The distance determination between the source and the observation point is performed using either phase based or time based measurements. The phase based calculations utilise measured differential phase at the observation point with reference to the antenna source which, when multiplied by the wavenumber, gives the value of the range. The time based measurements involve the multiplication of the measured propagation time delay and the group velocity for distance calculations.

This paper describes the modelling of phase and group velocities of propagation based on the concept of energy flow and the technique is demonstrated by considering two simple examples. The typical distance errors involved by using constant velocities of propagation are presented.

## Spherical Near-field to Far-field Transformation Using Equivalent Magnetic and Electric Current Approaches

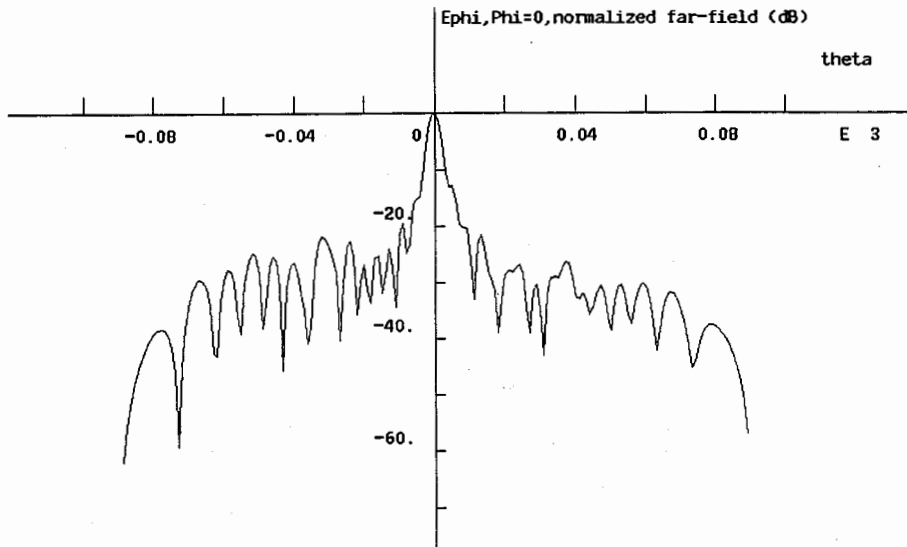
Ardalan Taághol  
Tapan K. Sarkar  
Mark Miller

### ABSTRACT

Two methods are presented to compute far-field antenna patterns from near-field measurements. These methods utilize near-field data to determine, first, an equivalent magnetic current source and, second, an equivalent electric current source over a fictitious planar surface which encompasses the antenna. These magnetic or electric currents are used to ascertain the far fields.

Under certain approximations, the currents should produce the correct far-fields in all regions in front of the antenna regardless of the geometry over which the near-field measurements are made. Two electric field integral equations are developed to relate the near-fields to the equivalent magnetic or electric currents. The Method of Moments is used to solve the integral equations by transforming them into matrix equations. These matrix equations are solved using Singular Value Decomposition.

Presented here is near-field to far-field transformation for spherical scanning.



Normalized far-field pattern of an aperture antenna determined from the measured near-field.

Thu. p.m.

## A DOMAIN DECOMPOSITION TECHNIQUE FOR ELECTRICALLY LARGE RADOMES

M.P. Hurst

McDonnell Douglas Corporation  
P.O. Box 516  
St. Louis, MO 63166

Analysis of the effects of radomes on the radiation patterns of enclosed antennas is typically done via asymptotic techniques, since most practical antenna/radome configurations are too large to apply more rigorous techniques such as the method of moments. In cases where boresight error is critical, however, asymptotic methods do not always yield sufficiently accurate predictions. Asymptotic methods do not adequately treat the effects of surface curvature, cusps, and guided waves, and significant error in the calculated beam direction and gain can occur. In this paper a method is proposed which captures the most significant of these effects while remaining numerically tractable.

The method proposed here involves spatial decomposition of an antenna/radome geometry into domains of manageable size for moment method analysis. The method assumes an excitation at one end of an elongated body such as the nose of a vehicle. The geometry is such that rays impinging on the walls of the radome are not reflected toward the excited end of the body, and thus the fields propagate from one end of the body to the other, possibly being partially reflected many times and eventually radiating into the space beyond the radome. Rays which *do* return to the antenna (due to scattering from the tip of the radome, for example) are assumed to have a negligible effect on the antenna pattern near the main beam direction. The assumption that fields only propagate in one general direction allows the various domains into which the radome is artificially divided to be decoupled. A cascade of isolated scattering problems is solved, one for each domain, with excitations derived from the fields calculated in the previous problem. Unlike the method of Umashankar, et al., (K.R. Umashankar, S. Nimmagadda, and A. Taflove, *IEEE Trans. Antennas Propagat.*, vol. AP-40, pp. 867-877, Aug. 1992) it is not necessary in the present method to compute the coupling between each pair of points on the body (or, equivalently, to fill a moment method matrix for the entire body). This feature provides considerable savings in computer storage and run time.

Two- and three-dimensional examples of problems involving thick dielectric radomes will be given in the presentation with comparison to direct moment method calculations.

## DIELECTRIC LENS ANTENNA AT EHF

A. Kumar  
AK Electromagnetique Inc.  
P. O. Box 240  
30 Rue Lippee  
Coteau Station  
Quebec  
Canada JOP 1EO

In recent years an increasing number of lens antennas have been designed and built at various microwave frequencies. A primary use of dielectric lens antennas is for multibeam applications such as satellite-born antennas where high gain and multibeam patterns can be generated by using the wide-angle characteristics of lens antennas.

In this paper, we have designed a dielectric lens using shaping techniques in the frequency range of 43.5 to 45.5 GHz. We have developed a software which is based on geometric optics with ray tracing techniques and the power conservation law.

The main design objective is to shape the lens to serve as an optical transformer, which transform the given feed pattern into the desired aperture distribution. A technique of coma-correction zoning including surface matching method is introduced in the software. The software predicts the optimum performance of the antenna including weight and loss reduction. The coverage of the beam depends on excitation of the horn array. In choosing the proper horn in an array, special care has been taken to minimize mutual coupling effects.

A dielectric lens antenna of stycast dielectric material (permittivity = 2.5) has been constructed to verify the computed results. The performance of the antenna is summarized as follows:

| Characteristics                 | Values  | Characteristics                 | Values   |
|---------------------------------|---------|---------------------------------|----------|
| Gain                            | 39 dBic | Polarization                    | RHCP     |
| Aperture effi.                  | 49%     | Scan loss                       | < 1 dB   |
| Antenna loss                    | < 2 dB  | Sidelobe level                  | < -32 dB |
| Cross-pol level<br>in main beam | < 24 dB | Cross-pol level<br>in side lobe | < -33 dB |

## THE USE OF MODEL BASED PARAMETER ESTIMATION (MBPE) FOR THE DESIGN OF CORRUGATED HORNS

L. R. Fermelia, G. Z. Rollins, P. Ramanujam  
Hughes Space and Communications Company Los Angeles, CA 90009.

The model based parameter estimation (MBPE) is an interesting approach to increase the efficiency of electromagnetic calculations (Miller, SCEEE, 1991). MBPE involves fitting physically motivated approximations to accurately computed or measured electromagnetic quantities from which unknown coefficients are numerically obtained. Thus, the performance of a component at a few frequencies can be used to interpolate the performance at a large number of frequencies and hence can be used to pick up any sharp resonances in the frequency response, which would otherwise be missed. This approach was used to detect resonance problems in wide-band corrugated conical horns. Furthermore, MBPE was used inside an optimization procedure whose cost function was based on the performance predicted by MBPE.

The horn under consideration operates over 3.7-4.2 GHz for transmit and 5.925-6.425 GHz for receive. The purpose of the current investigation is to determine what can be achieved with conventional corrugated horn. An accurate mode-matching analysis was embedded inside an optimization procedure, in which the slot depths were optimized to achieve the VSWR and the cross-pol performance. While the cross-pol performance was fairly smooth over the transmit and receive band, the VSWR performance exhibited some resonance in the transmit band. The number of frequencies used for optimization were 10 over transmit and 6 over receive. While the performance was satisfactory over the optimized frequencies, MBPE predicted a resonance in between these frequencies. Fig 1 shows the VSWR at the optimized frequencies and the values predicted by MBPE using these as samples. The sharp resonance near 3.9 GHz exhibited by MBPE, was confirmed by running mode-matching analysis of the horn at that frequency, thus verifying the validity of MBPE.

It was then decided to introduce MBPE inside the optimization. The cost function was modified to take into account the VSWR predicted by MBPE. Due to the simplicity of the calculations involved, the inclusion of MBPE did not increase the computation time for the optimization. Using this procedure a design free of resonances was achieved. Fig 2 shows the VSWR at the optimized frequencies and that predicted by MBPE. The mode-matching analysis was performed at many other frequencies to verify the absence of the resonances.

Fig 1.

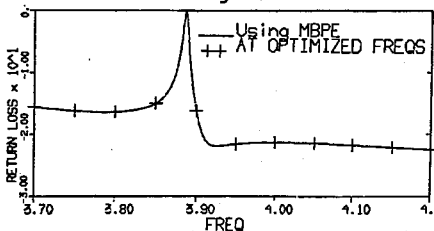
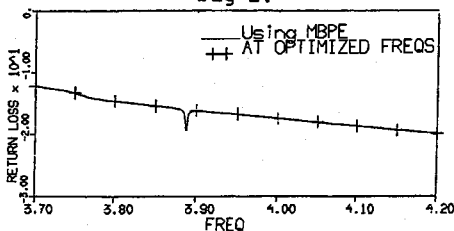


Fig 2.



Return loss for the optimization without MBPE (Fig 1.), and with MBPE (Fig 2.).

## Generalized Coordinate Transformation Matrix In Antenna Applications

Feng Cheng Chang \*  
 Department of Electrical Engineering  
 National Chung Cheng University  
 Taiwan, Republic of China

A coordinate transformation matrix relating any two coordinate systems is usually obtained by successively rotating angles about any of three major coordinate axes. These are well-known Eulerian angles. For some antenna applications, such as alignment of probe and gantry in nearfield measurement, an axis of rotation may not be exactly coincided with any of the major coordinate axes, determination of transformation matrix is therefore to be reformulated regarding this general case.

It is shown that a coordinate transformation matrix relating two coordinate systems can be expressed in a simple exponential form as  $\exp(-J\omega)$ , where  $\omega$  is an angle of rotation about the axis having directional cosine  $u = (u_x, u_y, u_z)$ , and  $J$  is called a "directional matrix", given by

$$J = \begin{bmatrix} 0 & -u_z & u_y \\ u_z & 0 & -u_x \\ -u_y & u_x & 0 \end{bmatrix}$$

In case a coordinate transformation matrix is obtained by rotating  $\omega_1$  around  $J_1$ , and then rotating  $\omega_2$  around  $J_2$ , the overall transformation may thus be expressed as

$$\exp(-J\omega) = \exp(-J_2\omega_2) \exp(-J_1\omega_1)$$

where for any given  $J_1, \omega_1$ , and  $J_2, \omega_2$ , the resulted  $J$  and  $\omega$  are then solved from the following two equations:

$$\cos \frac{\omega}{2} = \cos \frac{\omega_2}{2} \cos \frac{\omega_1}{2} + \sin \frac{\omega_2}{2} \sin \frac{\omega_1}{2} \operatorname{Tr} \left( \frac{1}{2} J_2 J_1 \right)$$

$$\sin \frac{\omega}{2} J = \sin \frac{\omega_2}{2} \cos \frac{\omega_1}{2} J_2 + \cos \frac{\omega_2}{2} \sin \frac{\omega_1}{2} J_1 + \sin \frac{\omega_2}{2} \sin \frac{\omega_1}{2} (J_2 J_1 - J_1 J_2)$$

The matrix written as  $\exp(-J\omega)$  is not of a convenient form for numerical computation, since a square matrix  $J$  appears in the exponential. We may find a more explicit and useful form by series expansion (Chang, Proc. IEEE 58, 145-146, 1970), and obtain

$$\exp(-J\omega) = I + (1 - \cos \omega) J J - \sin \omega J$$

$$= I + 2 \left( \sin \frac{\omega}{2} J \right) \left( \sin \frac{\omega}{2} J \right) - 2 \left( \cos \frac{\omega}{2} \right) \left( \sin \frac{\omega}{2} J \right)$$

Some other applications, such as in multi-reflector system, also will be discussed.

\* Formally with TRW Antenna Systems Lab., Redondo Beach, California. 121592.

Thu. p.m.

## L-BAND PATH LOSS MEASUREMENTS INSIDE A 350 CUBIC INCH ENGINE BLOCK CAVITY

Brian M. Bock\*, Richard Campbell, Douglas Brumm  
Department of Electrical Engineering  
Carl Anderson and Glen Barna  
Department of Mechanical Engineering  
Michigan Technological University  
Houghton, MI 49931

We have measured the path loss between a connecting rod mounted microwave transmitter and a receiving antenna in the oil pan of a 350 cubic inch Chevrolet V-8 engine. The pistons, connecting rods, crankshaft and camshaft are all installed in the block. All engine block and oil pan openings are covered flush with aluminum foil to prevent radiation leakage from the cavity and to simulate the enclosed environment of a running automobile engine. The coupling measurements were performed with several different receive antenna positions, and over a wide range of crankshaft angles.

The measurements show that the engine block propagation environment has the characteristics of an overmoded cavity, with deep nulls at a few crankshaft angles and an average received signal well above the "free space" value. We are currently running research engines with electronics packages mounted on connecting rods and inside the piston skirts. The measurements of L-band coupling show the feasibility of using a microwave link for telemetry from moving parts inside the engine to the external laboratory instrumentation.

**SPECIAL SESSION AP-S/URSI D-8****THURSDAY PM****DOWNSIZING TECHNOLOGY IN MOBILE COMMUNICATIONS**

Chairs: K. Kagoshima, NTT Radio Communications Systems Laboratories  
J. Huang, Jet Propulsion Laboratory

Room: Michigan League, Michigan Room

Time: 1:30-5:10

1:30 DOWNSIZING ANTENNA TECHNOLOGIES FOR MOBILE AND SATELLITE COMMUNICATIONS AP-S  
*J. Huang, A. Densmore, A. Tulintseff, V. Jamnejad, Jet Propulsion Laboratory*

1:50 REVIEW OF ESA MOBILE ANTENNA DEVELOPMENTS FOR SATELLITE COMMUNICATIONS AP-S  
*A.W. Jongejians, P.J. Rinous, A.G. Roederer, ESA-ESTEC*

2:10 ANALYSIS AND DESIGN OF A CIRCUMFERENTIAL WIDE SLOT CUT ON A THIN CYLINDER FOR MOBILE BASE STATION ANTENNAS AP-S  
*Jiro Hirokawa\*, Shun-ichi Sumikawa, Makoto Ando, Naohisa Goto, Tokyo Institute of Technology*

2:30 A THREE ELEMENT, SUPERDIRECTIVE ARRAY OF ELECTRICALLY SMALL, HIGH-TEMPERATURE SUPERCONDUCTING HALF LOOPS AT 500 MHZ AP-S  
*Donald R. Bowling, David J. Banks, Darry M. Kinman, Anna M. Martin, Naval Air Warfare Center; Robert J. Dinger, Naval Command, Control and Ocean Surveillance Center; Roger Forse, Superconductor Technologies; Greg Cook, University of Sheffield*

2:50 MINIATURIZATION OF ARRAY ANTENNAS WITH SUPERDIRECTIVE EXCITATION AP-S  
*Osamu Ishii, Keiichiro Itoh, Yasuhiro Nagai\*, NTT Interdisciplinary Research Laboratories; Kenichi Kagoshima, NTT Radio Telecommunication System Research Laboratory*

3:10 BREAK

3:30 ELECTRICAL ANTENNA VOLUME FOR A SCALE OF DOWNSIZING AP-S  
*Hiroyuki Arai, Yokohama National University*

3:50 ANALYSIS AND OPTIMIZATION OF REDUCED SIZE PRINTED MONOPOLE AP-S  
*H. Lebbar, M. Himdi, J.P. Daniel, University of Rennes I.U.R.A.*

4:10 MONOPOLE-LOADED SMALL LOOP ANTENNAS ELIMINATING A MATCHING CIRCUIT AP-S  
*Keizo Cho, Kenichi Kagoshima, NTT Radio Communication Systems Laboratories*

4:30 PRECISE MEASUREMENT OF INPUT IMPEDANCE AND RADIATION EFFICIENCY OF SMALL LOOP ANTENNAS AP-S  
*Ichiro Ida\*, Teruhiko Fujisawa, Koichi Ito, Jun-Ichi Takada, Chiba University*

4:50 DISCUSSION



## WAVEGUIDES II

Chairs: G.A. Thiele, University of Dayton; A.A. Oliner, Polytechnic University

Room: Michigan League, Henderson Room

Time: 1:30-5:30

|      |   |     |
|------|---|-----|
| 1:30 | CAPACITANCE OF A CIRCULARLY SYMMETRIC VIA FOR A MICROSTRIP TRANSMISSION LINE<br><i>Andrew W. Mathis*, Chalmers M. Butler, Clemson University</i>  | 394 |
| 1:50 | PROPERTIES OF BOUND AND LEAKY DOMINANT MODES ON STRIPLINE WITH UNIAXIAL ANISOTROPIC SUBSTRATES<br><i>David Nghiem, Jeffery T. Williams, David R. Jackson, University of Houston; Arthur A. Oliner, Polytechnic University</i> | 395 |
| 2:10 | ASYMMETRICAL FIN LINES CONTAINING ANISOTROPIC DIELECTRIC SUBSTRATE OR MAGNETIZED FERRITE<br><i>Z. Fan*, S.R. Pennock, University of Bath</i>  | 396 |
| 2:30 | THE TAPERED DIELECTRIC SLAB RADIATOR<br><i>Gerald M. Whitman*, New Jersey Institute of Technology; Felix Schwering, US Army CECOM; Wan-Yu Chen, New Jersey Institute of Technology</i>  | 397 |
| 2:50 | APERTURE COUPLED MICROSTRIP "MAGIC-T"<br><i>M.W. Katubse*, NDHQ; Y.M.M. Antar, Royal Military College; A. Ittipiboon, M. Cuhaci, Communications Research Center</i>   | 398 |
| 3:10 | BREAK   |     |
| 3:30 | A WAVEGUIDE POLARIZATION CONTROLLER<br><i>Kamal Sarabandi, The University of Michigan</i>   | 399 |
| 3:50 | COMPUTER AIDED DESIGN & OPTIMIZATION OF A CLASS OF WIDE BAND TURNSTILE COUPLING JUNCTIONS<br><i>Luiz Costa da Silva, Subir Ghosh, SG Microwaves Inc.</i>  | 400 |
| 4:10 | FULL WAVE ANALYSIS OF THREE-PLANE THREE-PORT RECTANGULAR WAVEGUIDE JUNCTIONS<br><i>J.M. Rebollar*, J. Esteban, J.E. Page, Universidad Politécnica de Madrid</i>   | 401 |
| 4:30 | FULL WAVE ANALYSIS OF STEPPED TWISTS IN RECTANGULAR WAVEGUIDES<br><i>J.M. Rebollar*, C. Vecino, J. Esteban, Universidad Politécnica de Madrid</i>   | 402 |
| 4:50 | RIGOROUS ANALYSIS OF RECTANGULAR WAVEGUIDE LOADED WITH DIELECTRIC POST BASED ON FEM-BEM<br><i>Zhang Feng, Fu Junmei, Xi'an Jiaotong University</i>  | 403 |
| 5:10 | THE NEW METHOD FOR ANALYSIS OF A RADIAL RESONATOR WAVEGUIDE DIODE MOUNTING STRUCTURE-SMC METHOD<br><i>Ling Chen, Yun-yi Wang, Southeast University</i>  | 404 |

## CAPACITANCE OF A CIRCULARLY SYMMETRIC VIA FOR A MICROSTRIP TRANSMISSION LINE

Andrew W. Mathis\* and Chalmers M. Butler

Department of Electrical and Computer Engineering

Clemson University, Clemson, SC 29634-0915

Vias connecting different traces of a multilayered circuit board generally cross at least one ground plane, and, in so doing, introduce a capacitance to a transmission-line circuit. At sufficiently low frequencies this capacitance can be ignored, but at high frequencies it must be taken into account in the design of a circuit. The via structure of interest in this paper consists of a hollow cylinder that passes through a circular hole in a ground plane. The cylinder has lips or washer-shaped flanges at its upper and lower ends that facilitate connection to a trace of a microstrip transmission line. Typically, the trace is supported by, and resides on, the surface of a dielectric slab which itself rests on the ground plane. Hence, the via extends from a surface of the dielectric slab through the hole in the ground plane.

An integral equation is derived for the charge induced on the cylindrical center of the via under the condition that the cylinder is raised to a potential  $V$  relative to that of the ground plane. The integral equation is solved numerically for the charge on the cylinder from which one can compute the via capacitance. In via analyses, the structure often is assumed to be in a homogeneous material, *i.e.*, the dielectric-air interface is ignored, but, in the present investigation, the presence of the dielectric substrate is accounted for by employing an appropriate Green's function. The partial differential equation for the Green's function is solved by a simple technique involving the Hankel transform. Consequently, this function is obtained in the form of an inverse Hankel transform which forces one to exercise care in carrying out the numerical evaluations of the Green's function in the solution of the integral equation.

Data depicting via capacitance and its dependence upon the dielectric constant of the slab and the via's geometric dimensions are presented for numerous cases of via configuration. Results show the difference in capacitance of a via in a homogeneous material and that of the same structure in the presence of a dielectric slab to be significant, especially if the thickness of the slab is the same as or larger than the radius of the hole in the ground plane. The presence of the lips or flanges on the via cylinder can introduce large increases in total charge on this composite central cylinder and, hence, can increase the via capacitance when the flange area is significant relative to that of the cylinder. This effect is particularly noticeable when the via is short relative to its diameter. Measurements to confirm these results are currently underway and, hopefully, can be completed in time to present.

## PROPERTIES OF BOUND AND LEAKY DOMINANT MODES ON STRIPLINE WITH UNIAXIAL ANISOTROPIC SUBSTRATES

David Nghiem<sup>†</sup>, Jeffery T. Williams<sup>†</sup>, David R. Jackson<sup>†</sup>, and Arthur A. Oliner<sup>††</sup>

† Applied Electromagnetics Laboratory  
Dept. of Electrical Engineering  
University of Houston  
Houston, TX 77204-4793

†† Weber Research Institute  
Dept. of Electrical Engineering  
Polytechnic University  
Brooklyn, NY 11201

Leaky modes have been found to exist on various planar transmission-line structures such as microstrip and stripline. Their presence is generally undesirable since they leak power away from the line, resulting in increased attenuation and possible spurious coupling between adjacent elements in the circuit. Recently, it was observed that a dominant leaky mode exists on ordinary stripline that has a small air gap above the strip conductor. This leaky mode is referred to as a "dominant" mode because the current on the strip conductor has a shape similar to that of the customary TEM mode on stripline with a homogeneous substrate. This leaky mode exists in addition to, and independently of, the proper (bound) mode on the air-gap structure. The attenuation constant  $\alpha$  of this mode is associated with leakage into the  $TM_0$  parallel-plate mode of the background structure (which has a propagation wavenumber  $k_{TM_0}$ ). One of the most important features observed for the leaky mode is that it has a field near the strip that closely resembles that of the conventional TEM stripline mode. On the other hand, for small air gaps, the proper mode has a field near the strip that resembles a  $TM_0$  parallel-plate mode. Therefore, it is the leaky mode that is a continuation of the conventional TEM stripline mode when a small air gap is introduced above the strip (D. Nghiem, J. T. Williams, D. R. Jackson, and A. A. Oliner, 1992 IEEE MTT-S Symp. Digest, pp. 491-494).

In the present work, the investigation is extended to a more general structure consisting of stripline with a *uniaxial anisotropic* substrate, with an air gap of arbitrary thickness  $\delta$  above the strip. For the case of a positive anisotropy ratio ( $\epsilon_{\parallel} > \epsilon_{\perp}$ ) it is found that there are two distinct proper modes (with  $\alpha = 0$ ) when  $\delta = 0$ . The first mode is the conventional  $TM_0$  parallel-plate mode having  $\beta = k_{TM_0}$ , which ignores the strip, and the second mode is a stripline-like mode having  $\beta < k_{TM_0}$ , despite the fact that there is no leakage. When a small air gap is introduced the first mode remains a proper mode with  $\beta > k_{TM_0}$ , while the second one becomes a leaky (complex improper) mode with  $\beta < k_{TM_0}$ . The leakage rate of this second mode is enhanced relative to the isotropic air-gap case. For the case of a negative anisotropy ratio ( $\epsilon_{\parallel} < \epsilon_{\perp}$ ), the behavior is very different. For  $\delta = 0$  there are again two proper modes. The first one is the  $TM_0$  parallel-plate mode and the second one is a stripline-like mode having  $\beta > k_{TM_0}$ . When a small air gap is introduced, however, these solutions part into three, a proper stripline-like mode with  $\beta > k_{TM_0}$ , and two real ( $\alpha = 0$ ) improper modes (one is stripline-like and the other, for very small air gaps, is parallel-plate like) which are nonphysical. When  $\delta$  increases to a critical value (dependent on the anisotropy ratio) the two real improper modal solutions merge to become a single leaky improper solution. This solution remains leaky up to another critical value of  $\delta$ , beyond which it again splits into two real improper solutions. In the region of leakage, this solution should be physically significant.

## ASYMMETRICAL FIN LINES CONTAINING ANISOTROPIC DIELECTRIC SUBSTRATE OR MAGNETIZED FERRITE

Z. Fan\* and S.R. Pennock

School of Electronic and Electrical Engineering  
University of Bath, Bath BA2 7AY, U. K.

Recently, asymmetrical fin lines have become attractive for microwave and millimeter wave integrated circuit applications. These asymmetrical structures offer several advantages over symmetrical (traditional) fin lines, such as ease of substrate and device mounting, wider single-mode bandwidth and an additional degree of freedom to obtain the characteristic parameters. A number of theoretical analyses for asymmetrical fin lines with isotropic dielectric substrates have been reported. It is well known that anisotropy is present in a variety of practical substrates used for microwave integrated circuits. Furthermore, a magnetized ferrite layer has to be inserted in the substrate in order to realize nonreciprocal devices. However, up until now, there seems to be no analysis developed for asymmetrical fin lines with anisotropic dielectric substrate or magnetized ferrite. Some of our recent studies in these areas are described as follows.

A theoretical and numerical method is presented for the analysis of the asymmetrical fin lines with anisotropic dielectric substrates. A couple of integral equations are first derived by expressing the field components in different regions in terms of different discrete Fourier transforms and applying the boundary conditions across interfaces. Galerkin's method is then applied to obtain the determinant equation for propagation constants of odd and even modes. In addition, characteristic impedance of the fundamental mode is derived based on the voltage-power definition. Numerical results are presented to show the effect of substrate anisotropy on the propagation constants and characteristic impedances. It is found that the effect on the propagation characteristics increases with the increase in the frequency. The results for the symmetrical cases are also presented and compared with theoretical data available in the literature, showing a very good agreement.

Asymmetrical fin lines containing a magnetized ferrite is also analyzed by means of the integral equation formulation and Galerkin's procedure with regards to their nonreciprocal properties. Convergence and numerical efficiency of the analysis is demonstrated to be good. Numerical results for the frequency dependent propagation constants of the forward and backward waves are obtained for various values of structural and material parameters. It is found that single-layer structures do not exhibit adequate nonreciprocity in the propagation characteristics, but the multi-layered structures such as sandwich ones give quite high differential phase shift for the realization of the efficient nonreciprocal devices. Numerical results are validated against the data previously published for the symmetrical one-layer and multilayer cases.

## THE TAPERED DIELECTRIC SLAB RADIATOR

Gerald M. Whitman\*, New Jersey Institute of Technology; Felix Schwering, US Army CECOM; Wan-Yu Chen, New Jersey Institute of Technology

Tapering the dielectric slab waveguide, as opposed to a sudden truncation, forms a dielectric radiator with increased directivity and reduced side lobe levels over a wider frequency band. The two dimensional structure consisting of a semi-infinite, lossless, dielectric waveguide feeding a dielectric wedge is studied.

The tapered portion of the structure is modeled by a sequence of several short slab waveguide segments of equal lengths and uniform cross-sectional areas of progressively smaller widths (staircase approximation). The fundamental, even, TE surface wave mode of the infinite, uniform, dielectric slab waveguide is assumed to be incident in the  $+z$  direction from  $z = -\infty$ . This mode does not experience cutoff and can propagate along very thin slab waveguides. The resultant fields are TE everywhere. They are represented in each distinct region as a superposition of guided and radiation modes whose expansion coefficients are determined by satisfaction of transverse field continuity conditions across each interface between slab waveguides of unequal cross-sections. The rigorous field solution is found by determining partial fields, first in the forward direction, i.e., in the  $+z$  direction, and then in the backward direction, i.e., in the  $-z$  direction. A forward partial field results by neglecting both the backward surface wave modes and the backward radiation modes which exist to the right of each interface. Hence, partial fields due to one step discontinuity can be completely determined before continuing on to the next step discontinuity. After the tip of the wedge is reached, the process is reversed; now the forward traveling modes to the left of each interface are neglected and the backward partial fields are determined. The total field is the sum of forward and backward partial fields. A desired accuracy for the total field is reached by repeating the procedure as often as required. Theoretical curves of the radiation pattern, expressed as a superposition of partial fields, will be presented for different wedge geometries and dielectric constants.

The analysis for the TM case is similar and is currently being done.

### APERTURE COUPLED MICROSTRIP "MAGIC-T"

\*Capt M.W. Katsube  
NDHQ  
101 Colonel By Drive  
Ottawa, Ontario  
Canada K1A 0K2

Y.M.M. Antar  
Dept. Elec/Comp Eng.  
Royal Military College  
Kingston, Ontario  
Canada K7K 5L0

A. Ittipiboon, M. Cuhaci  
Communications Research Center  
P.O. Box 11490, Station H  
Ottawa, Ontario  
Canada K2H 8S2

The advent of Monolithic Microwave Integrated Circuits (MMICs) has brought about the development of high performance, miniature microstrip devices. The light weight and conformability of these microstrip devices provide them with advantages over waveguides and make them very attractive for aircraft, missile, and satellite applications. With the maturing of MMIC's design and fabrication, the possibility of producing entire antennae and processing devices on a single or multilayer chip is becoming more feasible.

The "Magic-T" device is commonly found in waveguide form and is well known in the microwave field. This passive, reciprocal device has unique power division and isolation characteristics which are important and find wide applications in the microwave area. However, such a device does not exist in microstrip technology.

A new device (Fig. 1) in the form of a "Magic-T" type construction in microstrip technology, using aperture coupling, is investigated. Aperture coupling is a recent method for feeding electromagnetic energy from one substrate layer to another. It has a number of advantages including the separate integration of top and bottom layer circuitry, whereby the ground plane provides the isolation between the respective layers. Results indicate that this working device in microstrip exhibits the required properties of a "Magic-T".

Theoretical analysis is pursued to produce ideal circuit models based upon modal analysis. A first order approximation is made using the dominant mode, with Lorentz reciprocity and the Poynting theorem. Experimental findings show very good performance over a narrow band (~13-15 GHz) with possible broad band operation upon further optimization of the T-Branch, which at this stage, is the limiting factor. The slot coupling shows good characteristics from ~12-18 GHz.

This paper will present the most recent developments in improving the performance of this device over a wider bandwidth which includes modifications to the T-Branch and an open circuit termination of the feedline.

The aperture coupled microstrip "Magic-T" shows excellent potential in performance for future applications. Its integration into microstrip antennae and multi-layer processing systems may be useful for further MMIC technology advancement.

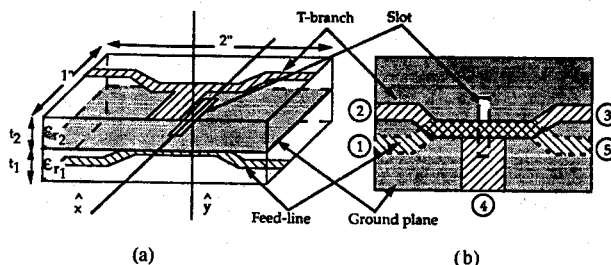


Fig. 1. Configuration of the aperture coupled microstrip "Magic-T." (a) 3-D view. (b) Top view.

## A WAVEGUIDE POLARIZATION CONTROLLER

Kamal Sarabandi  
Radiation Laboratory

Department of Electrical Engineering and Computer Science  
The University of Michigan, Ann Arbor, MI 48109-2122

### Abstract

Polarization agility in a military or remote sensing radar enhances the ability of the radar system in detection and measurement of a feature of interest in a radar scene. Traditionally, the desired polarization is generated by employing one or two dielectric septum polarizers or corrugated dielectric wave-plates. Since the output polarization of a septum polarizer depends on the relative orientation of the dielectric septum with respect to the polarization of the incident wave, waveguide rotary joints are required to generate a set of desired polarizations. The phase and amplitude variations as a function of orientation angle caused by the rotary joints degrade the performance of the polarizer. This problem becomes a limiting factor at millimeter and submillimeter wavelengths. The corrugated dielectric wave-plate limitations are its relatively large size and difficulties in machining narrow grooves for high frequencies.

In this paper a novel waveguide polarizer is introduced that does not require rotary joints and the frequency of operation can easily be adjusted by a few set screws. In this method the degenerate eigenvalues of a circular waveguide are separated by deforming the waveguide cross section slightly. For a specific finite length deformation over the extent of the circular waveguide, the desired phase difference ( $\pi/2$ ) between the two orthogonal modes is obtained. The deformation of the cylindrical shell is kept within the elastic region. In order to generate a desired polarization, the orientation angle of the deformation point with respect to the polarization of the incident wave can be adjusted by using a rotary roller mechanism concentric with the circular waveguide. Analysis of the problem based on the finite element method and an approximate analytical method is given. A prototype model at 34.5 GHz is built and tested. Experimental results shows excellent agreement with the theoretical prediction.

Thu. p.m.

**Computer Aided Design & Optimization  
of  
A Class of Wide Band Turnstile Coupling Junctions**

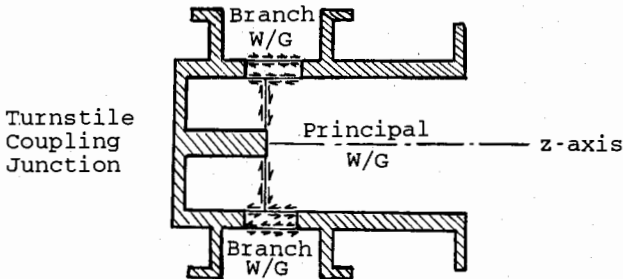
Luiz Costa da Silva & Subir Ghosh

SG Microwaves Inc.

1183 King Street East

Kitchener; Ontario N2G 2N3; Canada

Turnstile coupling junctions are widely used in devices such as ortho-mode transducers, diplexers, multiplexers etc. Traditionally, such designs have been implemented by experimental iteration of the design parameters to reach the desired electrical behaviour. Often observed deficiencies of such an approach are cost and performance compromises. In this paper, the design and optimization of a class of wide band turnstile coupling junctions are described based on precision computer aided MM modelling.



Above figure shows the coupling between a pair of branch waveguides and a principal waveguide. The coupling slots are oriented longitudinally on the side wall of the principal waveguide and along the broad side in the end wall of the rectangular branch waveguides. In order to achieve wide band response from a turnstile junction of this class, it is necessary to employ a vane like structure in the principal waveguide which partially overlaps with the length of the coupling slot along the z-axis. Fully computer aided design and optimization softwares have been developed for such turnstile junctions having any one of the following types of principal waveguide: circular, co-axial or rectangular. The equivalence of the problem as employed in the MM formulation is described in this figure. As is shown, the finite wall thickness at the coupling slot is taken into consideration.

Based on the above mentioned CAD procedure, results will be presented at the conference that demonstrate optimized electrical performance and elimination of experimental iterations in the design of turnstile coupling junctions.

## FULL WAVE ANALYSIS OF THREE-PLANE THREE-PORT RECTANGULAR WAVEGUIDE JUNCTIONS

J.M. Rebollar\*, J. Esteban, J.E. Page

Grupo de Electromagnetismo Aplicado y Microondas  
ETSI Telecomunicación. Universidad Politécnica de Madrid  
28040-Madrid. España.

Three-port junctions of rectangular waveguides play a very important role in the design of a wide number of microwave circuits. Many models, from monomodal (equivalent circuit) to multimodal description, have been proposed to simulate the behaviour of these structures.

An efficient and accurate technique for the analysis of three-port rectangular waveguide junctions is presented in this paper. The technique is based on a generalization of the well-known admittance matrix concept of circuit theory and yields a multimodal description of the junction by means of its Generalized Admittance Matrix (GAM). All the elements of the GAM can be obtained analytically in closed form.

Once the GAM is obtained, the Generalized Scattering Matrix (GSM) can be easily computed (after some algebraic manipulations) and combined with the GSM's of other blocks to characterize more complicated structures in a full wave mode. The proposed technique has been checked with numerical and experimental results from other authors, for the more classical cases of the E-plane and H-plane T-junctions.

In the general case considered in this paper of an E-/H-plane three port junction, both family of modes TE and TM are required in each waveguide port. A convergence study of the scattering parameters will be presented.

## FULL WAVE ANALYSIS OF STEPPED TWISTS IN RECTANGULAR WAVEGUIDES

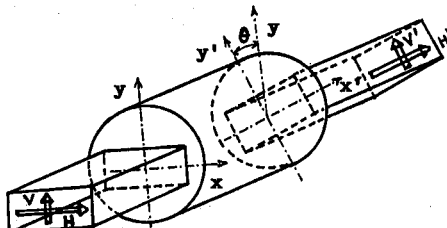
J.M. Rebollar\*, C. Vecino, J. Esteban

Grupo de Electromagnetismo Aplicado y Microondas  
ETSI Telecomunicación. Universidad Politécnica de Madrid  
28040-Madrid. España.

Variable stepped twists in rectangular waveguide can be easily implemented by inserting circular waveguide sections between the rectangular ones. This structure can be used as key building block in the design of polarization rotators.

A full wave and efficient analysis procedure is proposed to characterize the structure. Firstly, the Generalized Scattering Matrix (GSM) of the junction of a circular waveguide and a rectangular waveguide must be obtained. This GSM can be accurately and efficiently computed through the Mode Matching technique since all integrals to be evaluated can be solved analytically when the rectangular waveguide cross-section is smaller than circular waveguide one (R.H. MacPhie, R. Deleuil and A.K. Daoudia, URSI-Meeting, 216, 1992). Considering both polarizations (vertical and horizontal) as two electrical ports, the rectangular-circular discontinuity is a four-port structure and can be characterized by its GSM of generalized 2-port discontinuity. This procedure is advantageous when an adequate mixing of the GSM's for the vertical and horizontal polarizations ( $S^V$  and  $S^H$  respectively) is used.

Once the GSM of generalized 2-port of the two discontinuities are known, they are linked by the circular waveguide section in the usual way (J.M. Rebollar and J.A. Encinar, IEE Pt.H, 1-7, 1988) and taking into account the relationships due to the rotation angle  $\theta$  between the rectangular waveguides. Numerical and experimental results will be presented, showing the validity and efficiency of the proposed method.



RIGOROUS ANALYSIS OF RECTANGULAR WAVEGUIDE LOADED  
WITH DIELECTRIC POST BASED ON FEM-BEM

Zhang Feng      Fu Junmei

(Dept. of Information and Control Engineering  
Xi'an Jiaotong University, Xi'an 710049, P.R.C)

The study of inductive waveguide posts has been a subject of interest to researchers for many years. Cylindrical obstacles in a rectangular waveguide are used in many microwave device, i.e., dielectric materials with high relative permittivity are used to design microwave filter. A great number of papers for the H-plane discontinuity with theoretical or numerical methods are presented, but most of them are limited to the shape, location and number of posts.

The main purpose of this paper is to devise a procedure which is accurate, simple and general in that posts, lossless or lossy, of arbitrary shape, size, location and number can be analyzed effectively. Here, a combination of the finite element method(FEM) and boundary element method(BEM) is used. The waveguide of discontinuity will be divided into two regions,i.e., the inhomogeneous region with a dielectric and the homogeneous one without a dielectric. The FEM and BEM are applied to the inhomogeneous and homogeneous regions respectively.

In this paper, consider a rectangular waveguide containing a dielectric post, where the boundaries  $B_1$  and  $B_2$  connect the discontinuities to the rectangular waveguide,  $B_3$  encloses the the region  $\Omega_3$  containing the dielectrics. The region  $\Omega_4$  is surrounded by  $B_1$ ,  $B_2$ ,  $B_3$  and the short-circuit boundary  $B_0$ .

Unlike general procedures, the boundary  $B_1$  is located far enough to overlook the high-order harmonic wave, and this discontinuity is treated as network problem. Thus, when considering the excitation by  $TE_{11}$  mode, the incident field can be put on the boundary  $B_1$ , and the scattering matrix of the waveguide can be solved with FEM-BEM. A lossy dielectric post in a rectangular waveguide is investigated first, and the results are in agreement with data in literatures. Then a layer dielectric post is analyzed and the results are discussed.

A combination of FEM and BEM has been applied to the analysis of H-plane waveguide is loaded with dielectric post of arbitrary shape, size, number and location. Discontinuity problems with a large homogeneous region or with variations of the location of dielectrics can be handled easily by FEM-BEM. The validity and usefulness of this method is testified.

# THE NEW METHOD FOR ANALYSIS OF A RADIAL RESONATOR WAVEGUIDE DIODE MOUNTING STRUCTURE—SMC METHOD

Ling Chen      Yun-yi Wang

(State Key Laboratory of Millimeter Waves, Southeast University  
Nanjing 210018, P. R. C.)

## ABSTRACT

Radial resonator diode mounts have been widely used for Gunn and IMPATT oscillators where a local resonator is desirable for impedance matching between active devices and a standard rectangular waveguide. In the previous reports, for the theoretical analysis of diode mounts of oscillators, a simplified method is assuming a disc located above a ground plane in free space and not considering the effect of waveguide boundary conditions. A more accurate method is using a magnetic-current excitation to obtain admittance expressions from image theory. This method accounts accurately the effect of waveguide environment including either matched or short-circuited waveguide terminations. But, it requires the formulation of magnetic and electric field equations in each region and matching coefficients at each boundary. Recently, B.D.Bates extended this method and made it easy to formulate the analysis for CAD. However, his approach can be only used for single device or dual device axial mounts. In this paper, we present a new analysis method that is the Simulation Module Composition method (abbreviated: SMC method). In this method, firstly, eight fundamental elements to form multiple step radial-resonator waveguide multiple-diode mounts are found. Secondly, three simulation modules (radial transmission module, radial step module and waveguide-radial line match module) are established from the eight elements. The principle of SMC method is that, using the composition of three modules corresponding to the configuration to simulate field distribution of arbitrary oscillator or power combiner, by using algebraic operation of mathematical simulation matrices of the modules, the driving point and transfer admittances of device mounts are obtained. This method is also applicable to single device mounts. The application examples to oscillators and power combiners show this method is more accurate, more general and more flexible compared with the other method, and is very suitable to CAD.

## ROUGH SURFACES

Chairs: R.J. Marhefka, The Ohio State University; D.L. Jaggard, University of Pennsylvania

Room: Alumni Center, Room 2 Time: 1:30-5:30

|      |  |     |
|------|--|-----|
| 1:30 | RE-EXAMINATION OF THE KIRCHHOFF APPROXIMATION FOR SCATTERING FROM A ROUGH SURFACE<br><i>Yisok Oh*, Kamal Sarabandi, Fawwaz T. Ulaby, The University of Michigan</i>  | 406 |
| 1:50 | A SMOOTHING METHOD FOR ROUGH SURFACE SCATTERING<br><i>Akira Ishimaru, University of Washington</i>   | 407 |
| 2:10 | ON THE USE OF NORMALIZATION IN SMOOTHING BASED ROUGH SURFACE SCATTERING CALCULATIONS<br><i>Gary S. Brown, Virginia Polytechnic Institute &amp; State University</i>  | 408 |
| 2:30 | AN APPLICATION OF THE CONTOUR PATH FINITE DIFFERENCE TIME DOMAIN METHOD TO ROUGH SURFACE SCATTERING<br><i>Frank Hastings*, Shira L. Broschat, John B. Schneider, Washington State University</i>   | 409 |
| 2:50 | BISTATIC ELECTROMAGNETIC SCATTERING FROM SMALL CLUTTER CELLS FOR NON-GAUSSIAN CORRELATED SURFACES<br><i>L. Mockapetris*, Hanscom AFB; D. Tamasanis, ARCON Corporation</i>  | 410 |
| 3:10 | BREAK  |     |
| 3:30 | A GO+PO METHOD FOR COMPUTATION OF RANDOM ROUGH SURFACE SCATTERING<br><i>V. Santalla, M. Vera, A.G. Pino*, ETSI Telecomunicacion</i>  | 411 |
| 3:50 | K-DISTRIBUTED TERRAIN RADAR CLUTTER SIMULATION AND EXPERIMENTS<br><i>Z. Belhadj, S. El Assad, I. Lakkis, J. Saillard*, IRESTE</i>  | 412 |
| 4:10 | TERRAIN MODELLING USING PTD<br><i>S. Ananda Mohan*, University of Technology; Rao K.L. Narasimha, Osmania University</i>   | 413 |
| 4:30 | RADIOEMISSION OF A HOMOGENEOUS HALF-SPACE WITH A SLIGHTLY ROUGH BOUNDARY IN PRESENCE OF AN EXTERNAL SOURCE OF RADIATION<br><i>Oleg A. Tret'yakov, Alexander G. Yarovoy, Nickolay P. Zhuck*, Kharkov State University; Joseph M. Fuks, Alexander A. Puzenko, Radioastronomy Institute</i> | 414 |
| 4:50 | CALCULATING SCATTERED FIELD STATISTICS FROM SURFACE STATISTICS<br><i>Yu. I. Krutin, Yu.K. Sirenko, Institute of Radiophysics and Electronics</i>   | 415 |
| 5:10 | EFFECTIVE BACKSCATTERING DEPOLARIZATION RATIOS OF RANDOMLY ROUGH DIELECTRIC SURFACES<br><i>Jun Zhou, Da-Gang Fang, East China Institute of Technology</i>  | 416 |

## RE-EXAMINATION OF THE KIRCHHOFF APPROXIMATION FOR SCATTERING FROM A ROUGH SURFACE

Yisok Oh\*, Kamal Sarabandi, and Fawwaz T. Ulaby

Radiation Laboratory

Department of Electrical Engineering and Computer Science  
The University of Michigan, Ann Arbor, MI 48109-2122

### Abstract

The Kirchhoff approximation for the scattering of electromagnetic waves from a randomly rough surface has been studied extensively for several decades. In Kirchhoff approximation (KA), the total fields at any point on the surface are approximated by those of a plane interface tangent to the surface at that point. Aside from the tangent plane approximation, further simplifications are usually required to evaluate the ensemble averages involved in the diffraction integrals for a dielectric rough surface. A common simplification is achieved by expanding the integrands in terms of the local surface slopes and then evaluating these using integration by parts and discarding the "edge effect" contributions [P. Beckmann and A. Spizzichino, *The Scattering of Electromagnetic Waves from Rough Surfaces*, Macmillan, New York, 1963].

This simplification, however, is unnecessary since the ensemble average of the diffraction integrand can be evaluated exactly by employing the characteristic functions of random vectors specifying the surface and assuming Gaussian height and slope distributions. The ensemble average of the integrand can be evaluated exactly by using the spectral representation for the delta function and the characteristic function of a Gaussian random vector [A.H. Holzer and C.C. Sung, *J. Appl. Phys.*, 49, PP.1002-1011, 1978], at the expense of computing a four-folded integral for a one-dimensional random surface. In this paper, the four-folded integral is integrated analytically, and the final form of the scattering coefficients of the one-dimensional random surface is given in terms of a single integral in which the integrand is simply a function of the surface correlation function and its derivatives.

This technique is compared with the conventional KA and a numerical simulation for scattering from a randomly rough dielectric surface. The backscattering coefficients obtained by this technique (e.g., in case of Gaussian correlation function) agree better with the numerical simulation than those obtained by the conventional KA method.

## A SMOOTHING METHOD FOR ROUGH SURFACE SCATTERING

Akira Ishimaru  
Department of Electrical Engineering  
University of Washington  
Seattle, Washington 98195

A smoothing method is applied to rough surface scattering which extends the range of validity beyond the conventional perturbation method. The theory is based on equivalent boundary conditions. The Dyson equation is solved to obtain the coherent field and the result is identical to the Watson-Keller solution. It is noted that, even for a perfectly conducting surface, the surface exhibits an equivalent surface impedance due to the roughness, which can support a surface wave. The equivalent reflection coefficient is compared with those of the perturbation method and the phase perturbation method. The bistatic cross section consists of the first-order term and the second-order ladder and cyclic terms. The first-order term is obtained by the coherent incident field scattered by the surface with the coherent Green's function and is similar to the distorted Born approximation. This is similar but different from Watson-Keller results and reciprocity is satisfied. The second-order ladder term is obtained by considering the coherent field incident on the surface which is propagated along the surface with the coherent Green's function, and then scattered with the coherent Green's function. This is the Bethe-Salpeter equation and the solution is reciprocal. The cyclic term is similar to the ladder term except that the conjugate field is propagated in the reverse direction on the surface. The result shows that the cyclic term gives a peak in the backscattering direction. When the rms height is small, the second-order term is negligible and the first-order term is dominant. As the rms height increases, the second-order term becomes significant and enhanced backscattering takes place. Comparisons with numerical simulations are given to show the extended range of validity.

Thu. p.m.

## ON THE USE OF NORMALIZATION IN SMOOTHING BASED ROUGH SURFACE SCATTERING CALCULATIONS

Gary S. Brown

Bradley Department of Electrical Engineering  
Virginia Polytechnic Institute & State University  
Blacksburg, VA 24061-0111

Smoothing, as applied to rough surface scattering, is a technique that splits the surface current into its mean and fluctuating parts and uses approximate knowledge of the mean to generate a very accurate estimate of the fluctuating part. The method assumes that the average current is much larger than the fluctuating part; hence, the method is restricted to surfaces having small roughness height. This restriction applies even if the surface is a randomly elevated plane. To overcome this limitation, it has been proposed to normalize the basic integral equation for the surface current by the height-dependent phase factor which is the source of the small height restriction. Previous work has demonstrated that this approach to first normalize the integral equation and then apply smoothing is very effective when the roughness comprises small scale components superimposed on a large, gently undulating spectral component. It was further proposed that the method might be useful for other classes of surface roughness. This paper address this topic.

It was originally proposed that normalization might accelerate the rate of convergence of a standard iterative solution of the current integral equation. However, if the ratio test for convergence is applied to the normalized integral equation, one obtains exactly the same result as with the unnormalized equation. That is, exactly the same ratio of terms results. It would seem that normalization is not as robust as anticipated. This conclusion is incorrect because it assumes that the normalization is intended to improve the convergence of a standard iterative series which is not the case. Normalization is intended to work with smoothing not standard iteration. It is shown that when used in conjunction with smoothing, the success of normalization becomes very dependent on the spectral content of the part of the roughness used in the normalization process. For example, using low frequency components is very effective in the normalization process but the use of high frequencies (compared to  $k_0$ ) provides no improvement relative to a standard iterative approach. In this paper it is shown just how the spectral content of the normalizing height enters into the calculation of the fluctuating part of the current and how it controls the degree to which the method improves on standard iteration.

## AN APPLICATION OF THE CONTOUR PATH FINITE DIFFERENCE TIME DOMAIN METHOD TO ROUGH SURFACE SCATTERING

Frank Hastings\*, Shira L. Broschat, and John B. Schneider  
Electrical Engineering and Computer Science  
Washington State University  
Pullman, WA 99164-2752

The problem of modeling scattering from randomly rough surfaces has been approached through approximate and exact numerical methods. Both approaches have limitations: Approximate solutions are typically restricted to specific regions of validity and exact numerical solutions are hindered by the computational requirements inherent in the problem. Recently, the Finite Difference Time Domain (FDTD) method has been used to model rough surface scattering. This approach produces results with low computational cost; however, the original FDTD algorithm lacks sufficient numerical accuracy. A contour path (CP) modification of the FDTD algorithm has performed well in general scattering problems involving curved surfaces [Jurgens *et al.*, *IEEE Trans. Antennas Propagat.*, AP-40(4), 357-366, 1992]. In this work, the CP-FDTD method has been applied to the rough surface scattering problem. The results generated are accurate, while still maintaining modest computational costs.

In this paper, results are presented for the normal incidence excitation of one-dimensional Dirichlet surfaces with Gaussian statistics satisfying a Gaussian roughness spectrum. Monte Carlo simulations are used to compute the scattering cross sections as a function of scattered angle for various correlation lengths and rms surface heights. The method is similar to that of Thorsos [*J. Acoust. Soc. Am.*, 83(1), 78-92, 1988], using a tapered incident field. For each simulation, a large number of finite-length surfaces are generated. For each surface realization, the CP-FDTD simulation produces near-zone scattered field data which are transformed to the far field to obtain the scattered intensity. These individual results are then averaged over the total number of surfaces to obtain the cross sections.

Thu. p.m.

## BISTATIC ELECTROMAGNETIC SCATTERING FROM SMALL CLUTTER CELLS FOR NON-GAUSSIAN CORRELATED SURFACES

L. Mockapetris\*

Environmental Effects Branch  
Applied Electromagnetics Division  
Electromagnetics and Reliability Directorate  
Rome Laboratory, Hanscom AFB, MA 01731

D. Tamasanis

ARCON Corporation  
260 Bear Hill Road  
Waltham, MA 02154

Finite cell size scattering is increasingly becoming an important topic because the narrow pulse widths used in wide band radars result in small clutter cells. Decreasing the clutter cell size has been shown to alter the characteristics of the clutter power. In this paper, the impact that two different surface correlation functions have on scattered power for decreasing cell size is calculated. Both Gaussian and Bessel correlated surfaces are studied. Surface scattering is calculated using a model that combines small and large scale roughnesses introducing several aspects of the scattering which are affected by the cell size. Both the small and large scale scatterers have distinct polarization dependences which have to be combined. For Gaussian correlation, there are regions where the scattering is dominated by scattering from the small scale facets. For Bessel correlated surfaces the scattering from the small scale facets is usually considerably less than the large scale contribution. However, because the polarization state of the signal scattered by the small scale elements is significantly different from that scattered from the large scale elements, the small scale scattering will become dominant at the polarization angles where the large scale roughness has scattering minima.

The type of surface considered has a large number of similar scatterers that typically results in Rayleigh scattering. However, as the cell size is decreased, significant differences in behavior are observed. Small scale scattering will not be affected by decreasing the cell size because the dimensions of the clutter cell will remain much larger than the characteristic dimension of the small scale scatterers. The large scale scattering however, will be affected by reduction of the cell size because the cell dimensions will be on the order of a few large scale correlation lengths.

## A GO+PO Method for Computation of Random Rough Surface Scattering

V. Santalla, M. Vera, A.G Pino (\*)

Departamento de Tecnologias de las Comunicaciones  
ETSI Telecomunicacion  
Universidad de Vigo  
36200-VIGO, SPAIN

The problem of scattering from a rough surface has become of special interest in recent years. Many theories have been developed to explain and predict measured data. None of them is general and rigorous at the same time, usually several assumptions are used to simplify computational procedures [Beckmann and Spizzichino, "The scattering of electromagnetic waves from rough surfaces", Artech House, 1987].

The GO+PO method we have implemented is a high frequency model. This hybrid method combines principles of Geometric Optics (GO) and Physics Optics (PO). These procedures have already been applied successfully to radar cross section computation of arbitrary shaped cavities [H.Ling, R.C.Chou, S.W.Lee, "Shooting and bouncing rays: Calculating the RCS of an arbitrarily shaped cavity". IEEE Trans. on Ant. and Prop. Feb. 1989. A.G.Pino, F. Obelleiro, J.L. Rodriguez, A.M.Arias "A comparison of ray tracing methods for the analysis of high frequency scattering by arbitrarily shaped cavities." URSI Digest, Chicago, Jul. 1992.]. The plane wave that incides on the surface is modelled by rays, each one carrying information about amplitude, phase, trajectory and polarization. These rays are grouped in triads. Using ray tracing techniques the rays are driven (while changing their parameters depending on the travelled path and the reflection point on the surface) to the aperture plane in the far field region. Here, linear distributions of phase and amplitude on the triangular domains are used to compute by aperture integration the scattered field.

The main restriction of this method is that it applies only to surfaces with radius of curvature much greater than the wavelength of the incident radiation. However, in the microwave range, where the wavelength is rather small, one can use this model in most of the terrain types we are interested on. This method allows to consider multiple scattering and shadowing effects, (actually, taking them into account becomes a geometrical problem). Moreover, it is easy to include diffraction effects because it simply implies to consider the Geometrical Theory of Diffraction, an extension to GO.

The application of the method implies, inherently, a sampling of the surface, which allows to generate surfaces with a given statistical distribution and correlation function, avoiding the problems with the statistical parameters that come out with interpolation.

In this paper plane wave incidence will be investigated. Results will be presented for rough surfaces with Normal distribution and quadratic exponential correlation function ( $Ce^{-\frac{r^2}{R^2}}$ ).

## K-Distributed Terrain Radar Clutter Simulation and Experiments

Z. BELHADJ, S. EL ASSAD, I. LAKKIS and J. SAILLARD\*  
Laboratoire S2HF (Systèmes et Signaux Hautes Fréquences)  
La Chantrerie-CP 3003-44087 NANTES cedex 03 - FRANCE  
(Ph : (33) 40 68 30 64, Fax: 40 68 30 66)

When a radar illuminates a large area, the amplitude probability density function (PDF) of the clutter can be approximated by a Rayleigh distribution. However, measurements for high resolution radars reveal a substantial departure from the Rayleigh statistics. At present, non-Gaussian clutter models, (such as K-distributed clutters), are considered.

Under the multiplicative noise model assumption of the non-Gaussian clutter, it is assumed that the received polarimetric returns for a one-look image are the product of a complex Gaussian vector (which represents the speckle) and a gamma-distributed scaling factor which characterizes the spatial variability of the clutter.

In this paper, first, we use the Olivier, Novak and Burl algorithms for the clutter simulation, for which two types of clutter models are used. Therefore, based on a priori knowledge, we compare and interpret our results in relation to our predictions- such as the autocorrelation of some simulation steps, histograms of normalized amplitudes...

In practice, the K-distribution is derived with one parameter  $\alpha$ . The variation of this parameter will characterize each class of clutter (trees, grass, ...). Homogenous areas will be characterized by a high  $\alpha$ , whereas it will be small when concerning heterogeneous areas. The parameter  $\alpha$  isn't fixed for a specified type of clutter. In fact, it varies according to the frequency band, range resolution and radar look angle.... When the range resolution increases, this parameter also increases and can be explained by the decrease of the correlation between neighboring pixels. In addition, when the frequency increases,  $\alpha$  decreases. This is because the clutter fluctuation at the lower frequency band increases and the waves may penetrate into the crown region.

Experimental results obtained from data measurements of the MAESTRO-1 1989 campaign, which was done by Nasa/JPL, are presented. The measured target was a forest in the south of France. This forest consists of trees of different ages. The histogram of  $\alpha$  as a function of the age of the trees shows that when the trees are young, this parameter is small and when they are old,  $\alpha$  is large, which can be accounted for by the large number of fluctuations in young trees.

Results show how K-distribution can characterize amplitude distribution of pixel intensities when concerning a heterogeneous clutter. However, it will not agree when it concerns a homogenous clutter. This is clearly shown when we compare probability density function and cumulative density function (CDF) of amplitude and phase differences of theoretical and experimental results of various types of clutter.

Finally, we know that presence of the speckle in SAR images causes a major effect in image segmentation and consequently in terrain classification. For this reason, we will present theoretical and experimental results of various speckle reduction algorithms, such as the span image, the polarimetric whitening filter (PWF) image and the optimal weighted sum of the three simple polarimetric images.

## TERRAIN MODELLING USING P.T.D.

\*Ananda Mohan, S  
School of Electrical Engineering  
University of Technology, Sydney  
Australia

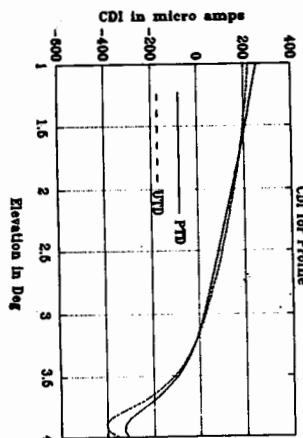
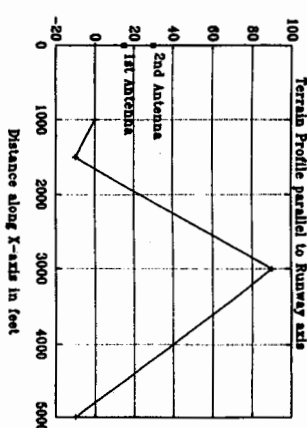
and Narasimha, Rao K.L.  
NERTU  
Osmania University  
Hyderabad, India

Aircraft Landing aids are generally affected by the multipath generated by the surrounding terrain and other obstructions such as buildings. In the case of ILS, the glidepath antennas use the surrounding terrain for forming overlapping signals in space. If the terrain is uneven, kinks will be formed in the glidepath thereby causing difficulties in the landing operation. Hence, a number of efforts have been made by the electromagnetic community to model and assess the electromagnetic scattering from an uneven terrain. The use of GTD and its uniform variant UTD [1] has so far been used to model the effects of uneven terrain on aircraft landing aids. In this paper we apply the physical theory of diffraction (PTD)-for the problem of terrain modelling. The total field at an observation point, according to PTD is given by

The terrain in front of the glidepath antenna mast is approximated as consisting of connected flat conducting plates, over the first Fresnel zone. The  $\bar{E}^{\text{dir}}$  is the field directly radiated by antenna to the receiver. The  $\bar{E}^{\text{scat}}$  contains the sum of singly and doubly scattered fields due Physical Optics Currents induced on the plates of the modelled terrain in the direction of observation point. The inclusion of double scattered fields take into consideration the effects of blockages. Detailed algorithms have been developed for systematically obtaining the illuminated regions for single and double scattered fields. The  $\bar{E}^{\text{PTD}}$  is the diffracted electric fields calculated using the PTD from the edges of the modelled terrain [2]. The integrations involved in the computation of Physical Optics Scattered fields and PTD diffracted fields have been simplified using the method of stationary phase. The total fields are evaluated by vectorially adding the contributions of fields from each antenna. Results on radiated fields as well as C.D.I. are computed for Null reference glidepath system. The computed results obtained using PTD have been compared with those of UTD [1] and the agreement appears to be satisfactory.

## References

[1] Luebbers et al, IEEE Trans, Vol AES-18, pp 11-19, Jan 1992  
[2] Pathak, PH, chapter 4, Antenna Handbook (edited by Lo and Lee), VanNostrand, 1988.



## RADIORMISSION OF A HOMOGENEOUS HALF-SPACE WITH A SLIGHTLY ROUGH BOUNDARY IN PRESENCE OF AN EXTERNAL SOURCE OF RADIATION

Oleg A.Tret'yakov, Alexander G.Yarovoy, Nickolay P.Zhuck,\*  
Department of Radiophysics, Kharkov State University,  
Svobody Sq., 4, Kharkov-77, 310077 Ukraine,  
and Joseph M. Fuks, Alexander A.Puzenko,  
Radioastronomy Institute,  
Krasnoznamyonnaia str., 4, Kharkov-2, 310002 Ukraine

The present report is a response to practical needs in the field of microwave remote sensing which in theoretical terms reduce to modelling of radioemission from a rough ground surface. We have developed a model that is more general than the already known ones in the following respects: (a) it takes account of radiation from external sources (the atmosphere and space), (b) the ground cover is assumed to be permeable to an electromagnetic field and to be a uniform dissipative dielectric.

In the report, a solution of the problem of the brightness temperature of the outgoing radiation is proposed and the results of an extensive computer-aided analysis of the radiobrightness contrast between smooth and rough boundaries are discussed.

Within the framework of the proposed solution the angular dependence of a brightness temperature of external sources is specified in the form typical of a nonisothermal atmosphere. The radioemission of soil is evaluated by means of the electrodynamic theory of equilibrium thermal fluctuations. The effect of roughness is allowed for by means of multiple scattering theory. The principal analytic results are obtained for the brightness temperature of the outgoing radiation at arbitrary polarization. They apply to the general case of statistically anisotropic roughness and can be used to derive equations for the Stokes parameters of the thermal radioemission.

In course of numerical calculations the roughness is assumed to be isotropic and Gaussian-correlated. The dependencies of brightness contrast on the geometric characteristics of the surface irregularities, the electrophysical characteristics of the dissipative half-space, and the viewing angle are investigated and physical explanation of the revealed effects are proposed.

## CALCULATING SCATTERED FIELD STATISTICS FROM SURFACE STATISTICS

Yu.I.Krutin' and Yu.K.Sirenko (PhD)  
Institute of Radiophysics and Electronics, Academy  
of Sciences of the Ukraine, 12 Acad. Proskury st.,  
Kharkov, 310085, Ukraine

Some efficient methods of numerical analysis of scattering by arbitrary and random surfaces are presented. A numerical algorithm free from restrictions on the surface inhomogeneities dimension, the configuration of these inhomogeneities (the function of height may be multiciphered), the nature of excitation and potential shadowing is suggested. By using this algorithm some data - both for the concrete surface realization and statistic - about the nature of the scattered field in any region of the space over a surface were obtained, the error being predictable.

This algorithm is based on the numerical methods of analytical regularization for the analysis of electromagnetic properties of periodic and compact closed media boundaries. The standard numerical realization of these methods at the increase of the range of the problem parameters (for example, a typical size of the radiated region) meets some restrictions arising computer resources. The authors see a way of overcoming these restrictions in using special iteration procedures and broadening of the approach which is based on the "S.-C.-R.P." and is methodologically substantiated (D.Maystre & J.P.Rossi, J.Opt.Soc.Am.A.8, 1276-1282, 1986).

In this report we confine ourselves to the case of horizontal polarization and perfectly reflective boundaries. This restriction nature. The authors are on the point of suggesting analogous algorithm for the case of another field polarization and arbitrary boundaries of dielectric media including the case when one medium is arbitrarily (randomly) inhomogeneous.

## EFFECTIVE BACKSCATTERING DEPOLARIZATION RATIOS OF RANDOMLY ROUGH DIELECTRIC SURFACES

Jun Zhou \* and Da-Gang Fang \*\*

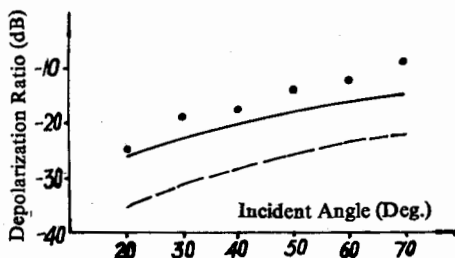
\* Doctoral class, Graduate School, East China Institute of Tech.

\*\* Dept. of Electrical Engineering, East China Institute of Tech.

Nanjing, P. R. of China 210014

Measuring backscattering Depolarization Ratios of surfaces is one powerful mean with which properties of randomly rough dielectric surfaces can be effectively detected. In the present theoretic models available to deal with the surface scattering topic, an actual scatterometer-transmitted polarized EM beam with certain angle-width is approximately treated as a plane EM wave or a scalar beam (F. T. Ulaby et al., *Microwave Remote Sensing*, V2, chapter12, 1982). However if a little careful, we can find that the measured backscattering Depolarization Ratios are sometimes much larger than the calculated upon the above approximation; the more small the ratio of a rough surface's rms height to the used wavelength is, the more larger the measured is than the calculated. Through elaborate analysis, the main cause responsible for the big error is revealed to be beam angle-width. The present generally-accepted plane wave or scalar beam approximation fails to deal with the cross-polarized backscattering of smoother surfaces in the calculation of backscattering Depolarization Ratios. To set up a direct relation between measurement and rigorous vector EM theory will be used, we introduce a new concept called effective backscattering Depolarization Ratio. On the basis of the rigorous vector EM theory, two exact analytic expressions of the effective backscattering Depolarization Ratios of a randomly rough dielectric surface for both horizontally and vertically polarized incident EM beams are driven, either is just the sum of both solution from the present theoretic models as an incident beam is approximated as an EM plane wave or a scalar beam and one modifying item resulting from the divergence of ray directions within the beam angle-width. The modifying item is independent of the rough surface's rms height.

The figure below shows the comparison between the actually measured backscattering Depolarization Ratio with a beam (expressed as black dots, from A. K. Fung et al., *IEEE T-GRS*, 2, 367-368, 1992) and both the solution from the Small Perturbation Model (dashed line) and this paper's effective backscattering Depolarization Ratios (solid line) at some different incident angles, for a randomly slightly rough bare soil surface with a rms height of 0.32cm. Two-way angle-width and central frequency of the incident EM beam used are  $12^\circ$  and 1.5GHz respectively (Y. Oh et al., *IEEE T-GRS*, 2, 371-372, 1992). Comparison inside the figure indicates that this paper's prediction is much closer to measurement than the solution from the Small Perturbation Model. The considerable volume scattering beneath the surface is mainly responsible for the high measured backscattering Depolarization Ratios.



## **Author Index**

## Author Index

Aberegg, K. R. .... 160  
 Abiri, H. .... 102  
 Alber, C. .... 39  
 Alexanian, A. .... 132  
 Alexopoulos, N. G. .... 264, 309  
 Ali, A. S. .... 347  
 Alishouse, J. C. .... 36  
 Allen, K. .... 113  
 Anastassiou, H. .... 194, 203  
 Anderson, C. .... 390  
 Andrade, O. M. .... 177  
 Angell, T. S. .... 229  
 Antar, Y. M. M. .... 398  
 Arvas, E. .... 361  
 Asari, E. .... 222  
 Badii, V. .... 209  
 Baker-Jarvis, J. R. .... 180  
 Bakhtazad, A. .... 102, 103  
 Balanis, C. A. .... 131  
 Balmain, K. G. .... 220  
 Bansal, R. .... 2  
 Bantin, C. C. .... 220  
 Bao, X. L. .... 79  
 Barakat, M. .... 85  
 Barber, G. C. .... 260  
 Barkdoll, T. L. .... 259  
 Barkeshli, K. .... 23  
 Barna, G. .... 390  
 Baron, J. .... 143  
 Bebermeyer, R. .... 215, 216, 219  
 Beck, F. B. .... 158  
 Belhadj, Z. .... 412  
 Benarroch, A. .... 111  
 Bermudez, L. A. .... 299  
 Besieris, I. M. .... 245, 362  
 Bhasin, K. B. .... 165  
 Bhattacharyya, A. K. .... 268, 271  
 Bleszynski, E. .... 10, 324  
 Bleszynski, M. .... 10, 319, 324  
 Blomme, K. .... 31  
 Bock, B. M. .... 390  
 Borderies, P. .... 263  
 Boric-Lubecke, O. .... 96  
 Bouche, D. .... 76  
 Bradley, R. .... 280  
 Bridges, G. E. .... 184  
 Bringhurst, S. .... 177  
 Broschat, S. L. .... 59, 409  
 Brown, G. S. .... 170, 408  
 Brumm, D. .... 390  
 Bryan, K. .... 234  
 Burke, G. J. .... 230  
 Burkholder, R. J. .... 202, 205  
 Burnside, W. D. .... 133  
 Butler, A. J. .... 100  
 Butler, C. M. .... 376, 394  
 Campbell, R. .... 113, 390  
 Cangellaris, A. .... 65, 258, 316  
 Cardama, A. .... 11  
 Carpentier, J. F. .... 20  
 Carvalho, M. C. R. .... 285  
 Casey, J. P. .... 2, 207  
 Castillo, S. P. .... 61, 217, 352  
 Catedra, M. F. .... 154  
 Catten, C. .... 127  
 Cendes, Z. .... 195, 196  
 Cha, C. C. .... 155, 156  
 Chambers, C. B. .... 350  
 Chan, B. .... 214  
 Chang, F. C. .... 389  
 Chang, T. .... 133  
 Chang, H.-C. .... 101  
 Chatterjee, D. .... 329, 337  
 Chaturvedi, P. .... 226  
 Chatzipetros, A. A. .... 362  
 Chen, J. T. .... 230  
 Chen, J. .... 141  
 Chen, K. M. .... 215, 216, 219, 381  
 Chen, L. .... 404  
 Chen, W.-Y. .... 397  
 Chen, H.-Y. .... 49  
 Chen, W. .... 17  
 Chew, W. C. .... 58, 228, 317  
 Chidambaram, S. .... 179  
 Chiou, V. .... 232  
 Chive, M. .... 52, 55, 56, 128  
 Cho, N. Y. .... 112  
 Choi-Grogan, Y. S. .... 197  
 Choudhary, S. .... 5  
 Chow, Y. L. .... 157  
 Chu, J.-Y. .... 75  
 Cockrell, C. R. .... 158  
 Compton, R. C. .... 167  
 Cone, G. .... 284  
 Constantinides, E. D. .... 333  
 Costa da Silva, L. .... 400  
 Cresson, P. Y. .... 52, 55  
 Croisant, W. J. .... 181  
 Crowgey, S. R. .... 349  
 Cuhaci, M. .... 351, 398  
 Cwik, T. .... 253  
 Dahle, J. S. .... 17  
 Daniel, E. M. .... 63  
 Davidson, D. B. .... 240  
 Davis, A. M. J. .... 368  
 De Zutter, D. .... 31  
 Deale, O. C. .... 53, 124  
 Dempsey, M. .... 314  
 Deshpande, M. D. .... 158  
 Di Massa, G. .... 18

|                        |                 |                   |                    |
|------------------------|-----------------|-------------------|--------------------|
| Diaz, R. E.            | 264, 309        | Grannemann, R. S. | 373                |
| Dinger, R. J.          | 172             | Gribbons, M.      | 65                 |
| Do-Nhat, T.            | 98, 99          | Griese, E.        | 159, 269           |
| Dominek, A.            | 135             | Grimm, J. M.      | 294                |
| Drachman, B.           | 294             | Grobic, D.        | 284                |
| Drewniak, J. L.        | 346             | Groom, R. W.      | 74                 |
| Duan, D.-W.            | 328             | Grosvenor, J. H.  | 178                |
| Dubois, L.             | 52, 55, 56, 128 | Guangyou, F.      | 223                |
| Duhamel, F.            | 56, 128         | Guoxiang, S.      | 161                |
| Duncan, S.             | 280             | Gupta, K. C.      | 347                |
| Dvir, I.               | 357             | Gutti, C. S.      | 272                |
| Dybdal, R. B.          | 136             | Gwynne, J. S.     | 348                |
| Eiken, S. D.           | 200             | Habashy, T. M.    | 74                 |
| Einziger, P. D.        | 357             | Hafner, Ch.       | 71, 72             |
| El Assad, S.           | 412             | Hall, W. F.       | 140                |
| Elsherbeni, A. Z.      | 16              | Han, Y.           | 40                 |
| Engheta, N.            | 50, 304, 305    | Han, H. C.        | 174                |
| Epp, L. W.             | 254             | Hanson, G.        | 179                |
| Esselle, K. P.         | 125             | Harfoush, F. A.   | 147                |
| Esteban, J.            | 401, 402        | Hartman, R. J.    | 126, 206, 290, 297 |
| Faché, N.              | 31              | Harrison          | 218                |
| Fallon, D.             | 173             | Hastings, F.      | 409                |
| Fan, Z.                | 300, 396        | Haupt, R. L.      | 230                |
| Fang, C.-C.            | 49              | Havrilla, M.      | 221                |
| Fang, D.-G.            | 416             | Hazen, D. A.      | 38                 |
| Farr, E. G.            | 345             | Heck, L.          | 77                 |
| Fedor, L. S.           | 38              | Hejase, H. A. N.  | 15, 201            |
| Feickert, C. A.        | 181             | Hermeline, F.     | 8                  |
| Felsen, L. B.          | 82, 263         | Heron, P.         | 84                 |
| Feng, Z.               | 325, 403        | Heyman, E.        | 356, 359, 360      |
| Fermelia, L. R.        | 388             | Hirvela, G. O.    | 350                |
| Fikioris, G.           | 83              | Hodges, R. E.     | 153                |
| Flood, K. M.           | 246             | Hood, R. E.       | 44                 |
| Fontana, T.            | 192, 193        | Hoppe, D. J.      | 254                |
| Foster, K. R.          | 50              | Houshmand, B.     | 306, 344           |
| Franklin Drayton, R.   | 30              | Howard, G. E.     | 157                |
| Franzese, N.           | 18              | Huang, C.         | 171, 276, 323      |
| Fröhlich, J.           | 73              | Huang, G.-T.      | 233                |
| Fukai, I.              | 148             | Hubing, T. H.     | 346                |
| Fuks, J. M.            | 414             | Hunsaker, J.      | 127                |
| Fukuchi, H.            | 109             | Hunsberger, F. P. | 364                |
| Gago-Ribas, E.         | 82              | Hurst, M. P.      | 386                |
| Garai, J. M.           | 298             | Hussar, P. E.     | 336                |
| Garcia-Castillo, L.-E. | 274, 275        | Hutchens, S. A.   | 16, 53             |
| Gasiewski, A. J.       | 45              | Ianconescu, R.    | 359, 360           |
| Ge, J. X.              | 168             | Ibrahim, K. A.    | 70                 |
| Gedney, S. D.          | 15, 201         | Ilavarasan, P.    | 215, 216           |
| Gerry, M. J.           | 363             | Infante, D.       | 221                |
| Geyer, R. G.           | 182             | Ishihara, T.      | 334                |
| Ghannouchi, F. M.      | 191             | Ishimaru, A.      | 310, 407           |
| Ghosh, S.              | 400             | Iskander, M. F.   | 120, 127, 146, 177 |
| Gilbert, B.            | 32              | Itoh, T.          | 96                 |
| Glisson, A. W.         | 3               | Ittipiboon, A.    | 19, 351, 398       |
| Goggans, P. M.         | 3               | Jackson, D. R.    | 395                |
| Goodberlet, M. A.      | 43              | Jaggard, D. L.    | 246, 247, 314      |
| Goorjian, P.           | 142             | Jakoby, R.        | 108                |
| Goto, K.               | 334             | Jamnejad, V.      | 253                |
| Gottumukkala, K. R.    | 272             | Janezic, M. D.    | 178, 180           |

|                    |                     |                   |                    |
|--------------------|---------------------|-------------------|--------------------|
| Jaroszewicz, T.    | 319                 | Larose, C.        | 6, 9               |
| Jary, P.           | 299                 | Lavenan, T.       | 78                 |
| Jaureguy, M.       | 263                 | Laxpati, S. R.    | 320                |
| Jedlicka, R. P.    | 217, 352            | Le Boulch, D.     | 78                 |
| Jeng, S.-K.        | 75                  | Le Martret, R.    | 8                  |
| Jensen, D.         | 127                 | Le Potier, C.     | 8                  |
| Jensen, M. A.      | 66                  | Leblebicioglu, K. | 236                |
| Jevtic, J.         | 188, 256            | Lecroart          | 56                 |
| Jiang, M.          | 34                  | Lee, H.-M.        | 374                |
| Jiang, X.          | 229                 | Lee, J.-F.        | 100, 254, 292      |
| Jianxin, L.        | 90, 286             | Lee, K. F.        | 17                 |
| Jiao, Y. C.        | 86                  | Lee, R.           | 188, 197, 256, 259 |
| Jin, J.            | 252                 | Lee, R. Q.        | 17, 185            |
| Jofre, L.          | 11                  | Lee, Y. H.        | 241                |
| John, W.           | 159                 | Lee, J. K.        | 241                |
| Johnson, J.        | 39                  | Legier, J. F.     | 28                 |
| Jones, C. A.       | 178                 | Lerman, B. B.     | 53, 124            |
| Joseph, R.         | 142                 | Li, C.-L.         | 381                |
| Judkins, J. B.     | 239, 240            | Li, Q.            | 215                |
| Junmei, F.         | 325, 403            | Li, H.-J.         | 232, 233           |
| Jurgens, T. G.     | 147                 | Li, L.            | 244                |
| Kao, P. S.         | 87                  | Liang, C. S.      | 373                |
| Kashiwa, T.        | 148                 | Liansheng, Y.     | 286                |
| Kastner, R.        | 318                 | Liepa, V.         | 234                |
| Katehi, L. P. B.   | 14, 29, 30, 33, 164 | Lim, J. S.        | 322                |
| Katsube, M. W.     | 398                 | Lin, H. P.        | 110                |
| Katz, D. S.        | 144                 | Lin, J. C.        | 118, 126           |
| Kawalko, S. F.     | 320                 | Lin, J.-H.        | 317                |
| Kaye, M.           | 291                 | Lin, M.-S.        | 75                 |
| Kempel, L. C.      | 321                 | Lin, T.-H.        | 101                |
| Kennis, P.         | 20, 28              | Lindell, I. V.    | 248                |
| Khebir, A.         | 191                 | Linder, J. E.     | 60                 |
| Khesbak, S.        | 281                 | Ling, H.          | 4                  |
| Khizhniiak, N. A.  | 312                 | Litva, J.         | 141, 145, 383      |
| Kiener, S.         | 9, 265              | Liu, J. C.        | 247                |
| Kimrey, H.         | 146                 | Liu, Q.-H.        | 227                |
| King, R. W. P.     | 83, 238             | Lucas, E.         | 192, 193           |
| Kinowski, D.       | 28                  | Luebbers, R.      | 134                |
| Klaus, G.          | 72, 73              | Luypaert, P.      | 293                |
| Kleinman, R. E.    | 229                 | Ma, Y.            | 311                |
| Kobayashi, R.      | 97                  | Maci, S.          | 94, 331            |
| Kobayashi, K.      | 375                 | Madsen, W. B.     | 38                 |
| Komar              | 218                 | Mallikarjun, T.   | 287, 288           |
| Kong, J. A.        | 87, 174             | Manara, G.        | 331, 332           |
| Kormanyos, B. K.   | 164                 | Manny Jr., C. W.  | 59                 |
| Koshikawa, S.      | 375                 | Margulies, W.     | 285                |
| Kotulski, J. D.    | 371                 | Marhefka, R. J.   | 333                |
| Kouki, A. B.       | 191                 | Marshall, L.      | 149                |
| Kouyoumjian, R. G. | 332                 | Martin, A. H.     | 48                 |
| Krauss, T. G.      | 155                 | Marzano, F. S.    | 44                 |
| Krutin, Yu. I.     | 415                 | Masero, A.        | 284                |
| Kuga, Y.           | 310                 | Mathis, A. W.     | 394                |
| Kumar, A.          | 208, 387            | Mautz, J. R.      | 206, 290, 297      |
| Kunz, K. S.        | 149                 | Maysire, D.       | 372                |
| Kuwabara, N.       | 97                  | Mazzetti, P.      | 284                |
| Laheurte, J.-M.    | 14                  | McArthur, P.      | 127                |
| Lakhtakia, A.      | 268                 | McCormack, C. J.  | 230                |
| Lakkis, I.         | 412                 | McInemey, M. K.   | 181                |

|                     |                         |                   |                    |
|---------------------|-------------------------|-------------------|--------------------|
| Meade, D. B.        | 255                     | Pan, G.           | 32                 |
| Mercader, L.        | 111                     | Papapolymerou, I. | 54                 |
| Michel, C.          | 52, 55                  | Papazian, P.      | 113                |
| Miller, M.          | 385                     | Parker, J. W.     | 190                |
| Miller, E. K.       | 230                     | Pathak, P. H.     | 202, 203, 205, 380 |
| Mink, J. W.         | 26, 27, 84              | Pennock, S. R.    | 67, 300, 396       |
| Mirotnik, M. S.     | 50                      | Peters, M. E.     | 308                |
| Mishra, S.          | 6, 9                    | Peters, Jr., L.   | 137                |
| Mitra, R.           | 62, 76, 200             | Peterson, A. F.   | 152, 160, 255      |
| Mitzner, K. M.      | 321, 330                | Pike, D.          | 204                |
| Mockapetris, L.     | 410                     | Piket-May, M.     | 143, 144           |
| Moghaddam, M.       | 306                     | Pino, A. G.       | 411                |
| Mohammadian, A. H.  | 140                     | Plumb, R. G.      | 226, 329, 337      |
| Mohan, S. A.        | 413                     | Pohle             | 218                |
| Moheb, H.           | 6                       | Pollock, M. A.    | 172                |
| Molinet, F.         | 335                     | Pop, I.           | 284                |
| Momose, T.          | 375                     | Prather           | 218                |
| Monahan, G. P.      | 27, 84                  | Pribetich, J.     | 52, 55, 56, 128    |
| Moore, T. G.        | 364                     | Pribetich, P.     | 20, 28             |
| Mortensen, G. E.    | 155, 156                | Prieto, F.        | 111                |
| Moses, C. A.        | 245                     | Puzenko, A. A.    | 414                |
| Moses, G. C.        | 48                      | Qi, S.            | 91                 |
| Moumneh, B.         | 16                      | Qi, Y. H.         | 86                 |
| Mugnai, A.          | 44                      | Qiu, Z.           | 376                |
| Muller, G.          | 335                     | Radnovic, I.      | 21, 22             |
| Murphy, J. A.       | 62                      | Rahmat-Samii, Y.  | 66, 153, 328, 330  |
| Nagode, T.          | 282                     | Rahnavard, M. H.  | 102, 103, 210      |
| Narasimha, R. K. L. | 413                     | Railton, C. J.    | 63, 64             |
| Natzke, J. R.       | 262                     | Raju, G. S. N.    | 272                |
| Nepa, P.            | 332                     | Ramahi, O.        | 200                |
| Nesic, A.           | 21, 22                  | Ramanujam, P.     | 388                |
| Nevels, R.          | 171, 276, 323           | Rao, K. V.        | 272                |
| Newkirk, M. H.      | 170                     | Rao, K. V. N.     | 173                |
| Newman, E. H.       | 260, 308                | Rao, P. M.        | 272                |
| Newman, M. B.       | 147                     | Rao, S. M.        | 322                |
| Ng, K. T.           | 53, 60, 124             | Rebeiz, G. M.     | 14, 164            |
| Nghiem, D.          | 395                     | Rebollar, J. M.   | 401, 402           |
| Ngo, T.             | 146                     | Reeves, M. M.     | 220                |
| Nguyen, T. X.       | 158                     | Remmert, R.       | 159                |
| Nguyen, C.          | 166, 283                | Reuster, D. D.    | 291                |
| Nishikata, A.       | 265                     | Rice, D. J.       | 310                |
| Niver, E.           | 115                     | Richard, M. A.    | 165                |
| Norgard             | 218                     | Richie, J. E.     | 70                 |
| Nyquist, D.         | 215, 216, 219, 221, 294 | Riley, D. J.      | 67                 |
| O'Keefe, S. G.      | 365                     | Rius, J. M.       | 11                 |
| Oh, Y.              | 406                     | Rivas, F.         | 154                |
| Okoniewski, M.      | 51, 313                 | Rivera, D. F.     | 207                |
| Oliner, A. A.       | 395                     | Robert G., R. G.  | 7                  |
| Olivier, J. C.      | 88, 89                  | Rohrer, N. J.     | 165                |
| Olsen, R. G.        | 257                     | Rojas, R. G.      | 260, 370           |
| Omick, S.           | 61                      | Rollins, G. Z.    | 388                |
| Orme, M.            | 127                     | Rong, A. S.       | 104, 105           |
| Otero, M. F.        | 370                     | Roper, D.         | 146                |
| Ott, R. H.          | 172                     | Roscoe, D. J.     | 351                |
| Otto, G. P.         | 228                     | Ross, J.          | 216, 221           |
| Page, J. E.         | 401                     | Ross, D. C.       | 189, 194           |
| Paker, S.           | 235                     | Ross, J.          | 215                |
| Paleczny, E.        | 28                      | Rothwell, E.      | 215, 216, 219      |

|                    |                      |
|--------------------|----------------------|
| Rowse, D. P.       | 62                   |
| Rudduck, R. C.     | 137                  |
| Saadoun, M. M.I.   | 304, 305             |
| Sabetfakhri, K.    | 29                   |
| Sadigh, A.         | 361                  |
| Said, R. A.        | 184                  |
| Saillard, J.       | 78, 231, 412         |
| Saillard, M.       | 372                  |
| Salazar-Palma, M.  | 274, 275             |
| Santalla, V.       | 411                  |
| Saoudy, S. A.      | 204, 382             |
| Sarabandi, K.      | 399, 406             |
| Sarkar, T. K.      | 274, 275, 385        |
| Sarmadi, H.        | 102                  |
| Sathiseelan, V.    | 121                  |
| Scharstein, R. W.  | 368, 369             |
| Schlecht, E.       | 280                  |
| Schnier, R. G.     | 266                  |
| Schneider, J. B.   | 59, 257, 409         |
| Schumacher, C. R.  | 79                   |
| Schuneman, A.      | 27                   |
| Schwering, F. K.   | 26, 27, 84, 112, 397 |
| Scott, Jr., W. R.  | 176                  |
| Sebak, A. A.       | 19                   |
| Sega               | 218                  |
| Sekellick, M. A.   | 267                  |
| Senior, T. B. A.   | 262                  |
| Sercu, J.          | 31                   |
| Shaarawi, A. M.    | 362                  |
| Shafai, L.         | 6, 85, 351           |
| Shamansky, H. T.   | 260                  |
| Shankar, V.        | 140                  |
| Shen, X.           | 71, 206              |
| Shin, R. T.        | 87                   |
| Simons, N. R. S.   | 19                   |
| Simons, R. N.      | 185                  |
| Sinha, M.          | 382                  |
| Sirenko, Yu. K.    | 415                  |
| Skirta, E. A.      | 312                  |
| Slade, G. W.       | 183                  |
| Smith              | 218                  |
| Smith, C. E.       | 16                   |
| Smith, E. A.       | 44                   |
| Snider, J. B.      | 37, 38, 41           |
| Sohos, G.          | 65                   |
| Solheim, F.        | 39                   |
| Somers, G. A.      | 380                  |
| Song, G. X.        | 86                   |
| Souza, J. R.       | 285                  |
| Speciale, R. A.    | 307                  |
| Speilman, T.       | 314                  |
| Spencer, R. W.     | 44                   |
| Spring, C. T.      | 316                  |
| Stach, J.          | 77                   |
| Stankov, B. B.     | 41                   |
| Steer, M. B.       | 27, 84               |
| Stepanescu, A.     | 284                  |
| Stevens, W. G.     | 173                  |
| Stirbat, I.        | 284                  |
| Stoyanov, A. J.    | 267                  |
| Stoyanov, Y. J.    | 267                  |
| Stuchly, M. A.     | 125                  |
| Sun, Z. L.         | 104, 105             |
| Sun, D. K.         | 195                  |
| Suratteau, J. Y.   | 372                  |
| Suvakov, S.        | 22                   |
| Swaminathan, M.    | 292                  |
| Swart, W. A.       | 88                   |
| Swift, C. T.       | 43                   |
| Taághol, A.        | 385                  |
| Taflove, A.        | 142, 143, 144        |
| Takagi, A.         | 296                  |
| Tamasanis, D.      | 410                  |
| Tame, B.           | 127                  |
| Tanaka, K.         | 296                  |
| Tanaka, M.         | 296                  |
| Tanyer, S. G.      | 7                    |
| Tashima, H.        | 296                  |
| Tatarskaia, M. S.  | 42                   |
| Tatarskii, V. I.   | 42                   |
| Tatarskii, V. V.   | 42                   |
| Taub, S. R.        | 185                  |
| Taute, B. J. E.    | 332                  |
| Telikepalli, R.    | 384                  |
| Tenforde, T. S.    | 119                  |
| Tertuliano, H.     | 299                  |
| Thiel, D. V.       | 365                  |
| Thiele, G. A.      | 291                  |
| Thomopoulos, E.    | 54                   |
| Thomson, D. J.     | 184                  |
| Tiberio, R.        | 94, 331              |
| Tice, T. E.        | 130, 172             |
| Tie, G.            | 90, 286              |
| Tillary, J. K.     | 350                  |
| Tilston, M. A.     | 220                  |
| Toccafondi, A.     | 94, 331              |
| Torres-Verdín, C.  | 74                   |
| Tran, H. B.        | 10, 324              |
| Tran, M.           | 166, 283             |
| Tranquilla, J. M.  | 384                  |
| Tret'yakov, O. A.  | 414                  |
| Trintinalia, L. C. | 4                    |
| Triolo, A.         | 112                  |
| Tripp, V. K.       | 349, 350             |
| Tsai, C. Y.        | 219                  |
| Turhan-Sayan, G.   | 236                  |
| Turk, J.           | 44                   |
| Tzeng, N.          | 133                  |
| Uberall, H.        | 79                   |
| Ufimtsev, P. Ya.   | 330, 377             |
| Ulaby, F. T.       | 406                  |
| Uslenghi, P. L. E. | 147, 244, 320        |
| Uzunoglu, N. K.    | 54                   |
| Valco, G. J.       | 165                  |
| Vall-llossera, M.  | 11                   |
| Valle, L.          | 154                  |

|                   |                    |
|-------------------|--------------------|
| Vandemark, D. C.  | 170                |
| VanDoren, T. P.   | 346                |
| VanHove, T.       | 39                 |
| Vanzura, E. J.    | 180                |
| Varadan, V. K.    | 242, 311           |
| Varadan, V. V.    | 242, 311           |
| Vecino, C.        | 402                |
| Ventouras, E.     | 54                 |
| Vera, M.          | 411                |
| Viitanen, A. J.   | 248                |
| Vivekanandan, J.  | 44                 |
| Vogel, W. J.      | 110                |
| Vogelius, M.      | 234                |
| Vogt, M.          | 159                |
| Volakis, J. L.    | 132, 189, 194, 321 |
| Walsh, J.         | 382                |
| Walsh, L.         | 146                |
| Walton, E. K.     | 363                |
| Wang, D.-S.       | 277                |
| Wang, H.-H.       | 49                 |
| Wang, T.-M.       | 4                  |
| Wang, W. T.       | 86                 |
| Wang, Y.          | 126                |
| Wang, Y.-Y.       | 34, 404            |
| Wang, J. J. H.    | 350                |
| Ware, R.          | 39                 |
| Wame, L. K.       | 217, 352           |
| Warren, G. S.     | 176                |
| Webb, K. J.       | 183, 255           |
| Weil, C. M.       | 180                |
| Weinreb, S.       | 280                |
| Welland, G.       | 277                |
| Wenbing, W.       | 223                |
| Westwater, E. R.  | 38, 40, 41, 42     |
| Whites, K. W.     | 201, 243           |
| Whitman, G. M.    | 112, 397           |
| Wilkes, D. L.     | 156                |
| Wilkins, G. M.    | 292                |
| Williams, J. T.   | 395                |
| Willis III, T. M. | 114                |
| Wilton, D. R.     | 322                |
| Winchester, T. A. | 358                |
| Wong, T. T. Y.    | 281, 282           |
| Wright, D. B.     | 258                |
| Wright, W.        | 167                |
| Wu, C.            | 141, 145           |
| Wu, K.            | 141, 145, 383      |
| Wu, T. T.         | 83, 238            |
| Wu, Z.            | 171, 276, 323      |
| Yang, Q.          | 91                 |
| Yarovoy, A. G.    | 414                |
| Yazgan, B.        | 235                |
| Yihong, Q.        | 161                |
| Ying, Z.          | 293                |
| Yokota, M.        | 295                |
| Yook, J.-G.       | 33                 |
| Yoshida, N.       | 270                |
| Young, J.         | 135, 348, 214      |
| Young, J. L.      | 257                |
| Young, P. G.      | 185                |
| Yuan, X.          | 195, 196           |
| Yuan, Y.          | 87                 |
| Yukutake, K.      | 334                |
| Zapata, J.        | 298                |
| Zeisberg, S.      | 27                 |
| Zhang, X.-Z.      | 353                |
| Zhou, J.          | 416                |
| Zhu, X.           | 32                 |
| Zhuang, Y.        | 383                |
| Zhuck, N. P.      | 414                |
| Zimmerman, M.     | 344                |
| Ziolkowski, R. W. | 239, 240           |
| Zogbi, G.         | 205                |
| Zouak, M.         | 231                |
| Zuffada, C.       | 253                |

# A MARRIAGE MADE IN HEAVEN



Imagine a symmetric model with *150,000 unknowns*. Now imagine solving it with two rank 75,000 matrices at a *sustained 4.6 GFLOPS*.

Lockheed Advanced Development Company (LADC) solved this problem—believed to be the largest Method of Moments problem ever using Intel's iPSC®/860 Parallel Supercomputer and an out-of-core slab solver developed by Intel for its family of ProSolver™ Parallel Linear Equation Solvers. Calculating the radar cross section of a signature-controlled stealth-technology vehicle, the code is unique not only in solving larger problems than any reported previously, but in accurately modeling all the materials involved in modern aircraft design.

We realize that all CEM problems cannot be solved using Method of Moments. Other customers have been equally successful at solving challenging problems using ray tracing, finite element, and time domain algorithms.

Intel's ProSolver family of linear equation solvers provides the optimized parallel routines needed for building, factoring, and solving the

large systems of linear equations common to CEM applications. The solvers are available for both the iPSC/860 Supercomputer and the Paragon™ XP/S Supercomputer, Intel's new 4th generation system based on the technology demonstrated in the Touchstone Delta System at Caltech.

According to Larry Dilger, senior project manager at LADC, Intel's combination of supercomputing hardware and ProSolver software is "*a marriage made in heaven for computational electromagnetics*." To find out how you can get to CEM Heaven, stop by our booth during the symposium or contact David Scott at 503-531-5347 or via Internet at [dscoff@ssd.intel.com](mailto:dscoff@ssd.intel.com).

The Intel logo, which consists of the word "intel" in a lowercase, sans-serif font. The letters are slightly slanted and have a bold, italicized appearance. The "i" is positioned at the top left, followed by "n", "t", "e", and "l" at the bottom right.

Supercomputer Systems Division

---

## Environmental Research Institute of Michigan

For almost 50 years ERIM has been a leader in imaging technologies: designing and developing advanced sensor systems and state-of-the-art image processing hardware and software.

That expertise in all aspects of image capture and processing has led to advances in a wide range of fields, including electro-optics and holography, imaging radars, and multi-spectral scanners, as well as powerful analog and digital image processing systems.

As an organization we are dedicated to adapting state-of-the-art technologies to military and civilian applications that encompass many of the most vexing problems facing our nation and the world. ERIM also helps enhance the economic competitiveness of the nation via its work in industrial machine vision for quality and process control in manufacturing.



ERIM's goal always is to employ the creativity of our research staff and the synergy that emerges from our many research activities to solve our customers' problems and to help keep our country safe, clean, and economically strong.



P.O. Box 134001  
Ann Arbor, MI 48113-4001

# **1994 IEEE AP-S International Symposium and URSI Radio Science Meeting**

**University of Washington  
Seattle, Washington USA  
June 19-24, 1994**

The 1994 AP-S International Symposium sponsored by the IEEE Antennas and Propagation Society and the URSI Radio Science Meeting sponsored by USNC Commissions A,B,D, and E of the International Union of Radio Science will be held on the campus of the University of Washington, Seattle, Washington, June 19-24, 1994. The technical sessions will cover the five-day period June 20-24 and will be coordinated among the two symposia to provide a comprehensive, well-balanced program.

- General information about the 1994 joint symposium can be obtained from:

**Dr. Gary Miller, Joint Symposia Chair  
c/o Engineering Continuing Education  
University of Washington, GG-13  
Seattle, WA 98195  
phone: (206) 543-5539  
fax: (206) 543-2352  
e-mail: kvamme@u.washington.edu**

- IEEE AP-S technical program inquiries should be directed to:

**Professor Leung Tsang  
Technical Program Committee Chair  
Department of Electrical Engineering  
University of Washington, FT-10  
Seattle, WA 98195  
phone: (206) 685-7537  
fax: (206) 543-3842  
e-mail: tsang@ee.washington.edu**

- URSI inquiries should be directed to:

**Professor Akira Ishimaru  
Department of Electrical Engineering  
University of Washington, FT-10  
Seattle, WA 98195  
phone: (206) 543-2169  
fax: (206) 543-3842  
e-mail: ishimaru@ee.washington.edu**

